Understanding Computer Use in Ground Water Science: An Anthology

24 papers on how computer technology can be used to better understand and illustrate ground water conditions.

September 1991

National Ground Water Association
6375 Riverside Drive
Dublin, OH 43017
614-761-1711

to replace 3897 free

Understanding Computer Use in Ground Water Science: An Anthology

This anthology contains 24 papers selected because the National Water Well Association believes they are among the best contributions on explaining the role computers can play in understanding and illustrating ground water concepts.

NWWA uses its anthologies as a means to disseminate information about narrow, but very important subjects.

All the articles presented within the anthology are available at the National Ground Water Information Center and are stored within Ground Water On-Line, the 65,000 record bibliographic data base operated by the Center. The National Ground Water Information Center was established in 1960 as a repository available to scientists, government, contractors, business and the public.

The NWWA, a not-for-profit professional society and trade association, represents all segments of the ground water industry. Its more than 23,000 members from nearly 70 nations include the world's leading ground water geologists and hydrologists, ground water contractors, engineers, manufacturers, and suppliers of ground water-related products and services. From its Dublin, Ohio headquarters NWWA provides the industry, government, business, and consumers guidance for sound scientific, economic, and beneficial development, protection and management of the world's ground water resources.

Understanding Computer Use in Ground Water Science: An Anthology

Order of Appearance

Contaminant Transport

13. An Idealized Ground-Water Flow and Chemical Transport Model (S-PATHS) (Ground Water, July/August 1984) by Phil L. Oberlander and R.W. Nelson

14. MOC Solutions of Convective-Dispersion Problems (Ground Water, November/December 1986) by Raz Khaleel and Donald L. Reddell

15. Applying the USGS Mass-Transport Model (MOC) to Remedial Actions by Recovery Wells (Ground Water, May/June 1988) by Aly I. El-Kadi

16. Modifying the USGS Solute Transport Computer Model to Predict High-Density Hydrocarbon Migration (Ground Water, November/December 1988) by M. Akhter Hossain and M. Yavuz Corapcioglu

17. Approximate and Analytical Solutions for Solute Transport from an Injection Well into a Single Fracture (Ground Water, January/February 1989) by Chia-Shyun Chen and S.R. Yates

Regional Hydrology

18. Ground-Water Modeling: Applications (Ground Water, September/October 1980) by James W. Mercer and Charles R. Faust

19. Microcomputer Model of Artificial Recharge Using Glover's Solution (Ground Water, January/February 1984) by D. Molden, D.K. Sunada, and J.W. Warner

20. Mapping Recharge Areas Using a Ground-Water Flow Model - A Case Study (Ground Water, March/April 1989) by Mary W. Stoertz and Kenneth R. Bradbury

Statistics

21. Three-Dimensional Cross-Semivariogram Calculations for Hydrogeological Data (Ground Water, September/October 1988) by Jonathan D. Istok, Richard M. Cooper, and Alan L. Flint

Unsaturated Zone

22. A Galerkin Finite-Element Program for Simulating Unsaturated Flow in Porous Media (Ground Water, January/February 1985) by R. Khaleel and T.C. Yeh

23. A Three-Dimensional Analytical Model to Aid in Selecting Monitoring Locations in the Vadose Zone (Ground Water Monitoring Review, Spring 1988) by C.R. McKee and A.C. Bumb

24. Simulation of Vapor Transport Through the Unsaturated Zone - Interpretation of Soil-Gas Surveys (Ground Water Monitoring Review, Spring 1988) by Lyle R. Silka

Aquifer Analysis / Pumping Tests

A Simple Computer Program for the Determination of Aquifer Characteristics from Pump Test Data

by Joseph C. Holzschuh III[a]

ABSTRACT

A computer program, based on the Hantush inflection method and designed for "desk top" computers is presented. The method assumes a leaky, isotropic, homogeneous aquifer of infinite areal extent. The language employed is BASIC, an interactive language used on the Wang Model 2200 programmable calculator. The program can be easily adapted to FORTRAN IV for use on larger machines.

INTRODUCTION

The staff at our Water Management District required a fast, approximate, and simple method for checking the analyses of pump test data submitted by various consultants in support of permit applications. Such a method would be used, not to replace type curve solutions but rather to provide initial estimates of aquifer characteristics, cross check other types of analyses and lend further support to them. Machine analysis was desirable, to eliminate human errors.

The equipment available was a Wang Model 2200 desk type calculator with 8K of memory and a cassette tape data storage system. A large IBM system was also available, but could not be directly used by our hydrologists in a "hands on" mode as could the Wang. Also, "turnaround" time for the larger system was typically 1 day or longer. Turnaround time for the desk top system was usually on the order of minutes. Many organizations have like or similar mini-computers available. Adapting the program to such machines would prove no problem.

METHODOLOGY

The method finally selected and adapted for machine use was the Hantush inflection point method (DeWiest, 1965). This method is based on determining the slope of a semi-log, drawdown versus time curve, at the inflection point (Figure 1). The inflection point (shown on Figure 1 at S feet of drawdown and occurring at time T) is assumed to be at one-half the maximum or equilibrium drawdown (Sϕ). The computation of the slope of the line should be done over a full-time log cycle centered about the inflection point. The program first determines the time (T) at which (S) occurs. Since the data points fed into the machine will probably not include point (T,S), T must be determined by interpolation from points (T1, S1) and (T2, S2). This is done by computing the slope (M1) between points (T1, S1) and (T2, S2) and

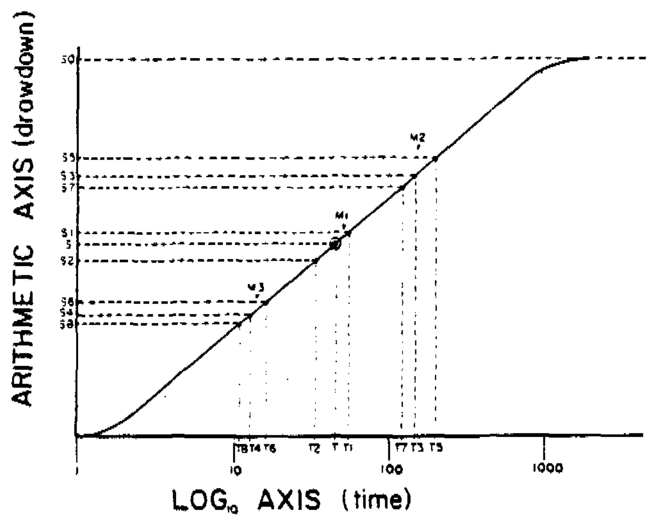

Fig. 1. Semi-log drawdown curve.

[a]Supervisory Hydrologist, Southwest Florida Water Management District, 5060 U.S. Highway 41 South, Brooksville, Florida 33512.

Discussion open until February 1, 1977.

utilizing that slope to compute (T). When point (T, S) has been determined, the value of T3 and T4 (+ and − 0.5 log cycle respectively) can be found. Since (T3, S3) and (T4, S4) are again probably not in the input data, they too must be interpolated from the closest input data points available, i.e. (T8, S8), (T6, S6), (T7, S7), and (T5, S5), utilizing slopes (M3) and (M2) respectively. The program determines the slope of the drawdown curve (M) over ½-log cycle and full-log cycle intervals. This was done because in rare instances equilibrium is reached so quickly that using a full-log cycle would include points outside the straight-line portion of the curve. Both slopes are printed out although only the full-log cycle slope is used. The investigator should check to see that both slopes agree closely. Any significant difference should be investigated.

Once the slope has been determined the only remaining difficulty is solving for $^r/B$. Hantush provides the following equation:

$$K = e^{r/B}\ K_0\ (r/B) \qquad (1)$$

where:

$$K = 2.3\ S/M \qquad (2)$$

Equation 1 is an implicit equation and cannot be solved directly. A solution is provided, however, by plotting values of $^r/B$ vs. K on semi-log paper, and approximating the curve so derived with a series of straight lines. Depending then on the value of K, the program selects the proper straight-line equation and solves for $^r/B$. Accuracy is usually sufficient for most purposes but the values of both K and $^r/B$ are printed out by the program so the investigator may consult a set of tables if so desired.

With $^r/B$ now known, transmissivity, storage and leakance can be solved for directly using the equations given by Hantush and shown in lines 950-970 in the program. The complete program is shown in Figure 2.

The inflection point method requires that equilibrium be reached during the pump test, and accordingly one of the assumptions made in the program is that the final data point entered is on the flat or equilibrium part of the curve. Experimenting with the program using data derived from local pump tests has indicated that if the test is terminated at a time when an appreciable portion of the equilibrium drawdown has already occurred, the transmissivity and storage coefficients reported by the program will differ only negligibly from their actual values. The leakance reported will tend to reflect a limiting value which will always be greater than the actual value. Such a limiting value for leakance can be useful when field conditions have prevented running the pump test to equilibrium.

```
10 REM    PROGRAMER HOLZSCHUH 7/25/75
20 PRINT "INFLECTION POINT METHOD"
30 DIM Z(2,100)
40 REM ---------------------------
50 REM --THIS SECTION INPUTS DATA--
60 REM ---------------------------
70 INPUT "HOW MANY MEASUREMENTS",N
80 INPUT "GIVE PUMPED WELL Q (GPM)",Q
90 INPUT "GIVE RADIUS TO OBS WELL (FT.)", R1
100 INPUT "DO YOU WISH TO ENTER DATA OR READ OFF TAPE
                    ENTER AND RECORD DATA - 1
                    READ OFF TAPE         - 2",A
110 ON A GOTO 120,130
120 PRINT "PLEASE LOAD BLANK DATA TAPE"
130 FOR C=1TO N
140 INPUT "GIVE TIME (MIN.), DRAWDOWN (FT)", Z(1,C),Z(2,C)
150 NEXT C
160 DATA SAVE Z()
170 GOTO 250
180 PRINT "PLEASE LOAD APPROPRIATE DATA TAPE"
190 STOP
200 PRINT :PRINT :PRINT :PRINT
210 DATA LOAD Z()
220 REM ----------------------------------------------
230 REM --COMPUTE DRAWDOWN AND TIME AT INFLECTION PT.--
240 REM ----------------------------------------------
250 S0=Z(2,N)
260 S=S0/2
270 FOR C=1TO N
280 IF S [ Z(2,C) THEN 300
290 NEXT C
300 S1=Z(2,C):S2=Z(2,C-1):T1=Z(1,C):T2=Z(1,C-1)
310 M1=   (S1-S2)/(.434294481903 3*(LOG(T1)-LOG(T2)))
320 B=S1-M1*.4342944819033*LOG(T1)
330 T=10!((S-B)/M1)
340 REM ---------------------------
350 REM --COMPUTE SLOPE OVER ONE HALF
          AND FULL LOG CYCLES--
360 REM ---------------------------
370 H=0
380 L=.4342944819033*LOG(T):L1=L+.25:L2=L-.25:T3=10!L1:T4=10!
390 GOTO 410
400 L=.4342944819033*LOG(T):L1=L+.5:L2=L-.5:T3=10!L1:T4=10!L2
410 FOR C=1TO N
420 IF T3 [ Z(1,C) THEN 440
430 NEXT C
440 T5=Z(1,C):T7=Z(1,C-1):S5=Z(2,C):S7=Z(2,C-1)
450 FOR C=1TO N
460 IF T4 [ Z(1,C) THEN 480
470 NEXT C
480 T6=Z(1,C):T8=Z(1,C-1):S6=Z(2,C):S8=Z(2,C-1)
490 M2=((S5-S7)/(.4342944819033*(LOG(T5)-LOG(T7))))
500 S3=(M2*(.4342944819033*(LOG(T3)-LOG(T7))))+S7
510 M3=((S6-S8)/(.4342944819033*(LOG(T6)-LOG(T8))))
520. S4=(M3*(.4342944819033*(LOG(T4)-LOG(T8))))+S8
530 IF H=1 THEN 570
540 M4=(S3-S4)*2
550 H=1
560 GOTO 400
570 M=S3-S4
580 K=(2.3*S)/M
590 REM ---------------
600 REM --COMPUTE R/B--
610 REM ---------------
620 IF K]4.763 THEN 680
630 IF K]2.682 THEN 700
640 IF K]1.352 THEN 720
650 IF K]1.144 THEN 740
660 IF K] .547 THEN 760
670 PRINT "ERROR R/B ] 5"
680 R=10!((K-.256)/(-2.256))
690 GOTO 800
700 R=10!((K-.596)/(-2.086))
710 GOTO 800
720 R=10!((K-.943)/(-1.739))
730 GOTO 800
740 R=10!((K-1.144)/(-1.354))
750 GOTO 800
760 R=10!((K-1.144)/(-.8530))
770 REM ----------------
780 REM --START OUTPUT--
790 REM ----------------
800 PRINT "R/B =",R
810 PRINT "K =",K
820 PRINT
830 PRINT "HALF LOG CYCLE SLOPE =",M4
840 PRINT "FULL LOG CYCLE SLOPE =",M
850 PRINT
860 PRINT "SLOPES SHOULD AGREE CLOSELY"
870 PRINT "IF THEY DO NOT, PLOT ON SEMI-LOG PAPER TO SEE IF"
880 PRINT "FULL LOG CYCLE SLOPE INCLUDES POINTS OUTSIDE"
890 PRINT "STRAIGHT LINE PART OF CURVE"
900 STOP
910 PRINT :PRINT :PRINT :PRINT
920 REM -------------------------
930 REM --COMPUTE TRANSMISSIVITY,
          STORAGE AND LEAKAGE--
940 REM -------------------------
950 T9=(264*Q*EXP(-R))/M     :REM  COMPUTE TRANSMISSIVITY
960 S9=(T9*T*R)/(3186*R1!2)  :REM  COMPUTE STORAGE
970 P=T9/((R1/R)!2)          :REM  COMPUTE LEAKANCE
980 REM ------------------
990 REM --COMPLETE OUTPUT--
1000 REM ------------------
1010 PRINT "AQUIFER CHARACTERISTICS ARE AS FOLLOWS"
1020 PRINT :PRINT
1030 PRINTUSING 1040,T9:PRINT
1040%     TRANSMISSIVITY         -     ########  GPD/FT.
1050 PRINTUSING 1060,S9:PRINT
1060%     STORAGE COEFFICIENT    -     #.######
1070 PRINTUSING 1080,P
1080%     LEAKANCE (P'/M')       -     #.######  GPD/FT.!3
1090 END
```

Fig. 2. Program listing.

```
RUN
INFLECTION POINT METHOD
HOW MANY MEASUREMENTS? 12
GIVE PUMPED WELL Q (GPM)? 1000
GIVE RADIUS TO OBS WELL (FT.)? 100

DO YOU WISH TO ENTER DATA OR READ OFF TAPE
        ENTER AND RECORD DATA - 1
        READ OFF TAPE         - 2? 1
PLEASE LOAD BLANK DATA TAPE
GIVE TIME (MIN.), DRAWDOWN (FT)? .2,1.76
GIVE TIME (MIN.), DRAWDOWN (FT)? .5,2.75
GIVE TIME (MIN.), DRAWDOWN (FT)? 1,3.59
GIVE TIME (MIN.), DRAWDOWN (FT)? 2,4.26
GIVE TIME (MIN.), DRAWDOWN (FT)? 5,5.23
GIVE TIME (MIN.), DRAWDOWN (FT)? 10,5.90
GIVE TIME (MIN.), DRAWDOWN (FT)? 20,6.47
GIVE TIME (MIN.), DRAWDOWN (FT)? 50,6.92
GIVE TIME (MIN.), DRAWDOWN (FT)? 100,7.11
GIVE TIME (MIN.), DRAWDOWN (FT)? 200,7.20
GIVE TIME (MIN.), DRAWDOWN (FT)? 500,7.21
GIVE TIME (MIN.), DRAWDOWN (FT)? 1000,7.21
R/B =              5.07672123E-02
K =                3.296153200416

HALF LOG CYCLE SLOPE =          2.500443771353
FULL LOG CYCLE SLOPE =          2.515508077402

SLOPES SHOULD AGREE CLOSELY
IF THEY DO NOT, PLOT ON SEMI-LOG PAPER TO SEE IF
FULL LOG CYCLE SLOPE INCLUDES POINTS OUTSIDE
STRAIGHT LINE PART OF CURVE

STOP
:CONTINUE


AQUIFER CHARACTERISTICS ARE AS FOLLOWS

    TRANSMISSIVITY          =        99753   GPD/FT.

    STORAGE COEFFICIENT     =     0.000095

    LEAKANCE (P'/M')        =     0.025709   GPD/FT.:3

END PROGRAM
FREE SPACE=10258

:
```

Fig. 3. Typical printout.

UNITS AND DATA ENTRY

All variables used in the program are in the gallon/foot/day system. The specific units used for input and output data are specified in the program and shown in the example.

Since much of the drawdown data that we work with are already stored on tape cassettes, provisions are made in the program to read the time-drawdown data directly from a tape and to write that data on a tape when they are initially entered. If only direct entry of data is desired

Table 1.

	Type Curve	*Inflection Point*
Transmissivity	100,000 gpd/ft.	99753 gpd/ft.
Leakance (P′/m′)	.025 gpd/ft.^{3}	.0257 gpd/ft.^{3}
Storage	.0001	.000095

with no provisions for tape storage, lines 100-120 and 160-210 of the program can be eliminated.

EXAMPLE

An example (employing generated data) used by Cooper (Bentall, 1963) to illustrate the use of type curves is used here to compare the two methods. Figure 3 is a print-out yielded by the program, when the data presented in Cooper's Table 6 (^{r} = 100 ft.) are inputed. The values obtained using the type curve method are shown here in Table 1 in comparison with those obtained by the program. The values in this case agreed closely, well within the limits of most field data.

CONCLUSION

Much has been said recently about the dangers of computerizing pump tests, with most of that fear probably well founded. The author wishes to emphasize that the program presented herein should not be used indiscriminantly, i.e. as a black box which grinds out answers of unquestionable reliability. The applicability of the inflection point method to the problem at hand must be considered, as well as other factors such as anisotropy and boundary conditions.

REFERENCES

Bentall, R. 1963. Shortcuts and special problems in aquifer tests. U.S. Geological Survey, Water-Supply Paper 1545-C.

DeWiest, J. M. 1965. Geohydrology. John Wiley and Sons.

Pumping Tests in Patchy Aquifers

by J. A. Barker and R. Herbert[a]

ABSTRACT

A numerical simulation and analytical study of a constant-rate pumping test, for a well situated at the centre of a disc of anomalous transmissivity and storage coefficient, have been used to aid in the interpretation of tests performed in a "patchy" aquifer in India. Equations describing the long-time behaviour of drawdown show that Jacob's method can be employed to estimate the regional transmissivity from drawdowns measured at any point in the aquifer or in the pumping well. However, these equations also show that an average storage coefficient should be calculated from drawdowns measured outside the aquifer discontinuity.

The results of this study support the hypothesis that the average transmissivity of a heterogeneous aquifer can be calculated from rates of drawdown observed after long periods of pumping.

INTRODUCTION

All aquifers are to some extent heterogeneous and this fact brings into question the validity of normal methods of pumping-test analysis which assume homogeneity. While it is perhaps obvious that pumping tests tend to "average out" the properties of aquifers, it is natural to be suspicious of results obtained when the pumping well is situated in a region of the aquifer which is considered to be atypical—especially if the only drawdown measured is that in the pumping well.

This paper describes (i) a field investigation that led to a consideration of the general problem of pumping tests in patchy aquifers, (ii) our attempts to gain insight into the problem by computer simulation and mathematical analysis of a simple form of heterogeneity, and (iii) a general hypothesis suggested by this study and previous work. Some particularly unusual pumping-test data, which appear to have a simple interpretation in the light of the analysis, are also presented.

BACKGROUND

The Overseas Section of the Hydrogeology Unit of the Institute of Geological Sciences is carrying out a study in the Deccan Traps of India which involves the drilling and pump-testing of many wells. Well yield has been found to be unpredictable. Typically, a test site would be centred on an established well yielding about 5 to 10 l/s (0.18 to 0.35 ft^3/s). It is quite common for an observation well subsequently drilled 20 metres away to yield less than 1 l/s (0.035 ft^3/s). This variability in yield has led to the conclusion that the aquifer is generally of low transmissivity but has within it pockets of relatively high transmissivity.

[a]Senior Scientific Officer and Principal Scientific Officer, respectively, Hydrogeology Unit, Institute of Geological Sciences, Maclean Building, Wallingford, Oxon, OX10 8BB, England.

Manuscript received August 1981, accepted October 1981.

Discussion open until September 1, 1982.

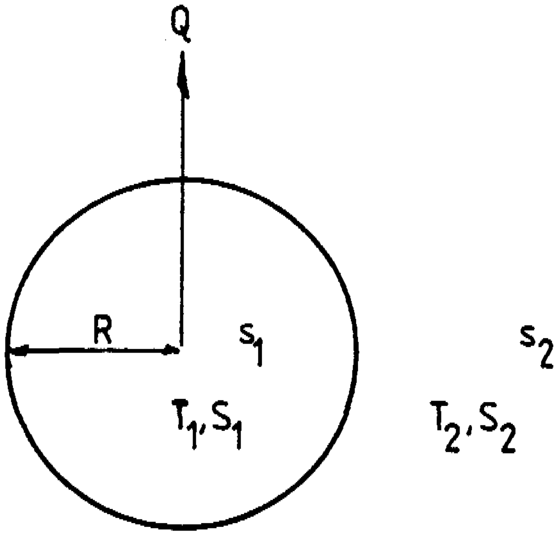

Fig. 1. Idealised heterogeneous aquifer studied.

The theoretical study described here was carried out to assist interpretation of the results of pumping tests performed in such an aquifer. In particular, the case of a pumping well situated in a high transmissivity pocket with observation wells both inside and outside the pocket, has been studied.

IDEALIZATION OF THE SYSTEM

In order to make the problem amenable to analytical as well as numerical methods, the system was chosen to have radial symmetry about the pumping well (see Figure 1). The aquifer is confined and consists of two regions with transmissivities T_1 for $r < R$ and T_2 for $r > R$, and corresponding storage coefficients S_1 and S_2. It is assumed that a constant pumping rate, Q, is maintained throughout the test in a fully penetrating well.

NUMERICAL STUDY

This idealized pumping test was simulated using a simple one-dimensional (radial) finite-difference model. Parameter values were chosen to approximate typical conditions encountered in the field tests in India. The values chosen were $T_1 = 80$ m²/d (0.01 ft²/s), $T_2 = 5$ m²/d (0.0006 ft²/s), $S_1 = S_2 = 0.001$, $R = 60$ m (197 ft), $Q = 5$ l/s (0.18 ft³/s). The pumping well was assumed to have a small finite diameter $2r_w = 0.2$ m (0.66 ft).

Figure 2 shows a semilog plot of simulated drawdown data, s, against time of pumping, t, for the test well ($r = r_w$) and for observation wells in both aquifer regions, r = 2 m (6.6 ft) and r = 62 m (203 ft).

For a fully-penetrating well pumping from a homogeneous, confined aquifer of transmissivity, T, well storage may have a significant effect on drawdowns if $Tt/r_w^2 < 25$ (Papadopulos and Cooper, 1967). This corresponds to times less than 4.5 minutes ($25r_w^2/T_1$) in the simulated test. Following this initial period there is a phase of the test when drawdowns in the outer aquifer region are negligible and the test results are consequently similar to those expected for a line sink in a homogeneous aquifer of transmissivity T_1. Further, since the quantity $u = r^2S_1/4T_1t$ is less than 0.01 for $t > 4.5$ minutes and $r < 10$ m (33 ft), drawdowns in both the production well and the inner observation well should follow the Jacob equation (Cooper and Jacob, 1946; Todd, 1959):

$$s_1 = \frac{Q}{4\pi T_1} \ln \frac{4T_1t}{Cr^2S_1} \qquad (1)$$

where C = 1.78 . . . .

The simulated data are approximated by equation (1) during the period 4.5 min. to 30 min.

As the radius of influence of the test moves into the outer aquifer region, drawdowns increase more rapidly until most of the water results from the lowering of heads in the outer region. It then seems reasonable to expect that rates of drawdown would become dominated by the transmissivity T_2. Figure 2 shows that all three curves tend to straight lines with roughly the same slope which, applying Jacob's equation, gives a transmissivity value close to the simulated values, T_2.

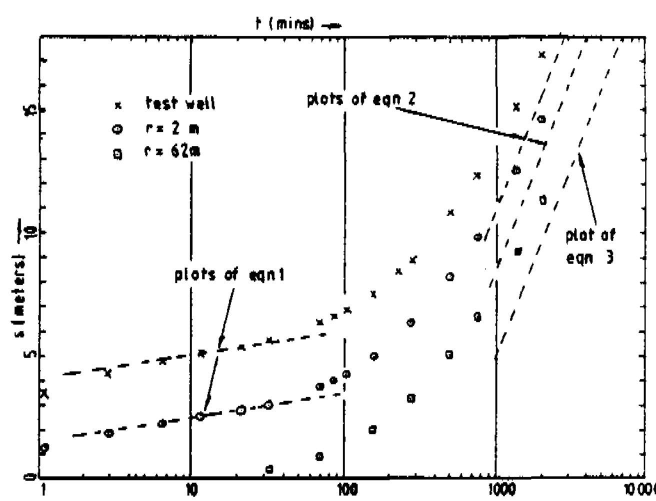

Fig. 2. Simulated drawdown data.

ANALYTICAL STUDY

The above numerical study suggests that Jacob's method can be used to obtain the transmissivity, T_2, from the rate of drawdown, measured in any part of the aquifer, after a sufficiently long time of pumping. In order to investigate this hypothesis, analytical expressions for the drawdown valid after long times were obtained by the method outlined in the Appendix. If s_1 and s_2 are the drawdowns in the inner and outer aquifer regions respectively, then for large t:

$$\frac{4\pi T_2}{Q} s_1 = \ln \frac{4T_2 t}{CS_2 R^2} + \frac{2T_2}{T_1} \ln \frac{R}{r} \qquad (2)$$

and

$$\frac{4\pi T_2}{Q} s_2 = \ln \frac{4T_2 t}{CS_2 r^2} \qquad (3)$$

A simple interpretation of these equations suggests that the inner aquifer region is in a quasi-steady-state with the drawdown described by the Thiem equation, while the drawdown in the outer region is described by the Theis equation for a homogeneous aquifer.

These equations confirm that a semilog plot of drawdown against time will tend to a straight line with slope $Q/4\pi T_2$. They further show that the intercept of this line on the t-axis can be used to estimate the storage coefficient S_2, but only if the drawdown is measured in the outer aquifer region (assuming R to be unknown). A plot of s against ln r should consist of two straight lines with slopes $Q/2\pi T_1$ for $r < R$ and $Q/2\pi T_2$ for $r > R$.

AN UNUSUAL FIELD RESULT

Figure 3 shows the results of a pumping test carried out in India in an aquifer known to have "patchy" properties. The results are unlike those usually obtained from a pumping test in that observed drawdowns are almost independent of the distance of the observation well from the pumping well.

All the wells drilled at this site had exceptionally high specific capacities which indicates that the wells lie within a zone of abnormally high transmissivity. If, as a first approximation, the pumping well is assumed to lie at the centre of a disc of high transmissivity, then equation (2) can be used to predict the drawdown after long times. If T_1 is much greater than T_2, the final term in equation (2) can be ignored, so the drawdown, s_1, will be independent of the radial distance (r) of the observation—on reflection, a fairly obvious result. The apparently anomalous data presented in Figure 3 thus can be explained, and the application of Jacob's method reveals a relatively low regional transmissivity of about 50 m^2/d (0.006 ft^2/s). The transmissivity of the inner region must, by contrast, be very high—possibly greater than 3,000 m^2/d (0.4 ft^2/s).

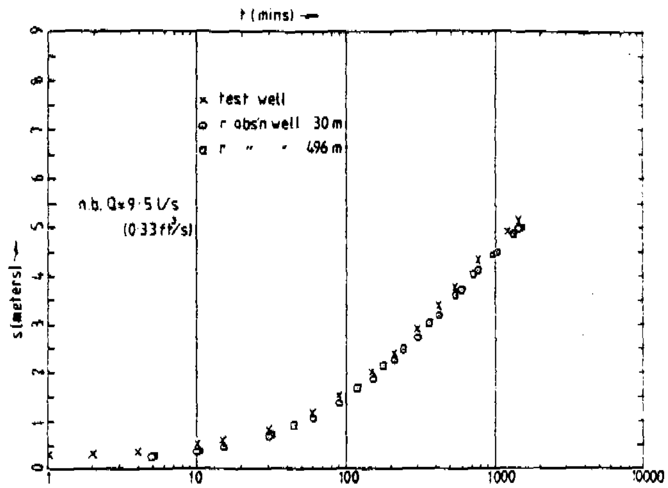

Fig. 3. Field data from a pumping test performed in India.

A GENERAL HYPOTHESIS

The results of these investigations lead to the following hypothesis concerning the interpretation of pumping-test data for heterogeneous aquifers: *The average transmissivity of an aquifer can be determined, using Jacob's method, from rates of drawdown measured at any point in the aquifer, or in the pumping well, after long times of pumping.*

We have only confirmed this hypothesis for a very special case of heterogeneity; Tóth (1967) argues the general case as follows: "Generally, pump tests indicate the presence of some kind of boundary. If, however, the pump test is long enough to permit a 'sampling' by the cone of influence of rock volumes which are large even on a regional scale, time-drawdown curves will behave again as if water was withdrawn from an infinite, homogeneous aquifer."

Vandenberg (1977) used a two-dimensional computer model to simulate a constant-rate pumping test in an aquifer with randomly distributed transmissivity but constant diffusivity. He concluded that the Theis curve-fitting method could be used to obtain average values of the transmissivity and storage coefficient, the fit to the simulated data being best for large values of t/r^2. Other work on the effects of statistical variations of properties on flow in porous media is reviewed by Freeze (1975).

From his own study of a one-dimensional model, Freeze concludes that a heterogeneous formation in general cannot be replaced by an equivalent homogeneous formation when considering transient flow. However, the "average transmissivity" referred to above is that which would be appropriate for use in a regional aquifer model with long time-scales; more precisely, for use when the characteristic time for changes of interest is much greater than x^2/κ, where x is the characteristic scale of spatial variation of transmissivity (e.g., R in Figure 1) and κ is the characteristic diffusivity. Here the implicit assumption is that the aquifer is essentially homogeneous when viewed on a sufficiently large scale.

DISCUSSION

In Figure 2 the transition between the two straight-line sections of the drawdown curves is characterized by a continuous increase in slope. Figure 4a shows an alternative form of the curve that may be observed when $T_2 < T_1$. Similarly, for the case $T_2 > T_1$, numerical simulations revealed the two forms of behaviour shown in Figures 4b and 4c. The form obtained depends on S_1/S_2 and r/R for a given value of T_1/T_2.

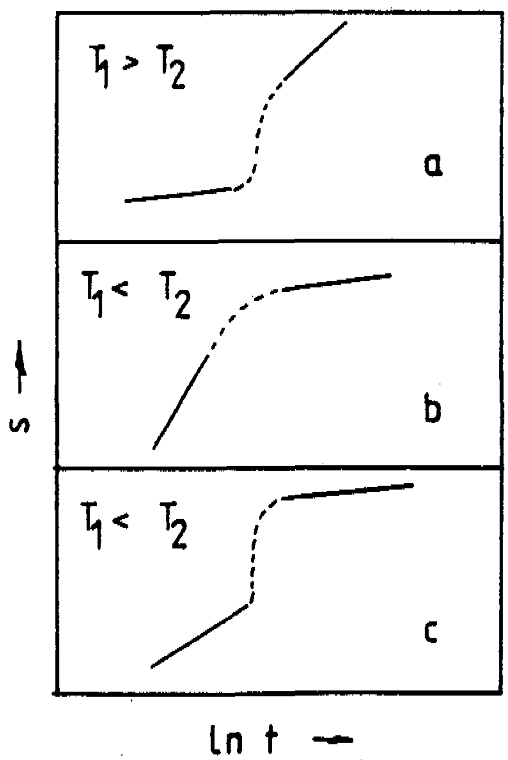

Fig. 4. Alternative forms of the drawdown variation for the idealised system. The form depends on T_1/T_2, S_1/S_2 and r/R.

In deriving equations (2) and (3), no assumption was made concerning the size of R, so these equations could be applied to a well where a cylindrically symmetrical region of formation damage is expected, or even to a well with a thick gravel pack. In both cases the equations show that the aquifer transmissivity can be calculated from rates of drawdown measured either in the pumping well or in observation wells, although the storage coefficient should be deduced from drawdowns measured some distance from the pumping well.

CONCLUSIONS

A pumping test performed in an aquifer with a radial discontinuity in its properties will result in time-drawdown curves of one of the forms shown in Figures 2 and 4; after long times of pumping the drawdown behaviour is described by equations (2) and (3).

When considered in conjunction with the results of previous studies of pumping tests in heterogeneous aquifers, the results of this study demonstrate that Jacob's method can be used with confidence to obtain a regional average for the aquifer transmissivity. An average storage coefficient should, however, be calculated from drawdowns measured at large distances from the pumping well.

NOMENCLATURE

C = $\exp \gamma$ (= 1.78 . . .).

I_0, I_1 modified Bessel functions of the first kind.

K_0, K_1 modified Bessel functions of the second kind.

p Laplace transform variable.

q = $(p\ S_1\ R^2/T_1)^{1/2}$.

Q well discharge rate.

r radial distance from the pumping well.

R radius of the boundary of the two aquifer regions (Figure 1).

s_1 drawdown for r < R.

$\bar{s}_1$ Laplace transform of s_1.

s_2 drawdown for r > R.

$\bar{s}_2$ Laplace transform of s_2.

S_1 storage coefficient for r < R.

S_2 storage coefficient for r > R.

t time after the start of pumping.

T_1	transmissivity for $r < R$.
T_2	transmissivity for $r > R$.
u	$= r^2S/4Tt$.
α	$= (S_2 T_1/S_1 T_2)^{1/2}$.
β	$= 2\pi T_1/Q$.
γ	= Euler's constant (= 0.5772 . . .).
θ	$= T_2/T_1$.
ϕ	$= pq [\theta\alpha K_1(\alpha q) I_0(q) - K_0(\alpha q) I_1(q)]$.

ACKNOWLEDGMENTS

The authors would like to thank the staff of the Indo-British Betwa ground-water project, in particular H. R. Versey and B. K. Singh, for identifying the "patchy" aquifer problem and for providing the pumping-test data (Figure 3). This paper is published by permission of the Director of the Institute of Geological Sciences, (N.E.R.C.).

REFERENCES

Cooper, H. H., and C. E. Jacob. 1946. A generalised geophysical method for evaluating formations constants and summarising well-field history. Trans. Amer. Geophys. Union. 27, 526-534.

Freeze, R. A. 1975. A stochastic-conceptual analysis of one-dimensional groundwater flow in nonuniform homogeneous media. Water Resour. Res. 11, 725-741.

Papadopulos, I. S., and H. H. Cooper. 1967. Drawdown in a large-diameter well. Water Resour. Res. 3, 241-244.

Todd, D. K. 1959. Ground Water Hydrology. John Wiley, New York. 336 pp.

Tóth, J. 1967. Groundwater in sedimentary (clastic) rocks. Proc. Symp. on Groundwater Hydrology, Am. Water Res. Assoc., San Francisco, Calif. 91-102.

Vandenberg, A. 1977. Pump testing in heterogeneous aquifers. J. Hydrol. 34, 45-62.

* * * * *

John Barker received a B.Sc. in Physics in 1969 from Sussex University, and a Ph.D. in Physics in 1974 from University College, London University. Since 1977, he has been Senior Scientific Officer, Hydrogeology Unit, Institute of Geological Sciences.

Robin Herbert received a B.Sc. in 1962, Ph.D. in 1966, and F.G.S. in 1973. He was awarded the Telford Premium by Institution of Civil Engineers in 1971. Since 1977, he has been Principle Scientific Officer to Institute of Geological Science, and adviser to Overseas Development Administration of UK. He is the author of over 20 technical papers in international journals and several project reports.

APPENDIX

Derivation of the Asymptotic Drawdown Equations

Referring to Figure 1, let s_1 and s_2 be the drawdowns in the inner and outer aquifer regions, respectively. Applying Darcy's law and the equation of continuity:

$$S_1 \frac{\partial s_1}{\partial t} = \frac{T_1}{r} \frac{\partial}{\partial r}\left(r \frac{\partial s_1}{\partial r}\right) \quad \text{for } r < R \qquad \text{(A1)}$$

and

$$S_2 \frac{\partial s_2}{\partial t} = \frac{T_2}{r} \frac{\partial}{\partial r}\left(r \frac{\partial s_2}{\partial r}\right) \quad \text{for } r > R \qquad \text{(A2)}$$

Assuming the well to be a line source with no storage:

$$\lim_{r \to 0} 2\pi r T_1 \frac{\partial s_1}{\partial r} = -Q \qquad \text{(A3)}$$

The drawdowns and radial fluxes in the two regions must be equal at $r = R$, so:

$$s_1(R,t) = s_2(R,t) \qquad \text{(A4)}$$

and:

$$T_1 \frac{\partial s_1}{\partial r}(R,t) = T_2 \frac{\partial s_2}{\partial r}(R,t) \qquad \text{(A5)}$$

The drawdown at a sufficiently large distance from the well will be zero:

$$s_2(\infty,t) = 0 \qquad \text{(A6)}$$

Initially, at the start of pumping, the drawdown will be zero everywhere:

$$s_1(r,o) = s_2(r,o) = 0 \qquad \text{(A7)}$$

The solution of equations (A1) to (A7) can be tackled by taking Laplace transforms and solving the resulting ordinary differential equations in terms of modified Bessel functions to give:

$$\beta\bar{s}_1(r,p) = \frac{K_0(qr/R)}{p} + \left[\frac{K_0(\alpha q)}{\phi} - \frac{K_0(q)}{p}\right] \frac{I_0(qr/R)}{I_0(q)} \qquad \text{..... (A8)}$$

$$\beta\bar{s}_2(r,p) = \frac{K_0(\alpha qr/R)}{\phi} \qquad \text{(A9)}$$

where

p is the Laplace transform variable,

$q^2 = p S_1R^2/T_1$,

$\phi = pq [\theta\alpha K_1(\alpha q) I_0(q) - K_0(\alpha q) I_1(q)]$,

$\alpha^2 = S_2T_1/S_1T_2$,

$\beta = 2\pi T_1/Q,$

$\theta = T_2/T_1.$

The transforms given by equations (A8) and (A9) are exact and could be inverted to give explicit expressions for the drawdown at all times; the inversion procedure would, however, be very complicated. Since only the long-time behaviour of the drawdown is of interest, equations (A8) and (A9) can be replaced by expressions that are valid for small values of p (and hence q). Now, for small x:

$$K_0(x) \simeq \ln(2/x) - \gamma$$

$$K_1(x) \simeq 1/x$$

$$I_0(x) \simeq 1$$

and

$$I_1(x) \simeq x/2$$

So, for small values of p, equations (A8) and (A9) become:

$$\beta\bar{s}_1 = \frac{1}{p}\left(\ln\frac{R}{r} + \frac{1}{\theta}\ln\frac{2}{\alpha q} - \frac{\gamma}{\theta}\right) \qquad \text{(A10)}$$

and:

$$\beta\bar{s}_2 = \frac{1}{\theta p}\left(\ln\frac{2R}{\alpha q r} - \gamma\right) \qquad \text{(A11)}$$

Equations (A10) and (A11) are easily inverted to give:

$$\frac{4\pi T_2 s_1}{Q} = \ln\frac{4T_2 t}{CS_2R^2} + \frac{2T_2}{T_1}\ln\frac{R}{r}. \qquad \text{(A12)}$$

and:

$$\frac{4\pi T_2 s_2}{Q} = \ln\frac{4T_2 t}{CS_2 r^2} \qquad \text{(A13)}$$

where $\ln C = \gamma$.

Equations (A12) and (A13) are the required expressions for the drawdown after long times.

Program HVRLV1 — Interactive Determination of Horizontal Permeabilities within Uniform Soils from Field Tests Using Hvorslev's Formulae

by K. U. Weyer and W. C. Horwood-Brown[a]

ABSTRACT

A computer program is presented for interactive, user-oriented calculation of permeabilities from slug tests using Hvorslev's formulae for filters in uniform soil. The analysis scheme is cost-efficient and allows for simple sensitivity analyses.

INTRODUCTION

In 1951 the U.S. Corps of Engineers (Hvorslev, 1951) presented a synopsis of methods and equations for the determination of permeabilities in granular material from laboratory and field tests. Although many different methods have been published since then, Hvorslev's methods still are used widely in practice for a calculation of permeabilities from "slug tests" in piezometers. In a slug test a rise of water level is caused in a well or piezometer by an instantaneous addition of material, be it water or solid material. The recession of the water level over time is used to calculate the permeability of the surrounding rock. In general, Hvorslev's methods are considered to be an adequate *tool for an estimation of the magnitude of* permeabilities in aquifers. For this reason the computer program HVRLV1 has been developed by the National Hydrology Research Institute (Calgary). The program has been written such that the calculations can be carried out interactively. This facilitates efficient evaluation and permits sensitivity analyses of field data obtained.

The terms permeability and hydraulic conductivity are used interchangeably in this paper.

METHODS OF PERMEABILITY DETERMINATION

The theory of Hvorslev's permeability determination has been summarized in Hvorslev's (1951) original figure 18 which also presents the field methods and equations used.

The program HVRLV1 applies to field conditions where the well point filter is installed in uniform soil (see Figure 1). Three basic methods for permeability determination are considered: the constant head method, the variable head method and the basic time lag method. Assumptions are as follows:

- Soil at filter intake.
- Infinite depth and directional isotropy (k_h and k_v constant).
- No disturbance, segregation, swelling or consolidation of the soil.

---

[a]National Hydrology Research Institute, Ground Water Division, 101-4616 Valiant Drive N.W., Calgary, Alberta, Canada T3A OX9.

Received October 1981, revised December 1981, accepted December 1981.

Discussion open until November 1, 1982.

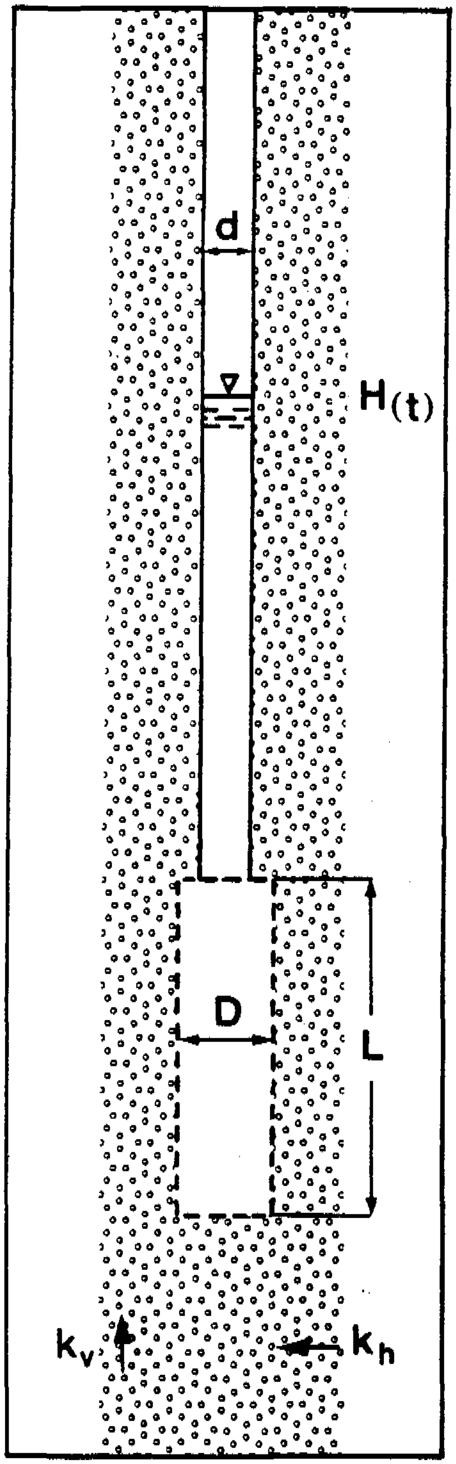

Fig. 1. Field arrangement for Hvorslev slug tests calculated by program HVRLV1. See Table 1 for explanation of variables.

• No air or gas entrapped in soil, well point or pipe.

• Hydraulic losses in pipes, well point or filter negligible.

• No sedimentation or leakage.

Constant Head Method

The calculation makes use of the equation

$$k_h = \frac{q \cdot \ln\left[\frac{mL}{D} + \sqrt{1 + \left(\frac{mL}{D}\right)^2}\right]}{2 \cdot \pi \cdot L \cdot H_c}$$

Before commencement of calculation the following parameters need to be known: q, H_c, L, D, and the ratio k_h/k_v. The notations, dimensions and names of input variables are listed and explained in Table 1.

Variable Head Method

The calculation makes use of two equations

$$k_h = \frac{d^2 \cdot \ln\left[\frac{mL}{D} + \sqrt{1 + \left(\frac{mL}{D}\right)^2}\right]}{8 \cdot L \cdot (t_2 - t_1)} \ln \frac{H_1}{H_2} \quad \text{for } \frac{mL}{D} \leqslant 4$$

$$k_h = \frac{d^2 \cdot \ln\left(\frac{2mL}{D}\right)}{8 \cdot L \cdot (t_2 - t_1)} \ln \frac{H_1}{H_2} \quad \text{for } \frac{mL}{D} > 4$$

Before commencement of calculation the following parameters need to be known: H_1, H_2, t_1, t_2, d, L, D, and the ratio k_h/k_v.

Basic Time Lag Method

The calculation makes use of the equations

$$k_h = \frac{d^2 \cdot \ln\left[\frac{mL}{D} + \sqrt{1 + \left(\frac{mL}{D}\right)^2}\right]}{8 \cdot L \cdot T} \quad \text{for } \frac{mL}{D} \leqslant 4$$

$$k_h = \frac{d^2 \cdot \ln\left(\frac{2mL}{D}\right)}{8 \cdot L \cdot T} \quad \text{for } \frac{mL}{D} > 4$$

Before commencement of calculation the following parameters need to be known: d, L, D, the ratio k_h/k_v, and T. The determination of the basic time lag is outlined in Figure 2. The basic time lag T is the time t at which H is equivalent to 0.37 H_0.

PROGRAM STRUCTURE AND OPERATION

The program HVRLV1 has been listed in Appendix 1. It has been written in Multics FORTRAN which is an extension to ANSI Standard FORTRAN, 1966. The program has been tested at the University of Calgary Honeywell computer. The computer operates on a DPS Level 2 running Multics Release 8.2. The program can be operated

Table 1. List of Notations and Data Input Parameters

Notation	*Name of Input Variable*[1]	*Dimensions of Input*
D	DSCREEN	Diameter of intake area, [cm]
d	DPIPE	Inside diameter of piezometer pipe, [cm]
L	LSCREEN	Length of intake, [m]
H_c	HC	Constant piezometer head, [m]
H_1	H1	Piezometric head for $t = t_1$, [m]
H_2	H2	Piezometric head for $t = t_2$, [m]
q	Q	Flow of water, [cm^3/s]
t	T1, T2	Time, [s]
T	TLAG	Basic time lag, [s]
k_v		Vertical permeability of soil
k_h		Horizontal permeability of soil
m		Transformation ratio: $m = \sqrt{k_h/k_v}$
k_h/k_v	RATIO	
	IDENT	Name of piezometer (up to 8 characters)

[1] Input is format free. Variables are separated by a semicolon, data values by blanks or commas.

in interactive and in batch mode. Table 2 shows the hierarchy of subroutines used.

After program and data files have been set up in the mass storage area of the computer system, the program can be operated simply following the logic and steps outlined in Figures 3 and 4. The control commands used are listed and explained in Table 3. Within the execution of the program they are submitted as outlined in Figures 3 and 4. Necessary data variables are listed and

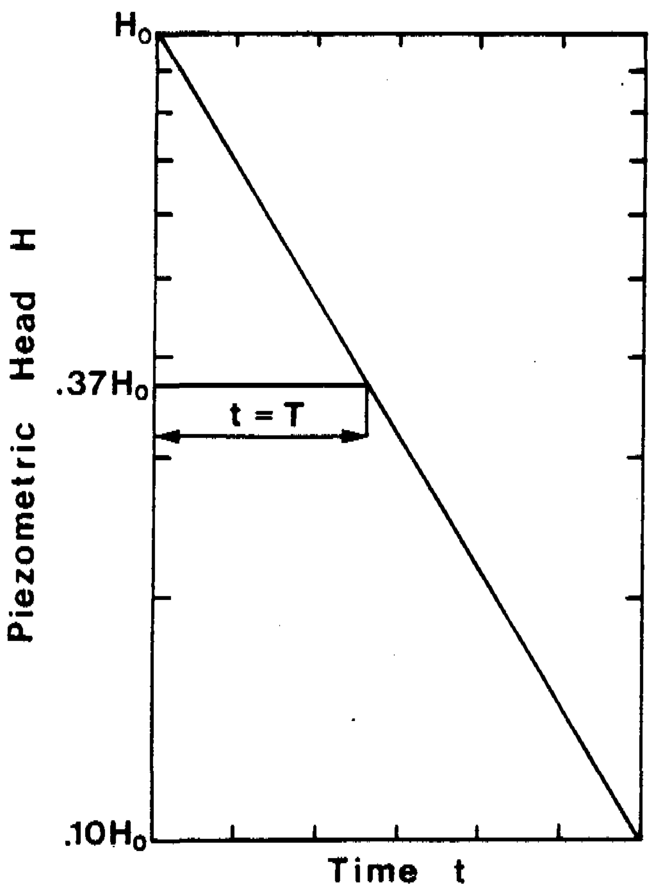

Fig. 2. Determination of basic time lag T from semilog plot of time vs. head. H_0 is the piezometric head H at the time t = 0.

Table 2. Hierarchy of Subroutines in Program HVRLV1

```
HVRLV1 - MAINLINE
  BLOCK DATA
  DRIVER          ]
      INTERP      ]
      SKIP        ]-   INTERACTIVE AND BATCH
      RDTITL      ]    CONTROL STRUCTURE
      RDVAL       ]
      CHEAD       ]
      VHEAD       ]-   PERMEABILITY CALCULATION
      BTLAG       ]    AND PRINTING OF RESULTS
         PRTITL   ]
```

Table 3. List of Control Commands for Program HVRLV1

INPUT=X1	- X1=5 interactive mode - X1≠5 batch mode, data on file specified
OUTPUT=X2	- X2=6 output to terminal - X2≠6 output to file X2, X2≠6
TITLE(....)	- general heading for output table, 72 characters maximum.
CHEAD	- use constant head method of calculation
VHEAD	- use variable head method of calculation
BTLAG	- use basic time lag method of calculation
PROC or PROCEED	- proceed with calculation
STOP	- no further calculation

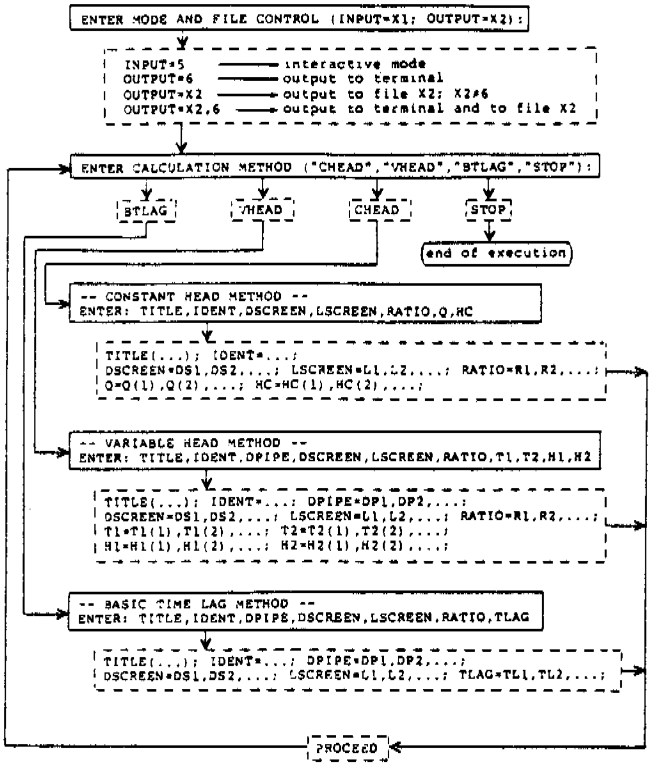

Fig. 3. Operation of program HVRLV1 in interactive mode. Program messages are in solid boxes, user responses in boxes with broken lines. Use of TITLE (. . . .) is facultative. STOP can be submitted at any response time.

explained in Table 1. Error messages generated by the program are listed in Table 4. Figures 5 and 6 are examples of interactive and batch executions, respectively.

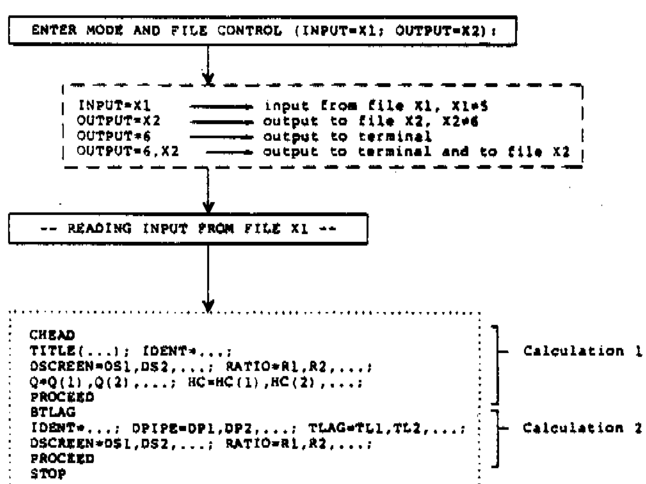

Fig. 4. Operation of program HVRLV1 in batch mode. Program messages are in solid boxes; user responses are in the broken-line box. An example of a batch input file for two different calculations is in the dotted box.

To terminate the program the command STOP can be submitted at any time when response is required. The use of TITLE(. . . .) is facultative. The sequence of data variables is not restricted. Data variables are format free; commas and blanks serve as dividers for data, semicolons as dividers for variables.

AUTOMATIC LOOPING FACILITY

Up to 10 values can be assigned to a data variable, (e.g. DSCREEN = X1, X2, ... , X10). Where more than one value is assigned, the program will automatically loop through all possible combinations of data, within one input set. The looping sequence is outlined in Table 5. Within the table the looping sequence follows the rows before progressing vertically.

PROGRAM OUTPUT

Output can be routed to a terminal, a separate output file or both as outlined in Figures 3 and 4. Separate output files are automatically structured by pages and paginated, with column headings and titles printed on each page (see Figure 6). The tables contain the input data, the ratio (mL)/D and the calculated permeabilities in cm/s and m/s.

Tables can be built up interactively from a terminal or by using batch files. If use is made of the automatic looping facility, interactive output at the terminal is in the form of a table (see Figure 5). Otherwise the output at the terminal is interspersed with the record of interactive communication. Using the output parameter OUTPUT = 6, X2 will build up a table in file X2 which does not contain the record of the inter-

Table 4. List of Error Messages

MESSAGES DURING FILE CONTROL SPECIFICATION:

```
* ERROR * UNEXPECTED END OF DATA INPUT
  INPUT AND OUTPUT FILE MUST BE SPECIFIED, OR "STOP"

* ERROR * UNABLE TO READ FILE CONTROL CARD
  RE-ENTER INPUT AND OUTPUT STATEMENTS

* ERROR * UNIT NUMBER MUST BE FROM 1 TO 99

* ERROR * CONFLICTING INPUT/OUTPUT SPECIFICATION
  RE-ENTER INPUT AND OUTPUT STATEMENTS
```

MESSAGES FROM SUBROUTINE DRIVER:

```
* ERROR * CALCULATION METHOD MUST BE SPECIFIED

* ERROR * UNEXPECTED END OF DATA INPUT

* ERROR * PARAMETER NAME NOT RECOGNIZED

* ERROR * MISSING EQUAL SIGN

* ERROR * UNABLE TO READ DATA VALUE AT COLUMN ..

* ERROR * MISSING VALUE FOR PARAMETER .......
```

```
ASSIGN INPUT-OUTPUT FACILITIES:

ENTER MODE AND FILE CONTROL (INPUT=X1; OUTPUT=X2):
? INPUT=5; OUTPUT=6

CHOOSE CALCULATION METHOD AND SUPPLY DATA:

ENTER CALCULATION METHOD ("CHEAD","VHEAD","BTLAG","STOP"):
? BTLAG

-- BASIC TIME LAG METHOD --
ENTER: TITLE,IDENT,DPIPE,DSCREEN,LSCREEN,RATIO,TLAG
? TITLE(EXAMPLE 1. INTERACTIVE SESSION USING PROGRAM HVRLV1)
? IDENT=PIEZO; DPIPE=4.93; DSCREEN=4.93,10.16; LSCREEN=9.3; RATIO=1.
? TLAG=1.,10.; PROC

RESULT OF CALCULATIONS:

                 EXAMPLE 1. INTERACTIVE SESSION USING PROGRAM HVRLV1

     HORIZONTAL HYDRAULIC CONDUCTIVITY  (HVORSLEV'S BASIC TIME LAG METHOD)

PIEZO      DPIPE  DSCREEN  LSCREEN  RATIO   TLAG     ML/D    ------- PERM --------
 NO.       (CM)    (CM)      (M)    (H/V)   (S)                (M/S)       (CM/S)
----------------------------------------------------------------------------------

PIEZO       4.93    4.93     9.30    1.00    1.00   168.36   2.13E-04    2.13E-02
PIEZO       4.93    4.93     9.30    1.00   10.00   168.36   2.13E-05    2.13E-03

PIEZO       4.93   10.16     9.30    1.00    1.00    91.69   1.87E-04    1.87E-02
PIEZO       4.93   10.16     9.30    1.00   10.00    91.69   1.87E-05    1.87E-03

STOP EXECUTION:

ENTER CALCULATION METHOD ("CHEAD","VHEAD","BTLAG","STOP"):
? STOP
```

Fig. 5. Example of interactive communication at a terminal using the automatic looping facility for basic time lag calculations. The figure shows data input and the results of calculations.

```
CONTENTS OF FILE1:

BTLAG
TITLE(EXAMPLE 2. BATCH SESSION USING PROGRAM HVRLV1)
IDENT=PIEZO2; DPIPE=1.39; DSCREEN=1.39; RATIO=.5,1.,10.
LSCREEN=.3; TLAG=10.,20.; PROC
STOP

EXECUTION OF PROGRAM HVRLV1 USING FILE1:

ENTER MODE AND FILE CONTROL (INPUT=X1; OUTPUT=X2):
? INPUT=1; OUTPUT=2


  -- READING INPUT DATA FROM FILE  1 --

CALCULATION RESULTS STORED IN FILE2:

                 EXAMPLE 2. BATCH SESSION USING PROGRAM HVRLV1

     HORIZONTAL HYDRAULIC CONDUCTIVITY  (HVORSLEV'S BASIC TIME LAG METHOD)

PIEZO      DPIPE  DSCREEN  LSCREEN  RATIO   TLAG     ML/D    ------- PERM --------
 NO.       (CM)    (CM)      (M)    (H/V)   (S)                (M/S)       (CM/S)
----------------------------------------------------------------------------------

PIEZO2      1.39    1.39     0.30    0.50   10.00    15.26   2.75E-05    2.75E-03
PIEZO2      1.39    1.39     0.30    0.50   20.00    15.26   1.38E-05    1.38E-03

PIEZO2      1.39    1.39     0.30    1.00   10.00    21.58   3.03E-05    3.03E-03
PIEZO2      1.39    1.39     0.30    1.00   20.00    21.58   1.52E-05    1.52E-03

PIEZO2      1.39    1.39     0.30   10.00   10.00    68.25   3.96E-05    3.96E-03
PIEZO2      1.39    1.39     0.30   10.00   20.00    68.25   1.98E-05    1.98E-03
```

Fig. 6. Example of batch execution using the automatic looping facility for basic time lag calculations. The figure shows data input and the results of calculations.

active communication. All tables printed are suitable for direct inclusion in reports without further typing. An example of the procedure and results is given in Figure 5.

Table 5. Looping Sequence for the Three Types of Data Input. Looping Sequence Is in Order of Listing. Data Pairs Are Treated as One Variable. Horizontal Progress Precedes Vertical Progress.

1. Constant head method

Q } data	:	Q_1, Q_2, ..., Q_{10}
HC } pair	:	H_1, H_2, ..., H_{10}
RATIO	:	R_1, R_2............, R_{10}
LSCREEN	:	L_1, L_2, ..., L_{10}
DSCREEN	:	DS_1, DS_2.........., DS_{10}

2. Variable head method

T1, T2 } data pair	:	Δt_1, Δt_2, ..., Δt_{10}
H1, H2 }	:	ΔH_1, ΔH_2, ..., ΔH_{10}
RATIO	:	R_1, R_2, ..., R10
LSCREEN	:	L_1, L_2, ..., L_{10}
DSCREEN	:	DS_1, DS_2, ..., DS_{10}
DPIPE	:	DS_1, DS_2, ..., DS_{10}

3. Basic time lag method

TLAG	:	T_1, T_2, ..., T_{10}
RATIO	:	R_1, R_2, ..., R_{10}
LSCREEN	:	LS_1, LS_2, ..., LS_{10}
DSCREEN	:	DS_1, DS_2, ..., DS_{10}
DPIPE	:	DP_1, DP_2, ..., DP_{10}

ACKNOWLEDGMENTS

Preparation of this report was in part supported by Cominco Ltd. through a Joint Research Project dealing with the hydrogeology south of Great Slave Lake. Our appreciation is extended to the management of Pine Point Mines, Ltd. The manuscript was proofread by Dr. H. Ryckborst; Dr. A. Vonhof, Calgary; and G. Grove, Ottawa. Their comments were greatly appreciated.

DISCLAIMER

The program has been tested repeatedly against hand-calculated data and results of calculations published elsewhere. Nevertheless, the authors and NHRI do not accept responsibility for applications of this program.

REFERENCE

Hvorslev, M. J. 1951. Time lag and soil permeability in groundwater observations. U.S. Corps of Engineers, Waterways Experimental Stn. Bull. No. 36.

* * * * *

K. U. Weyer received the equivalents of a B.Sc. (Geology), M.Sc. (Engineering Geology), and Ph.D. (Hydrogeology) from the Universities of Munich and Bonn in West Germany. He has worked on various research and consultant assignments in several countries of Europe and Asia. Since 1975 he has been a Research Scientist with the National Hydrology Research Institute (NHRI) in Calgary, focusing on research in hydrodynamics and mining hydrology.

W. C. Horwood-Brown received a B.Sc. in Ecology from the University of Toronto in 1974. Since 1975 she has worked with Environment Canada in Ottawa and Calgary (NHRI). Currently she is responsible for computer applications and program development within a Joint Research Project with a major Canadian mining company.

APPENDIX 1. HVRLV1 PROGRAM

```
C************************   H V R L V 1   ***************************C
C                                                                    C
C      PROGRAM HVRLV1 CALCULATES, IN INTERACTIVE AND BATCH MODE,     C
C      HORIZONTAL HYDRAULIC CONDUCTIVITIES FOR CASE "G" IN           C
C      FIGURE 18 OF HVORSLEV,M.J.,1951, TIME LAG AND SOIL            C
C      PERMEABILITY IN GROUNDWATER OBSERVATIONS.                     C
C                                                                    C
C                  AUTHORS - W.C.HORWOOD + K.U.WEYER                 C
C                                                                    C
C                            APRIL, 1981                             C
C                                                                    C
C********************************************************************C
      CHARACTER*1 CARD, FILPAR(3,6), COMMA, SCOLAN
      COMMON /C1000/ IN, IOUT, IAIN, IAOUT, INTER
     *       /C2000/ CARD(80), ICOL
     *       /C3100/ COMMA, SCOLAN
      DATA FILPAR/ 1HI, 1HO, 1HS,
     *             1HN, 1HU, 1HT,
     *             1HP, 1HT, 1HO,
     *             1HU, 1HP, 1HP,
     *             1HT, 1HU, 1H ,
     *             1H , 1HT, 1H /
      IAIN=5
      IAOUT=6
C.....OPEN STATEMENTS IN MULTICS FORTRAN CONNECT A FILE OR DEVICE
C     TO A UNIT AND ASSIGN CONTROL ATTRIBUTES FOR A CONNECTED UNIT
      OPEN(IAIN,FORM="formatted",MODE="in",PROMPT=.TRUE.)
      OPEN(IAOUT,FORM="formatted",MODE="out",CARRIAGE=.TRUE.)
C
   90 IC1=0
      IC2=0
      IN=0
      IOUT=0
      INTMP=0
      IOUTMP=0
      INTER=6
C
C.....READ MODE AND FILE CONTROL PARAMETERS
  100 WRITE(IAOUT,110)
  110 FORMAT(/' ENTER MODE AND FILE CONTROL (INPUT=X1; OUTPUT=X2):')
  120 READ(IAIN,130,END=800) CARD
  130 FORMAT(80A1)
      ICOL=1
C.....THE SIGN "$" INDICATES A MULTIPLE RETURN OPTION
      CALL SKIP(1,0,$800)
C
C.....READ PARAMETERS
  140 CALL INTERP(FILPAR,3,6,IC)
      IF(IC.EQ.0) GO TO 840
      IF(IC.EQ.3) GO TO 999
C
C.....SKIP TO EQUAL SIGN
      CALL SKIP(4,1,$840)
C
C.....SKIP TO NUMBER
  150 CALL SKIP(1,1,$840)
C
C.....READ NUMBER
      CALL RDVAL(REALF,IERR)
      IF(IERR.EQ.1) GO TO 840
      IUNT=IFIX(REALF)
      IF(IUNT.LE.0.OR.IUNT.GT.99) GO TO 860
C
C.....ASSIGN NUMBER ACCORDINGLY
      IF(IC.EQ.2) GO TO 160
C
C....."INPUT"
      IC1=IC1+1
      IF(IUNT.NE.5) IN=IUNT
      IF(IUNT.EQ.5) INTMP=5
      GO TO 170
C
C....."OUTPUT"
  160 IC2=IC2+1
      IF(IUNT.NE.6) IOUT=IUNT
      IF(IUNT.EQ.6) IOUTMP=6
C
C.....CHECK FOR ADDITIONAL UNIT NUMBER
  170 CONTINUE
      CALL SKIP(1,1,$180)
      IF(CARD(ICOL).EQ.COMMA) GO TO 150
      IF(CARD(ICOL).NE.SCOLAN) GO TO 840
C
C....SKIP TO NEXT PARAMETER
      CALL SKIP(1,1,$180)
      GO TO 140
C
C.....CHECK ASSIGNMENT OF UNIT NUMBERS
  180 CONTINUE
      IF(INTMP.GT.0.AND.IN.GT.0) GO TO 880
      IF(IN.EQ.0) GO TO 200
      IF(IN.EQ.IOUT.OR.IN.EQ.IOUTMP) GO TO 880
  200 IF(INTMP.EQ.0) GO TO 210
      IF(INTMP.EQ.IOUT.OR.INTMP.EQ.IOUTMP) GO TO 880
  210 CONTINUE
      IF(IN.EQ.0.AND.INTMP.EQ.0) GO TO 120
      IF(IOUT.EQ.0.AND.IOUTMP.EQ.0) GO TO 120
      IAIN=INTMP
      IAOUT=IOUTMP
      IF(IOUT.GT.0) OPEN(IOUT,FORM="formatted",MODE="out",
     *    CARRIAGE=.TRUE.)
C
      IF(IN.GT.0) WRITE(INTER,220) IN
  220 FORMAT(//'    -- READING INPUT DATA FROM FILE ',I2,' --'/)
C
C.....FILE CONTROL PARAMETERS AND MODE HAVE  BEEN SPECIFIED
      CALL DRIVER
C
C.....STOP EXECUTION
  999 STOP
C
C.....ERROR MESSAGES
  800 WRITE(IAOUT,810)
  810 FORMAT(' * ERROR * UNEXPECTED END OF DATA INPUT'/
     *       '       INPUT AND OUTPUT FILE MUST BE SPECIFIED, OR "STOP" ')
      GO TO 100
  840 WRITE(IAOUT,850)
  850 FORMAT(' * ERROR * UNABLE TO READ FILE CONTROL CARD'/
     *       '       RE-ENTER INPUT AND OUTPUT STATEMENTS')
      GO TO 90
  860 WRITE(IAOUT,870)
  870 FORMAT(' * ERROR * UNIT NUMBER MUST BE FROM 1 TO 99')
      GO TO 100
  880 WRITE(IAOUT,890)
  890 FORMAT(' * ERROR * CONFLICTING INPUT/OUTPUT SPECIFICATION'/
     *       '       RE-ENTER INPUT AND OUTPUT STATEMENTS')
      GO TO 90
      END
```

```
C**********************   B L O C K   D A T A   *********************C
C                                                                    C
C      BLOCK DATA INITIALIZES PARAMETERS IN COMMON BLOCKS            C
C                                                                    C
C********************************************************************C
      BLOCK DATA
      CHARACTER*1 BLANK, COMMA, SCOLAN, LBRACK, RBRACK, CVEC, PLUS,
     *            MINUS
      COMMON /C3000/ BLANK
     *       /C3100/ COMMA, SCOLAN
     *       /C3200/ LBRACK, RBRACK
     *       /C3300/ CVEC(12), PLUS, MINUS
      DATA BLANK/1H /, COMMA/1H,/, SCOLAN/1H;/, LBRACK/1H(/,
     *     RBRACK/1H)/, PLUS/1H+/, MINUS/1H-/
      DATA CVEC/1H0, 1H1, 1H2, 1H3, 1H4, 1H5, 1H6, 1H7, 1H8, 1H9, 1H.,
     *          1HE/
      END
```

```
C************************   D R I V E R   ***************************C
C                                                                    C
C      SUBROUTINE DRIVER DIRECTS THE READING OF COMMANDS AND         C
C      PARAMETER VALUES AND CALLS THE CALCULATION SUBROUTINES        C
C                                                                    C
C********************************************************************C
      SUBROUTINE DRIVER
      CHARACTER*1 CARD, PARA(15,7), AMETHD(4,5), IDENT, BLANK, SCOLAN,
     *            COMMA, TITLE
      DIMENSION NVCH(5), NVVH(8), NVBTL(5)
      COMMON /C1000/ IN, IOUT, IAIN, IAOUT, INTER
     *       /C2000/ CARD(80), ICOL
     *       /C3000/ BLANK
     *       /C3100/ COMMA, SCOLAN
     *       /C4000/ IDENT(8), DATPAR(11,10), NVAL(11)
     *       /C4200/ IMETH, IAOFLG, IOFLG
     *       /C4300/ TITLE(72), NTITL, NWTITL
     *       /C4400/ NLINE, NLINEX
      DATA AMETHD/ 1HC, 1HV, 1HB, 1HS,
     *             1HH, 1HH, 1HT, 1HT,
     *             1HE, 1HE, 1HL, 1HO,
     *             1HA, 1HA, 1HA, 1HP,
     *             1HD, 1HD, 1HG, 1H  /
      DATA PARA /
     *1HD,1HD,1HL,1HR,1HT,1HT,1HT,1HH,1HH,1HH,1HQ,1HI,1HT,1HP,1HS,
     *1HP,1HS,1HS,1HA,1HL,1H1,1H2,1H1,1H2,1HC,1H ,1HD,1HI,1HR,1HT,
     *1HI,1HC,1HC,1HT,1HA,1H ,1H ,1H ,1H ,1H ,1H ,1HE,1HT,1HO,1HO,
     *1HP,1HR,1HR,1HI,1HG,1H ,1H ,1H ,1H ,1H ,1H ,1HN,1HL,1HC,1HP,
     *1HE,1HE,1HE,1HO,1H ,1H ,1H ,1H ,1H ,1H ,1H ,1HT,1HE,1H ,1H  ,
     *1H ,1HE,1HE,1H ,1H ,1H ,1H ,1H ,1H ,1H ,1H ,1H ,1H ,1H ,1H  ,
     *1H ,1HN,1HN,1H ,1H ,1H ,1H ,1H ,1H ,1H ,1H ,1H ,1H ,1H ,1H  /
      DATA NVCH/ 2, 3, 4, 10, 11/ ,
     *     NVVH/ 1, 2, 3, 4, 6, 7, 8, 9/ ,
     *    NVBTL/ 1, 2, 3, 4, 5/
      NLINE=0
      NLINEX=35
      IAOFLG=0
      IOFLG=0
      IF(IAOUT.GT.0) IAOFLG=1
      IF(IOUT.GT.0)  IOFLG=1
      IMETH=0
    1 DO 2 I=1,11
    2 NVAL(I)=0
      NWTITL=0
      NTITL=0
      DO 5 I=1,8
    5 IDENT(I)=BLANK
C
      IF(IAIN.GT.0) WRITE(INTER,10)
   10 FORMAT(//  ' ENTER CALCULATION METHOD ("CHEAD","VHEAD","BTLAG","ST
     *OP"): ')
      IF(IAIN.GT.0) READ(IAIN,20,END=3000) CARD
      IF(IN.GT.0) READ(IN,20,END=3000) CARD
   20 FORMAT(80A1)
      ICOL=1
      IMETHO=IMETH
      CALL SKIP(1,0,$2900)
      CALL INTERP(AMETHD,4,5,IMETH)
      IF(IMETH.EQ.0) GO TO 2900
      IF(IMETH.EQ.IMETHO) GO TO 25
      IF(IAOUT.GT.1) IAOFLG=1
      IF(IOUT.GT.0)  IOFLG=1
   25 CONTINUE
      IF(IOUT.GT.0.AND.NLINE.GT.NLINEX) IOFLG=1
      IF(IMETH.EQ.4) GO TO 600
C
      IF(IAIN.LE.0) GO TO 60
      IF(IMETH.EQ.1) WRITE(INTER,30)
   30 FORMAT(/' -- CONSTANT HEAD METHOD --'/
     *       ' ENTER: TITLE,IDENT,DSCREEN,LSCREEN,RATIO,Q,HC')
      IF(IMETH.EQ.2) WRITE(INTER,40)
   40 FORMAT(/' -- VARIABLE HEAD METHOD --'/
     *       ' ENTER: TITLE,IDENT,DPIPE,DSCREEN,LSCREEN,RATIO,T1,T2,H1,H
     *2' )
      IF(IMETH.EQ.3) WRITE(INTER,50)
   50 FORMAT(/' -- BASIC TIME LAG METHOD --'/
     *       ' ENTER: TITLE,IDENT,DPIPE,DSCREEN,LSCREEN,RATIO,TLAG')
   60 IF(IAIN.GT.0) READ(IAIN,20,END=3000) CARD
      IF(IN.GT.0)    READ(IN,20,END=3000) CARD
      ICOL=1
      CALL SKIP(1,0,$3000)
C
   70 CALL INTERP(PARA,15,7,IP)
      IF(IP.EQ.0) GO TO 3020
      IF(IP.GE.13) GO TO 90
C.....SKIP TO EQUAL SIGN
      CALL SKIP(4,1,$3040)
   90 CONTINUE
      IF(IP.GT.11) GO TO 200
C
C.....READ PARAMETER VALUES
      NVAL(IP)=0
  100 CALL SKIP(2,1,$60)
      IF(CARD(ICOL).EQ.SCOLAN) GO TO 700
      CALL RDVAL(REALF,IERR)
      IF(IERR.EQ.1) GO TO 3060
C     UP TO 10 VALUES FOR EACH PARAMETER ARE PERMITTED, SKIP REST
      IF(NVAL(IP).EQ.10) GO TO 100
      NVAL(IP)=NVAL(IP)+1
      DATPAR(IP,NVAL(IP))=REALF
      GO TO 100
C
  200 CONTINUE
      I1=IP-11
      GOTO(300,400,500,600),I1
C
C....."IDENT"
  300 CONTINUE
      NID=0
```

```
      CALL SKIP(1,1,$60)
  310 NID=NID+1
      IDENT(NID)=CARD(ICOL)
      ICOL=ICOL+1
      IF(ICOL.GT.80) GO TO 60
      IF(CARD(ICOL).EQ.SCOLAN) GO TO 700
      IF(NID.LT.8) GO TO  310
      CALL SKIP(5,0,$60)
      GO TO 700
C
C....."TITLE"
  400 CONTINUE
      CALL SKIP(3,1,$3000)
      CALL RDTITL
      NWTITL=1
      CALL SKIP(5,1,$60)
      GO TO 700
C
C....."PROC"
  500 CONTINUE
      IF(IOUT.GT.0.AND.NWTITL.EQ.1) IOFLG=1
      IF(IAOUT.GT.0.AND.NWTITL.EQ.1) IAOFLG=1
      GOTO(510,530,550),IMETH
  510 DO 520 I=1,5
      N=NVCH(I)
      IF(NVAL(N).LE.0) GO TO 3080
      IF(IAOUT.GT.0.AND.NVAL(N).GT.1) IAOFLG=1
  520 CONTINUE
      CALL CHEAD
      GO TO 1
  530 DO 540 I=1,8
      N=NVVH(I)
      IF(NVAL(N).LE.0) GO TO 3080
      IF(IAOUT.GT.0.AND.NVAL(N).GT.1) IAOFLG=1
  540 CONTINUE
      CALL VHEAD
      GO TO 1
  550 DO 560 I=1,5
      N=NVBTL(I)
      IF(NVAL(N).LE.0) GO TO 3080
      IF(IAOUT.GT.0.AND.NVAL(N).GT.1) IAOFLG=1
  560 CONTINUE
      CALL BTLAG
      GO TO 1
C
C....."STOP"
  600 STOP
C
C.....ADDITIONAL INPUT
  700 CALL SKIP(1,1,$60)
      GO TO 70
C
C.....ERROR MESSAGES
 2900 WRITE(INTER,2910)
 2910 FORMAT(' * ERROR * CALCULATION METHOD MUST BE SPECIFIED')
      IMETH=IMETHO
      IF(IAIN.GT.0) GO TO 1
      GO TO 4000
 3000 WRITE(INTER,3010)
 3010 FORMAT(' * ERROR * UNEXPECTED END OF DATA INPUT')
      GO TO 4000
 3020 WRITE(INTER,3030)
 3030 FORMAT(' * ERROR * PARAMETER NAME NOT RECOGNIZED')
      GO TO 4000
 3040 WRITE(INTER,3050)
 3050 FORMAT(' * ERROR * MISSING EQUAL SIGN')
      GO TO 4000
 3060 WRITE(INTER,3070) ICOL
 3070 FORMAT(' * ERROR * UNABLE TO READ DATA VALUE AT COLUMN ',I2)
      GO TO 4000
 3080 WRITE(INTER,3090) (PARA(N,N1),N1=1,7)
 3090 FORMAT(' * ERROR * MISSING VALUE FOR PARAMETER ',7A1)
      IF(IAIN.GT.0) GO TO 60
      GO TO 600
 4000 CONTINUE
      IF(IAIN.GT.0) GO TO 60
      WRITE(INTER,4010) (CARD(I),I=1,80)
 4010 FORMAT('   LAST CARD READ:',80A1/
     *       '   EXECUTION TERMINATED')
      END


C************************   I N T E R P   *************************C
C                                                                  C
C     SUBROUTINE INTERP READS COMMANDS AND PARAMETERS              C
C                                                                  C
C******************************************************************C
      SUBROUTINE INTERP(CMND,NCMND,NMX,ICMND)
      CHARACTER*1 CARD, CMND, BLANK
      DIMENSION CMND(NCMND,NMX)
      COMMON /C2000/ CARD(80), ICOL
     *       /C3000/ BLANK
C.....ICOL POINTS TO FIRST CHARACTER OF PARAMETER OR COMMAND
      ICMND=0
C.....MATCH FIRST CHARACTER OF PARAMETER, THEN MATCH THE REST
C     OF THE PARAMETER
      DO 30 I=1,NCMND
      IF(CARD(ICOL).NE.CMND(I,1)) GO TO 30
      IF(NMX.EQ.1) GO TO 15
      ICOLO=ICOL
      DO 10 J=2,NMX
      IF(CMND(I,J).EQ.BLANK) GO TO 10
      ICOL=ICOL+1
      IF(ICOL.GT.80) GO TO 20
      IF(CARD(ICOL).NE.CMND(I,J)) GO TO 20
   10 CONTINUE
C
C.....WORD HAS BEEN MATCHED
   15 ICMND=I
      RETURN
C
C.....WORD HAS NOT BEEN MATCHED
   20 ICOL=ICOLO
C
   30 CONTINUE
      RETURN
      END


C**************************   S K I P   ***************************C
C                                                                  C
C     SUBROUTINE SKIP SKIPS BLANKS AND/OR CHARACTERS TO LOCATE THE C
C     NEXT CHARACTER TO BE READ.                                   C
C                                                                  C
C******************************************************************C
      SUBROUTINE SKIP(ISKIP,IADD1,*)
      CHARACTER*1 CARD, LBRACK, RBRACK, BLANK, EQUALS, COMMA, SCOLAN
      COMMON /C2000/ CARD(80), ICOL

     *       /C3000/ BLANK
     *       /C3100/ COMMA, SCOLAN
     *       /C3200/ LBRACK, RBRACK
      DATA EQUALS/1H=/
C
C     ISKIP DETERMINES THE CHECKING PROCEDURE FOR SUBROUTINE SKIP
C         ISKIP=1   SKIP BLANKS TO FIRST NON-BLANK
C         ISKIP=2   SKIP BLANKS AND COMMAS TO FIRST NON-BLANK
C         ISKIP=3   SKIP ANY CHARACTER TO A LEFT BRACKET
C         ISKIP=4   SKIP ANY CHARACTER TO AN EQUAL SIGN
C         ISKIP=5   SKIP ANY CHARACTER TO A SEMICOLAN
C
C.....IADD1 (0 OR 1) MOVES POINTER ICOL IADD1 COLUMNS TO A STARTING
C     POINT
      ICOL=ICOL+IADD1
C
      GOTO(100,200,300,400,500),ISKIP
C
  100 CONTINUE
      IF(ICOL.GT.80) GO TO 1000
      IF(CARD(ICOL).NE.BLANK) GO TO 900
      ICOL=ICOL+1
      GO TO 100
C
  200 CONTINUE
      IF(ICOL.GT.80) GO TO 1000
      IF(CARD(ICOL).NE.BLANK.AND.CARD(ICOL).NE.COMMA) GO TO 900
      ICOL=ICOL+1
      GO TO 200
C
  300 CONTINUE
      IF(ICOL.GT.80) GO TO 1000
      IF(CARD(ICOL).EQ.LBRACK) GO TO 900
      ICOL=ICOL+1
      GO TO 300
C
  400 CONTINUE
      IF(ICOL.GT.80) GO TO 1000
      IF(CARD(ICOL).EQ.EQUALS) GO TO 900
      ICOL=ICOL+1
      GO TO 400
C
  500 CONTINUE
      IF(ICOL.GT.80) GO TO 1000
      IF(CARD(ICOL).EQ.SCOLAN) GO TO 900
      ICOL=ICOL+1
      GO TO 500
C
  900 RETURN
C
C.....END OF DATA ENCOUNTERED
 1000 RETURN 1
      END


C************************   R D T I T L   *************************C
C                                                                  C
C     SUBROUTINE RDTITL READS TITLE OF DATA TABLES                 C
C                                                                  C
C******************************************************************C
      SUBROUTINE RDTITL
      CHARACTER*1 CARD, TITLE, RBRACK, LBRACK, BLANK
      COMMON /C1000/ IN, IOUT, IAIN, IAOUT, INTER
     *       /C2000/ CARD(80), ICOL
     *       /C3000/ BLANK
     *       /C3200/ LBRACK, RBRACK
     *       /C4300/ TITLE(72), NTITL, NWTITL
C
C.....CLEAR TITLE VECTOR
      DO 10 I=1,72
   10 TITLE(I)=BLANK
      NTITL=0
C
C.....SKIP TO FIRST CHARACTER OF TITLE
      CALL SKIP(1,1,$100)
C
C.....READ TITLE
   20 IF(ICOL.GT.80.OR.CARD(ICOL).EQ.RBRACK) GO TO 100
      NTITL=NTITL+1
      IF(NTITL.GT.72) GO TO 50
      TITLE(NTITL)=CARD(ICOL)
      ICOL=ICOL+1
      GO TO 20
C
C.....WARNING MESSAGE
   50 WRITE(INTER,60)
   60 FORMAT(' * WARNING * TITLE HAS BEEN TRUNCATED TO 72 CHARACTERS')
      NTITL=72
C
  100 RETURN
      END


C**************************   R D V A L   *************************C
C                                                                  C
C     SUBROUTINE RDVAL READS DATA FROM DATA SOURCE FILE            C
C                                                                  C
C******************************************************************C
      SUBROUTINE RDVAL (REALF,IERR)
      INTEGER RSIGN,ESIGN,ERSW
      CHARACTER*1 CARD, LBRACK, RBRACK, BLANK, COMMA,  SCOLAN,
     *               PLUS, MINUS, CVEC
      COMMON /C2000/ CARD(80), ICOL
     *       /C3000/ BLANK
     *       /C3100/ COMMA, SCOLAN
     *       /C3200/ LBRACK, RBRACK
     *       /C3300/ CVEC(12), PLUS, MINUS
      IERR=0
      ISW=1
      EXP=0.0
      ICT=0
      REAL=0.0
      RSIGN=0
      ESIGN=0
C
      IF(CARD(ICOL).EQ.PLUS) GO TO 5
      IF(CARD(ICOL).NE.MINUS) GO TO 10
      RSIGN=-1
    5 ICOL=ICOL+1
      IF(ICOL.GT.80) GO TO 110
C
   10 ICT=ICT+1
C
      DO 20 I=1,12
      RP=I
      IF(CARD(ICOL).EQ.CVEC(I)) GO TO 30
   20 CONTINUE
      GO TO 100
C
   30 IF(RP.EQ.11.0) GO TO 70
      IF(RP.EQ.12.0) GO TO 80
C
      GOTO(40,50,60),ISW
```

```
C
   40 REAL=REAL*10.0+RP-1.0
      GO TO 90
C
   50 REAL=REAL+(RP-1.0)/10.0**IP
      IP=IP+1
      GO TO 90
C
   60 EXP=EXP*10.0+RP-1.0
      GO TO 90
C
   70 IF(ISW.GT.1) GO TO 110
      ISW=2
      IP=1
      GO TO 90
C
   80 IF(ISW.EQ.3) GO TO 110
      ISW=3
      ICOL=ICOL+1
      IF(ICOL.GT.80) GO TO 110
      IF(CARD(ICOL).EQ.PLUS) GO TO 90
      IF(CARD(ICOL).NE.MINUS) GO TO 10
      ESIGN=-1
C
   90 ICOL=ICOL+1
      IF(ICOL.GT.80) GO TO 105
      GO TO 10
C
  100 IF(ICT.EQ.1.OR.CARD(ICOL).NE.COMMA.AND.CARD(ICOL).NE.BLANK.
     *    AND.CARD(ICOL).NE.RBRACK.AND.CARD(ICOL).NE.SCOLAN) GO TO 110
  105 IF(RSIGN.EQ.-1) REAL=-REAL
      IF(ESIGN.EQ.-1) EXP=-EXP
      IEXP=EXP
      REAL=REAL*10.0**IEXP
      REALF=REAL
      ICOL=ICOL-1
      RETURN
C
C.....ERROR MESSAGES
  110 IERR=1
      RETURN
      END


C*************************   C H E A D   ***************************C
C                                                                   C
C     SUBROUTINE CHEAD CALCULATES HORIZONTAL HYDRAULIC CONDUCTIVITY  C
C     USING THE CONSTANT HEAD METHOD                                C
C                                                                   C
C*******************************************************************C
      SUBROUTINE CHEAD
      CHARACTER*1 IDENT, TITLE
      COMMON /C1000/ IN, IOUT, IAIN, IAOUT, INTER
     *        /C4000/ IDENT(8), DATPAR(11,10), NVAL(11)
     *        /C4200/ IMETH, IAOFLG, IOFLG
     *        /C4300/ TITLE(72), NTITL, NWTITL
     *        /C4400/ NLINE, NLINEX
C
      PI=3.141593
      ISKIP=1
      IF(IAOFLG.EQ.1.OR.IOFLG.EQ.1) CALL PRTITL(79)
C
C.....PERMEABILITY CALCULATION
      DO 200 I2=1,NVAL(2)
      IF(I2.EQ.1.AND.NVAL(2).GT.1) ISKIP=ISKIP+1
      DO 200 I3=1,NVAL(3)
      IF(I3.EQ.1.AND.NVAL(3).GT.1) ISKIP=ISKIP+1
      DO 200 I4=1,NVAL(4)
      IF(I4.EQ.1.AND.NVAL(4).GT.1) ISKIP=ISKIP+1
      DO 200 I10=1,NVAL(10)
      IF(I10.EQ.1.AND.NVAL(10).GT.1) ISKIP=ISKIP+1
      IF(ISKIP.LE.0) GO TO 175
      IF(IOUT.GT.0) WRITE(IOUT,165)
      IF(IAOUT.GT.0) WRITE(IAOUT,165)
  165 FORMAT(1X)
      NLINE=NLINE+1
      ISKIP=0
      IF(NLINE.LT.NLINEX.OR.IOUT.EQ.0) GO TO 175
      IOFLG=1
      CALL PRTITL(79)
C
C.....AVOID DIVISION BY ZERO
  175 CONTINUE
      IF(DATPAR(2,I2).LE.0.OR.DATPAR(3,I3).LE.0..OR.DATPAR(10,I10).LE.0)
     *    GO TO 250
      Q=DATPAR(11,I10)*.000001
      D=DATPAR(2,I2)*.01
      RM=DATPAR(4,I4)**.5
      RLD=RM*DATPAR(3,I3)/D
      PERMM=Q*ALOG(RLD+(1.-(RLD**2.))**.5)/(2.*PI*DATPAR(3,I3)*
     *  DATPAR(10,I10))
      PERMCM=PERMM*100.
C
C.....PRINT RESULTS
      IF(IOUT.GT.0) WRITE(IOUT,300) (IDENT(I),I=1,8),DATPAR(2,I2),
     *  DATPAR(3,I3),DATPAR(4,I4),DATPAR(11,I10),DATPAR(10,I10),
     *  PERMM, PERMCM
      NLINE=NLINE+1
      IF(IAOUT.GT.0) WRITE(IAOUT,300) (IDENT(I),I=1,8),DATPAR(2,I2),
     *  DATPAR(3,I3),DATPAR(4,I4),DATPAR(11,I10),DATPAR(10,I10),
     *  PERMM, PERMCM
  300 FORMAT(1X,8A1,3X,F5.2,4X,F5.2,3X,F5.2,2X,F6.1,2X,F7.1,
     *        9X,1PE8.2,4X,1PE8.2)
      GO TO 200
C
C.....DENOMINATOR EQUALS ZERO, CALCULATION DISCONTINUED
  250 CONTINUE
      IF(IOUT.GT.0) WRITE(IOUT,350) (IDENT(I),I=1,8),DATPAR(2,I2),
     *  DATPAR(3,I3),DATPAR(4,I4),DATPAR(11,I10),DATPAR(10,I10)
      NLINE=NLINE+1
      IF(IAOUT.GT.0) WRITE(IAOUT,350) (IDENT(I),I=1,8),DATPAR(2,I2),
     *  DATPAR(3,I3),DATPAR(4,I4),DATPAR(11,I10),DATPAR(10,I10)
  350 FORMAT(1X,8A1,3X,F5.2,4X,F5.2,3X,F5.2,2X,F6.1,2X,F7.1,
     *9X,'    --     ',2X,'    --     ')
  200 CONTINUE
      RETURN
      END


C*************************   V H E A D   ***************************C
C                                                                   C
C     SUBROUTINE VHEAD CALCULATES PERMEABILITY USING THE VARIABLE    C
C     HEAD METHOD                                                   C
C                                                                   C
C*******************************************************************C
      SUBROUTINE VHEAD
      CHARACTER*1 IDENT, TITLE
      COMMON /C1000/ IN, IOUT, IAIN, IAOUT, INTER
     *        /C4000/ IDENT(8), DATPAR(11,10), NVAL(11)
     *        /C4200/ IMETH, IAOFLG, IOFLG
     *        /C4300/ TITLE(72), NTITL, NWTITL
     *        /C4400/ NLINE, NLINEX
C
      ISKIP=1
      IF(IAOFLG.EQ.1.OR.IOFLG.EQ.1) CALL PRTITL(97)
C
C.....PERMEABILITY CALCULATION
      DO 200 I1=1,NVAL(1)
      IF(I1.EQ.1.AND.NVAL(1).GT.1) ISKIP=ISKIP+1
      DO 200 I2=1,NVAL(2)
      IF(I2.EQ.1.AND.NVAL(2).GT.1) ISKIP=ISKIP+1
      DO 200 I3=1,NVAL(3)
      IF(I3.EQ.1.AND.NVAL(3).GT.1) ISKIP=ISKIP+1
      DO 200 I4=1,NVAL(4)
      IF(I4.EQ.1.AND.NVAL(4).GT.1) ISKIP=ISKIP+1
      DO 200 I6=1,NVAL(6)
      IF(I6.EQ.1.AND.NVAL(6).GT.1) ISKIP=ISKIP+1
      IF(ISKIP.LE.0) GO TO 175
      IF(IOUT.GT.0) WRITE(IOUT,165)
      IF(IAOUT.GT.0) WRITE(IAOUT,165)
  165 FORMAT(1X)
      NLINE=NLINE+1
      ISKIP=0
      IF(NLINE.LT.NLINEX.OR.IOUT.EQ.0) GO TO 175
      IOFLG=1
      CALL PRTITL(97)
C
C.....AVOID DIVISION BY ZERO
  175 CONTINUE
      IF(DATPAR(2,I2).LE.0..OR.DATPAR(3,I3).LE.0..OR.DATPAR(9,I6).LE.0.
     * .OR.(DATPAR(7,I6)-DATPAR(6,I6)).LE.0.) GO TO 250
      DPIPE=DATPAR(1,I1)*.01
      D=DATPAR(2,I2)*.01
      RM=DATPAR(4,I4)**.5
      RLD=RM*DATPAR(3,I3)/D
      IF(RLD.GT.4) GO TO 180
C
C.....RL/D LESS THAN OR EQUAL TO 4
      PERMM=(DPIPE**2.)*ALOG(RLD+(1.+RLD**2.)**.5)/(8.*DATPAR(3,I3)*
     *     (DATPAR(7,I6)-DATPAR(6,I6)))*ALOG(DATPAR(8,I6)/DATPAR(9,I6))
      GO TO 190
C
C.....RL/D GREATER THAN 4
  180 PERMM=(DPIPE**2.)*ALOG(2.*RLD)/(8.*DATPAR(3,I3)*(DATPAR(7,I6)-
     *  DATPAR(6,I6)))*ALOG(DATPAR(8,I6)/DATPAR(9,I6))
C
C.....PRINT RESULTS
  190 PERMCM=PERMM*100.
      IF(IOUT.GT.0) WRITE(IOUT,300) (IDENT(I),I=1,8), DATPAR(1,I1),
     *  DATPAR(2,I2),DATPAR(3,I3),DATPAR(4,I4),DATPAR(6,I6),
     *  DATPAR(7,I6),DATPAR(8,I6),DATPAR(9,I6),RLD,PERMM,PERMCM
      NLINE=NLINE+1
      IF(IAOUT.GT.0) WRITE(IAOUT,300) (IDENT(I),I=1,8),DATPAR(1,I1),
     *  DATPAR(2,I2),DATPAR(3,I3),DATPAR(4,I4),DATPAR(6,I6),
     *  DATPAR(7,I6),DATPAR(8,I6),DATPAR(9,I6),RLD,PERMM,PERMCM
  300 FORMAT(1X,8A1,1X,F5.2,2X,F5.2,3X,F5.2,2X,F5.2,1X,F8.2,1X,F8.2,
     *        1X,F6.2,1X,F6.2,1X,F7.2,2X,1PE8.2,2X,1PE8.2)
      GO TO 200
C
C.....DENOMINATOR EQUALS ZERO, CALCULATION DISCONTINUED
  250 CONTINUE
      IF(IOUT.GT.0) WRITE(IOUT,350) (IDENT(I),I=1,8),DATPAR(1,I1),
     *  DATPAR(2,I2),DATPAR(3,I3),DATPAR(4,I4),DATPAR(6,I6),
     *  DATPAR(7,I6),DATPAR(8,I6),DATPAR(9,I6)
      NLINE=NLINE+1
      IF(IAOUT.GT.0) WRITE(IAOUT,350) (IDENT(I),I=1,8),DATPAR(1,I1),
     *  DATPAR(2,I2),DATPAR(3,I3),DATPAR(4,I4),DATPAR(6,I6),
     *  DATPAR(7,I6),DATPAR(8,I6),DATPAR(9,I6)
  350 FORMAT(1X,8A1,1X,F5.2,2X,F5.2,3X,F5.2,2X,F5.2,1X,F8.2,1X,F8.2,
     *        1X,F6.2,F6.2,9X,'    --     ','    --     ')
  200 CONTINUE
      RETURN
      END


C*************************   B T L A G   ***************************C
C                                                                   C
C     SUBROUTINE BTLAG CALCULATES HORIZONTAL HYDRAULIC CONDUCTIVITY  C
C     USING THE BASIC TIME LAG METHOD                               C
C                                                                   C
C*******************************************************************C
      SUBROUTINE BTLAG
      CHARACTER*1 IDENT, TITLE
      COMMON /C1000/ IN, IOUT, IAIN, IAOUT, INTER
     *        /C4000/ IDENT(8), DATPAR(11,10), NVAL(11)
     *        /C4200/ IMETH, IAOFLG, IOFLG
     *        /C4300/ TITLE(72), NTITL, NWTITL
     *        /C4400/ NLINE, NLINEX
C
      ISKIP=1
      IF(IAOFLG.EQ.1.OR.IOFLG.EQ.1) CALL PRTITL(82)
C
C.....PERMEABILITY CALCULATION
      DO 200 I1=1,NVAL(1)
      IF(I1.EQ.1.AND.NVAL(1).GT.1) ISKIP=ISKIP+1
      DO 200 I2=1,NVAL(2)
      IF(I2.EQ.1.AND.NVAL(2).GT.1) ISKIP=ISKIP+1
      DO 200 I3=1,NVAL(3)
      IF(I3.EQ.1.AND.NVAL(3).GT.1) ISKIP=ISKIP+1
      DO 200 I4=1,NVAL(4)
      IF(I4.EQ.1.AND.NVAL(4).GT.1) ISKIP=ISKIP+1
      DO 200 I5=1,NVAL(5)
      IF(I5.EQ.1.AND.NVAL(5).GT.1) ISKIP=ISKIP+1
      IF(ISKIP.LE.0) GO TO 175
      IF(IOUT.GT.0) WRITE(IOUT,165)
      IF(IAOUT.GT.0) WRITE(IAOUT,165)
  165 FORMAT(1X)
      NLINE=NLINE+1
      ISKIP=0
      IF(NLINE.LT.NLINEX.OR.IOUT.EQ.0) GO TO 175
      IOFLG=1
      CALL PRTITL(82)
C
C.....AVOID DIVISION BY ZERO
  175 CONTINUE
      IF(DATPAR(2,I2).LE.0..OR.DATPAR(3,I3).LE.0..OR.DATPAR(5,I5).LE.0.)
     *  GO TO 250
      DPIPE=DATPAR(1,I1)*.01
      D=DATPAR(2,I2)*.01
      RM=DATPAR(4,I4)**.5
      RLD=RM*DATPAR(3,I3)/D
      IF(RLD.GT.4.) GO TO 180
C
C.....RL/D LESS THAN OR EQUAL TO 4
      PERMM=(DPIPE**2.)*ALOG(RLD+(1.+RLD**2.)**.5)/(8.*DATPAR(3,I3)*
     *  DATPAR(5,I5))
      GO TO 190
C
C.....RL/D GREATER THAN 4
  180 PERMM=(DPIPE**2.)*ALOG(2.*RLD)/(8.*DATPAR(3,I3)*DATPAR(5,I5))
```

```
C
C.....PRINT RESULTS
  190 PERMCM=PERMM*100.
      IF(IOUT.GT.0) WRITE(IOUT,300) (IDENT(I),I=1,8),DATPAR(1,I1),
     *  DATPAR(2,I2),DATPAR(3,I3),DATPAR(4,I4),DATPAR(5,I5),RLD,
     *  PERMM,PERMCM
      NLINE=NLINE+1
      IF(IAOUT.GT.0) WRITE(IAOUT,300) (IDENT(I),I=1,8),DATPAR(1,I1),
     *  DATPAR(2,I2),DATPAR(3,I3),DATPAR(4,I4),DATPAR(5,I5),RLD,
     *  PERMM,PERMCM
  300 FORMAT(1X,8A1,3X,F5.2,3X,F5.2,4X,F5.2,2X,F6.2,1X,F7.2,2X,F7.2,2X,
     *          1X,1PE8.2,4X,1PE8.2)
      GO TO 200
C
C.....DENOMINATOR EQUALS ZERO, CALCULATION DISCONTINUED
  250 CONTINUE
      IF(IOUT.GT.0) WRITE(IOUT,350) (IDENT(I),I=1,8),DATPAR(1,I1),
     *  DATPAR(2,I2),DATPAR(3,I3),DATPAR(4,I4),DATPAR(5,I5)
      NLINE=NLINE+1
      IF(IAOUT.GT.0) WRITE(IAOUT,350) (IDENT(I),I=1,8),DATPAR(1,I1),
     *  DATPAR(2,I2),DATPAR(3,I3),DATPAR(4,I4),DATPAR(5,I5)
  350 FORMAT(1X,8A1,3X,F5.2,3X,F5.2,4X,F5.2,2X,F6.2,1X,F7.2,11X,
     *    '     --     ',2X,'     --     ')
  200 CONTINUE
      RETURN
      END

C*************************    P R T I T L   **************************C
C                                                                      C
C     SUBROUTINE PRTITL PRINTS THE TITLE OF TABLES                     C
C                                                                      C
C**********************************************************************C
      SUBROUTINE PRTITL(NLTOT)
      CHARACTER*1 TITLE, ATITLE(132), BLANK
      COMMON /C1000/ IN, IOUT, IAIN, IAOUT, INTER
     *       /C3000/ BLANK
     *       /C4200/ IMETH, IAOFLG, IOFLG
     *       /C4300/ TITLE(72), NTITL, NWTITL
     *       /C4400/ NLINE, NLINEX
C
      IF(IOFLG.EQ.0) GO TO 20
      NLINE=0
      WRITE(IOUT,60)
   60 FORMAT(1H1)
C
C.....PRINT MAIN TITLE
   20 CONTINUE
      IF(IAOFLG.EQ.1) WRITE(IAOUT,10)
   10 FORMAT(/)
C
      IF(NTITL.EQ.0) GO TO 95
      DO 70 I=1,132
   70 ATITLE(I)=BLANK
      NX1=(NLTOT-NTITL)/2
      IF(NX1.LE.0) NX1=0
      NI=0
      NX2=NX1+NTITL
      NX1=NX1+1
      DO 80 I=NX1,NX2
      NI=NI+1
   80 ATITLE(I)=TITLE(NI)
      IF(IOFLG.EQ.1) WRITE(IOUT,90) (ATITLE(I),I=1,NX2)
      IF(IAOFLG.EQ.1) WRITE(IAOUT,90) (ATITLE(I),I=1,NX2)
      NLINE=NLINE+4
   90 FORMAT(//1X,132A1/)
C
C.....PRINT CALCULATION METHOD AND APPROPRIATE COLUMN HEADINGS
   95 CONTINUE
      GOTO(100,200,300),IMETH
C
C....."CONSTANT HEAD METHOD"
  100 CONTINUE
      IF(IOFLG.EQ.1) WRITE(IOUT,110)
      IF(IAOFLG.EQ.1) WRITE(IAOUT,110)
      GO TO 500
  110 FORMAT(/ 6X,68HHORIZONTAL HYDRAULIC CONDUCTIVITY  (HVORSLEV'S CONS
     *TANT HEAD METHOD) //
     *1X,'PIEZO',5X,'OSCREEN',2X,'LSCREEN',2X,
     *        'RATIO',5X,'Q',8X,'HC',8X,'-------- PERM --------'/
     *        2X,'NO.',7X,'(CM)',6X,'(M)',4X,'(H/V)',
     *        3X,'(CC/S)',5X,'(M)',9X,'(M/S)',7X,'(CM/S)'/
     *        1X,79('-') )
C
C....."VARIABLE HEAD METHOD"
  200 CONTINUE
      IF(IOFLG.EQ.1) WRITE(IOUT,210)
      IF(IAOFLG.EQ.1) WRITE(IAOUT,210)
      GO TO 500
  210 FORMAT(/15X,68HHORIZONTAL HYDRAULIC CONDUCTIVITY  (HVORSLEV'S VARI
     *ABLE HEAD METHOD) //
     *1X,'PIEZO',4X,'DPIPE',1X,'OSCREEN',1X,'LSCREEN',2X,
     *        'RATIO',4X,'T1',6X,'T2',7X,'H1',5X,'H2',4X,'ML/D',2X,
     *        '------ PERM -------'/
     *        2X,'NO.',5X,'(CM)',3X,'(CM)',5X,'(M)',4X,'(H/V)',4X,
     *       '(S)',5X,'(S)',6X,'(M)',4X,'(M)',11X,'(M/S)',
     *        5X,'(CM/S)'/
     *      97('-') )
C
C....."BASIC TIME LAG METHOD"
  300 CONTINUE
      IF(IOFLG.EQ.1) WRITE(IOUT,310)
      IF(IAOFLG.EQ.1) WRITE(IAOUT,310)
      GO TO 500
  310 FORMAT(/7X,69HHORIZONTAL HYDRAULIC CONDUCTIVITY  (HVORSLEV'S BASIC
     * TIME LAG METHOD) //
     *1X,'PIEZO',6X,'DPIPE',2X,'OSCREEN',2X,'LSCREEN',2X,
     *        'RATIO',3X,'TLAG',5X,'ML/D',4X,'------- PERM --------'/
     *        2X,'NO.',7X,'(CM)',4X,'(CM)',6X,'(M)',4X,'(H/V)',
     *        3X,'(S)',16X,'(M/S)',6X,'(CM/S)'/
     *       1X,82('-') )
C
C.....RESET FLAGS
  500 CONTINUE
      IAOFLG=0
      IOFLG=0
      RETURN
      END
```

Analysis of Leaky Aquifer Pumping Test Data: An Automated Numerical Solution Using Sensitivity Analysis

by P. M. Cobb, C. D. McElwee, and M. A. Butt[a]

ABSTRACT

The Kansas Geological Survey is pursuing an effort to automate some of the more common methods of aquifer pumping-test analysis. This paper discusses the results of work done on the leaky artesian aquifer as defined by Hantush and Jacob (1955). The paper covers the basic theory of the aquifer type, the numerical solution of the leaky artesian-well function, and the methodology of achieving the "best fit" parameters in the least squares' sense. Several data sets are used to demonstrate the applicability of the proposed technique. These examples indicate the generally satisfactory results produced by the automated analysis documented here.

The algorithm has good convergence properties. Initial estimates for the aquifer parameters may vary by about three orders of magnitude above or below the correct values. For typical data sets the rms fitting error should be less than a few tenths of a foot. If this is not the case, one is probably not dealing with a simple leaky aquifer. This method of pumping-test analysis does not eliminate the role of an experienced hydrologist to define the local hydrogeology and aquifer type. However, once the decision is made as to which aquifer configuration is being observed, this program will, in a quick and unbiased fashion, give an accurate assessment of the leaky-aquifer parameters within the limits of the theoretical approximations and the data quality.

[a]Kansas Geological Survey, 1930 Ave. A, Campus W., The University of Kansas, Lawrence, Kansas 66044.

Received September 1981, revised January 1982, accepted January 1982.

Discussion open until November 1, 1982.

INTRODUCTION

The Kansas Geological Survey is in the process of fabricating a series of computer programs designed to analyze pumping-test data. The program discussed in this paper solves the inverse problem for a leaky-artesian aquifer system proposed by Hantush and Jacob (1955). The leaky-artesian aquifer problem considered here is not the most general configuration (see Hantush, 1960; Neuman and Witherspoon, 1969a); however, the limited number of data sets available for analysis tend to be for this simple case. The limits of the theory used in this paper are outlined by Neuman and Witherspoon (1969b). The automated analysis of the simple confined-aquifer pumping test has been published previously by the Survey (McElwee, 1980a). The methodology used in the present study involves sensitivity analysis and a least-squares' fitting technique to analyze the time-drawdown data while satisfying the equations developed by Hantush and Jacob (1955). These techniques will be outlined in the text. More information may be found in McElwee (1980a, 1980b), McElwee and Yukler (1978), and Cobb, McElwee and Butt (1978).

Because of the limited number of available data sets for this aquifer configuration, this technique is being published after extensive but not exhaustive testing. However, we have tested it for several hypothetical data sets and for seven real data sets readily available to us. At this point, we feel quite confident in the algorithm's capabilities.

It is hoped that, by setting this algorithm out for public scrutiny, new data sets will be tested and the program more thoroughly verified. A more detailed report with program listings is available from the authors. Using the available data sets, we have been able to establish that, for fairly smooth data sets (those that conform generally to the shape of the leaky type curves), the model has excellent convergence properties. Initial estimates of the storage coefficient, transmissivity, and leakage coefficient may be in the range of plus or minus three orders of magnitude of the correct value and still obtain successful convergence.

This method of pumping-test analysis does not remove the requirement of having an experienced hydrologist evaluate the local hydrogeology and pumping-test data to identify the aquifer type. However, once the decision is made as to which aquifer configuration is being observed, this program will, in a quick and unbiased fashion, give an accurate assessment of the leaky-aquifer parameters within the limits of the theoretical approximations. After using this model for the pumping-test analysis, the hydrologist should always look at the root-mean-square (rms) deviation in drawdown and the "best fit" drawdowns calculated by the program. The experimental and theoretical drawdowns should not differ greatly anywhere and the rms deviation should be less than a few tenths of a foot in order to have confidence in the analysis. If this is not the case, one is probably not dealing with a simple leaky aquifer.

THEORY AND ANALYTICAL SOLUTION FOR THE LEAKY CONFINED AQUIFER PROBLEM

The aquifer system defined by Hantush and Jacob (1955), as depicted in Figure 1, is composed of a level, isotropic, homogeneous, porous medium of infinite areal extent. The lower aquifer boundary is assumed to be impervious, while the upper boundary is assumed to be a leaky confining bed. A source bed overlies the leaky confining bed. Water is derived from the aquifer by elastic expansion of the water and compression of the aquifer matrix as pumping occurs. Leakage through the semiconfining bed is assumed to be proportional to the drawdown in the semiconfined aquifer. It is assumed that no water is removed from storage in the semiconfining unit and that no drawdown occurs in the source bed.

These assumptions lead to the following differential equation (Jacob, 1946)

$$\frac{\partial^2 s}{\partial r^2} + \frac{1}{r}\frac{\partial s}{\partial r} - \frac{s}{B^2} = \left(\frac{S}{T}\right)\frac{\partial s}{\partial t}\,, \qquad (1)$$

where

$s(r,t)$ is the drawdown at any distance from the well at any time,

r is the radial distance measured from the well,

S is the storage coefficient of the artesian aquifer,

$T = Km$ is the transmissivity of the artesian aquifer,

$B^2 = T/(K'/m')$; and

K and K' are the respective permeabilities of the artesian aquifer and the semiconfining bed,

m and m' are the respective thicknesses of the artesian aquifer and the semiconfining bed,

K'/m' is the leakance or specific leakage of the semiconfining bed (Hantush, 1949); and

Q is the well discharge.

With appropriate boundary conditions, an analytical solution is obtainable.

$$s = (Q/4\pi T)\cdot\int_u^\infty \exp(-y-z)/y\,dy \qquad (2)$$
$$u = r^2S/4Tt,\quad z = r^2/4B^2y$$

NUMERICAL SOLUTION PROCEDURE

Our first attempt at evaluating equation (2) involved the Laguerre Quadrature formula. Integral functions of the form

$$\int_0^\infty f(x)\,e^{-x}\,dx$$

may be approximated by the method of Laguerre integration:

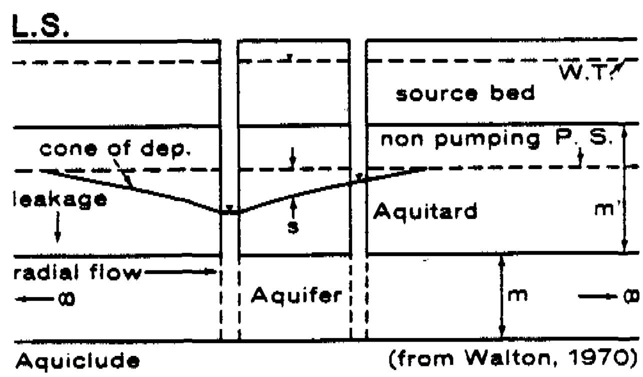

Fig. 1. Diagram of ideal leaky aquifer.

$$\int_0^\infty f(x)\,e^{-x}\,dx \approx \sum_{i=1}^{n} w_i f(x_i) \qquad (3)$$

where the w_i's are weighting factors, and the x_i's correspond to zeros of the n^{th} order Laguerre polynomials. The values of w_i and x_i are catalogued in Abramowitz and Stegun (1968).

To perform the integration in equation (2), a transformation of variables must occur in order to make the limits of integration compatible with the Laguerre Quadrature formula, equation (3). This transformation is a straightforward substitution of the form $y = x + u$. The integral takes the form

$$G(r/B,u) = \int_0^\infty \exp\left\{-u - r^2/[4B^2(x+u)]\right\}/(x+u) \cdot \exp(-x) \cdot dx$$

and is solved numerically by the appropriate substitutions in the Laguerre integration formula. The function $G(r/B,u)$ was evaluated by Laguerre integration of order 15. We found that evaluating equation (2) with Laguerre integration did not give the desired accuracy for small values of u. Therefore, an alternate evaluation scheme had to be developed.

Hantush and Jacob (1955) give several forms of the solution to equation (1) for different ranges of u and r/B. The alternate evaluation scheme we use involves three equations, which are solved numerically in order to cover the complete range of u and r/B. The equations are listed here, along with the appropriate ranges of u and r/B.

$$s = Q/(4\pi T) \cdot G(r/B,u)$$
$$u = r^2 S/4Tt, \quad u \geqslant 1.0, \quad \text{any value of } r/B \qquad (4)$$

$$s = Q/(4\pi T) \cdot [2K_o(r/B) - G(r/B,p)]$$
$$p = Tt/SB^2 \geqslant 1, \quad (r/B)^2 \geqslant u \leqslant 1.0 \qquad (5)$$

$$s = Q/4\pi T \cdot \left\{2K_o(r/B) + I_o(r/B) \cdot Ei(-r^2/4B^2u)\right.$$
$$+ \exp(-r^2/4B^2u) \cdot [0.5772 + \ln(u) - Ei(-u)$$
$$- u + u \cdot (I_o(r/B) - 1)/(r^2/4B^2)$$
$$\left.- u^2 \sum_{n=1}^{\infty} \sum_{m=1}^{n} \frac{(-1)^{n+m}(n-m+1)!}{((n+2)!)^2} (r^2/4B^2)^m u^{n-m}]\right\}$$
$$(r/B)^2 \leqslant u \leqslant 1 \qquad (6)$$

$Ei(x)$ is the exponential integral; I_o and K_o are the zero order modified Bessel functions of the first and second kind.

The numerical solution of the exponential integral, $Ei(x)$, is described in detail by McElwee (1980b, p. 3). Solutions for the zero-order modified Bessel functions of the first and second kinds, $I_o(x)$ and $K_o(x)$, were obtained by polynomial approximations. Abramowitz and Stegun (1968) catalog several forms for each function. Each form is suitable for a particular range of x. The double summation in equation (6) is solved numerically by a truncated summation, since only a finite number of terms is required to approximate a convergent series. $G(r/B,u)$ and $G(r/B,p)$ were evaluated using the Laguerre integration procedure described earlier. The numerical computational routines involving these functions were checked by generating the table published in Walton (1970), page 146. This table could be produced accurately to the fourth decimal place.

SENSITIVITY ANALYSIS

Parametric sensitivity analysis is a method of examining the stability of a mathematical representation of a dynamic system with respect to variations in the values of the system's physical parameters. The theoretical basis of this technique is outlined by Tomovic (1962), while the application to hydrologic problems has been examined by Vemuri, *et al.* (1969), McCuen (1973), Yukler (1976), and McElwee and Yukler (1978).

In formulating the sensitivity analysis of the leaky confined aquifer problem, the following mathematical model was used:

$$F(h_{xx}, h_{yy}, h_t, h; S,T,L,Q) = 0 \qquad (7)$$

where $h_{xx} = \frac{\partial^2 h}{\partial x^2}$, $h_{yy} = \frac{\partial^2 h}{\partial y^2}$, $h_t = \frac{\partial h}{\partial t}$

h = hydraulic head,

S = storage coefficient,

T = transmissivity,

L = inverse leakage coefficient ($L = 1/B$), and

Q = pumpage.

The solution may be written as

$$h = h(x,y,t; S,T,L,Q)$$

Variation of any single parameter such as T produces a new solution

$$F(h^*_{xx}, h^*_{yy}, h^*_t, h^*; S,T+\Delta T,L,Q) = 0 \qquad (8)$$

where ΔT is the incremental change in T and h^* is the perturbed head. The solution to this expression is of the form $h^* = h^*(x,y,t; S,T+\Delta T,L,Q)$. The stability of the system to small changes in the parameter T may be expressed by

$$\frac{\Delta h}{\Delta T} = \frac{h^* - h}{\Delta T}$$

If the limit to this expression exists as ΔT approaches zero, it may be written as

$$U_T (x,y,t;\ S,T,L,Q) = \frac{\partial h}{\partial T} = \lim_{\Delta T \to 0} \frac{\Delta h}{\Delta T} \qquad (9)$$

Also

$$U_S (x,y,t;\ S,T,L,Q) = \frac{\partial h}{\partial S} = \lim_{\Delta S \to 0} \frac{\Delta h}{\Delta S} \qquad (10)$$

and

$$U_L (x,y,t;\ S,T,L,Q) = \frac{\partial h}{\partial L} = \lim_{\Delta L \to 0} \frac{\Delta h}{\Delta L} \qquad (11)$$

which are, respectively, the sensitivity coefficients with respect to changes in S and the sensitivity coefficient with respect to changes in L.

The solution to the flow equation is assumed to depend analytically upon the independent parameters, S, T, L, and Q. The function $h^*(x,y,t;\ S,T+\Delta T, L,Q)$, which is perturbed in the parameter T, may be expanded in a Taylor's series (Tomovic, 1962). If ΔT is small, all nonlinear terms can be neglected as follows:

$$h^*(x,y,t;S,T+\Delta T,L,Q) = h(x,y,t;S,T,L,Q) + U_T \Delta T \qquad \ldots\ldots (12)$$

where $U_T = (\partial h)/(\partial T)$. Thus, new hydraulic heads, resulting from incremental changes in T, can be computed directly if the unperturbed head is known and U_T can be computed. Similar expressions may be derived for perturbation with respect to S and L:

$$h^*(x,y,t;S+\Delta S,T,L,Q) = h(x,y,t;S,T,L,Q) + U_S \Delta S \qquad \ldots\ldots (13)$$

$$h^*(x,y,t;S,T,L+\Delta L,Q) = h(x,y,t;S,T,L,Q) + U_L \Delta L \qquad \ldots\ldots (14)$$

These are correct to first order in ΔS and ΔL, respectively.

For this technique to be useful, it is only necessary to be able to compute U_S, U_T, and U_L, since $h(x,y,t;\ S,T,L,Q)$ may be computed by previously discussed techniques. This computation may be done by analytical or numerical techniques. In this work, it was found to be convenient to obtain U_S and U_T by direct analytical means and U_L by a numerical method.

Recall that the basic equation describing the solution to the leaky confined aquifer is

$$s = \frac{Q}{4\pi T} \int_u^\infty \frac{1}{y} \exp\left(-y - \frac{L^2 r^2}{4y}\right) dy, \qquad u = \frac{r^2 S}{4Tt}, \quad L = B^{-1} \qquad (2)$$

By applying Leibnitz's rule for differentiating an integral (Hildebrand, 1962), it is easy to obtain the sensitivity coefficients with respect to S and T:

$$U_S = \frac{\partial s}{\partial S} = -\frac{Qr^2}{16\pi T^2 t} \left[\frac{1}{u} \exp\left(-u - \frac{L^2 r^2}{4u}\right)\right] \qquad (15)$$

$$U_T = \frac{\partial s}{\partial T} = -\frac{Q}{4\pi T^2} \int_u^\infty \frac{1}{y} \exp\left(-y - \frac{L^2 r^2}{4y}\right) dy + \frac{Qr^2 S}{16\pi T^3 t} \left[\frac{1}{u} \exp\left(-u - \frac{L^2 r^2}{4u}\right)\right] = -\frac{s}{T} - \frac{S}{T} U_S \qquad (16)$$

These equations may be evaluated easily by standard numerical functions on a high-speed computer once s is known.

U_L was computed by a direct numerical technique, rather than by formulating an analytical solution, to conserve program simplicity while retaining computational accuracy. Note that the argument of the exponential within the integral of equation (2) contains the parameter L. Hence, differentiation will transform the entire function within the integral and will define

$$U_L = \int_u^\infty \frac{\partial}{\partial L} \left\{\exp(-y - L^2 r^2/4y)/y\right\} dy = \int_u^\infty \left\{-Lr^2/2y^2\right\} \exp(-y - L^2 r^2/4y)\, dy \qquad (17)$$

Note that both U_S and U_T in equations (15) and (16) can be expressed in such a manner that, after the drawdown s is computed, no further numerical integration is required. The sensitivity with respect to leakage, U_L in equation (17), can be computed only by additional numerical integration that would involve the formulation of a more complex subroutine. Therefore, the decision was made to generate U_L by a finite difference approximation. The approximation

$$\partial s/\partial L \simeq \left\{s(L+\Delta L) - s(L-\Delta L)\right\}/2\Delta L \qquad (18)$$

where

$$s(L\mp\Delta L) = Q/4\pi T \int_u^\infty \exp\left\{-y - r^2 (L\mp\Delta L)^2/4y\right\}/y \cdot dy \qquad \ldots\ldots (19)$$

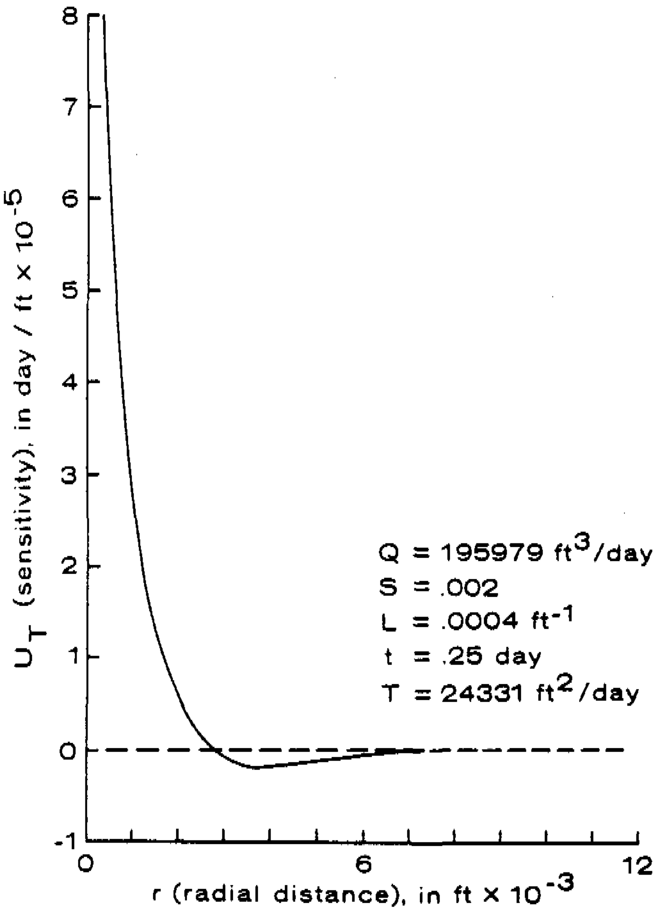

Fig. 2. Radial dependence of U_T.

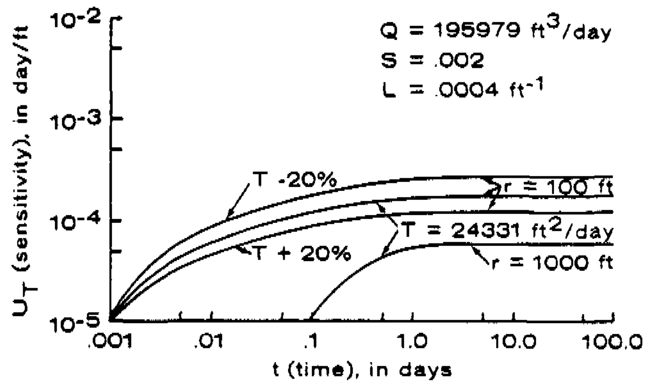

Fig. 3. Effect of radius and transmissivity on the time dependence of U_T.

The radial dependence of U_S is shown in Figure 4. This coefficient does not diverge at the well, nor does its sign change. It is inversely proportional to S. The constancy of algebraic sign indicates that as S changes there is a general raising or lowering of the cone of depression.

The time dependence of U_S is presented in Figure 5. Radial variation is indicated by the presence of three curves. Each curve reaches its maximum value for U_S at a time directly proportional to its radial value. At some finite value of time each curve approaches zero in value, indicating that a steady state is achieved. Until steady

becomes increasingly accurate as ΔL approaches zero. Satisfactory evaluation of U_L occurred for ΔL set equal to .01 L. The methodology for computing the sensitivity coefficients is now complete.

DISCUSSION OF THE LEAKY AQUIFER SENSITIVITY COEFFICIENTS

The radial dependence of U_T is shown in Figure 2. The function diverges logarithmically near the well. U_T changes sign at some finite value of radius. This demonstrates the fact that when T is changed, the cone of depression deepens in some areas and shallows in others. (Note that radial distances in the figures are measured in *thousands* of feet. The radius r has been multiplied by 10^{-3} to give small integers.)

Figure 3 depicts the time dependence of positive values of U_T for variations in r and T. Note that U_T is inversely proportional to T. The curves represent a transmissivity of 24,331 ft²/day and ±20% of that value at a radius of 100 feet and a T of 24,331 ft²/day at a radius of 1,000 feet. Note that all curves flatten after three to four days. This describes the steady condition caused by deriving the discharge Q totally from leakage.

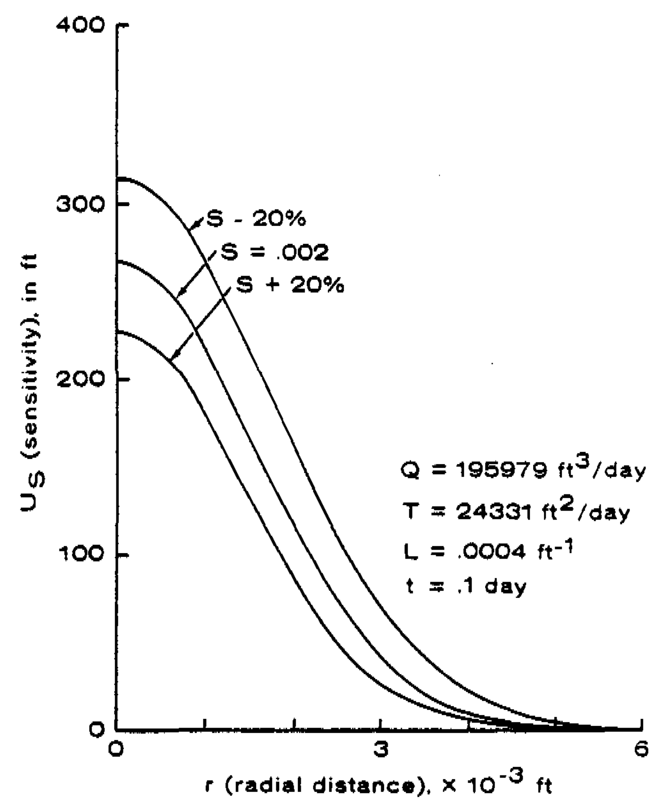

Fig. 4. Effect of changes in S on the radial dependence of U_S.

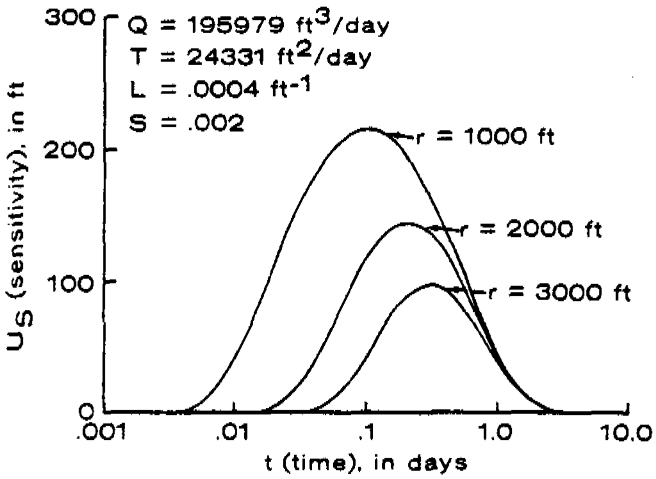

Fig. 5. Effect of radius on the time dependence of U_S.

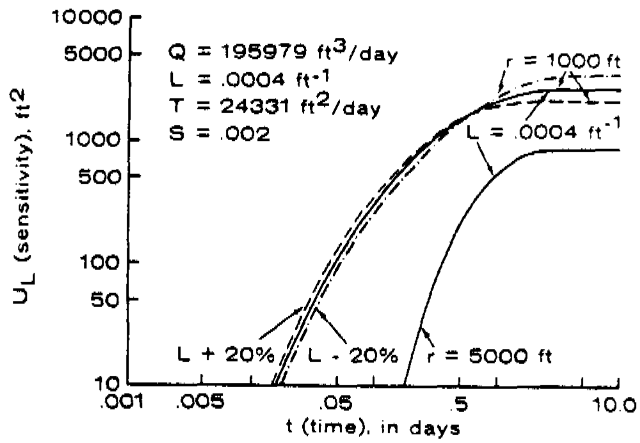

Fig. 7. Effect of changes in L and radius on the time dependence of U_L.

state is attained, there is a dual source supplying the pumpage, namely water released from storage and leakage. The curves roll over as leakage starts to dominate the source mechanism. U_S is zero outside the cone of depression and at any time after steady state is attained.

Figure 6 shows the radial dependence of U_L. The sensitivity coefficient U_L does not diverge at the well and approaches zero for large values of r. These are similar to the curves for U_S.

The time dependence of U_L is shown in Figure 7 for two values of r. All curves grow with time until a steady state is achieved where leakage is supplying the entire discharge Q. The set of curves labeled L = .0004 ft^{-1} and ±20% of that value are of interest. Observe that at t less than .6 days, U_L is directly proportional to L; while for t greater than .6 days, U_L is inversely proportional to L. As indicated before, Q is supplied by a dual source in the leaky artesian aquifer—water taken from storage in the aquifer and water supplied by leakage through the aquitard. This dual source mechanism results in the changing dependence on L.

THE FITTING PROCEDURE

The objective of any curve-fitting technique, whether performed manually or by computer, is to fit a theoretical type curve to an experimental data set as accurately as possible, evaluating in the process a corresponding set of physical parameters. To perform this task successfully, a mechanism is required for judging the error in the fit. Classical manual curve-fitting relies basically on the best "eye ball" fit. The computer method described here allows the fitting error to be accurately and meaningfully determined as the rms error.

In order to apply the parametric sensitivity method to the fitting problem, it is necessary to define an error function

$$E = \sum_i \left[s_e(t_i) - s^*(t_i)\right]^2$$

where E is the summation over i discrete samples of the squared difference between the experimental drawdown (s_e) and the updated drawdown (s^*), which is computed from the truncated Taylor's Series

$$s^* = s + U_T \Delta T + U_S \Delta S + U_L \Delta L$$

The argument t_i represents the i^{th} value of time. Expansion of the squared error function, taking partial derivatives with respect to the perturbed parameters, and setting the partial derivatives equal to zero, yields a set of three simultaneous linear equations that must be satisfied to obtain the best fit.

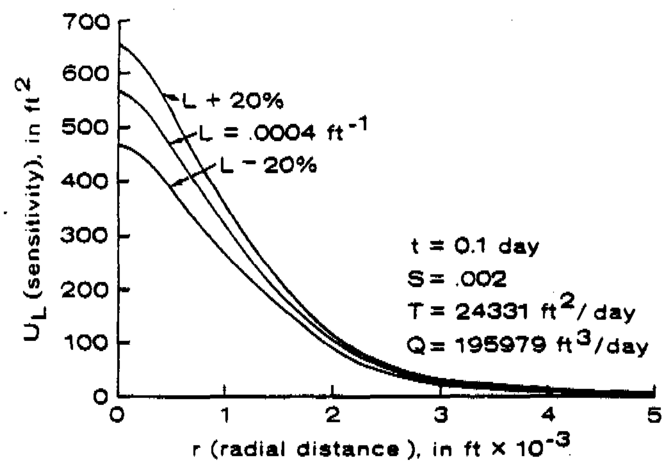

Fig. 6. Effect of changes in L on the radial dependence of U_L.

More specifically, for minimizing E, it is required that

$$\frac{\partial E}{\partial \Delta T} = \frac{\partial E}{\partial \Delta S} = \frac{\partial E}{\partial \Delta L} = 0 \qquad (20)$$

The linear system of equations that results is

$$\begin{bmatrix} \sum_i U_L^2 & \sum_i U_L U_S & \sum_i U_L U_T \\ \sum_i U_S U_L & \sum_i U_S^2 & \sum_i U_S U_T \\ \sum_i U_T U_L & \sum_i U_T U_S & \sum_i U_T^2 \end{bmatrix} \begin{bmatrix} \Delta L \\ \Delta S \\ \Delta T \end{bmatrix} = \begin{bmatrix} \sum_i U_L (s-s_e) \\ \sum_i U_S (s-s_e) \\ \sum_i U_T (s-s_e) \end{bmatrix} \quad \ldots\ldots (21)$$

and can be solved explicitly for ΔL, ΔS, and ΔY. The quantity s is the theoretical drawdown at time t calculated from the previous values of L, S, and T. The new values of the parameters are simply

$$\begin{aligned} L_{i+1} &= L_i + \Delta L_i \\ S_{i+1} &= S_i + \Delta S_i \\ T_{i+1} &= T_i + \Delta T_i \end{aligned} \qquad (22)$$

This process continues until the values of ΔL_i, ΔS_i, and ΔT_i simultaneously satisfy a specified convergence criteria. The goodness of fit obtained at the termination of the last iteration is indicated by the value of the rms error

$$\sqrt{\frac{\sum_i (s - s_e)^2}{n}}$$

where n is the number of discrete samples of s.

The success of this methodology is dependent to a degree upon the initial estimates of the parameters S, T, and L. However, numerical experiments conducted with the most recent version of the computer program indicate that the initial estimates may be as much as three orders of magnitude above or below the final solution values and convergence will still be obtained.

In order to maintain physical reality and improve numerical stability, the algorithm requires that the parameters S, T, and L must always be positive. Furthermore, the relative increments $\Delta T/T$, $\Delta S/S$, and $\Delta L/L$ are never allowed to exceed 0.5 or be less than −0.2 in any one iteration. This subterfuge insures that the algorithm proceeds in an orderly fashion to the minimum error. In the tests we have run the algorithm converges to the global minimum; however, it is possible that only a local minimum will be found. By trying several initial guesses, it should be possible to find the global minimum, if there is any doubt.

Table 1. Comparison of Aquifer Parameters for Typical Data Sets Obtained by Graphical Analysis and by Automated Analysis

Data Source Code		*Graphical Analysis Values*		*Automated Analysis Values*	*Automated rms Error*
1		T = 182000 gpd/ft S = .002 B = 2500 ft		202000 gpd/ft .002 3300 ft	.007 ft
2*	a		a	99000 .000097 2000	.038
	b	T = 99400 S = .0001 B = 2000	b	100000 .000097 1980	.016
	c		c	97800 .0001 1950	.010
3		T = 1500 S = .00020 B = 430		1800 .00017 650	.125
4	a	T = 49000 S = .000090 B = 4100		44000 .000086 3900	.378
	b	T = 41000 S = .000080 B = 4000		46000 .000084 4800	.030

T = Transmissivity
S = Storage coefficient
B = Leakage coefficient
* The values obtained by graphical analysis represent an average of three sets of data taken for different values of radius. Each data set was independently analyzed and tabulated for the automated analysis.

APPLICATION TO TYPICAL DATA

Table 1 lists the best-fit aquifer parameter values for several data sets analyzed by fitting leaky artesian type curves, both graphically and using the technique discussed here. The data sources are listed by number in the Appendix. The lower case letters indicate that data was taken for different observation wells at the same pumping test, or that several independent pumping tests were listed in the same source. The principal feature of this table is the quite good agreement between the automated-analysis values and the graphical-analysis values. All values are well within the same order of magnitude; in fact the differences are not over 35% and most of them are in the 10-20% range. The largest rms error is about .4 feet for set 4a. The smallest rms error is .007 feet for data set 1. Note that data sets with the lowest rms error do not necessarily have the closest agreement between sets of parameters. This fact is related to the sensitivities of the various parameters and the subjectivity of a graphical fit.

Table 2 is a comparison of parameter values derived from data sets analyzed by a confined aquifer model and by a leaky artesian model. Although the rms errors are satisfactory, there is a discrepancy of several orders of magnitude in the storage value for example 6. These examples demonstrate the fact that imperfect data can still lead to convergence in this algorithm. This points out that in addition to analyzing the drawdown curve from an aquifer test one must carefully examine the hydrogeology of a site because of the ambiguity of analyzing real data by theoretical curves. A compilation of the data sources referenced in Tables 1 and 2 is contained in the Appendix.

DISCUSSION AND SUMMARY

This paper has set forth a methodology for analyzing the leaky artesian-aquifer pumping test by using a numerical regression algorithm built on sensitivity analysis. A by-product is the solution to the drawdown equation.

The algorithm presented in this paper has proven consistently its ability to converge to the "correct" set of aquifer parameters for a typical data set. In this case "correct" means the values obtained by manual curve matching methods for real data, or the values used in generating the hypothetical data. These best-fit values are achieved over a range of initial estimates ranging from three orders of magnitude above to three orders of magnitude below the converged values. The number of iterations is reduced as the estimated parameter values approach the true values. For typical data sets the rms error tends to be only a few tenths of a foot, while for fairly idealized sets of data, the rms error is a few hundredths of a foot. Iterations can be reduced by increasing the size of the acceptable error criteria, but only at the cost of increased rms error. Memory size and computing time are relatively small for this algorithm. The typical analysis costs only a few dollars or less.

If the data diverges too much from ideal data, convergence may not occur. In this case, if convergence does occur, the rms error may be unacceptable. Although this algorithm gives a unique solution to any data set for which it can achieve a converged set of values, it cannot distinguish absolutely between different types of aquifers. Since the three degrees of freedom (three aquifer parameters) give the algorithm considerable latitude in achieving convergence, an imperfect data set may be run successfully and a set of values for transmissivity, storage, and leakage produced. This fact points to several cautions. First, only the best data available should be analyzed. Second, the geohydrology should be examined carefully by experienced personnel to aid in classifying the aquifer type. Third, if doubt exists about the validity of the converged values, the rms error value should be noted and individual best-fit drawdowns should be compared to the field data for gross deviations. While this type of automated analysis can ease the burden of the hydrologist, it does not appear that it will reduce his role.

Table 2. Comparison of Data Analyzed Two Ways (Nonleaky and Leaky)

Data Source Code	*Confined Aquifer Values*	*Leaky Aquifer Values*	*Leaky rms Error*
5	T = 44000 gpd/ft S = .00046 B = 0 ft	T = 42000 gpd/ft S = .00044 B = 8600 ft	0.240 ft
6	T = 42000 S = .00004 B = 0	T = 9800 S = .0045 B = 65	.036

REFERENCES

Abramowitz, M., and I. A. Stegun. 1968. Handbook of Mathematical Functions. Dover Publications, New York. p. 231.

Cobb, P. M., C. D. McElwee, and M. A. Butt. 1978. Leaky aquifer parameter identification by sensitivity analysis. Transactions of the American Geophysical Union. v. 60, no. 6, p. 67.

Hantush, M. S. 1949. Plain potential flow of ground water with linear leakage. Doctoral dissertation, University of Utah.

Hantush, M. S. 1960. Modification of the theory of leaky aquifers. Journal of Geophysical Research. v. 65, no. 11, pp. 3713-3725.

Hantush, M. S., and C. E. Jacob. 1955. Non-steady radial flow in an infinite leaky aquifer. Transactions of the American Geophysical Union. v. 36, pp. 95-100.

Hildebrand, F. B. 1962. Advanced Calculus for Applications. Prentice-Hall, Englewood Cliffs, New Jersey. p. 360.

Jacob, C. E. 1946. Radial flow in a leaky artesian aquifer. Transactions of the American Geophysical Union. v. 27, pp. 198-208.

Kreysig, E. 1972. Advanced Engineering Mathematics. John Wiley and Sons, Inc., New York. pp. 329-331.

McCuen, R. H. 1973. Component sensitivity: a tool for the analysis of complex water resources systems. Water Resources Research. v. 9, no. 1, pp. 243-246.

McElwee, C. D. 1980a. Theis parameter evaluation from pumping tests by sensitivity analysis. Ground Water. v. 18, no. 1, pp. 56-60.

McElwee, C. D. 1980b. The Theis equation: evaluation, sensitivity to storage and transmissivity, and automated fit of pump test data. Kansas Geological Survey, Groundwater Series No. 3. 39 pp.

McElwee, C. D., and M. A. Yukler. 1978. Sensitivity of groundwater models with respect to variations in transmissivity and storage. Water Resources Research. v. 14, no. 3, p. 451.

Neuman, S. P., and P. A. Witherspoon. 1969a. Theory of flow in a confined two aquifer system. Water Resources Research. v. 5, no. 4, pp. 803-816.

Neuman, S. P., and P. A. Witherspoon. 1969b. Applicability of current theories of flow in leaky aquifers. Water Resources Research. v. 5, no. 4, pp. 817-829.

Tomovic, R. 1962. Sensitivity analysis of dynamic systems. McGraw-Hill, New York. 141 pp.

Vemuri, V., J. A. Dracup, R. C. Erdmann, and N. Vemuri. 1969. Sensitivity analysis method of system identification and its potential in hydrologic research. Water Resources Research. v. 5, no. 2, pp. 341-349.

Walton, W. C. 1970. Groundwater Resource Evaluation. McGraw-Hill, New York. 664 pp.

Yukler, M. A. 1976. Analysis of error in groundwater modeling. Ph.D. dissertation, The University of Kansas. 182 pp.

* * * * *

Patrick M. Cobb received B.S. degree in Geophysics in 1976 and M.S. degree in Water Resources Science in 1980, both from the University of Kansas. The thesis topic was natural salt-water intrusion in the Great Bend Prairie in south-central Kansas. Since 1979 he has been employed by the Kansas Geological Survey in the Geohydrology Section. The hydrology of the Great Bend Prairie and applied numerical modeling are continuing topics of interest.

Carl D. McElwee graduated in 1965 from William Jewell College with a B.A. in Physics. He received M.A. and Ph.D. degrees from the University of Kansas in 1967 and 1971, respectively. His research area was solid-state physics. From 1971 to 1974 he worked for Texaco, Inc. in Houston, Texas as a research geophysicist. Since 1974 he has worked for the Kansas Geological Survey in the Geohydrology Section. His area of special interest is ground-water models.

Munir A. Butt graduated in 1969 from Regional Engineering College, Kashmir, with B.E. (Civil). He received M.E. degree from Roorkee University, India in 1973 and M.S. degree in Water Resources Engineering from the University of Kansas in 1977. From 1969 to 1975 he worked as Assistant Engineer, Kashmir Irrigation and Flood Control Department. Presently, he is at the University of Kansas and works as research assistant for the Kansas Geological Survey in the Geohydrology Section.

APPENDIX. TEST DATA SOURCES

1. Groundwater Resource Evaluation. Walton, W. C. McGraw-Hill. 1970. (page 286, Problem 4.5.)
2. Cooper, H. H. 1963. In Ground Water Hydraulics, Lohman, S. W. 1972. USGS Prof. Paper 708. (page 31, Table II.)
3. Illinois State Water Supply, Bulletin 49. Walton, W. C. 1962. Department of Registration and Education, Urbana, Ill. (page 32, Table 5.)
4. Aquifer test in the Ogallala Formation (26-37-21ddd). Gutentag, E. D. 1965. USGS, Garden City, Kansas. (USGS data file.)
5. Results of aquifer tests in the Wellington Aquifer near Salina, Kansas. Gillespie, J. B. 1979. USGS, Lawrence, Kansas. (unpublished data.)
6. Pump test data at Test Well #1. (In Groundwater Resources Investigation of the Spratt Site for Sunflower Electric Cooperative.) 1977. Burns and McDonnel Consultants, Kansas City, Missouri.

FIELD REPORTS

NUMERICAL METHOD OF PUMPING TEST ANALYSIS USING MICROCOMPUTERS

by K. S. Rathod and K. R. Rushton[a]

Abstract. This paper describes how a numerical method of pumping test analysis, which has proved to be useful in many practical situations, can be run on microcomputers. Full details of a program in BASIC and a test problem are provided. The need to perform all the calculations to a sufficient accuracy is stressed, and the choice of suitable mesh spacings and time steps is discussed.

Introduction

A numerical technique of representing the radial flow towards a pumped well (Rushton and Redshaw, 1979) has proved to be valuable in analysing and interpreting pumping test data. Features that can be included in this approach include well storage, boundary effects, variable saturated depth, leakage, delayed yield, variations in hydraulic conductivity and storage coefficient with depth or radius, and variable abstraction rates. Examples of particular studies include gravel aquifers (Rushton and Booth, 1976), sandstone aquifers with delayed yield (Rushton and Chan, 1977), artesian overflowing boreholes (Rushton and Rathod, 1980), test in which data are only available in the pumped well (Rushton, 1978), long-term tests lasting up to 70 days (Gonzalez and Rushton, 1981), and pumping tests in large-diameter wells (Rushton and Holt, 1981).

The basis of the numerical approach is to solve the time-variant differential equation using a finite difference approach in which the radial dimension is divided into discrete intervals which increase logarithmically from small values near the well to large values towards the boundary. The time dimension is also divided into discrete steps which increase logarithmically. This leads to a set of simultaneous equations for each time step; these equations can be solved using an elimination routine. Details of the technique including a program in FORTRAN can be found in Rushton and Redshaw (1979).

With the increasing availability of inexpensive microcomputer systems, it is advantageous to transfer this program to run on these computers. There are, however, certain limitations of these microcomputers when they are used for complex scientific calculations. The authors have been in correspondence with a number of workers who have attempted to prepare microcomputer programs for this numerical model, and several have encountered major difficulties.

This paper presents a version of the numerical model program written in BASIC. It has been tested thoroughly on a Radio Shack TRS 80 system but, because there are crucial differences between the accuracy of working and operation of the various systems, sufficient information about a typical problem is presented to enable independent checks to be made. Possible difficulties in computation are highlighted, and the importance of small radial mesh spacings and time increments is discussed.

Numerical Model

In this section a brief summary of the formulation of the numerical model is given; full details including a derivation from the differential equation are given by Rushton and Redshaw (1979). The symbols used in this section are chosen to coincide with those used in the BASIC program (Figure 1).

---

[a]Civil Engineering Department, University of Birmingham, P.O. Box 363, Birmingham B15 2TT, United Kingdom.

Received April 1984, accepted May 1984.
Discussion open until March 1, 1985.

```
0010 REM:*******************************************************
0015 REM:   NUMERICAL MODEL FOR RADIAL FLOW TO A WELL          *
0020 REM:                    K.R. RUSHTON.                     *
0025 REM:FOR GIVEN TRIAL PARAMETERS FOR AN AQUIFER,THE MODEL *
0030 REM:CALCULATES DRAWDOWNS IN THE AQUIFER.WITH THESE      *
0035 REM:DRAWDOWNS AND FIELD OBSERVATIONS SUCCESSIVELY BETTER*
0040 REM:ESTIMATES OF THE AQUIFER PARAMETERS CAN BE MADE AND *
0045 REM:SENSITIVITY ANALYSIS CARRIED OUT. VARIOUS FEATURES  *
0050 REM:SUCH AS WELL LOSSES,WELL STORAGE,LEAKAGE ETC. CAN BE*
0055 REM:EASILY INCLUDED IN THE MODEL.                       *
0060 REM:*******************************************************
0065 REM:  ***   THIS VERSION IS CONFIGURED TO SUITE   ***   *
0070 REM:  *** RADIO SHACK TRS-80 MICROCOMPUTER SYSTEM ***   *
0075 REM!!!!!!******!!!!!******!!!!!******!!!!!******!!!!!
0080 REM!!!!   INPUT INITIAL CONDITIONS          ******!!!!!
0085 REM!!!!!******!!!!!******!!!!!******!!!!!******!!!!!
0090 REM:P=PERM,S1=CONFINED STORAGE AND S2=UNCONFINED STORAGE
0095 REM:R1=WELL RADIUS,R9=RADIUS TO OUTER BOUNDARY
0099 DEFINT I,J,K,M,N : DEFDBL A-H,L,O-Z
0100 INPUT "PERM,SCON,SUNC,RW,RMAX";P,S1,S2,R1,R9
0105 LPRINT USING"PERM=###.### CONF-STOR=###.#####";P,S1,
0110 LPRINT USING"  UNCONF-STOR=###.####";S2
0115 LPRINT USING"RWELL=##.####   RMAX=#.###^^^^";R1,R9
0120 REM:LOGARITHMIC MESH. FIVE MESH INTERVALS PER
0125 REM:TENFOLD INCREASE IN RADIAL DISTANCE.
0130 C=1.5848932D00
0135 R3=R1
0140 N1=2
0145 N1=N1+1
0150 R3=R3*C
0155 IF R3<R9  THEN GOTO 0145
0160 REM:DECLARE DIMENSIONS FOR THE VARIABLES.
0165 DIM R(N1),R2(N1),D(N1),D1(N1),S(N1),H(N1),Q(N1)
0170 DIM U(N1),V(N1),O1(4),O2(4)
0175 REM:R=RADIAL DISTANCE, R2=R*R, D=DRAWDOWN
0180 REM:D1=DRAWDOWN FROM PREVIOUS TIME STEP.
0185 REM:S=TIME/STORAGE COEFF. H=EQUIV. HYD. RESISTANCE.
0190 REM:Q1=RECHARGE. U AND V COEFF. USED  IN GAUSSIAN
0195 REM:ELIMINATION ROUTINE. O1 AND O2 LOCATION OF FOUR
0200 REM:OBH'S AND DRAWDOWNS AT THESE BOREHOLES.
0205 REM:CALCULATE RADIAL DISTANCES FOR THE MESH POINTS
0210 R(1)=R1/C
0215 R2(1)=R(1)*R(1)
0220 FOR N=2 TO N1
0225   R(N)=C*R(N-1)
0230   R2(N)=R(N)*R(N)
0235 NEXT N
0240 R(N1)=R9
0245 R2(N1)=R9*R9
0250 N2=N1-1
0255 N3=N2-1
0260 REM: A  IS NATURAL LOG OF THE RATIO OF
0265 REM: TWO SUCCESSIVE RADII.  A2=A*A
0270 A=4.60517D-01
0275 A2=A*A
0280 REM:U1=TOP AND L1=BASE OF AQUIFER;W=WATER LEVEL;Q1=RECH
0285 INPUT "TOP,BASE,IWL,RECH";U1,L1,W,Q1
0290 REM:INITIALIZE ARRAYS
0295 FOR N=1 TO N1
0300   Q(N)=Q1
0305   D(N)=W
0310   D1(N)=W
0315 NEXT N
0320 LPRINT USING"TOP OF AQUIFER= +###.##";U1,
0325 LPRINT USING"  BASE OF AQUIFER= +###.##";L1
0330 LPRINT USING"INITIAL WATER LEVEL= +###.##";W,
0335 LPRINT USING"  RECHARGE= ###.###";Q1
0340 REM: READ 1 FOR RECHARGE BOUNDARY OR 2 FOR IMPERMEABLE.
0345 INPUT "RECHARGE BOUNDARY=1,IMPERMEABLE=2";J1
0350 IF J1=1 THEN LPRINT "*****  RECHARGE BOUNDARY  *****"
0355 IF J1<>1 THEN LPRINT "*****  IMPERMEABLE BOUNDARY  *****"
0360 REM:INPUT NODE NOS. OF FOUR OBSERVATION WELLS.
0365 INPUT "FOUR OBSERVATION NODES";O1(1),O1(2),O1(3),O1(4)
0370 REM:P1=PUMPING RATE, T9=OPERATION TIME FOR THE PHASE
0375 REM: DATA FOR NEXT PUMPING PHASE CAN BE PROVIDED HERE
0380 INPUT "GIVE PUMPING RATE AND DURATION";P1,T9
0385 GOSUB 7000
0390 IF P1<0.0D00 THEN STOP
0395 REM:CONVERT P1 TO P2 FOR USE IN CALCULATIONS
0400 REM: P2=P1/(2*PI*A)
0405 P2=0.125D00*P1/(CDBL(ATN(0.1D01))*A)
0410 GOSUB 8000
0415 REM:T=CURRENT TIME,T9=TIME FOR WHICH PHASE OPERATES
0420 REM:I1=100 FOR THE LAST TIME STEP, OTHERWISE ZERO.
0425 I1=0
0430 T=0.0D00
0435 REM:SET INITIAL TIME STEP SUCH THAT U<1.0 AT WELL FACE.
0440 T0=2.5D-01*R2(2)*S1/(P*(L1-U1))
0445 IF T0>1.0D-06 THEN T0=1.0D-06
1000 REM:
1005 REM!!!!!!******!!!!!******!!!!!******!!!!!******!!!!!
1010 REM!!!!!! CALCULATIONS FOR EACH TIME STEP    ******!!!!!
1015 REM!!!!!******!!!!!******!!!!!******!!!!!******!!!!!
1020 REM:
1025 T=T + T0
1030 IF T<T9 THEN GOTO 2000
1035 REM:TIME STEP JUST BEFORE THE END OF THE PHASE IS REACHED.
1040 REM:LAST TIME STEP FOR THE CURRENT PHASE.
1045 T0=T9-(T-T0)
1050 T=T9
1055 I1=100
```

Fig. 1. Program in BASIC.

```
1060 REM:LOOP K, K2 TIMES FOR CONVERGENCE .
1065 REM:FOR UNCONFINED CONDITION K2 SHOULD EQUAL FOUR BUT
1070 REM:TO ECONOMISE, K2 IS SET TO ONE .
1075 REM:Z = AVERAGE SATURATED THICKNESS FOR A NODE.
2000 K2=1
2005 FOR K=1 TO K2
2010   FOR N=1 TO N2
2015     REM:SELECT APPROPRIATE STORAGE COEFF. DEPENDING
2020     REM:ON WHETHER THE CONDITION IS CONF. OR UNCONF.
2025     Z=L1 - 0.50D00*(D(N)+D(N+1))
2030     S3=S2
2035     IF Z < (L1-U1) THEN GOTO 2050
2040     Z=L1-U1
2045     S3=S1
2050     H(N)=A2/(Z*P)
2055     S(N)=T0/(S3*R2(N))
2060   NEXT N
2065   REM:MODIFY COEFFICIENTS TO TAKE INTO ACCOUNT
2070   REM:WELL STORAGE AND CONDITION NEAR WELL FACE.
2075   H(1)=1.0D-04 * H(1)
2080   S(1)=2.0D00*T0*A/R2(2)
2085   S(2)=2.0D00*S(2)
2090   REM:MODIFY COEFF.S FOR CONDITION ON OUTER BOUNDARY
2095   H(N2)=(LOG(R(N1)/R(N2)))*(LOG(R(N1)/R(N2)))/(Z*P)
2100   H(N1)=1.0D+10
2105   S(N2)=2.0D0*T0*A/((R(N1)-R(N2-1))*S3*R(N2))
2110   S(N1)=2.0D0*T0*A/((R(N1)-R(N2))*S3**R(N1))
2115   REM:LARGE STORAGE ON LAST NODE IF IT IS RECH. BOUNDARY
2120   IF J1=1 THEN S(N1)=1.0D-10 * S(N1)
2125   REM:
3000   REM: GAUSSIAN ELIMINATION
3010   U(1)=1.0D00/H(1) + 1.0D00/S(1)
3015   V(1)=D1(1)/S(1) + P2
3020   FOR N=2 TO N2
3025     U(N)=1.0D0/H(N-1)+1.0D0/H(N)+1.0D0/S(N)
3030     U(N)=U(N)-(1.0D0/H(N-1))*(1.0D0/H(N-1))/U(N-1)
3035     V(N)=D1(N)/S(N)-R2(N)*Q(N)+(1.0D0/H(N-1)*V(N-1))/U(N-1)
3040   NEXT N
3045   V(N2)=D1(N2)/S(N2)-0.5D00*R(N2)*(R(N1)-R(N3))*Q(N2)/A
3046   V(N2)=V(N2)+(V(N3)/H(N3))/U(N3)
3050   U(N1)=1.0D00/H(N2) + 1.0D00/S(N1)
3051   U(N1)=U(N1) - (1.0D00/H(N2))*(1.0D00/H(N2))/U(N2)
3055   V(N1)=D1(N1)/S(N1)-0.5D00*R(N1)*(R(N1)-R(N2))*Q(N1)/A
3056   V(N1)=V(N1)+(V(N2)/H(N2))/U(N2)
3060   REM:
3070   REM:
3075   D(N1)=V(N1)/U(N1)
3080   FOR J=1 TO N2
3085     N=N2-J+1
3090     D(N)=(V(N)+1.0D0/H(N)*D(N+1))/U(N)
3095   NEXT J
3100   REM:IF DRAWDOWN IN THE WELL BELOW THE TOP OF AQUIFER
3105   REM:REACHES MORE THAN 90% OF AQUIFER THICKNESS THEN
3110   REM:THE WELL RUNS DRY AND THE PROGRAM STOPS.
3115   IF D(1)< (9.0D-01*L1 + 1.0D-01*U1) THEN GOTO 3135
3120   LPRINT "*** EXCESSIVE DRAWDOWN ***"
3125   GOSUB 9000
3130   STOP
3135 NEXT K
3500 REM:DRAWDOWNS AT FOUR OBSERVATION BOREHOLES
3505 FOR M=1 TO 4
3510   K1=O1(M)
3515   O2(M)=D(K1)
3520 NEXT M
3525 LPRINT USING"#.###^^^^  ";T,D(2),O2(1),O2(2),O2(3),O2(4),D(N1)
3530 REM:TRANSFER VALUES OF DRAWDOWNS TO OLD DRAWDOWNS.
3535 FOR N=1 TO N1
3540   D1(N)=D(N)
3545 NEXT N
3550 REM:
3555 REM!!!!!******!!!!!******!!!!!******!!!!!******!!!!!
3560 REM!!!!!!***  END OF CALCULATION FOR ONE TIME STEP !!!!!
3565 REM!!!!!******!!!!!******!!!!!******!!!!!******!!!!!
3570 REM:
3575 REM:
4000 REM:CALCULATE NEW TIME STEP
4005 T0=T*0.5848932D00
4010 IF I1=0 THEN GOTO 1025
4015 GOSUB 9000
4020 GOTO 0380
7000 LPRINT
7010 LPRINT USING"PUMPING RATE= #.###^^^^ CU.METRES/DAY ";P1,
7020 LPRINT USING"   FOR  #.###^^^^ DAYS ";T9
7030 RETURN
8000 FOR M=1 TO 4
8010   K1=O1(M)
8020   O2(M)=R(K1)
8030 NEXT M
8040 LPRINT "TIME(DAYS) ";
8050 LPRINT USING"#####.###  ";R(2),O2(1),O2(2),O2(3),O2(4),R(N1)
8060 RETURN
9000 LPRINT
9010 LPRINT "NODE  RADIUS          RADIUS       HORIZ.HYD";
9020 LPRINT "      TIME/STORAGE  DRAWDOWN"
9030 LPRINT " NO                   SQUARED      RESISTANCE     ";
9040 LPRINT "COEFFICIENT"
9050 FOR N=1 TO N1
9060   LPRINT USING"###";N,
9070   LPRINT USING" #.####^^^^   ";R(N),R2(N),H(N),S(N),D1(N)
9080 NEXT N
9090 RETURN
```

Discrete Space Mesh

As water is pumped from a well, the water level in the well falls and the influence within the aquifer is reflected by reductions in the ground-water heads. Consequently, in a pumping test, ground-water heads change with radial distance from the pumped well and with time.

It is convenient to define ground-water heads at a series of radial distances from the pumped well axis. Since rapid changes occur close to the pumped well with slower changes at larger radii, the spacing between the mesh (or nodal) points, where the heads are defined, increases logarithmically.

If the radius of the well is 0.15 m, it is possible to have five mesh intervals between the well face and 1.5 m. Thus the nodal positions are 0.15 m, 0.2377 m, 0.3768 m, 0.5972 m, 0.9464 m, and 1.5 m. Between 1.5 m and 15 m there are a further five intervals, and the same pattern is repeated between 15 m and 150 m, and between 150 m and 1500 m. If the outer boundary is at 2000 m, this is taken as the last nodal point.

In the mesh, each radius is $10^{0.2}$ times the preceding one. This mesh can be generated by statement number 225 of the program

$$R(N) = C*R(N-1)$$

where $C = 10^{0.2}$. In the example to be described in detail later, the final nodal point is N = 23, R = 2000 m. Node N = 1 represents the water within the well and can be used to simulate the well storage.

Discrete Time Steps

Just as drawdowns are calculated at a series of increasing radii from the well, the times at which the drawdowns are calculated also increase logarithmically. A very small time increment, T0, is used initially so that at the well face the standard parameter $u = r^2S/4Tt = 1.0$. In several of the examples quoted in this paper, five time intervals for a tenfold increase in time are used.

Lumping Model

It is helpful to introduce a lumping model which summarizes the numerical technique. Figure 2(a) indicates how the area is divided into a discrete mesh, and three typical nodes N-1, N and N+1 are drawn schematically in Figure 2(b). The radial distances from the pumped well to these nodes are R(N-1), R(N), and R(N+1), respectively.

The resistance to flow caused by the transmissivity of the aquifer is represented by equivalent hydraulic resistances H(N-1) and H(N). These hydraulic resistances can represent both changes in the saturated depth and variations in hydraulic conductivities with saturated depth.

In addition to the horizontal flow of water, another component of the flow balance is the recharge. This can be simulated as a lumped inflow with the quantity at node N depending on the square of the radius.

A further inflow, similar to the recharge, is the water released from storage. During a time step from time T to time T + T0 where T0 is the time increment (usually written as Δt), the drawdown at node N increases from D1(N) to D(N). The quantity of water released from storage depends on the change in head, the area represented by the node, the time increment, and the storage coefficient. Consequently, a time/storage coefficient can be introduced with S(N) = T0/(S3*R2(N)) where R2(N) signifies the square of the radius. S3 is the appropriate storage coefficient, either confined or unconfined. Since the radii can vary from 0.15 to 2000 m in a typical problem, the factor S(N) varies

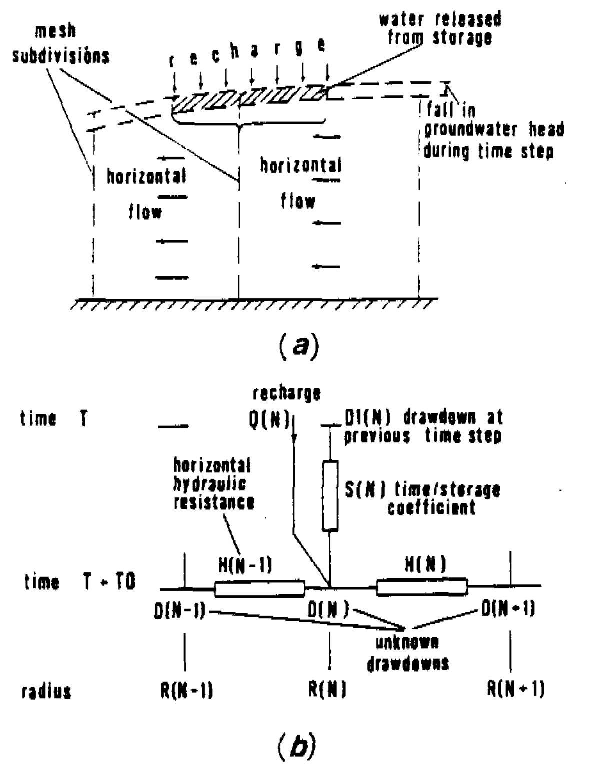

Fig. 2. Derivation of numerical model (a) section showing hydraulic problem with mesh subdivisions and (b) equivalent hydraulic parameters for the discrete model.

Table 1. Main Sections of the Program

Statement numbers	*Section of program*
10- 200	Description of program; input of aquifer dimensions and parameters.
205- 365	Set up radial mesh; specify initial drawdowns and condition on outer boundary. Select observation well positions.
370- 445	Input pumping rate and duration of phase; calculate initial time step.
1000-2125	Calculation for time increment; determine saturated depth and equivalent hydraulic parameters.
3000-3575	Gaussian elimination; stop if drawdown is excessive; output heads at observation wells.
4000-4020	Either perform calculation for another time step or at the end of the phase print full output. Read in data for next phase.
7000-9090	Printing subroutines.

by about eight orders of magnitude. This can lead to computational difficulties.

Further Features

There are many other features that can be represented in the model including well storage, well losses, varying abstraction rates, changes between the confined and unconfined states, leaky aquifer behaviour, delayed yield, and different conditions on the outer boundaries. The inclusion of these features in the numerical model is described by Rushton and Redshaw (1979).

Solution of Equations

Referring to Figure 2(b), the drawdowns D(N-1), D(N), and D(N+1) are unknowns, but the drawdowns D1(N) were calculated at the previous time step. Consequently, when a flow balance is written for node N, there are three unknowns. This is repeated at each nodal point; therefore, a set of simultaneous equations result. These equations can be solved using a simple elimination routine.

The only drawback of this elimination routine is that errors can occur if the arithmetic is not carried out to a sufficient accuracy. Consequently, double precision arithmetic is used which, for this particular computer, means that variables are handled in the computer to accuracy of 16 significant figures, whereas single precision only uses 6 significant figures.

Computer Program

Detailed comments and explanations are made within the program listing (Figure 1). However, Table 1 has been prepared to identify the main sections of the program. The accuracy of the program will be discussed later.

Particular Example

When ascertaining whether a program is correct, it is helpful to have an example against which checks can be made. This section describes an example which tests most aspects of the program. Figure 3 sketches the problem.

An aquifer, which is initially confined, has a well of 0.15 m radius and extends to an outer recharge boundary at 2000 m. The initial position of the ground-water head is chosen as datum, and all depths and drawdowns are measured vertically downwards. Thus, the confining layer is at 2 m below the initial ground-water head, and the base of the aquifer is at 12 m. The hydraulic conductivity is 65 m/d giving an initial transmissivity of 650 m^2/d. Due to an abstraction rate of 2500 m^3/d, the ground-water heads fall, and the region in the vicinity of the well becomes unconfined with the storage coefficients changing from confined values of 0.0001 to the specific yield of 0.01.

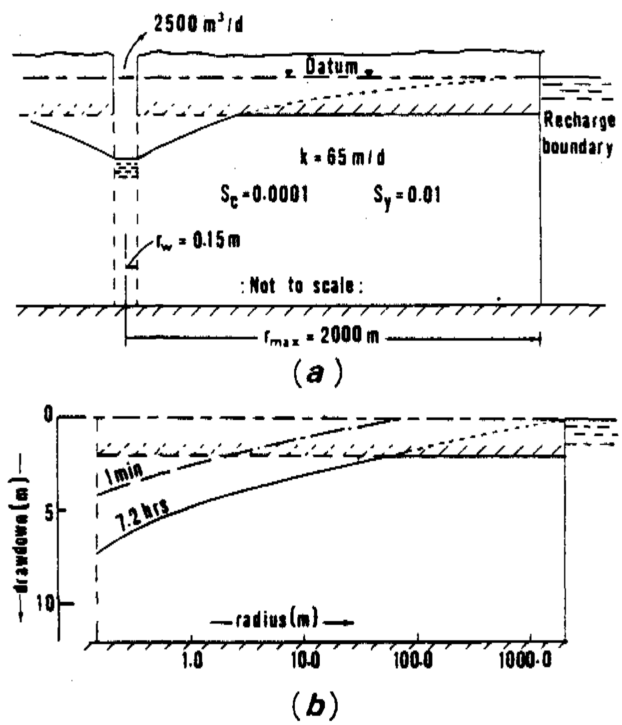

Fig. 3. Typical problem (a) with change from confined to unconfined conditions and (b) drawdown results for 1 min and 7.2 hours plotted against logarithm of radius.

Table 2. Input Data for Computer Program

```
6.50D01,0.10D-03,0.10D-01,1.5D-01,2.0D04
2.0D00,1.2D01,0.0D00,0.0D00
1
7,12,17,22
2.50D03,3.0D-01
0.00D00,1.0D00
-1.0D00,2.0D00
```

Input data to the program is listed in Table 2, and this is repeated as the first seven lines of the output in Table 3. Referring to Table 2, the third and fourth numbers of line two indicate that the initial drawdown is zero and that there is no recharge. The third line records that there is a constant head on the outer boundary which will provide a varying recharge depending on conditions within the aquifer. An impermeable boundary is indicated by J1=2. The abstraction rate of 2500 m^3/d for 0.3 days is followed by a recovery phase of 1.0 day; this is indicated by lines five and six. The last line with negative abstraction rate signifies the end of the calculations. Full details of the drawdown variation with time are provided at nodes 7, 12, 17, and 22 which correspond to the radial distances of 1.5 m, 15 m, 150 m, and 1500 m from the pumped well.

A complete output of the first phase is presented as Table 3. The first part of the printout records the input data; the main section records time-drawdown data at the well, four observation wells, and the outer boundary. At the end of the printout is a detailed record of the coefficients used in the calculation for the final time step. Certain important features should be noted.

a. As the drawdown in the well exceeds 2.0 m after a time of 0.865×10^{-4} day, the storage coefficient at that node changes from 10^{-4} to 10^{-2}.

b. After a time of 0.3 day, the unconfined region spreads beyond 37.68 m (see the section at the bottom of Figure 3). This is reflected by a discontinuity in the values of the time/storage coefficient.

c. A consequence of the aquifer becoming unconfined is that the saturated depth *decreases*. This results in *increases* in the horizontal hydraulic resistances for nodes 2 to 14. The nonstandard values at nodes 22 and 23 occur because of the modification of the mesh intervals at the boundary.

d. At the outer boundary the condition is zero drawdown. The drawdown according to the computer program is 0.146×10^{-9} which, compared to a drawdown of 0.0967 m at the next node into the aquifer, is effectively zero.

e. As indicated in the sketch of Figure 3, the well-water level coincides with the level within the aquifer; therefore, the seepage face is ignored. However, the effect of the seepage face could be included by increasing the horizontal hydraulic resistance between nodes 2 and 3 by a factor of about five. This can be achieved by including an extra statement in the program

```
2077     H(2) = 5.0D00*H(2)
```

Table 3. Part of Output from the Program Using Data of Table 2

```
PERM= 65.000 CONF-STOR= 0.00010 UNCONF-STOR= 0.0100
RWELL= 0.1500   RMAX=0.2000D+04
TOP OF AQUIFER=   +2.00  BASE OF AQUIFER=  +12.00
INITIAL WATER LEVEL=   +0.00  RECHARGE=   0.000
*****  RECHARGE BOUNDARY  *****

PUMPING RATE= 0.2500D+04 CU.METRES/DAY    FOR  0.300D+00 DAYS
```

TIME(DAYS)	0.150	1.500	15.000	150.000	1500.000	2000.000
0.365D-09	0.306D-04	0.220D-10	0.492D-26	0.000D+00	0.000D+00	0.000D+00
0.137D-08	0.485D-04	0.510D-10	0.118D-25	0.000D+00	0.000D+00	0.000D+00
0.217D-08	0.769D-04	0.215D-09	0.338D-25	0.000D+00	0.000D+00	0.000D+00
0.345D-08	0.122D-03	0.144D-08	0.300D-23	0.000D+00	0.000D+00	0.000D+00
0.546D-08	0.193D-03	0.108D-07	0.202D-21	0.000D+00	0.000D+00	0.000D+00
0.865D-08	0.306D-03	0.753D-07	0.139D-19	0.000D+00	0.000D+00	0.000D+00
0.137D-07	0.485D-03	0.457D-06	0.842D-18	0.000D+00	0.000D+00	0.000D+00
0.217D-07	0.768D-03	0.235D-05	0.431D-16	0.708D-37	0.000D+00	0.000D+00
0.345D-07	0.122D-02	0.102D-04	0.183D-14	0.295D-34	0.000D+00	0.000D+00
0.546D-07	0.193D-02	0.371D-04	0.635D-13	0.103D-31	0.000D+00	0.000D+00
0.865D-07	0.305D-02	0.116D-03	0.179D-11	0.294D-29	0.000D+00	0.000D+00
0.137D-06	0.484D-02	0.316D-03	0.411D-10	0.678D-27	0.000D+00	0.000D+00
0.217D-06	0.766D-02	0.766D-03	0.758D-09	0.127D-24	0.000D+00	0.000D+00
0.345D-06	0.121D-01	0.170D-02	0.113D-07	0.190D-22	0.000D+00	0.000D+00
0.546D-06	0.192D-01	0.351D-02	0.134D-06	0.229D-20	0.000D+00	0.000D+00
0.865D-06	0.303D-01	0.686D-02	0.128D-05	0.222D-18	0.000D+00	0.000D+00
0.137D-05	0.477D-01	0.129D-01	0.983D-05	0.171D-16	0.000D+00	0.000D+00
0.217D-05	0.750D-01	0.233D-01	0.607D-04	0.106D-14	0.221D-35	0.000D+00
0.345D-05	0.117D+00	0.411D-01	0.304D-03	0.519D-13	0.109D-32	0.000D+00
0.546D-05	0.183D+00	0.705D-01	0.124D-02	0.203D-11	0.429D-30	0.000D+00
0.865D-05	0.283D+00	0.118D+00	0.424D-02	0.627D-10	0.134D-27	0.000D+00
0.137D-04	0.431D+00	0.194D+00	0.122D-01	0.153D-08	0.330D-25	0.000D+00
0.217D-04	0.647D+00	0.309D+00	0.305D-01	0.294D-07	0.642D-23	0.375D-36
0.345D-04	0.946D+00	0.477D+00	0.672D-01	0.443D-06	0.980D-21	0.905D-34
0.546D-04	0.134D+01	0.709D+00	0.133D+00	0.518D-05	0.116D-18	0.171D-31
0.865D-04	0.182D+01	0.100D+01	0.236D+00	0.469D-04	0.107D-16	0.249D-29
0.137D-03	0.234D+01	0.134D+01	0.381D+00	0.325D-03	0.756D-15	0.279D-27
0.217D-03	0.284D+01	0.168D+01	0.558D+00	0.172D-02	0.407D-13	0.239D-25
0.345D-03	0.328D+01	0.198D+01	0.745D+00	0.694D-02	0.166D-11	0.155D-23
0.546D-03	0.364D+01	0.223D+01	0.928D+00	0.216D-01	0.512D-10	0.762D-22
0.865D-03	0.394D+01	0.243D+01	0.110D+01	0.533D-01	0.120D-08	0.286D-20
0.137D-02	0.418D+01	0.260D+01	0.125D+01	0.107D+00	0.215D-07	0.821D-19
0.217D-02	0.442D+01	0.280D+01	0.141D+01	0.185D+00	0.299D-06	0.152D-17
0.345D-02	0.463D+01	0.296D+01	0.156D+01	0.281D+00	0.320D-05	0.313D-16
0.546D-02	0.485D+01	0.314D+01	0.171D+01	0.393D+00	0.265D-04	0.413D-15
0.865D-02	0.505D+01	0.329D+01	0.184D+01	0.512D+00	0.170D-03	0.435D-14
0.137D-01	0.527D+01	0.347D+01	0.200D+01	0.641D+00	0.846D-03	0.353D-13
0.217D-01	0.548D+01	0.363D+01	0.212D+01	0.770D+00	0.325D-02	0.224D-12
0.345D-01	0.570D+01	0.381D+01	0.228D+01	0.906D+00	0.971D-02	0.112D-11
0.546D-01	0.592D+01	0.397D+01	0.240D+01	0.104D+01	0.227D-01	0.443D-11
0.865D-01	0.615D+01	0.415D+01	0.256D+01	0.117D+01	0.426D-01	0.143D-10
0.137D+00	0.637D+01	0.431D+01	0.268D+01	0.129D+01	0.655D-01	0.382D-10
0.217D+00	0.658D+01	0.446D+01	0.280D+01	0.139D+01	0.857D-01	0.880D-10
0.300D+00	0.672D+01	0.455D+01	0.287D+01	0.144D+01	0.967D-01	0.146D-09

NODE NO	RADIUS	RADIUS SQUARED	HORIZ.HYD RESISTANCE	TIME/STORAGE COEFFICIENT	DRAWDOWN
1	0.9464D-01	0.8957D-02	0.6015D-07	0.3362D+01	0.6724D+01
2	0.1500D+00	0.2250D-01	0.5760D-03	0.7344D+03	0.6724D+01
3	0.2377D+00	0.5652D-01	0.5324D-03	0.1462D+03	0.6225D+01
4	0.3768D+00	0.1420D+00	0.4973D-03	0.5820D+02	0.5766D+01
5	0.5972D+00	0.3566D+00	0.4683D-03	0.2317D+02	0.5337D+01
6	0.9464D+00	0.8957D+00	0.4437D-03	0.9224D+01	0.4932D+01
7	0.1500D+01	0.2250D+01	0.4227D-03	0.3672D+01	0.4549D+01
8	0.2377D+01	0.5652D+01	0.4043D-03	0.1462D+01	0.4184D+01
9	0.3768D+01	0.1420D+02	0.3881D-03	0.5820D+00	0.3834D+01
10	0.5972D+01	0.3566D+02	0.3737D-03	0.2317D+00	0.3499D+01
11	0.9464D+01	0.8957D+02	0.3608D-03	0.9224D-01	0.3177D+01
12	0.1500D+02	0.2250D+03	0.3492D-03	0.3672D-01	0.2865D+01
13	0.2377D+02	0.5652D+03	0.3387D-03	0.1462D-01	0.2565D+01
14	0.3768D+02	0.1420D+04	0.3291D-03	0.5820D-02	0.2274D+01
15	0.5972D+02	0.3566D+04	0.3263D-03	0.2317D+00	0.1995D+01
16	0.9464D+02	0.8957D+04	0.3263D-03	0.9224D-01	0.1718D+01
17	0.1500D+03	0.2250D+05	0.3263D-03	0.3672D-01	0.1442D+01
18	0.2377D+03	0.5652D+05	0.3263D-03	0.1462D-01	0.1166D+01
19	0.3768D+03	0.1420D+06	0.3263D-03	0.5820D-02	0.8906D+00
20	0.5972D+03	0.3566D+06	0.3263D-03	0.2317D-02	0.6182D+00
21	0.9464D+03	0.8957D+06	0.3263D-03	0.9224D-03	0.3517D+00
22	0.1500D+04	0.2250D+07	0.1273D-03	0.4815D-03	0.9666D-01
23	0.2000D+04	0.4000D+07	0.1000D+11	0.7610D-13	0.1458D-09

Accuracy

As with all numerical solutions, errors do arise and it is not always clear whether the errors are acceptable. Errors can arise because the numerical method is unreliable, because the size of the mesh intervals or time steps is too large, or because of limitations due to the computer.

Microcomputer Errors

Microcomputers do not usually have the same arithmetic accuracy as large computer systems. For instance, the accuracy of the TRS 80 on single and double precision is illustrated by the numbers 1.123456 and 1.123456789012345. However, the accuracy to which arithmetic is performed can vary from one computer to another. In most microcomputers the arithmetic is performed by software, and information is not usually available about the accuracy of the software arithmetic. In particular, it is advisable to avoid the routine which raises a variable to a power.

Certain problems were solved using single and double precision. For some of the problems there was little difference between single and double precision but for other problems, single precision produced drawdowns which were only one-third of those for double precision. Such errors could be anticipated when note is taken of the wide range of magnitudes of the time/storage coefficients of Table 3.

Theis Solution

The exact Theis solution is a good check on the accuracy of the computer simulation. By taking a small well radius of, say 0.0001 m, and a large outer radius of 100 km and ensuring that confined conditions apply, the assumptions of the Theis solution can be met in the numerical model. Comparisons can then be made with the analytical results. Particular attention should be paid to the earlier times when the Jacob approximation is not valid. Errors in W(u) should all be less than 0.1 when there are five mesh intervals for a tenfold increase in radius and five time steps for a tenfold increase in time. In practical problems the number of mesh and time intervals can be crucial.

Mesh and Time Intervals

Certain workers using this numerical model for pumping test analysis have obtained inadequate results because they have used radial increments or time increments that are too large. The increments used in the program presented here are the maximum acceptable. For certain problems such as large-diameter wells, significant decreases in saturated depth, leaky aquifers, and delayed yield, particular care needs to be taken.

Table 4. Selected Results for a Leaky Aquifer, Transmissivity 650 m^2/d, Storage Coefficient 10^{-4}, Well Radius 0.15 m, Leakage Coefficient 60 m, Abstraction Rate 2500 m^3/d

No. of mesh intervals per decade	20	5	2.5
No. of time steps per decade	20	5	2.5
Time (days)	*Drawdown (m) at 15 m from pumped well*		
8.65×10^{-5}	0.2317	0.2296	0.2275
5.46×10^{-4}	0.8231	0.8166	0.8188
1.37×10^{-3}	0.9326	0.9407	0.9609*
3.44×10^{-3}	0.9438	0.9457*	0.9307*
8.65×10^{-3}	0.9438	0.9435*	0.9436*
5.46×10^{-2}	0.9444*	0.7256*	1.664*
1.37×10^{-1}	1.698*	0.5255*	0.5211*

* Values exhibiting instabilities.

Table 4 contains results for a leaky aquifer solution with a variety of mesh and time intervals. Before the steady drawdown of 0.9438 is reached adequate results were obtained, but when there are only 2.5 intervals per decade in time and space, instabilities occur quickly. Even with 20 intervals per decade in time and space, instabilities eventually arise. These instabilities occur because of the sensitive balance between the water leaking through the overlying strata and the abstraction.

For delayed yield problems a response similar to that of a leaky aquifer occurs with the drawdown increasing only slightly with time. Using the approach suggested by Rushton and Redshaw (1979) for the inclusion of delayed yield, adequate results can be obtained provided that five mesh intervals and five time increments are used for each tenfold increase in radius and time.

To summarize the requirements for adequate accuracy, the computer program should use double precision throughout, even for constants such as 1.0. The minimum number of intervals for a tenfold increase in both space and time should be five. Only three statements need to be changed to modify the size of intervals.

1. If n is the number of mesh intervals per tenfold increase in radius

Statement 130 $\quad C = 10^{(1/n)}$

Statement 270 $\quad A = \ell n(10)/n$

2. If there are t time intervals per tenfold

increase in time, the factor in statement 4005 is modified to $10^{(1/t)} - 1.0$.

Conclusions

Provided that sufficient care is taken, it is possible to carry out a pumping test analysis using numerical methods on microcomputers. It is essential, however, to check the program thoroughly since the accuracy of computation varies for different microcomputer systems. A typical problem which is designed to test the accuracy of the computation is presented.

Details are presented in the references listed at the end of this paper. The use of this numerical model is both for the analysis of pumping tests which are difficult to interpret using conventional methods, and for the prediction of the likely response due to extensive pumping from an aquifer.

References

Gonzalez, Maria del Mar and K. R. Rushton. 1981. Deviations from classical behaviour in pumping test analysis. Ground Water. v. 19, no. 5, pp. 510-516.

Rushton, K. R. 1978. Estimating transmissivity and storage coefficient from abstraction well data. Ground Water. v. 16, pp. 81-85.

Rushton, K. R. and S. J. Booth. 1976. Pumping test analysis using a discrete time-discrete space numerical method. Journal of Hydrology. v. 28, pp. 13-27.

Rushton, K. R. and Y. K. Chan. 1977. Numerical pumping test analysis in unconfined aquifers. ASCE, no. IR1, pp. 1-12.

Rushton, K. R. and S. M. Holt. 1981. Estimating aquifer parameters for large-diameter wells. Ground Water. v. 19, pp. 505-509.

Rushton, K. R. and K. S. Rathod. 1980. Overflow tests analysed by theoretical and numerical methods. Ground Water. v. 18, pp. 61-69.

Rushton, K. R. and S. C. Redshaw. 1979. Seepage and Groundwater Flow. Wiley, Chichester. 332 pp.

* * * * *

K. S. Rathod received his B.E. (Civil) degree from the M.S. University, Baroda, India, and his M.Sc. degree from the Strathclyde University, Glasgow. He is currently involved in ground-water modeling work at the University of Birmingham, England.

K. R. Rushton is Professor of Civil Engineering at the University of Birmingham. He has been involved in developing both analogue and digital modeling techniques in ground-water flow.

FIELD REPORTS

COMPUTING DRAWDOWN DISTRIBUTIONS USING MICROCOMPUTERS

by James M. King[a]

Abstract. Using known or estimated values of transmissivity and storativity, the distribution of drawdowns at any time within a discretized flow field can be generated by applying simple trigonometry and numerical approximations of the exponential integral to the Theis equation. Single- and multiple-well systems, as well as image boundaries, are readily simulated with this method. A program employing this technique is presented in BASIC for use with microcomputers. The availability, low cost, and computational power of many small computers makes them ideal for this type of application. Their user-oriented features allow many possible combinations of wells, boundaries, and hydraulic properties to be analyzed in a short time.

Introduction

Microcomputers are rapidly filling the void between programmable hand-held calculators and main-frame systems for many hydrologic applications. Attractive features of these small computers are their remarkable computational power, their use of the BASIC language which facilitates interactive programming, and instant screen graphics. In terms of hydrologic studies, these features cooperate to allow a large number of analyses to be made in a short time.

This paper describes an interactive BASIC program with a great deal of utility for examining pumping and boundary effects in studies which do not warrant a more complex numerical model. The program uses known or estimated aquifer parameters to compute the drawdown at every point in a grid representing the area of influence in a confined aquifer. It determines the drawdown distribution resulting from a single well or the combined effects of several interfering wells and is capable of simulating moderately complex combinations of recharge and discharge boundaries using image-well theory. The version of the code listed in the Appendix is efficient, has minimal memory requirements, and is fully compatible with TRS-80 Model III and Model 4 microcomputers. It is useable with many other small computers in its present form or can be made so with only slight modifications.

Computational Scheme

The model algorithm is based on the non-equilibrium equation of Theis (1935) for radial flow to and from wells that fully penetrate homogeneous and isotropic confined aquifers:

$$s = \frac{114.59\,Q}{T} W(u) \qquad (1)$$

where s is the drawdown in the potentiometric surface (ft), Q is the constant rate of well discharge (gpm), and T is the aquifer transmissivity (gpd/ft). A negative Q may be used in (1) for recharging wells. W(u) is the exponential integral, the argument of which is given by

$$u = \frac{1.87\,r^2 S}{Tt} \qquad (2)$$

where r is the radial distance from the pumping well to a point at which drawdown is measured (ft), S is the aquifer storativity, and t is the pumping time (days). There are other forms of (1) and (2) for use with different units of length, volume, and time (see, for example, Freeze and Cherry, 1979, p. 344). The above forms were chosen because of their compatibility with practical field units, but the program can be easily modified to accommodate any set of units.

[a]Staff Hydrogeologist, GAI Consultants, Inc., 570 Beatty Rd., Monroeville, Pennsylvania 15146.

Received August 1983, revised June 1984, accepted July 1984.

Discussion open until May 1, 1985.

Examples of applications using (1) and (2) are abundant in the literature and are found in most ground-water hydrology texts.

The solution method requires discretizing the area of influence into a mesh-centered grid with either a uniform or variable node spacing. All wells and observation points are located at the grid nodes, and the ability to use nonuniform node spacings permits more flexibility in locating wells and boundaries. This feature also allows the nodal density to be increased or decreased in parts of the discretized area where differing degrees of resolution are desired.

The algorithm first determines the argument u for a given node using (2) in line 350 (see Appendix). To do this, the radius from the pumping well to the node is computed using the Pythagorean theorem (line 330). When the computational process reaches the node at which the pumping well is located, the well radius is used. W(u) is then calculated numerically (lines 1800 to 1870) using polynomial approximations which are given in Gautschi and Cahill (1964) in algebraic form. These approximations are also presented in Huntoon (1980). The determination of W(u) is expedited for long pumping times and/or small radii by invoking the approximation of Cooper and Jacob (1946), plus an additional term of the infinite series for $u \leq 0.01$ (lines 1820 and 1830). The computed W(u) value is then used in (1) to compute the drawdown at the node (line 370). The algorithm is applied successively until the drawdown is computed at each node in the grid.

For multiple wells, including image wells, a separate solution is computed for each well and superposed at every node to simulate additive interference effects. The total drawdown at each node is thus given by

$$s_{i,j,n} = \frac{114.59}{T} \sum_{m=1}^{n} Q_m W(u)_{i,j,m} \qquad (3)$$

where $s_{i,j,n}$ is the drawdown at the node in row i and column j of the grid due to n wells, and m is the well index. The pumping rate Q is well-specific, and the value of W(u) is dependent on the location of each node with respect to each well.

The polynomial approximations of W(u) used in the program are efficient and accumulate less roundoff error than methods which compute successive terms of the infinite series within the exponential integral. The series methods (see, for example, Picking, 1979; Dumble and Cullen, 1983) are theoretically capable of unlimited precision but are burdened with a large number of multiplications and divisions which are the slowest arithmetic operations in most computers. The approximations used here owe their efficiency to their nested-multiplication form which requires fewer multiplications and divisions. Even so, the calculation of W(u) is the slowest part of the algorithm.

Table 1. Comparison of Published and Computed Values of W(u)

u	*Publ. W(u)**	*Computed W(u)*
6.13757×10^{-10}	20.6342	20.63421
3.12209×10^{-7}	14.4025	14.40238
8.83810×10^{-4}	6.4549	6.454937
5.79278×10^{-2}	2.3285	2.328442
3.59957×10^{-1}	7.746×10^{-1}	7.745455×10^{-1}
2.87965	1.524×10^{-2}	1.521546×10^{-2}

* Interpolated from Ferris and others (1962).

The approximating routine for W(u) was tested over a wide range of function arguments by comparing computed values with corresponding interpolated values from Ferris and others (1962, p. 96). Table 1 shows that the model approximations compare quite favorably and fall well within the range of accuracy needed for most hydrologic applications.

Example Application of the Program

The input and units required by the program are listed in Table 2 in order of entry. The grid dimensions, node spacings, hydraulic parameters, and well information are specified by the user in response to prompts by the program. Row and column spacings are entered beginning at the upper left corner of the grid. As written, the code permits up to 20 wells and a primary matrix of up to 25 rows and columns (line 40). The dimensions of the main matrix may be increased or reduced according to the problem size and amount of available memory. The output is a matrix composed of drawdowns at all nodes within the discretized region and may be used to generate contour maps.

Table 2. Required Program Inputs in Order of Their Entry

Data, units	
1. Title	6. Duration of pumping, days
2. Grid dimensions	7. Number of wells
3. Node spacings, ft	8. Well coordinates
4. Storativity	9. Pumping rates, gpm
5. Transmissivity, gpd/ft	10. Well radii, ft

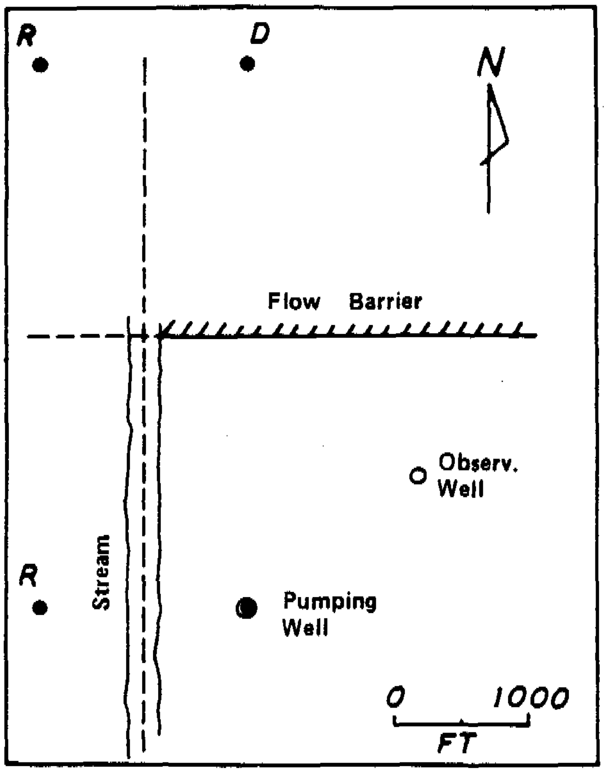

Fig. 1. Test scheme for the program. Solid circles are image wells; R = recharge wells, D = pumping wells.

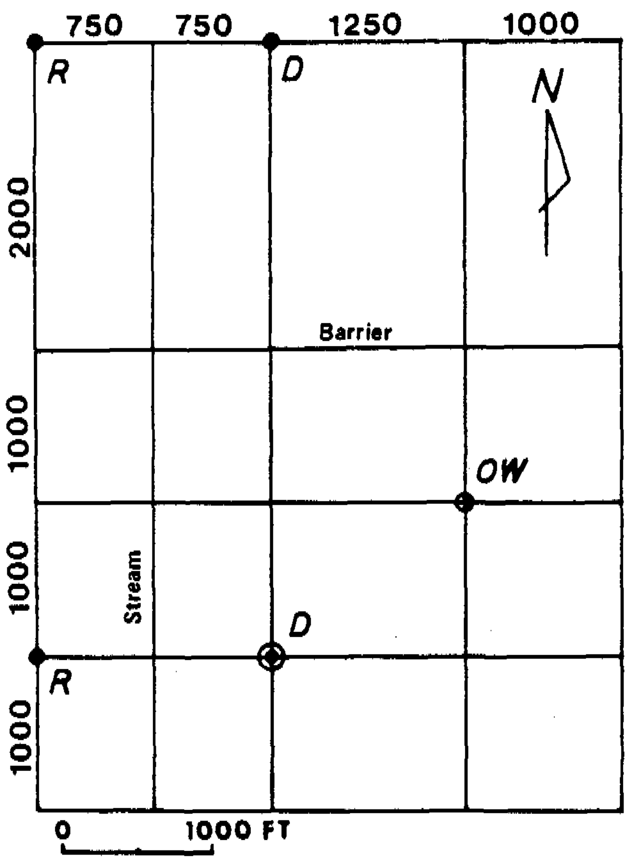

Fig. 2. Variable grid representing Figure 1. Numbers at the top and left are the grid spacings. OW = observ. well.

To demonstrate simultaneously the simulation of multiple-well systems and the treatment of boundaries, a hypothetical test situation is presented in Figure 1. The test scheme consists of a 12-inch diameter well discharging for 0.5 days at 250 gpm from a confined aquifer with a storativity of 2.5×10^{-4} and a transmissivity of 7.8×10^{4} gpd/ft. Two mutually perpendicular boundaries are located within the area of influence—a flow barrier 2,000 ft north of the test well and a fully penetrating stream 750 ft to the west.

The problem area is represented by the variable 5×5 grid in Figure 2 with the grid spacings as shown. Each boundary is represented by a grid line so that drawdowns at the boundaries are computed. Three image wells at nodes (1,1), (1,3), and (4,1) are used to simulate the effects of the boundaries. The discharge well is at node (4,3). Note that the number of nodes outside the problem domain is minimized by extending the grid only to the image wells and by using a single large row spacing north of the flow barrier.

The test scheme yields a manually computed Theis drawdown of 0.56 ft at the observation well 1,600 ft northeast of the pumping site. Simulating the same scheme using the grid in Figure 2 and the program results in an identical drawdown at the observation point (OW) and also provides the drawdowns at all other nodes south and east of the boundary intersection. The determination of the areal distribution of drawdown allowed the map in Figure 3 to be constructed. Map preparation may be facilitated by coupling the program to a plotting routine.

Figure 4 is the model output for the above example problem from which Figure 3 was constructed. Drawdowns at nodes corresponding to wells and boundaries may be noted by comparing Figures 4 and 2. Note that the drawdown along the recharge boundary in column 2 is zero. The output statements in the program may be modified to route the results to a printer for more flexibility in formatting. Some tab statements (e.g., line 210) may also require modification for monitor screens with 80 columns (the code is based on a monitor width of 64 columns).

Closing Remarks

If appropriate aquifer conditions exist and boundaries are adequately representable with image wells, the program presented here permits the entire drawdown distribution due to pumping to be reproduced or predicted. Many possible combinations of conditions can be examined in a

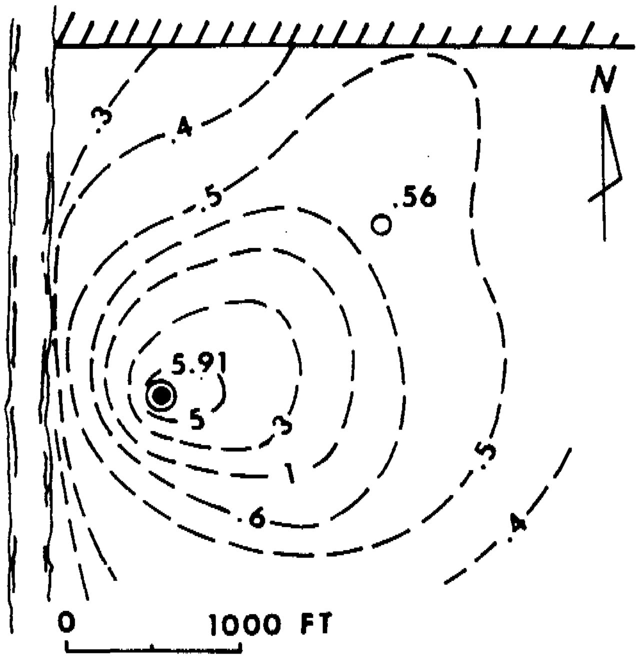

Fig. 3. Contour map of the drawdown distribution for the example problem. Contours are in feet.

```
PROJECT: EXAMPLE PROBLEM

   DATE: 11 JUNE 84


          STORATIVITY = 2.5E-04

       TRANSMISSIVITY = 78000

         NO. OF WELLS = 4


TOTAL DRAWDOWN AFTER  .5 DAYS

1  -5.91   0.00   5.91   0.64   0.43

2  -0.31   0.00   0.31   0.49   0.43

3  -0.50   0.00   0.50   0.56   0.44

4  -5.91   0.00   5.91   0.64   0.43

5  -0.45   0.00   0.45   0.47   0.36
```

Fig. 4. Output from the example problem.

short time since the code allows the number and locations of wells and boundaries and the hydraulic properties of the aquifer to be varied easily. The availability, low cost, and computational capabilities of microcomputers makes them well suited for this type of application and the rapid performance of multiple simulations is enhanced by interactive BASIC programming.

Regarding practical applications, the program has been used to define optimal well spacings for multiple-well dewatering schemes and to delineate the drawdown distributions of pumping centers under varying boundary conditions. Using other simple numerical techniques and function approximations, the program can be modified to generate drawdown distributions in leaky and unconfined aquifers.

References Cited

Cooper, H. H., and C. E. Jacob. 1946. A generalized graphical method for evaluating formation constants and summarizing well field history. Amer. Geophys. Union Trans. v. 27, pp. 526-534.

Dumble, J. P., and K. T. Cullen. 1983. The application of a microcomputer in the analysis of pumping test data in confined aquifers. Ground Water. v. 21, pp. 79-83.

Ferris, J. G., D. B. Knowles, R. H. Brown, and R. W. Stallman. 1962. Theory of Aquifer Tests. U.S.G.S. Water-Supply Paper 1536-E.

Freeze, R. A., and J. A. Cherry. 1979. Groundwater. Prentice-Hall, Englewood Cliffs, New Jersey.

Gautschi, W., and W. F. Cahill. 1964. Exponential integral and related functions. In Abramowitz, M., and I. A. Stegun, eds., Handbook of Mathematical Functions with Formulas, Graphs, and Mathematical Tables. U.S. Dept. of Commerce, National Bureau of Standards Applied Math. Series 55. pp. 227-251.

Huntoon, P. W. 1980. Computationally efficient polynomial approximations used to program the Theis equation. Ground Water. v. 18, pp. 134-136.

Picking, L. W. 1979. Programming a pocket calculator for solving multiple well, variable pumping rate problems. Ground Water. v. 17, pp. 205-208.

Theis, C. V. 1935. The relationship between lowering of the piezometric surface and the rate and duration of discharge of a well using ground-water storage. Amer. Geophys. Union Trans. v. 16, pp. 519-524.

• • • • •

James M. King earned an M.S. degree in Hydrogeology from the University of Toledo in 1977, and completed a Ph.D. in Hydrogeology at Indiana University in 1983. He has been employed with a State agency regulating waste disposal, and is now a Hydrogeologist with GAI Consultants specializing in waste disposal problems, mine hydrology, the numerical modeling of ground-water systems, and computer applications.

```
10 REM DRAWDOWN DISTRIBUTION PROGRAM
20 REM By James M. King
30 REM
40 DIM A(25,25),Z(4,20),RQ(24),CQ(24): DE
FINT I,J,L,N
50 CLS: INPUT "ENTER THE TITLE OF THE SIM
ULATION";A$: PRINT
60 INPUT "ENTER THE CURRENT DATE (NO COMM
AS)";DAT$: PRINT
70 INPUT "ENTER THE NUMBER OF ROWS IN THE
 GRID";R: PRINT
80 INPUT "ENTER THE NUMBER OF COLUMNS";CL
: PRINT
90 PRINT "ENTER EACH ROW SPACING (FT):"
100 FOR I=1 TO R-1: INPUT RQ(I): NEXT I:
PRINT
110 PRINT "ENTER EACH COLUMN SPACING (FT)
:"
120 FOR I=1 TO CL-1: INPUT CQ(I): NEXT I:
 PRINT
130 INPUT "ENTER THE STORATIVITY & TRANSM
ISSIVITY (GPD/FT) (S,T)";S,T: PRINT
140 PRINT "ENTER THE LENGTH OF THE PUMPIN
G PERIOD (DAYS) AND THE NUMBER OF"
150 INPUT "WELLS (TIME,NO.)";TM,NW: PRINT
160 PRINT "ENTER THE GRID COORDINATES, PU
MPING RATES (GPM), AND RADIUS": PRINT "(F
T) OF EACH WELL (R,C,Q,RAD):"
170 FOR C=1 TO NW
180 INPUT Z(1,C),Z(2,C),Z(3,C),Z(4,C): NE
XT C
190 ST=1.87*S/(TM*T): TQ=114.59/T
200 CLS: PRINT: PRINT: PRINT: PRINT
210 PRINT TAB(16) "*-*-* COMPUTATIONS IN
PROGRESS *-*-*"
220 FOR C=1 TO NW
230 FOR I=1 TO R: DR=0
240 IF I=Z(1,C) THEN 280
250 IF I < Z(1,C) THEN Q1=Z(1,C)-1: MI=I:
 GOTO 270
260 MI=Z(1,C): Q1=I-1
270 FOR L=MI TO Q1: DR=DR+RQ(L): NEXT L
280 FOR J=1 TO CL: DC=0
290 IF J=Z(2,C) THEN 330
300 IF J < Z(2,C) THEN Q2=Z(2,C)-1: NI=J:
 GOTO 320
310 NI=Z(2,C): Q2=J-1
320 FOR L=NI TO Q2: DC=DC+CQ(L): NEXT L
330 RD=SQR(DR[2+DC[2)
340 IF RD=0 THEN RD=Z(4,C)
350 U=ST*RD[2
360 GOSUB 1810
370 DD=TQ*Z(3,C)*WU
380 A(I,J)=A(I,J)+DD: NEXT J: NEXT I: NEX
T C
390 REM --- PRINT ROUTINE ---
400 CLS: PRINT "PROJECT: ";A$: PRINT "
DATE: ";DAT$: PRINT
410 PRINT TAB(10) "STORATIVITY =";S
420 PRINT TAB(7) "TRANSMISSIVITY =";T
430 PRINT TAB(9) "NO. OF WELLS =";NW: PRI
NT: PRINT
440 PRINT "PRESS ANY KEY TO CONTINUE . .
."
450 D$=INKEY$: IF D$="" GOTO 450 ELSE CLS
460 PRINT "TOTAL DRAWDOWN AFTER ";TM;"DAY
S"
470 FOR I=1 TO R
480 PRINT: PRINT USING "##";I;
490 FOR J=1 TO CL
500 PRINT TAB(J*8-8) USING "####.##";A(I,
J);
510 NEXT J: PRINT: NEXT I
520 PRINT: PRINT "ANOTHER SIMULATION WITH
 THE SAME T & S? (Y/N):"
525 FOR I=1 TO R: FOR J=1 TO CL: A(I,J)=0
: NEXT J: NEXT I
530 D$=INKEY$: IF D$="" GOTO 530
540 CLS: IF D$="Y" THEN 140
550 PRINT "RUN TERMINATED."
560 END
1800 REM --- COMPUTE EXPONENTIAL INTEGRAL
 ---
1810 IF U > 10 OR U < 0 THEN WU=0: RETURN
1820 TY=-.5772156649-LOG(U)+U*.99999193
1830 IF U <= .01 THEN WU=TY: RETURN
1850 IF U < 1.0 THEN 1870
1855 E=2.718281828
1860 WU=(.2677737343+U*(8.6347608925+U*(1
8.059016973+U*(8.5733287401+U))))/(U*E[U*
(3.9584969228+U*(21.0996530827+U*(25.6329
561486+U*(9.5733223454+U))))): RETURN
1870 WU=TY+U[2*(-.24991055+U*(.05519968+U
*(-.00976004+U*.00107857))): RETURN
```

NOTE: "[" indicates exponentiation.

GROUND WATER

COMPUTER NOTES

A COMPUTERIZED TECHNIQUE FOR ESTIMATING THE HYDRAULIC CONDUCTIVITY OF AQUIFERS FROM SPECIFIC CAPACITY DATA

by Kenneth R. Bradbury[a] and Edward R. Rothschild[b]

Abstract. Specific capacity data obtained from well construction reports can provide useful estimates of hydraulic conductivity (K). A simple computer program has been developed which can correct specific capacity data for partial penetration and well loss and, using an iterative technique, provide rapid estimates of K at hundreds of data points. The program allows easy data handling and is easily linked with existing statistical programs or contour mapping routines. The method was tested at two field sites in Wisconsin, one underlain by a sandy outwash aquifer, the other by fractured dolomite. In both areas, estimates of K from corrected specific capacity data agree reasonably well with data from pumping tests.

Introduction

Hydrogeologists continually seek and test simple, quick, and inexpensive methods for determining aquifer characteristics. The use of specific capacity tests to determine transmissivity (T), and ultimately hydraulic conductivity (K), is one such tool. Although the use of specific capacity data in estimating aquifer parameters is certainly not new (Theis *et al.*, 1963; Lohman, 1972), commonly used estimation techniques (described below) are somewhat slow and cumbersome. In this paper we describe a computer program which rapidly and accurately provides estimates of aquifer transmissivity at hundreds of points where specific capacity data are available, and we demonstrate that the technique gives excellent results at two field sites in Wisconsin. Because the solution is performed with the use of a computer, data can be manipulated easily and linked with available graphical and statistical packages.

[a]Wisconsin Geological and Natural History Survey, 1815 University Avenue, Madison, Wisconsin 53705.

[b]CH2M Hill, 310 Wisconsin Avenue, Suite 700, Milwaukee, Wisconsin 53201.

Received December 1983, revised October 1984, accepted November 1984.

Discussion open until September 1, 1985.

A specific capacity test involves pumping a well (of known construction) at a known rate and period of time, and measuring the drawdown within the well at the end of the test period. The length of the test is determined by how long it takes for the water level in the well to reach a state of apparent equilibrium, that is, when the change in drawdown is minimal with time. Specific capacity is defined as the discharge divided by the drawdown in the well, and the units generally used are gallons per minute per foot of drawdown (GPM/FT).

Theis *et al.* (1963) present a method of estimating transmissivity from specific capacity. They treat a specific capacity test as a short nonequilibrium pumping test, and utilize a graphical solution to estimate transmissivity. Several other workers, including Walton (1970), Lohman (1972), and Gabrysch (1968) have applied Theis' method to field problems. In this study, we replace the graphical approach with a short computer program utilizing an iterative procedure.

Estimating T from specific capacity involves a series of assumptions. These assumptions include a known storage coefficient (S), minimal well loss, full penetration, and a nonleaky, homogeneous and isotropic, artesian aquifer of infinite areal extent. (These assumptions are essential to use of the Theis equation, and are described in many basic texts.) Fortunately, because specific capacity varies with the logarithm of l/S, the solution is not very sensitive to variations in S, which can be estimated with sufficient accuracy from previous studies in an area, or by using representative values for a given aquifer type. If appropriate data are available, well loss corrections can be made. Corrections for partial penetration may be very important because few wells fully penetrate an aquifer. A method adopted from Brons and Marting (1961) is used in this study to correct for partial penetration.

To demonstrate the method, specific capacity data were used to estimate hydraulic conductivities for aquifers in two large field areas in Wisconsin (see Figure 1). One aquifer is a confined, fractured dolomite (area A), and the other consists of unconfined, unconsolidated sands and gravels (area B). In Wisconsin, specific capacity tests are generally performed by drillers at the time of well installation. Reports of the tests, as well as geologic logs and well construction reports for most wells are available at the Wisconsin Geological and Natural History Survey. In this study, we use available information to determine aquifer transmissivity, corrected for partial penetration of the wells, and

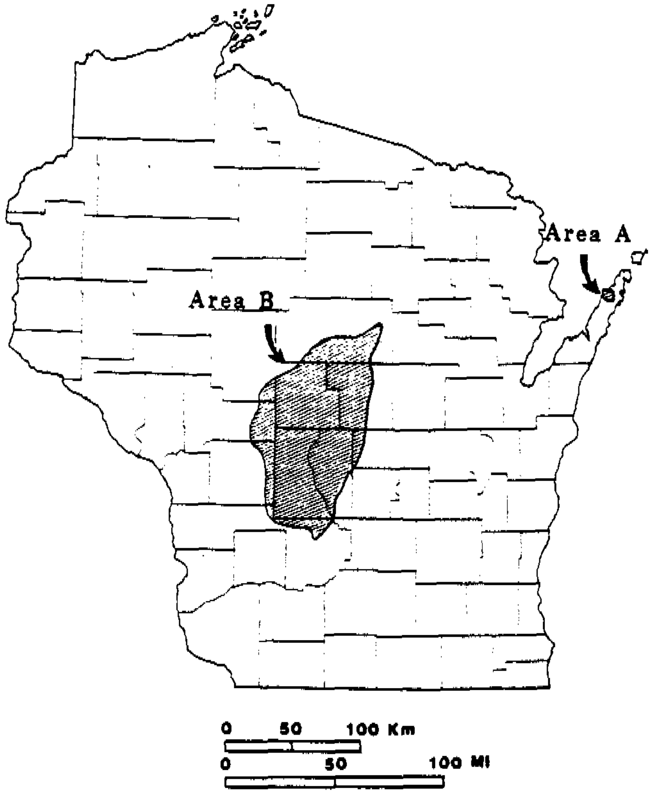

Fig. 1. Map of Wisconsin showing locations of field areas A (fractured dolomite) and B (sand and gravel).

then produce maps of hydraulic conductivity. The maps agree well with the more limited data available from pumping tests.

There are many advantages of using specific capacity information to compute hydraulic conductivity. The data are generally readily available and abundant: for area A, 224 specific capacity tests were available versus 5 pumping tests; for area B, 268 specific capacity tests were available versus 11 pumping tests. Estimates of hydraulic conductivity, based on specific capacity data, are quick, easy, and inexpensive, and when used in conjunction with limited pumping test data, may be the best method for mapping aquifer characteristics over large areas.

Computer Program Development

Theis *et al.* (1963) describe a method for estimating the transmissivity of an aquifer from the specific capacity of wells. Their analysis is based on the Jacob equation, given in consistent units as:

$$T = \frac{Q}{4\pi s} \ln \left(\frac{2.25\ Tt}{r_w{}^2 S} \right) \qquad (1)$$

where

T = transmissivity (L^2/t),

Q = discharge (L^3/t),

s = drawdown in the well (L),

t = pumping time (t),

S = storage coefficient (dimensionless), and

r_w = radius of the well (L).

Because T appears twice, this formula cannot be solved directly, and Theis *et al.* (1963) and Walton (1970) (among others) propose graphical solutions involving matching the specific capacity data to a family of curves. The graphical methods have the disadvantage of requiring a different set of curves for every possible combination of well radius, pumping period, and storage coefficient. In addition, any corrections for partial penetration or well loss require additional calculations.

Well loss is an increase in drawdown in the well bore over drawdown in the aquifer adjacent to the well. It is due to turbulent flow as water enters the well bore and pump, and depends on the pumping rate, construction of the well, and hydraulic properties of the tested aquifer. It is possible to correct specific capacity data for well loss using the equation (Csallany and Walton, 1963):

$$S_W = CQ^2 \qquad (2)$$

where

S_W = well loss (L),

C = well loss constant (t^2/L^5), and

Q = discharge (L^3/t).

Csallany and Walton present an equation with which to evaluate C from step-drawdown data.

Most private wells penetrate less than the full thickness of aquifers. During a specific capacity test, partially penetrating wells may yield anomalously low values of specific capacity, depending on the ratio of penetration (L) to aquifer thickness (b). In Wisconsin, the L/b ratio is sometimes as low as 0.1. Thus, a correction for partial penetration is necessary before estimating transmissivity from specific capacity. For unsteady drawdown in a partially penetrating well, Sternberg (1973) shows that

$$s = \frac{Q}{4\pi T} \left[\ln \left(\frac{2.25\ Tt}{r_w{}^2 S} \right) + 2\ s_p \right] \qquad (3)$$

where s_p is a "partial penetration factor" given by Brons and Marting (1961) as

$$s_p = \frac{1 - L/b}{L/b} \left(\ln \frac{b}{r_w} - G\{L/B\} \right) \qquad (4)$$

where

b = aquifer thickness (L),

L = length of open interval (L), and

G = a function of the L/b ratio.

Brons and Marting evaluate G(L/b) for various values of (b/r_w). In the present study the polynomial equation

$$G\{L/b\} = 2.948 - (7.363\ L/b) + 11.447\ \{L/b\}^2 - 4.675\ \{L/b\}^3 \qquad (5)$$

was fitted to the data of Brons and Marting by multiple regression, with a correlation coefficient of 0.992. Rewriting equation (3) to incorporate equation (2), we have

$$T = \frac{Q}{4\pi(s - s_w)}\left[\ln\left(\frac{2.25\ Tt}{r_w^2 S}\right) + 2\ s_p\right] \qquad (6)$$

The solution of equation (6) yields an estimate of T which is corrected for well loss and partial penetration, and incorporates t, S, and r_w.

Figure 2 shows a flow chart for a computer program which solves equation (6). The program first reads the data in the inconsistent units (gallons per minute, inches, feet, etc.) which are customarily used on driller's logs. After converting to consistent units (feet, seconds), the program solves equations (2), (4), and (5) directly. It then solves equation (6) iteratively, using an initial estimate of T (TGUESS) to calculate an updated estimate (TCALC). The program then substitutes the updated estimate for the original guess, and repeats the process until TGUESS and TCALC agree within a small error criterion (ERR). Finally the program prints the results.

Appendix A is a simple BASIC computer code written for an Apple IIe computer illustrating the estimation technique for a single well. A sample output is included in Appendix B. In practice, we expand this program to do several hundred estimations. The program is easily modified to change the types and methods of input and output. Currently it is designed to accept input either interactively or via a data file that has been merged with the program file. By including well coordinates in the input data, the output can be used directly in graphics plotting packages, as well as in statistical routines. The variables ERR and TGUESS have been assigned values of 0.1E-5 and 0.1, respectively. These can be altered by changing lines 300 and 320 of the program. The program also has been written in FORTRAN and is available from the authors.

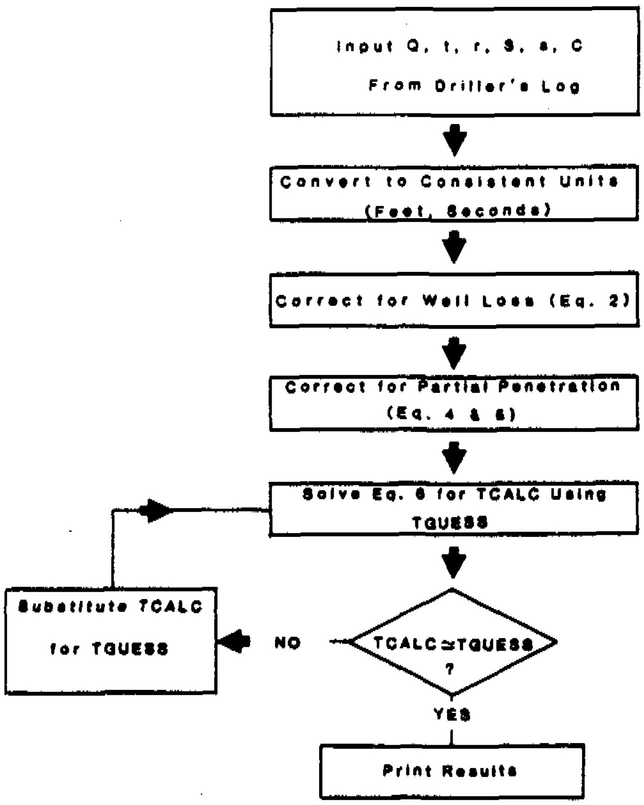

Fig. 2. Computer program flow chart.

Description of Field Sites

The aquifer analysis method described above was utilized for the two study areas in Wisconsin shown in Figure 1. The first (area A), called the Peninsula site, is in Door County, northeastern Wisconsin, and encompasses 17.8 mi^2 (46.1 km^2). The aquifer at the Peninsula site is a highly fractured Silurian dolomite. Studies of the interactions of ground water at the site with surface water in adjacent Green Bay used computer modeling (Bradbury, 1982). The computer models required extensive data on transmissivity and hydraulic conductivity of the dolomite aquifer. Because the results of five available pumping tests in the area (Sherrill, 1978) might not adequately describe spatial variability of the fractured dolomite aquifer, the transmissivity estimation technique was applied to specific capacity data from 224 local wells. The use of specific capacity tests increased the average density of hydraulic conductivity data from 0.3 to 12.6 points/mi^2 (0.78 to 32.6 points/km^2).

The second site (area B) encompasses a large portion of the Central Sand Plain of Wisconsin, which is underlain by an aquifer of sandy glacial outwash, and has an area of approximately 612 mi^2 (1585 km^2). The sand and gravel aquifer in the

Table 1. Statistical Results of Estimates of Hydraulic Conductivity (K) from Specific Capacity for Two Areas in Wisconsin. Geometric Means, Standard Deviations (σ), and 95 Percent Confidence Limits Are Given

	K (ft/sec)
AREA A: Fractured dolomite (N = 223)	
Geometric mean	7.8×10^{-5}
σ	0.61
95% C.I.	$6.5 \times 10^{-5} - 9.3 \times 10^{-5}$
AREA B: Sandy outwash (N = 266)	
Geometric mean	2.1×10^{-3}
σ	0.25
95% C.I.	$1.6 \times 10^{-3} - 2.2 \times 10^{-3}$

area is widely utilized for spray irrigation of crops, especially potatoes. Recent indications of groundwater contamination by pesticides in the area (Rothschild *et al.*, 1982) prompted further study of the aquifer, including computer modeling (Rothschild, 1982). Specific capacity data for the area are abundant (268 points) in comparison to the number of pumping tests (11), and the transmissivity estimation technique was used to help describe the hydraulic characteristics of the aquifer. By utilizing specific capacity data the density of data points for transmissivity was increased from 0.018 points/mi^2 (pumping tests) to 0.44 points per mi^2 (0.045 to 1.14 points/km^2).

Results

Reliability of Estimates

Results of the computer estimation of hydraulic conductivities from specific capacity data agree well with values calculated using full-scale pumping tests. Table 1 gives a statistical summary of hydraulic conductivity estimates for 223 wells in fractured dolomite (area A) and 266 wells in sandy outwash (area B). Because hydraulic conductivity data are generally log-normally distributed (Freeze, 1975), the geometric mean gives a good measure of the central tendency of the data, and sigma (σ) represents the standard deviation of the log-transformed data. Table 1 shows that, using many data points, the specific capacity estimates give a lower mean hydraulic conductivity for fractured dolomite (7.8×10^{-5} ft/sec) than for sandy outwash (2.1×10^{-3} ft/sec). Standard deviation values show that the fractured dolomite has statistically more variation in hydraulic conductivity than does the sandy outwash, and that the range of variation in both materials is small enough to make the results useful. Freeze (1975) reports that computer models can give meaningful estimates of hydraulic head when hydraulic conductivity "σ of K" values are less than 0.5, but that meaningful head predictions are impossible when σ is greater than 2.0. Thus the σ values of 0.61 and 0.25 reported here give confidence of reasonable results when using the data in computer simulations to predict hydraulic heads.

In spite of the well-known difficulties in estimating hydraulic conductivities from specific capacity data, the range of values predicted by our method is relatively small. Figure 3 presents average hydraulic conductivities for various materials, and shows the range of values obtained from our computer estimates. As noted by Winter (1981) the standard error in estimating values of hydraulic conductivity is often close to 100 percent or even higher. Thus the ranges of values shown on Figure 3 are quite narrow when compared to the possible ranges of hydraulic conductivity values, and the variation in K is less than one order of magnitude for the sandy outwash and just over an order of magnitude for the fractured dolomite.

Comparing estimates from individual wells, the results of the computer program are surprisingly close to data determined by pumping tests (Table 2). In the fractured dolomite of area A (wells 1-5), specific capacity data give hydraulic conductivity estimates which are slightly smaller than but of the

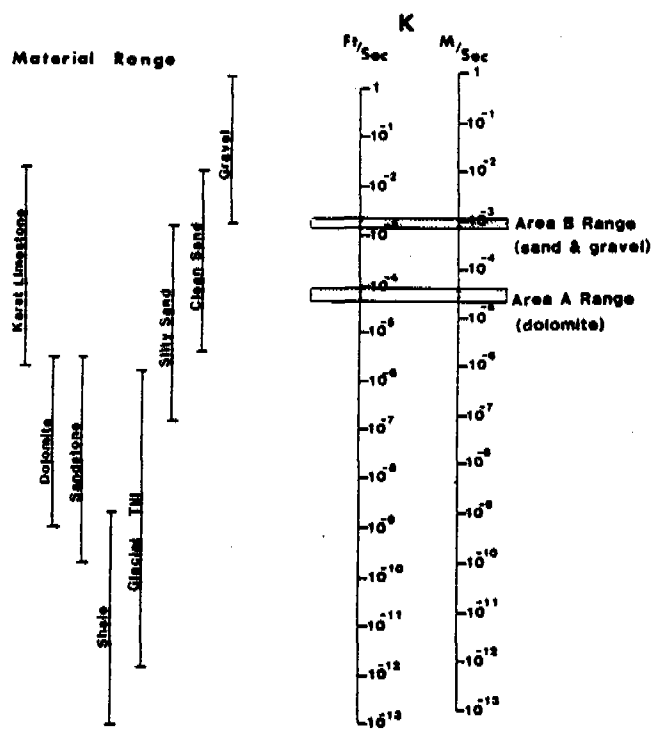

Fig. 3. Ranges of hydraulic conductivity (K) for various geologic materials, showing ranges determined from specific capacity estimates in this study (after Freeze and Cherry, 1979).

Table 2. Comparison of Values of Hydraulic Conductivity (K) Obtained from Pumping Tests with Values Estimated from Specific Capacities for Wells in Two Different Areas in Wisconsin

Well	*Pumping test K (ft/sec)*	*Specific capacity estimate K (ft/sec)*
AREA A: Fractured dolomite		
1	2.8×10^{-4}	7.3×10^{-4}
2	1.7×10^{-4}	1.0×10^{-5}
3	3.0×10^{-4}	5.0×10^{-4}
4	8.8×10^{-4}	2.8×10^{-4}
5	3.9×10^{-4}	1.0×10^{-4}
Geometric mean	3.5×10^{-4}	1.6×10^{-4}
σ	0.26	0.75
AREA B: Sandy outwash		
6	2.9×10^{-3}	1.5×10^{-3}
7	3.4×10^{-3}	1.5×10^{-3}
8	2.7×10^{-3}	2.8×10^{-3}
9	2.2×10^{-3}	1.8×10^{-3}
10	2.8×10^{-3}	1.8×10^{-3}
11	2.4×10^{-3}	2.0×10^{-3}
12	2.1×10^{-3}	1.8×10^{-3}
13	3.3×10^{-3}	2.7×10^{-3}
14	1.5×10^{-3}	1.9×10^{-3}
15	2.4×10^{-3}	2.2×10^{-3}
16	1.5×10^{-3}	2.8×10^{-3}
Geometric mean	2.4×10^{-3}	2.0×10^{-3}
σ	0.12	0.10

same order of magnitude as values derived from full-scale pumping tests using identical wells. In the sandy outwash of area B (wells 6-16), slight variations in K were also detected by specific capacity tests. Wells 9-12 in area B are radial collector wells. These wells are larger in diameter and are more efficient than the high capacity wells used for other specific capacity tests (Karnauskas, 1977). This efficiency difference is evident in consistently lower K values as determined by specific capacity tests, and highlights the importance of knowledge of well construction when interpreting such data. One of the poorer comparisons is for well 16. Due to the nature of outwash in this area the observation wells for the pumping test may not have been in full hydraulic connection with the pumping well. Much of the variation in values for the Central Sand Plain (area B) is explained by poor depth-to-bedrock control. Due to the high transmissivity of the overlying sands and gravels, few area wells are drilled to bedrock. In general, comparisons are poorer for the fractured dolomite of area A than for the sandy outwash of area B. The fractured dolomite is less homogeneous than the outwash, and the fracture system there may not truly approximate a porous media.

Contour Mapping

Contour maps of hydraulic conductivity for the two study areas are a valuable product of the computer program (Figures 4 and 5). The maps are produced by estimating T from specific capacity, then calculating K from aquifer thickness. Because all data are computerized, it is relatively simple to plot and contour the data using standard software packages. Interpolation, graphing, and smoothing packages were used to produce the maps in Figures 4 and 5 for the two study areas.

Distinct trends and differences are discernible in both areas. Figure 4 shows the hydraulic conductivity distribution in the fractured dolomite of the Peninsula area (area A). Because of the logarithmic distribution of K in the fractured dolomite the data are contoured by base 10 logs. As would be expected for a fractured dolomite aquifer, the areal distribution of K appears almost random with the exception of an area of higher K near the center of the area. The likelihood of this area having a higher K was confirmed by additional modeling efforts using a parameter estimation model (Bradbury, 1982).

In the sandy outwash of area B (Figure 5) the areal variation in K is less, and arithmetic contours are plotted. Variations in K shown on the map may be related to known depositional outwash facies in the area (Rothschild, 1982). The statistical inter-

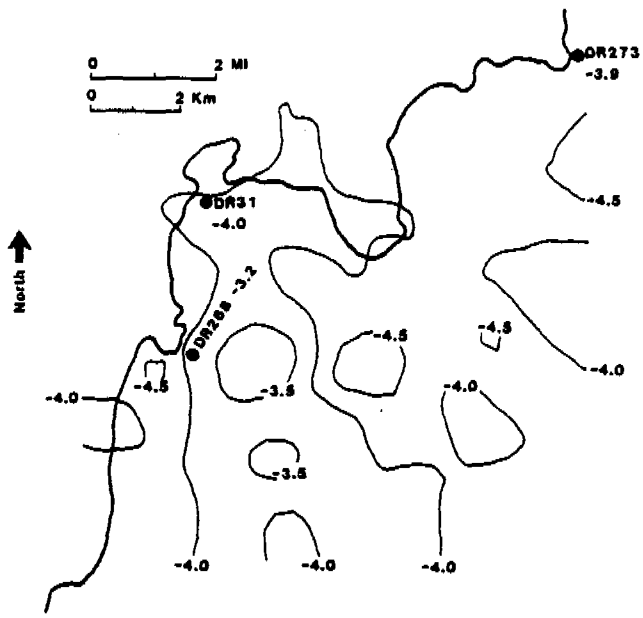

Fig. 4. Contour plot of hydraulic coqductivity in study area A based on specific capacity and aquifer thickness data. Base 10 logs are plotted; contour interval is 0.5 log unit. Locations and log hydraulic conductivity values are shown for three wells where pumping tests were conducted.

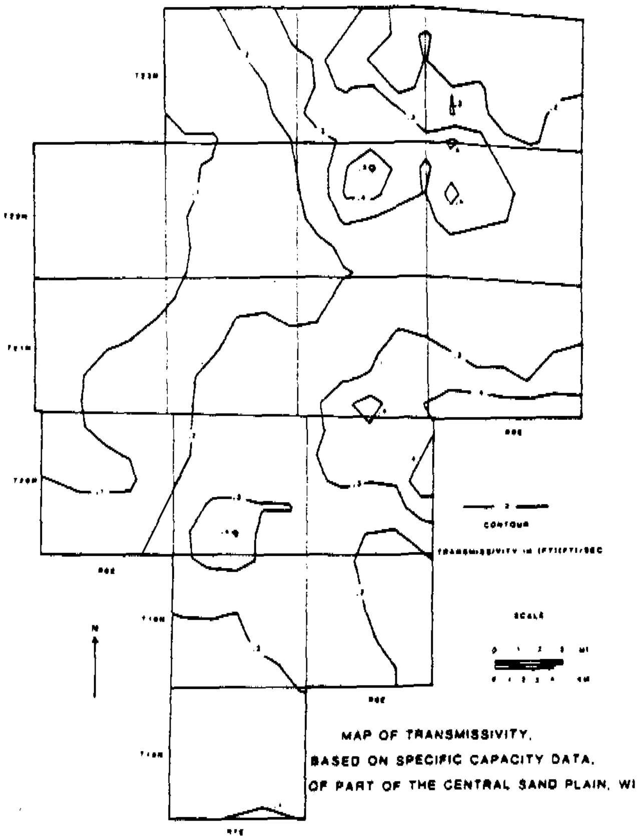

Fig. 5. Map of hydraulic conductivity based on specific capacity data for area B.

pretations of Figures 4 and 5 might be aided by advanced statistical techniques such as kriging which are beyond the scope of the present study.

Conclusions

Although the use of specific capacity data for estimating aquifer characteristics is not new, computer techniques can produce reliable estimates at more points and with less effort than in the past. Computers allow the rapid evaluation and manipulation of specific capacity data from large numbers of data points. The ability to use such data to describe the transmissivity and hydraulic conductivity of aquifers statistically or graphically is an important tool. The method described here has been successfully tested for sandy outwash and fractured dolomite aquifers at two field areas in Wisconsin.

Acknowledgments

This research has been supported by the University of Wisconsin Water Resources Center, the University of Wisconsin Sea Grant Program, the Wisconsin Geological and Natural History Survey, and Martin Marietta Energy Systems, Inc. under contract DE-AC05-84OR21400 with the U.S. Department of Energy.

References

Bradbury, K. R. 1982. Hydrogeologic relationships between Green Bay of Lake Michigan and onshore aquifers in Door County, Wisconsin. Ph.D. thesis, Dept. of Geol. and Geophys., Univ. of Wisconsin-Madison. 274 pp.

Brons, F., and V. E. Marting. 1961. The effect of restricted fluid entry on well productivity. J. Petrol. Technol. v. 13, no. 2, pp. 172-174.

Csallany, S. and W. C. Walton. 1963. Yields of shallow dolomite wells in northern Illinois. Rept. of Inv. 46. Ill. State Water Survey, Champaign, IL. p. 14.

Freeze, R. A. 1975. A stochastic-conceptual analysis of one-dimensional groundwater flow in nonuniform homogeneous media. Water Resour. Res. v. 11, no. 5, pp. 725-741.

Freeze, R. A., and J. A. Cherry. 1979. Groundwater. Prentice-Hall, Englewood Cliffs, NJ. 604 pp.

Gabrysch, R. K. 1968. The relationship between specific capacity and aquifer transmissibility in the Houston area, Texas. Ground Water. v. 6, no. 4, pp. 9-14.

Karnauskas, R. J. 1977. The hydrogeology of the Nepco Lake watershed in central Wisconsin with a discussion of management implications. M.S. thesis, Dept. of Geol. and Geophys., Univ. of Wisconsin-Madison.

Lohman, S. W. 1972. Ground-water hydraulics. U.S. Geol. Surv. Prof. Paper 708. pp. 45-46.

Rothschild, E. R. 1982. Hydrogeology and contaminant transport modeling of the Central Sand Plain, Wisconsin. M.S. thesis, Dept. of Geol. and Geophys., Univ. of Wisconsin-Madison. 135 pp.

Rothschild, E. R., R. J. Manser, and M. P. Anderson. 1982. Investigation of aldicarb in ground water in selected areas of the Central Sand Plain of Wisconsin. Ground Water. v. 20, no. 4, pp. 437-445.

Sherrill, M. G. 1978. Geology and ground water in Door County, Wisconsin with emphasis on contamination potential in the Silurian dolomite. U.S. Geol. Surv. Water Supply Paper 2047. 38 pp.

Sternberg, Y. M. 1973. Efficiency of partially penetrating wells. Ground Water. v. 11, no. 3, pp. 5-7.

Theis, C. V., R. H. Brown, and R. R. Meyer. 1963. Estimating the transmissivity of aquifers from the specific capacity of wells. pp. 331-340. In: R. Bental (ed.), Methods of determining permeability, transmissivity, and drawdown. U.S. Geol. Surv. Water Supply Paper 1536-I.

Walton, W. C. 1970. Groundwater Resource Evaluation. McGraw-Hill, New York. 664 pp.

Winter, T. C. 1981. Uncertainties in estimating the water balance of lakes. Water Res. Bull. v. 17, no. 1, pp. 82-115.

* * * * *

Kenneth Bradbury received his B.A. in Geology from Ohio Wesleyan University, his A.M. in Geology from Indiana University, and his Ph.D. in Geology from the University of Wisconsin-Madison. He has worked as a Hydrologist for the Southwest Florida Water Management District and is currently a Research Hydrogeologist with the Wisconsin Geological and Natural History Survey. His current interests include ground-water parameter estimation and field techniques in ground-water studies.

Edward Rothschild received a Bachelor's Degree in Geology from the University of Vermont, and a Master's Degree in Geology at the University of Wisconsin-Madison.

He has worked for the IEC Corp as an Environmental Engineer at an in situ uranium mining operation, and as a Research Scientist in the Environmental Sciences Division of Oak Ridge National Laboratory. He is currently a Hydrogeologist with CH2M Hill. Current interests include modeling and investigation of organics and radionuclides in ground water.

Appendix A

```
10  PRINT : PRINT : PRINT :
20  PRINT "A PROGRAM TO ESTIMATE AQUIFER TRANSMISSIVITY"
30  PRINT "AND HYDRAULIC CONDUCTIVITY"
40  PRINT "FROM SPECIFIC CAPACITY TESTS"
50  PRINT ""
60  PRINT "WRITTEN BY K. BRADBURY AND E. ROTHSCHILD, SEPTEMBER 1981"
70  PRINT ""
80  PRINT "************************************************************"
90  PRINT "****************** LIST OF VARIABLES ******************"
100  PRINT
110  PRINT "NUM = IDENTIFICATION NUMBER OF WELL"
120  PRINT "DIAM = DIAMETER OF WELL (INCHES)"
130  PRINT "LGTH = LENGTH OF OPEN INTERVAL OR WELL SCREEN (FEET)"
140  PRINT "LVL = STATIC WATER LEVEL...NEGATIVE FOR FLOWING WELL (DEPTH I
     N FEET)"
150  PRINT "PUMP = DEPTH TO WATER WHILE PUMPING DURING SPECIFIC CAPACITY
     TEST (FEET)"
160  PRINT "LN = LENGTH OF TEST (HOURS)"
170  PRINT "GPM = PUMPING RATE DURING TEST (GALLONS/MINUTE)"
180  PRINT "AQTHIC = THICKNESS OF AQUIFER (FEET)"
190  PRINT "S = ESTIMATED OR MEASURED STORAGE COEFFICIENT (UNITLESS)"
200  PRINT "C = WELL LOSS COEFFICIENT (WALTON, BULL 49)... USE 1 IF UNKNO
     WN"
210  PRINT "SC = SPECIFIC CAPACITY CORRECTED FOR WELL LOSS (GALLONS/MINUT
     E/FOOT)"
220  PRINT "T = TRANSMISSIVITY (FEET * FEET/SECOND)"
230  PRINT "K = HYDRAULIC CONDUCTIVITY (FEET/SECOND)"
240  PRINT "ERR = CONVERGENCE CRITERIA FOR T ESTIMATE (FEET * FEET/SECOND
     )"
250  PRINT "**************************************************************
     "
260  PRINT "HOW MANY WELLS WILL BE ANALYZED?"
270  INPUT XX
280  DIM NUM(XX),DIAM(XX),LGTH(XX),LVL(XX),PUMP(XX),LN(XX),GPM(XX),AQTHIC
     (XX)
290  DIM SC(XX),S(XX),C(XX),T(XX),K(XX),KOUNT(XX),FLUB(XX),ITER(XX)
300 ERR = 0.1E - 5
310 KOUNT = 0
320 TGUESS = 0.1
330  REM  ************************************************************
340  REM  READ IN RAW DATA IN UNITS GIVEN ON DRILLERS LOGS
350  REM  ************************************************************
360  PRINT "DO YOU WANT TO ENTER DATA INTERACTIVELY OR FROM A FILE?"
370  PRINT "ENTER 0 IF INTERACTIVELY OR 1 IF FROM FILE"
380  INPUT A
390  IF A = 1 THEN  GOTO 530
400  FOR Z = 1 TO XX
410  PRINT "WELL NUMBER="; INPUT NUM(Z)
420  PRINT "WELL DIAMETER (IN)= "; INPUT DIAM(Z)
430  PRINT "STATIC WATER LEVEL (FT)= "; INPUT LVL(Z)
440  PRINT "DEPTH TO WATER DURING TEST (FT)= "; INPUT PUMP(Z)
450  PRINT "THE LENGTH OF THE TEST (HR)= "; INPUT LN(Z)
460  PRINT "PUMPING RATE (GPM)= "; INPUT GPM(Z)
470  PRINT "THICKNESS OF AQUIFER (FT)= "; INPUT AQTHIC(Z)
480  PRINT "OPEN INTERVAL (FT)= "; INPUT LGTH(Z)
490  PRINT "STORAGE COEFFICIENT= "; INPUT S(Z)
500  PRINT "WELL LOSS COEFFICIENT= "; INPUT C(Z)
510  NEXT Z
520  GOTO 560
530  FOR Z = 1 TO XX
540  READ NUM(Z),DIAM(Z),LVL(Z),PUMP(Z),LN(Z),GPM(Z),AQTHIC(Z),LGTH(Z),S(
     Z),C(Z)
550  NEXT Z
560  REM  ************************************************************
570  REM  DO ANALYSIS FOR EACH WELL
580  REM  ************************************************************
590  FOR Y = 1 TO XX
600 FLUB(Y) = 0:ITER(Y) = 0
610  REM  ************************************************************
620  REM  CHANGE TO CONSISTENT UNITS AND CALCULATE DRAWDOWN
630  REM  ************************************************************
640 R = DIAM(Y) / 24.0
650 TIME = LN(Y) * 3600.0
660 Q = GPM(Y) / 449.0
670 DD =  - (LVL(Y) - PUMP(Y))
680  IF (DD    = 0.0) GOTO 1090
690 KOUNT = KOUNT + 1
700  REM  ************************************************************
710  REM  CORRECT DRAWDOWN FOR WELL LOSS USING THE EQUATION SW=CQQ
720  REM  SEE WALTON, BULL. 49, PAGE 27
730  REM  C IS ESTIMATED FROM STEP DRAWDOWN TESTS.
740  REM  ************************************************************
750 SW = C(Y) * Q * Q
760 DD = DD - SW
770 SC(Y) = GPM(Y) / DD
780  REM  ************************************************************
790  REM  CALCULATE AQUIFER TRANSMISSIVITY USING THE JACOB EQUATION
800  REM  USING A CORRECTION FOR PARTIAL PENETRATION AS GIVEN BY
810  REM  STERNBURG (1973)
820  REM  ************************************************************
830  REM  FIRST CALCULATE SP PARAMETERS FOR USE IN THE EQUATION
840  REM  ************************************************************
850 B = LGTH(Y) / AQTHIC(Y)
860  IF (B . 1.0) GOTO 1090
870 HRW = AQTHIC(Y) / R
880 GB = 2.9480 - (7.363 * B) + (11.447 * B * B) - (4.675 * B * B * B)
890 SP = ((1.0 - B) / B) * ( LOG (HRW) - GB)
900  REM  ************************************************************
910  REM  NOW SOLVE FOR T USING ITERATIONS
920  REM  ************************************************************
930 TGUESS = 0.1
940  FOR W = 1 TO 25
950 F1 = Q / (4.0 * 3.1416 * DD)
960 F2 = (2.25 * TGUESS * TIME) / (R * R * S(Y))
970 TCALC = F1 * ( LOG (F2) + (2.0 * SP))
980 TEST =  ABS (TCALC - TGUESS)
990 TGUESS =  ABS (TCALC)
1000  IF (TEST    = ERR) THEN  GOTO 1060
1010 KOUNT(Y) = W
1020  NEXT W
1030  IF (KOUNT(Y) = 25) AND (TEST   ERR) THEN  GOTO 1050
1040  GOTO 1060
1050 ITER(Y) = 1: GOTO 1100
1060 T(Y) = TCALC
1070 K(Y) = T(Y) / AQTHIC(Y)
1080  GOTO 1100
1090 FLUB(Y) = 1
1100  NEXT Y
1110  REM  ************************************************************
1120  REM  PRINT OUTPUT
1130  REM  ************************************************************
1140  PR# 1
1150  PRINT "************************************************************"
1160  PRINT "AQUIFER PROPERTIES AS DETERMINED BY ANALYSIS OF "
1170  PRINT "              SPECIFIC CAPACITY TESTS"
1180  PRINT "************************************************************"
1190  PRINT ""
1200  FOR V = 1 TO XX
1210  IF FLUB(V) = 1 GOTO 1330
1220  IF ITER(V) = 1 GOTO 1390
1230  PRINT ""
1240  PRINT "WELL NUMBER ";NUM(V)
1250  PRINT "SPECIFIC CAPACITY (GPM/FT) = ";SC(V)
1260  PRINT "TRANSMISSIVITY (FT*FT/SEC) = ";T(V)
1270  PRINT "              USING A STORAGE COEFFICIENT = ";S(V)
1280  PRINT "              NUMBER OF ITERATIONS = ";KOUNT(V)
1290  PRINT "HYDRAULIC CONDUCTIVITY (FT/SEC) = ";K(V)
1300  NEXT V
1310  PRINT "THE NUMBER OF WELLS IN THIS RECORD IS ";XX
1320  GOTO 1430
1330  PRINT ""
1340  PRINT "WELL NUMBER ";NUM(V)
1350  PRINT "INPUT ERROR, EITHER:"
1360  PRINT "     1. WATER LEVEL WAS HIGHER DURING TEST THAN BEFORE, OR:"
1370  PRINT "     2. THE SCREEN LENGTH IS LONGER THAN THE AQUIFER THICKNE
     SS."
1380  GOTO 1300
1390  PRINT ""
1400  PRINT "WELL NUMBER ";NUM(V)
1410  PRINT "SOLUTION DID NOT CONVERGE WITHIN 25 ITERATIONS"
1420  GOTO 1300
1430  END
```

Appendix B

As an example of computer program input and output, the following data from area A were input into the interactive computer program (Appendix A).

Number of wells to be analyzed = 2
Interactive data entry
Well number 1
Well diameter = 6 in.
Static water level = 42 ft
Depth to water during test = 57 ft
Length of test = 8 hr
Pumping rate = 10 gpm
Aquifer thickness = 205 ft
Open interval = 47 ft
Storage coefficient = 0.0002
Well loss coefficient = 32.7
Well number 2
Well diameter = 6 in.
Static water level = 132 ft
Depth to water during test = 141 ft
Length of test = 8 hr
Pumping rate = 10 gpm
Aquifer thickness = 115 ft
Open interval = 68 ft
Storage coefficient = 0.0002
Well loss coefficient = 32.7

Figure A1 is the computer output generated by these data.

```
************************************************************
AQUIFER PROPERTIES AS DETERMINED BY ANALYSIS OF
          SPECIFIC CAPACITY TESTS
************************************************************
WELL NUMBER 1
SPECIFIC CAPACITY (GPM/FT) = .666688713
TRANSMISSIVITY (FT*FT/SEC) = 5.93317103E-03
          USING A STORAGE COEFFICIENT = 2E-04
          NUMBER OF ITERATIONS = 3
HYDRAULIC CONDUCTIVITY (FT/SEC) = 2.89422977E-05

WELL NUMBER 2
SPECIFIC CAPACITY (GPM/FT) = 1.11117235
TRANSMISSIVITY (FT*FT/SEC) = 4.56944391E-03
          USING A STORAGE COEFFICIENT = 2E-04
          NUMBER OF ITERATIONS = 3
HYDRAULIC CONDUCTIVITY (FT/SEC) = 3.97342949E-05
THE NUMBER OF WELLS IN THIS RECORD IS 2
```

Fig. A-1. Example of computer printout.

COMPUTER NOTES

A GENERAL PURPOSE MICROCOMPUTER AQUIFER TEST EVALUATION TECHNIQUE

by C. J. Hemker[a]

Abstract. Although determination of aquifer characteristics from pumping test data is generally carried out using type curves or other graphical techniques, a number of computer methods have been developed recently for this purpose. Based on the principle of least squares, these methods of nonlinear regression analysis can be applied to any flow system for which analytical expressions of the drawdown distribution are known. In view of the growing general interest in the application of microcomputers in ground-water hydrology, a BASIC routine has been developed for estimating any number of aquifer parameters. The least squares solution is calculated by Marquardt's algorithm, using the singular-value decomposition of the Jacobian matrix. The robust computing method obtained can be applied to all kinds of pumping tests. Aquifer characteristics as well as their standard deviations are computed with optimal speed and accuracy. The technique is demonstrated by a simple application to steady flow in a leaky aquifer and an example is provided. Other applications are easily implemented and programs for unsteady-state aquifer tests, recovery tests and multiple aquifer tests are available.

Introduction

Conventional methods of aquifer test analysis cannot cope with complicating circumstances, as often encountered in field situations. More sophisticated techniques have to be used in these cases to obtain reliable results. Since computer methods for aquifer evaluation, based on the principle of least squares, can be applied to any flow system for which analytical expressions for the drawdown distribution are known (Saleem, 1970), this type of solution has a large potential.

Superposition of any number of pumping (injection) wells and pumping schemes, less common drawdown formulae, e.g. solutions for systems with storage in semipervious layers (Hantush, 1964) and multiple aquifer solutions (Hemker, 1984), all come within reach of practical aquifer test analysis. Not only the wide range of possible applications, but also the speed and accuracy and the possibility to calculate the reliability of the resulting values are advantages that contribute to the increasing use of computer techniques for the identification of aquifer characteristics.

Positive experiences with parameter estimation from aquifer tests using a main-frame computer, together with the increasing availability of a spectrum of microcomputer types, raised the question whether some well-tested algorithms could be implemented in BASIC to obtain similar results with relatively inexpensive equipment. In the Autumn of 1983 the Acorn-BBC microcomputer was chosen for this purpose.

In this paper the resulting computing technique is described and the related complete BASIC code is presented. The method is demonstrated by a simple application to steady flow in a leaky aquifer.

Estimation of Aquifer Parameters

The procedure for computer determination of numerical values of aquifer characteristics from pumping test data is in many ways comparable with the well-known type curve technique. Five steps may be distinguished:

1. An appropriate drawdown formula (model) must be selected which considers the type of aquifer, the kind of flow and other simplifying assumptions.

2. Starting from some arbitrary position, an iterative procedure is used to improve the fit between observed drawdown and theoretical (type curve) values by adjusting, directly or indirectly, the values for the unknown aquifer parameters.

3. When adjustments have become sufficiently small to not influence the corresponding parameters in a sensible way, the iterative process is stopped. It is possible, however, that many combinations of parameter values can be found which result in an equally good fit.

4. Depending on the goodness of fit an impression of the accuracy of calculated parameter values is obtained.

5. A decision needs to be made with respect to how far the calculated values may be regarded as realistic representations of actual aquifer characteristics; this depends on a comparison between results obtained by the fitting procedure and the

[a]Institute of Earth Sciences, Free University, P.O. Box 7161, 1007 MC, Amsterdam, The Netherlands; and Water Supply Company "A & V," Meerkerk, The Netherlands.

Received June 1984, revised September 1984, accepted November 1984.

Discussion open until September 1, 1985.

physical reality of model assumptions.

Only steps 2, 3, and 4 can be carried out by computer, leaving both model selection and interpretation of results to the experience of the hydrologist.

An important difference between the two techniques is that in contrast with the judgement by eye in traditional curve fitting, the computer method needs a well-defined criterion for goodness of fit. In similar problems on nonlinear regression analysis, the sum of squares of differences between observed and calculated values is generally used. If a hydrogeologic situation can be represented by an appropriate drawdown formula and the errors in measured drawdown values are not influenced by systematic disturbances, the parameter values obtained by minimizing this sum of squares may be regarded as the best estimates.

Several computer methods have been developed to estimate aquifer characteristics from pumping test data, based on essentially the same least squares technique (Saleem, 1970; Labadie and Helweg, 1975a; Leijnse, 1980, 1982; McElwee, 1980; Chander *et al.*, 1981). The problem of how the best estimates are determined is very important in relation to the efficiency and robustness of the computing method, but the principle of minimizing least squares should always yield the same results when the same data are processed.

Another difference between graphical curve fitting and the least squares technique is the transformation to logarithmic drawdowns, which makes the type curve method less sensitive to the deeper measurements (Labadie and Helweg, 1975b).

Minimization Method

The theory of methods available for finding a least squares fit of experimental data to a nonlinear function of several variables has been discussed extensively in the literature (e.g. Luenberger, 1973; Bard, 1974; Gill *et al.*, 1981). The algorithm used for the Microcomputer Aquifer Test Evaluation (MATE) programs is a derivative of the ALGOL 60 procedure MARQUARDT from the numerical program library NUMAL (Hemker, 1981). As the name of this procedure indicates, it is based on the method proposed by Marquardt (1963).

By starting with some initial estimate for all the unknown parameter values x_j ($j = 1, \ldots, n$), the sum of m ($m \geqslant n$) squares $F(x)$ is minimized in an iterative way. During the k-th iteration step, a vector d_k is defined as the solution of the equations

$$(J_k^T J_k + \lambda_k I)\, d_k = -J_k^T f_k \qquad (1)$$

where

d = step vector by which the new vector of parameters is calculated: $x_{k+1} = x_k + d_k$;

f = m vector of differences between calculated and observed drawdowns, termed the residual vector;

I = unit matrix;

J = Jacobian matrix, an $m \times n$ matrix, whose (i,j)-th element is the partial derivative of f_i with respect to x_j ($i = 1, \ldots, m$); J^T is the transpose of J;

λ = non-negative scalar for which an appropriate value must be chosen during iteration;

m = number of observations;

n = number of parameters.

The starting value for λ is fixed at 1% of the sum of eigenvalues of $J^T J$ and this is halved in each iteration if

$$F_k - F_{k+1} \geqslant -10^{-2}\, d_k^T J_k^T f_k \qquad (2)$$

If this condition is not satisfied, λ is multiplied by a factor of 10, more than once if necessary.

Using this strategy, it is possible that equation (1) has to be solved for more than one value of λ. To do this in an easy way, the singular-value decomposition of the Jacobian is calculated:

$$J_k = U_k\, \Sigma_k\, V_k^T \qquad (3)$$

where

U = m-th order orthonormal matrix;

Σ = the $m \times n$ diagonal matrix of singular values;

V = n-th order orthonormal matrix.

Substituting equation (3) into (1) and rearranging leads to

$$d_k = -V_k(\Sigma_k^2 + \lambda_k I)^{-1}\, \Sigma_k\, U_k^T f_k \qquad (4)$$

which shows that once the singular-value decomposition has been performed, d is easily calculated for different values of λ. The decomposition can be further used to derive information about the statistics of the problem.

The iterative procedure is terminated when the absolute and relative improvement in sum of squares is less than a given tolerance.

A detailed description of the ALGOL 60 procedure MARQUARDT is given by Bus *et al.* (1975).

Application

In this paper only a single application of the described parameter estimation method for aquifer test evaluation is presented. The relatively simple De Glee-Hantush formula has been selected. This drawdown equation for steady-state well flow in a semiconfined aquifer can be expressed as

$$s = \frac{Q}{2\pi KD} K_0(r/L) \tag{5}$$

where the steady-state drawdown s is a function of two independent variables: Q (discharge) and r (distance from the pumped well), and two aquifer characteristics: KD (transmissivity) and L (leakage factor). According to the definition of the leakage factor, $L = \sqrt{KDc}$, the hydraulic resistance of the semipervious layer (c) and the transmissivity of the aquifer (KD) can be chosen as unknown parameters.

Implementation

The microcomputer program presented (MATE-DEGLEE) has been written in extended BASIC and can be run on an Acorn-BBC computer with 32 K memory. As the complete listing (see Appendix) contains only few REMark statements, to keep its length within bounds, additional information about the program structure and the algorithms used will be helpful to explain its operation and allow any required adaptations. No explanation will be given for specific statements and other commands available with the BBC-BASIC language. The user is referred to the BBC User Guide (Coll, 1982) or other books on this subject.

The program has been split into a main body and several separately defined functions and procedures. The purpose of the main part (lines 100-280) is the interactive input of data and the dimensioning of arrays, while all computation and output of results are left to the procedure PROCCAL. A subroutine is added (300-330) to enable the user to go back to the start by pressing the Escape-key, retaining the present values of all variables. By means of a flexible interactive data input (500-640) and three successive pages of information concerning the values requested, all necessary aquifer test data can be supplied to the computer with ample possibilities to correct typing errors. The contents of these pages are shown in Figures 1 to 3. To find values for the required starting estimate (page 3), default values are calculated from the first and last given values of distance

```
PUMPING TEST ANALYSIS      DATA INPUT 1

For a leaky aquifer and steady-state
drawdown data, using De Glee's formula

Two parameters (aquifer characteristics)
will be calculated
 - KD : aquifer transmissivity (m2/day)
 - c  : hydraulic resistance of semi-
        pervious layer (day)

Pumping rate (m3/day) = 761

Number of piezometers = 8


Type C (Change data) or SPACE (continue)
```

Fig. 1. Screen display. Data pumping test "Dalem," page 1.

```
PUMPING TEST ANALYSIS      DATA INPUT 2

Type for each piezometer
- distance to pumping well (m)
- steady state drawdown  (cm)

1   distance = 10     drawdown = 31
2   distance = 10     drawdown = 25.2
3   distance = 30     drawdown = 23.5
4   distance = 30     drawdown = 21.3
5   distance = 60     drawdown = 17
6   distance = 90     drawdown = 14.7
7   distance = 120    drawdown = 13.2
8   distance = 400    drawdown = 5.9


Type C (Change data) or SPACE (continue)
```

Fig. 2. Screen display. Data pumping test "Dalem," page 2.

```
PUMPING TEST ANALYSIS      DATA INPUT 3



Give an estimate for both unknown
parameters


  KD-value = 1758

   c-value = 367



Type C (Change data) or SPACE (continue)
```

Fig. 3. Screen display. Calculated initial estimate for both parameters.

and drawdown using approximations based on the well-known equations given by Thiem and Cooper-Jacob.

Procedure PROCCAL (2000-2170) prints the input data, calculates the least squares solution (PROCMARQ) and the standard deviation of the parameters (PROCS) and finally prints the results by calling PROCRES and PROCOUT. Five elements of array "I" are to control the iterative curve fitting process. I(1) is a starting value, used for the relation between the gradient and the Gauss-Newton direction and I(2) is the maximum number of calls of PROCFUN by PROCMARQ. The iterative process is stopped if the improvement in the sum of squares is sufficiently small [i.e. less than I(3) × (sum of squares) + I(4) × I(4)]. A fifth control parameter is the machine precision, set at $5\ 10^{-9}$ at the start of PROCMARQ.

The De Glee-Hantush formula is implemented in PROCFUN (3000-3080). To prevent either parameter from becoming negative in any iteration, minimum values are chosen: $KD \geqslant 1$ m²/day and $c \geqslant 1$ day. The Bessel function K_0 is evaluated in function FNK (9000-9160) by means of either a Taylor series approximation (argument < 4) or a finite Chebyshev series expansion.

The procedure PROCJAC (7000-7100) yields the Jacobian matrix obtained using current estimates of the unknown parameters. Although all derivatives can be computed analytically in this case, a forward finite-difference approximation is applied using intervals of 10^{-3} of the parameter value. In this way the procedure is applicable to all kinds of aquifer tests, provided that the drawdowns can be computed with sufficient accuracy.

To calculate the singular-value decomposition of the Jacobian, the matrix is first reduced to bidiagonal form by Householder's transformation in PROCHSH (6000-6480). The corresponding postmultiplying and premultiplying matrices are subsequently computed in the same procedure. From these intermediate results the complete decomposition is calculated by PROCQR (6500-6880). The algorithms used are derived from the NUMAL procedure QRISNGVALDEC (Hemker, 1981).

When, according to the given stopping criterion, iterations are completed by PROCMARQ, the resulting estimated parameters, together with their standard deviations as determined by PROCS (8000-8050), are displayed on the screen by procedure PROCRES (2200-2300). The same procedure also presents a table with all calculated, observed and residual drawdowns. A separate procedure, called PROCOUT (2400-2500), is used to give additional information on the iterative process: viz., the sum of squares and its improvement from the last iteration, the number of iterations performed and the running time. The condition number, also shown at this time, is defined as the ratio of the largest to the smallest eigenvalue of the matrix $J^T J$. This number gives an impression of how well-defined the least squares solution is. Very large values ($> 10^7$) indicate useless results, such as may be obtained when the data provided do not contain sufficient information to determine the parameters required.

The resulting observed and calculated drawdowns can easily be presented graphically on the monitor screen, but since several plotting techniques can be selected, this is left to the user's preference and no such procedure is included in the program listing.

Example

Data from the pumping test "Dalem," presented by Kruseman and de Ridder (1970) to illustrate the method of type curves, are used here as an example of the MATE-program. Figures 1 to 3 show the data input pages as they appear on the screen and all computer results are given in Figure 4. A comparison of the computed parameters with those obtained by the graphical method ($KD = 2114$ m²/day and $c = 572$ days), shows a moderate difference, within the calculated standard deviations. The reason for the rather high calculated standard deviations can be found in the heterogeneity of the aquifer, demonstrated by the difference in drawdown between both piezometers at 10-meter distance. Apparently only three iterations are required, while the running time is less than half a minute. Starting with much worse initial estimates the calculation is almost as quick, while the results are the same.

Conclusions

Marquardt's algorithm has been successfully implemented on a microcomputer. The resulting least squares method can be applied to find aquifer characteristics and their individual standard deviations from pumping test data. The microcomputer appears to be well suited for this purpose: accurate results may be obtained within a few minutes depending on the drawdown equation used and the number of data. The BASIC routine presented in this paper is applicable to a large number of aquifer test problems, all of which may be solved in the same way as long as the appropriate drawdown formula can be evaluated with sufficient accuracy.

```
    Distance    Drawdown
      (m)         (cm)

      10.0        31.0
      10.0        25.2
      30.0        23.5
      30.0        21.3
      60.0        17.0
      90.0        14.7
     120.0        13.2
     400.0         5.9

    Discharge rate   761.0    m3/day


    Results of successive iterations

    KD-value      c-value
     (m2/d)        (day)

      1758.0       367.0
      1910.7       363.2
      1941.8       380.9
      1945.8       385.6


 THE CALCULATED LEAST SQUARES SOLUTION

 Parameter   value + Standard deviation

 KD-value     1945 +    197    ( 10% )
  c-value      385 +    222    ( 57% )


 Calculated   Observed    Cal-Obs

      28.49      31.00      -2.51
      28.49      25.20       3.29
      21.66      23.50      -1.84
      21.66      21.30       0.36
      17.37      17.00       0.37
      14.87      14.70       0.17
      13.12      13.20      -0.08
       6.17       5.90       0.27

 The sum of squares is 20.9
 Improvement last iteration 4.1E-8
 Number of iterations 3
 Condition number 27.3
 Running time 0.279 minutes
```

Fig. 4. Results pumping test "Dalem," as obtained by the computer program MATE-DEGLEE.

Acknowledgments

Appreciation is expressed to Dr. P. W. Hemker, who provided valuable support on the application of NUMAL procedures and to Professor N. A. de Ridder and Professor I. Simmers for reading and amending the manuscript.

Note

Considerable effort has been expended in an attempt to provide an error-free program, but the author, being a ground-water hydrologist rather than a programmer, does not accept responsibility for the consequences of any errors that may have been overlooked.

A floppy disk for the BBC-computer (40/80 tracks), containing programs for the analysis of steady and unsteady-state aquifer tests, recovery tests, and multiple aquifer tests is available from the author at duplication and mailing costs.

References

Bard, Y. 1974. Nonlinear Parameter Estimation. Academic Press, London and New York. 341 pp.

Bus, J.C.P., B. van Domselaar, and J. Kok. 1975. Nonlinear Least Squares Estimation. Stichting Mathematisch Centrum, NW 17/75, Amsterdam. 42 pp.

Chander, S., P. N. Kapoor, and S. K. Goyal. 1981. Analysis of pumping test data using Marquardt algorithm. Ground Water. v. 19, no. 3, pp. 275-278.

Coll, J. 1982. The BBC Microcomputer User Guide. British Broadcasting Corporation, London. 518 pp.

Gill, P. E., W. Murray, and M. H. Wright. 1981. Practical Optimization. Academic Press, London and New York. 401 pp.

Hantush, M. S. 1964. Hydraulics of wells. Advances in Hydroscience. v. 1, pp. 281-432. Academic Press, New York.

Hemker, C. J. 1984. Steady groundwater flow in leaky multiple-aquifer systems. J. Hydrol. v. 72, pp. 355-374.

Hemker, P. W. 1981. NUMAL numerical procedures in ALGOL 60. Mathematisch Centrum. MCS 47.1-47.7, Amsterdam.

Kruseman, G. P. and N. A. de Ridder. 1970. Analysis and evaluation of pumping test data. Bulletin 11, Institute for Land Reclamation and Improvement, Wageningen. pp. 69-73.

Labadie, J. W. and O. J. Helweg. 1975a. Step-drawdown test analysis by computer. Ground Water. v. 13, no. 5, pp. 438-444.

Labadie, J. W. and O. J. Helweg. 1975b. Reply to the Discussion by N. T. Sheahan. Ground Water. v. 13, no. 5, pp. 449-450.

Leijnse, A. 1980. Berekening van bodemconstanten uit pompproefgegevens met behulp van niet-lineaire regressieanalyse. RID (Nat. Inst. for Water Supply) -Meded. no. 80-3, Voorburg, 22 pp.

Leijnse, A. 1982. Evaluation of pumping tests; identification of parameter values and their reliability. Proceedings of the Exeter Symposium, July 1982, IAHS Publ. no. 136, pp. 195-203.

Luenberger, D. G. 1973. Introduction to Linear and Nonlinear Programming. Addison-Wesley, Reading, Mass. 356 pp.

Marquardt, D. W. 1963. An algorithm for least-squares estimation of nonlinear parameters. J. Soc. Indust. Appl. Math. v. 11, no. 2, pp. 431-441.

McElwee, C. D. 1980. Theis parameter evaluation from pumping tests by sensitivity analysis. Ground Water. v. 18, no. 1, pp. 56-60.

Saleem, Z. A. 1970. A computer method for pumping-test analysis. Ground Water. v. 8, no. 5, pp. 21-24.

* * * * *

Christiaan J. Hemker received his B.Sc. degree in Physical Geography from the Municipal University of

Amsterdam in 1975 and a M.Sc. degree in Hydrology from the Free University of Amsterdam in 1980. In 1979 he joined the Water Supply Company "A & V" as a Geohydrologist, and since 1982 has been temporarily employed at the Free University to teach courses in ground-water hydraulics. His fields of special interest are ground-water modeling and (micro)computer applications to ground-water hydrology.

Appendix. Program Listing MATE-DEGLEE

```
  10 REM Microcomputer Aquifer Test Evaluation     ** MATE **
  20 REM for steady-state semi-confined flow       * DEGLEE *
  30 REM by Christiaan J.Hemker 1983
  40 REM last update  6-5-1984
  50
 100 MODE7:D%=0:N%=2:ON ERROR GOTO 250
 110 M%=15:MX%=20:Q=800:REM Default values
 120 @%=&40A:K%=0:REPEAT PROCH(1):PROCPAGE1:K%=1:UNTIL FNEND
 130 IF M%<N% THEN PRINT"Insufficient data    Try again":END
 140 IF D%>0 THEN GOTO 160 ELSE D%=1
 150 DIM P(2),P$(2),PD$(2),R(MX%),S(MX%)
 160 H%=(M%-1)DIV10:FOR L%=0 TO H%
 170   K%=0:REPEAT PROCH(L%+2):PROCPAGE2(L%):K%=1:UNTIL FNEND
 180   NEXT:K%=0:REPEAT PROCH(H%+3):PROCPAGE3:K%=1:UNTIL FNEND
 190  IF D%>3 THEN GOTO 220 ELSE D%=4
 200 DIM A(MX%,N%),B(N%),C(N%),D(N%),E(7),F(MX%),G(MX%)
 210 DIM I(4),O(7),Q(N%),V(N%,N%),Z(N%)
 220 PROCCAL:REM Calculation and output
 230
 250 IF ERR=17 OR ERR=0 THEN GOTO 300 ELSE REPORT
 260 END
 290
 300 REM Subroutine to re-start by pressing ESCAPE
 310 PRINT'"      Stop or Repeat? (S/R)"
 320 A$=GET$:IF A$="S" THEN PRINT:END
 330 IF A$="R" THEN GOTO 120 ELSE GOTO 320
 350
 500 REM Function for interactive data input
 510 DEF FNP(M%,LL%,L%,P$,V):LOCAL P%,V%,V$
 520 PRINTTAB(LL%,L%);P$;" = ";V;
 530 IF M%>0 THEN PRINT" ? ";:P%=POS:V%=VPOS
 540 PRINT SPC(40);:IF M%=0 THEN =V
 550 INPUT TAB(P%,V%) V$
 560 IF LEN(V$)>0 THEN V=VAL(V$) ELSE M%=0
 570 GOTO 520
 590
 600 REM Function end page
 610 DEF FNEND:LOCAL A$
 620 PRINTTAB(0,23)"Type C (Change data) or SPACE (continue)";
 630 A$=GET$:IF A$=" " THEN =TRUE
 640 IF A$="C" THEN =FALSE ELSE GOTO 630
 660
 700 DEF FNMAX(A,B):IF B>A THEN =B ELSE =A
 720
 900 DEF PROCH(I%):REM heading
 910 CLS:PRINT'"PUMPING TEST ANALYSIS      DATA INPUT ";I%
 920 ENDPROC
 930
1000 DEF PROCPAGE1:REM Read data page 1
1010 PRINT'''"For a leaky aquifer and steady-state"
1020 PRINT"drawdown data, using De Glee's formula"
1030 PRINT'"Two parameters (aquifer characteristics)";
1040 PRINT"will be calculated"
1050 PRINT" - KD : aquifer transmissivity (m2/day)"
1060 PRINT" - c  : hydraulic resistance of semi-"
1070 PRINT"             pervious layer (day)"
1080 Q=FNP(K%,0,15,"Pumping rate (m3/day)",Q)
1090 M%=FNP(K%,0,18,"Number of piezometers",M%)
1100 IF D%=0 THEN MX%=FNMAX(MX%,M%)
1110 IF M%<=MX% THEN ENDPROC
1120 PRINTTAB(0,17)"If number>";MX%;" stop and start again"
1130 GOTO 1090
1140
1300 DEF PROCPAGE2(L%):REM Read data page 2+
1310 IF K%+L%+D%>1 THEN GOTO 1330
1320 FOR I%=1 TO M%:R(I%)=10*I%:S(I%)=1:NEXT:D%=2
1330 PRINT'''"Type for each piezometer"
1340 PRINT"- distance to pumping well (m)"
1350 PRINT"- steady state drawdown  (cm)"
1360 J%=0:REPEAT J%=J%+1:I%=L%*10+J%
1370   PRINTTAB(0,9+J%);I%
1380   R(I%)=FNP(K%,4,9+J%,"distance",R(I%))
1390   S(I%)=FNP(K%,21,9+J%,"drawdown",S(I%))
1400   UNTIL J%=10 OR I%=M%
1410 ENDPROC
1600 DEF PROCPAGE3:LOCAL T,L:REM Read starting guess
1610 IF K%=1 OR D%>2 THEN GOTO 1670 ELSE D%=3
1620 P$(1)="KD-value":PD$(1)="(m2/d)"
1630 P$(2)=" c-value":PD$(2)="(day)"
1640 T=1+LN(R(M%)/R(1))*50*Q/(1+PI*(S(1)-S(M%)))
1650 L=R(1)*EXP(PI*T*S(1)/(50*Q))/1.123
1660 P(1)=INT(T):P(2)=1+INT(L*L/T)
1670 PRINT''''"Give an estimate for both unknown"
1680 PRINT"parameters"
1690 P(1)=FNP(K%,2,11,P$(1),P(1))
1700 P(2)=FNP(K%,2,13,P$(2),P(2))
1710 ENDPROC
1720
2000 DEF PROCCAL:REM write input, calculate and write output
2010 LOCAL I%,A$:CLS:@%=&2010B
2020 PRINT'"   Distance   Drawdown"
2030 PRINT"      (m)        (cm)"'
2040 FOR I%=1 TO M%:PRINT R(I%),S(I%)
2050   IF I%MOD10=0 THEN A$=INKEY$(500):PRINT
2060   NEXT:PR=TRUE:TIME=0
2070 PRINT'"   Discharge rate  ";Q;"  m3/day"''
2080 PRINT"  Results of successive iterations"'
2090 PRINTTAB(3)P$(1)TAB(14)P$(2)'TAB(5)PD$(1)SPC(6)PD$(2)'
2100 I(1)=0.01:REM value used for the calculation of labda
2110 I(2)=50:  REM max number of iterations
2120 I(3)=1E-4:REM relative stopping criterion
2130 I(4)=1E-4:REM absolute stopping criterion
2140 PROCMARQ:PROCS
2150 TM=TIME:SOUND 1,-14,200,10
2160 IF O(1)=0 THEN PROCRES:PROCOUT ELSE PROCOUT:PROCRES
2170 ENDPROC
2180
2200 DEF PROCRES:REM write solution
2210 PRINT''"THE CALCULATED LEAST SQUARES SOLUTION"
2220 PRINT'"Parameter  value   Standard deviation"'
2230 FOR I%=1 TO N%:@%=&8:PRINTP$(I%),INT(P(I%));
2240   @%=&3:PRINT" ¯ ",INT(Z(I%))TAB(27)"(";
2250   PRINT INT(Z(I%)*100/ABS(P(I%)))"% )":NEXT
2260 *FX 15,1
2270 A$=GET$:PRINT''"Calculated  Observed   Cal-Obs"'
2280 @%=&2020A:FOR I%=1 TO M%
2290   PRINT(S(I%)+G(I%)),S(I%),G(I%):NEXT:A$=GET$
2300 ENDPROC
2310
2400 DEF PROCOUT:REM write additional information
2410 @%=&308:IF O(1)=0 THEN GOTO 2440
2420 PRINT''"Nonlinear regression calculation"
2430 PRINT"has been BROKEN OFF"
2440 PRINT'"The sum of squares is ";O(2)*O(2)
2450 PRINT"Improvement last iteration ";O(6)*O(6)
2460 PRINT"Number of iterations ";O(5)
2470 PRINT"Condition number ";O(7)
2480 PRINT"Running time ";TM/6000;" minutes"
2490 A$=GET$
2500 ENDPROC
2510
3000 DEF PROCFUN:REM DeGlee's formula
3010 LOCAL I%,B
3020 IF P(1)<1 THEN P(1)=1:REM transmissivity
3030 IF P(2)<1 THEN P(2)=1:REM hydraulic resistance
3040 IF PR THEN FOR I%=1 TO N%:PRINT P(I%);:NEXT:PRINT
3050 FOR I%=1 TO M%
3060   B=R(I%)/SQR(P(2)*P(1))
3070   G(I%)=Q*FNK(B)*50/(PI*P(1))-S(I%):NEXT
3080 ENDPROC
3090
5000 DEF PROCMARQ:REM Marquardt's algorithm
5010 LOCAL E%,F%,G%,I%,J%,K%,P%,Q%,S%
5015 LOCAL A,B,E,F,L,M,R,S,V,W,X,Y,Z
5020 V=10:W=0.5:M=0.01
5025 I(0)=5E-9:REM machine precision
5030 IF I(1)<1E-7 THEN Y=1E-8 ELSE Y=I(1)/10
5040 E(0)=I(0):E(2)=I(0):E(6)=I(0):E(4)=10*N%
5050 B=I(3):A=I(4)*I(4)
5060 G%=I(2):E%=0:F%=1:S%=0:P%=0
5070 Q%=-INT(LOG(Y*I(0)))
5080 FOR I%=1 TO N%:Q(I%)=P(I%):NEXT
5090 PROCFUN
5100 GOSUB 5500:F=Z:O(3)=SQR(F)
```

```
5110 S%=S%+1
5120 PROCJAC:REM calculate jacobian
5125 PROCHSH:PROCQR:REM singular-value decomposition
5130 IF S%=1 THEN GOSUB 5510:L=I(1)*Z:GOTO 5140
5135 IF P%=0 THEN L=L*W ELSE P%=0
5140 FOR I%=1 TO N%:Z=0:FOR K%=1 TO M%
5150      Z=A(K%,I%)*G(K%)+Z:NEXT
5160   C(I%)=D(I%)*Z:NEXT
5170 FOR I%=1 TO N%:Z(I%)=C(I%)/(D(I%)*D(I%)+L):NEXT
5180 FOR I%=1 TO N%:Z=0:FOR K%=1 TO N%
5190      Z=V(I%,K%)*Z(K%)+Z:NEXT
5200   P(I%)=Q(I%)-Z:NEXT
5210 F%=F%+1:IF F%>=G% THEN E%=1:GOTO 5300
5220 PROCFUN
5230 GOSUB 5500:S=Z:R=F-Z
5240 GOSUB 5520:IF R>M*Z THEN GOTO 5280
5250 P%=P%+1:L=V*L
5260 IF P%=1 THEN GOSUB 5510:E=Y*Z:IF L<E THEN L=E
5270 IF P%<Q% THEN GOTO 5170 ELSE E%=4:GOTO 5300
5280 FOR I%=1 TO N%:Q(I%)=P(I%):NEXT:F=S
5290 IF F>A AND R>B*F+A THEN GOTO 5110
5300 FOR I%=1 TO N%:X=D(I%)+I(0)
5310   FOR K%=1 TO N%:A(K%,I%)=V(K%,I%)/X:NEXT:NEXT
5320 FOR I%=1 TO N%:FOR J%=1 TO I%:Z=0
5330     FOR K%=1 TO N%:Z=A(I%,K%)*A(J%,K%)+Z:NEXT
5340     V(I%,J%)=Z:V(J%,I%)=Z:NEXT:NEXT
5350 E=D(1):L=E:IF N%=1 THEN GOTO 5380
5360 FOR I%=2 TO N%
5370   IF D(I%)>L THEN L=D(I%) ELSE IF D(I%)<E THEN E=D(I%)
5375   NEXT
5380 Z=L/(E+I(0)):O(7)=Z*Z
5390 O(2)=SQR(F):Z=R+F:IF Z>0 THEN O(6)=SQR(Z)-O(2)
5400 O(4)=F%:O(5)=S%:O(1)=E%
5420 ENDPROC
5500 Z=0:FOR K%=1 TO M%:X=G(K%):Z=X*X+Z:NEXT:RETURN
5510 Z=0:FOR K%=1 TO N%:X=D(K%):Z=X*X+Z:NEXT:RETURN
5520 Z=0:FOR K%=1 TO N%:Z=C(K%)*Z(K%)+Z:NEXT:RETURN
5530
6000 DEF PROCHSH
6010 LOCAL I%,J%,H%,T%,C,F,G,H,R,S,V,W
6020 R=0:FOR I%=1 TO M%:W=0
6030   FOR J%=1 TO N%:W=ABS(A(I%,J%))+W:NEXT
6040   IF W>R THEN R=W
6050   NEXT:C=E(0)*R:E(1)=R
6060 FOR I%=1 TO N%:H%=I%+1:S=0
6070   IF H%>M% THEN GOTO 6090
6080   FOR T%=H% TO M%:V=A(T%,I%):S=S+V*V:NEXT
6090   IF S<C THEN D(I%)=A(I%,I%):GOTO 6170
6100   F=A(I%,I%):S=F*F+S
6110   IF F<0 THEN G=SQR(S) ELSE G=-SQR(S)
6120   D(I%)=G:H=F*G-S:A(I%,I%)=F-G
6130   IF H%>N% THEN GOTO 6170
6140   FOR J%=H% TO N%:S=0
6150     FOR T%=I% TO M%:S=S+A(T%,I%)*A(T%,J%):NEXT:S=S/H
6160     FOR T%=I% TO M%
6165       A(T%,J%)=A(T%,J%)+A(T%,I%)*S:NEXT:NEXT
6170   IF I%=N% THEN GOTO 6270
6180   S=0:IF H%=N% THEN GOTO 6200
6190   FOR T%=H%+1 TO N%:S=S+A(I%,T%)*A(I%,T%):NEXT
6200   IF S<C THEN B(I%)=A(I%,H%):GOTO 6270
6210   F=A(I%,H%):S=F*F+S
6220   IF F<0 THEN G=SQR(S) ELSE G=-SQR(S)
6230   B(I%)=G:H=F*G-S:A(I%,H%)=F-G
6240   FOR J%=H% TO M%:S=0
6250     FOR T%=H% TO N%:S=S+A(I%,T%)*A(J%,T%):NEXT:S=S/H
6260     FOR T%=H% TO N%:A(J%,T%)=A(J%,T%)+A(I%,T%)*S:NEXT
6265     NEXT
6270   NEXT
6280 H%=N%:V(N%,N%)=1
6290 FOR I%=N%-1 TO 1 STEP -1
6300   H=B(I%)*A(I%,H%):IF H>=0 THEN GOTO 6350
6310   FOR J%=H% TO N%:V(J%,I%)=A(I%,J%)/H:NEXT
6320   FOR J%=H% TO N%:S=0:FOR T%=H% TO N%
6330       S=S+A(I%,T%)*V(T%,J%):NEXT
6340     FOR T%=H% TO N%:V(T%,J%)=V(T%,J%)+V(T%,I%)*S:NEXT
6345     NEXT
6350   FOR J%=H% TO N%:V(I%,J%)=0:V(J%,I%)=0:NEXT
6360   V(I%,I%)=1:H%=I%:NEXT
6370 FOR I%=N% TO 1 STEP -1
6380   H%=I%+1:G=D(I%):H=G*A(I%,I%)
6390   IF H%<=N% THEN FOR J%=H% TO N%:A(I%,J%)=0:NEXT
6400   IF H>=0 THEN GOTO 6460
6410   IF H%>N% THEN GOTO 6450
6420   FOR J%=H% TO N%:S=0:FOR T%=H% TO M%
6430       S=S+A(T%,I%)*A(T%,J%):NEXT:S=S/H
6440     FOR T%=I% TO M%:A(T%,J%)=A(T%,J%)+A(T%,I%)*S:NEXT
6445     NEXT
6450   FOR J%=I% TO M%:A(J%,I%)=A(J%,I%)/G:NEXT:GOTO 6470
6460   FOR J%=I% TO M%:A(J%,I%)=0:NEXT
6470   A(I%,I%)=A(I%,I%)+1:NEXT
6480 ENDPROC
6500 DEF PROCQR
6510 LOCAL C%,I%,J%,K%,L%,R%,T%,U%,V%,X%
6515 LOCAL B,C,F,G,H,M,S,T,V,W,X,Y,Z
6520 T=E(2)*E(1):C%=0:B=0:X%=E(4):M=E(6):R%=N%:U%=N%
6530 K%=U%:V%=U%-1
6540 K%=K%-1:IF K%=0 THEN GOTO 6650
6550 IF ABS(B(K%))>T THEN GOTO 6580
6560 IF ABS(B(K%))>B THEN B=ABS(B(K%))
6570 GOTO 6650
6580 IF ABS(D(K%))>T THEN GOTO 6540
6590 C=0:S=1
6600 FOR I%=K% TO V%:F=S*B(I%):B(I%)=C*B(I%):J%=I%+1
6610   IF ABS(F)<T THEN I%=V%:GOTO 6640
6620   G=D(J%):H=SQR(F*F+G*G):D(J%)=H:C=G/H:S=-F/H
6630   FOR T%=1 TO M%:V=A(T%,K%):W=A(T%,J%)
6635     A(T%,K%)=V*C+W*S:A(T%,J%)=W*C-V*S:NEXT
6640   NEXT
6650 IF K%<>V% THEN GOTO 6690
6660 IF D(U%)<0 THEN D(U%)=-D(U%) ELSE GOTO 6670
6665 FOR I%=1 TO N%:V(I%,U%)=-V(I%,U%):NEXT
6670 IF D(U%)<M THEN R%=R%-1
6680 U%=V%:GOTO 6860
6690 C%=C%+1:IF C%>X% THEN GOTO 6870
6700 L%=K%+1:Z=D(U%):X=D(L%):Y=D(V%)
6710 IF V%=1 THEN G=0 ELSE G=B(V%-1)
6720 H=B(V%):F=((Y-Z)*(Y+Z)+(G-H)*(G+H))/(2*H*Y)
6730 G=SQR(F*F+1)
6740 IF F<0 THEN C=F-G ELSE C=F+G
6750 F=((X-Z)*(X+Z)+H*(Y/C-H))/X:C=1:S=1
6760 FOR I%=L%+1 TO U%:J%=I%-1:G=B(J%)
6770   Y=D(I%):H=S*G:G=C*G
6780   Z=SQR(F*F+H*H):C=F/Z:S=H/Z
6790   IF J%<>L% THEN B(J%-1)=Z
6800   F=X*C+G*S:G=G*C-X*S:H=Y*S:Y=Y*C
6810   FOR T%=1 TO N%:V=V(T%,J%):W=V(T%,I%)
6815     V(T%,J%)=V*C+W*S:V(T%,I%)=W*C-V*S:NEXT
6820   Z=SQR(F*F+H*H):D(J%)=Z:C=F/Z:S=H/Z
6830   F=C*G+S*Y:X=C*Y-S*G
6840   FOR T%=1 TO M%:V=A(T%,J%):W=A(T%,I%)
6845     A(T%,J%)=V*C+W*S:A(T%,I%)=W*C-V*S:NEXT:NEXT
6850 B(V%)=F:D(U%)=X
6860 IF U%>0 THEN GOTO 6530
6870 E(3)=B:E(5)=C%:E(7)=R%
6880 ENDPROC
6890
7000 DEF PROCJAC:REM calculate jacobian
7010 LOCAL I%,J%,D,P:PR=FALSE
7020 FOR I%=1 TO M%:F(I%)=G(I%):NEXT
7030 FOR J%=1 TO N%:D=P(J%)*1.001:P=P(J%)
7040   P(J%)=D:PROCFUN:P(J%)=P
7050   FOR I%=1 TO M%
7060     A(I%,J%)=(G(I%)-F(I%))/(D-P):NEXT
7070   NEXT
7080 FOR I%=1 TO M%:G(I%)=F(I%):NEXT
7090 PR=TRUE
7100 ENDPROC
7110
8000 DEF PROCS:REM statistics
8010 LOCAL Z:IF M%=N% THEN Z=0:GOTO 8030
8020 Z=SQR((O(2)*O(2))/(M%-N%))
8030 FOR I%=1 TO N%:Z(I%)=Z*SQR(V(I%,I%))
8040   NEXT
8050 ENDPROC
8060
9000 DEF FNK(B):REM Bessel function K0
9010 LOCAL K%,U,V,W,X,Y,Z
9020 IF B>4 THEN GOTO 9100
9030 IF B<1E-37 THEN B=1E-37
9040 X=LN(2/B)-.577215665:U=X
9050 V=1:W=1:Y=B*B/4:K%=0
9060 K%=K%+1:W=W*Y*V*V:U=U+V
9070 V=1/(K%+1):Z=W*U:X=X+Z
9080 IF ABS(Z/X)>5E-8 THEN GOTO 9060
9090 =X
9100 Y=10/B-1:Z=Y+Y:U=-4.5E-8
9110 W=Z*U+6.32575E-7:V=U:U=W
9120 W=Z*U-V-1.1106685E-5:V=U:U=W
9130 W=Z*U-V+2.6953261E-4:V=U:U=W
9140 W=Z*U-V-1.1310504E-2:V=U:U=W
9150 X=SQR(PI/(2*B))*EXP(-B)
9160 =X*(Y*U-V+0.988408174)
```

COMPUTER NOTES

SPEEDING IT UP IN BASIC

by John Logan[a]

Abstract. Execution time of many programs can be markedly shortened by (a) defining frequently used constants in assignment statements or placing them in arrays and by (b) avoiding or minimizing the use of exponentials.

Microcomputers work so rapidly that it is often of little concern whether a problem is solved in two seconds or in one. However, there may be hundreds of calls to lengthy algorithms in certain programs, and shortening of execution time can become important. Examples include the development of drawdown distributions around a well field, sensitivity analyses, regional flow models and investigations of optimization. In such problems, a well function—particularly our old friends W(u) and W(u, r/B)—may be solved by polynomial approximation, and attention to a few simple programing procedures can have a material effect upon execution time.

Consider the following example of a polynomial contrived to represent the type we often use:

$$x = .0011\,u + .0022\,u^2 + .0033\,u^3 + .0044\,u^4$$

Let us do this 1000 times with different values of u and accumulate the total:

```
10 SX=0
20 FOR U=1 TO 1000
30 X=.0011*U+.0022*U↑2+.0033*U↑3+.0044*U↑4
40 SX=SX+X
50 NEXT U
60 PRINT SX
70 END                                        ....(1)
```

Line 30 directly tracks the equation, and this style appears in many published programs. My micro requires 244 seconds to run this example.

Exponentiation is rather slow. By eliminating that operation and rewriting line 30 to

```
30 X=.0011*U+.0022*U*U+.0033*U*U*U
      +.0044*U*U*U*U                          ....(2)
```

execution lowers to 92 seconds.

As the program cycles through the FOR/NEXT loop, each of the four constants must be "translated" to machine language 1000 times. It is much faster that this be done only once through the use of assignment statement. We may add line 15 and modify line 30 as follows:

```
15 C1=.0011:C2=.0022:C3=.0033:C4=.0044
30 X=C1*U+C2*U*U+C3*U*U*U+C4*U*U*U*U
                                              ....(3)
```

Execution time reduces to 39 seconds, a dramatic improvement over the original 244.

Sample program (1) above is simplified almost to the point of absurdity: our usual problems are much more complex. My program for determining W(u, r/B) uses 38 constants and exponentiations to the power of 12. In such conditions, the methods of example (3)—although rapid—require tortuous programing. The constants should be placed in an array that is loaded with READ/DATA statements and the repetitive multiplications can best be handled by assignments as in line 25 below. With those modifications, the program of the example becomes:

```
10 DIM C(4): SX=0
15 FOR J=1 TO 4: READ C(J): NEXT
20 FOR U=1 TO 1000
25 U1=U:U2=U*U:U3=U2*U:U4=U3*U
30 X=C(1)*U1+C(2)*U2+C(3)*U3+C(4)*U4
40 SX=SX+X
50 NEXT
60 PRINT SX
70 END
80 DATA .0011,.0022,.0033,.0044
```

This version runs in 54 seconds and is an acceptable compromise between minimum execution time and practical programing.

These suggestions may not work on all micros nor will the stated running times be the same. However, persons interested in shortening the execution of complex programs might try placing frequently used constants in arrays (or in assignment statements) and eliminating (or at least minimizing) exponentiations.

* * * * *

John Logan began working in the ground-water specialty in the Upper Neolithic. Following employment with the Bureau of Reclamation, the Agency for International Development, the United Nations, UNESCO, and county government, he decided to make an honest living and has been a consulting geologist for the last ten years.

[a]Consulting Geologist, P.O. Box 2096, Carmel, California 93921.

Received December 1985, accepted February 1986.
Discussion open until November 1, 1986.

An Automated Numerical Evaluation of Slug Test Data

by M. W. Kemblowski and C. L. Klein[a]

ABSTRACT

Development of a numerical algorithm to analyze slug test data is described. This type of test is very popular for aquifer testing, primarily because of its simplicity. Many such tests are performed to estimate the hydraulic conductivity values of ground-water-bearing formations. Those values in turn are used to calculate pore-water velocities. The algorithm was coded and successfully tested for a hypothetical data set. It has also been applied at a number of field locations. One such application is presented.

INTRODUCTION

This paper is a summary of the development and testing of a numerical algorithm designed to analyze slug test data. This type of test is very popular for aquifer testing, primarily because of its simplicity. Many such tests are performed as part of hydrogeologic assessments. The algorithm utilizes the slug test analysis presented by Bouwer and Rice (1976) and uses a sensitivity analysis for parameter estimation (McElwee, 1985).

THEORY AND ANALYTICAL SOLUTION OF THE SLUG TEST PROBLEM

The theory of the slug test problem is based on the Thiem equation which describes the relationship between the inflow into the borehole and the drawdown.

$$Q = \frac{2\pi K L_e (h - h_w)}{\ln (r/r_w)} \qquad (1)$$

where h_w = piezometric head in the well (ft); h = piezometric head at distance r (ft); r_w = effective radius of the well, including the gravel pack (ft); r = distance from the well center (ft); K = hydraulic conductivity (ft/day); Q = inflow into the borehole (ft^3/day); and L_e = effective aquifer thickness, in this case, height of open section of well (ft).

The rate at which the well-water level will rise depends on the inflow into the well and may be expressed as:

$$\frac{dy}{dt} = - \frac{Q}{\pi r_c^2} \qquad (2)$$

where r_c = internal radius of the well; and y = drawdown at the well. Assuming that at some distance R (radius of influence), the drawdown is dissipated ($h = 0$), one can substitute equation (1) into equation (2) and solve the resulting equation for y to obtain:

$$y_t = y_0 \exp \left[- \frac{2 K L_e t}{r_c^2 \ln (R/r_w)} \right] \qquad (3)$$

$$K = \frac{r_c^2 \ln (R/r_w)}{2 L_e t} \ln \frac{y_0}{y_t} \qquad (3a)$$

where R = effective radial distance at which the drawdown is dissipated; y_0 = drawdown in well at time zero; y_t = drawdown in well at time t; and t = time since y_0.

[a]Shell Development Company, Westhollow Research Center, P.O. Box 1380, Houston, Texas 77001.

Received June 1987, revised November 1987, accepted November 1987.

Discussion open until January 1, 1989.

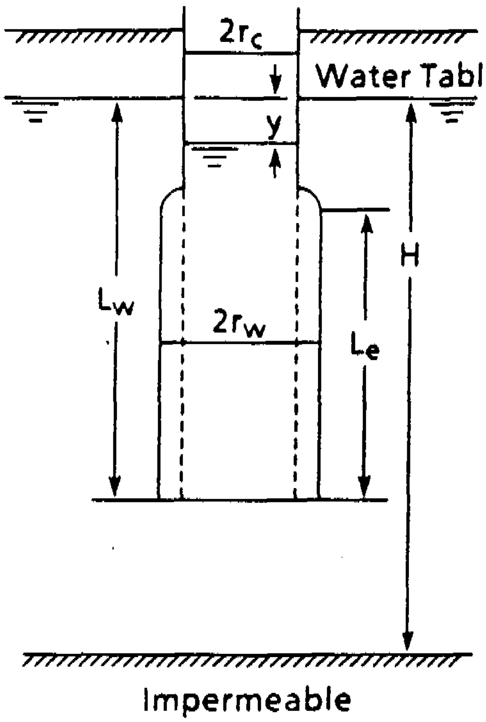

Fig. 1. Geometry and symbols of slug test.

Values of R were experimentally determined (Bouwer and Rice, 1976) for different values of r_w, L_e, L_w, and H (see Figure 1). For a partially penetrating well, the following empirical equation was developed:

$$\ln \frac{R}{r_w} = 1/[\ \frac{1.1}{\ln(L_w/r_w)} + \frac{A + B \ln((H - L_w)/r_w)}{(L_e/r_w)}\ ] \quad (4)$$

where A and B are dimensionless parameters shown in Figure 2 as functions of L_e/r_w. The experiments indicated the effective upper limit of $\ln((H - L_w)/r_w)$ is 6. This upper limit is included in the program.

For a fully penetrating well ($H = L_w$), R is calculated using the following relation:

$$\ln \frac{R}{r_w} = 1/[\ \frac{1.1}{\ln(L_w/r_w)} + \frac{C}{(L_e/r_w)}\ ] \quad (5)$$

where C is a dimensionless coefficient shown in Figure 2 as a function of L_e/r_w.

PARAMETER ESTIMATION BY SENSITIVITY ANALYSIS

For simplicity, equation (3) is rewritten as follows:

$$K = \frac{D}{t} \ln \frac{y_0}{y_t} \quad (6a)$$

where

$$D = \frac{r_c^2 \ln(R/r_w)}{2L_e}, \quad (6b)$$

D is a known constant for a given test. Using equation (6a), we can express drawdown y_t as a function of time and hydraulic conductivity.

$$y_t(K) = y_0\, e^{-Kt/D} \quad (7)$$

The basic idea of parameter estimation technique is to calculate a value of K that would minimize the difference between observed and calculated values of drawdown. This is done by iterations. After each iteration, the "old" value of K is updated.

$$K^* = K + \Delta K \quad (8)$$

The sensitivity analysis provides a tool to calculate ΔK.

Using the Taylor expansion and neglecting the terms of the order higher than one, we can estimate the value of drawdown $y_t(K + \Delta K)$ as a function of $y_t(K)$.

$$y_t(K + \Delta K) = y_t(K) + \frac{\partial y}{\partial K} \Delta K =$$

$$y_0\, e^{-Kt/D} - y_0 (\frac{t}{D})\, e^{-Kt/D} \Delta K = y_t(K)(1 - \frac{t}{D} \Delta K) \quad (9)$$

Using equation (9), we may now develop an expression for the total square error between the observed drawdown y_i^0 and the drawdown calculated by equation, $y_i^* = y_t(K + \Delta K)$ (subscript i refers to time).

$$E = \sum_{i=1}^{N} (y_i^0 - y_i^*)^2 = \sum_{i=1}^{N} (y_i^0 - y_i + y_i \frac{t_i}{D} \Delta K)^2 =$$

$$\sum_{i=1}^{N} [(y_i^0 - y_i)^2 + 2(y_i^0 - y_i) y_i \frac{t_i}{D} \Delta K + (y_i \frac{t_i}{D} \Delta K)^2] \quad (10)$$

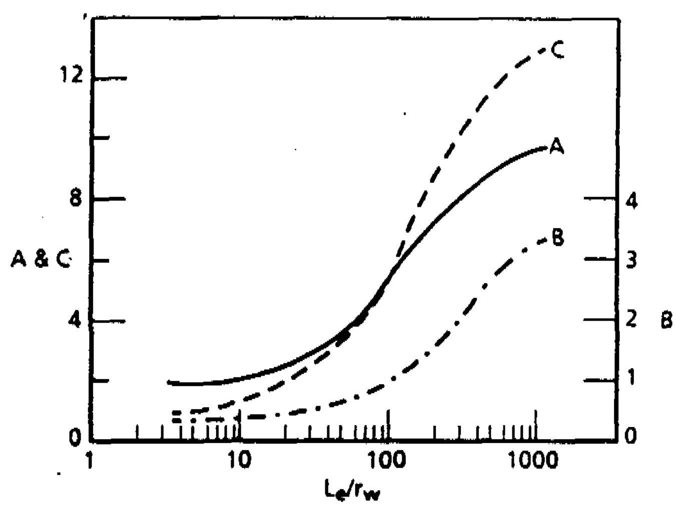

Fig. 2. Curves relating coefficients A, B, and C to L_e/r_w (after Bouwer and Rice, 1976).

where N is the number of observations.

This total square error may be minimized with respect to ΔK.

$$\frac{\partial E}{\partial \Delta K} = 2 \sum_{i=1}^{N} \left[(y_i^0 - y_i) y_i \frac{t_i}{D} + y_i^2 \frac{t_i^2}{D^2} \Delta K \right] \equiv 0 \quad (11)$$

Equation (11) is used to estimate the conductivity correction.

$$\Delta K = -D \sum_{i=1}^{N} \left[(y_i^0 - y_i) y_i t_i \right] / \sum_{i=1}^{N} y_i^2 t_i^2 \quad (12)$$

The numerical algorithm consists of the following steps:

1. Read the input data.
2. Calculate the effective radius using equation (4) (partially penetrating well) or (5) (fully penetrating well).
3. Calculate D [equation (6b)].
4. Calculate simulated drawdown $\{y_i\}$ [equation (7)].
5. Calculate the conductivity correction [equation (12)].
6. Calculate "new" conductivity [equation (8)].
7. Calculate total square error [equation (10)].
8. Estimate the standard deviation σ using the following expression:

$$\sigma = \left[\frac{1}{N-1} (E) \right]^{1/2} \quad (13)$$

9. If the number of iterations $<$ NITER, go back to step 4 (NITER = maximum number of iterations).
10. Print out the results.
11. Stop.

This algorithm was coded in FORTRAN for IBM PC. In order to use it, the user has to provide the test geometry and drawdown data, and estimate parameters A and B or parameter C using Figure 2. The program does not have a weighing system that would consider early data more important than the late ones (Bouwer, 1978). However, the user can limit the number of data points.

MODEL TESTING

The numerical solution was tested using a computer-generated data set. This set of drawdown data was calculated for a fully penetrating, partially screened well of the internal radius $r_c = 0.05$ m, and the external radius $r_w = .1$ m. The initial saturated thickness of the aquifer was $L_w = 15$ m, and the screen height was $L_e = 10$ m. For these conditions, dimensionless parameter C was estimated from Figure 2 to be C = 1.5. To generate the drawdown data using equation (7), the value of the hydraulic conductivity was assumed to be K = .288 m/day (.0002 m/min). The initial drawdown was $y_0 = 1$ m. The drawdown values were calculated for 10 minutes, with a one-minute interval (Figure 3). This data set was then used to calculate the hydraulic conductivity of the system using the developed numerical procedure. The initial estimated value of hydraulic conductivity was .0144 m/day (0.00001 m/min). It took the program five iterations to calculate the correct value of hydraulic conductivity (Figure 3). Table 1 shows the results for the five iterations.

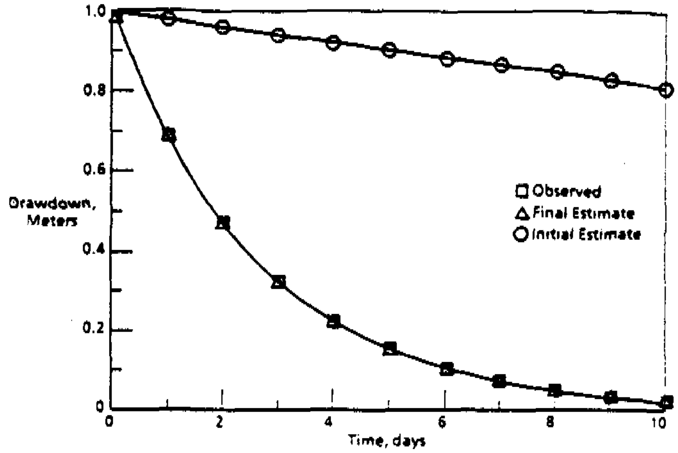

Fig. 3. Model testing.

MODEL APPLICATION

The automated evaluation procedure has been used successfully at a number of locations to interpret slug test data. One recent application was done to estimate the hydraulic conductivity at a

Table 1. Model Application and Results

Iteration	K (m/min)	σ(m)
0	0.100E-04	0.79
1	0.779E-04	0.031
2	0.144E-03	0.01
3	0.188E-03	0.0018
4	0.199E-03	0.0007
5	0.200E-03	0.00003
6	0.200E-03	0.00003

site in Kalkaska, Michigan. The field test was performed using a partially penetrating well with inner radius $r_c = 0.104$ ft and external radius $r_w = 0.281$ ft. The well penetration depth L_w was equal to 3.115 ft. The length of the screen under the water table L_e was equal to L_w. The total saturated thickness was estimated to be 100 ft. The dimensionless parameters A and B, estimated from Figure 2, were 1.8 and 0.25, respectively. The test was performed by submerging a closed bailer into the well, thus creating a negative drawdown. The initial value of the negative drawdown was 0.68 ft. Figure 4 shows the field data and the simulated drawdown for the estimated hydraulic conductivity $K = 0.000611$ ft/sec which was obtained after five iterations. It can be seen that the simulated results fit the field data quite well.

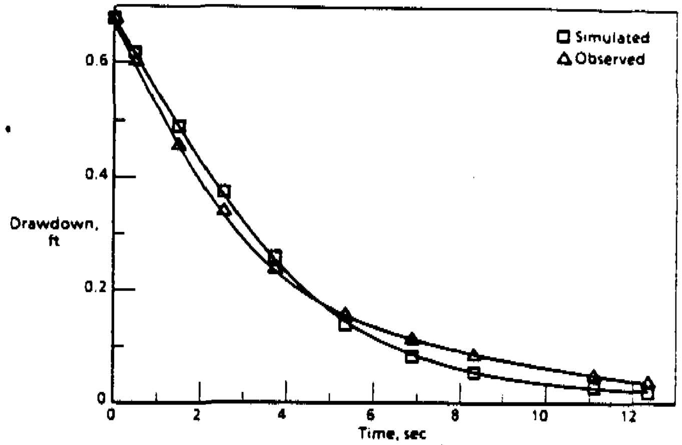

Fig. 4. Model application.

SUMMARY

An automated numerical procedure was developed to analyze slug test data. The procedure is based on the sensitivity analysis for parameter estimation. The solution was validated using computer-generated data. It also has been used successfully at a number of locations. One such application at a Kalkaska, Michigan site is described.

ACKNOWLEDGMENTS

The authors gratefully acknowledge helpful discussions with J. D. Colthart of Shell Development Company. We thank the management of Shell Oil Company for permission to publish this paper.

REFERENCES

Bouwer, H. 1978. Groundwater Hydrology. McGraw-Hill, New York.

Bouwer, H. and R. C. Rice. 1976. A slug test for determining hydraulic conductivity of unconfined aquifers with completely or partially penetrating wells. Water Res. Research. v. 12, pp. 423-428.

McElwee, C. 1985. Sensitivity analysis. In NATO Advanced Study Institute on Fundamentals of Transport Phenomena in Groundwater. Newark, Delaware (ed., Jacob Bear).

* * * * *

Marian W. Kemblowski is a Research Engineer with Shell Development Company, Houston, Texas. He received his M.S. in Civil Engineering from the Technical University of Warsaw, Poland, and his Ph.D. in Hydrology from the Institute of Land Reclamation, Warsaw, Poland. His current research interests are in the area of quantitative analysis of miscible and immiscible hydrocarbon transport in the subsurface.

Catherine L. Klein is a Research Technician with Shell Development Company. She is a B.S. student at the University of Houston, University Park, Texas, with double majors in Chemical Engineering and Computer Science. She has extensive experience in applying computer models to characterizing pollutant transport in ground water.

GROUND WATER

Computer Notes

A Method to Determine the Formation Constants of Leaky Aquifers, and Its Application to Pumping Test Data

by F. Kohlbeck[a] and A. Alvarez[b]

Abstract. A method to calculate aquifer transmissivity, storage coefficient, and the leakage coefficient from pumping test data for a leaky aquifer is presented. The method is carried out by a computer program and is based on a minimization of the sum of squares of differences between drawdown in the observation well and the theoretical values from the Hantush and Jacob formula. No user defined starting points are necessary. Random error estimates for the parameters are given. Applications of the method are illustrated using data from pumping tests performed in leaky aquifers at the Cauca River Valley, Colombia.

Introduction

A great number of computer programs exist for the calculation of aquifer parameters from pumping test data. The parameters are found by fitting theoretical drawdowns as a function of time to measured values. Most of the programs use the Theis (1935) equation for confined aquifers. An overview can be taken from Yeh (1987). Only a few methods use the more general equation of Hantush and Jacob (1955) for leaky aquifers.

The first program for this purpose was published by Saleem (1970). He used standard routines of a FORTRAN library on an IBM mainframe to perform a nonlinear least-squares approach. These routines are not available for personal computers. The methods used within these subroutines are not described in the publication. The program does not contain special features for treating the specific shape of Hantush equation. Cobb et al. (1982) used the gradient (Newtonian) method for the optimization. This method fails if the normal equations are ill-conditioned. Chander et al. (1981a) fit an approximation of the well function for leaky aquifers to experimental data. The approximation was first published by Hantush (1956) and does not match well at early time values to the exact solution. The optimization is performed by a quasi-Newtonian method (Marquardt algorithm) for solving with nonlinear least squares. This method is superior to the simple Newtonian approach. The same authors (1981b) also used Kalman filtering with success. Another method has been given by Şen (1986) who used the slopes of successive data points to calculate the parameters directly from Hantush approximation.

The result of a nonlinear least-squares procedure frequently is not the optimum solution of the problem. It may happen that the calculation terminates at a local minimum. In this case, another starting point can lead to another solution. However, a good program should always result in the best solution one can obtain from the data. Therefore, one has to test extensively with real and with perturbed data to determine whether the final solution depends on the starting point or not.

The method presented in this paper is based on the Hantush and Jacob (1955) equation for leaky aquifers. This equation does not account for storage in the leaking unit as was treated later by Hantush (1960) and Neuman and Witherspoon (1969a). The method uses special techniques of

[a]Techn. Univ. Vienna, Abt. Geophysics, Gusshausstrasse 27-29, A1040 Vienna, Austria.

[b]Universidad Nacional de Colombia, Dpto. de Geociencias, Apartado Aereo 14490, Bogotá D.E., Colombia.

Received April 1989, revised April and July 1990, accepted August 1990.

Discussion open until November 1, 1991.

Table 1. Comparison of Results from Examples of Yeh (1988), Walton (1962), and Saleem (1970) with the Presented Method

Author	*Transmiss.* T	*Stor. coeff.* S	*Vert. perm.* K'	*Stand. dev.* σ
	m^2/d	$E\text{-}04$	$E\text{-}03\ m/d$	m
Yeh original	1139	1.93	—	0.00547
present	1134 ± 2	1.94 ± 0.02	0.27 ± 0.20	0.00557
	$gal/d/ft$	$E\text{-}04$	$E\text{-}02\ g/d/ft^2$	ft
Walton orig.	1510	2.	11.0	0.200
Saleem	1801	1.8	6.6	0.156
present	1856 ± 16	1.66 ± 0.1	6.0 ± 0.4	0.147

nonlinear least-squares fitting to obtain the best fit independent of the starting point. The case of a nonleaky aquifer is considered a special case of a leaky aquifer with leakage trending towards zero.

Computer Program

The program is written in FORTRAN 77 and contains more than 3600 lines of source code. The majority of the subroutines are taken from CERNLIB and are described in detail by James and Roos (1971). The tests were performed on an AT-compatible personal computer with math coprocessor. The computation time increases approximately linearly with the number of data pairs and takes less than two minutes on AT-compatible computer with 8 MHz clock and 60 data pairs. The input data consist of a text line, a line with the code for the units, and a line that contains the distance r, the pumping rate Q, and the thickness of the semiconfining bed b′. Further lines contain the observation times and drawdowns. No starting values for the parameters are needed. A further option calculates the theoretical drawdowns for given values of storage coefficient S, transmissivity T, and permeability K′ at given times.

The output contains the input data, the calculated values for S, T, and K′, with their standard errors and a table of calculated and observed drawdowns.

The errors of the parameters S, T, and K′ are calculated with the assumption that the differences between calculated and observed drawdowns are random errors with normal distribution. In practical cases the assumptions for the validity of the well function for leaky aquifers [see equation (1) later in this context] are not fulfilled exactly, and the errors consist of a systematic and a random part. Therefore, the calculated standard errors of the parameters can be seen as a lower limit. The real errors will be much higher in most of the cases.

Examples

Published Data

The program was tested with already published data for the purpose of comparison with known methods and with unpublished data to demonstrate the practical application.

The published data of well 19 from Walton (1962) and from Yeh (1987) who used Todd (1980) values were used to test the program. The results are compared in Table 1. The calculations of Yeh are based on nonleaky aquifers.

For reasons of compatibility, the thickness of the semiconfining bed b′ has been set to 10 m, so vertical permeability K′ could be calculated. The standard deviation σ in Table 1 is defined by:

$$\sigma = \sqrt{G/(N - n)}$$

with G the sum of squares of the differences between calculated and measured values of drawdown (s), the number of observations (N), and the number of parameters (n). For the leaky aquifer $n = 3$, while for the nonleaky case $n = 2$. Therefore, σ is less for the calculation of Yeh than with the present calculation because n is smaller for Yeh's method.

Data from Cauca River Valley

Practical examples were taken from measurements at the Cauca River Valley, Colombia, which covers an area of 4,600 km^2. The tests were performed in the southern part of the valley and are reported by Alvarez and Tenjo (1971). Data are presented here (Table 2) to provide published data from a leaky system that other researchers can use when comparing computer programs.

The Cauca River Valley has a tectonic origin and is underlain with alluvial sediments that have become the richest aquifers of the Colombian Andean zone. The total thickness of the alluvium is unknown. However, it has been classified in three hydrogeological units with the following characteristics:

Unit A is from the surface to 110 m depth. Its upper 70 m are largely clay and silt, individual lenses of which can reach 36 m of thickness. The lower 40 m are composed of sand and gravel with some lenses of clay. This lower part contains several types of aquifers, i.e., free, confined, and leaky aquifers. The yields range from 10 to 264 l/s, with a median yield of 130 l/s. The measured specific capacities range from 4 to 13 l/(sm), with a median value of 8 l/(sm). The transmissivities range from 300 to 2800 m^2 per day, while the storage coefficients range from 7×10^{-4} to 1.05×10^{-2}. For the leaky aquifers, the leaky coefficients range from 5.03×10^{-4} to 3.9×10^{-2} per day.

Unit B underlies unit A. It is mainly composed of clay with a thickness of about 80 m, and is considered as the confining bed.

Table 2a. Computer Evaluation of Colombian Pumping Test Data: Pumping Test No. 1

Input parameters:

	r(m)	Q(l/s)	b'(m)
Value	105.0	145.0	1.000

Calculated parameters:

	$T(m^2/d)$	S	K'(m/d)
Value	1994.	0.1379E-02	0.2913E-02
Error	2.538	0.1073E-04	0.3134E-04

Observed (s_o) and calculated (s_c) drawdowns:

Time min.	s_o m	s_c m	$s_o - s_c$ m
1.000	0.1000E-01	0.9013E-02	0.9870E-03
2.000	0.5000E-01	0.6041E-01	−0.1041E-01
3.000	0.1100	0.1263	−0.1631E-01
4.000	0.1800	0.1910	−0.1104E-01
5.000	0.2400	0.2510	−0.1099E-01
6.000	0.2900	0.3057	−0.1575E-01
7.000	0.3500	0.3557	−0.5708E-02
8.000	0.3900	0.4014	−0.1145E-01
9.000	0.4400	0.4435	−0.3522E-02
10.00	0.4800	0.4824	−0.2410E-02
16.00	0.6500	0.6677	−0.1772E-01
20.00	0.7700	0.7609	0.9101E-02
25.00	0.8600	0.8564	0.3646E-02
30.00	0.9500	0.9355	0.1445E-01
35.00	1.020	1.003	0.1694E-01
40.00	1.060	1.062	−0.1774E-02
43.00	1.100	1.094	0.6384E-02
45.00	1.140	1.114	0.2637E-01
50.00	1.170	1.160	0.9997E-02
55.00	1.220	1.202	0.1813E-01
60.00	1.260	1.240	0.2001E-01
70.00	1.320	1.307	0.1285E-01
80.00	1.380	1.365	0.1519E-01
90.00	1.420	1.415	0.4855E-02
100.0	1.470	1.460	0.1033E-01
110.0	1.510	1.499	0.1054E-01
120.0	1.520	1.535	−0.1535E-01
150.0	1.620	1.625	−0.5092E-02
180.0	1.690	1.696	−0.5515E-02
210.0	1.740	1.753	−0.1264E-01
240.0	1.780	1.800	−0.2008E-01
270.0	1.820	1.840	−0.2017E-01
300.0	1.860	1.875	−0.1454E-01
330.0	1.890	1.904	−0.1431E-01
347.0	1.880	1.919	−0.3947E-01
360.0	1.920	1.930	−0.1034E-01
420.0	1.970	1.974	−0.3594E-02
454.0	1.970	1.994	−0.2398E-01
480.0	2.000	2.008	−0.7933E-02
510.0	2.010	2.023	−0.1252E-01
540.0	2.030	2.036	−0.5689E-02
560.0	2.040	2.044	−0.3765E-02
600.0	2.070	2.058	0.1156E-01
615.0	2.060	2.063	−0.3479E-02
660.0	2.090	2.077	0.1271E-01
720.0	2.110	2.093	0.1695E-01
780.0	2.130	2.106	0.2366E-01
840.0	2.150	2.118	0.3239E-01
900.0	2.140	2.127	0.1279E-01
910.0	2.150	2.129	0.2133E-01
960.0	2.160	2.135	0.2456E-01
1020.	2.160	2.143	0.1747E-01
1080.	2.160	2.149	0.1136E-01
1140.	2.150	2.154	−0.3941E-02
1260.	2.150	2.163	−0.1255E-01
1320.	2.150	2.166	−0.1606E-01
1380.	2.150	2.169	−0.1912E-01
1410.	2.150	2.171	−0.2051E-01

Table 2b. Computer Evaluation of Colombian Pumping Test Data: Pumping Test No. 2

Input parameters:

	r(m)	Q(l/s)	b'(m)
Value	109.0	123.0	1.000

Calculated parameters:

	$T(m^2/d)$	S	K'(m/d)
Value	1086.	0.3571E-02	0.7116E-02
Error	3.257	0.4137E-04	0.1166E-03

Observed (s_o) and calculated (s_c) drawdowns:

Time min.	s_o m	s_c m	$s_o - s_c$ m
1.000	0.1000E-01	0.0000	0.1000E-01
1.500	0.1500E-01	0.0000	0.1500E-01
2.000	0.2000E-01	0.6206E-04	0.1994E-01
2.500	0.3000E-01	0.4054E-03	0.2959E-01
3.000	0.4000E-01	0.1261E-02	0.3874E-01
3.500	0.5000E-01	0.2840E-02	0.4716E-01
4.000	0.6000E-01	0.5269E-02	0.5473E-01
4.500	0.7000E-01	0.8596E-02	0.6140E-01
5.000	0.8000E-01	0.1281E-01	0.6719E-01
6.000	0.1000	0.2367E-01	0.7633E-01
7.000	0.1150	0.3729E-01	0.7771E-01
8.000	0.1300	0.5302E-01	0.7698E-01
9.000	0.1500	0.7031E-01	0.7969E-01
10.00	0.1500	0.8870E-01	0.6130E-01
15.00	0.2500	0.1872	0.6275E-01
20.00	0.3200	0.2843	0.3570E-01
25.00	0.3900	0.3741	0.1592E-01
30.00	0.4500	0.4559	−0.5857E-02
35.00	0.5200	0.5302	−0.1021E-01
40.00	0.5800	0.5980	−0.1802E-01
45.00	0.6350	0.6601	−0.2511E-01
50.00	0.6900	0.7172	−0.2723E-01
55.00	0.7400	0.7700	−0.3003E-01
60.00	0.7900	0.8190	−0.2903E-01
70.00	0.8750	0.9074	−0.3236E-01
80.00	0.9500	0.9851	−0.3506E-01
90.00	1.025	1.054	−0.2917E-01
100.0	1.090	1.116	−0.2622E-01
110.0	1.150	1.172	−0.2236E-01
120.0	1.210	1.224	−0.1351E-01
150.0	1.350	1.353	−0.3431E-02
180.0	1.460	1.457	0.2757E-02
210.0	1.545	1.543	0.2438E-02
240.0	1.620	1.614	0.5848E-02
270.0	1.680	1.675	0.4822E-02
300.0	1.740	1.728	0.1215E-01
330.0	1.785	1.774	0.1122E-01
360.0	1.820	1.814	0.5843E-02
420.0	1.890	1.882	0.8252E-02
480.0	1.950	1.936	0.1411E-01
540.0	1.995	1.980	0.1501E-01
600.0	2.040	2.016	0.2359E-01
660.0	2.070	2.047	0.2321E-01
720.0	2.100	2.072	0.2763E-01
780.0	2.130	2.094	0.3594E-01
840.0	2.145	2.113	0.3244E-01
900.0	2.160	2.128	0.3156E-01
960.0	2.170	2.142	0.2788E-01
1020.	2.175	2.154	0.2105E-01
1080.	2.175	2.164	0.1077E-01
1140.	2.175	2.173	0.1817E-02
1200.	2.180	2.181	−0.1006E-02
1260.	2.185	2.188	−0.2857E-02
1320.	2.185	2.194	−0.8872E-02
1380.	2.190	2.199	−0.9165E-02
1440.	2.190	2.204	−0.1382E-01
1500.	2.190	2.208	−0.1795E-01
1560.	2.185	2.212	−0.2659E-01
1620.	2.180	2.215	−0.3482E-01
1680.	2.180	2.218	−0.3769E-01
1681.	2.180	2.218	−0.3773E-01

Unit C underlies unit B. It is composed of sand, gravel, and some clay of unknown thickness. It is a confined aquifer tapped by several flowing artesian wells. Below unit C follow sedimentary, metamorphic, and igneous rocks.

In the pumping tests presented in this paper, leakage was obtained from unit A.

The constants of five different pumping tests are presented in Table 3. The calculation of hydraulic parameters was carried out with the type curve method, with the inflection point method after Hantush (1956) and with the computer program. The results are listed in Table 3.

It can be seen that the computer method compares well with the conventional methods and that the standard deviation is always lowest with the computer's least-squares approximation. Furthermore, the computer method has incorporated an error estimation for the parameters. As already mentioned, these error estimates have little practical relevance because they assume that the data are distributed normally around the well function. However, the assumptions for a leaky aquifer made by Hantush and Jacob (1955) are not fulfilled completely in any one of the examples. This can be gathered from the Tables 2a and 2b which show a partial output of the computer program for two pumping tests of the Cauca Valley. One recognizes that the differences between measured and calculated drawdowns (last column) are not randomly distributed over the time scale: one can divide the series of measurements into sections that contain exclusively positive or negative differences. The series of pumping test No. 1 (Table 2a) consists of five and that of No. 2 (Table 2b) consists of four such sections. This bias cannot be removed by selecting other aquifer parameters but only by applying another, more realistic well function as discussed by Neuman and Witherspoon (1969b).

Method

The drawdown, s, in an observation well caused by a constant pumping rate Q in a production well can be written as (Hantush and Jacob, 1955):

$$s_c(t) = z_1 \cdot F(t; z_2, z_3) \tag{1a}$$

with

$$F(t; z_2, z_3) = \int_{z_2/t}^{\infty} (1/x) \cdot \exp[-x - 0.25(z_3)^2/x]\,dx \tag{1b}$$

The constants z_1, z_2, z_3 are related to the transmissivity T, the aquifer storage coefficient S, and the vertical permeability of the semiconfined bed K′ by:

$$\begin{aligned} z_1 &= \alpha \cdot Q/T \\ z_2 &= S \cdot \beta \cdot r^2/T \\ (z_3)^2 &= K' \cdot r^2/(b' \cdot T) \end{aligned} \tag{2}$$

in which r = distance between the observation well and the pumping well; b′ = saturated thickness of the semiconfining bed; and α and β are constants whose values are dependent on the units used. For metric units, $\alpha = 1./(4\pi)$, and $\beta = 0.25$. This formula holds only for certain restrictions on the parameters (see Walton, 1979).

Table 3. Comparison of Results from Type Curve Interpretation (T), Hantush (1956) Inflection Point Evaluation (I), and Least-Squares Calculation (C) with Examples of Field Measurements

Pumping test no.		*Transmiss. T m^2/d*	*Stor. coeff. S E-03*	*Leakance K′/b′ E-03/d*	*Stand. dev. σ^2 E-03 m*
	T	1847	1.54	3.77	26
1	I	1900	1.44	3.88	28
	C	1994 ± 3	1.38 ± 0.01	2.91 ± 0.03	16
	T	1302	3.62	7.82	38
2	I	1037	3.76	5.78	111
	C	1086 ± 3	3.57 ± 0.04	7.12 ± 0.12	35
	T	1408	2.35	3.17	24
3	I	1400	2.27	1.69	50
	C	1321 ± 4	2.36 ± 0.04	4.00 ± 0.13	20
4	T	2807	1.47	0.169	56
	C	3088 ± 8	1.27 ± 0.01	0.00 ± 0.00	35
5	T	893	2.53	1.03	39
	C	907 ± 2	2.37 ± 0.02	1.04 ± 0.03	28

If one has a series of observed drawdowns $s_o(t_i)$ at observation times t_i, optimal estimates $\hat{z}_1, \hat{z}_2, \hat{z}_3$ for the parameters z_1 to z_3 can be determined by minimizing the sum of squares

$$G = \sum_i \epsilon_i^2 \tag{3a}$$

of the differences

$$\epsilon_i = s_o(t_i) - s_c(t_i) \tag{3b}$$

between calculated and measured values of s. From equation (2), T and S can be calculated from z_1 and z_3. With a known value for b′ also, K′ can be calculated from z_3. Because equation (1) obviously is not a linear combination of z_1 to z_3, a simple linear least-squares technique cannot be used for obtaining the optimum values. The program uses a nonlinear optimization procedure as follows:

Starting with arbitrary estimates for z_2 and z_3 and substituting equations (1) into equation (3b) one obtains:

$$y_i = z_1 a_i + \epsilon_i \tag{4}$$

with known values of $a_i = F(t_i; z_2, z_3)$; and $y_i = s_o(t_i)$.

From equation (4), one obtains the normal equation

$$\sum_i (y_i - z_1 a_i) a_i = 0$$

and the optimal estimate $\hat{z}_1(z_2, z_3)$ for z_1:

$$\hat{z}_1(z_2, z_3) = \frac{\sum y_i a_i}{\sum_i a_i a_i} \tag{5}$$

Equation (5) reduces the three-dimensional nonlinear optimization problem to a two-dimensional one, whereby computation effort is considerably shortened.

The nonlinear optimization searches for the minimum of G from equation (3a) with respect to z_2 and z_3, and uses

$z_1 = \hat{z}_1$ from equation (5). It is first carried out with a Monte Carlo method to give rough estimates of z_2 and z_3 and then continues with the simplex method of Nelder and Mead (1965). Both methods are described by James (1972). They offer some advantages compared with the conventional Newtonian and variable metric methods that are most frequently used for function minimization. The matrix of normal equations that is used with the Newtonian methods frequently is ill-conditioned, and the algorithm will diverge in this case (Marquardt, 1963). The presented method will find the best solution also when the Newtonian ends at a local minimum.

The integral of equation (1b) is solved numerically by a modified Romberg algorithm. The direct application of numerical integration to the integral is not favorable, because the intermediate values which are necessary for integration are not selected properly by usual methods. With the substitution of $x = \exp(y)$, equation (1b) can be written:

$$F(t; z_2, z_3) = \int_{\ln(z_2/t)}^{\infty} \cdot \exp[-\exp(y) - 0.25 \cdot (z_3)^2 \cdot \exp(-y)]\,dy \qquad (6)$$

which is integrated much faster and with higher accuracy than expression (1b). The upper bound for x in equation (1b) can be taken from Hantush (1956) to be 8 instead of infinite with sufficient accuracy. The lower bound is taken to be $u = 0.5 \cdot (z_3)^2/[b + |\ln(z_2/t)|]$ where b denotes a constant (a proper value is 4) which depends on the accuracy of the calculations. The lower boundary u is selected only when $u < z_2/t$.

The speed of calculation of the whole number of integrations for different time values t_i can be increased further if the areas beyond the integral overlap each other for different time values. It follows that equation (6) can also be written:

$$F(t_{i+1}) = F(t_i) + \int_{\ln(z_2/t_{i+1})}^{\ln(z_2/t_i)} \cdot \exp[-\exp(y) - 0.25 \cdot (z_3)^2 \cdot \exp(-y)]\,dy$$

The second part of the right side is computed much faster than the whole integral equation (6). The first part, $F(t_i)$, is already known from the previous calculation.

Errors

The basic statistical formula for calculating the random errors of the parameters z_i can be taken from Linnik (1961).

$$\delta z_i = v_{ii} \sqrt{G/(N - n)}$$

where δz_i = standard error of z_i; N = number of observations; n = number of parameters (n = 3); G = sum of squared differences between calculated and measured drawdowns [from equation (3a)]; v_{ii} = diagonal element of variance matrix V; $V = W^{-1}$; and $w_{ik} = (\partial^2 G)/(\partial z_i\, \partial z_k)$, element of matrix W. The derivatives are calculated by finite differences of function values.

Availability

Authorized users of CERNLIB may obtain a copy of the program by request to one of the authors. Permission for using CERNLIB can be obtained by writing to Program Library Division DD, CERN, CH-1211, Geneve 23, Switzerland with reference to program package D506 Minuit.

References

Alvarez, A. and S. Tenjo. 1971. Hydrogeology of the Cauca River Valley southern part. Unpublished field data. Ingeominas-CVC, Colombia.

Chander, S., P. N. Kapoor, and S. K. Goyal. 1981a. Analysis of pumping test data using Marquardt algorithm. Ground Water. v. 19, no. 3, pp. 275-278.

Chander, S., P. N. Kapoor, and S. K. Goyal. 1981b. Aquifer parameter estimation using Kalman filters. Journal of Irrigation and Drainage Division, ASCE. Proc. Paper 16101. v. 107, no. IR1, pp. 25-33.

Cobb, P. M., C. D. McElwee, and M. A. Butt. 1982. Analysis of leaky aquifer pumping test data: An automated numerical solution using sensitivity analysis. Ground Water. v. 20, no. 3, pp. 325-333.

Hantush, M. S. and C. E. Jacob. 1955. Non-steady radial flow in an infinite leaky aquifer. Trans. Amer. Geophys. Union. v. 36, no. 1, pp. 95-100.

Hantush, M. S. 1956. Analysis of data from pumping tests in leaky aquifers. Trans. Amer. Geophys. Union. v. 37, no. 6, pp. 702-714.

Hantush, M. S. 1960. Modification of the theory of leaky aquifers. J. Geophys. Res. v. 65, no. 11, pp. 3713-3725.

James, F. 1972. Function minimization. Proceedings of the 1972 CERN Computing and Data Processing School, Pertisau, Austria, September 10-24, 1972. CERN 72-21. 50 pp.

James, F. and M. Roos. 1971. Minuit. Long write-up. CERN Program Library. CERN CH1211 Genf 23, Switzerland.

Linnik, J. W. 1961. Methode der kleinsten Quadrate in moderner Darstellung. VEB, Berlin. 315 pp.

Marquardt, D. W. 1963. An algorithm for least-squares estimation of nonlinear parameters. J. Soc. Indust. Appl. Math. v. 11, pp. 431-441.

Nelder, J. A. and R. Mead. 1965. A simplex method for function minimisation. Comput. J. v. 7, p. 308.

Neuman, S. P. and P. A. Witherspoon. 1969a. Theory of flow in a two aquifer system. Water Resour. Res. v. 5, no. 4, pp. 803-817.

Neuman, S. P. and P. A. Witherspoon. 1969b. Applicability of current theories of flow in leaky aquifers. Water Resour. Res. v. 3, no. 4, pp. 817-829.

Saleem, Z. A. 1970. A computer method for pumping-test analysis. Ground Water. v. 8, no. 5, pp. 21-24.

Şen, Z. 1986. Determination of aquifer parameters by slope-matching method. Ground Water. v. 24, no. 2, pp. 217-223.

Theis, C. V. 1935. The relation between the lowering of piezometric surface and the rate and duration of discharge of a well using groundwater storage. Trans. Amer. Geophys. Union. v. 16, pp. 519-524.

Todd, D. K. 1980. Groundwater Hydrology. 2nd ed. John Wiley & Sons, New York. 535 pp.

Walton, W. C. 1962. Selected analytical methods for well and aquifer evaluation. State of Illinois, State Water Survey Division. Bull. 49. 81 pp.

Walton, W. C. 1979. Review of leaky artesian aquifer test evaluation methods. Ground Water. v. 17, no. 3, pp. 270-283.

Yeh, Hund-Der. 1987. Theis solution by nonlinear least-squares and finite-difference Newton's method. Ground Water. v. 25, no. 6, pp. 710-715.

Chemistry

A Computer Program for a Trilinear Diagram Plot and Analysis of Water Mixing Systems[a]

by Michael D. Morris, Jeffrey A. Berk,
Joseph W. Krulik, and Yoram Eckstein[b]

ABSTRACT

The Piper (1953) trilinear diagram has been widely used to graphically represent the dissolved constituents of natural waters and to test for apparent mixtures of waters from different sources. Because of the time required to plot points and calculate the proportional values of mixing, this treatment of data was often quite tedious, particularly in studies involving large numbers of chemical analyses. The PIPER program was written in BASIC to be run on a Hewlett-Packard desktop computer with an X-Y plotter. Data input is in ppm units. The program plots points in all three fields of the trilinear diagram, draws at each point within the central diamond field a circle with a radius correspondent to the concentrations expressed in meq/l, checks for points that fall on a straight line (or within a predetermined tolerance of a straight line) representing postulated mixtures with two end members, and/or within a triangle representing mixtures of three end members. Finally, the program does a numerical analysis of the mixing ratios of the constituents for postulated mixing systems according to the methodology as presented by Piper (1953).

[a]Department of Geology, Kent State University Contribution No. 241.

[b]Department of Geology, Kent State University, Kent, Ohio 44242.

Received April 1982, revised August 1982, accepted September 1982.

Discussion open until July 1, 1983.

INTRODUCTION

In a graphical treatment of chemical analyses of ground water developed by Piper (1953), the character of a ground water can be expressed by three points located in three different fields. The points represent: (1) percentage-reacting equivalents of three major cation constituents (Mg^{++}, Na^{+} and Ca^{++}) in a cation triangular field; (2) percentage-reacting equivalents of three major anion constituents (Cl^{-}, $SO_4^{=}$ and HCO_3^{-}) in an anion triangular field; and (3) the point in the diamond-shaped field representing the overall chemical character of the solution. The last point is plotted at the intersection of rays projected from the points in the anion and cation triangular fields into the diamond field (Figure 1).

Piper's graphical treatment of the chemical analysis allows for an easy discrimination of distinct water types by their plottings in various subareas of the diamond field (Figure 2). Piper (1953) also suggested that water analysis represented by points aligning along a straight line in all three fields should be tested for the possibility that they represent a part of a mixing system. A solution produced by a mixture of two end members is represented in each of the three fields as a point which is located on a straight line in between the points representing the two end members. Moreover, the individual ionic constituents in the mixture will all have been mixed in the same proportions. Similarly, in the case of a mixture from three sources, the solution will be

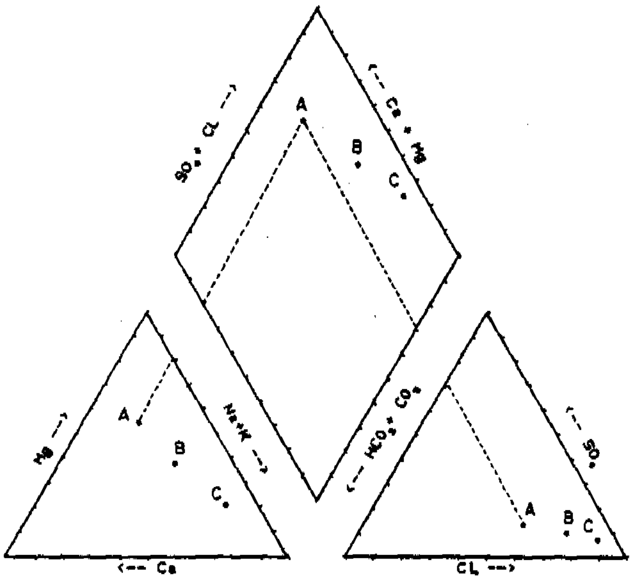

Fig. 1. Piper's (1953) trilinear diagram.

represented in each of the three fields by a point located inside a triangle defined by the three end members. Again, all the ionic constituents will have been mixed in the same proportions.

When only a few points are plotted on a trilinear diagram, it is rather easy to discern and confirm a binary mixing by "eyeballing" of three points aligned on a straight line in all three fields and to make the appropriate computations (Piper, 1953). To discern and confirm a ternary mixing system is more complex. When the number of chemical analyses involved is large, the task of

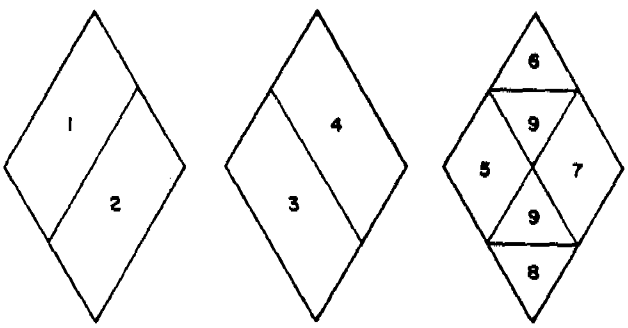

Fig. 2. Water types on a trilinear diagram:
area 1 – $(Ca^{+2} + Mg^{+2}) > (Na^{+} + K^{+})$;
area 2 – $(Ca^{+2} + Mg^{+2}) < (Na^{+} + K^{+})$;
area 3 – $(HCO_3^{-} + CO_3^{-2}) > (Cl^{-} + SO_4^{-2})$;
area 4 – $(HCO_3^{-} + CO_3^{-2}) < (Cl^{-} + SO_4^{-2})$;
area 5 – carbonate hardness (secondary alkalinity) > 50%;
area 6 – noncarbonate hardness (secondary salinity) > 50%;
area 7 – noncarbonate alkali (primary salinity) > 50%;
area 8 – carbonate alkali (primary alkalinity) > 50%;
area 9 – no dominant cation-anion pair.

singling out all possible mixing systems and testing each for validity is extremely tedious, as well as is the mere task of production of a trilinear diagram for a large number of analyses. The following computer program is designed to plot up to 100 chemical analyses on a trilinear diagram and then scan simultaneously all the analyses, testing for all the possible combinations in binary and ternary mixing systems.

The program was designed to place points in all three fields and to calculate and test the proportions needed to postulate possible mixing relationships. Although this program produces reliable calculations for a wide variety of chemical compositions, the user is cautioned that the results can be significantly affected by the selection of input values and certain user-specified options. The user is further cautioned that interpretations must reflect the specific field conditions and locations from which the water samples were collected.

Our computer program is based on Piper's (1953) original assumptions:

1. All of the major constituents have been included in the calculations.

2. All ions are assumed to remain in solution.

3. All the Fe, Al, and Si are present in the water in a colloidal state as oxides and are not in chemical equilibrium with the ionized constituents. Therefore, these elements are not included in calculations of total concentration.

4. Minor constituents of ground water are summed with the six major constituents to which they are respectively related in chemical properties.

5. Water consisting of substantial quantities of free acid cannot be fully represented on the diagram.

The program was written in Hewlett-Packard enhanced BASIC for use on a HP 9845A desktop computer with an optional 9872B X-Y plotter. Options within the program allow graphics to be produced on the cathode-ray-tube (CRT) display, the thermal printer, or the X-Y plotter. Minor variations should allow this program to be adapted to other computers using BASIC. Due to memory limitations on the HP 9845A, the program is actually subdivided into two smaller routines linked together. "PIPER," the first portion of the program, is used to input and store data, compute unit conversions and to plot the resulting percentage values on the trilinear diagram. The mixing calculations may then be performed by the second portion of the program named "MIXING." The transfer of control to the second routine is accomplished in line 3680 of "PIPER" utilizing the LINK command in order to conserve all variables defined earlier. Depending on the computer capabilities that the program is going to be adapted to, it may be stored as one long program or several smaller routines. A flow diagram of the program is shown in Figure 3.

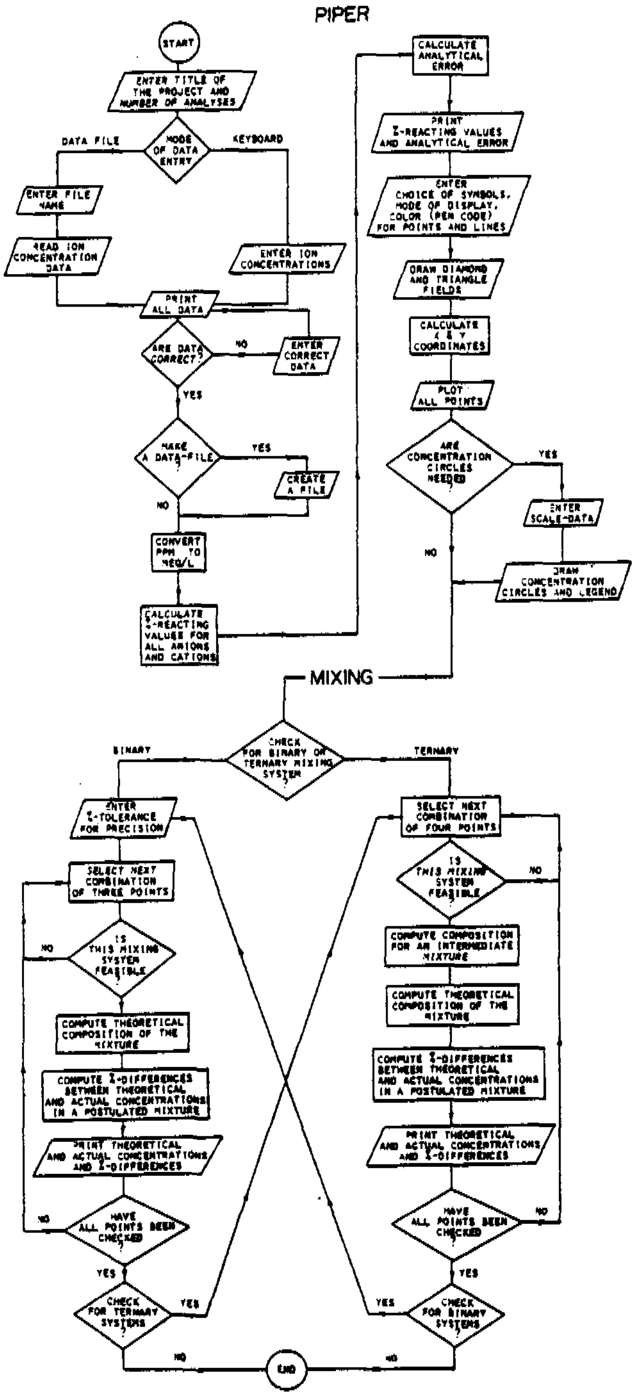

Fig. 3. Flow chart of "PIPER" and "MIXING."

INPUT OF RAW DATA

Input concentrations of various constituents must be in units of parts per million (ppm). The program will convert these units to meq/l, and further to percentage of total dissolved solids.

The program asks for the six major constituents: (Ca^{++}, Mg^{++}, Na^{+}, Cl^{-}, SO_4^{--} and HCO_3^{-}) and only K^{+}, CO_3^{--} and NO_3^{-} as second-rank constituents. Other second-rank constituents can be added with only minor changes in the program. In a single run of the program, data from a maximum of 100 sources may be entered, stored, plotted and tested for mixing trends.

Data input can come from keyboard or data previously stored on a data file. Creation of a data file after input from the keyboard is a user's option.

PLOTTING AND COMPUTATIONAL PROCEDURES

The plotting of points and the drawing of the outline of the triangles and diamond both are done in cartesian coordinates on the H-P graphics system. All trilinear coordinates must be converted to X-Y coordinates. The units used are millimeters for the CRT and will vary on the X-Y plotter depending on the size of the plot. The plotting field is 184.47 by 149.82 units. The primary trilinear diagram is an equilateral triangle with sides divided into 100 units. For ease in reading, cation and anion subtriangles are offset from the upper diamond. The subtriangles are equilateral with sides of 50 units representing a range of 0 to 100% of a specified constituent.

The height of a triangle (Figure 4) is calculated in the following manner:

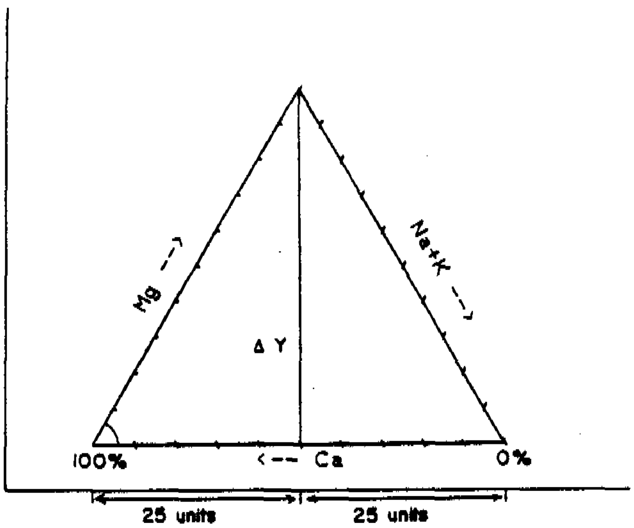

Fig. 4. Dimensional relationship in a triangular field of a trilinear diagram.

$$\tan 60^\circ = \Delta Y/(50/2)$$

$$\Delta Y = 25(\tan 60^\circ)$$

$$\Delta Y \cong 43.30 \text{ units}$$

In similar fashion, the dimensions of the diamond field are found to be 50 units wide and 86.60 units in height.

Points within the cation triangle, if plotted by hand, are based on the percentage-reacting values of Ca^{+2}, Mg^{+2}, Na^{+} and K^{+}; if plotted by this program, the points (Figure 5) are based on the percentage of Ca^{+2} and Mg^{+2} compared to the total cations. Points within the anion triangle are calculated and plotted in a similar fashion based on the percentages of SO_4^{-2} and HCO_3^{-}. The relevant equations are as follows:

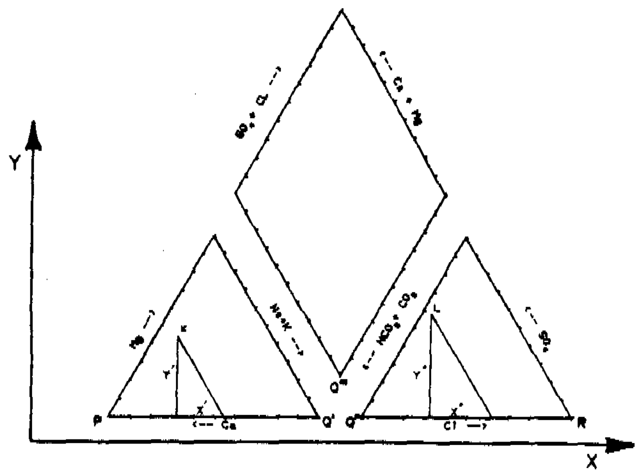

Fig. 5. Coordinate system in the triangular fields of a trilinear diagram.

$$\frac{Y'}{25(\tan 60^\circ)} = \frac{Mg^{+2}(\%)}{100}$$

$$100\,Y' = 25 \tan 60^\circ\, Mg^{+2}(\%)$$

$$Y' = \tan 60^\circ \frac{Mg^{+2}(\%)}{4}$$

$$\tan 60^\circ = Y'/X'$$

$$X' = Y'/\tan 60^\circ$$

$$\frac{Y''}{25(\tan 60^\circ)} = \frac{SO_4^{-2}(\%)}{100}$$

$$100\,Y'' = 25 \tan 60^\circ\, SO_4^{-2}(\%)$$

$$Y'' = \tan 60^\circ \frac{SO_4^{-2}(\%)}{4}$$

$$\tan 60^\circ = Y''/X''$$

$$X'' = Y''/\tan 60^\circ$$

Recalling the conversion: 2% ion concentration = 1 unit on the plotting field

$$X_K = X_{Q'} - Ca^{+2}(\%)\frac{1 \text{ unit}}{2\%} - X'$$

$$X_K = X_{Q'} - \frac{Ca^{+2}(\%)}{2} - \frac{Y'}{\tan 60^\circ}$$

$$X_K = X_{Q'} - \frac{Ca^{+2}(\%)}{2} - \frac{\tan 60^\circ\, Mg^{+2}(\%)/4}{\tan 60^\circ}$$

$$X_K = X_{Q'} - \frac{Ca^{+2}(\%)}{2} - \frac{Mg^{+2}(\%)}{4}$$

$$Y_K = Y_{Q'} + Y'$$

$$Y_K = Y_{Q'} + \tan 60^\circ \frac{Mg^{+2}(\%)}{4}$$

$$X_L = X_R - HCO_3^{-}(\%)\frac{1 \text{ unit}}{2\%} - X''$$

$$X_L = X_R - \frac{HCO_3^{-}(\%)}{2} - \frac{Y''}{\tan 60^\circ}$$

$$X_L = X_R - \frac{HCO_3^{-}(\%)}{2} - \frac{\tan 60^\circ\, SO_4^{-2}(\%)/4}{\tan 60^\circ}$$

$$X_L = X_R - \frac{HCO_3^{-}(\%)}{2} - \frac{SO_4^{-2}(\%)}{4}$$

$$Y_L = Y_R + Y''$$

$$Y_L = Y_R + \tan 60^\circ \frac{SO_4^{-2}(\%)}{4}$$

The location of points in the diamond is at the intersection of rays projected from points in the anion and cation triangles. In the computer program it is calculated and plotted based on the reacting percentages of HCO_3^{-} and $(Na^{+}) + (K^{+})$ (Figure 6).

To plot the point in the diamond field as shown in Figure 6, the following equations were derived:

$$X_{R'} - X_{P'} = 100 \text{ units}$$

$$X_S - X_{P'} = (Na^{+} + K^{+})(\%)\frac{1 \text{ unit}}{2\%}$$

$$X_{R'} - X_U = HCO_3^-(\%)\,\frac{1\text{ unit}}{2\%}$$

$$(X_U - X_T) = (X_T - X_S) = \tfrac{1}{2}[(X_{R'} - X_{P'}) - (X_{R'} - X_U) - (X_S - X_{P'})]$$

$$(X_T - X_S) = 50 - \frac{HCO_3^-(\%)}{4} - \frac{(Na^+ + K^+)(\%)}{4}$$

$$X_J = X_T = X_{P'} + (X_{R'} - X_{P'}) - (X_{R'} - X_U) - (X_T - X_S)$$

$$X_J = X_{P'} + 100 - \frac{HCO_3^-(\%)}{2} - [50 - \frac{HCO_3^-(\%)}{4} - \frac{(Na^+ + K^+)(\%)}{4}]$$

$$X_J = X_{P'} + 50 - \frac{HCO_3^-(\%)}{4} + \frac{(Na^+ + K^+)(\%)}{4}$$

$$\measuredangle\, TSJ = 60^\circ$$

$$\tan 60^\circ = \frac{Y_J - Y_T}{X_T - X_S}$$

$$Y_J - Y_T = \tan 60^\circ\,(X_T - X_S)$$

$$= \tan 60^\circ\,[50 - \frac{HCO_3^-(\%)}{4} - \frac{(Na^+ + K^+)(\%)}{4}]$$

$$= \frac{\tan 60^\circ}{4}\,[200 - HCO_3^-(\%) - (Na^+ + K^+)(\%)]$$

$$= 86.60 - .4330\,[HCO_3^-(\%) + (Na^+ + K^+)(\%)]$$

$$Y_J = Y_{Q'''} + 86.60 - .4330\,[HCO_3^-(\%) + (Na^+ + K^+)(\%)]$$

Analyses may be plotted with a point, an identification number, or by choice of five other symbols. There has not been a provision for overprints.

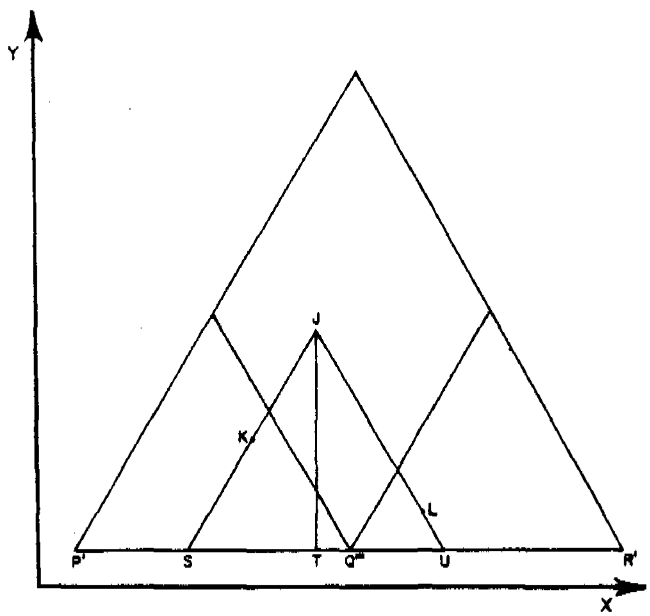

Fig. 6. Coordinate system in the diamond field of a trilinear diagram.

Piper proposed using circles, whose areas are proportional to the absolute concentrations of the sources, plotted around points in the central diamond field. Our program plots circles whose radii are based on the sum of meq/l and are proportionally represented with either an arithmetic scale at a user-defined proportion or a logarithmic scale.

DETERMINATION OF MIXING BETWEEN TWO END MEMBERS

Primary criterion for ground-water mixing is that the flow directions must physically bring waters from two sources together. This criterion cannot be judged by the computer program and must not be overlooked by the operator. The second criterion for determination of a binary mixing system is based on the assumption that when two waters mix in any proportion and all products remain in solution, the mixture will plot somewhere on a straight line between the two end members in all three fields of the trilinear diagram. The total concentration for the mixture in the diamond field must be intermediate between the total concentration of the two end members, whereas the concentration of the mixture (the absolute concentration and the concentration of the specific constituents) must all be in equal proportionate volumes (Figure 7; Piper, 1953). Our computer program analyzes all the elements of this criterion and either confirms or disproves apparent mixtures.

One of the most important decisions required from the user of this program is to determine the acceptable tolerance away from a straight line for a group of any three points being considered as a possible mixing combination. A user-specified

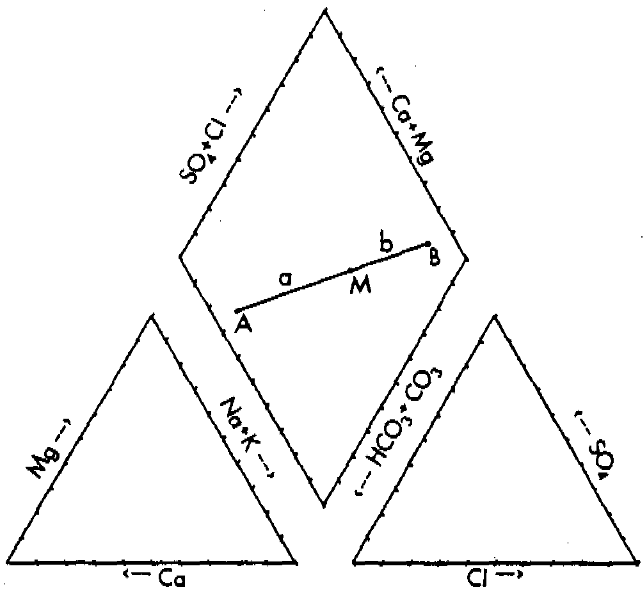

Fig. 7. Binary mixing system in the diamond field of the *trilinear diagram.*

$$a/b = (V_b \times E_b)/(V_a \times E_a)$$

$$V_a/V_b = (b \times E_b)/(a \times E_a)$$

$$E_m = [E_a \times E_b \times (a + b)]/[(a \times E_a) + (b \times E_b)]$$

$$V_a = (b \times E_b)/[(a \times E_a) + (b \times E_b)]$$

$$V_b = (a \times E_a)/[(a \times E_a) + (b \times E_b)]$$

$$C_m = (C_a \times V_a) + (C_b \times V_b)$$

where:

a;b	–	**distances measured on the diagram;**
E_a, E_b, E_m	–	**concentrations of respective waters having compositions A, B and M;**
V_a	–	**proportionate volume in mixture M of water having composition A;**
V_b	–	**proportionate volume in mixture M of water having composition B;**
C_m	–	**calculated concentration of the mixture M.**

tolerance away from a true straight line is incorporated. Based on an acceptable analytical error, a five percent tolerance is normally used. Deviation allowed away from a straight line is a function of the length of that line and the user-specified tolerance. Possible mixing points must fit inside a tolerance window. If a point falls more than the preset percentage away from the straight line, the tested combination of three points is rejected as not a mixing system. For example, when a five percent tolerance has been specified, a mixing point on a line seven units long would be considered if the point was within .35 units off the line. In clusters of points (i.e., very short lines) even very small analytical errors would cause mixtures to be disqualified. All points representing a postulated mixing system may deviate from their plotted positions. The maximum amount they may deviate is assumed to be the same as the user-defined percent tolerance. If both end points in a binary mixing system have maximum variance in opposing directions, the line is either lengthened or shortened. The length of the line is compared to the maximum possible variation. If that amount of possible variance is greater than the length of the line, the program considers these points a cluster. The allowed tolerance away from the cluster of points, representing similar percentage of reacting concentrations, is equal to the user-specified percentage.

To test for possible mixtures, all points are considered in all combinations of pairs as end members, and the remaining points are tested to see if they fit within a "tolerance window" around the line. The limits of the window are the maximum plus the tolerance, and the minimum minus the tolerance for both the X and Y values of the end points (Figure 8). The window is further limited within two parallel lines on either side of, and at the specified tolerance away from the line under consideration.

The user should be cautioned that the mixing systems identified by the computer program conform with the mathematical criteria only (Piper, 1953).

THREE-WAY MIXING

Piper also suggested a method to check for a ternary mixture resulting from three end members. This technique treats the three end-member compositions, when plotted, as apexes of a hypothetical triangle in each plotting field. The first criterion for a hypothetical mixture point for the program to consider is that it must plot within the

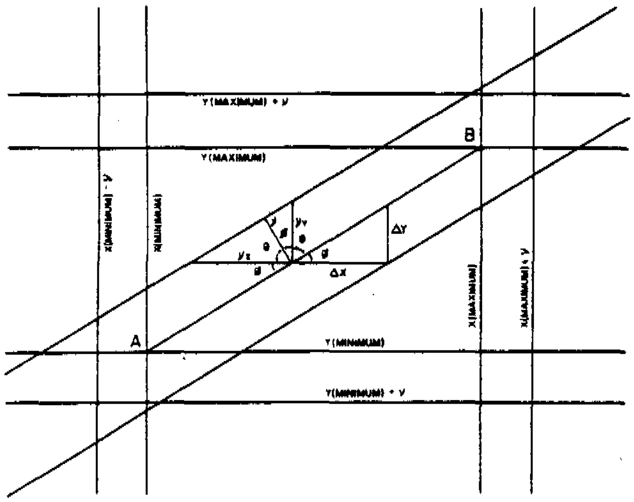

Fig. 8. Coordinate system for the experimental error tolerance in a binary mixing system.

$\cos \phi = v/v_Y$ $\cos \phi = v/v_X$

triangles in all three fields. The second criterion is that its total concentration must be less than the total concentration of the most saline end member and more than the least saline end member. Any source that meets the above criteria has its individual ions compared then to a theoretical mixture based on the correct proportions for its location.

The theoretical perfect mixture is calculated in the following manner. A line is drawn from one of the end members (Point A, Figure 9) through the point of the hypothetical mixture (point M). The point (M') where this line intersects the opposite side of the triangle on the line CB is considered an intermediate mixing point between end

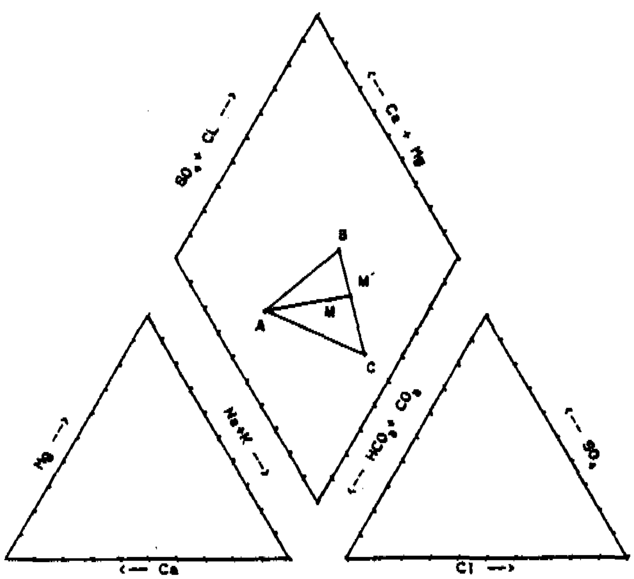

Fig. 9. Ternary mixing system.

members C and B. The program calculates the theoretical concentrations for this intermediate point M' based on its proportional distance from points B and C in the same manner as used in the two-end-member mixing. The calculated concentrations for M' and the concentrations for point A are used as end points for the calculations of values for a theoretical mixture located at point M. These calculated values of a theoretical mixing point for the three end members are then compared to the actual values of M. If the calculations demonstrate that mixing between the three end members may produce the mixing point examined, the results are included in the output. If this point fails to meet the graphical or analytical criteria, the program proceeds to another set of end points.

OUTPUT

The Piper trilinear diagram can be produced on the CRT, thermal printer, or the X-Y plotter. Plotting on the CRT is the fastest and can be used in preliminary work where no hard copy is required. If a hard copy is required, a thermal printer copy may be produced after using the CRT. The thermal printer copy is limited in size, clarity and accuracy of point locations. These are merely limits on the display of the diagram and do not affect the accuracy of the mixing tests. Plotting on the X-Y plotter may produce diagrams in a wide variety of sizes and colors with high accuracy of point locations. Overhead projection transparencies may also be produced with an optional pen set. Overprints of several different sets of data may be run with different symbols or colors. Concentration circles are optional and may be left off some copies for simplification and clarity.

Hard copies of the input data along with percentage-reacting values, absolute concentrations and analytical error may be obtained as an output. Binary mixing systems are represented in an output as a series of tables listing the points lying on straight lines in all three fields, the preset percentage tolerance and a percentage error computed from the difference between the concentrations (total and of individual constituents) in the water plotted as the intermediate point and a theoretical perfect mixture for that point.

The output of a ternary mixing system is also given as a table, listing all the points representing all the mixing systems. The tables display the comparisons for absolute and individual constituent concentrations. A complete listing of the program is given in Appendix I, and an example of input and output is shown in Appendix II.

APPENDIX I. PROGRAM LISTING*

```
10   REWIND '              <PIPER>                   update: 9-22-82JB
11   OPTION BASE 1
12   COM Imax,Outprinter,Find_quest$,Err_extreme,Save$
20    PRINTER IS 16
40    PRINT PAGE;"THIS PROGRAM WAS DEVELOPED FOR KSU DEPT. OF GEOLOGY"
50    PRINT "THIS PROGRAM IS DESIGNED TO:"
60    PRINT " (1) CALCULATE MILLIEQUIVALENTS AND PERCENTAGES"
70    PRINT " (2) PLOT EACH SOURCE ON A PIPER DIAGRAM"
80    PRINT " (3) CHECK FOR POSSIBLE MIXTURES"
90    WAIT 3000
100   PRINT PAGE
110   INPUT "Is the PIPER overlay on the keys?",Quest$
120   IF Quest$<>"YES" THEN 110
130   PRINT "Is the printed output from this program to be printed on the interna
l printer";LIN(1);"or the external printer ('AGILE' terminal)?"
150   PRINT LIN(1),TAB(10),"INTERNAL";TAB(30),"0";LIN(1),TAB(10),"EXTERNAL";TAB(3
0),"1"
160   INPUT Outprinter
170   PRINT PAGE
180   INPUT "WHAT IS THE TITLE OF YOUR PROJECT ? (MAX 16 LETTERS )",Title$
190   PRINTER IS Outprinter
200   PRINT USING 220
220   IMAGE 80("*")
240   IMAGE 2X,3D,6(3X,5D.DD)
250   PRINT TAB(30);Title$
260   PRINT USING 220
270   PRINTER IS 16
300   DEG
330   DIM Pma(100),Pca(100),Pnak(100),Pso(100),Pcl(100),Phco(100)
340   DIM Eqfe(100),Eqca(100),Eqmg(100),Eqna(100),Eqk(100),Eqhco(100),Eqcl(100),E
qso(100),Eqno(100),Eqpo(100),Eqco(100)
360   DIM Ca(100),Mg(100),Na(100),K(100),Hco(100),Cl(100),So(100),No(100),Co(100)
370   SHORT Xd(100),Yd(100),Yrt(100),Xlf(100),Ylf(100)
380   DIM Po(100),Err(100),Fe(100),Dif(100),Si(100)
390   DIM Totnak(100),Totcl(100),Tothco(100),Tcat(100),Tanio(100),Cat(100)
400   DIM Tds(100),Nsum(100),Ani(100)
410   INPUT "DATA ENTRY MODE:KEYBOARD(1) OR DATA FILE:T14(2)",Q
420   ON Q GOTO 510,430
424   PRINT "IMPROPER RESPONSE     ---try again"
425   WAIT 3000
426   PRINT PAGE
430   MASS STORAGE IS ":T14"
440   INPUT "WHAT IS DATA FILE NAME?",File_name$
441   ON ERROR GOTO 424
450   ASSIGN #1 TO File_name$
451   OFF ERROR
455   READ #1;Imax
460   FOR I=1 TO Imax
470     READ #1;Ca(I),Mg(I),Na(I),K(I),Hco(I),Co(I),Cl(I),So(I),No(I),Po(I),Fe(I)
,Si(I)
480   NEXT I
490   REWIND
500   GOTO 670
510   INPUT " FROM HOW MANY SOURCES DO YOU HAVE SAMPLES?",Imax
512   PRINT "NUMBER OF SOURCES = ";Imax
513   FOR I=1 TO Imax
520     PRINTER IS 16
530     PRINT "GIVE YOUR VALUES FOR SOURCE #";I
540     INPUT "VALUE OF Ca ?",Ca(I)
550     INPUT "VALUE OF Mg ?",Mg(I)
560     INPUT "VALUE OF Na ?",Na(I)
570     INPUT "VALUE OF K ?",K(I)
580     INPUT "VALUE OF HCO3?",Hco(I)
590     INPUT "VALUE OF CO3 ?",Co(I)
600     INPUT "VALUE OF SO4 ?",So(I)
610     INPUT "VALUE OF Cl ?",Cl(I)
620     INPUT "VALUE OF NO3 ?",No(I)
630     INPUT "VALUE OF PO4 ?",Po(I)
640     INPUT "VALUE OF Si ?",Si(I)
650     INPUT "VALUE OF Fe ?",Fe(I)
660   NEXT I
670   GOSUB List
690   INPUT "ARE YOUR VALUES ALL CORRECT?",Q$              ' Corrects values
700   IF Q$="YES" THEN GOTO 1000
710   PRINTER IS 16
720 Correct: INPUT "WHICH SOURCE IS IT FROM?",I
730   PRINT "WHICH ION DO YOU WANT TO CHANGE ?";LIN(2);TAB(9);"ION";TAB(30);"#";T
AB(10);"Ca";TAB(30);"1";TAB(10);"Mg";TAB(30);"2"
740   PRINT TAB(10);"Na";TAB(30);"3";TAB(10);"K";TAB(30);"4";TAB(10);"HCO3";TAB(3
0);"5";TAB(10);"CO3";TAB(30);"6";TAB(10);"Cl";TAB(30);"7";TAB(10);"SO4";
750   PRINT TAB(30);"8";TAB(10);"NO3";TAB(30);"9";TAB(10);"PO4";TAB(29);"10";TAB(
10);"Fe";TAB(29);"11";TAB(10);"Si";TAB(29);"12"
770   INPUT "Type in the number corresponding to the ion to be changed.",Ion
780   PRINT PAGE
790   IF Ion=1 THEN INPUT "NEW VALUE ?",Ca(I)
800   IF Ion=2 THEN INPUT "NEW VALUE ?",Mg(I)
810   IF Ion=3 THEN INPUT "NEW VALUE ?",Na(I)
820   IF Ion=4 THEN INPUT "NEW VALUE ?",K(I)
830   IF Ion=5 THEN INPUT "NEW VALUE ?",Hco(I)
840   IF Ion=6 THEN INPUT "NEW VALUE ?",Co(I)
850   IF Ion=7 THEN INPUT "NEW VALUE ?",Cl(I)
860   IF Ion=8 THEN INPUT "NEW VALUE ?",So(I)
870   IF Ion=9 THEN INPUT "NEW VALUE ?",No(I)
880   IF Ion=10 THEN INPUT "NEW VALUE ?",Po(I)
890   IF Ion=11 THEN INPUT "NEW VALUE ?",Fe(I)
900   IF Ion=12 THEN INPUT "NEW VALUE ?",Si(I)
910   PRINTER IS Outprinter
920   PRINT LIN(1),"Source is #";I;LIN(1)
930   PRINT " SOURCE         Ca            Mg            Na            K            HCO3          CO
3"
940   PRINT USING 240;I,Ca(I),Mg(I),Na(I),K(I),Hco(I),Co(I)
950   PRINT " SOURCE         SO4           Cl            NO3           PO4          Si            Fe"
960   PRINT USING 240;I,So(I),Cl(I),No(I),Po(I),Si(I),Fe(I)
970   PRINTER IS 16
980   INPUT "ANY MORE CORRECTIONS ? (YES/NO)",Q$
990   IF Q$="YES" THEN 720
1000  INPUT "Is printout of the data required? (YES/NO)",Q$
1010  IF Q$="YES" THEN GOSUB List
1020  INPUT "DO YOU WANT YOUR DATA STORED IN A DATA FILE ? (YES/NO)",Q$
1030  IF Q$="YES" THEN GOSUB Data
1031  FOR I=1 TO Imax
1040    Eqca(I)=PROUND(Ca(I)*.0499,-2)                  ' COMPUTES MEQ FROM PPM
1050    Eqmg(I)=PROUND(Mg(I)*.08226,-2)
1060    Eqna(I)=PROUND(Na(I)*.04350,-2)
1070    Eqk(I)=PROUND(K(I)*.02557,-2)
1080    Eqhco(I)=PROUND(Hco(I)*.01639,-2)
1090    Eqco(I)=PROUND(Co(I)*.03333,-2)
1100    Eqcl(I)=PROUND(Cl(I)*.02821,-2)
1110    Eqso(I)=PROUND(So(I)*.02082,-2)
1120    Eqno(I)=PROUND(No(I)*.01613,-2)
1125    Eqpo(I)=PROUND(Po(I)*.03159,-2)
1126    Eqfe(I)=PROUND(Fe(I)*.03581,-2)
1127  NEXT I
1128  INPUT "Are the meq/l values to be printed? (YES/NO)",Quest$
1129  IF Quest$="NO" THEN GOTO 1145
1130  PRINTER IS Outprinter
1132  PRINT LIN(2);"EQUIVALENTS PER MILLION:";LIN(1)
1133  PRINT "SOURCE       Ca            Mg            Na            K             HCO3"
1134  FOR I=1 TO Imax
1135    PRINT USING 1142;I,Eqca(I),Eqmg(I),Eqna(I),Eqk(I),Eqhco(I)
1136  NEXT I
1137  PRINT LIN(1)
1138  PRINT "SOURCE       CO            CL            SO4           NO3           PO4"
1139  FOR I=1 TO Imax
1140    PRINT USING 1142;I,Eqco(I),Eqcl(I),Eqso(I),Eqno(I),Eqpo(I)
1141  NEXT I
1142  IMAGE 2X,3D,5(3X,4D.3D)
1143  PRINT LIN(1)
1145  INPUT "Are the percent values to be printed? (YES/NO)",Q$
1155  IF Q$="YES" THEN PRINTER IS Outprinter
1156  IF Q$<>"YES" THEN PRINTER IS 16
1157  PRINT LIN(2);"PERCENT OF TDS:MEQ.";LIN(1)
1158  PRINT "SOURCE  %Ca    %Mg     %Na+K   %Cl     %SO     %HCO   ABS.CONC.   ERR";L
IN(1)
1159  FOR I=1 TO Imax                       ' COMPUTATION OF %
1160    Totnak(I)=Eqna(I)+Eqk(I)
1170    Totcl(I)=Eqcl(I)+Eqno(I)
1180    Tothco(I)=Eqhco(I)+Eqpo(I)+Eqco(I)
1190    Tcat(I)=Eqca(I)+Eqmg(I)+Totnak(I)
1200    Tanio(I)=Tothco(I)+Eqso(I)+Totcl(I)
1210    Cat(I)=Ca(I)+Mg(I)+Na(I)+K(I)+Fe(I)
1220    Ani(I)=Hco(I)+Co(I)/2.03+So(I)+Cl(I)+No(I)+Po(I)+Si(I)
1230    Tds(I)=Cat(I)+Ani(I)
1240    Nsum(I)=Tcat(I)+Tanio(I)
1250    IF Tcat(I)>Tanio(I) THEN Dif(I)=Tcat(I)-Tanio(I)
1260    IF Tcat(I)>Tanio(I) THEN Err(I)=Dif(I)/Nsum(I)*100
1270    IF Tcat(I)<Tanio(I) THEN Dif(I)=Tanio(I)-Tcat(I)
1280    IF Tcat(I)<Tanio(I) THEN Err(I)=Dif(I)/Nsum(I)*100
1290    Pca(I)=Eqca(I)/Tcat(I)*100
1300    Pmg(I)=Eqmg(I)/Tcat(I)*100
1310    Pnak(I)=Totnak(I)/Tcat(I)*100
1320    Pcl(I)=Totcl(I)/Tanio(I)*100
1330    Pso(I)=Eqso(I)/Tanio(I)*100
1340    Phco(I)=Tothco(I)/Tanio(I)*100
1380    PRINT USING "2X,3D,6(X,3D.DD),2X,5D.DD,3X,3D.DD";I,Pca(I),Pmg(I),Pnak(I),
Pcl(I),Pso(I),Phco(I),Nsum(I),Err(I)
1390  NEXT I
1400  PRINTER IS 16
1410  PRINT PAGE;"HOW SHOULD THE POINTS BE PLOTTED?"
1430  PRINT "            NUMBER            DISPLAY METHOD"
1440  PRINT "              1               NUMBERS"
1450  PRINT "              2               POINTS (.)"
1460  PRINT "              3               ASTERISKS (*)"
1470  PRINT "              4               PLUSES (+)"
1480  PRINT "              5               POUND SIGN (#)"
1490  PRINT "              6               LETTER O (O)"
1500  INPUT Chartype
1510  PRINT PAGE;"ENTER PLOTTER DEVICE NUMBER AS INDICATED BELOW"
1530  PRINT "            NUMBER           DEVICE"
1540  PRINT "              1              CRT (screen)"
1550  PRINT "              2              PLOTTER"
1560  FIXED 0
1570  INPUT Plottype
1580  IF (Plottype<1) OR (Plottype>2) THEN GOTO 1520
1590  IF Plottype=1 THEN 1630
1600  INPUT "Is the plotter on and is P1 & P2 set?",Q$
1602  IF Q$="NO" THEN GOTO 1600
1605  INPUT "Should the plotter be run at half speed?(recommended for overheads)"
,Qa$
1606  IF Qa$="NO" THEN OUTPUT 705;"VS36"        'SET PEN SPEED TO 360mm/sec
1607  IF Qa$="YES" THEN OUTPUT 705;"VS18"       'SET PEN SPEED TO 180mm/sec
1610  PRINT PAGE
1630  IF Plottype=1 THEN GOTO 1670
1640  PEN 0
1650  INPUT "ENTER NUMBER OF THE PEN TO BE USED IN PLOTTING POINTS",Pena
1660  INPUT "ENTER THE NUMBER OF THE PEN TO BE USED IN DRAWING THE GRAPH",Penb
1670  IF Plottype=1 THEN PLOTTER IS 13,"GRAPHICS"
1680  IF Plottype=2 THEN PLOTTER IS 7,5,"9872A"
1690  GRAPHICS
1700  CSIZE 2,.3                       ' Changes the height to width ratio of slashes
1710  IF (Penb=0) AND (Plottype=2) THEN GOTO 2620
1720  PEN Penb
1730  MOVE 10,3                        ' DRAWS TRIANGLES
1740  LINE TYPE 1
1750  FOR Triangle=1 TO 2
1760   IF Triangle=1 THEN MOVE 10,3
1770   IF Triangle=2 THEN MOVE 70,3
1780   FOR T=1 TO 3
1790     L=-2.5
1800     M=0
1810     IF T=1 THEN L=5
1820     IF T=2 THEN M=4.33
1830     IF T=3 THEN M=-4.33
1840     LORG 2
1850     FOR I=1 TO 10
1860       WHERE Xcoord,Ycoord
1870       DRAW Xcoord+L,Ycoord+M
1880       IF (T=1) AND (Triangle=1) THEN LABEL USING "K";"\"
1890       IF (T=1) AND (Triangle=2) THEN LABEL USING "K";"/"
1900       IF (T=2) AND (Triangle=1) THEN LABEL USING "K";"/"
1910       IF (T=2) AND (Triangle=2) THEN LABEL USING "K";"-"
1920       IF (T=3) AND (Triangle=1) THEN LABEL USING "K";"-"
1930       IF (T=3) AND (Triangle=2) THEN LABEL USING "K";"\"
1940       MOVE Xcoord+L,Ycoord+M
1950     NEXT I
1960   NEXT T
1970  NEXT Triangle
1980  MOVE 55,13                       ' DRAWS DIAMOND
1990  FOR T=1 TO 4
2000    L=-2.5
2010    M=4.33
2020    IF (T=1) OR (T=4) THEN L=2.5
2030    IF (T=3) OR (T=4) THEN M=-4.33
2040    FOR I=1 TO 10
2050      WHERE Xcoord,Ycoord
2060      DRAW Xcoord+L,Ycoord+M
2070      IF (T=1) OR (T=3) THEN LABEL USING "K";"\"
2080      IF (T=2) OR (T=4) THEN LABEL USING "K";"/"
2090      MOVE Xcoord+L,Ycoord+M
2100    NEXT I
2110  NEXT T
2120  LDIR 0
2130  CSIZE 3                          ' LABEL DIAGRAM
2140  LORG 3
2150  MOVE 30,2
2160  LABEL "<-- Ca";
2170  MOVE 90,2
2180  LABEL "Cl -->";
2190  LDIR 300
2200  MOVE 50,30
2210  LABEL "Na+K -->";
2220  MOVE 75,90
2230  LABEL "<-- Ca + Mg";
2240  MOVE 110,30
2250  LABEL "<-- SO";
2260  CSIZE 2
2270  LABEL "4";
2280  CSIZE 3
2290  LDIR 60
2300  MOVE 70,15
2310  LABEL "<-- HCO";
2320  CSIZE 2
2330  LABEL "3";
2340  CSIZE 3
```

---

* Copies of the program may be obtained on disc (single, or double density) or tape-cassette for a nominal fee by contacting Dr. Yoram Eckstein, Department of Geology, Kent State University, Kent, Ohio 44242.

```
2350 MOVE 77,27
2360 LABEL "+ CO";
2370 CSIZE 2
2380 LABEL "3";
2390 CSIZE 3
2400 MOVE 40,70
2410 LABEL "SO";
2420 CSIZE 2
2430 LABEL "4";
2440 CSIZE 3
2450 MOVE 42,73
2460 LABEL " + CL -->";
2470 MOVE 15,20
2480 LABEL "Mg -->";
2490 LDIR 0
2500 MOVE 5,85                               ! Print title of plot.
2510 CSIZE 3
2520 LORG 2
2530 LABEL USING "K";Title$
2540 PEN Pena
2550 Plot=Plot+1
2560 IF Plot=1 THEN GOTO 2590            ! All pts. must be plotted the first time
2561 PRINT PAGE
2570 INPUT "Are all data points to be plotted on the diagram?",O1$
2580 IF O1$="NO" THEN GOTO 2620
2590 Imin=1
2600 Imax1=Imax
2610 GOTO 2640
2620 INPUT "At what observation should the plotting begin?",Imin
2621 PEN Pena
2630 INPUT "At what observation should the plotting stop?",Imax1
2640 FOR I=Imin TO Imax1                  ! PLOTS POINTS LEFT TRIANGLE
2650   Ylf(I)=Pmg(I)*.4330+3              ! CALCULATES Y FROM Mg% + OFFSET
2660   Xlf(I)=60-Pca(I)/2-Pmg(I)/4        ! CALCULATES X FROM Mg% + Ca% + OFFSET
2670   MOVE Xlf(I),Ylf(I)
2680   CSIZE 2
2690   GOSUB 3720
2700 NEXT I
2710 FOR I=Imin TO Imax1                  ! PLOTS POINTS ON RIGHT TRIANGLE
2720   Yrt(I)=Pso(I)*.4330+3              ! CALCULATES Y FROM SO4% + OFFSET
2730   Xrt(I)=120-Pso(I)/4-Phco(I)/2      ! CALCULATES X FROM SO4 + HCO3%+OFFSET
2740   MOVE Xrt(I),Yrt(I)
2750   GOSUB 3720
2760 NEXT I
2770 FOR I=Imin TO Imax1                  ! PLOTS POINTS IN DIAMOND
2780   Xd(I)=65-Phco(I)/4+Pnak(I)/4       ! CALCULATES X FROM HCO+Na+K% + OFFSET
2790   Yd(I)=99.6-.4330*(Phco(I)+Pnak(I)) ! CALCULATES Y FROM HCO+Na+K% + OFFSET
2800   MOVE Xd(I),Yd(I)
2810   GOSUB 3720
2820 NEXT I
2830 PEN 0
2840 BEEP
2850 PAUSE
2860 Dump$="NO"
2870 IF Plottype=1 THEN INPUT "DO YOU WANT A COPY ON THE INTERNAL PRINTER?",Dump
$
2880 IF Dump$="YES" THEN DUMP GRAPHICS
2890 IF Dump$="YES" THEN PRINT LIN(5)
2900 PRINTER IS 16
2910 PRINT PAGE
2920 INPUT "DO YOU WANT TO DRAW CONCENTRATION CIRCLES ?",Cir$
2930 IF Cir$="NO" THEN 3620
2940 IF Cir$<>"YES" THEN 2920
2960 IF Plottype=2 THEN INPUT "WHAT PEN NUMBER DO YOU WISH TO DRAW THE CIRCLES ?
",Ques
2970 PEN Ques
2980 INPUT "DO YOU WISH THE CIRCLES PLOTTED ARITHMATICALLY(1) OR LOGRITHMATICALL
Y(2) ?",Ans
2990 IF Ans=1 THEN 3290
3000 FOR I=Imin TO Imax1
3010  Circle=LGT(Nsum(I))*4
3020  MOVE Xd(I),Yd(I)
3030  FOR Angle=0 TO 360 STEP 10
3040   DRAW Xd(I)+Circle*SIN(Angle),Yd(I)+Circle*COS(Angle)
3050  NEXT Angle
3060 NEXT I
3080 MOVE 105,85
3090 LORG 4
3100 LABEL "SCALE OF CONCENTRATION CIRCLE RADII(MEQ)"
3110 MOVE 105,84
3120 LINE TYPE 9
3130 DRAW 105+4*LGT(1),84
3140 DRAW 105+4*LGT(10),84
3150 DRAW 105+4*LGT(100),84
3160 DRAW 105+4*LGT(1000),84
3170 LINE TYPE 1
3180 LORG 2
3190 LDIR 270
3200 MOVE 105,82
3210 LABEL "1"
3220 MOVE 105+4*LGT(10),82
3230 LABEL "10"
3240 MOVE 105+4*LGT(100),82
3250 LABEL "100"
3260 MOVE 105+4*LGT(1000),82
3270 LABEL "1000"
3280 GOTO 3560
3290 INPUT "WHAT IS THE MIN. ABS. CONCENTRATION(MEQ) TO BE USED",Amin
3300 INPUT "WHAT IS THE MAX. ABS. CONCENTRATION(MEQ) TO BE USED",Amax
3310 IF Amin>=Amax THEN 3290
3320 FOR I=Imin TO Imax1
3330   Conv=30*Nsum(I)/(Amax-Amin)
3340   MOVE Xd(I),Yd(I)
3350     FOR Angle=0 TO 360 STEP 10
3360     DRAW Xd(I)+Conv*SIN(Angle),Yd(I)+Conv*COS(Angle)
3370   NEXT Angle
3380 NEXT I
3400 MOVE 105,85
3410 LORG 4
3420 LABEL "SCALE OF CONCENTRATION CIRCLE RADII(MEQ)"
3440 MOVE 95,83
3450 LINE TYPE 9
3460 FOR I=0 TO 30 STEP 6
3470   DRAW 95+I,83
3480 NEXT I
3490 LINE TYPE 1
3500 LORG 2
3510 FIXED 0
3520 FOR I=0 TO 5
3530   MOVE 93+I*6,80
3540   LABEL I*((Amax-Amin)/5)+Amin
3550 NEXT I
3560 PEN 0
3570 PAUSE
3580 IF Plottype=1 THEN INPUT "Do you need a hard copy?(YES/NO).",Quest$
3590 IF (Quest$<>"YES") OR (Plottype<>1) THEN 3620
3600 DUMP GRAPHICS
3601 PRINTER IS 0
3610 PRINT LIN(3)
3620 INPUT "Is another plot of this same data needed? (YES/NO)",Plot$
3630 IF Plot$<>"NO" THEN GOTO 1400
3640 EXIT GRAPHICS
3650 PLOTTER 13 IS OFF
3660 PLOTTER 7.5 IS OFF
3670 PRINTER IS 16
3671 PRINT PAGE;"What would you like to do now?";LIN(2);TAB(10);"Find mixing lin
es";TAB(40);"1";TAB(10);"Correct a data value & replot";TAB(40);"2"
3672 PRINT TAB(10);"Store data";TAB(40);"3";TAB(10);"Draw Stiff diagrams";TAB(40
);"4";TAB(10);"End program";TAB(40);"5"
3673 INPUT Q
3674 ON Q GOTO Mixing,Correct,Store,Stiff,End
3675 Stiff:LINK "STIFF:T15",10,10
3680 Mixing:LINK "MIXING:T15",10,10
3690 Store:GOSUB Data
3691 GOTO 3671
3700 End:STOP
3710 STOP
3720 LORG 5
3730 IF Chartype=1 THEN LABEL USING "K";I
3740 IF Chartype=3 THEN LABEL USING "K";"+"
3750 IF Chartype=4 THEN LABEL USING "K";"-"
3760 IF Chartype=5 THEN LABEL USING "K";"#"
3770 IF Chartype=6 THEN LABEL USING "K";"O"
3780 LORG 4
3790 IF Chartype=2 THEN LABEL USING "K";"."
3800 RETURN
3860 Data:INPUT "DATA WILL BE STORED IN T:14,IS THERE A TAPE IN T:14",Ans$
3870 IF Ans$="YES" THEN 3890
3890 MASS STORAGE IS ":T14"
3900 INPUT "FILE NAME TO STORE DATA?",File_name$
3910 CREATE File_name$,INT(Imax*.4+1)
3920 ASSIGN #1 TO File_name$
3930 PRINTER IS 16
3931 PRINT #1;Imax
3940 FOR I=1 TO Imax
3950  PRINT #1;Ca(I),Mg(I),Na(I),K(I),Hco(I),Co(I),Cl(I),So(I),No(I),Po(I),Fe(I)
,Si(I)
3960 NEXT I
3965 PRINT "SOURCE        Cl          SO4         NO3         PO4          Fe          Si"
3970 FOR I=1 TO Imax
3990  PRINT USING 240;I,Cl(I),So(I),No(I),Po(I),Fe(I),Si(I)
4000 NEXT I
4010 PRINTER IS Outprinter
4020 PRINT Title$;" DATA STORED AS",File_name$;"--containing ";Imax;" sources"
4030 PRINTER IS 16
4040 DISP "Press continue to proceed. CONT"
4050 PAUSE
4060 RETURN
4070 List:! THIS SUBROUTINE LIST THE PPM VALUES
4080 INPUT "Is the data to be printed on the printer?",Quest$
4090 IF Quest$="YES" THEN PRINTER IS Outprinter
4100 IF Quest$="NO" THEN PRINTER IS 16
4101 PRINT LIN(1);"PARTS PER MILLION:";LIN(1)
4105 PRINT " SOURCE        Ca          Mg          Na          K          HCO3          CO
3"
4110 FOR I=1 TO Imax
4130   PRINT USING 240;I,Ca(I),Mg(I),Na(I),K(I),Hco(I),Co(I)
4140 NEXT I
4150 PRINT LIN(1)
4155 PRINT " SOURCE        Cl          SO4          NO3          PO4          Fe          Si"
4160 FOR I=1 TO Imax
4180   PRINT USING 240;I,Cl(I),So(I),No(I),Po(I),Fe(I),Si(I)
4190 NEXT I
4200 PRINT LIN(1)
4210 RETURN
4220 SUBEND
4230 END
```

```
10    ! *******The title of this program is MIXING*******
20    DEG
30    REWIND ":T15"
40    COM Imax,Outprinter,Conc_quest$,Err_extreme,Save$
50    OVERLAP
60    DIM J(2)
70    INPUT "Is the mixture from two or three end points? (2 or 3)",Mixtype
80    PRINTER IS 16
90    GOSUB Output_options
100   IMAGE 80("-")
110   IMAGE 2X,3D,6(3X,5D.DD)
120   IF Mixtype=2 THEN Two_way
130   IF Mixtype=3 THEN Three_way
140   GOTO 70
150 Two_way: INPUT "WHAT %TOLERANCE AWAY FROM A STRAIGHT LINE IS TO BE ALLOWED?"
,Tol
160   PRINTER IS Outprinter,WIDTH(132)
170   IF Outprinter=11 THEN PRINTER IS Outprinter,WIDTH(132)  !ADJUSTS FOR AGILE
WIDTH
180   PRINT "                    CHECK FOR MIXTURES FROM 2 SOURCES";LIN(2);"THESE SOURCE
S FORM STRAIGHT LINES IN ALL THREE FIELDS WITHIN ±";Tol;"%"
190   T=1
200   Tol=Tol/100
210   FOR A=1 TO Imax
220   FOR B=A TO Imax
230   FOR C=1 TO Imax
240   IF A=B THEN 590
250   IF (C=A) OR (C=B) THEN 560
260   Test=FNCk2pt1(Tol,Xd(*),Yd(*),A,B,C)                   ! CHECKS DIAMOND
270   IF Test=1 THEN 560
280   Test=FNCk2pt1(Tol,Xlf(*),Ylf(*),A,B,C)                 ! CHECKS LFT TRIANGLE
290   IF Test=1 THEN 560
300   Test=FNCk2pt1(Tol,Xrt(*),Yrt(*),A,B,C)                 ! CHECKS RT TRIANGLE
310   IF Test=1 THEN 560
320   Lad=SQR((Xd(A)-Xd(C))^2+(Yd(A)-Yd(C))^2)              ! FINDS a IN DIAMOND
330   Lbd=SQR((Xd(B)-Xd(C))^2+(Yd(B)-Yd(C))^2)              ! FINDS b IN DIAMOND
340   Lalf=SQR((Xlf(A)-Xlf(C))^2+(Ylf(A)-Ylf(C))^2)         ! FINDS a IN LEFT TRI
350   Lblf=SQR((Xlf(B)-Xlf(C))^2+(Ylf(B)-Ylf(C))^2)         ! FINDS b IN LEFT TRI
360   Lart=SQR((Xrt(A)-Xrt(C))^2+(Yrt(A)-Yrt(C))^2)         ! FINDS a IN RT. TRI
370   Lbrt=SQR((Xrt(B)-Xrt(C))^2+(Yrt(B)-Yrt(C))^2)         ! FINDS b IN RT. TRI
380   Va=Lbd*Nsum(B)                                         ! VOLUME OF A IN C
390   Vb=Lad*Nsum(A)                                         ! VOLUME OF B IN C
400   Vcomb=Va+Vb                                            ! COMBINED VOLUMES
410   Fa=Va/Vcomb                                           ! %A OF MIX C
420   Fb=Vb/Vcomb                                           ! %B OF MIX C
430   Fm=PROUND(Nsum(A)*Nsum(B)*(Lad+Lbd)/(Lad*Nsum(A)+Lbd*Nsum(B)),-2)! FINDS FM
440   Perrorem=(Fm-Nsum(C))/Nsum(C)*100                      ! FINDS % ERROR FM
450   Valf=Lblf*Nsum(B)/(Lalf*Nsum(A)+Lblf*Nsum(B))          ! FINDS VA IN LF TRI
460   Vblf=Lalf*Nsum(A)/(Lalf*Nsum(A)+Lblf*Nsum(B))          ! FINDS VB IN LF TRI
470   Vart=Lbrt*Nsum(B)/(Lart*Nsum(A)+Lbrt*Nsum(B))          ! FINDS Va IN RT TRI
480   Vbrt=Lart*Nsum(A)/(Lart*Nsum(A)+Lbrt*Nsum(B))          ! FINDS Vb IN RT TRI
490   Totnakt=PROUND(Totnak(A)*Valf+Totnak(B)*Vblf,-2)       ! FINDS Cm OF Na+K
500   Totclt=PROUND(Totcl(A)*Vart+Totcl(B)*Vbrt,-2)            ! FINDS Cm OF Cl
510   Totcot=PROUND(Tothco(A)*Vart+Tothco(B)*Vbrt,-2)          ! FINDS Cm OF HCO3+CO
3
520   Eqcat=PROUND(Eqca(A)*Valf+Eqca(B)*Vblf,-2)               ! FINDS Cm OF Ca
530   Eqmgt=PROUND(Eqmg(A)*Valf+Eqmg(B)*Vblf,-2)               ! FINDS Cm OF Mg
540   Eqsot=PROUND(Eqso(A)*Vart+Eqso(B)*Vbrt,-2)               ! FINDS Cm OF SO4
550   CALL Calc_mix(Totnakt,Totclt,Totcot,Eqcat,Eqmgt,Eqsot,Fm,Perrornak,Perrorem
,Nsum(*),Totcl(*),Totnak(*),Tothco(*),Eqca(*),Eqmg(*),Eqso(*),A,B,C,0,T,Fa,Fb,0)
560   DISP "Searching completed on points:";A;" and ";B
570   NEXT C
580   NEXT B
590   NEXT A
600   PRINT LIN(2);TAB(10);"N/A = Not applicable to two component mixing";LIN(1)
610   PRINT "SEARCH IS COMPLETED"
620   PRINTER IS 16
630   PRINT PAGE;"What would you like to do now?";LIN(2);TAB(10);"2-Way mixing";T
AB(40);"1";TAB(10);"3-Way mixing";TAB(40);"2";TAB(10);"Store data";TAB(40);
640   PRINT "3";TAB(10);"End program";TAB(40);"4";TAB(10);"Change output options"
;TAB(40);"5"
650   INPUT Q
660   ON Q GOTO Two_way,Three_way,Store,End,Output
670 End: STOP
680 Store: GOSUB Data
690   GOTO 620
700 Output: GOSUB Output_options
710   GOTO 620
```

```
720   STOP
730 Three_way: FIXED 0
740   Type=3
750   PRINTER IS Outprinter,WIDTH(132)
760   FOR A=1 TO Imax-2                                    ! THREE POINT MIXING
770    FOR B=A+1 TO Imax-1                                 ! Points A,B and D make-up
780     FOR D=B+1 TO Imax                                  !   the triangle. Point C
790      IF (D=A) OR (D=B) THEN 1450                       !   is being tested.
800      FOR C=1 TO Imax
810       IF (C=A) OR (C=B) OR (C=D) THEN 1430
820       Test=0
830       Test=FNMix3(Xd(A),Xd(B),Xd(D),Xd(C),Yd(A),Yd(B),Yd(D),Yd(C))
840       IF Test=1 THEN 1430
850       CALL Intersection(A,B,D,C,New_x,New_y,Xd(*),Yd(*))! The 'New_' variable
860       Newd_x=New_x
870       Newd_y=New_y
880       Lad=SQR((Xd(A)-Newd_x)^2+(Yd(A)-Newd_y)^2)       !  denotes the coord.
890       Lbd=SQR((Xd(B)-Newd_x)^2+(Yd(B)-Newd_y)^2)       !  of the projected pt.
900       Test=FNMix3(Xrt(A),Xrt(B),Xrt(D),Xrt(C),Yrt(A),Yrt(B),Yrt(D),Yrt(C))
910       IF Test=1 THEN 1430
920       Va=Lbd*Nsum(B)
930       Vb=Lad*Nsum(A)
940       CALL Intersection(A,B,D,C,New_x,New_y,Xrt(*),Yrt(*))
950       Newrt_x=New_x
960       Newrt_y=New_y
970       Lart=SQR((Xrt(A)-Newrt_x)^2+(Yrt(A)-Newrt_y)^2)
980       Lbrt=SQR((Xrt(B)-Newrt_x)^2+(Yrt(B)-Newrt_y)^2)
990       Test=FNMix3(Xlf(A),Xlf(B),Xlf(D),Xlf(C),Ylf(A),Ylf(B),Ylf(D),Ylf(C))
1000      IF Test=1 THEN 1430
1010      CALL Intersection(A,B,D,C,New_x,New_y,Xlf(*),Ylf(*))
1020      Newlf_x=New_x
1030      Newlf_y=New_y
1040      Lalf=SQR((Xlf(A)-Newlf_x)^2+(Ylf(A)-Newlf_y)^2)
1050      Lblf=SQR((Xlf(B)-Newlf_x)^2+(Ylf(B)-Newlf_y)^2)
1060      I=0
1070      Valf=Lblf*Nsum(B)/(Lalf*Nsum(A)+Lblf*Nsum(B))
1080      Vblf=Lalf*Nsum(A)/(Lalf*Nsum(A)+Lblf*Nsum(B))
1090      Vart=Lbrt*Nsum(B)/(Lart*Nsum(A)+Lbrt*Nsum(B))
1100      Vbrt=Lart*Nsum(A)/(Lart*Nsum(A)+Lbrt*Nsum(B))
1110      Em=PROUND(Nsum(A)*Nsum(B)*(Lad+Lbd)/(Lad*Nsum(A)+Lbd*Nsum(B)),-2)
1120      Totnakt=PROUND(Totnak(A)*Valf+Totnak(B)*Vblf,-2)! THESE ARE THE CONC.
1130      Totclt=PROUND(Totcl(A)*Vart+Totcl(B)*Vbrt,-2)   !   AT THE PROJECTED
1140      Totcot=PROUND(Tothco(A)*Vart+Tothco(B)*Vbrt,-2) !   END POINTS
1150      Eqcat=PROUND(Eqca(A)*Valf+Eqca(B)*Vbrt,-2)
1160      Eqmgt=PROUND(Eqmg(A)*Valf+Eqmg(B)*Vblf,-2)
1170      Eqsot=PROUND(Eqso(A)*Vart+Eqso(B)*Vbrt,-2)
1180      Lad=SQR((Xd(D)-Xd(C))^2+(Yd(D)-Yd(C))^2)          ! FINDS NEW DISTANCES
1190      Lbd=SQR((Xd(C)-Newd_x)^2+(Yd(C)-Newd_y)^2)        !  USING PROJECTED PT
1200      Vd=Lbd*Em                                        ! VOL OF D IN C
1210      Vnew=Lad*Nsum(D)
1220      Vcom=Vnew+Vd
1230      Pa=Vnew/Vcom*(Va/(Va+Vb))
1240      Pb=Vnew/Vcom*(Vb/(Va+Vb))
1250      P=Vd/Vcom                                        ! % D IN C
1260      Lalf=SQR((Xlf(D)-Xlf(C))^2+(Ylf(D)-Ylf(C))^2)
1270      Lblf=SQR((Xlf(C)-Newlf_x)^2+(Ylf(C)-Newlf_y)^2)
1280      Lart=SQR((Xrt(D)-Xrt(C))^2+(Yrt(D)-Yrt(C))^2)
1290      Lbrt=SQR((Xrt(C)-Newrt_x)^2+(Yrt(C)-Newrt_y)^2)
1300      Valf=Lblf*Em/(Lalf*Nsum(D)+Lblf*Em)
1310      Vblf=Lalf*Nsum(D)/(Lalf*Nsum(D)+Lblf*Em)
1320      Vart=Lbrt*Em/(Lart*Nsum(D)+Lbrt*Em)
1330      Vbrt=Lart*Nsum(D)/(Lart*Nsum(D)+Lbrt*Em)
1340      Em=PROUND(Nsum(D)*Em*(Lad+Lbd)/(Lad*Nsum(D)+Lbd*Em),-2)
1350      Perrorem=(Em-Nsum(C))/Nsum(C)*100
1360      Totnakt=PROUND(Totnak(D)*Valf+Totnakt*Vblf,-2) ! THESE ARE THE CONC.
1370      Totclt=PROUND(Totcl(D)*Vart+Totclt*Vbrt,-2)    !   EXPECTED AT PT. C
1380      Totcot=PROUND(Tothco(D)*Vart+Totcot*Vbrt,-2)
1390      Eqcat=PROUND(Eqca(D)*Valf+Eqcat*Vbrt,-2)
1400      Eqmgt=PROUND(Eqmg(D)*Valf+Eqmgt*Vblf,-2)
1410      Eqsot=PROUND(Eqso(D)*Vart+Eqsot*Vbrt,-2)
1420 CALL Calc_mix(Totnakt,Totclt,Totcot,Eqcat,Eqmgt,Eqsot,Em,Perrornak,Perrorem
,Nsum(*),Totcl(*),Totnak(*),Tothco(*),Eqca(*),Eqmg(*),Eqso(*),A,B,C,D,T,Pa,Pb,P)
1430      NEXT C
1440      DISP "Searching completed on points:";A,B,D
1450     NEXT D
1460    NEXT B
1470 NEXT A
1480 BEEP
1490 GOTO 510
1500 END
1510 !                  ******* SUBROUTINES *********
1520 Output_options:PRINT PAGE;"Do you want those tables where the concentration
 of the mixture point is too   high or too low to be considered a mixture ";
1530 PRINT "resulting from the end members in the printed output? (YES/NO)"
1540 INPUT Conc_quest$
1550 PRINT PAGE;"Do you want individual ion concentrations printed along with th
e total concentrations? (YES/NO)"
1560 INPUT Save$
1570 PRINT PAGE;"What should the cutoff value be for maximum concentration error
."
1580 INPUT Err_extreme
1590 PRINT PAGE;"What output device should be used for printed output. (AGILE 11
,thermal printer 0"
1600 INPUT Outprinter
1610 RETURN
1620 STOP
1630 Data:INPUT "DATA WILL BE STORED IN T:14.IS THERE A TAPE IN T:14",Ans$
1640 IF Ans$="YES" THEN 1660
1650 IF Ans$<>"YES" THEN 1630
1660 MASS STORAGE IS ":T14"
1670 INPUT "FILE NAME TO STORE DATA?",File_name$
1680 CREATE File_name$,INT(Imax*.4+1)
1690 ASSIGN #1 TO File_name$
1700 PRINTER IS 16
1710 PRINT #1:Imax
1720 PRINT " SOURCE       Ca          Mg          Na          K          HCO3        CO
3"
1730 FOR I=1 TO Imax
1740  PRINT #1:Ca(I),Mg(I),Na(I),K(I),Hco(I),Co(I),Cl(I),So(I),No(I),Po(I),Fe(I)
,Si(I)
1750  PRINT USING 110;I,Ca(I),Mg(I),Na(I),K(I),Hco(I),Co(I)
1760  NEXT I
1770  PRINT " SOURCE       Cl          SO4         NO3         PO4         Fe          Si"
1780  FOR I=1 TO Imax
1790  PRINT USING 110;I,Cl(I),So(I),No(I),Po(I),Fe(I),Si(I)
1800  NEXT I
1810  PRINTER IS Outprinter
1820  PRINT "DATA ";"STORED AS",File_name$;"---containing ";Imax;"sources"
1830  PRINTER IS 16
1840  DISP "Press continue to proceed. CONT"
1850  PAUSE
1860 RETURN
1870 DEF FNCk2ptl(Tol,SHORT X(*),Y(*),REAL A,B,C)     ! Determines if point C
1880 DEG                                               ! is located on line AB
1890 Test=2
1900 N=0
1910 IF X(A)=X(B) THEN Angley=90                       ! EXCEPTION FOR 90 SLOPE
1920 IF X(A)=X(B) THEN M=999999999999                  ! EXCEPTION FOR 90 SLOPE
1930 IF X(A)=X(B) THEN 1980                            ! EXCEPTION FOR 90 SLOPE
1940 IF Y(A)=Y(B) THEN Angley=0                        ! EXCEPTION FOR 0 SLOPE
1950 IF Y(A)=Y(B) THEN 1980                            ! EXCEPTION FOR 0 SLOPE
1960 M=(Y(B)-Y(A))/(X(B)-X(A))                         ! CALCULATES SLOPE
1970 Angley=ATN(M)                                     ! FINDS ANGLE OF SLOPE
1980 N=Y(A)-M*X(A)                                     ! FINDS INTERCEPT
1990 L=SQR((X(B)-X(A))^2+(Y(A)-Y(B))^2)                ! FINDS LENGTH OF LINE
2000 Anglex=90-ABS(Angley)                             ! FINDS COMP. ANGLE
2010 IF Angley=90 THEN Ytol=Tol*L                      ! AVOIDS /0
2020 IF Angley=90 THEN 2040
2030 Ytol=Tol*L/COS(Angley)                            ! FINDS Y TOLERANCE
2040 IF Angley=0 THEN Xtol=Tol*L                       ! AVOIDS /0
2050 IF Angley=0 THEN 2070
2060 Xtol=Tol*L/COS(Anglex)                            ! FINDS X TOLERANCE
2070 IF L<Tol*96.60 THEN Ytol=Tol*43.30                ! CHECKS CLUSTER
2080 IF L<Tol*96.60 THEN Xtol=Tol*43.30                ! CHECKS CLUSTER
2090 IF X(C)>MAX(X(A),X(B))+Xtol THEN Test=1           ! SETS X MAX OF WINDOW
2100 IF X(C)<MIN(X(A),X(B))-Xtol THEN Test=1           ! SETS X MIN OF WINDOW
2110 IF Y(C)>MAX(Y(A),Y(B))+Ytol THEN Test=1           ! SETS Y MAX OF WINDOW
2120 IF Y(C)<MIN(Y(A),Y(B))-Ytol THEN Test=1           ! SETS Y MIN OF WINDOW
2130 IF Angley=90 THEN 2160                            ! AVOIDS /0
2140 IF Y(C)>M*X(C)+N+Ytol THEN Test=1                 ! CHECKS Y DISTANCE FROM LINE
2150 IF Y(C)<M*X(C)+N-Ytol THEN Test=1                 ! CHECKS Y DISTANCE FROM LINE
2160 IF Angley=0 THEN 2180                             ! AVOIDS /0
2170 IF X(C)>(Y(C)-N)/M+Xtol THEN Test=1               ! CHECKS X DISTANCE FROM LINE
2180 IF X(C)<(Y(C)-N)/M-Xtol THEN Test=1               ! CHECKS X DISTANCE FROM LINE
2190 RETURN Test
2200 FNEND
2210 SUB Intersection(A,B,D,C,New_x,New_y,SHORT X(*),Y(*))! Subroutine finds the
2220 OPTION BASE 1                                     !  intersection of 2 lines.
2230 Denomab=Denomcd=Numab=Numcd=.0001
2240 IF X(A)<>X(B) THEN Denomab=X(A)-X(B)              ! Avoids division by zero
2250 IF X(C)<>X(D) THEN Denomcd=X(C)-X(D)              !  and infinite slopes.
2260 IF Y(A)<>Y(B) THEN Numab=Y(A)-Y(B)
2270 IF Y(C)<>Y(D) THEN Numcd=Y(C)-Y(D)
2280 M(1)=Numab/Denomab
2290 M(2)=Numcd/Denomcd
2300 B(1)=-(M(1)*X(A)-Y(A))
2310 B(2)=-(M(2)*X(D)-Y(D))
2320 New_x=(B(1)-B(2))/(M(2)-M(1))                     ! New X-Y coordinates
2330 New_y=M(2)*New_x+B(2)
2340 SUBEND
2350 DEF FNMix3(SHORT Xi,Xj,Xk,Xl,Yi,Yj,Yk,Yl)         ! Determines if a point C
2360  Slopecheck(1)=Xi-Xj                              ! is located within a
2370  Slopecheck(2)=Yi-Yj                              !  triangle formed by pts
2380  Slopecheck(3)=Xj-Xk                              !  A,B & D
2390  Slopecheck(4)=Yj-Yk
2400  Slopecheck(5)=Xk-Xi
2410  Slopecheck(6)=Yk-Yi
2420  FOR N=1 TO 5 STEP 2
2430   Zapped=0
2440   IF (Slopecheck(N)<>0) AND (Slopecheck(N+1)<>0) THEN GOSUB Pos
2450   IF Zapped=1 THEN 2510                           ! Zapped is set to one in
2460   IF Slopecheck(N)=0 THEN GOSUB Vert              ! the subroutine if the
2470   IF Zapped=1 THEN 2510                           ! point C is outside the
2480   IF Slopecheck(N+1)=0 THEN GOSUB Hor             ! triangle ABD.
2490   IF Zapped=1 THEN 2510
2500  NEXT N
2510  RETURN Zapped
2520 Pos: M=Slopecheck(N+1)/Slopecheck(N)              ! Compares point C with a
2530 IF N=1 THEN GOTO 2610                             !  line of slope M and an
2540 IF N=3 THEN GOTO 2580                             !  end point 'Bline' by
2550 Bline=-(M*Xk-Yk)                                  !  examining the Y intercepts
2560 Bcomp=-(M*Xj-Yj)
2570 GOTO 2630
2580 Bline=-(M*Xj-Yj)
2590 Bcomp=-(M*Xi-Yi)
2600 GOTO 2630
2610 Bline=-(M*Xi-Yi)
2620 Bcomp=-(M*Xk-Yk)
2630 Btest=-(M*Xl-Yl)
2640 IF (Btest>Bline) AND (Bcomp<Bline) THEN Zapped=1
2650 IF (Btest<Bline) AND (Bcomp>Bline) THEN Zapped=1
2660 RETURN
2670 Vert: IF N=1 THEN Bline=Xi                        ! Same, but with vertical lines
2680 IF N=1 THEN Bcomp=Xk
2690 IF N=3 THEN Bline=Xj
2700 IF N=3 THEN Bcomp=Xi
2710 IF N=5 THEN Bcomp=Xj
2720 IF N=5 THEN Bline=Xk
2730 IF (Xl<Bline) AND (Bcomp>Bline) THEN Zapped=1
2740 IF (Xl>Bline) AND (Bcomp<Bline) THEN Zapped=1
2750 RETURN
2760 Hor: IF N=1 THEN Bline=Yi                         ! Same, but with horizontal lines
2770 IF N=1 THEN Bcomp=Yk
2780 IF N=3 THEN Bline=Yj
2790 IF N=3 THEN Bcomp=Yi
2800 IF N=5 THEN Bline=Yk
2810 IF N=5 THEN Bcomp=Yj
2820 IF (Yl>Bline) AND (Bcomp<Bline) THEN Zapped=1
2830 IF (Yl<Bline) AND (Bcomp>Bline) THEN Zapped=1
2840 RETURN
2850 FNEND
2860 ! This subprogram prints the errors of the mixing test.
2870 SUB Calc_mix(Totnakt,Totclt,Totcot,Eqcat,Eqmgt,Eqsot,Em,Perrornak,Perrorem,
Nsum(*),Totcl(*),Totnak(*),Tothco(*),Eqca(*),Eqmg(*),Eqso(*),A,B,C,D,T,Pa,Pb,P)
2880 COM Imax,Outprinter,Conc_quest$,Err_extreme,Save$
2890 IMAGE 80("_")
2900 IF ABS(Perrorem)>Err_extreme THEN GOTO 3310  ! SCREENS OUT UNWANTED OUTPUT
2910 Conc_check=0
2920 IF Nsum(C)>MAX(Nsum(A),Nsum(B),Nsum(D)) THEN Conc_check=1
2930 IF Nsum(C)<MIN(Nsum(A),Nsum(B),Nsum(D)) THEN Conc_check=2
2940 IF (Conc_check>0) AND (Conc_quest$="NO") THEN GOTO 3310
2950 PRINT USING 2890
2960 IF Conc_check=1 THEN PRINT "CONCENTRATION OF MIXTURE IS TOO HIGH FOR THE NE
XT SET OF POINTS"
2970 IF Conc_check=2 THEN PRINT "CONCENTRATION OF MIXTURE IS TOO LOW FOR THE NEX
T SET OF POINTS"
2980 Perrornak=(Totnakt-Totnak(C))/Totnak(C)*100       ! FINDS % ERROR Na+k
2990 Perrorcl=(Totclt-Totcl(C))/Totcl(C)*100           ! FINDS % ERROR Cl
3000 Perrorco=(Totcot-Tothco(C))/Tothco(C)*100         ! FINDS % ERROR HCO3+CO3
3010 Perrorca=(Eqcat-Eqca(C))/Eqca(C)*100              ! FINDS % ERROR Ca
3020 Perrormg=(Eqmgt-Eqmg(C))/Eqmg(C)*100              ! FINDS % ERROR Mg
3030 Perrorso=(Eqsot-Eqso(C))/Eqso(C)*100              ! FINDS % ERROR SO4
3040 PRINT USING 3050;A,B,D,C
3050 IMAGE      "Ion      Point #",2D,"   Point #",2D,"   Point #",2D,"      Calcula
ted   Point #",2D,"    %Error"
3060 PRINT "______________________________________________mix__________
______________"
3070 FIXED 2
3080 Eqmgc$=VAL$(Eqmg(D))
3090 Eqcac$=VAL$(Eqca(D))
3100 Totnakc$=VAL$(Totnak(D))
3110 Tothcoc$=VAL$(Tothco(D))
3120 Eqsoc$=VAL$(Eqso(D))
3130 Totclc$=VAL$(Totcl(D))
3140 Nsumc$=VAL$(Nsum(D))
3150 IF T<>2 THEN P$=VAL$(P*100)&" %"
3160 IF T=2 THEN Eqmgc$=Eqcac$=Totnakc$=Tothcoc$=Eqsoc$=Totclc$=Nsumc$="N/A"
3170 IF T=2 THEN P$=""
3180 IMAGE 9A,X,5D.DD,4X,5D.DD,4X,8A,4X,5D.DD,4X,5D.DD,4X,4D.DD
3190 PRINT USING 3180;"CONC.",Nsum(A),Nsum(B),Nsumc$,Em,Nsum(C),Perrorem
3200 IF Save$="NO" THEN GOTO 3310
3210 PRINT USING 3180;"   Mg",Eqmg(A),Eqmg(B),Eqmgc$,Eqmgt,Eqmg(C),Perrormg
3220 PRINT USING 3180;"   Ca",Eqca(A),Eqca(B),Eqcac$,Eqcat,Eqca(C),Perrorca
3230 PRINT USING 3180;"  Na+K",Totnak(A),Totnak(B),Totnakc$,Totnakt,Totnak(C),Pe
rrornak
3240 PRINT USING 3180;"HCO3+CO3",Tothco(A),Tothco(B),Tothcoc$,Totcot,Tothco(C),P
errorco
3250 PRINT USING 3180;"  SO4",Eqso(A),Eqso(B),Eqsoc$,Eqsot,Eqso(C),Perrorso
3260 PRINT USING 3180;"   Cl",Totcl(A),Totcl(B),Totclc$,Totclt,Totcl(C),Perrorcl
3270 Pa=Pa*100
3280 Pb=Pb*100
3290 PRINT "Mixing          "
3300 PRINT "Factors      ";Pa;"%      ";Pb;"%      ";P$
3310 SUBEND
```

APPENDIX II. INPUT AND OUTPUT

The data analyzed by Piper (1953) was chosen as a test problem to evaluate the validity of the computer program. Both graphical and computational results were compared. Table 1 lists the water chemistry of the eight water samples as presented by Piper (1953). The sample notation used in Piper (1953) and the computer program sample numbers are both listed.

We could not discern any difference in locations of points on the manually produced graph by Piper (1953) and the computer plotted graph (Figure 10). Comparison of percent-reacting values tabulated by Piper (Table 2) with the values obtained as an output of the computer program (Table 3) shows very minor discrepancies, caused by difference between the values of atomic weight used by Piper in 1953 and more accurate values

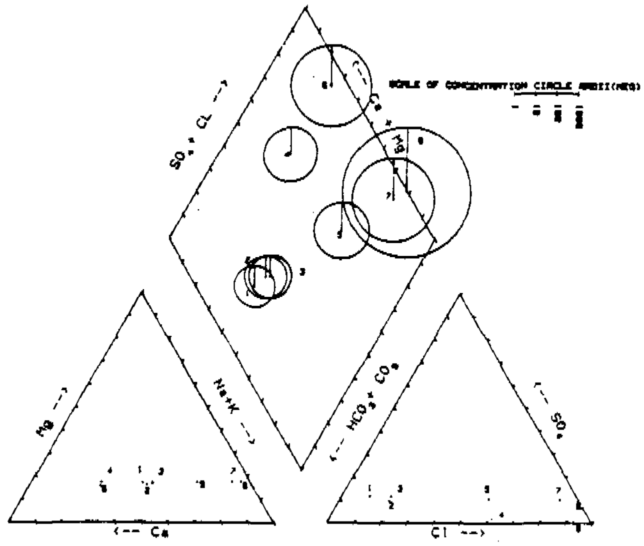

Fig. 10. Graphic output. Numbers correspond with "Source" in Table 3.

Table 1. Chemical Constituents Analyzed by Piper (1953) – Input

Constituent (ppm)								
Piper identifier:	A1	B1	b1	A2	a2	B2	b2	C
Program identifier:	*1*	*2*	*3*	*4*	*5*	*6*	*7*	*8*
Calcium (Ca)	39	40	39	102	42	466	65	393
Magnesium (Mg)	10	10	11	19	22	77	98	1228
Sodium (Na) / Potassium (K)	47	52	56	54 / 3.6	152	255	808	10220 / 353
Bicarbonate (HCO_3)	204	207	204	203	203	166	199	139
Sulfate (SO_4)	24	21	26	6.7	49	0	207	2560
Chloride (Cl)	16	32	32	199	199	1346	1346	18360

Table 2. Percent-Reacting Values Computed by Piper (1953)

Constituent	A1	B1	b1	A2	a2	B2	b2	C
Calcium	40.4	39.3	36.8	56.0	19.9	57.2	7.0	3.4
Magnesium	17.1	16.2	17.1	17.2	17.2	15.6	17.3	17.6
Sodium + Potassium	42.5	44.5	46.1	26.8	62.9	27.2	75.7	79.0
TOTALS	100.0	100.0	100.0	100.0	100.0	100.0	100.0	100.0
Bicarbonate	77.9	71.7	69.9	36.7	33.4	6.7	7.1	0.4
Sulfate	11.6	9.2	11.3	1.5	10.2	0	9.5	9.3
Chloride	10.5	19.1	18.8	61.8	56.4	93.3	83.4	90.3
TOTALS	100.0	100.0	100.0	100.0	100.0	100.0	100.0	100.0

Table 3. Percent-Reacting Values Computed by the PIPER Program

Source	% Ca^{++}	% Mg^{++}	%($Na^+ + K^+$)	% Cl^-	% SO_4^{--}	% HCO_3^-	*Absolute Conc.* (TDS, mg/l)	*% Error*
1	40.54	17.05	42.41	10.49	11.66	77.86	9.10	5.71
2	39.37	16.14	44.49	19.03	9.30	71.67	9.81	3.57
3	36.86	17.01	46.12	18.83	11.30	69.87	10.07	5.06
4	56.00	17.16	26.84	61.78	1.54	36.67	18.17	.06
5	19.96	17.21	62.83	56.33	10.24	33.43	20.48	2.73
6	57.17	15.56	27.27	93.32	0.00	6.68	81.36	.02
7	6.98	17.35	75.67	83.38	9.46	7.16	91.99	.99
8	3.42	17.59	78.99	90.31	9.29	.40	1147.75	.06

Table 4. A Portion of the Computer Output of the Test for Mixing Systems

CHECK FOR MIXTURES FROM 2 SOURCES
THESE SOURCES FORM STRAIGHT LINES IN ALL THREE FIELDS WITHIN ±2%

Ion	*Point #1*	*Point #8*	*Point #1*	*Calculated mix*	*Point #3*	*% Error*
CONC.	9.10	1147.75	N/A	10.14	10.07	.70
Mg	.82	101.02	N/A	.91	.90	1.11
Ca	1.95	19.61	N/A	1.97	1.95	1.03
Na+K	2.04	453.60	N/A	2.44	2.44	0.00
HCO3+CO3	3.34	2.28	N/A	3.34	3.34	0.00
SO4	.50	53.30	N/A	.55	.54	1.85
Cl	.45	517.94	N/A	.92	.90	2.22
Mixing Factors	99.91%	.09%				

Ion	*Point #1*	*Point #8*	*Point #1*	*Calculated mix*	*Point #5*	*% Error*
CONC.	9.10	1147.75	N/A	21.12	20.48	3.13
Mg	.82	101.02	N/A	1.81	1.81	0.00
Ca	1.95	19.61	N/A	2.12	2.10	.95
Na+K	2.04	453.60	N/A	6.48	6.61	−1.97
HCO3+CO3	3.34	2.28	N/A	3.33	3.33	0.00
SO4	.50	53.30	N/A	1.06	1.02	3.92
Cl	.45	517.94	N/A	5.92	5.61	5.53
Mixing Factors	98.94%	1.06%				

Ion	*Point #1*	*Point #8*	*Point #1*	*Calculated mix*	*Point #7*	*% Error*
CONC.	9.10	1147.75	N/A	96.32	91.99	4.71
Mg	.82	101.02	N/A	7.97	8.06	−1.12
Ca	1.95	19.61	N/A	3.21	3.24	−.93
Na+K	2.04	453.60	N/A	34.27	35.15	−2.50
HCO3+CO3	3.34	2.28	N/A	3.26	3.26	0.00
SO4	.50	53.30	N/A	4.55	4.31	5.57
Cl	.45	517.94	N/A	40.18	37.97	5.82
Mixing Factors	92.34%	7.66%				

N/A = Not applicable to two component mixing
SEARCH IS COMPLETED

used in present computations. These discrepancies are also due to differences in precision of calculations of the percentage-reaction values. Table 4 shows an output example of evaluation of a mixing system.

REFERENCES

Hem, J. D. 1964. Study and interpretation of the chemical characteristics of natural water, 2nd ed. U.S. Geological Survey Water-Supply Paper 1473. 363 pp.

Piper, A. M. 1953. A graphic procedure in the geochemical interpretation of water analyses. U.S. Geological Survey, Water Res. Div. Ground Water Notes, Geochemistry. no. 12, 14 pp.

* * * * *

Michael D. Morris, Jeffrey A. Berk, and Joseph W. Krulik are currently completing their graduate studies at the Department of Geology, Kent State University. Michael D. Morris works on a part-time basis for Snell Environmental Group of Akron, Ohio, evaluating the hydrogeological conditions of a waste disposal site in old strip mine pits in Stark County, Ohio, as his M.S. degree thesis. Jeffrey A. Berk is developing a finite-difference model of the aquifer, serving the City of Kent water-supply system, as his M.S. degree thesis. Joseph W. Krulik is working on completion of his M.S. thesis on the ground-water resources of Franklin Township, Portage County, Ohio.

Yoram Eckstein is Professor of Geology at Kent State University. He is a Hydrogeologist who has been active in teaching, research and consulting for the past 20 years. He graduated in 1959 with a B.S. in Geology, and also received M.S. and Ph.D. degrees from Hebrew University of Jerusalem, Israel. Professional experience ranges from consulting activities in ground-water and geothermal exploration, evaluation and development in the U.S., Israel, Iran, South Korea, Honduras and Nicaragua, to research appointments with the Department of Hydrogeology, Geological Survey of Israel and Department of Earth and Planetary Sciences, Massachusetts Institute of Technology.

COMPUTER NOTES

TRILINEAR DIAGRAM REVISITED: APPLICATION, LIMITATION, AND AN ELECTRONIC SPREADSHEET PROGRAM

by Songlin Cheng[a]

Abstract. The trilinear diagram has been used extensively in hydrochemical studies. The concept of hydrochemical facies based on the trilinear diagram can effectively characterize the chemical composition of water in a qualitative manner. However, its application is rather limited for quantitative and precise study, because it is difficult, if not impossible, to distinguish various mechanisms that may cause similar change in water chemistry by this diagram alone. This limitation is illustrated with various hypothetical water-rock interactions and mixing trends plotted on the trilinear diagram.

Introduction

The trilinear diagram (Hill, 1940; Piper, 1944) has been used extensively in hydrochemical studies. It effectively delineates the change of water types as the water migrates from one region of an aquifer to the other. In case of mixing between waters, the data distribution on the diagram may reveal the end members of the intermediate mixtures. Simple mixing between two end members should result in a straight line in all three fields of the trilinear diagram, provided all ions remain in the solution. However, the assumption that all ions remain in the solution may not be valid in most ground-water systems. For example, dissolution and precipitation of minerals are rather common in ground-water systems. Any post-mixing reaction may cause deviation from a straight mixing line. Besides, a straight line may be caused by reaction, rather than mixing. Therefore, identifying a mixing situation from straight alignment on a trilinear diagram is not an accurate approach. In this paper, the data distribution on the trilinear diagram as a result of water-rock interactions and mixing will be illustrated.

The speed and accuracy of computer plotting can relieve the tedium and remove the chance of error of hand plotting. Morris *et al.* (1983) published a BASIC program for plotting data on the trilinear diagram. This program also checks for the possibility of mixing. They applied the tangent function to convert a tertiary system to X-Y coordinates. In this paper, a sine and cosine function set for coordinate conversion are presented. This approach has the advantage of assigning 100 units to the side length of triangles of the trilinear diagram and easily scaling the diagram on the X-Y coordinate system.

As it is becoming increasingly common to maintain chemical databases on electronic spreadsheets, it is desirable to be able to use the same database for various applications and manipulations. Based on these considerations and available programs on our computer the LOTUS 1-2-3 (TM) is ideal for trilinear application, as it has the spreadsheet, plotting routines, and capability for programming. The macros on a floppy diskette and users' instructions are available from the author upon request.

---

[a] Laboratory of Isotope Geochemistry, Department of Geosciences, University of Arizona, Tucson, Arizona 85721.

Received April 1987, revised December 1987, accepted January 1988.

Discussion open until January 1, 1989.

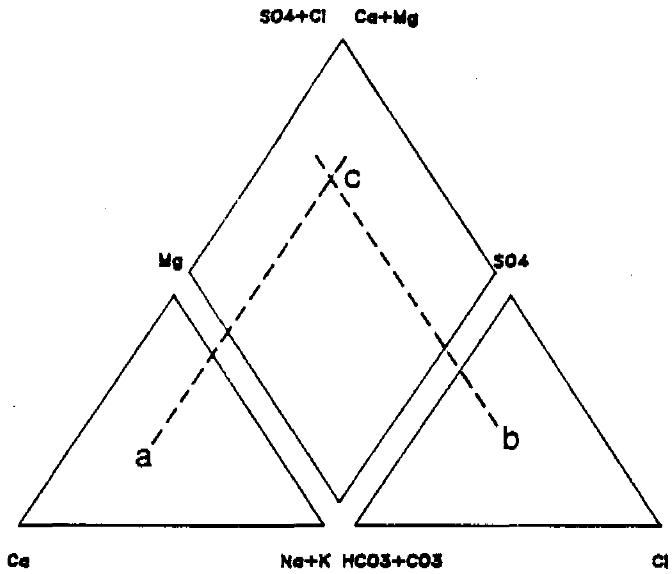

Fig. 1. The trilinear diagram. The cation and anion ratios of each sample are plotted in the cation (lower left) and anion (lower right) triangles (points a and b, respectively). The data point in the center diamond field is the intersection of the lines extended from the ion ratios and parallel to the sides of the triangles.

The Geometry of Trilinear Diagram

Hill and Piper's trilinear diagram (Figure 1) consists of a cation triangle on the lower left, an anion triangle on the lower right, and a diamond field in the center. The equivalent percentage of cations and anions are plotted first on the correspondent triangles (points a and b, respectively). Lines parallel to the sides of the triangles are drawn through these percentage points and extended into the diamond field. The intersection (point c) represents the sample in the diamond field.

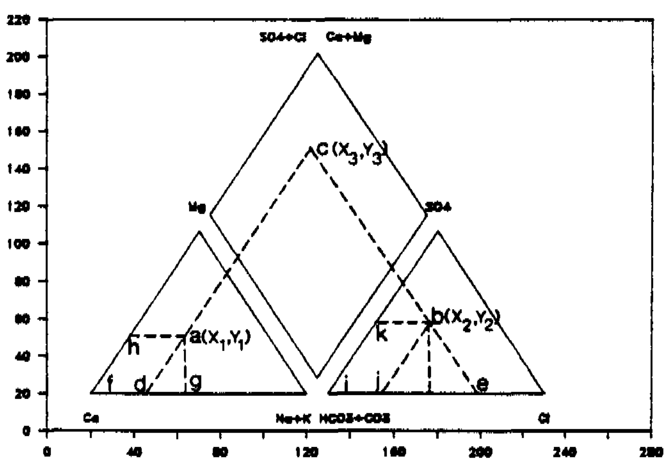

Fig. 2. The tertiary plot of trilinear diagram can be converted to X-Y plot by trigonometric function (see text for detail).

Referring to Figure 2, if the triangles of the trilinear diagram are drawn as equilateral, the mathematics of computation will be simple. If a, b, and c on Figure 2 are sample points on the trilinear diagram, then the triangle cde is equilateral. The tertiary system can be converted easily to two-dimensional X-Y coordination. The data points in cation and anion triangles, and in the diamond field are then located by correspondent (Xi,Yi) pairs. If the lower left apex of the cation triangle, f, is located on (20,20), the X-axis runs parallel to the base of the triangle, and the Y-axis is perpendicular to the X-axis; then, ion ratios and (Xi,Yi)'s on the new X-Y coordination system have the following mathematical relationship (assuming side length equals 100 units and spacing between triangles is 10 units):

Cation triangle:

$$\begin{aligned} X1 &= 20 + fg = 20 + fd + dg = 20 + fd + ad \times \sin 30^\circ \\ &= 20 + fd + fh \times \sin 30^\circ \\ &= 20 + (Na + K\%) + (Mg\%) \times \sin 30^\circ \\ Y1 &= 20 + ag = 20 + ad \times \cos 30^\circ = 20 + fh \times \cos 30^\circ \\ &= 20 + (Mg\%) \times \cos 30^\circ \end{aligned}$$

Anion triangle:

$$\begin{aligned} X2 &= 20 + (\text{side length}) + (\text{spacing}) + ij + bj \times \sin 30^\circ \\ &= 20 + (\text{side length}) + (\text{spacing}) + ij + ik \times \sin 30^\circ \\ &= 20 + 100 + 10 + (Cl\%) + (SO_4\%) \times \sin 30^\circ \\ Y2 &= 20 + bj \times \cos 30^\circ \\ &= 20 + ki \times \cos 30^\circ \\ &= 20 + (SO_4\%) \times \cos 30^\circ \end{aligned}$$

Diamond field:

$$\begin{aligned} cd &= de \text{ (equilateral triangle)} \\ &= [(\text{side length}) - fd] + (\text{spacing}) + ie \\ &= [100 - (Na + K\%)] + 10 \\ &\qquad + [100 - (HCO_3 + CO_3\%)] \\ &= [100 - (Na + K\%)] + 10 + [SO_4\% + Cl\%] \\ X3 &= 20 + fd + cd \times \sin 30^\circ \\ &= 20 + (Na + K\%) + cd \times \sin 30^\circ \\ Y3 &= 20 + cd \times \cos 30^\circ \end{aligned}$$

The apex, f, can be any convenient location on the X-Y coordinate system. The trilinear diagram macro locates this apex on (20,20), and therefore, 20 units is included in each of the above equations for calculating (Xi,Yi). The spacing between triangles can be other than the 10 units selected here.

Application of Trilinear Diagram

Many graphic methods are commonly used for representing hydrochemical data, such as the Schoeller diagram, Stiff diagram, and Hill and Piper's trilinear diagram. The trilinear diagram has the advantage of representing multiple parameters

Table 1. Chemical Compositions of Water Generated from Computer Simulation with the Program PHREEQE
[See text section "Application of Trilinear Diagram: I. Gypsum Dissolution" for detail. Ion concentrations are in meq/l. This table also includes the column designation (alphabetic) and row number (numeric) of the worksheet.]

	A	B	C	D	E	F	G	H	I	J	K	L	M
1:	SAMPLE #		TEMP(°C)	pH	ALKAL.	SiO2	Ca	Mg	Na	K	Cl	SO4	NO3
2:													
3:													
4:													
5:	END MEMBER A		22.50	7.40	2.82	0.55	2.54	0.34	1.16	0.04	0.23	0.66	0.11
6:	A+GYP1		22.50	7.46	2.88	0.55	3.10	0.34	1.16	0.04	0.23	1.16	0.11
7:	A+GYP2		22.50	7.42	2.85	0.55	3.57	0.34	1.16	0.04	0.23	1.66	0.11
8:	A+GYP3		22.50	7.39	2.82	0.55	4.04	0.34	1.16	0.04	0.23	2.16	0.11
9:	END MEMBER B		22.50	7.36	2.79	0.55	4.51	0.34	1.16	0.04	0.23	2.66	0.11
10:													
11:	END MEMBER A		22.50	7.40	2.82	0.55	2.54	0.34	1.16	0.04	0.23	0.66	0.11
12:	MIX1		22.50	7.39	2.81	0.55	2.94	0.34	1.16	0.04	0.23	1.06	0.11
13:	MIX2		22.50	7.38	2.81	0.55	3.33	0.34	1.16	0.04	0.23	1.46	0.11
14:	MIX3		22.50	7.38	2.80	0.55	3.53	0.34	1.16	0.04	0.23	1.66	0.11
15:	MIX4		22.50	7.37	2.80	0.55	3.73	0.34	1.16	0.04	0.23	1.86	0.11
16:	MIX5		22.50	7.37	2.80	0.55	4.12	0.34	1.16	0.04	0.23	2.26	0.11
17:	END MEMBER B		22.50	7.36	2.79	0.55	4.51	0.34	1.16	0.04	0.23	2.66	0.11

of a quantity of data on the same graph without losing clarity of data points; therefore, it is the most frequently used graphic method for hydrochemical study.

Because the locations of the data points in the trilinear diagram reflect the chemical characteristics of the water, the concept of hydrochemical facies is frequently used to describe the chemical property of water. This concept has been discussed in many hydrogeology textbooks. The concept of hydrochemical facies is very useful to illustrate the change in chemical characteristics as water migrates down the hydraulic gradient. The trend observed on the trilinear diagram would give an indication of the type of reactions that are responsible for the change in a qualitative way. For example, dissolution of gypsum ($CaSO_4 \cdot 2H_2O$) may change a Ca-HCO_3 type water to a Ca-SO_4 water. However, it is dangerous to define the mechanism responsible for the change of water type solely by the trend observed on the trilinear diagram. Alternative mechanisms should be considered and tested by other means.

In addition to the concept of hydrochemical facies, a straight line on the trilinear diagram may indicate a mixing system. Recently, Morris *et al.* (1983) published a program in BASIC which plots a trilinear diagram and tests for the possibility of mixing. The two end-members mixing line bears the assumption that all the ions remain in the solution after mixing. Therefore, a mixing line conclusion hinges on the validity of this assumption. Precipitation, dissolution of minerals, and ion exchange reaction are very common in natural water, and they may cause deviation from a straight line. Therefore, it is risky to base a mixing conclusion on a straight line on the trilinear diagram. Besides, pure mineral dissolution can also result in a straight line on the trilinear diagram, i.e. a straight line on the trilinear diagram may not definitely indicate mixing. Therefore, this approach should be used with great care when searching for mixing in a ground-water system.

In order to illustrate the above generalized statements, we used the computer program PHREEQE (Parkhurst, Thorstenson, and Plummer, 1980) to generate a series of water compositions along mixing and/or reaction trends. Two mixing/reaction paths will be examined in the next two sections.

I. Gypsum Dissolution

Gypsum ($CaSO_4 \cdot 2H_2O$) is a common mineral in most ground-water systems and dissolution of gypsum may cause calcite to precipitate. For example, Back *et al.* (1983) found that dolomite dissolution and concurrent precipitation of calcite in the Mississippian Pahasapa Limestone aquifer is driven by gypsum dissolution. Table 1 lists the results of computer simulation with PHREEQE. One mmole/liter of gypsum is added to end member A in four equal steps to generate end member B. Calcite equilibrium is maintained at each step. Intermediate waters are designated A+GYP1, A+GYP2, and A+GYP3. Table 1 also lists intermediate mixtures (MIX1 through MIX5) between end members A and B. Both products of gypsum dissolution (□) and mixtures (+) between

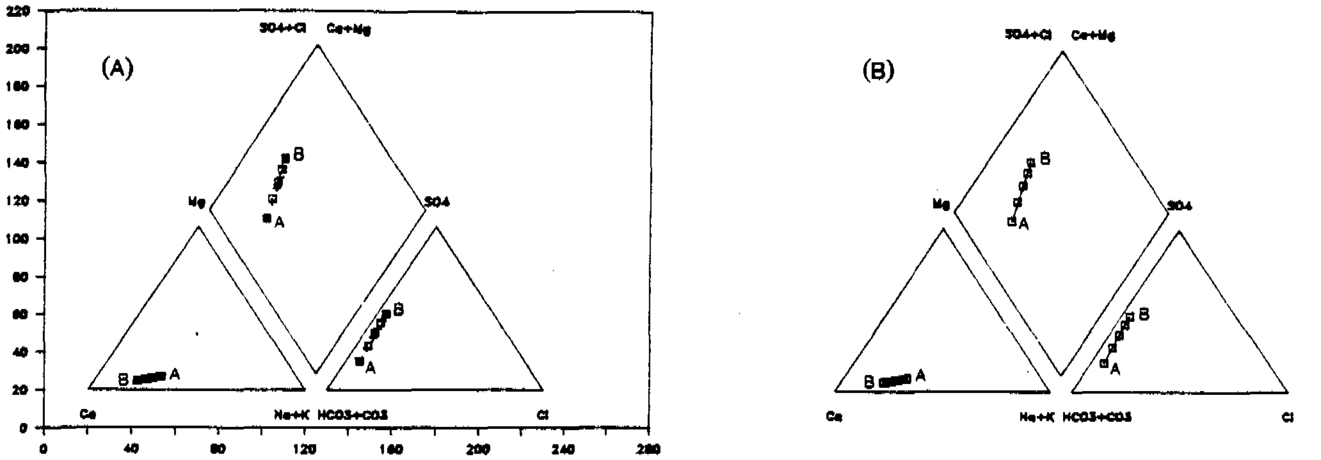

Fig. 3. (A): Trilinear diagram of water A with progressive gypsum dissolution to B (symbol □). Intermediate mixtures between A and B are also plotted (symbol +).

(B): Same as Figure 3(A). Mixing trend is shown as a line by redefining the plotting format. The X-Y coordination was eliminated by specifying different colors for grid and by not loading the pen during plotting. However, this trick cannot be used if a dot matrix printer is used rather than a pen plotter.

end members A and B as listed in Table 1 are plotted on Figure 3. Figure 3(A) is the trilinear diagram generated from LOTUS 1-2-3 macros. Figure 3(B) is generated by redefining the plotting format of Figure 3(A). The mixing trend between end members A and B is plotted as a line on Figure 3(B). It is clear from this figure that a straight line on the trilinear diagram does not prove "mixing." The mixing line is indistinguishable from the gypsum-dissolution-calcite equilibrium trend.

II. Ca-Na Ion Exchange Reaction

Ca-Na ion exchange reaction is a common and important reaction in many aquifers. In the central San Juan Basin, New Mexico, dissolution of calcite driven by Ca-Na ion exchange explain the high Na, low Ca, high alkalinity, and high pH of the water (Phillips *et al.*, 1987). Similar reaction has been observed in Maryland (Chapelle and Knobel, 1983).

Table 2 lists a computer-simulated chemical

Table 2. Chemical Compositions of Water Generated from Computer Simulation with the Program PHREEQE
[See text section "Application of Trilinear Diagram: II. Ca-Na Ion Exchange Reaction" for detail. Ion concentrations are in meq/l. This table also includes column designation (alphabetic) and row number (numeric) of the worksheet.]

	A	B	C	D	E	F	G	H	I	J	K	L	M
1:	SAMPLE #		TEMP(^{o}C)	pH	ALKAL.	SiO2	Ca	Mg	Na	K	Cl	SO4	NO3
2:													
3:													
4:													
5:	END MEMBER A		22.50	7.40	2.82	0.55	2.54	0.34	1.16	0.04	0.23	0.66	0.11
6:	A+EXCH1		22.50	8.32	3.33	0.55	0.37	0.34	3.84	0.04	0.23	0.66	0.11
7:	A+EXCH2		22.50	8.72	3.54	0.55	0.15	0.34	4.27	0.04	0.23	0.66	0.11
8:	A+EXCH3		22.50	9.12	3.98	0.55	0.07	0.34	4.80	0.04	0.23	0.66	0.11
9:	A+EXCH4		22.50	9.46	4.87	0.55	0.03	0.34	5.72	0.04	0.23	0.66	0.11
10:	END MEMBER B		22.50	9.76	6.47	0.55	0.02	0.34	7.33	0.04	0.23	0.66	0.11
11:													
12:	END MEMBER A		22.50	7.40	2.82	0.55	2.54	0.34	1.16	0.04	0.23	0.66	0.11
13:	MIX1+CALC.-EQ		22.50	7.71	3.06	0.55	1.55	0.34	2.39	0.04	0.23	0.66	0.11
14:	MIX2+CALC.-EQ		22.50	8.17	3.27	0.55	0.52	0.34	3.63	0.04	0.23	0.66	0.11
15:	MIX3+CALC.-EQ		22.50	8.69	3.52	0.55	0.16	0.34	4.24	0.04	0.23	0.66	0.11
16:	MIX4+CALC.-EQ		22.50	9.15	4.04	0.55	0.06	0.34	4.86	0.04	0.23	0.66	0.11
17:	MIX5+CALC.-EQ		22.50	9.55	5.24	0.55	0.03	0.34	6.10	0.04	0.23	0.66	0.11
18:	END MEMBER B		22.50	9.76	6.47	0.55	0.02	0.34	7.33	0.04	0.23	0.66	0.11
19:													
20:	END MEMBER A		22.50	7.40	2.82	0.55	2.54	0.34	1.16	0.04	0.23	0.66	0.11
21:	MIX1		22.50	8.60	3.55	0.55	2.04	0.34	2.39	0.04	0.23	0.66	0.11
22:	MIX2		22.50	9.16	4.28	0.55	1.54	0.34	3.63	0.04	0.23	0.66	0.11
23:	MIX3		22.50	9.31	4.64	0.55	1.28	0.34	4.24	0.04	0.23	0.66	0.11
24:	MIX4		22.50	9.43	5.01	0.55	1.03	0.34	4.86	0.04	0.23	0.66	0.11
25:	MIX5		22.50	9.62	5.74	0.55	0.53	0.34	6.10	0.04	0.23	0.66	0.11
26:	END MEMBER B		22.50	9.76	6.47	0.55	0.02	0.34	7.33	0.04	0.23	0.66	0.11

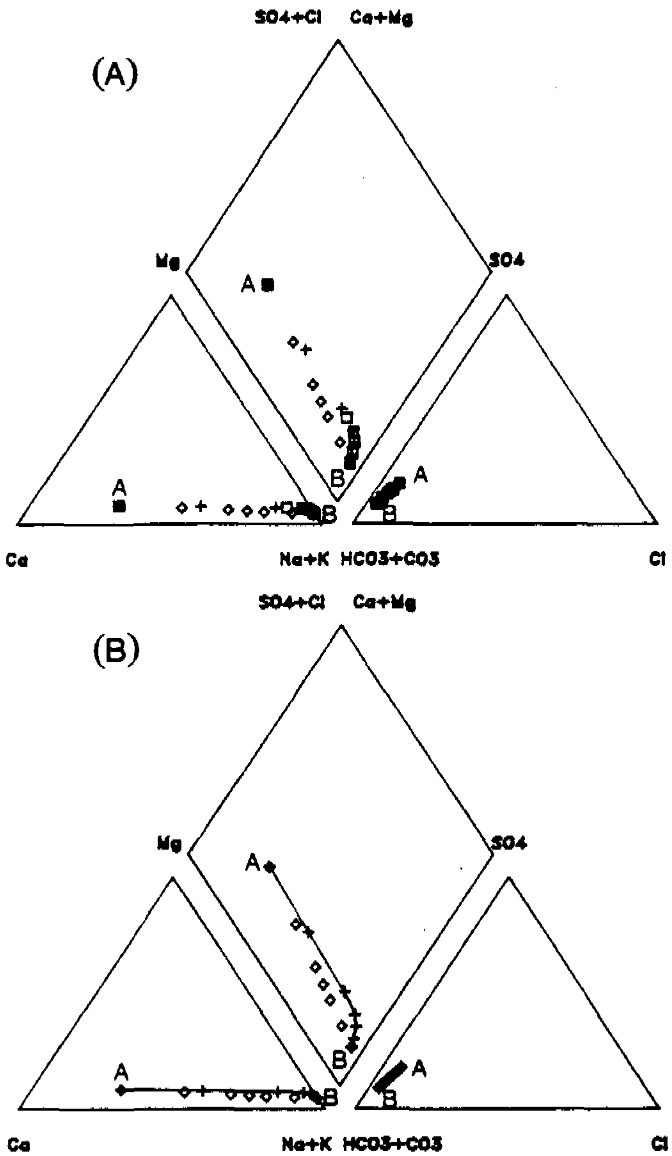

Fig. 4. (A): *Trilinear diagram of water A with progressive* Ca-Na ion exchange reaction (symbol □). Various mixtures between A and B are represented by symbol ◇. Post-mixing equilibration with calcite (symbol +) would deviate the mixing trend from the original straight line and become indistinguishable from the Ca-Na ion exchange reaction. Calcite equilibrium is maintained during the Ca-Na ion exchange reaction.

(B): Same as Figure 4(A). The Ca-Na ion exchange trend is represented as a line by redefining the graph format.

composition of water. End member B is generated by progressive Ca-Na ion exchange while maintaining calcite-equilibrium (rows 5 through 10, Table 2). Also listed in Table 2 are chemical composition of mixtures between end members A and B. Calcite-equilibrium is maintained for the waters on rows 13 through 17.

Figure 4 is a trilinear diagram of the three groups of water listed in Table 2. Although simple mixing (symbol ◇) is distinguishable from a Ca-Na ion exchange trend (symbol □), post-mixing equilibration with calcite deviates from a simple mixing line (symbol +). Therefore, mixing may also take place in a series of waters plotted on a curved line on the trilinear diagram.

In this example, the similarity in chemical composition between a Ca-Na ion exchange trend (first group, Table 2) and post-mixing calcite-equilibration trend (second group, Table 2) does not mean that it is impossible to identify the correct mechanism. Other parameters, such as stable isotopes of hydrogen, oxygen, carbon, and sulfur, should help solve the puzzle.

Summary and Conclusions

Hill and Piper's trilinear diagram is a valuable graphic tool for representing hydrochemical data. It effectively illustrates the chemical characteristics of a ground-water system from recharge to the deeper portion of the aquifer. The tedious plotting task can be greatly reduced if one takes advantage of the speed and accuracy of a computer. A set of simple equations is presented to transfer the tertiary system of the trilinear diagram to X-Y coordination and electronic spreadsheet macros for plotting a trilinear diagram.

The concept of hydrochemical facies is useful in characterization of the chemical nature of water. However, it can be misleading to define hydrogeochemical reactions based on changes in hydrochemical facies.

Although mixing may be a common phenomenon, post-mixing reactions may obscure the mixing trend on a trilinear diagram. Reactions such as dissolution, precipitation, ion exchange reaction, and even CO_2 outgassing, are common in natural waters. The assumption that all ions remain in solution after mixing for a linear mixing line on a trilinear diagram cannot be adopted unconditionally. On the other hand, simple mineral dissolution may result in a straight line on a trilinear diagram, and therefore, a straight line on the diagram does not necessarily indicate mixing. In reality, due to the heterogeneity of most ground-water systems, the chemical composition of the end member may not be well defined. Analytical errors may introduce additional uncertainty. All of these would make it difficult to recognize a mixing line on a trilinear diagram.

Based on the above considerations, the trilinear diagram is a useful tool to characterize the chemical composition of a ground-water system, that is, hydrochemical study. However, for detailed hydro*geo*chemical investigations, such as water-rock interaction, quantitative hydrogeochemical study, one should include efforts such as consideration of the isotopic composition, mineralogy, and reaction path simulation for screening hypotheses. The real mechanism(s) that is (are) operating in a ground-water system may elude the researcher if these hydrogeochemical approaches are ignored.

Acknowledgments

The author wishes to thank Dr. Austin Long and the Laboratory of Isotope Geochemistry, Department of Geosciences, University of Arizona, for supporting this study.

References

Back, W., B. B. Hanshaw, L. N. Plummer, P. H. Rahn, C. T. Rightmire, and M. Rubin. 1983. Process and rate of dedolomitization: Mass transfer and ^{14}C dating in a regional carbonate aquifer. Geol. Soc. Am. Bull. v. 94, pp. 1415-1429.

Chapelle, F. H. and L. L. Knobel. 1983. Aqueous geochemistry and the exchangeable cation composition of glauconite in the Aquia aquifer, Maryland. Ground Water. v. 21, no. 3, pp. 343-352.

Hill, R. A. 1940. Geochemical patterns in Coachella Valley, Calif. Trans. Amer. Geophys. Union. v. 21.

Morris, M. D., J. A. Berk, J. W. Krulik, and Y. Eckstein. 1983. A computer program for a trilinear diagram plot and analysis of water mixing systems. Ground Water. v. 21, no. 1, pp. 67-78.

Parkhurst, D. L., D. C. Thorstenson, and L. N. Plummer. 1980. PHREEQE—A computer program for geochemical calculations. U.S. Geol. Surv. Water-Resources Invest. 80-96. 210 pp.

Phillips, F. M., M. K. Tansey, L. A. Peeters, S. Cheng, and A. Long. 1987. An isotopic investigation of ground-water in the central San Juan Basin, New Mexico: I. ^{14}C dating as a basis for a numerical flow model. (Submitted to Water Resour. Res.)

Piper, A. M. 1944. A graphic procedure in the geochemical interpretation of water analyses. Trans. Amer. Geophys. Union. v. 25, pp. 914-923.

Plummer, L. N., B. F. Jones, and A. H. Truesdell. 1976. WATEQF—A FORTRAN IV version of WATEQ, a computer program for calculating chemical equilibrium of natural water. U.S. Geol. Surv. Water-Resources Invest. 76-13. 61 pp.

* * * * *

Songlin Cheng received his B.S. (1972) in Geology from Cheng Kung University, Taiwan, M.S. (1979) in Geology from Wright State University, and Ph.D. (1984) in Geosciences from the University of Arizona. He is currently Research Associate at the Laboratory of Isotope Geochemistry, Department of Geosciences, University of Arizona. His professional interests include isotope geochemistry, hydrogeochemical modeling, and carbon-14 ground-water dating.

Contaminant Transport

An Idealized Ground-Water Flow and Chemical Transport Model (S-PATHS)

by Phil L. Oberlander and R. W. Nelson[a]

ABSTRACT

The number of studies on the actual and potential environmental consequences of contaminated ground water is growing. One means of studying these consequences is through an idealized flow and transport model, S-PATHS, which allows the hydrologist to determine the salient features of contaminant migration with a minimum of data.

The transport of contaminants by ground water from many waste disposal sites can be geometrically idealized as flow between a line and a circle. The flow system adjacent to the disposal site can be represented as a contaminant line source, and a downgradient pumping well as a circular sink. To study waste disposal sites on a larger scale the model geometry is reversed and the disposal site is represented as a circular source, and a river or other convenient line of evaluation is represented as a line sink. This idealization allows S-PATHS to describe the flow and transport process directly by a single partial differential expression. S-PATHS considers transmissivity, effective porosity, sorption, source strength, source concentration, decay, potentiometric gradient, circle size, and distance to the line. Coding for the model is not lengthy and can be run on a large-capacity, hand-held calculator.

INTRODUCTION

The environmental consequences of ground-water contamination are being studied more often today as actual and potential waste sites are identified. To assess the environmental consequences at a disposal site, we must identify the time- and location-dependent flow rate of the contaminant into the biosphere. We can determine these values approximately, without using a complex digital model, by considering an idealized flow system and by using analytical expressions.

An evaluation of contaminant transport by ground water can often be geometrically simplified by considering the transport as migration between a circle and a line. For example, the regional movement of contaminant from a leaking tank or landfill to a nearby river can be conceptualized as flow from a circular source to a line sink. Likewise, the local movement of contaminant from a linear disposal pit to a pumping well can be considered as flow from a line source to a circular sink. This idealization of the ground-water flow system allows the hydrologist to perform preliminary calculations that describe the location of the contaminant plume and to determine quantities of contaminant reaching the biosphere. This approach is also useful for parameter sensitivity studies and when a lack of field data does not justify a more complex model.

We idealize the transport process by assuming that a uniform potentiometric gradient normal to the line (source-sink) exists before pumping or injection, as well as steady-state, two-dimensional flow. The hydrologic zone receiving the contaminant is characterized as a medium of a constant thickness that is isotropic and homogeneous. Contaminant retardation along the flow path by sorption is assumed to take place under chemical equilibrium conditions. The contaminant is assumed to be vertically mixed in the hydrologic unit receiving the waste material. We also use the diameter of the circle, distance between the line and the circle, head at the circle, initial concentration, and decay to describe the contaminant migration. The hydrologic unit is assumed to be infinite in the direction normal to the gradient. The given boundary conditions result in a simple mathematical description of the flow system. The flow description also provides a maximum contaminant arrival flux because contaminant spreading by inhomogeneous, anisotropic media and

[a]Geosciences Research and Engineering Department, Battelle-Northwest Laboratories, P.O: Box 999, Richland, Washington 99352.

Received October 1983, revised March 1984, accepted April 1984.

Discussion open until January 1, 1985.

dispersion is not considered. In unfractured and nonkarstic aquifers, this level of analysis can often be used to determine the environmental severity of a liquid release and the need for further modeling.

In this article we present the analytical expressions for flow and transport, but do not necessarily detail the numerous intermediate steps. These expressions define the contaminant plume and answer the three essential questions concerning contaminants entering the biosphere: where, when, and how much. Model results are plotted as location-, time-, and quantity-dependent graphs that characterize the contaminant arrival at the discharge location (Nelson, 1978). S-PATHS performs the necessary calculations on a hand-held calculator which allows simple use and rapid access to the model.

TWO-DIMENSIONAL FLOW EQUATIONS

The beginning point for this development is a reduced form of equation (A-1) found in Nelson and Schur (1980). The dimensional potential, ϕ', is given as:

$$\phi' = H_0 - U_0 x' - \frac{H_0}{\ln(R/r_0')} \ln\left[\frac{\sqrt{(x')^2 + (y')^2}}{r_0'}\right] \quad (1)$$

where

ϕ' = $\phi'(x',y')$ is the potential energy head function that satisfies Laplace's equation,

H_0 = the head in the circular source-sink of approximate radius r_0' with center at the origin,

U_0 = the uniform lateral flow gradient in the positive x direction,

R = the distance from the center of the circle to the line boundary,

r_0' = the dimensional approximate radius of the circular source-sink located at the origin, and

x',y' = the dimensional Cartesian coordinates of an arbitrary point with the origin at the center of the circular source-sink.

Equation (1) is based on the boundary conditions presented in the introduction. Conceptually, equation (1) describes a two-dimensional potential surface by combining the potential formed by the regional gradient and the potential formed by injection or withdrawal at the circle. The geometry of the flow system is illustrated in Figure 1 as flow from a circular source to a line sink.

A convenient set of dimensionless variables for this flow system is:

$$x = \frac{x'}{R}, \quad y = \frac{y'}{R}, \quad r_0 = \frac{r_0'}{R}, \quad \phi = \frac{\phi'}{H_0}, \quad t = \frac{K_0 H_0}{R^2} t' \quad (2)$$

where

x,y = the dimensionless Cartesian coordinates,

t' = the dimensional time,

t = the dimensionless time, and

K_0 = the hydraulic conductivity of the confined porous stratum.

Use of the expressions from equations (1) and (2) gives the dimensionless potential, ϕ, as:

$$\phi = 1 - \frac{U_0 R}{H_0} x - \frac{1}{\ln(1/r_0)} \ln\left[\frac{\sqrt{x^2 + y^2}}{r_0}\right] \quad (3)$$

The expression for potential given in equation (3) was derived by making two approximations. The circle and the line are used as equipotentials, which under some circumstances require that limits be imposed on model use. In most field studies, however, the limits do not preclude the use of the model.

The first approximation for which a limit is needed involves the circular equipotential at the origin. Equation (3) introduces some distortion to the potentiometric surface in that the equipotential at approximate radius, r_0, is not always a circle. We describe the amount of distortion at the circle by considering the shape of the actual equipotential as compared to a circle with radius,

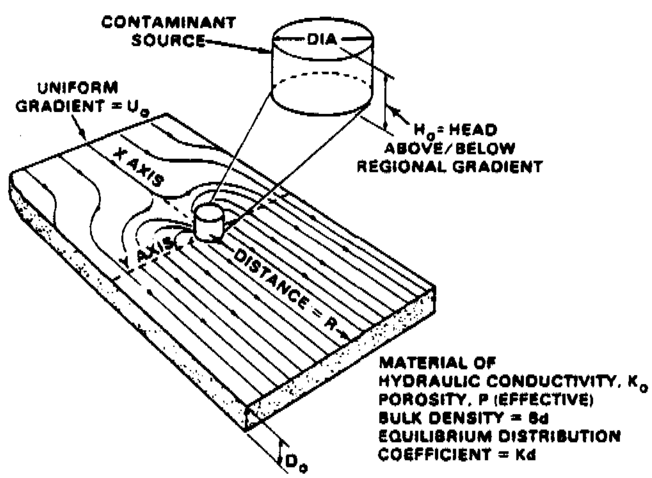

Fig. 1. Illustration of model geometry and example streamlines. Shown as flow from a circular source to a line sink.

EQUIVALENT EQUIPOTENTIAL SHAPE

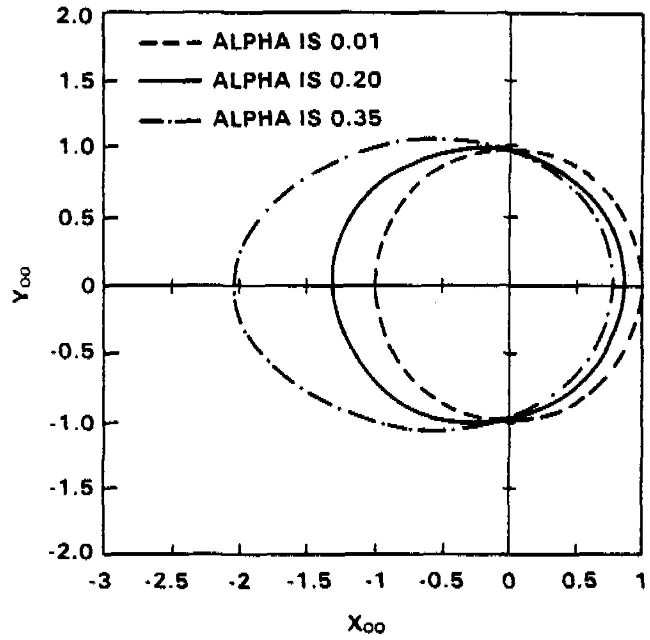

Fig. 2. Distortion of circle as a function of parameter scale factors. The shape is considered essentially circular when alpha is $\leqslant$0.2.

r_0. If we let $\phi = 1$ and allow x'_{00}, y'_{00} to denote the coordinates defining the approximate equipotential representing the circle, then:

$$y'_{00}/r'_0 = \pm\sqrt{\exp\left[-\alpha(x'_{00}/r'_0)\right] - (x'_{00}/r'_0)^2} \qquad (4)$$

where
$$\alpha = \frac{2\,U_0 r'_0 \ln(R/r'_0)}{H_0} \qquad (5)$$

which expresses the shape of the equipotential boundary only as a function of α.

Figure 2 shows the shape of the equipotential boundary for different values of α. The results in the figure show that when $\alpha \leqslant 0.2$ the boundary is essentially circular, but the center is displaced upgradient or to the left from the $\alpha = 0$ or exact boundary. The displacement upgradient effectively provides slightly longer flow paths to a discharge location and hence slightly longer calculated travel times than pathlines originating at $\alpha = 0$. For this reason, equation (3) is a good approximation of ϕ for all $\alpha \leqslant 0.2$. The distortion at the circle increases with large values of U_0 (gradient) and r'_0 (circle size) and with small values of H_0 (head).

The second approximation occurs along the line boundary because the line is not precisely an equipotential. We describe the relative distortion by dividing the model-predicted potential along the y axis by the exact potential at $x = R$, $y = 0$, using equation (3). The distortion factor increases exponentially with distance along the y axis under conditions of small R (distance to line), H_0, U_0, and large r'_0. However, as long as the relative distortion is less than 1.10, the effect to calculated travel times and outflow locations is negligible. Setting the relative distortion limit at 1.10 and solving for y_l with equation (3) gives:

$$y_l = \sqrt{\{e[(\frac{-1.10\,U_0R}{H_0} + \frac{U_0R}{H_0})\ln(\frac{U_0}{R})]\}^2 - 1} \qquad (6)$$

which is the maximum distance (dimensionless) along the line boundary for which the model will produce reliable results. Our model checks for potentiometric distortion at the circle and the line, and prints a message to the user when the limitations are exceeded.

THE STREAM FUNCTION

We use the stream function to obtain pathlines and travel times for this flow system. The stream function describes steady-state flow, and is available as the complex conjugate of the previously defined potential in equation (3), specifically:

$$\xi = \frac{U_0R}{H_0}y - \frac{1}{\ln(1/r_0)}\arctan\left(\frac{y}{x}\right) \qquad (7)$$

The terms on the right-hand side of the equation are the imaginary parts of the complex potential $\Phi = \phi + i\xi$, which satisfies the Laplace equation. Furthermore, the Cauchy-Riemann condition:

$$\frac{\partial\xi}{\partial x} = -\frac{\partial\phi}{\partial y} \quad \text{and} \quad \frac{\partial\xi}{\partial y} = \frac{\partial\phi}{\partial x} \qquad (8)$$

is satisfied. This verifies that equation (7) is analytic (Boas, 1966).

The stream function is conveniently expressed as the fraction of the total outflow from the discharge location. This is possible because the idealized flow system is symmetric about the x axis. Half of the flow will occur in the positive y quadrants and the other half will occur in the negative y quadrants with the x axis functioning as the line of symmetry. The contaminant plume is bounded by the outermost streamlines (ξ max) which surround the entire flow between the source and the sink. The flow problem is simplified when we consider the flow only in the positive y quadrants, with the remainder of the solution available as the mirror image. This allows the substitution of $\xi_m = \xi\,\text{max}/2$. Expressing the ratio of the positive y source outflow flux in dimensionless form as the ratio $\Psi = \xi/\xi_m$ gives:

$$\Psi = \frac{y}{2\pi\gamma} + \frac{1}{2\pi}\arctan\left(\frac{y}{x}\right) \tag{9}$$

where
$$\gamma = \frac{H_0}{U_0 R \ln(1/r_0)} \tag{10}$$

The stream function Ψ defines a steady pathline location, and also provides the ratio of the outflow flux as:

$$\Psi_i = \frac{Q_i}{Q_T} \tag{11}$$

where

Ψ_i = a particular streamline,

Q_i = cumulative flow from Y = 0 to a particular streamline Ψ_i, and

Q_T = total flow at circular source-sink.

The flow at the circle is defined as:

$$Q_T = \frac{2\pi D_0 K_0 H_0}{\ln(1/r_0)} \tag{12}$$

where D_0 = thickness of contaminated zone, K_0 = hydraulic conductivity, and other terms are as previously defined. A revised form of equation (12) which solves for H_0 can be used when the flow rate (Q_T) is known. Our model uses either a known flow rate or a known head at the circle as input and then calculates and displays the remaining parameter. The zero relative head occurs on the regional gradient at the circle before a hydraulic source-sink is imposed.

A discussion of the physical significance of equation (9) may be helpful. Physically, Ψ is the cumulative fraction of the entire source flux obtained by integrating all of the flow crossing any line connecting a point on the positive x axis, with the specific point having coordinates (x,y) appearing in the right-hand side of equation (9). At any point, Ψ equals a constant, is perpendicular to the potential function, and traces out the entire streamline. By selecting a range of x_{oo} and y_{oo} values on the circle and calculating corresponding values of Ψ_i, the steady-state pathlines are defined for the entire flow field.

STREAMLINE LOCATION AT THE LINE BOUNDARY

The streamline terminates at two locations: a point on the circle and at the line boundary. The maximum value of y for any streamline Ψ_i occurs at the line boundary. Substitution of $y = y_m$ and $x = 1$ into equation (9) yields:

$$\Psi_i = \frac{y_m}{2\pi\gamma} + \frac{1}{2\pi}\arctan(y_m) \tag{13}$$

Equation (13) does not algebraically solve for y_m; therefore, the y_m root is extracted using a simple iterative method. We obtain an initial estimate for y_m by setting the tangent of a small angle approximately equal to the angle in radians; therefore:

$$y_m \sim 2\pi\left(\frac{\gamma}{\gamma+1}\right)\Psi_i \tag{14}$$

and the improvement expression is:

$$y_{m,k+1} = \left[\frac{\Psi_i}{\frac{y_{m,k}}{2\pi\gamma} + \frac{1}{2\pi}\arctan(y_{m,k})}\right] y_{m,k} \tag{15}$$

The hydraulic flux for a streamline can be computed once we know y_m, and is defined as:

$$q = D_0 K_0 U_0 \left[1 + \left(\frac{\gamma}{1 + y_m^2}\right)\right] \tag{16}$$

The hydraulic flux (L^2/T) is used to compute the contaminant outflow flux (M/LT), which is given as:

$$m = qC_0(2^{-t/\S}) \tag{17}$$

where

C_0 = contaminant concentration or radionuclide activity at source,

t = contaminant travel time to discharge location, and

§ = radioactive half life.

The cumulative contaminant outflow rate (M/T) is given as:

$$M_C = \Psi_i Q C_0(2^{-t/\S}) \tag{18}$$

The concentration of contaminant at the source can be expressed as either a mass per volume or a radiological activity per volume. For nonradioactive sources the half-life is assumed to be large (1×10^{99}), and decay is essentially zero. The mass outflow flux provides the basis for computing the mass of contaminant being discharged to the biosphere. We can determine the outflow mass by integrating the mass outflow flux over the length of the line.

TRAVEL TIME FROM SOURCE TO SINK

To determine travel time we integrate the x and y components of velocity with time. By expressing as a ratio the shortest travel time (t_s)

where $y = 0$, to the travel time for streamlines (t_i), we determine the dimensionless travel time. The resultant equation is presented without development as:

$$\frac{t_i}{t_s} = \frac{1}{[1 - r_0 - \gamma \ln(\frac{1+\gamma}{r_0+\gamma})]} \left\{ y_{mi} \cot(2\pi\Psi_i - \frac{y_{mi}}{\gamma}) - y_{oi} \cot(2\pi\Psi_i - \frac{y_{oi}}{\gamma}) + \gamma \ln\left[\frac{|\sin(2\pi\Psi_i - \frac{y_{mi}}{\gamma})|}{|\sin(2\pi\Psi_i - \frac{y_{oi}}{\gamma})|} \right] \right\} \quad (19)$$

where y_{oi} = y position on circle boundary for streamline (Ψ_i), and y_{mi} = y position on line boundary for streamline (Ψ_i).

Equation (19) is used to calculate the fluid travel time for varying values of y for each streamline. A reduced form of this equation can also be used to locate contaminant position between the circle and the line boundaries. By choosing a time t and solving for x and y, the position of the contaminant plume is defined with time. This allows us to observe the advance of contaminant and illustrates the time-dependence of contaminant quantity at the discharge boundary. The time that contaminant will arrive at a known point between the source and the sink can be determined by successive estimations of t. A reduced form of equation (19) is solved for y by the Regula Falsi Method (Rektorys, 1969) of successive iteration given as:

$$Z_{k+2} = \frac{Z_k\, f(Z_{k+1}) - (Z_{k+1})\, f(Z_k)}{f(Z_{k+1}) - f(Z_k)} \quad (20)$$

where

Z_{k+2} = 0 at a root (y),

Z_k = root estimates, and

$$f(Z_k) = y \cot(2\pi\Psi_i - \frac{y}{\gamma}) + \ln[|\sin(2\pi\Psi_i - \frac{y}{\gamma})/ \sin(2\pi\Psi_i - \frac{y_{oi}}{\gamma})|] - \frac{U_0 R_t}{H_0 P} - y_{oi} \cot(2\pi\Psi_i - \frac{y_{oi}}{\gamma}).$$

When $Z_{k+2} \neq 0$, Z_{k+2} is used to replace either Z_k or Z_{k+1}, depending on whether the sign of $f(Z_k)$ or $f(Z_{k+2})$ is respectively positive or negative. Convergence is usually slow with this method. Solving equation (9) for x gives:

$$x = y \cot(2\pi\Psi_i - \frac{y}{\gamma}) \quad (21)$$

where $-\frac{\pi}{2} < (2\pi\Psi_i - \frac{y}{\gamma}) < \frac{\pi}{2}$.

The restriction on equation (21) is needed to allow the cotangent to be defined.

CHEMICAL RETARDATION

Contaminants that are in chemical equilibrium and sorbed on the porous media are retarded with respect to water travel time. The retardation factor (S) is defined in Freeze and Cherry (1979) as:

$$S = 1 + (\frac{B_d K_d}{P}) \quad (22)$$

where

B_d = mass bulk density,

K_d = equilibrium distribution coefficient, and

P = effective porosity.

The retardation factor is a constant multiplier to the kinematic equations already presented. The contaminant travel time is defined as:

$$t_c = S t_w \quad (23)$$

where t_c = travel time for a particular contaminant, and t_w = water travel time as defined by equation (18). If the contaminant transport is water-coincident and not solute-sorbed, then $K_d = 0$, and the problem reduces to equation (18).

MODEL S-PATHS

The equations presented above have been combined to form the ground-water model S-PATHS. As noted previously the analytical expressions are symmetrical about the x axis. The coding for the model S-PATHS calculates the positive y portion of the problem. The negative y results are available as the mirror image. Flow quantities and fluxes are therefore given with respect to the positive y axis and are not the total flow from the source. The program has a user-interactive format that allows several input and output options. Table 1 details the options and also serves as an input worksheet and model illustration.

Upon final data input, the program generates 14 representative streamlines and calculates the time, location, and quantity of contaminant reach-

Table 1. Two-Dimensional Steady-State Analytical Flow and Transport Model

LOCATION ______ CASE ______ USER ______

REMARKS ______

Parameters must be in consistent units. Flow is either from circular source to line sink, or from line source to circular sink. Program generates streamlines and calculates flow paths, travel times, and discharge quantities. Enter values, then press R/S. Memory size = 033, and calculator is in radians mode.

1.	______ 1 or 0	=	Flow is from 0 = line to well, 1 = well to line.
2.	______ DIA	=	Well diameter (L).
3.	______ U_0	=	Uniform regional gradient (L/L).
4.	______ R	=	Distance between well and line boundary (L).
5.	______ P	=	Effective porosity of aquifer (L^3/L^3).
6.	______ K_0	=	Hydraulic conductivity (L/T).
7.	______ D_0	=	Thickness of contaminant zone (L).
8.	______ 1 or 0	=	Known flow rate Q(L^3/T) enter 1, known head at circle H_0(L) enter 0. Program calculates and prints nonentered value.
9.	______ $(K_d)(B_D)$	=	Equilibrium distribution coefficient times bulk mass density. For zero sorption enter 0.
10.	______ C_0	=	Contaminant concentration at source (M/L^3).
11.	______ Decay	=	Radioactive half life (T), enter 0 for nonradioactive contaminants.
12.	______ 1 or 0	=	Contaminant position 1 = Yes, Ø = No. At times ______, ______, ______, enter 0 for unwated times.
13.	______ 1 or 0	=	Potentiometric heads at times from No. 12 above? To initiate next model run enter GTO OO, then R/S.

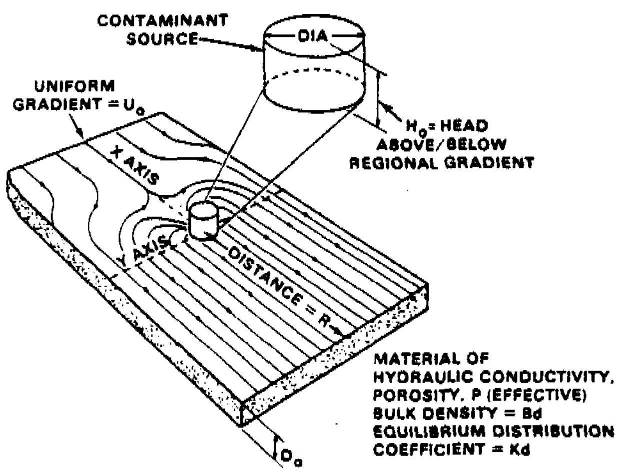

ing the biosphere. Program running time ranges from 5 to 25 minutes depending on the complexity of the output options. The coding presented in Appendix A is written for a Hewlett-Packard 41-CV hand calculator and a peripheral printer (product brand name is used for purposes of identification only; it does not represent endorsement by Battelle-Northwest Laboratories.) A set of test data and results are provided in Tables 2 and 3 to help the user verify keypunch accuracy.

As with all ground-water models, the accuracy of the predictions is directly related to the quality of input data and the validity of the simplifying assumptions. Areal two-dimensional contaminant transport models, such as S-PATHS, are sensitive to the thickness of the hydrologic unit. Ideally, the thickness of the contaminant zone (D_0) is the same as that of a distinct hydrologic unit. In cases where D_0 is a fraction of the total aquifer thickness, the computed values may not be representative. For example, assuming all of the water being discharged from a well comes from a thin contaminated layer may result in an unrealistic value of drawdown. Model results should be interpreted by the hydrologist as an approximate solution to a complex real-world situation.

Table 2. Input Verification Data

Worksheet line no.	*Input parameters*	*Input data*
1	Flow direction (flow is toward line)	1
2	DIA (circle diameter)	0.5
3	U_0 (gradient)	0.005
4	R (distance to line)	1850
5	P (effective porosity)	0.2
6	K_0 (hydraulic conductivity)	1425
7	D_0 (contaminated zone thickness)	200
	At well (known flow rate)	1
8	QT (discharge rate)	1.4063×10^6
9	(K_d B_d) (Distribution coef bulk density)	0.95
10	C_0 (concentration)	500
11	Half life	30.23
12	Contaminant position? (Yes)	1
	T1	210
	T2	400
	T3	0
13	Potential at time T? (Yes)	1

INTERPRETATION OF MODEL RESULTS

The combination of model output parameters allows a variety of interpretive graphs to be constructed. A complete description of these techniques using the output available from S-PATHS is presented in Nelson (1978). One analysis useful to the hydrologist is the determination of time and quantity of peak contaminant outflow. This is accomplished by plotting the cumulative contaminated outflow rate versus arrival time as shown in Figure 3. The figure shows the cumulative arrival of a contaminant of constant concentration at the discharge location. Of importance are the delay time, which is the time from contaminant release to the first contaminant outflow, and the spread time, which is the time period over which the leading edge of the plume is discharged. The maximum outflow rate occurs at 25 years in Figure 3.

A contaminant source often enters the ground-water flow system for a time period (T_x)

Table 3. Model Output

Calculated value	*Sample streamlines*	
	Streamline 1	*Streamline 14*
X at circle	0.250	−0.250
Y at circle	1.118×10^{4}	1.118×10^{-4}
Y at line	1850	1850
Y at line	0.065	455.454
Time to discharge location	234.008	457.885
Q/QT (from Y = 0 to Y) = Ψ_i	7.127×10^{-5}	0.500
ΣQ (from Y = 0 to Y) L**3/T	100.223	703050.096
Σ contaminant (from Y = 0 to Y) M/T	234.254	9690.38
Hydraulic flux (at Y) L**2/T	1545.984	1539.070
Contaminant flux (at Y) M/TL	3613.481	21.214
At time	210.000	210.000
Y =	0.064	296.524
X =	1688.031	97.457
Head equals	−8.368	0.910
At time	400.000	400.000
Y =	"Point beyond discharge location"	446.718
X =		1459.569
Head equals	No output	−7.147

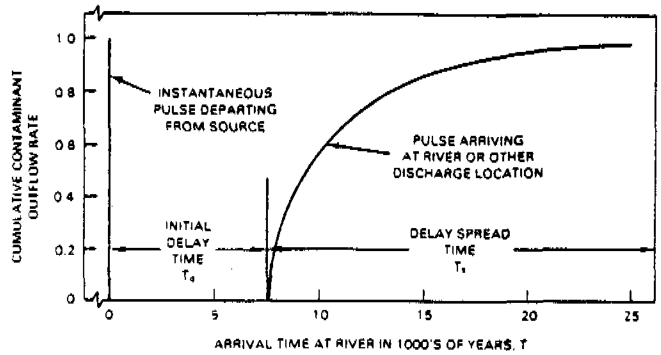

Fig. 3. Cumulative contaminant outflow versus time for an instantaneous source. The contaminant arrives over a period of time due to hydraulic spreading.

which is less than the spread time. These cases are analyzed by replotting the contaminant outflow rate versus time curve shifted along the x-axis a positive distance of T_x. This procedure is shown in Figure 4 in which the left-most curve represents the arrival of the leading edge of the contaminant plume and the shifted curve (solid line) represents the trailing edge. The time of contaminant flow at any point is limited to the time T_x. Therefore, the contaminant outflow rate becomes the difference between the first arrival curve and the last arrival curve. The resultant contaminant outflow rate is shown as the dashed line in Figure 4. The maximum discharge rate now occurs at the delay time plus T_x and then attenuates as shown. When radionuclides are modeled, the peak outflow rate is affected by decay, and the curve representing the trailing edge of the contaminant plume must be modified to account for decay during time T_x. Knowing the contaminant outflow rate with time allows the calculation of contaminant mass outflow by graphically determining the area under the curve (shaded area) in Figure 4. The mass outflow with time is particularly useful when evaluating concentration of contaminant in a downgradient surface-water body.

The above example is based on the contaminant outflow rate and time variables. The analysis could be continued by examining contaminant outflow flux with respect to location. It becomes obvious that by combining the linking variables of time, location, cumulative relative water-discharge rate (Q/QT), cumulative water-flow rate (ΣQ), location-dependent water-discharge flux (Q flux), cumulative contaminant outflow rate (Σ Contam), and location-dependent contaminant outflow flux (Contam Flux), a suite of analyses can be performed that will provide a technical description of contaminants entering the environment. Our experience in the application of this technique has demonstrated its flexibility, simplicity, and ability to facilitate communication between the technical evaluator and the decision maker.

ACKNOWLEDGMENTS

The authors wish to thank Mr. Kenneth T. Key, formerly of Pacific Northwest Laboratory, for the initial coding of some sections of S-PATHS.

REFERENCES

Boas, M. W. 1966. Mathematical Methods in the Physical Sciences. John Wiley and Sons, Inc., New York. 778 pp.

Freeze, R. A., and J. A. Cherry. 1979. Ground Water. Prentice Hall, Inc. 604 pp.

Nelson, R. W. 1978. Evaluating the environmental consequences of groundwater contamination, 1, an overview of contaminant arrival distributions and general evaluation requirements, 2, obtain location/arrival time and location/outflow quantity distributions for steady flow systems. Water Resources Research. v. 14, no. 3, pp. 409-415, pp. 416-428.

Nelson, R. W., and J. A. Schur. 1980. PATHS Groundwater Hydrologic Model. PNL-3162, Pacific Northwest Laboratory, Richland, Washington.

Rektorys, K. 1969. Survey of Applicable Mathematics. The Massachusetts Institute of Technology Press, Cambridge, Massachusetts. 1369 pp.

* * * * *

Phil L. Oberlander is a Research Scientist with Battelle Northwest Laboratories operated by Battelle Memorial Institute in Richland, Washington. His current research interests include hydrogeologic characterization of nuclear core melt accidents, environmental consequence analysis of contaminant transport, and coupled geostatistical-hydrologic modeling. He has a B.S. in Geology from Western Illinois University and an M.S. in Hydrology from

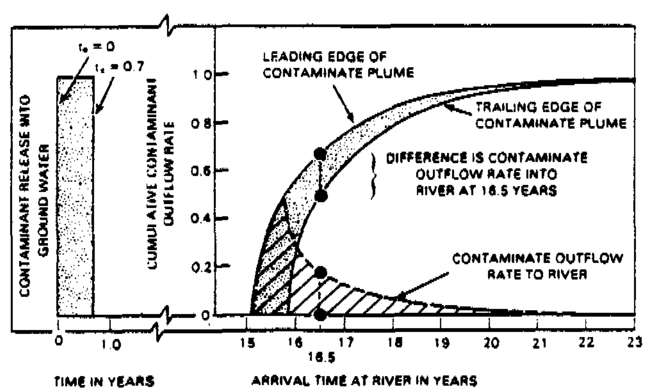

Fig. 4. Cumulative contaminant outflow versus time for a continuous source. Contaminant outflow is limited by time period of contaminant entry to aquifer.

the University of Nevada. He has experience in aquifer analysis, geophysics, and ground-water regulation.

R. William Nelson is a Staff Scientist with Battelle-Northwest Laboratories in Richland, Washington. He is the author of over 60 papers on the evaluation of contaminant movement in aquifers and analysis of the subsequent environmental consequences. In 1978, Mr. Nelson received the O. E. Meinzer Award from the Geological Society of America in recognition of his contributions to research in contaminant hydrology. He is currently conducting research on the ground-water hazards associated with the disposal of uranium mill tailings.

APPENDIX A. S-PATHS CODE LISTING

```
01*LBL "S-PATHS"
02*LBL 00
"MODEL S-PATHS"
XEQ "PRA" RAD CLRG
ADV "FLOW IS TOWARD"
PRA "0 = CIRCLE" PRA
"1 = LINE" PRA
"ENTER 1 OR 0" PRA
CF 00 STOP X=0? SF 00
"ENTER CIRCLE"
XEQ "PRA" "DIAMETER"
PRA STOP 2 / STO 11
"ENTER GRADIENT" PRA
STOP STO 13
"ENTER DISTANCE" PRA
"TO LINE" PRA STOP
STO 14 "ENTER POROSIT"
XEQ "PRA" STOP STO 16
"ENTER HYDRAULIC" PRA
"CONDUCTIVITY"
XEQ "PRA" STOP STO 17
"ENTER THICKNESS" PRA
"OF CONTAM. ZONE" PRA
STOP STO 19
"AT CIRCLE" PRA
"0=KNOWN HEAD" PRA
"1=KNOWN Q" PRA STOP
X=0? GTO 01 SF 01
RCL 14 RCL 11 / LN
"ENTER QT L**/T" PRA
STOP STO 22 * RCL 17
RCL 19 * 2 * PI *
/ "HEAD AT CIRCLE="
PRA PRX STO 12

65*LBL 02
"ENTER BULK" PRA
"DENSITY*KD" PRA STOP
STO 18
"ENT CONTAMINANT" PRA
"CONCENTRATION" PRA
STOP STO 31
"ENT RADIOACTIVE" PRA
"HALF LIFE" PRA .693
STOP X=0? + STO 33
"CONTAMINANT" XEQ "PRA"
"POSITION ?" XEQ "PRA"
"1=YES 0=NO" XEQ "PRA"
CF 02 CF 03 CF 04
STOP X=0? GTO 03
"ENTER TIME 1"
XEQ "PRA" STOP STO 23
SF 02 "ENTER TIME 2"
XEQ "PRA" STOP STO 24
SF 03 "ENTER TIME 3"
XEQ "PRA" STOP STO 25
SF 04 "HEAD AT TIME T?"
PRA "1=YES 0=NO" PRA
CF 05 STOP X=0?
GTO 03 SF 05 GTO 03

144*LBL 01
FS? 01 GTO 03 RCL 19
RCL 17 *
"ENTER HEAD L" PRA
STOP STO 12 * PI *
2 * RCL 14 RCL 11 /
LN / STO 22
"QT L**3/T=" PRA PRX
GTO 02

169*LBL 03
CF 01 .01401 STO 20
ADV RCL 13 RCL 14 *
RCL 12 / STO 01 -1.1
* RCL 01 / RCL 11
RCL 14 / LN * E↑X
X↑2 1 - SQRT RCL 14
* STO 30 RCL 14
RCL 11 / LN RCL 11 *
RCL 13 * 2 * RCL 12
/ .2 X>Y? GTO 04
"CIRCLE DISTORT" ADV
XEQ "PRA" GTO 00

216*LBL 04
ISG 20 GTO 05 ADV ADV
ADV ADV ADV PSE PSE
BEEP STOP

228*LBL 05
ADV ADV
"STREAMLINE NO."
XEQ "PRA" RCL 20 INT
XEQ "PRX" 1 RCL 20
INT X=Y? GTO 06 5
RCL 20 INT X>Y?
GTO 07 .39269908
ST+ 21 RCL 21 COS
RCL 11 * STO 00
GTO 10

254*LBL 06
RCL 11 .9999999 *
STO 00 GTO 10

260*LBL 07
13 RCL 20 INT X=Y?
GTO 08 14 RCL 20 INT
X=Y? GTO 09 .19634954
ST+ 21 RCL 21 COS
RCL 11 * STO 00
GTO 10

279*LBL 08
RCL 11 -.9999 *
STO 00 GTO 10

285*LBL 09
RCL 11 -.9999999 *
STO 00

290*LBL 10
"X AT CIRCLE" XEQ "PRA"
RCL 00 XEQ "PRX"
RCL 14 / STO 00
RCL 11 RCL 14 /
STO 01 RCL 13 RCL 17
* STO 07 RCL 19 *
STO 09 RCL 18 RCL 16
+ RCL 14 * RCL 07 /
STO 08 RCL 01 1/X LN
RCL 14 * RCL 13 *
RCL 12 X<>Y - STO 06
1 + RCL 06 RCL 01 -
/ LN RCL 06 * RCL 01
+ CHS 1 + STO 02
ST* 00 RCL 01 X↑2
RCL 00 X↑2 - SQRT
STO 26 RCL 14 *
"Y AT CIRCLE" XEQ "PRA"
PRX RCL 26 RCL 00 /
RAD ATAN X<0? XEQ 11
RCL 06 * RCL 26 +
STO 00 2 / PI /
RCL 06 / STO 15
RCL 00 RCL 06 1 + /
STO 04

381*LBL 12
RCL 04 PI 2 * RCL 06
* / RCL 04 ATAN 2
PI * / + RCL 15
X<>Y - RCL 04 *
STO 03 RCL 04 X<>Y -
ABS 1 E-9 X>Y? GTO 13
RCL 03 STO 04 GTO 12

412*LBL 13
"X AT LINE" XEQ "PRA"
RCL 14 XEQ "PRX"
"Y AT LINE" XEQ "PRA"
RCL 03 STO 10 RCL 14
* XEQ "PRX" RCL 30
X<=Y? GTO 28 X<>Y
RCL 00 RCL 03 -
RCL 06 / STO 04 SIN
ABS RCL 00 RCL 26 -
RCL 06 / STO 01 SIN
ABS / LN RCL 06 *
RCL 01 TAN 1/X RCL 26
CHS * + RCL 04 TAN
1/X RCL 03 * +
RCL 02 / RCL 08 *
STO 27
"TIME TO DISCHAR" PRA
" LOCATION" XEQ "PRA"
PRX RCL 15
"Q/QT=Q FROM Y=0"
XEQ "PRA"
" TO Y /TOTAL Q" PRA
XEQ "PRX" RCL 22 *
"CUMULATIVE Q"
XEQ "PRA"
"Y=0 TO Y L**3/T" PRA
XEQ "PRX" 2 RCL 27
RCL 28 / CHS Y↑X
RCL 31 * STO 32 *
"CUM. CONTAM."
XEQ "PRA"
"Y=0 TO Y M/T"
XEQ "PRA" XEQ "PRX"
RCL 06 RCL 03 X↑2 1
+ / 1 + RCL 03 *
"HYDRAULIC FLUX"
XEQ "PRA"
" AT Y L**2/T" PRA
XEQ "PRX" RCL 32 *
"CONTAM. FLUX" PRA
" AT Y M/TL" PRA PRX
FC? 02 GTO 04

523*LBL 14
FS? 02 GTO 15 FS? 03
GTO 16 FS? 04 GTO 17
SF 02 SF 03 SF 04
GTO 04

534*LBL 11
PI + RTN

538*LBL 15
CF 02 RCL 23 GTO 18

542*LBL 16
CF 03 RCL 24 GTO 18

546*LBL 17
CF 04 RCL 25

549*LBL 18
X=0? GTO 14 "AT TIME"
PRA PRX RCL 27 X<=Y?
GTO 27 X<>Y FS? 00 -
RCL 12 * RCL 17 *
RCL 14 X↑2 / STO 09
RCL 13 RCL 14 *
RCL 09 * RCL 18
RCL 16 / 1 + /
RCL 12 RCL 16 * /
STO 00 RCL 15 PI * 2
* STO 02 RCL 26
RCL 06 / - STO 01
RCL 10 STO 03 CF 07
CF 06

600*LBL 19
RCL 02 RCL 03 RCL 06
/ - STO 04 SIN
RCL 01 SIN / ABS LN
RCL 06 * RCL 04 TAN
1/X RCL 03 * +
RCL 00 - RCL 01 TAN
1/X RCL 26 * -
STO 05 ABS 1 E-5 X>Y?
GTO 25 RCL 05 FS? 06
GTO 23 GTO 20

638*LBL 22
RCL 10 RCL 08 *
RCL 29 RCL 07 * -
RCL 08 RCL 07 - /
STO 03 GTO 19

652*LBL 20
FS? 07 GTO 21 STO 07
RCL 26 STO 29 STO 03
SF 07 GTO 19

661*LBL 21
STO 08 SF 06 GTO 22

665*LBL 23
STO 09 RCL 08 * 0
X>Y? GTO 24 RCL 03
STO 29 RCL 09 STO 08
GTO 22

677*LBL 24
RCL 03 STO 10 RCL 09
STO 07 GTO 22

683*LBL 25
"Y =" XEQ "PRA" RCL 03
RCL 14 * STO 00
XEQ "PRX" RCL 02
RCL 03 RCL 06 / -
TAN 0 X>Y? GTO 29
X<>Y 1/X RCL 03 *
RCL 14 * STO 01 "X ="
XEQ "PRA" XEQ "PRX"
FS? 05 GTO 26 GTO 14

713*LBL 26
RCL 12 FS? 00 CHS
RCL 13 FS? 00 CHS
RCL 01 * - RCL 12
FS? 00 CHS RCL 14
RCL 11 / LN RCL 01
X↑2 RCL 00 X↑2 +
SQRT RCL 11 / LN *
- "HEAD AT TIME T="
PRA PRX GTO 14

746*LBL 27
"POINT BEYOND" PRA
"DISCHARGE LOC"
XEQ "PRA" GTO 14

752*LBL 28
"LINE DISTORT" PRA
"MAXIMUM Y =" XEQ "PRA"
RCL 30 XEQ "PRX" ADV
GTO 00

761*LBL 29
"X UNDEFINED" PRA
"IN REGION" PRA ADV
GTO 14 .END.
```

GROUND WATER

COMPUTER NOTES

MOC SOLUTIONS OF CONVECTIVE-DISPERSION PROBLEMS

by Raz Khaleel[a] and Donald L. Reddell[b]

Abstract. The method of characteristics is used to solve the one- and two-dimensional convective-dispersion equations in steady, uniform flow fields. Fully documented listings of the FORTRAN programs are presented. Comparison of numerical results with existing analytical solutions show excellent agreement.

Introduction

When convection and dispersion are considered simultaneously, conventional finite-difference techniques introduce artificial numerical dispersion (Peaceman and Rachford, 1962). The artificial dispersion may dominate low physical dispersion especially if dispersivities are small. Garder *et al.* (1964) developed the method of characteristics (MOC) to overcome the numerical dispersion problem. The MOC does not introduce numerical dispersion and has been widely used for solving miscible displacement problems (e.g., Reddell and Sunada, 1970; Bredehoeft and Pinder, 1973; Konikow and Bredehoeft, 1974, 1978). On the other hand, a number of researchers (e.g., Lam, 1977; van Genuchten, 1977; Huyakorn and Taylor, 1977) have shown that in certain convection-dominated flow systems, the standard Galerkin finite-element formulation will produce excessive numerical dispersion and/or oscillation even if higher order elements are used.

In this paper, MOC solutions of one- and two-dimensional convective-dispersion equations for a conservative tracer are presented for steady, uniform flow fields. Fully documented listings of the FORTRAN programs are presented and numerical examples are included to illustrate the basic use of the MOC. The accuracy of the computer codes is tested by comparison with available analytical solutions.

Numerical Model

The convective-dispersion equation for a conservative tracer in fluid flow through a saturated porous medium is given as (Scheidegger, 1961):

$$\frac{\partial C}{\partial t} + \frac{\partial}{\partial x_i}(V_i C) = \frac{\partial}{\partial x_i}\left(D_{ij}\frac{\partial C}{\partial x_j}\right) \quad i = 1 \text{ and } 3 \qquad (1)$$

where C = tracer concentration (ML^{-3}); V_i = components of velocity vector (LT^{-1}) in a Cartesian coordinate system of x_i; D_{ij} = coefficient of hydrodynamic dispersion, a second rank tensor (L^2T^{-1}); and t = time (T). The double summation convention of tensor notation is implied in the use of equation (1). The coefficient of hydrodynamic dispersion, D_{ij}, depends on the flow pattern and medium characteristics. It is formed from the contraction of a fourth rank tensor and a second rank tensor which is a function of flow (Bear, 1972):

$$D_{ij} = a_{ijmn}\frac{V_m V_n}{|V|} \qquad (2)$$

where a_{ijmn} = dispersivity of the medium, a fourth rank tensor (L); V_m, V_n = velocity components in the m and n directions, respectively (LT^{-1}); and $|V|$ = magnitude of velocity (LT^{-1}).

Scheidegger (1961) showed that for an isotropic medium, the longitudinal and lateral dispersion coefficients (D_L and D_T, respectively) are related to the dispersivities by

$$D_L = \alpha_L\,|V| \qquad (3a)$$

and

$$D_T = \alpha_T\,|V|. \qquad (3b)$$

[a] Staff Engineer, Rockwell Hanford Operations, P.O. Box 800, Richland, Washington 99352.

[b] Professor of Agricultural Engineering, Texas A&M University, College Station, Texas 77843.

Received November 1984, revised March 1986, accepted April 1986.

Discussion open until May 1, 1987.

Combining equations (2) and (3), the tensorial forms of the dispersion coefficient for two-dimensional flow in an isotropic aquifer are (Konikow and Bredehoeft, 1978):

$$D_{11} = D_L \frac{V_1 V_1}{V^2} + D_T \frac{V_3 V_3}{V^2} \tag{4a}$$

$$D_{33} = D_T \frac{V_1 V_1}{V^2} + D_L \frac{V_3 V_3}{V^2} \tag{4b}$$

$$D_{31} = D_{13} = (D_L - D_T) \frac{V_1 V_3}{V^2} \tag{4c}$$

The MOC algorithm is not described here in detail because it has already been discussed in the literature (Garder *et al.*, 1964). Briefly, equation (1) approaches a hyperbolic equation as the second-order dispersion term becomes small with respect to the convective term. According to the MOC, we can associate with a given hyperbolic equation a simplified system of equations in terms of an arbitrary curve parameter, the solutions of which are called the characteristic curves of the differential equation. Detailed derivations of characteristic curves for a homogeneous, linear partial differential equation and for a nonlinear, nonhomogeneous partial differential equation were given by Garder *et al.* (1964).

In the MOC, in addition to the usual division of the flow region into a grid system, a set of moving points is introduced into the numerical solution. The location of each moving point is specified by its coordinates in the finite-difference grid. Initially, the moving points are uniformly distributed throughout the grid system. The initial concentration assigned to each point is the initial concentration associated with the stationary node of the grid block containing the point. At each time interval, the moving points in a two-dimensional system are relocated using:

$$x_{1\ell}^{t+\Delta t} = x_{1\ell}^{t} + \Delta t \, V_{1\ell}^{t+\Delta t} \tag{5a}$$

and

$$x_{3\ell}^{t+\Delta t} = x_{3\ell}^{t} + \Delta t \, V_{3\ell}^{t+\Delta t} \tag{5b}$$

where $t + \Delta t$ = new time level; t = old time level; Δt = time increment; $x_{1\ell}$ and $x_{3\ell}$ = coordinates of the ℓ-th moving point in the x_1 and x_3 directions; and $V_{1\ell}$ and $V_{3\ell}$ = velocities of the ℓ-th moving point in the x_1 and x_3 directions. When all the moving points have been relocated, each block in the grid system is temporarily assigned a concentration, $C^{t+\Delta}$, which is the average of the concentrations $C_\ell^{t+\Delta}$ of all the moving points lying inside the grid block at time $t + \Delta t$. Next, the change in concentration due to dispersion, ΔC, is calculated using an explicit, centered-in-space finite-difference approximation to the dispersive term on the right-hand side of equation (1). Each moving point is then assigned a concentration according to:

$$C_\ell^{t+\Delta t} = C_\ell^{t+\Delta} + \Delta C. \tag{6}$$

To complete the step from time t to $t + \Delta t$, the solute concentration at the stationary grid nodes is calculated according to

$$C^{t+\Delta t} = C^{t+\Delta} + \Delta C. \tag{7}$$

Computer Programs

Listings of the MOC programs for solving one-dimensional and two-dimensional tracer flow problems are given in Appendices A and B, respectively. The following steps in the MOC procedure are valid for both one- and two-dimensional problems.

Step 1: In addition to assigning nodal coordinates and concentrations, initial coordinates and concentrations are assigned to the moving points in each grid block.

Step 2: Determine which grid block the moving point is located in, and relocate the point using the assigned flow velocity. Also, if during a time step, any point moves out of the system, it is reentered at an inflow boundary with the appropriate boundary concentration and coordinates. Minor changes in the programs must be made when boundary conditions are changed to allow for the proper removal and reintroduction of the moving points. After the moving points have been relocated, a count is made of the number of moving points in each grid block.

Step 3: A temporary concentration equal to the average of the concentrations of moving points inside the grid block is assigned to each grid block.

Step 4: A change in grid block concentration due to dispersion is calculated based on the temporary grid block concentration calculated in Step 3.

Step 5: Each grid block concentration is updated based on the change in concentration calculated in Step 4.

Step 6: Each moving point concentration is also updated based on the change in concentration calculated in Step 4.

Steps 2 through 6 are repeated for each simulated time step. Each step is clearly identified in both programs in Appendices A and B.

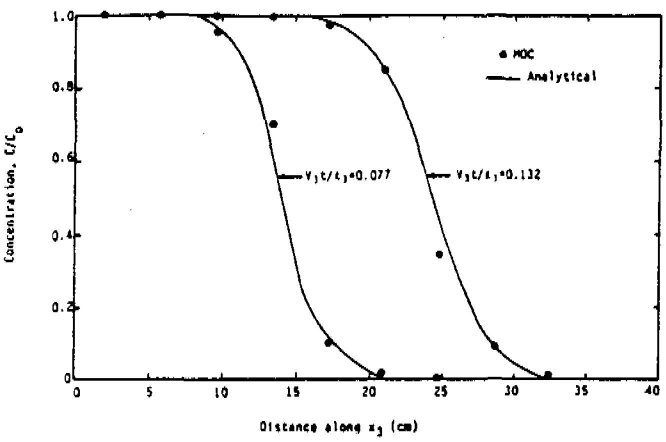

Fig. 1. Comparison of analytical and numerical solutions to the longitudinal dispersion problem in one-dimensional flow.

Numerical Testing

Longitudinal Dispersion in One-Dimensional Flow

Numerical simulation results based on the computer code in Appendix A were compared with those obtained from the solution of the following form of the convective-dispersion equation:

$$\frac{\partial C}{\partial t} = D_L \frac{\partial^2 C}{\partial x_3^2} - V_3 \frac{\partial C}{\partial x_3}. \tag{8}$$

The appropriate initial and boundary conditions for the problem considered are:

$$\begin{aligned} C(x_3, 0) &= 0; \quad x_3 \geqslant 0 \\ C(0, t) &= C_O; \quad t \geqslant 0 \\ C(\infty, t) &= 0; \quad t \geqslant 0. \end{aligned} \tag{9}$$

Ogata and Banks (1961) used Laplace transforms with equation (8) to obtain the solution

$$\frac{C}{C_O} = \tfrac{1}{2}\left[\operatorname{erfc}\left\{\frac{x_3 - V_3 t}{2(D_L t)^{1/2}}\right\} + \exp\left\{\frac{V_3 x_3}{D_L}\right\} \operatorname{erfc}\left\{\frac{x_3 + V_3 t}{2(D_L t)^{1/2}}\right\}\right]. \tag{10}$$

A numerical solution was obtained using the following data for the one-dimensional program (Appendix A):

number of grid blocks (NR) = 49.
total number of moving points (NP1) = 196.
number of moving points per grid block (NPZ) = 4.
maximum number of time steps (MAXST) = 18.

simulation finish time (FINTIM) = 1710 sec.
time increment, Δt (DELT) = 100 sec.
spatial increment, Δx_3 (DELZ) = 3.81 cm.
total depth of model, ℓ_3 (TZ) = 182.88 cm.
longitudinal dispersion coefficient,
D_L (DL) = 2.94×10^{-3} cm^{2}s^{-1}.
seepage velocity, V_3 (VEL) = 0.01411 cms^{-1}.
dimensionless concentration (C/C_O) at input boundary (CO) = 1.0.
dimensionless initial concentration, C/C_O (CINTL) = 0.0.

Note that the required number of grid blocks for a total length of 182.88 cm is 48. However, in the input data, NR has been increased by one to accommodate the upper boundary condition. This also resulted in an increase in the total number of moving points. The results shown in Figure 1 indicate excellent agreement between the numerical and analytical solutions.

Longitudinal Dispersion in Two-Dimensional Flow

To check the numerical solution using the tensorial form of the dispersion coefficient [equation (4)], a coordinate transformation was performed (Figure 2). The coordinate axes were rotated so that an angle of 45° existed between the velocity vector and the transformed coordinate axes. The problem was solved numerically in the rotated coordinate system (x_1', x_3'). This forced the numerical model to use the tensor transformation for the dispersion coefficient. However, the physics of the problem was not changed, and equation (10) still provides an analytical solution to the problem in the (x_1, x_3) coordinate system.

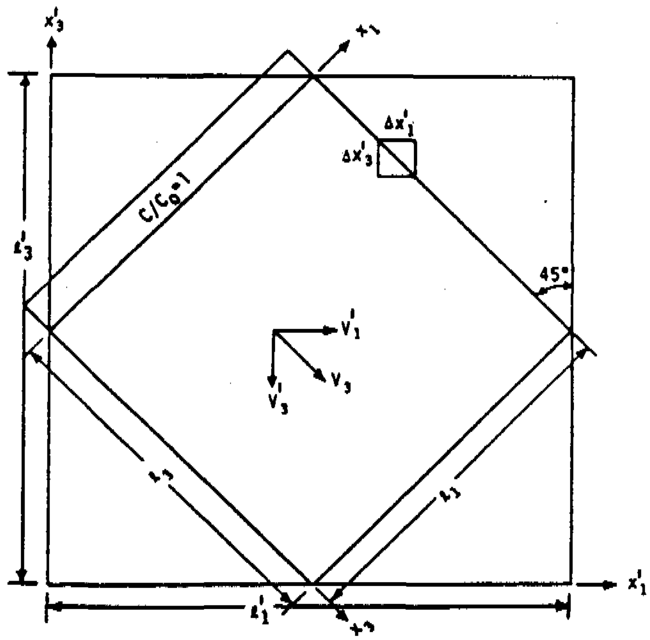

Fig. 2. Schematic diagram of coordinate axes rotation used for comparing numerical and analytical solutions of the longitudinal dispersion problem in two-dimensional flow.

A rectangular region, $0 \leqslant x_3 \leqslant \ell_3$ and $0 \leqslant x_1 \leqslant \ell_1$, was considered in which the flow is along the x_3 axis with a steady, uniform seepage velocity, V_3 (Figure 2). With the coordinates rotated 45 degrees with respect to the velocity vector V_3, the numerical solution was carried out in the rectangular region defined by $0 \leqslant x'_3 \leqslant \ell'_3$ and $0 \leqslant x'_1 \leqslant \ell'_1$. A steady, uniform seepage velocity with components $V'_3 = 0.707\ V_3$ and $V'_1 = 0.707\ V_3$ existed in the transformed region. A fluid with a relative concentration of $C/C_o = 1.0$ was injected across the entire interface $0 \leqslant x_1 \leqslant \ell_1$. Data used to numerically solve the problem (Figure 2) were: $\Delta x'_3 = 0.4$ cm, $\Delta x'_1 = 0.4$ cm, $\Delta t = 2$ sec, $V'_3 = 0.071$ cm sec^{-1}, $V'_1 = 0.071$ cm sec^{-1}, $V_3 = 0.10$ cm sec^{-1}, grid dimensions = 20 × 20, $D_L = 0.01$ cm^2 sec^{-1}, $D_T = 0.001$ cm^2 sec^{-1}, $\ell_3 = 5.66$ cm, $\ell_1 = 5.66$ cm, and the number of moving points per grid block = 4. Some modifications to the code listed in Appendix A were necessary to run the longitudinal dispersion problem with and without the tensor transformation in two-dimensional flow. The modified code is not listed because the modifications are minor. It is available on request from the authors.

Two solutions were obtained for this problem; one solution used the tensorial transformations for the dispersion coefficients, D_L and D_T, given by equations (4), and the other solution used no tensor transformation. With the tensor transformation, the longitudinal dispersion coefficient (D_{33}) is oriented parallel to the velocity vector (V_3) and the lateral dispersion coefficient (D_{11}) is oriented perpendicular to the velocity vector (V_3). For the case with no tensor transformation, the longitudinal dispersion coefficient (D_{33}) is oriented parallel to the x'_3 coordinate axis and the lateral dispersion coefficient (D_{11}) is oriented parallel to the x'_1 coordinate axis.

The results from the numerical solution of this longitudinal dispersion problem with and without the tensor transformation are shown in Figure 3. The analytical solution as given by equation (10) is also plotted. The results indicate an excellent agreement between the numerical and analytical solution when the tensor transformation is used. The solution without the tensor transformation yielded a steeper concentration profile than the analytical solution. Thus, a significant error results in the numerical solution of the dispersion equation when the tensor transformation is not used and the cross-derivative terms in equation (4) are ignored.

Figure 4 shows the lateral concentration distribution after 0.71 pore volumes of fluid were injected. Again, the numerical solution using the tensor transformation provides more accurate

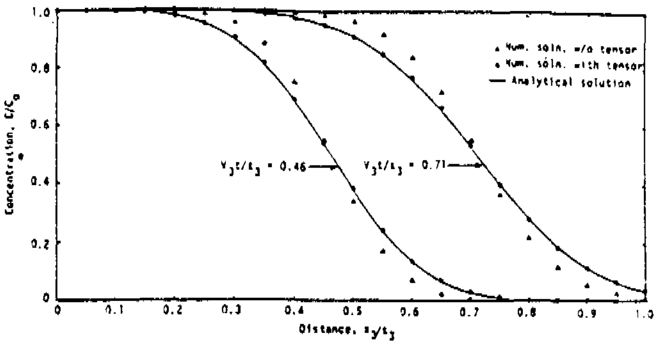

Fig. 3. Comparison of longitudinal concentration distribution calculated with and without the tensor transformation for the longitudinal dispersion problem in two-dimensional flow.

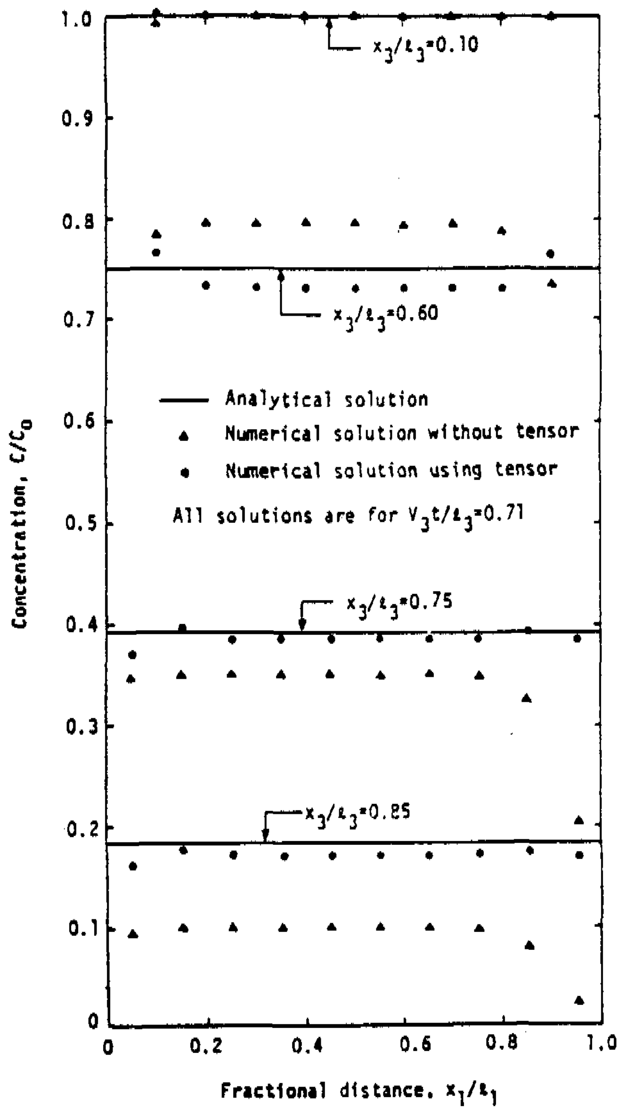

Fig. 4. Comparison of lateral concentration distribution with and without the tensor transformation for the longitudinal dispersion problem in two-dimensional flow.

results than that without the tensor transformation. Some error in the numerical solution occurs near the boundaries ($x_1 = 0$ and $x_1 = \ell_1$). This occurs because the straight boundaries of the column in the (x_1, x_3) coordinate system must be approximated by a series of rectangles or squares in the rotated coordinate system (x_1', x_3') (Figure 2). As $\Delta x_1'$ and $\Delta x_3'$ become very small, a better approximation of the boundary conditions can be expected. The numerical results for any value of x_3/ℓ_3 were generally the same for $0.3 \leq x_1/\ell_1 \leq 0.7$. No dispersion (or mass flow) was allowed to occur across the boundary columns $x_1 = 0$ and $x_1 = \ell_1$. This condition was approximated numerically by setting the dispersion coefficients equal to zero for all nodes on these two boundaries.

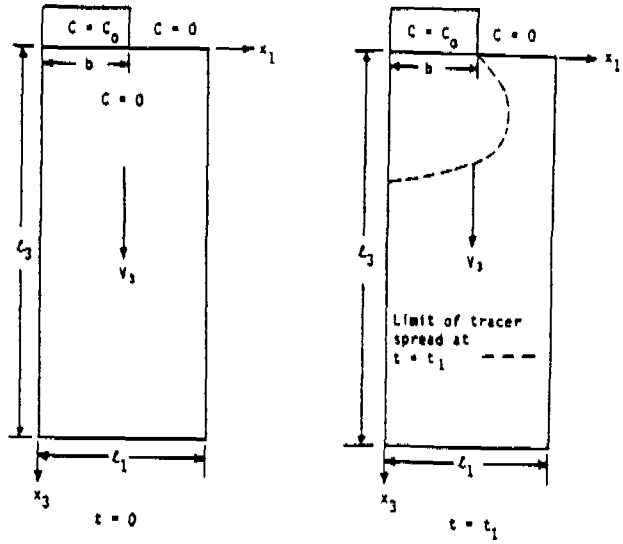

Fig. 5. Schematic diagram of longitudinal and lateral dispersion problem in one-dimensional flow.

Longitudinal and Lateral Dispersion in One-Dimensional Flow

If a rectangular column ($0 \leq x_3 \leq \ell_3$, $0 \leq x_1 \leq \ell_1$) is used and a tracer source is maintained over a portion of the input area ($0 \leq x_1 \leq b$) as shown on Figure 5, then both longitudinal and lateral dispersion will occur. Assuming a homogeneous and isotropic saturated medium with unidirectional flow in the x_3 direction and $\partial C/\partial x_1 = 0$, equation (1) becomes

$$\frac{\partial C}{\partial t} = D_L \frac{\partial^2 C}{\partial x_3^2} + D_T \frac{\partial^2 C}{\partial x_1^2} - V_3 \frac{\partial C}{\partial x_3}. \qquad (11)$$

The initial and boundary conditions are given by

$$C(x_1, 0, t) = C_0; \qquad 0 \leq x_1 \leq b; \quad t \geq 0$$

$$C(x_1, 0, t) = 0; \qquad b < x_1 < \ell_1; \quad t \geq 0$$

$$\frac{\partial C}{\partial x_1}(0, x_3, t) = 0, \qquad t > 0$$

$$\frac{\partial C}{\partial x_1}(\ell_1, x_3, t) = 0, \qquad t > 0$$

$$C(x_1, \infty, t) = \text{Bounded}$$

$$C(x_1, x_3, 0) = 0 \qquad 0 \leq x_1 \leq \ell_1; \quad x_3 > 0. \quad (12)$$

Harleman and Rumer (1963) gave the following approximate steady-state solution to equations (11) and (12).

$$\frac{C}{C_0} = \tfrac{1}{2} \operatorname{erfc} \left[\frac{x_1 - b}{2\sqrt{D_T x_3/V_3}} \right]. \qquad (13)$$

A problem of longitudinal and lateral dispersion in unidirectional flow was run using the code in Appendix B and the following data:

number of grid blocks (rows) in the vertical (x_3) direction (NR) = 26.
total number of moving points in vertical (x_3) direction (NP1) = 52.
number of moving points/grid block in x_3 direction (NPZ) = 2.
number of grid blocks (columns) in horizontal (x_1) direction (NC) = 20.
total number of moving points in horizontal (x_1) direction (NP2) = 40.
number of moving points/block in x_1 direction (NPX) = 2.
maximum number of time steps (MAXST) = 100.
initial value of counter for printing numerical solution (KPRINT) = 1.
number of intervals at which results are printed (IFAC) = 100.

simulation finish time (FINTIM) = 200 sec.
time increment, Δt (DELT) = 2.0 sec.
vertical spatial increment, Δx_3 (DELZ) = 0.40 cm.
total depth of model in x_3 direction, ℓ_3 (TZ) = 10.0 cm.
horizontal spatial increment, Δx_1 (DELX) = 0.20 cm.
total width of model in x_1 direction, ℓ_1 (TX) = 4.0 cm.

longitudinal dispersion coefficient, D_L (DL) = 0.01 cm^2 sec^{-1}.
lateral dispersion coefficient, D_T (DT) = 0.001 cm^2 sec^{-1}.
length of tracer source in x_1 direction, b (B) = 2.20 cm.
velocity in x_3 direction, V_3 (VEL) = 0.10 cm sec^{-1}.

dimensionless concentration (C/C_0) at input boundary (CO) = 1.0.
dimensionless initial concentration, C/C_0 (CINTL) = 0.0.

As in the one-dimensional program, NR was increased by one to accommodate the upper boundary condition.

The results from the numerical solution of the longitudinal and lateral dispersion problem are shown in Figures 6 and 7, at t = 200 sec and after an approximate steady-state condition was achieved. For comparison, the approximate analytical solutions for the steady-state case as determined from (13) are also plotted in Figures 6 and 7 as the solid lines. In general, the accuracy of the numerical solution is excellent. The region close to the source, i.e., $x_3 = 0$, is a problem area where the accuracy is not as good. This occurs because of the very steep concentration gradient in the x_1 direction which approaches a step function. Reddell and Sunada (1970) discussed the problem of achieving accurate numerical solutions along steep concentration profiles or when step-input functions are used. They reported that much smaller grid dimensions are necessary to obtain accurate results in these areas. It should also be noted that equation (13) is only an approximate analytical solution and not an exact one. Also, equation (13) is a steady-state solution, but the numerical solutions are transient. The numerical solutions were terminated after 200 sec of simulation, and the results were changing only slightly with each additional time step, and a true steady state had not been achieved.

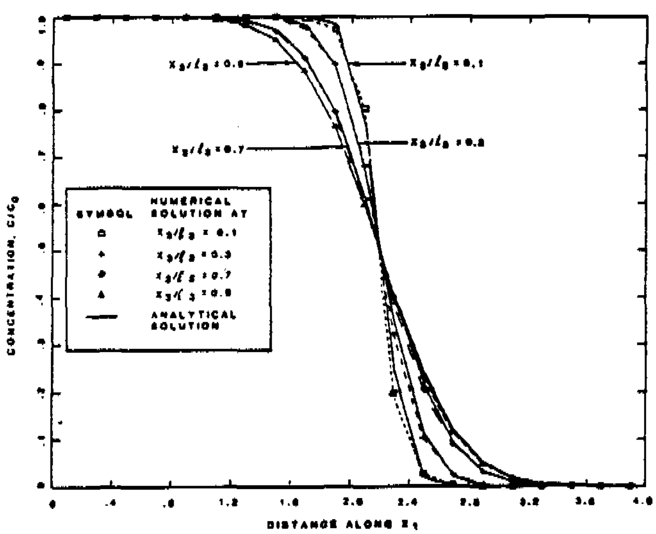

Fig. 6. Comparison of lateral concentration distribution at steady state as calculated numerically and by an approximate analytical solution for the two-dimensional dispersion problem in one-dimensional flow.

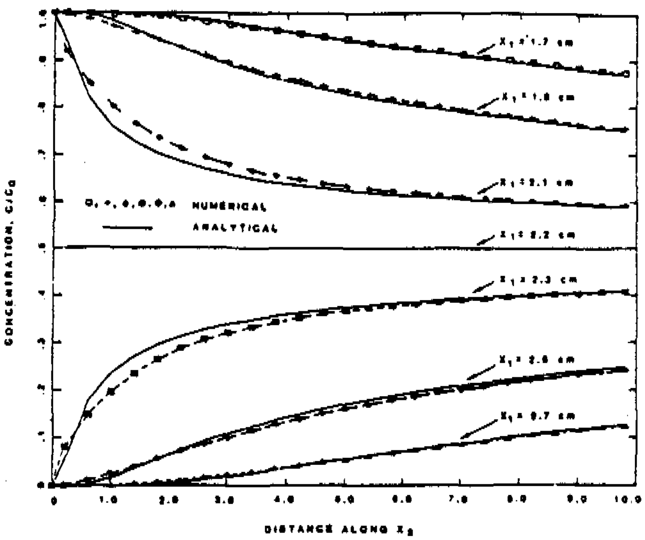

Fig. 7. Comparison of longitudinal concentration distribution at steady state as calculated numerically and by an approximate analytical solution for the two-dimensional dispersion problem in one-dimensional flow.

Longitudinal and Lateral Dispersion in Two-Dimensional Flow

A longitudinal and lateral dispersion problem was also solved numerically in the rotated coordinate system (x'_1, x'_3) as shown in Figure 8. A fluid with a relative concentration of C/C_0 = 1.0

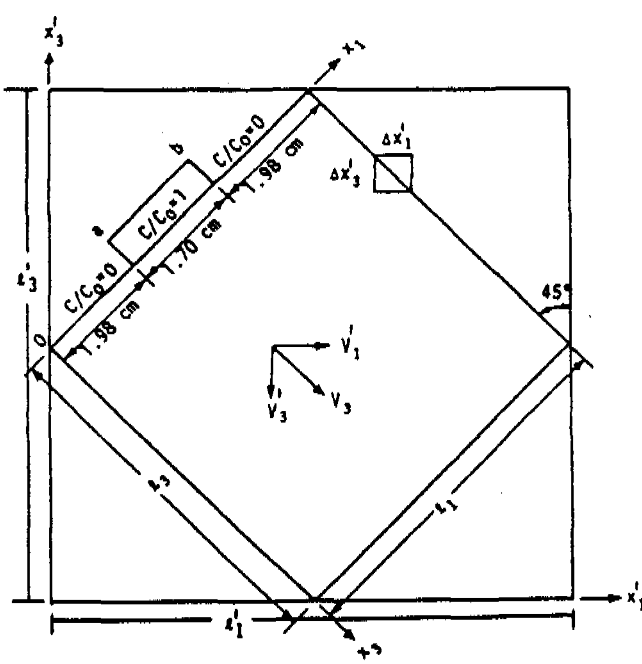

Fig. 8. Schematic diagram of coordinate axes rotation used for comparing numerical and analytical solutions of the longitudinal and lateral dispersion problem in two-dimensional flow.

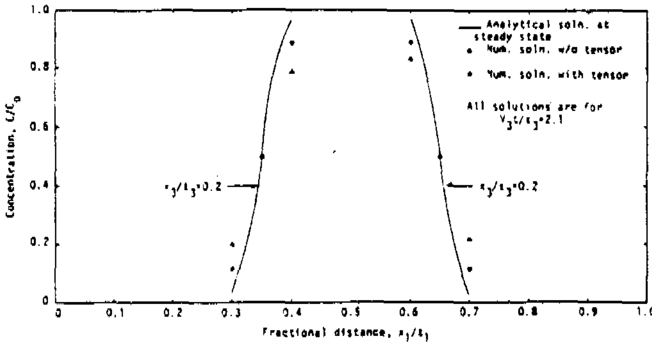

Fig. 9. Comparison of lateral concentration distribution at $x_3/\ell_3 = 0.2$ as calculated by using the tensor transformation, without the tensor transformation, and by an approximate analytical solution for steady-state conditions for the two-dimensional dispersion and flow problem.

was injected over the interval $a \leqslant x_1 \leqslant b$ and fluid with a relative concentration of $C/C_O = 0.0$ was injected over the intervals $0 \leqslant x_1 \leqslant a$ and $b \leqslant x_1 \leqslant \ell_1$. Data used to numerically solve this problem were the same as for the previously described longitudinal dispersion problem.

Again, some minor modifications to the code listed in Appendix B were necessary to run the longitudinal and lateral dispersion problem with and without the tensor transformation in two-dimensional flow. The modified code is available on request from the authors.

The results from the numerical solution of the longitudinal and lateral dispersion problem with and without the tensor transformation are shown in Figures 9 through 12 after 2.1 pore volumes of fluid were injected and an approximate steady-state condition was achieved. For comparison, the approximate analytical solution for the steady case as determined from equation (13) is also plotted.

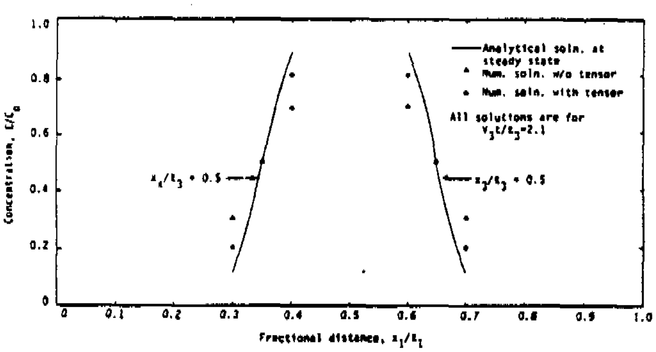

Fig. 10. Comparison of lateral concentration distribution at $x_3/\ell_3 = 0.5$ as calculated by using the tensor transformation, without the tensor transformation, and by an approximate analytical solution for steady-state conditions for the two-dimensional dispersion and flow problem.

Figure 12 shows that the numerical solutions obtained using the tensor transformation are much closer to the analytical solution than those without the tensor transformation. However, the accuracy of the numerical solution is not as good as was achieved in the longitudinal dispersion problem described earlier. As discussed earlier, this occurs because of the very steep concentration gradient in the x_1 direction.

The concentration profiles as plotted do not show any "overshoot" or "undershoot." However, overshoot and undershoot did occur but were generally on the order of 10^{-3} to 10^{-4} C/C_O. Since the numerical solution without the tensor transformation did not produce any overshoot, the use of a "nine-star" grid pattern to estimate the cross derivatives for the tensor transformation is believed to be the source of this small amount of overshoot.

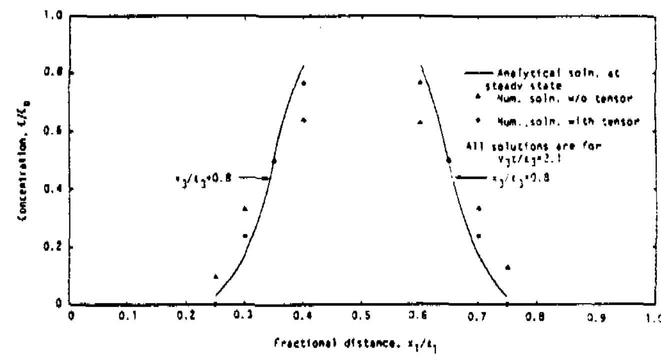

Fig. 11. Comparison of lateral concentration distribution at $x_3/\ell_3 = 0.8$ as calculated by using the tensor transformation, without the tensor transformation, and by an approximate analytical solution for steady-state conditions for the two-dimensional dispersion and flow problem.

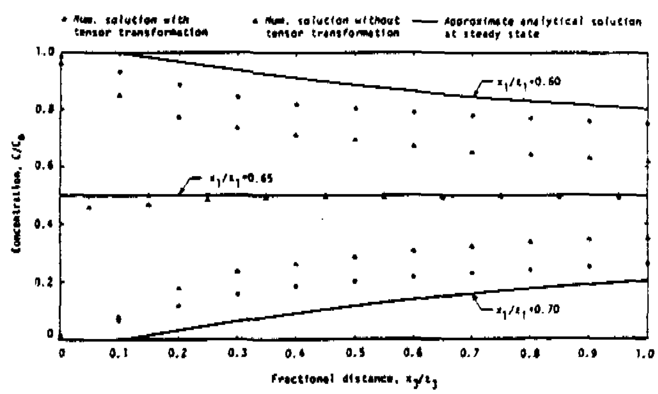

Fig. 12. Comparison of longitudinal concentration distribution at steady state as calculated by using the tensor transformation, without the tensor transformation, and by an approximate analytical solution for the two-dimensional dispersion and flow problem.

Summary and Conclusions

Four different convective-dispersion problems were considered: (1) longitudinal dispersion in one-dimensional flow; (2) longitudinal dispersion with and without the tensor transformation in two-dimensional flow; (3) longitudinal and lateral dispersion in unidirectional flow; and (4) longitudinal and lateral dispersion with and without the tensor transformation in two-dimensional flow. A steady, uniform flow field was assumed and the porous medium was homogeneous and isotropic. A coordinate transformation was necessary to check the numerical solution using the tensorial form of the dispersion coefficient. The MOC was used to solve the convective-dispersion equations. The results from the numerical solutions of the dispersion problems were compared with available analytical solutions. Excellent agreement was obtained between the numerical and analytical solutions when the tensor transformation was used. This provides strong evidence for the accuracy of the MOC and the numerical tensor transformation used.

The MOC appears to be capable of solving the longitudinal dispersion as well as the longitudinal and lateral dispersion problems. No problems with overshoot occurred and no numerical dispersion resulted from the numerical process. The small amount of overshoot that occurred in the numerical solution is believed to be the result of using a nine-star grid pattern to estimate the cross derivatives for the tensor transformation.

The FORTRAN programs presented in the paper are intended to illustrate the basic use of the MOC in solving convective-dispersion problems for a conservative tracer in a saturated porous medium. For specific applications to real-world field problems involving fluid sources and sinks in confined/unconfined heterogeneous aquifers, other FORTRAN programs (e.g., Konikow and Bredehoeft, 1978) are available.

References

Bear, J. 1972. Dynamics of Fluids in Porous Media. Elsevier Publ. Co., NY. 764 pp.

Bredehoeft, J. D. and G. F. Pinder. 1973. Mass transport in flowing groundwater. Water Resources Research. v. 9, no. 1, pp. 194-210.

Garder, A. O., Jr., D. W. Peaceman, and A. L. Pozzi, Jr. 1964. Numerical calculation of multidimensional miscible displacement by the method of characteristics. Society of Petroleum Engineers Journal. v. 4, no. 1, pp. 26-36.

Harleman, D.R.F. and R. R. Rumer. 1963. Longitudinal and lateral dispersion in an isotropic porous medium. Journal of Fluid Mechanics. v. 16, pp. 385-394.

Huyakorn, P. S. and D. Taylor. 1977. Finite element models for coupled groundwater flow and convective dispersion. In Finite Elements in Water Resour., Gray, W. G., G. F. Pinder, and C. A. Brebbia, eds. Pentech Press, London. pp. 1.131-1.152.

Konikow, L. F. and J. D. Bredehoeft. 1974. Modeling flow and chemical quality changes in an irrigated stream-aquifer system. Water Resources Research. v. 10, no. 3, pp. 546-562.

Konikow, L. F. and J. D. Bredehoeft. 1978. Computer model of two-dimensional solute transport and dispersion in ground water. U.S.G.S. Techniques of Water Resource Investigations. Chapter C2, Book 7, 90 pp.

Lam, D.C.L. 1977. Comparison of finite element and finite difference methods for nearshore advection-diffusion transport model. In Finite Elements in Water Resour., Gray, W. G., G. F. Pinder, and C. A. Brebbia, eds. Pentech Press, London. pp. 1.115-1.130.

Ogata, A. and R. B. Banks. 1961. A solution of the differential equation of longitudinal dispersion in porous media. U.S. Geol. Survey Prof. Paper 411-A. U.S. G.P.O., Washington, DC. 7 pp.

Peaceman, D. W. and H. H. Rachford, Jr. 1962. Numerical calculation of multidimensional miscible displacement. Society of Petroleum Engineers Journal. v. 2, no. 4, pp. 327-339.

Reddell, D. L. and D. K. Sunada. 1970. Numerical simulation of dispersion in groundwater aquifers. Colorado State University, Hydrology Papers, No. 41. 79 pp.

Scheidegger, A. E. 1961. General theory of dispersion in porous media. Journal of Geophysical Research. v. 66, no. 10, pp. 3273-3278.

van Genuchten, M. T. 1977. On the accuracy and efficiency of several numerical schemes for solving the convective-dispersion equation. In Finite Elements in Water Resources, Gray, W. F., G. F. Pinder, and C. A. Brebbia, eds. Pentech Press, London. pp. 1.71-1.90.

* * * * *

Raz Khaleel is a Staff Engineer with Rockwell Hanford Operations, Rockwell International, Richland, Washington. He is also an adjunct faculty member in the Department of Civil Engineering at Washington State University, Pullman. He obtained his Ph.D. in Soil and Water Engineering from Texas A&M University, College Station. His research interests are in numerical modeling of subsurface flow systems.

Donald L. Reddell is a Professor in the Department of Agricultural Engineering at Texas A&M University, College Station. He obtained his Ph.D. in Soil and Water Engineering from Colorado State University, Fort Collins. His research interests are in ground-water hydrology and numerical simulation of fluid flow and transport in saturated and unsaturated flow systems.

Appendix A. Solution of One-Dimensional Convective-Dispersion Equation by the Method of Characteristics

```
C---------------------- INPUT INFORMATION ---------------------------------
C
C     ***NOTE:  TO RUN PROGRAM YOU MUST USE THE COMMAND:
C               EX MOC.FOR,SYS:IMSLIB/LIB
C
C     NR = NUMBER OF GRIDS (ROWS) IN THE VERTICAL (X3) DIRECTION
C     NP1= NUMBER OF MOVING POINTS IN THE VERTICAL DIRECTION
C     NPZ= NUMBER OF MOVING POINTS/GRID IN X3 DIRECTION
C     MAXST= MAXIMUM NUMBER OF TIME STEPS
C
C     FINTIM= SIMULATION FINISH TIME IN SECONDS
C     DELT   = TIME INCREMENT IN SECONDS
C     DELZ   = SPATIAL INCREMENT IN CM.
C     TZ     = TOTAL DEPTH OF MODEL IN X3 DIRECTION
C
C     DL = LONGITUDINAL DISPERSION COEFFICIENT IN CM**2/SEC.
C     VEL= VELOCITY IN X3 DIRECTION
C     CO = DIMENSIONLESS CONCENTRATION AT THE INPUT BOUNDARY
C     CINTL = DIMENSIONLESS INITIAL CONCENTRATION
C-------------------------------------------------------------------------
C              ********** PROGRAM VARIABLES **********
C
C     ALENZ = TOTAL LENGTH IN X3 DIRECTION
C     MAXST = MAX. NO. OF TIME STEPS DURING SIMULATION
C     ZC ( )= X3 COORDINATE AT GRID CENTER
C     Z( )   = X3 COORDINATE OF MOVING POINTS
C     C( )   = CONCENTRATION OF MOVING POINTS
C     V( )   = VELOCITY OF EACH MOVING POINT
C     SUMC( ) = SUMMATION OF CONCENTRATION OF MOVING POINTS IN A GRID
C     COUNT( )= A COUNT OF NUMBER OF MOVING POINTS IN A GRID
C     CAVG ( )= AVERAGE CONCENTRATION OF TRACER FOR A GRID AND IS
C               DETERMINED AS SUMC/COUNT
C     DELC ( )= CHANGE IN CONCENTRATION FOR A GRID DUE TO DISPERSION
C     CCOA( ) = DIMENSIONLESS CONCENTRATION BY ANALYTICAL SOLUTION
C     NI1      = ROW NUMBER OF GRID IN WHICH MOVING POINT IS LOCATED
C     DOG      = INCREMENTING FACTOR USED IN DO-LOOP
C-------------------------------------------------------------------------
C
      INTEGER TSTEP
      DIMENSION Z(196),CAVG(49),COUNT(49),SUMC(49),V(196),DELC(196),
     $ CCOA(49),C(196),ZC(49)
      DATA NPRINT,IPRINT,NREAD/3,5,5/
      WRITE (IPRINT,100)
100   FORMAT (/,2X,' THE FOLLOWING VARIABLES HAVE I5 FORMATS',
     $ /,2X,' GIVE VALUES FOR: NR, NP1, NPZ, MAXST',/)
      READ (NREAD,1) NR, NP1, NPZ, MAXST
      WRITE (NPRINT,2) NR, NP1, NPZ, MAXST
      WRITE (IPRINT,200)
200   FORMAT (/,2X, ' THE NEXT 4 VARIABLES HAVE FREE FORMATS',/,
     $ 2X, ' GIVE VALUES FOR FINTIM, DELT, DELZ, TZ',/)
      READ (NREAD,*) FINTIM,DELT,DELZ,TZ
      WRITE (IPRINT,300)
300   FORMAT (/,2X, ' THE LAST FOUR VARIABLES HAVE FREE FORMATS',/,
     $ 2X, ' GIVE VALUES FOR DL, VEL, CO, CINTL',//)
      READ (NREAD,*) DL, VEL, CO, CINTL
      WRITE (IPRINT,400)
400   FORMAT (//,2X,' OUTPUT DISPOSED TO LINE PRINTER')
      WRITE (NPRINT,4) FINTIM, DELT, DELZ, TZ, DL, VEL, CO, CINTL
      PZ = FLOAT(NPZ)
      AD = DELT*DL/DELZ/DELZ
      ALENZ = DELZ * FLOAT(NR)
      ADISZ = DELZ/PZ
      NRM1 = NR - 1
C-------------------------------------------------------------------------
C
C     *** STEP 1: ASSIGN INITIAL COORDINATES AND CONCENTRATIONS TO
C                             MOVING POINTS ***
      ZC(1) = 0.0
      ZC(2) = DELZ/2.
      DO 80 I = 3, NR
80    ZC(I) = ZC(I - 1) + DELZ
      DO 67 I = 1, NR
      SUMC(I) = 0.0
      COUNT(I)= 0.0
67    DELC(I) = 0.0
      DO 10 I = 1, NP1
      DOG = FLOAT (I - 1)
      Z(I)= (DELZ/PZ) * (0.5 + DOG)
      C(I)= CINTL
      IF (I .LE. NPZ) C(I) = 1.0
      V(I) = VEL
      NI1 = Z(I)/DELZ + 1.0
      SUMC(NI1) = SUMC(NI1) + C(I)
      COUNT(NI1)= COUNT(NI1)+ 1.0
10    CONTINUE
C
      DO 11 I = 1,NR
      IF (COUNT(I) .EQ. 0.) COUNT(I)=1.0
      CAVG(I) = SUMC(I)/COUNT(I)
11    CONTINUE
C
C*******PRINT INITIAL CONCENTRATION FOR EACH GRID POINT*******
C
      TSTEP = 0
      TIME = 0.0
      WRITE (NPRINT, 17)
      DO 500 I = 1,NR
500   WRITE (NPRINT, 16) I, SUMC(I), COUNT(I), DELC(I), CAVG(I)
1000  CONTINUE
C
C---------------- START SIMULATION OVER TIME STEPS -------------------------
C
      TSTEP = TSTEP + 1
      IF (TIME + DELT .GT. FINTIM) DELT = FINTIM - TIME
      TIME = TIME + DELT
C
C------ STEP 2: DETERMINES WHICH GRID THE MOVING POINT IS LOCATED, AND
C                RELOCATES THE POINT USING ASSIGNED FLOW VELOCITY ------
C
      DO 20 I = 1, NP1
      NI1 = Z(I)/DELZ + 1.0
      Z(I) = Z(I) + DELT*V(I)
20    CONTINUE
C-------------------------------------------------------------------------
C*******IF DURING A TIME STEP, ANY MOVING POINT MOVES OUT OF THE SYSTEM, IT IS
C       RE-ENTERED AT THE INFLOW BOUNDARY; ASSIGNED APPROPRIATE COORDINATES AND
C       CONCENTRATION **********
C
      DO 66 I = 1, NP1
      IF (Z(I) .LT. ALENZ) GO TO 66
      NPM1 = NP1 - 1
      DO 52 J = 1, NPM1
      NN = NP1 + 1 - J
      Z(NN) = Z(NN - 1)
      V(NN) = V(NN - 1)
      C(NN) = C(NN - 1)
52    CONTINUE
      Z(1) = Z(2) - ADISZ
      IF (Z(1) .LT. 0.01) Z(1) = 0.01
      V(1) = VEL
      C(1) = CO
66    CONTINUE
C*************************************************************************
C  **** INITIALIZE THE SUMC AND COUNT ARRAYS ****
C
      DO 54 I = 1, NR
      SUMC (I) = 0.0
      COUNT(I) = 0.0
54    CONTINUE
C  ***********************************************************************
C  **** COMPUTE SUMC AND COUNT FOR MOVING POINTS IN A GRID ****
C
      DO 40 I = 1, NP1
      NI1 = IFIX (Z(I)/DELZ + 1.0)
      SUMC (NI1) = SUMC (NI1) + C (I)
      COUNT (NI1) = COUNT (NI1) + 1.0
40    CONTINUE
C-------------------------------------------------------------------------
C-------STEP 3: ASSIGN A TEMPORARY CONCENTRATION TO EACH GRID, EQUAL TO THE
C                AVERAGE OF CONCENTRATIONS OF MOVING POINTS INSIDE THE GRID-----
      DO 30 I = 1, NR
      IF (COUNT(I) .EQ. 0.) COUNT(I) = 1.0
      CAVG(I) = SUMC(I)/COUNT(I)
30    CONTINUE
C-------------------------------------------------------------------------
C     STEP 4: COMPUTE CHANGE IN GRID CONCENTRATION DUE TO DISPERSION
C
      DO 38 I = 2, NRM1
      DELC(I) = AD * (CAVG(I-1) - 2.*CAVG(I) + CAVG(I+1))
      DELC(NR)= AD * (CAVG(NR+1) - CAVG(NR))
38    CONTINUE
C-------------------------------------------------------------------------
C     STEP 5: UPDATE GRID POINT CONC. BASED ON DELC
C
      DO 48 I = 1, NR
      CAVG(I) = CAVG(I) + DELC(I)
48    CONTINUE
C-------------------------------------------------------------------------
C     STEP 6: MODIFY MOVING POINT CONC. BASED ON DELC
C
      DO 22 I = 1, NP1
      NI1 = Z(I)/DELZ + 1.0
      C(I)= C(I) + DELC(NI1)
22    CONTINUE
C-------------------------------------------------------------------------
C****** ERROR FUNCTION ANALYTICAL SOLUTION ******
C
      A = 2.*SQRT(DL*TIME)
      DO 81 I = 1, NR
      S1 = ERFC((ZC(I)-V(I)*TIME)/A)
      S2 = ERFC((ZC(I)+V(I)*TIME)/A)
      CCOA(I)=0.5*(S1+EXP(V(I)*ZC(I)/DL)*S2)
81    CONTINUE
C-------------------------------------------------------------------------
C****** PRINTS SIMULATION RESULTS ******
C
      WRITE (NPRINT,303) TIME
      WRITE (NPRINT,32)
      WRITE (NPRINT,31) (I,ZC(I),CAVG(I),CCOA(I), I=1,NR)
      IF (TSTEP .EQ. MAXST) STOP
      GO TO 1000
1     FORMAT (4(I5))
2     FORMAT (/1X,' NR=',I5,3X,' MOVING PTS. IN Z-DIRECTION=',
     $ I5/1X,' MOVING POINTS PER GRID = ',I5,3X,' MAX. TIME STEPS =',I5
     $ )
3     FORMAT (4(F10.2))
4     FORMAT (/1X,'FINTIM=' ,F10.2,3X,' DELT=',F10.2,3X,
     $ ' DELZ=', F10.2,3X,' Z=', F10.3,3X,' DL=',E10.3,
     $ 3X,' VEL=',E16.8,3X,' CO=',F10.3/1X,'CINITIAL=',F10.3)
8     FORMAT (2(F10.6))
17    FORMAT (/8X, '=================FOR THE GRID POINTS=======',
     $ '==========',/7X,' I',5X,
     $ ' SUMC',8X,' COUNT',7X,' DELC',7X,' CAVG'/)
16    FORMAT (1X, I8, 4(E14.6))
32    FORMAT (/4X,'I',3X,'ZC(I)',5X,'CCO(I)',7X,'CCOA(I)',6X,'I',3X,
     $ 'ZC(I)',5X,'CCO(I)',7X,'CCOA(I)',6X,'I',3X,'ZC(I)',5X,'CCO(I)',
     $ 7X,'CCOA(I)'/15X,'(NUMERICAL)',2X,'(ANALYTICAL)',14X,
     $ '(NUMERICAL)',3X,'(ANALYTICAL)',14X,'(NUMERICAL)',3X,
     $ '(ANALYTICAL)')
31    FORMAT (3(2X,I3,F7.2,2E14.6))
303   FORMAT (/1X,' SIMULATION TIME = ',E10.3/)
      STOP
      END
```

Appendix B. Solution of Two-Dimensional Convective-Dispersion Equation by the Method of Characteristics

```
C-------------------- INPUT INFORMATION ---------------------------
C
C        *** NOTE: TO RUN THE PROGRAM YOU MUST USE THE COMMAND:
C                  EX MOC2D.FOR,SYS:IMSLIB/LIB
C
C------ NR = NO. OF GRIDS(ROWS) IN THE VERTICAL(X3) DIRECTION
C        NP1 = NO. OF MOVING POINTS IN VERTICAL(X3) DIRECTION
C        NPZ = NO. OF MOVING POINTS PER GRID IN X3 DIRECTION
C        NC = NO. OF GRIDS(COLUMNS) IN HORIZONTAL (X1) DIRECTION
C        NP2 = NO. OF MOVING POINTS IN HORIZONTAL (X1) DIRECTION
C        NPX = NO. OF MOVING POINTS PER GRID IN X1 DIRECTION
C        MAXST = MAXIMUM NO. OF TIME STEPS USED IN SIMULATION
C        KPRINT=INITIAL COUNTER FOR PRINTING NUMERICAL SOLUTION
C        IFAC=NUMBER OF INTERVALS AT WHICH RESULTS ARE PRINTED
C
C------ FINTIM = SIMULATION FINISH TIME IN SECONDS
C        DELT = TIME INCREMENT IN SECONDS
C        DELZ = VERTICAL (X3) SPATIAL INCREMENT IN CM.
C        TZ = TOTAL DEPTH OF MODEL IN VERTICAL (X3) DIRECTION
C        DELX = HORIZONTAL (X1) SPATIAL INCREMENT IN CM.
C        TX = TOTAL WIDTH OF MODEL IN HORIZONTAL (X1) DIRECTION
C
C------ DL = LONGITUDINAL DISP. COEFF. (CM**2/SEC)
C        DT = LATERAL DISP. COEFF. (CM**2/SEC)
C        B = LENGTH OF TRACER SOURCE IN X1 DIRECTION IN CM.
C        VEL = VELOCITY IN VERTICAL (X3) DIRECTION (CM/SEC)
C        CO = DIMENSIONLESS CONC. AT INPUT BOUNDARY
C        CINTL = DIMENSIONLESS INITIAL CONC.
C-------------------------------------------------------------------
C
C    ****************** PROGRAM VARIABLES ******************
C
C        ALENZ = TOTAL LENGTH OF MODEL IN VERTICAL (X3) DIRECTION
C        Z = VERTICAL (X3) COORDINATE OF MOVING POINTS
C        X = HORIZONTAL (X1) COORDINATE OF MOVING POINTS
C        C = DIMENSIONLESS CONC. OF MOVING POINTS
C        V = VELOCITY OF EACH MOVING POINT
C        DOGZ, DOGX = INCREMENTING FACTORS USED IN DO LOOPS
C        SUMC = SUMMATION OF CONCENTRATION OF MOVING POINTS IN A GRID
C        COUNT = A COUNT OF NO. OF MOVING POINTS IN A GRID
C        NI1 = ROW NO. OF A GRID IN WHICH A MOVING POINT IS LOCATED
C        NI2 = COLUMN NO. OF A GRID IN WHICH A MOVING POINT IS LOCATED
C        DELC = CHANGE IN CONCENTRATION FOR A GRID DUE TO DISPERSION
C---------------------------------------------------------------------
         INTEGER TSTEP
         DIMENSION Z(52),CAVG(26,21),DISP(26,21),COUNT(26,21)
         DIMENSION SUMC(26,21),V(52),DELC(26,21),CCO(26,21),C(52,42)
         DIMENSION ZC(26),CCOA(26,21),XC(21),X(42)

         DATA NPRINT,IPRINT,NREAD/3,5,5/
```

```
      WRITE(IPRINT,100)
100   FORMAT(/,2X,' THE FOLLOWING VARIABLES HAVE I5 FORMAT'/,2X,
     $ ' GIVE VALUES FOR: NR,NP1,NPZ,NC,NP2,NPX,MAXST,KPRINT,IFAC'./)
      READ(NREAD,1)NR, NP1, NPZ, NC, NP2, NPX, MAXST, KPRINT, IFAC
      WRITE(NPRINT,2)NR, NP1, NPZ, NC, NP2, NPX, MAXST, KPRINT, IFAC
      WRITE(IPRINT,200)
200   FORMAT(/,2X,' THE NEXT 6 VARIABLES HAVE FREE FORMAT',/,
     $ 2X, ' GIVE VALUES FOR FINTIM, DELT, DELZ, TZ, DELX, TX',/)
      READ(NREAD,*)FINTIM, DELT, DELZ, TZ, DELX, TX
      WRITE(IPRINT,300)
300   FORMAT(/,2X,' THE LAST 6 VARIABLES HAVE FREE FORMAT',/,
     $ 2X, ' GIVE VALUES FOR: DL, DT, B, VEL, CO, CINTL',//)
      READ(NREAD,*) DL, DT, B, VEL, CO, CINTL
      WRITE(IPRINT,400)
400   FORMAT(//,2X,' OUTPUT DISPOSED TO LINE PRINTER')
      WRITE(NPRINT,4)FINTIM,DELT,DELZ,TZ,DL,VEL,DELX,TX,DT,B,
     $ CO, CINTL
C----------- INITIALIZE VARIABLES ---------------------------------
      PZ=FLOAT(NPZ)
      PX=FLOAT(NPX)
      ADZ=DELT * DL/DELZ/DELZ
      ADX=DELT * DT/DELX/DELX
      NCB=IFIX(B/DELX)
      NCB1=NCB + 1
      NPXB=IFIX(B*NPX/DELX)
      NPXB1=NPXB + 1
      ALENZ=DELZ * FLOAT(NR)
      ADISZ=DELZ/PZ
      NRM1=NR - 1
      NCM1=NC - 1
C
C------- COORDINATES FOR STATIONARY GRID SYSTEM ---------------
C
      ZC(1) = 0.
      ZC(2) = DELZ/2.
      XC(1) = DELX/2.
      DO 80 I=3,NR
80    ZC(I)=ZC(I-1) + DELZ
      DO 81 I=2,NC
81    XC(I)=XC(I-1) + DELX
C
C------- INITIALIZE SUMC AND COUNT -----------------------------
C
      DO 67 J=1,NC
      DO 67 I=1,NR
      SUMC(I,J) = 0.
      COUNT(I,J) = 0.
67    DELC(I,J) = 0.
C
C--- STEP 1: ASSIGN INITIAL COORDINATES AND CONCENTRATIONS TO MOVING POINTS --
C
      DO 10 J=1,NP2
      DO 10 I=1,NP1
      DOGZ=FLOAT(I-1)
      DOGX=FLOAT(J-1)
      Z(I)=(DELZ/PZ) * (0.5 + DOGZ)
      X(J)=(DELX/PX) * (0.5 + DOGX)
      C(I,J)=CINTL
      IF(I .LE. NPZ .AND. J .LE. NPXB) C(I,J)=CO
C
C------- CALCULATE INITIAL VALUES OF SUMC AND COUNT -----------
C
      V(I)=VEL
      NI1=IFIX(Z(I)/DELZ +1.0)
      NI2=IFIX(X(J)/DELX +1.0)
      SUMC(NI1,NI2)=SUMC(NI1,NI2) + C(I,J)
      COUNT(NI1,NI2) = COUNT(NI1,NI2) + 1.0
10    CONTINUE

C
C------- ASSIGN INITIAL CONCENTRATIONS TO STATIONARY GRID POINTS ------
C
      DO 11 J=1,NC
      DO 11 I=1,NR
      IF(COUNT(I,J) .EQ. 0.) COUNT(I,J) =1.0
      CAVG(I,J)=SUMC(I,J)/COUNT(I,J)
11    CONTINUE
      TSTEP=0
      TIME=0.
C
C------- PRINT INITIAL CONCENTRATIONS FOR EACH GRID POINT -----------
C
      WRITE(NPRINT,17)
      DO 500 I=1,NR
      DO 500 J=1,NC
500   WRITE(NPRINT,16)I,J,SUMC(I,J),COUNT(I,J),DELC(I,J),CAVG(I,J)
1000  CONTINUE

C
C------- SIMULATION STARTS ------------------------------------------
C
      TSTEP = TSTEP +1
      IF( TIME + DELT .GT. FINTIM) DELT=FINTIM-TIME
      TIME = TIME +DELT

C
C--- STEP 2: DETERMINE WHICH GRID EACH MOVING POINT IS IN, AND RELOCATE
C          USING VELOCITY --------
C
      DO 20 I=1,NP1
      Z(I)=Z(I) + DELT * V(I)
20    CONTINUE

C
C------- RE-ASSIGN COORDINATES AND CONCENTRATIONS TO MOVING POINTS WHICH
C          HAVE MOVED OUT OF THE SYSTEM. i.e., INPUT THEM AGAIN AT THE
C          INFLOW BOUNDARY ---------
C
      DO 66 I=1,NP1
      IF(Z(I) .LT. ALENZ) GOTO 66
      NPM1=NP1 - 1

      DO 66 K=1,NPM1
      NN=NP1 + 1 - K
      Z(NN) = Z(NN-1)
66    CONTINUE

      DO 68 J=1,NP2
      DO 68 K=1,NPM1
      NN=NP1 + 1 -K
      C(NN,J) = C(NN-1,J)
68    CONTINUE
      Z(1)=Z(2) - ADISZ
      IF(Z(1) .LT. .01) Z(1)=.01

      DO 65 J=1,NPX
      C(1,J) = CO
      IF(J .GT. NPXB) C(1,J)=CINTL
65    CONTINUE

C
C------- RESET SUMC AND COUNT ---------------------------------
C
      DO 54 I=1,NR
      DO 54 J=1,NC
      SUMC(I,J)=0.
      COUNT(I,J)=0.
54    CONTINUE

C
C------- FOR EACH GRID, SUM UP THE TOTAL CONCENTRATION (SUMC) AND THE
C         NUMBER OF MOVING POINTS (COUNT) --------
C
      DO 40 J=1,NP2
      DO 40 I=1,NP1
      NI1=IFIX(Z(I)/DELZ +1.0)
      NI2=IFIX(X(J)/DELX + 1.0)
      SUMC(NI1,NI2)=SUMC(NI1,NI2) + C(I,J)
      COUNT(NI1,NI2)=COUNT(NI1,NI2) + 1.0
40    CONTINUE

C
C--- STEP 3: CALCULATE A TEMPORARY AVERAGE CONCENTRATION FROM SUMC AND COUNT
C
      DO 30 J=1,NC
      DO 30 I=1,NR
      IF(COUNT(I,J) .EQ. 0.) COUNT(I,J) = 1.0
      CAVG(I,J)=SUMC(I,J)/COUNT(I,J)
30    CONTINUE

C
C--- STEP 4: CALCULATE CHANGE IN CONCENTRATION DUE TO DISPERSION -----------
C                     ***** INTERIOR GRIDS ****
C
      DO 38 J=2,NCM1
      DO 38 I=2,NRM1
38    DELC(I,J)=ADX * (CAVG(I,J-1) -2.*
     $ CAVG(I,J) + CAVG(I,J+1)) + ADZ * (CAVG(I-1,J)
     $ -2. * CAVG(I,J) + CAVG(I+1,J))
C
C                     **** SIDE BOUNDARIES ****
C
      DO 70 I=2,NRM1
      DELC(I,1) = ADZ * (CAVG(I-1,1)-2. *CAVG(I,1) +
     $ CAVG(I+1,1)) + ADX * (CAVG(I,2) - CAVG(I,1))
70    DELC(I,NC) = ADZ * (CAVG(I-1,NC) - 2. * CAVG(I,NC)+
     $ CAVG(I+1,NC)) + ADX * (CAVG(I,NC-1) - CAVG(I,NC))

C
C                     **** LOWER BOUNDARY ****
C
      DO 72 J=2,NCM1
72    DELC(NR,J)=ADZ * (CAVG(NR-1,J) -CAVG(NR,J)) + ADX*
     $ (CAVG(NR,J-1) - 2. * CAVG(NR,J) + CAVG(NR,J+1))
C
C                     ****   CORNERS   ****
C
      DELC(NR,NC) = ADX * (CAVG(NR,NC-1) -
     $ CAVG(NR,NC)) + ADZ * (CAVG(NR+1,NC) -
     $ CAVG(NR,NC))

      DELC(NR,1) = ADZ * (CAVG(NR,1) - CAVG(NR-1,1)) + ADX *
     $ (CAVG(NR,2) - CAVG(NR,1))

C
C------ STEP 5: UPDATE CONCENTRATIONS FOR STATIONARY GRID POINTS -------
C
      DO 48 J=1,NC
      DO 48 I=1,NR
      CAVG(I,J)=CAVG(I,J) + DELC(I,J)
      CCO(I,J)=CAVG(I,J)/CO
48    CONTINUE

C
C------ STEP 6: UPDATE CONCENTRATIONS FOR MOVING POINTS ---------------
C
      DO 22 J=1,NP2
      DO 22 I=1,NP1
      NI1=IFIX(Z(I)/DELZ + 1.0)
      NI2=IFIX(X(J)/DELX + 1.0)
      C(I,J) = C(I,J) + DELC(NI1,NI2)
22    CONTINUE

C
C ****** TIME STEP HAS BEEN COMPLETED ******
C
C------ WRITE OUT INTERMEDIATE STEPS --------
C
      IF (TSTEP .NE. KPRINT*IFAC) GO TO 601
      KPRINT=KPRINT+1
      WRITE(NPRINT,788) (XC(J),J=1,NC)
788   FORMAT(1X,'Z    X=',20F6.2/)
      WRITE(NPRINT,303) TIME
      WRITE(NPRINT,600)(ZC(I),(CCO(I,J),J=1,NC),I=1,NR)
600   FORMAT(1X,21F6.3)
601   CONTINUE
C
C------ COMPARE ANALYTICAL AND NUMERICAL SOLUTIONS -------------
C
      IF(TSTEP .EQ. MAXST) GOTO 90
      GOTO 91
C
C     ******  ANALYTICAL SOLUTION  ******
C
90    DO 83 J=1,NC
      DO 83 I=2,NR
      CCOA(I,J)=0.5 * ERFC((XC(J) -B)/(2. * SQRT(DT *
     $ ZC(I)/VEL)))
83    CONTINUE

      DO 75 J=1,NC
      IF(J .LE. NCB) CCOA(1,J)=CO
75    IF(J .GT. NCB1) CCOA(1,J)=CINTL

      WRITE(NPRINT,880)
880   FORMAT(/,,,3X,'FINAL TIME STEP'///)
      WRITE(NPRINT,303)TIME
      WRITE(NPRINT,32)
      WRITE(NPRINT,31)((I,J,ZC(I),XC(J),CCO(I,J),CCOA(I,J),J=1,NC)
     $ ,I=1,NR)
91    CONTINUE
C
C   ****** CHECK IF MAXIMUM NUMBER OF TIME STEPS IS EXCEEDED *******
C
      IF(TSTEP .EQ. MAXST) STOP
      GOTO 1000
C
C--------- LIST OF PRINT STATEMENTS ----------------------------------
C
1     FORMAT(9(I5))
2     FORMAT( 1X,' NR =',I4,3X,' MOVING PTS. IN Z-DIRECTION =',
     $ I4,3X,' MOVING POINTS PER GRID = ',I3//,1X,' NC = ',I4,3X,
     $ ' MOVING PTS. IN X-DIRECTION = ',I4,3X,' MOVING PTS. PER
     $ GRID = ',I3,3X,'MAX. NO. OF TIME STEPS = ',I5//1X,
     $ 'PRINTING COUNTER =',I5,3X,'PRINTING INTERVAL =',I5)
3     FORMAT(6(F10.2))
4     FORMAT(/1X,' FINTIM = ',F8.2,3X,'DELT =',F6.1,3X,
     $ ' DELZ =', F6.2,3X,' Z =', F6.1,3X,' DL =',F7.2,
     $ 3X,' VEL =',F6.1//,1X,' DELX = ',F6.2,3X,'TX = ',
     $ F6.1,3X,'DT = ',E10.3,3X,' B = ',F4.2//,1X,'CO =',
     & F5.1,3X,'INITIAL CONC. = ',F5.1///)
17    FORMAT( 5X,' FOR THE GRID POINTS'/,/4X,'I',3X,'J'
     $ ,6X,' SUMC',7X,' COUNT',7X,' DELC ',8X,' CAVG'/)
16    FORMAT(1X,2I4,4(E14.6))
32    FORMAT( 2X,' I, J, ZC, XC,  CCO(NUM),CCO(ANAL)',/)
31    FORMAT(3(1X,2I3,2F4.1,2E14.6))
303   FORMAT(,,/1X,' SIMULATION TIME = ',E10.3/)
      STOP
      END
```

Applying the USGS Mass-Transport Model (MOC) to Remedial Actions by Recovery Wells

by Aly I. El-Kadi[a]

ABSTRACT

The USGS two-dimensional mass-transport model (MOC) is widely used in the analysis of ground-water contamination problems. A need exists to examine the accuracy of the code in situations dominated by radially convergent and divergent flow around wells. The model is applied here to situations that commonly exist in remedial actions involving recovery wells. The cases simulated are a recharge/recovery single well, a recharge/recovery doublet, and plume capture by one or two production wells. The results were tested against analytical and semianalytical solutions. Inaccuracies in model results occurred especially for the doublet case under continued long-time simulation. Inaccuracies are caused not only by the mainly radial-flow situation, or by the curvature nature of streamlines, but also by the arrival of contamination at the sink nodes. Better agreement of numerical and analytical solutions was obtained for the single-well and plume-capture situations. However, a large mass-balance error exists for the single-well case. Inaccuracies can be reduced by modifying the code and reducing the finite-difference mesh (e.g., Erickson, 1985). However, the use of a very fine mesh (i.e., on the order of a few feet) may prevent the use of the code in large-scale problems. Care must be taken in applying the model to situations where production or injection wells are close to each other.

INTRODUCTION

The U.S. Geological Survey two-dimensional mass-transport model, known also as MOC and developed originally by Konikow and Bredehoeft (1978), utilizes the method of characteristics and the finite-difference approach in the solution of the mass-transport problem. The model has undergone numerous modifications and revisions (e.g., Sanford and Konikow, 1985). It has been applied in a large number of field studies (e.g., Bouvette, 1983; Chapelle, 1986; and Sophocleous, 1984) and tested against analytical and alternative numerical approaches (e.g., Sophocleous *et al.*, 1982). The well-documented code is relatively easy to use. Various options can be applied to describe different hydrological conditions. The recent introduction of a microcomputer version and a preprocessor for input data preparation has increased the popularity of the code.

The model is tested here in situations dominated by radially convergent and divergent flow around wells. The authors of the code do not encourage the application of the model to such problems, especially when using a grid that is too coarse (L. Konikow, pers. comm., 1987). However, some applications of the code to similar situations have been reported in the literature (e.g., Freeberg *et al.*, 1987). Erickson (1985), realizing that problems arise in the use of MOC for these situations, modified the code for use in the analysis of single-well tracer tests. The major changes include simulating the converging/diverging flow field resulting from wells; eliminating the hydrodynamic dispersion in the well during the pumping phase; changing the manner in which particle concentration is estimated from node concentration; changing the way mass is removed by pumpage; and adding new particles before the pumping phase. A finer mesh (one square foot) was also used. Better accuracy as well as better mass conservation was obtained following these changes.

Note, however, that the use of such a fine mesh is impractical due to the limited area that can be handled by the code in this case. If we consider the large number of particles that must be handled and the limit imposed on the size of the time step, computational costs could be prohibitive. A need exists to examine the suitability of the code in the analysis of relatively large problems of a practical nature.

In general, accuracy of numerical results can be judged using various criteria relevant to the purpose of model application and the expected use of results. For example, when professional judgment is needed, an order-of-magnitude analysis of concentration values or travel times is generally acceptable, especially under uncertainty in data and processes involved. On the other hand, more accurate estimates are needed in some situations involving, for example, the assessment of exposure levels of toxic chemicals in the environment. In the present analysis, both visual inspection and esti-

---

[a]Associate Director for Research, Water Sciences Program, Holcomb Research Institute, Butler University, 4600 Sunset Avenue, Indianapolis, Indiana 46208.

Received May 1987, revised October 1987, accepted October 1987.

Discussion open until November 1, 1988.

mates of root-mean-squared error are used to assess the accuracy of the model. "Reasonable" or "good" results are defined in practical terms; "unacceptable" results are based on severe fluctuations.

The objective for the study is to verify MOC for situations pertinent to remedial actions by recovery wells. The cases simulated are a recharge/recovery single well, a recharge/recovery doublet, and plume capture by one or two production wells. The model is not completely tested in the terms described, for example, by van der Heijde *et al.* (1985). These authors define a three-level testing approach that ranges between testing against analytical solutions and history matching.

REMEDIAL ACTIONS

Remedial actions include the use of systems to contain spilled or leaked contaminants and to recover and treat ground water. [For details of different techniques see, e.g., U.S. Environmental Protection Agency (1985) and Ehrenfeld and Bass (1984).] Containment systems interfere with transport mechanisms by means of hydraulic barriers such as recovery wells, interceptor trenches, grout curtains, and slurry walls. Treatment systems include the use of physical, chemical, and biological activities. Physical/chemical processes include *in situ* air stripping and activated carbon absorption; both are effective in reducing volatile organic compounds. Air stripping helps remove volatile chemicals from the soil by drawing or venting air through the unsaturated soil layer. Another form of air stripping passes contaminated water through a packed column or tower with counterflowing air and water. The effectiveness of carbon absorption depends on the type of competing compounds (e.g., Engineering-Science, 1986).

Aboveground and *in situ* biological methods have been employed recently in the treatment of contaminated ground water. Aboveground processes include fixed film treatment such as trickling filters, or suspended-growth systems such as activated sludge (Jensen *et al.*, 1986). *In situ* biodegradation can be performed by using existing soil microorganisms or by adding microorganisms and nutrients to the contaminated aquifer. Such treatment is presently in the experimental stage; its effectiveness depends on a number of factors such as type and concentration of contaminants, hydrogeology, nutrient availability, dissolved oxygen, pH, temperature, and salinity (Engineering-Science, 1986).

Recovery wells are the most commonly used remediation techniques. In aquifer cleanup, they extract the polluted ground water and either reinject it after treatment or release it to a surface-water body. In some cases, recovery wells are combined with injection wells to improve recovery by altering the hydraulic gradient. The recovery well system should be designed to intercept the contaminant plume such that no further degradation of the aquifer occurs. Modeling is a very useful tool in the design of such systems (Boutwell *et al.*, 1985).

TESTING THE MODEL

Case 1: A Recharge/Recovery Single Well

A recharge-pumping cycle for a fully penetrating well in a confined aquifer is used to test MOC. Water of a known concentration (C_o) is injected into the well. After some time, the flow is reversed and the contaminated water is pumped out. Such a process can be used in field work to define the dispersive properties of aquifers (see e.g., Güven *et al.*, 1985). The situation may also represent a cleanup process following extended contamination.

Gelhar and Collins (1971) derived an approximate analytical solution for the distribution of the relative concentration in the well during the withdrawal period. By neglecting the effects of well radius and molecular diffusion, this expression reads:

$$\frac{C}{C_o} = \tfrac{1}{2}\,\mathrm{erfc}\left\{\frac{V}{\left[\frac{16}{3}\frac{\alpha}{R_1}\left(2+|V|^{1/2}\,V\right)\right]^{1/2}}\right\} \qquad (1)$$

With i = 1 and 2 representing the indices for the recharge and discharge period, respectively, V is given by:

$$V = 1 - \frac{V_2}{V_1} \qquad (2)$$

where $V_i = Q_i t_i$ is the recharge or discharge volume of water, Q_i is the recharge or discharge rate, and t_i is time. In equation (1), α is the radial dispersivity, erfc is the complementary error function, and R_1 is given by:

$$R_1 = \left(\frac{Q_1 t_1}{\pi n B}\right)^{1/2} \qquad (3)$$

where B is the aquifer thickness (assumed constant), and n is porosity. For the special case of $Q_1 = Q_2$, equation (2) reduces to:

$$V = -\frac{t}{t_1} \qquad (4)$$

in which $t = t_1 + t_2$ is the total time.

Table 1. Common Parameters for Test Cases 1.A, 1.B, 1.C, and 1.D

Parameter	*Symbol*	*Value*	*Units*
Saturated conductivity	K	0.005	ft/s
Aquifer thickness	B	20.0	ft
Porosity	n	0.30	–
Ratio of longitudinal to transverse dispersivity	α_t/α_ℓ	1.0	–
Mesh increments in x direction	Δx	900.	ft
Mesh increments in y direction	Δy	900.	ft
Number of increments in x direction	N_x	9	–
Number of increments in y direction	N_y	11	–
Initial concentration	C_i	0.0	%
Concentration of injected water	C_o	100.	%

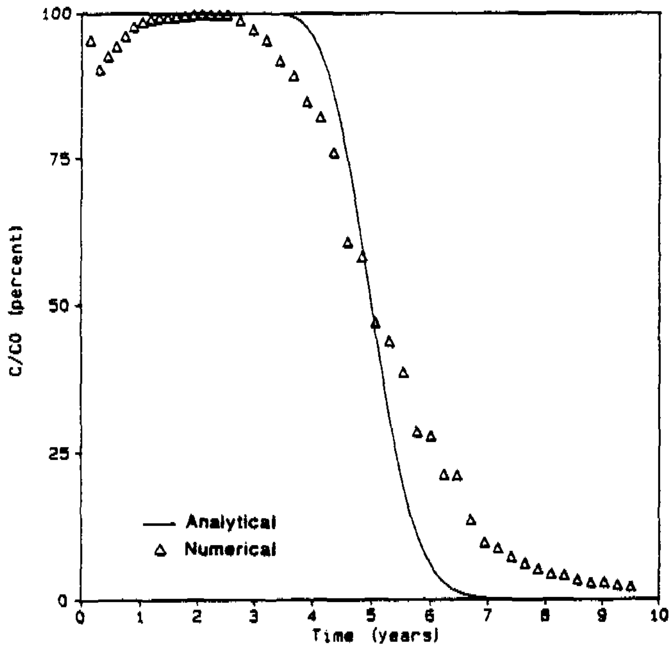

Fig. 1. Time change of relative concentration in the well as estimated both numerically and analytically for case 1.A.

Table 2. Values of α_ℓ, t_1, Q_1 (= Q_2) for Test Cases 1.A, 1.B, 1.C, and 1.D

Case	α_ℓ *(ft)*	t_1 *(year)*	$Q_1 = Q_2$ *(cfs)*
1.A	100.	2.5	1.0
1.B	100.	1.0	1.0
1.C	0.001	2.5	1.0
1.D	100.	2.5	0.5

A number of hypothetical experiments were simulated, and the results were compared to the analytical solution as given by equation (1). The input data for MOC are shown in Tables 1 and 2.

Figures 1 through 4 illustrate results of the analysis for experiments 1.A to 1.D. The root-mean-squared error for the four cases is, respectively, 1.9, 2.9, 3.4, and 1.4. Despite the severity of the

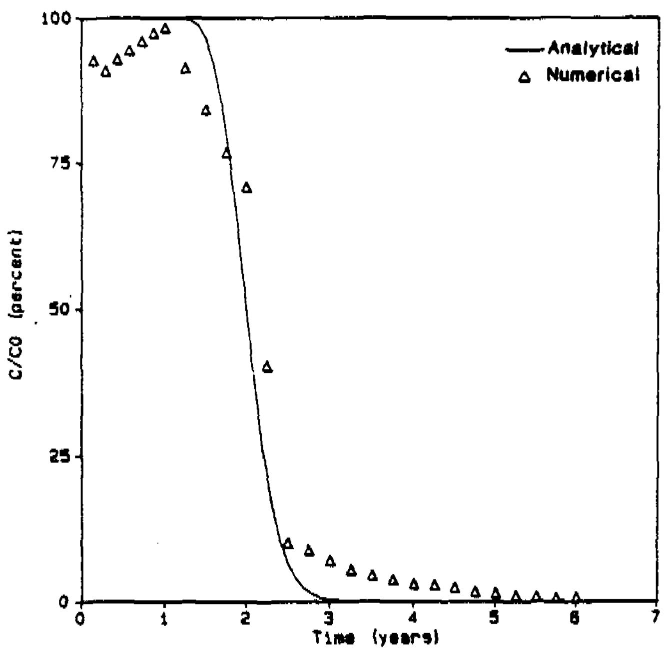

Fig. 2. Time change of relative concentration in the well as estimated both numerically and analytically for case 1.B.

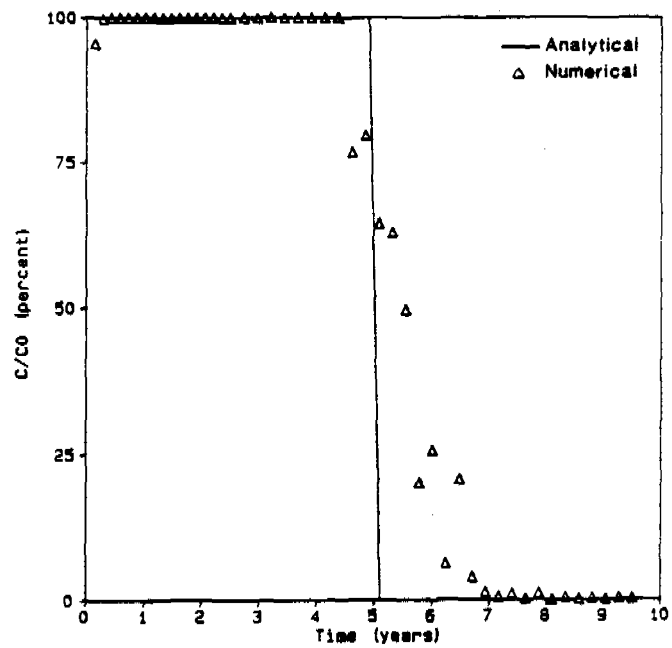

Fig. 3. Time change of relative concentration in the well as estimated both numerically and analytically for case 1.C.

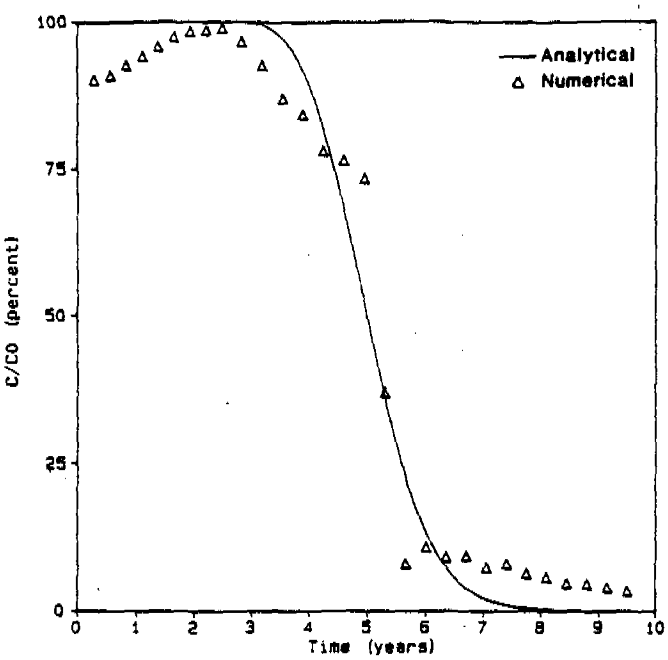

Fig. 4. Time change of relative concentration in the well as estimated both numerically and analytically for case 1.D.

test, a radial flow case, reasonable match can be observed for all cases. Some fluctuations can be noticed, yet the overall behavior of the numerical results is good. The largest deviation of the numerical results from the analytical solution exists for case 1.C. The deviations appear in the form of numerical dispersion; errors are most severe for larger well fluxes or longer injection periods. The inclusion of large physical dispersion (Figure 1) did not mask the numerical dispersion effects, suggesting that most of the error is due to poor representation of radial flow near the well rather than to numerical dispersion, i.e., by inaccuracies in predicting the flow field, rather than inaccuracies in estimating the advection term. The percentage mass-balance error is illustrated for all cases in Figure 5 as a function of time. The maximum value of error is about −16%, −22%, −23%, and −13% for cases 1.A, 1.B, 1.C, and 1.D, respectively.

Considering the reasonably good results shown in Figures 1 through 4, it seems that, as explained by Konikow and Bredehoeft (1978), the large mass error is caused also by the method of estimating the solute mass removed from the aquifer at sink nodes during each time increment. It appears also that the radial flow does not cause serious problems for MOC in the single-well test, e.g., in terms of large fluctuations leading to unacceptable results. Continuous injection, simulated earlier by Konikow and Bredehoeft (1978), also shows good accuracy. For a similar experiment (results not shown here), the relative mass error ranged approximately between +12% to −19%. It can be concluded that, for practical purposes, MOC is reasonably accurate for continuous injection and for the recharge-pumping cycle. However, the mass conservation in the model should be improved. The introduction of a large number of particles as well as the use of a smaller grid size did not improve the mass error encountered. (The results of these simulations are not shown here.)

Case 2: A Recharge/Recovery Doublet

The second MOC test involved application to a recharge/recovery doublet. A semianalytical solution to the purely convective transport case was introduced and programmed by Javandel *et al.* (1984). The model, called RESSQ, uses the complex velocity potential to estimate the concentration distribution in the aquifer. The technique is applicable to a two-dimensional flow in a homogeneous confined aquifer in the absence of dispersion and diffusion effects. The calculation steps are as follows (Javandel *et al.*, 1984):

The technique identifies, first, simple flow components such as sources and sinks. Second, the overall complex velocity potential of the system is obtained by combining the expressions for each individual component. Third, the velocity field is identified by taking the derivative of the velocity potential. Fourth, locations of contaminant fronts and flow patterns are estimated at various values of time. Finally, stream function of the system is used to calculate the time variation of the rate at which

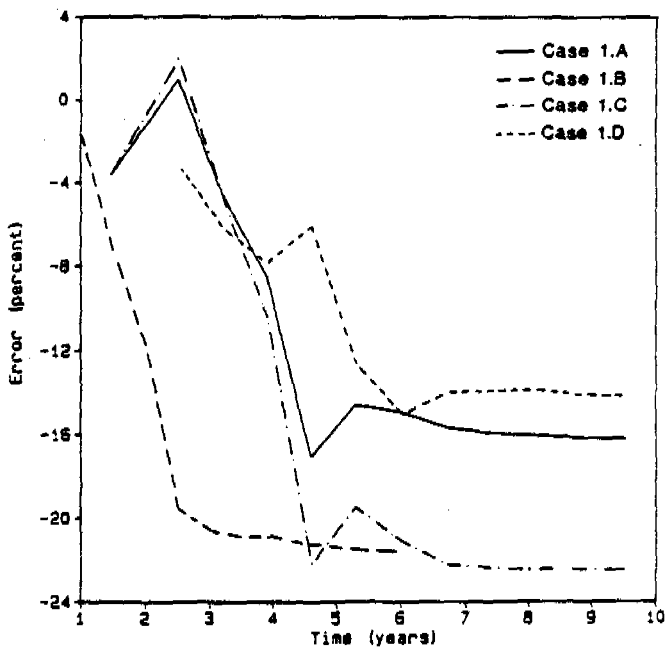

Fig. 5. Relative mass-balance error for cases 1.A, 1.B, 1.C, and 1.D, as function of time.

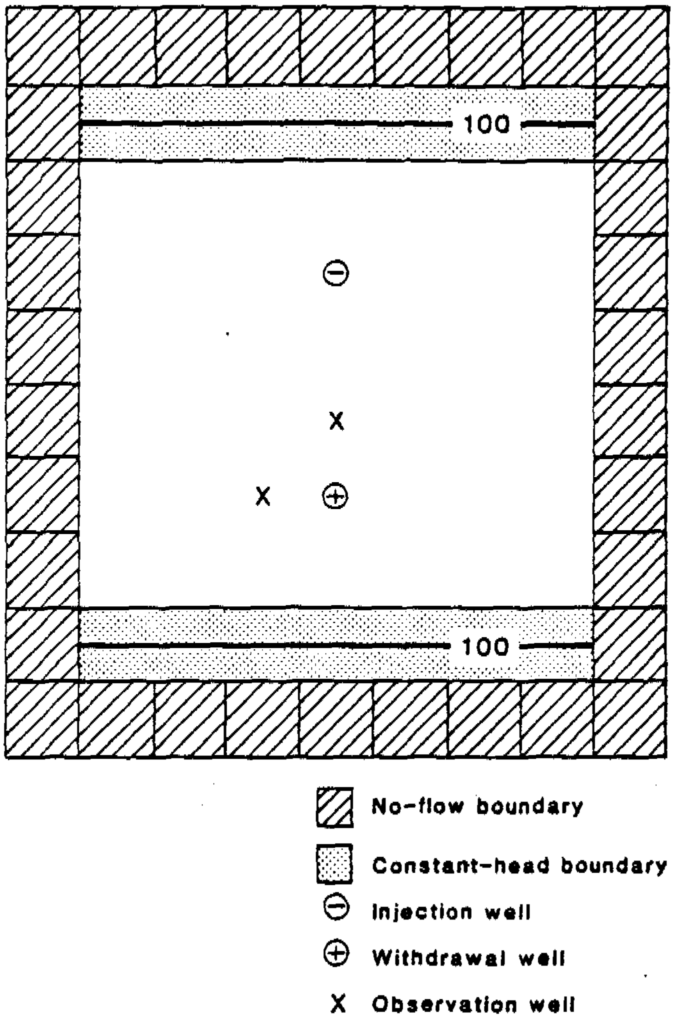

Fig. 6. The aquifer model for the recharge/discharge doublet.

a contaminant reaches any desired outflow boundary.

Figure 6 illustrates the aquifer model for the test problem simulated. Model parameters are given in Table 1. The values of α_ℓ and α_t were set equal to zero. The rate of withdrawal or recharge was taken as 1.0 cfs.

Figure 7 compares the time change of concentration in the withdrawal well estimated using MOC, with that estimated using RESSQ. The figure shows reasonable match for a short time period (less than 2.0 years). The two models predicted the same value for the time at which the contaminant reaches the production well (about 1.5 years). This value agrees with the available analytical solution (Javandel *et al.*, 1984). For a time larger than 2.0 years, the numerical solution is not accurate and shows large fluctuations for which the analytical solution represents the upper envelope. The time change of concentration in two observation wells is also shown in Figure 8. The concentration in the well upstream of the production well

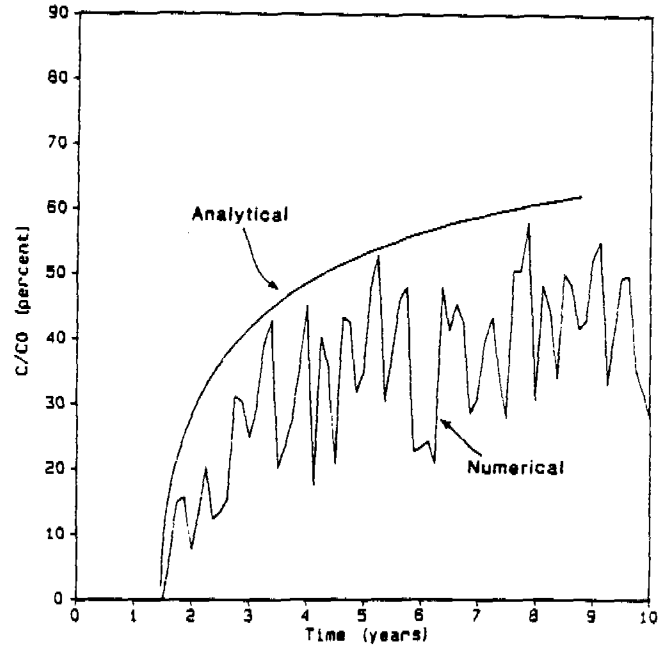

Fig. 7. Time change of relative concentration in the production well for the aquifer model shown in Figure 5.

[at node (5,6)] shows much less fluctuation than the concentration for the well immediately to the left of the production well [at node (4,7)]. The relative mass-balance error was reasonably small, approximately between −10% to +2%. The error fluctuates between −10% and +2% to reach minimum at about 2.0 years, and then grows to about −8%. It can be concluded that MOC is accurate in dealing with similar problems for a relatively short time; the accuracy then declines as the simulation

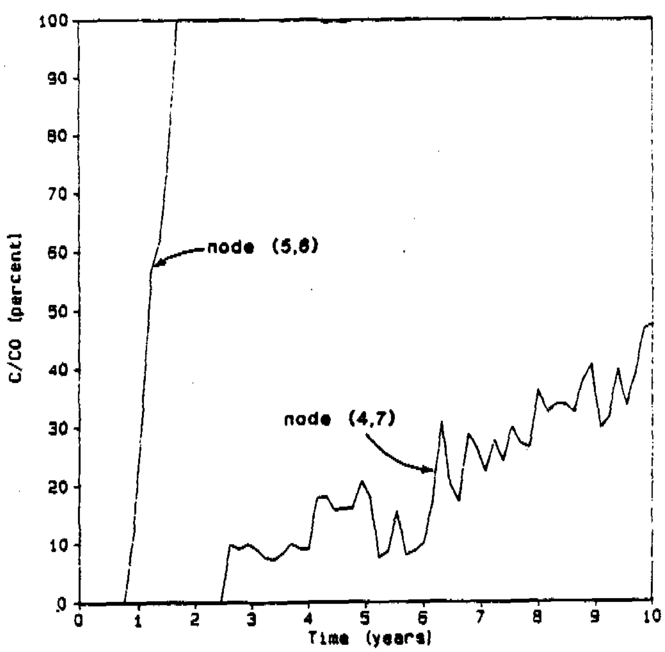

Fig. 8. Time change of relative concentration in the two observation wells shown in Figure 5.

continues for longer times due to the arrival of contamination at the sinks. Again, as indicated by Konikow and Bredehoeft (1978), the decline in accuracy is a direct effect of the manner in which concentrations are computed at sink nodes and the method of estimating the mass of solute removed from the aquifer at sink nodes during each time increment.

Case 3: Plume Capture

Plume capture is a technique that prevents further degradation of the aquifer by using a number of pumping wells. The optimum number of pumping wells and their discharge rates and locations must be specified in advance. Recently, Javandel and Tsang (1986) introduced a technique, based on the complex potential theory, to define the equations for the streamlines separating the capture zone of one or more pumping wells from the rest of the aquifer. The cases of a single well and of two wells are used here to test MOC.

For the single-well case, assuming that the well is located at the origin, the equation of the dividing streamlines reads (Javandel and Tsang, 1986):

$$y = \pm \frac{Q}{2BU} - \frac{Q}{2\pi BU} \tan^{-1} \frac{y}{x} \qquad (5)$$

in which y and x are locations on the dividing streamline, Q is well flux, B is aquifer thickness, and U is Darcy's velocity for the regional flow. The test problem for this case is illustrated in Figure 9. The parameters used are given in Table 1. The simulation considers only convective transport. A number of problems were simulated considering different values for $\Delta H = H_1 - H_2$, with H_1 fixed at 100 ft. [H_1 and H_2 are the values of the hydraulic head at the upper and lower constant-head boundaries, respectively (Figure 9).] Equation (5) can be used to estimate the minimum value of Q to capture the plume. The velocity U can be estimated using the head gradient and the hydraulic conductivity. In this case the values x and y represent the coordinate of the right (or left) corner of the landfill relative to the well location.

With a steady-state flow situation, the numerical model was run long enough to represent the steady-state condition for mass transport. An iterative procedure was needed to estimate the well flux. Figure 10 illustrates the node concentrations, as obtained numerically, superimposed on the analytical solution representing the dividing streamlines as calculated using equation (5). The concentrations shown were estimated for the case

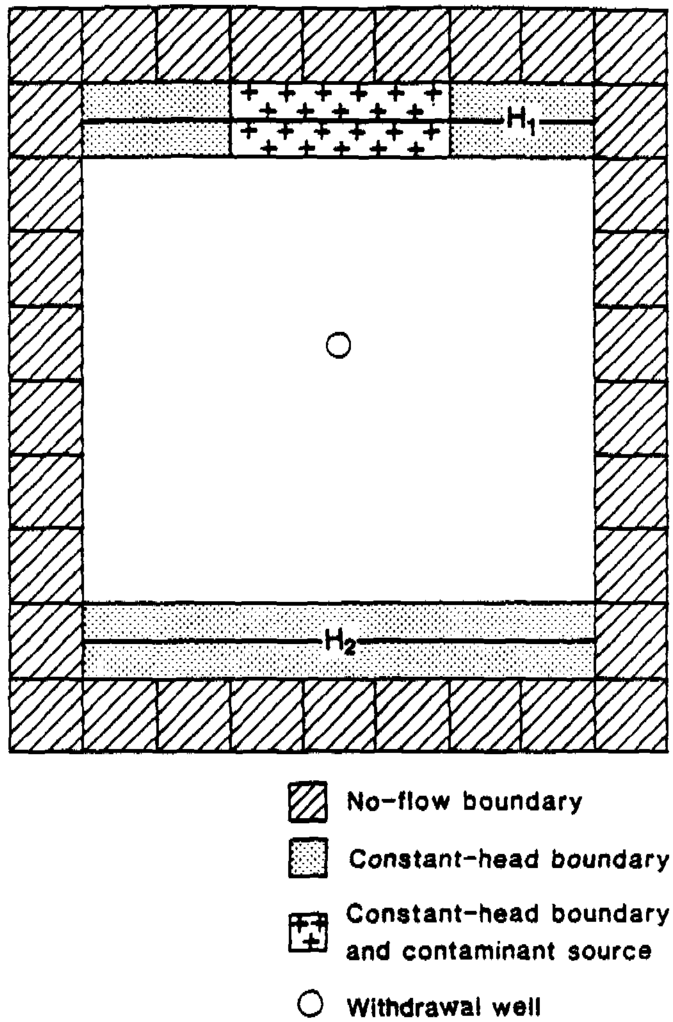

Fig. 9. The aquifer model for plume capture by a single production well.

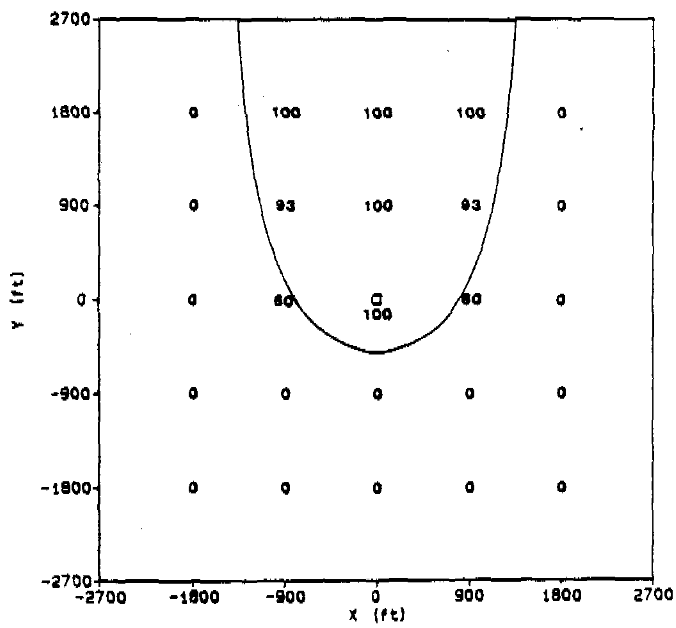

Fig. 10. Relative concentrations at nodes of a part of the aquifer superimposed on the analytical solution for the dividing streamline. The production well is located at the origin.

with $\Delta H = 50$ ft. The figure shows that MOC is capable of approximating the capture area for this case and also for all values of ΔH considered.

Figure 11 compares the well flux obtained analytically [via equation (5)] with that estimated numerically using MOC for different values of ΔH. The numerical model predicted higher values for well flux over the entire range of ΔH. The value needed to capture the plume numerically was about 1.5 times the respective analytical value. Sensitivity of results to the mesh size was not studied; it is expected, however, that closer agreement can be achieved as the mesh size decreases.

Figure 12 illustrates the time change of the relative concentration in the well for three selected values of ΔH: 20, 50, and 90 ft. Some fluctuations exist, yet their extent is not severe.

The case of a plume capture by two wells also was simulated for $\Delta H = 20$ ft. The case is represented by Figure 9, with two wells located at nodes (4,5) and (5,6). The landfill extended over five nodes, (3,2) to (7,2). The theoretical discharge as estimated analytically by the equation of Javandel and Tsang (1986) is about 1.8 cfs. Although MOC was also able to approximate the capture area, larger fluctuations in the pumping wells were observed. The well flux, 2.3 cfs for this case, was also larger than the theoretical value.

MOC is, in general, accurate in simulating plume capture by recovery wells. The relative mass error for all cases considered was acceptable, with a value between −2.7% to −6.4%.

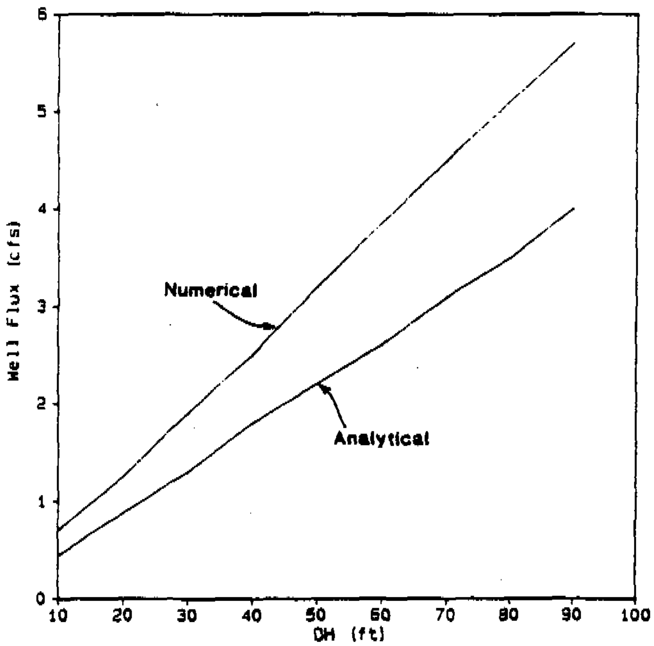

Fig. 11. Comparison between the well flux needed to capture the plume obtained numerically and analytically for different $\Delta H = H_1 - H_2$.

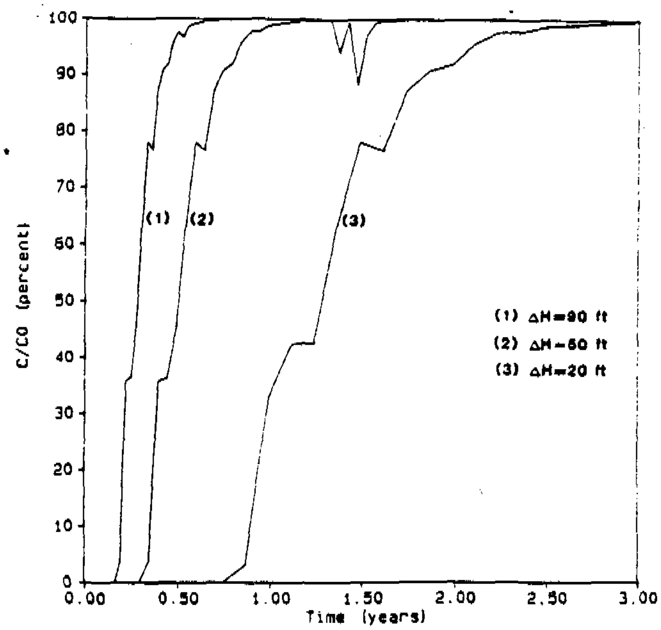

Fig. 12. Time change of relative concentration in the well for three selected values of ΔH (20, 50, and 90 ft).

CONCLUSIONS

The study examined the application of the USGS two-dimensional mass-transport model MOC in the analysis of some remedial actions involving recovery wells. Three situations were examined: a recharge/recovery single well, a recharge/recovery doublet, and plume capture by one or two wells. Solutions were compared to available analytical or semianalytical solutions. The cases considered involve mainly radial flow and curved flow lines; these are considered to be severe tests for the model. However, due to the popularity of the model, it was felt necessary to quantify the errors that may arise during its application to remedial actions.

The study indicates that the results are acceptable in situations involving a recovery/recharge single well. The radial flow nature caused some inaccuracies and fluctuations in the well-concentration estimates, with relatively high mass-balance errors; yet the overall behavior of results is reasonable. Some inaccuracies are also attributable—as Konikow and Bredehoeft indicated—to the manner in which concentrations are computed at sink nodes. Acceptable results also were obtained for plume capture where the cases involved a single well or two wells. In these cases, the model overestimated the value of well flux needed to capture the plume. However, for practical purposes, the model can be used in the analysis of such situations, especially under cases where analytical solutions do not exist, as under heterogeneous conditions or physical dispersion.

The analysis of a recharge/recovery doublet indicates that the model is accurate only for a short time after the start of the simulation. The results are not acceptable for larger simulation times.

Efforts are presently underway to improve on the mass-balance calculations (L. Konikow, pers. comm., 1987; see also Sanford and Konikow, 1985). In addition, improvement of model prediction for radially convergent and divergent flows has been considered (e.g., Erickson, 1985). Major modifications include the simulation of the converging/diverging flow field around the well, and changing the way mass is removed by pumping. A reduced mesh size is needed because the area of the cell should approximate that of the well (on the order of one foot). However, such discretization will reduce drastically the application of the model to large problems. Considering the coarse mesh used here, and the possible trade-off between computer costs and accuracy, the results obtained for the single-well case and for the plume capture case appear quite reasonable.

ACKNOWLEDGMENT

The author acknowledges the input of Dr. L. Konikow of the USGS, Reston, Virginia, who reviewed an earlier version of this manuscript.

REFERENCES

Boutwell, S. H., S. M. Brown, B. R. Roberts, and Atwood Anderson-Nichols & Co., Inc. 1985. Modeling remedial actions at uncontrolled hazardous waste sites. Office of Solid Waste and Emergency Response, U.S. Environmental Protection Agency, Washington, DC.

Bouvette, T. C. 1983. The characterization of hazardous waste sites with analytical and numerical models. M.S. thesis, Rice University, Houston, TX.

Chapelle, F. H. 1986. A solute transport simulation of brackish water intrusion near Baltimore, Maryland. Ground Water. v. 24, no. 6, pp. 741-751.

Ehrenfeld, J. and J. Bass. 1984. Evaluation of Remedial Action Unit Operations at Hazardous Waste Disposal Sites. Noyes Publications, Park Ridge, NJ. Pollution Technology Review No. 10. 434 pp.

Engineering-Science. 1986. Cost model for selected technologies for removal of gasoline components from groundwater. Health and Environ. Sciences Dept., American Petroleum Inst., Washington, DC. API Pub. No. 4422.

Erickson, J. R. 1985. Parameter-estimation technique for the analysis of single-well tracer tests. M.Sc. thesis, Colorado State University, Fort Collins, CO.

Freeberg, K. M., P. B. Bedient, and J. A. Connor. 1987. Modeling of TCE contamination and recovery in a shallow sand aquifer. Ground Water. v. 25, no. 1, pp. 70-80.

Gelhar, L. W. and M. A. Collins. 1971. General analysis of longitudinal dispersion in nonuniform flow. Water Resources Research. v. 7, no. 6, pp. 1511-1521.

Güven, O., R. W. Felta, F. J. Molz, and J. G. Melville. 1985. Analysis and interpretation of single-well tracer tests in stratified aquifers. Water Resources Research. v. 21, no. 5, pp. 676-684.

Javandel, I., C. Doughty, and C. F. Tsang. 1984. Groundwater Transport: Handbook of Mathematical Models. American Geophysical Union, Washington, DC. Water Resources Monograph 10. 228 pp.

Javandel, I. and C. F. Tsang. 1986. Capture-zone type curves: A tool for aquifer cleanup. Ground Water. v. 24, no. 5, pp. 616-625.

Jensen, B., E. Arvin, and A. T. Gundersen. 1986. The degradation of aromatic hydrocarbons with bacteria from oil-contaminated aquifers. Proc. of Petroleum Hydrocarbons and Organic Chemicals in Ground Water Prevention, Detection, and Restoration. National Water Well Association, Dublin, OH.

Konikow, L. F. and J. D. Bredehoeft. 1978. Computer model of two-dimensional solute transport and dispersion in ground water. U.S. Geological Survey, Techniques of Water-Resources Investigation. Bk. 7, Ch. C2.

Sanford, W. E. and L. F. Konikow. 1985. A two-constituent solute-transport model for ground water having variable density. U.S. Geological Survey, Water-Resources Investigations Report 85-4270. Denver, CO.

Sophocleous, M. A. 1984. Groundwater flow parameter estimation and quality modeling of the equus beds aquifer in Kansas, U.S.A. J. Hydrology. v. 69, pp. 197-222.

Sophocleous, M. A., M. Heidari, and C. D. McElwee. 1982. Water quality modeling of the equus beds aquifer in south-central Kansas. Techn. Completion Rep., Kansas Water Resources Research Institute, Univ. of Kansas, Lawrence, KS.

U.S. Environmental Protection Agency. 1985. Remedial action at waste disposal sites. (Revised). Office of Emergency and Remedial Response, U.S. Environmental Protection Agency, Washington, DC.

van der Heijde, P.K.M., P. S. Huyakorn, and J. W. Mercer. 1985. Testing and validation of ground water models. Proc. Practical Applications of Ground Water Modeling, National Water Well Assoc., Columbus, OH.

* * * * *

Aly I. El-Kadi is Associate Director for Research in Holcomb Research Institute's Water Sciences Program, Butler University. He received his B.S. and M.S. degrees in Civil Engineering from Ain Shams University, Cairo, Egypt, and his Ph.D. degree in Ground-Water Hydrology from Cornell University in 1982. His current research includes modeling the effects of parameter variability on mass transport in soil and ground water, and the transport of contaminants in partially frozen soil. He has authored or coauthored papers on saturated and unsaturated flow in uniform and fractured porous media, and on stochastic analysis of flow in heterogeneous porous media. His publications include state-of-the-art reports on modeling infiltration and variability studies as they apply to groundwater systems.

Modifying the USGS Solute Transport Computer Model to Predict High-Density Hydrocarbon Migration

by M. Akhter Hossain and M. Yavuz Corapcioglu[a]

ABSTRACT

Chlorinated hydrocarbons, such as trichloroethylene (TCE), trichloroethane (TCA), tetrachloroethylene (PCE), chloroform, and carbon tetrachloride, enter soils and ground water from chemical waste disposal sites and from accidents. The migration of such high-density hydrocarbons in a natural gradient unconfined gravel aquifer is studied. The Buckley-Leverett approach is extended to a two-dimensional case to simulate a high-density immiscible hydrocarbon displacing ground water in a gravity-driven system. Governing equations that were developed earlier by Corapcioglu and Hossain (1988) are solved by modifying the U.S.G.S. solute transport model (Konikow and Bredehoeft, 1978). The modification incorporates the fractional flow curves of water and their saturation derivatives in vertical and horizontal directions as functions of degree of water saturation. The details of the modification techniques are given, and the numerical results are presented for a hydrocarbon spill. Numerical results show that high-density, low-viscosity immiscible chlorinated hydrocarbons can travel deeper and further in contrast to lower-density, higher-viscosity compounds, and that the migration is dominated by gravity largely uncoupled from the horizontal component until the plume reaches the lower boundary.

INTRODUCTION

Chlorinated hydrocarbons are widely used in the chemical industry as metal degreasers and dry cleaning compounds among other uses. As a result of spills or past mismanagement, they are frequently encountered as contaminants in ground water. Dense chlorinated hydrocarbon groups include halogenated aliphatics such as trichloroethylene (TCE) with specific gravities from 1.2 to 2.2. In contrast to light hydrocarbons like gasoline that float on the water table, dense hydrocarbons sink into the aquifer and remain at the bottom for extended periods of time. The migration of these hydrocarbons is generally governed by the vertical component instead of lateral advective transport as for low-density hydrocarbons (Corapcioglu and Baehr, 1987). Limited solubility of high-density hydrocarbons furthermore poses a greater potential risk allowing the compound to dissolve into the ground water over a very long period of time. Meanwhile, the residual amount of hydrocarbon left in the pores during the downward migration continues to leach. Byer *et al.* (1981) provide an overview of the problem and note that the limited solubility allows chlorinated hydrocarbons to stay on the bottom for extended periods of time. Villaume (1985) describes various case histories involving dense nonaqueous phase liquids (NAPLs) such as coal tar and PCBs.

In this research, we study the migration of a high-density hydrocarbon in an unconfined gravel aquifer. In other words, the transport of an immiscible phase in a natural gradient gravity-driven system is investigated. Any chemical (e.g., adsorption, dissolution) or biological (e.g., biodegradation, biotransformation) processes are neglected in favor of studying density and viscosity effects. These objectives are achieved by presenting the system of equations for modeling dense hydrocarbon contaminant migration in a water-saturated porous medium. Then, governing equations are solved by modifying the solute transport model developed by Konikow and Bredehoeft (1978) at the U.S. Geological Survey. The main emphasis of this paper is to present the modifications introduced into the software for study of high-density immiscible hydrocarbon migration in an unconfined aquifer. Since the USGS program is well-documented and widely available for use in PCs, such a modification to study a timely, but a problem of different nature, would be a welcoming convenience for the practicing hydrogeologist.

TRANSPORT EQUATIONS OF HIGH-DENSITY HYDROCARBONS

Corapcioglu and Hossain (1988) developed the governing equations for high-density hydrocarbon migration in ground water. They assumed

---

[a] Department of Civil and Environmental Engineering, Washington State University, Pullman, Washington 99164-3001.

Received January 1987, revised March 1988, accepted March 1988.

Discussion open until May 1, 1989.

that in contamination of gravity-driven natural gradient systems by dense hydrocarbons ($\rho_{nw} > \rho_w$), the volumetric rate of ground-water flow is much larger than that of hydrocarbons. In such a system, ground-water flow is essentially horizontal along the impervious bed, and the flow of dense hydrocarbon contaminant is dominated by a sinking mechanism due to density difference. The contaminant penetrates the aquifer essentially in the vertical direction. This conclusion is confirmed by observations of Schwille (1981) and Faust (1985) who states that "For an immiscible fluid more dense than water, we expect gravity effects to be dominant. As a consequence we might anticipate downward migration of the contaminant in both the unsaturated zone and below the water table." Furthermore, Corapcioglu and Hossain (1986) reported the migration of a TCE plume in a plexiglass laboratory flume of 30 inches deep, and note the development of the plume essentially in the vertical direction, independent of lateral flow component. Their results show that it takes around 11 hours to reach the lower boundary.

Corapcioglu and Hossain (1988) obtained the governing equation for two-dimensional flow of high-density hydrocarbons in a homogeneous inclined reservoir with uniform properties (see Figure 1). Ground-water contamination by a dense hydrocarbon can be formulated by a two-phase fluid flow in a porous medium. TCE (hydrocarbon) is referred as the immiscible (nonwetting) phase and the water as the miscible (wetting) phase. In their formulations, Corapcioglu and Hossain neglected capillary pressures, liquid and soil compressibilities to obtain

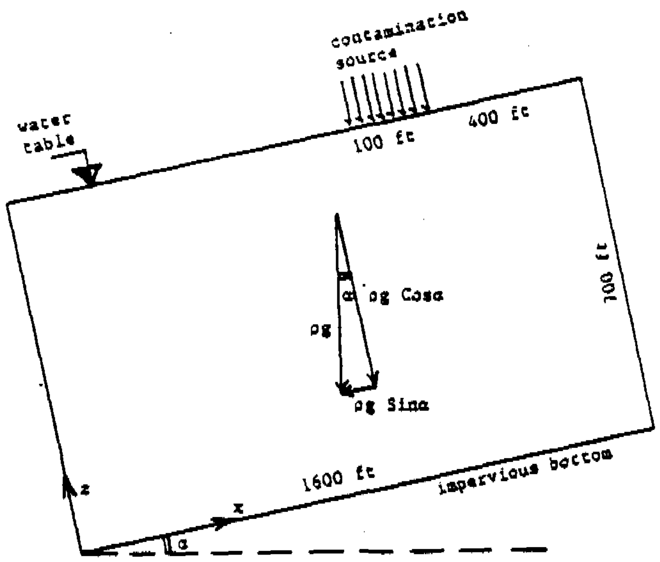

Fig. 1. Definition sketch of the problem.

$$q_x \frac{\partial r_{wx}}{\partial x} + q_z \frac{\partial r_{wz}}{\partial z} + n \frac{\partial S_w}{\partial t} = 0 \qquad (1)$$

where q_x and q_z are the total (water plus hydrocarbon) volumetric flow rates in lateral and vertical directions, respectively. Fractional flow expressions r_{wx} and r_{wz} in the lateral and vertical directions, respectively, are defined as

$$r_{wx} = \frac{q_{wx}}{q_x}, \qquad r_{wz} = \frac{q_{wz}}{q_z} \qquad (2)$$

where q_{wx} and q_{wz} are the volumetric flow rate of water in the lateral and vertical directions. In terms of degree of water saturations S_w

$$r_{wx} \simeq \frac{1}{1 + \dfrac{k_{nw}}{k_w} \dfrac{\mu_w}{\mu_{nw}}} \qquad (3)$$

$$r_{wz} \simeq \frac{1 - \dfrac{k_{nw}\Delta\rho}{\mu_{nw} q_z} g \cos\alpha}{1 + \dfrac{k_{nw}}{k_w} \dfrac{\mu_w}{\mu_{nw}}} \qquad (4)$$

where k_w and k_{nw} are the relative permeabilities of water and hydrocarbon, respectively;
μ_w and μ_{nw} are respective viscosities;
$\Delta\rho$ is the density difference ($= \rho_w - \rho_{nw}$); and
n is the porosity of the aquifer.

We note that in equations (3) and (4), capillary pressure differences are neglected, and in equation (3), the gravity term due to the magnitude of angle of inclination, α, of aquifers in nature is neglected. Since our purpose is to model the migration of TCE spill in a highly pervious gravel aquifer, we can assume capillary pressure gradients have a negligible effect on the flow. However, in other types of aquifers, capillary pressure gradients may be important. Furthermore, Corapcioglu and Hossain (1988) showed $q_x\ \partial r_{wx}/\partial x$ and $q_z\ \partial r_{wz}/\partial z$ to be larger than $r_{wx}\ \partial q_x/\partial x$ and $r_{wz}\ \partial q_z/\partial z$, respectively, to obtain equation (1). We should also note that for an instantaneous hydrocarbon spill of relatively small quantity, the volumetric flow rate of water would be much larger than that of hydrocarbon.

Permeability terms k_{nw} and k_w, in equations (3) and (4) are functions of degree of water saturation, S_w. Permeability expressions $k_w\ (S_w)$ and $k_{nw}\ (S_{nw})$ are obtained from laboratory experiments under no-flow conditions. For example, Lin *et al.* (1982) obtained relative permeability data for the case of trichloroethylene imbibition in a TCE-water system. We fitted the following relative permeability expressions to Lin's data. Curves of similar forms were also employed by Faust (1985). Thus, the permeability expressions are

$$k_{rw} = \frac{(S_w - 0.331)^3}{(1 - 0.331)^3}, \quad k_{rnw} = \frac{(0.83 - S_w)^{2.5}}{(0.83)^{2.5}} \qquad (5)$$

It is known that

$$k_w = k_o k_{rw}, \quad k_{nw} = k_o k_{rnw} \qquad (6)$$

where k_o is the porous medium's intrinsic permeability. Therefore, fractional water flow expressions r_{wx} and r_{wz} are functions of degree of water saturation S_w only. The viscosity ratio (μ_w/μ_{nw}) is assumed to be constant at isothermal soil conditions. Furthermore, $(\Delta\rho g \cos\alpha/q_z)$ in equation (4) is taken constant based on the assumption of constant vertical flow due to gravity dominance. Then, we can rewrite equation (1) as

$$\frac{q_x}{n} \frac{dr_{wx}}{dS_w} \frac{\partial S_w}{\partial x} + \frac{q_z}{n} \frac{dr_{wz}}{dS_w} \frac{\partial S_w}{\partial z} + \frac{\partial S_w}{\partial t} = 0 \qquad (7)$$

Equation (7) is a quasi-linear first-order partial differential equation with a single variable S_w. For a one-dimensional case (horizontal x-direction), it reduces to the Buckley-Leverett (1942) equation. Buckley and Leverett addressed the oil production problem encountered as a result of linear displacement of oil in the reservoir by water. They considered a homogeneous inclined reservoir with uniform, constant thickness, and solved the governing equation for one-dimensional flow by neglecting capillary pressures, gravity, and liquid compressibilities.

By definition, the material derivative of S_w is

$$\frac{dS_w}{dt} = \frac{\partial S_w}{\partial t} + \frac{\partial S_w}{\partial x} \frac{dx}{dt} + \frac{\partial S_w}{\partial z} \frac{dz}{dt} \qquad (8)$$

A comparison of equations (7) and (8) shows that

$$\left.\frac{dx}{dt}\right|_{S_w} = \left.\frac{q_x}{n} \frac{dr_{wx}}{dS_w}\right|_{S_w} \qquad (9)$$

$$\left.\frac{dz}{dt}\right|_{S_w} = \left.\frac{q_z}{n} \frac{dr_{wz}}{dS_w}\right|_{S_w} \qquad (10)$$

Note that $dx/dt|_{S_w}$ and $dz/dt|_{S_w}$ are velocity components of an advancing surface of a given value of the degree of water saturation. On curves $x = x(t)$ and $z = z(t)$ which coincide with moving curves of constant S_w, $x(t)$ and $z(t)$ are called characteristic curves of equation (7). Then, equation (7) yields

$$\frac{dS_w}{dt} = 0 \qquad (11)$$

The solution of equation (11) can be obtained by employing the method of characteristics. This method was successfully used by Konikow and Bredehoeft (1978) to solve the conventional solute transport equation.

REVIEW OF USGS MODEL

Konikow and Bredehoeft (1978) developed a two-dimensional digital computer model to predict the concentration of a dissolved chemical species in flowing ground water. In addition to concentration values, the program simultaneously calculates ground-water velocities in two lateral directions. The program solves two coupling partial differential equations, the ground-water flow equation (in terms of head distribution in the aquifer) and the solute transport equation (in terms of mass concentration).

Konikow and Bredehoeft express the solute transport equation as

$$\frac{\partial C}{\partial t} = \frac{1}{b} \frac{\partial}{\partial x_i} (bD_{ij} \frac{\partial C}{\partial x_j}) - V_x \frac{\partial C}{\partial x} - V_y \frac{\partial C}{\partial y} + F \qquad (12)$$

where $$F = \frac{C(S \frac{\partial h}{\partial t} + W - \epsilon \frac{\partial b}{\partial t}) - C'W}{\epsilon b} \qquad (13)$$

and C is the mass concentration of the dissolved chemical species; D_{ij} is the coefficient of hydrodynamic dispersion; b is the saturated thickness of the aquifer; and C′ is the mass concentration of the dissolved chemical in a source or sink fluid. V_x and V_y are components of velocity in the x and y directions, respectively; h is the hydraulic head; S is the storage coefficient; t is the time; $W = W(x,y,t)$ is the volume flux per unit area; and x_i and x_j are the Cartesian coordinates. $W(x,y,t)$ can be expressed as $W(x,y,t) = Q(x,y,t) - K_z(H_s - h)/m$ where Q is the rate of withdrawal or recharge; K_z is the vertical hydraulic conductivity of the confining layer, streambed, or lakebed; m is the thickness of the confining layer; ϵ is the porosity; and H_s is the hydraulic head in the source bed, stream, or lake. The material derivative of concentration is defined by

$$\frac{dC}{dt} = \frac{\partial C}{\partial t} + \frac{\partial C}{\partial x} \frac{dx}{dt} + \frac{\partial C}{\partial y} \frac{dy}{dt} \qquad (14)$$

A comparison of the second and third terms on the right-hand side of equation (14) with the second and third terms on the right-hand side of equation (12) shows that

Table 1. Correspondence Between Equations in Our Model and USGS Model

Equation # for high-density hydrocarbon migration	*Equation # for USGS model*
(1)	(12)
F=0	(13)
(8)	(14)
(9)	(15)
(10)	(16)
(11)	(17)

$$V_x = dx/dt \qquad (15)$$

$$V_y = dy/dt \qquad (16)$$

Substitution of equations (15), (16), and (12) into equation (14) gives

$$\frac{dC}{dt} = \frac{1}{b}\frac{\partial}{\partial x_i}\left(bD_{ij}\frac{\partial C}{\partial x_j}\right) + F \qquad (17)$$

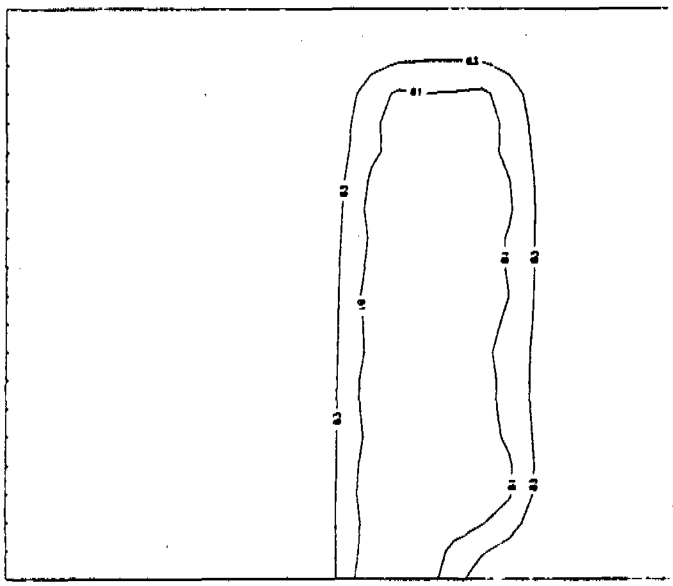

Fig. 2. Water saturation profiles for μ_w/μ_{nw} = 1.72, and ρ_{nw} = 1.46 g/cm^3 (TCE) at three years with initial slug injection. Note that $S_{nw} = 1 - S_w$.

Solutions to equations (15)-(17) can be expressed in a general form as x = x(t), y = y(t), and C = C(t) which are called the characteristic curves of equation (12). A comparison of equation (17) with equation (11) shows that the right-hand side of equation (17) is equal to zero for an identical match. Correspondence between equations in our model and USGS model is summarized in Table 1. The general solution technique by the method of characteristics is given by Konikow and Bredehoeft (1978), and the reader is referred to this reference for a more detailed discussion.

In this study, we use an IBM-PC version of the USGS program that is marketed by Scientific Publications Company. Their version incorporates several changes that were necessary to accommodate the main-frame program in the IBM-PC. The details of the modification of the USGS model are given in the Appendix.

RESULTS AND CONCLUSIONS

The numerical model was applied to simulate the formation of a TCE plume in a gravel aquifer due to an instantaneous spill from a buried source in the saturated zone (e.g., storage tank rupture). A spill of a relatively small volume of contaminant can be modeled as a slug injection (i.e., pulse source) into a sloping natural gradient unconfined aquifer. The aquifer is 700 ft thick and 1600 ft wide, inclined at an angle of 10° to the horizontal. The domain includes 162 nodes spaced 100 ft apart in each direction. Note that the figure illustrating the results (Figure 2) shows only a portion of the domain which is 700 ft thick and 800 ft wide. The initial conditions included the assumption of 100% water saturation throughout the domain.

Figure 2 shows the contour plot of the water saturation distribution at three years using data given in Table 2. The results clearly indicate the dominance of gravity effects in the vertical direction; due to the high density of the contaminant,

Table 2. Model Parameters Used

Density of water	ρ_w = 1 g/cm^3
Density of TCE	ρ_{nw} = 1.46 g/cm^3
Density difference	$\Delta\rho = \rho_w - \rho_{nw}$ = −0.46 g/cm^3
Dynamic viscosity of water	μ_w = 1.0019 × 10^{-2} poise
Dynamic viscosity of TCE	μ_{nw} = 0.58 × 10^{-2} poise
Intrinsic permeability of soil	k_o = 5.823 × 10^{-7} cm^2
Porosity of soil	n = 0.4
Angle of inclination	α = 10°
Residual saturation of water in a water-TCE system	S_{wr} = 0.331
Residual saturation of TCE in a water-TCE system	S_{wnr} = 0.170
Shock front saturation or cutoff saturation	S_{wc} = 0.675

spreading takes place only after the TCE plume reaches the bottom.

In summary, we study the migration of a high-density hydrocarbon in an unconfined aquifer. The Buckley-Leverett approach is extended to a two-dimensional case to simulate a high-density immiscible hydrocarbon displacing ground water in a gravity-driven natural gradient aquifer. Governing equations are solved by modifying the USGS solute transport model developed by Konikow and Bredehoeft (1978). The modification incorporated the fractional flow curves of water and their saturation derivatives in vertical and horizontal directions as functions of degree of water saturation. Results show that high-density, low-viscosity immiscible chlorinated hydrocarbons can travel deeper and further in contrast to lower-density, higher-viscosity compounds, and that the migration is dominated by gravity largely uncoupled from the horizontal component until the plume reaches the lower boundary.

APPENDIX – MODIFICATIONS OF THE USGS PROGRAM

In this appendix, we continuously refer to Konikow and Bredehoeft (1978) by indicating specific page and program line numbers. Therefore, the reader should obtain an original copy of that publication to follow the modifications needed for modeling high-density hydrocarbon migration.

First, the two-dimensional areal problem is modified to run for a two-dimensional vertical one. Vertical z-coordinate replaces the lateral y-coordinate. To achieve this, the input data are modified as shown in Attachment IV on page 79 of Konikow and Bredehoeft (1978). In the original program (20.0) in Data Set 4 for test problem number 3 stands for the vertical thickness of the aquifer (THCK = 20 ft). To rotate the flow field, we take a unit width in the lateral direction normal to the plane of paper. Thus, (20.0) is replaced by (1.00) (see Table 3). Then, on the same page (p. 79) in Data Set 3, VPRM = (0.1), which is a dummy variable in our case, is replaced by an arbitrary constant, e.g., 2×10^{-5} ft/sec.

In the program, the subroutine VELO calculates the flow velocities at nodes and cell boundaries, dispersion coefficients and the minimum number of particle moves required to solve the solute transport equation. In our modified version of VELO, we calculate dx/dt and dz/dt at a given S_w as expressed by equations (9) and (10). Note that in equations (9) and (10), we enter the values of q_x and q_z calculated by considering gravity terms only. The changes made at VELO are on page 55 between lines E410 and E460. Lines E410-E460 are replaced by

```
    IF (CONC(IX,IY).GE.82.9) CONC(IX,IY)=82.9
    IF (CONC(IX,IY).LE.33.2) CONC(IX,IY)=33.2
    WRITE(*,*)'CONC(IX,IY)=',CONC(IX,IY)
    BB=(0.83)**2.5
    AA=(0.669)**3
    RKNW(IX,IY)=((0.83-0.01*CONC(IX,IY))**2.5)/BB
    WRITE (*,*)'RKNW(IX,IY)=',RKNW(IX,IY)
    RKW(IX,IY)=((0.01*CONC(IX,IY)-0.331)**3)/AA
    WRITE(*,*)'RKW(IX,IY)=',RKW(IX,IY)
    DKRNW(IX,IY)=-2.5/BB*((0.83-0.01*CONC(IX,IY))**1.5)
    DKRW(IX,IY)=3/AA*((0.01*CONC(IX,IY)-0.331)**2)
    ALPHA=.175
    grdx=-SIN(ALPHA)
    write(*,*)'grdx=',grdx
    DENMX(IX,IY)=RKW(IX,IY)+1.72*RKNW(IX,IY)
    WRITE(*,*)'DENMX(IX,IY)=',DENMX(IX,IY)
    DDENMX(IX,IY)=DKRW(IX,IY)+1.72*DKRNW(IX,IY)
    DRWX(IX,IY)=(DENMX(IX,IY)*DKRW(IX,IY)-RKW(IX,IY)*DDENMX(IX,
1IY))/(DENMX(IX,IY)**2)
    WRITE(*,*)'DRWX(IX,IY)=',DRWX(IX,IY)
 VX(IX,IY)=PERM(IX,IY)*GRDX*PORINV*DRWX(IX,IY)
    WRITE(*,*)'VX=',VX(IX,IY)
```

to calculate dx/dt as given by equation (9). Note that the parameter grdx (which calculates the hydraulic gradient in the x-direction) is equal to $-\sin\alpha$, since the hydraulic gradient can be assumed to be constant in a gravity-driven natural gradient system. Furthermore, the first and second lines of this new program segment keep the water saturation values above the residual water saturation $S_{wr} = 0.33$ and below $S_{wc} = 0.67$ behind the front as explained by Corapcioglu and Hossain (1986). Note that this restriction on S_w is imposed only in this program segment while calculating dr_{wx}/dS_w and not while calculating S_w by subroutine CNCON which computes the change in water saturation in the aquifer. Since this restriction is imposed at the very beginning, it also applies to calculate dr_{wz}/dS_w which is handled by the program segment given below. Such a restriction allows us to avoid the existence of double water saturation at the saturation front due to bulbous saturation profile. A discussion of this phenomenon has been explained by Corapcioglu and Hossain (1986).

One should note that Konikow and Bredehoeft solved the solute transport problem in terms of concentration, C. In this study we solve the high-density hydrocarbon migration problem in terms of water saturation, S_w. Thus, the parameter termed CONC (IX, IY) in the USGS program denotes the degree of water saturation, S_w in our modification.

Similarly, dr_{wz}/dS_w and dz/dt are calculated by

```
    DRO=-0.465
    QZ=0.028
    UMNW=0.0058
    CT=(5.71E-4)*COS(ALPHA)*DRO/(QZ*UMNW)
    WRITE(*,*)'CT=',CT
    UP(IX,IY)=RKW(IX,IY)-CT*RKNW(IX,IY)*RKW(IX,IY)
    WRITE(*,*)'UP=',UP(IX,IY)
    DUP(IX,IY)=DKRW(IX,IY)-CT*(RKNW(IX,IY)*DKRW(IX,IY)
1+RKW(IX,IY)*DKRNW(IX,IY))
    DN(IX,IY)=RKW(IX,IY)+1.72*RKNW(IX,IY)
    WRITE(*,*)'DN=',DN(IX,IY)
    DDN(IX,IY)=DKRW(IX,IY)+1.72*DKRNW(IX,IY)
    DRWZ(IX,IY)=(DN(IX,IY)*DUP(IX,IY)-UP(IX,IY)*DDN(IX,IY))/
3(DN(IX,IY)**2)
    grdy=COS(ALPHA)
    WRITE(*,*)'DRWZ(IX,IY)=',DRWZ(IX,IY)
 VY(IX,IY)=PERM(IX,IY)*GRDY*PORINV*ANFCTR*DRWZ(IX,IY)
```

Table 3. Input Data for the Problem Studied

time limit; # of time limits; convergence criterion; # of pumping periods; # of nodes in the x-direction; # of nodes in the y-direction; max # of particles; NUMOBS; NREC; 3 of identification codes

```
  15   1   18   93200   1   7   0 100   0   9   1   0   1   0   0   0
 25.0.0001 0.40   0.  6e-3   1.61.2e6  100  100  0.3 0.50    1
0 2E-05   VPRM=2x10^-5 ft/sec
0  1.0    THCK=1 ft
0 0.0
1 1.0
000000000000000000
000000000000000000
000000000001100000
000000000000000000
000000000000000000   pulse source points(DATA SET 6)
000000000000000000
000000000000000000   should be same
000000000000000000   source concentration(water saturation)
000000000000000000
1          1.0        83.0        0.0 0    DATA SET 7
1 1.0 — DATA SET 8 (dummy water table data to start the run)
  0.  0.  0.  0.  0.  0.  0.  0.  0.  0.  0.  0.  0.  0.  0.  0.  0.  0.
  0.100.100.100.100.100.100.100.100.100.100.100.100.100.100.100.100.
  0. 96. 96. 96. 96. 96. 96. 96. 96. 96. 96. 96. 96. 96. 96. 96. 96.  0.
  0. 87. 87. 87. 87. 87. 88. 88. 88. 88. 88. 88. 89. 89. 89. 89. 89.  0.
  0. 83. 83. 83. 83. 83. 84. 84. 84. 84. 84. 84. 84. 84. 85. 85. 85.  0.
  0. 80. 80. 80. 80. 80. 80. 81. 81. 81. 81. 81. 81. 82. 82. 82. 82.  0.
  0. 77. 77. 77. 77. 78. 78. 78. 78. 78. 78. 78. 78. 78. 79. 79. 79.  0.
  0. 75. 75. 75. 75. 75. 75. 75. 75. 76. 76. 76. 76. 76. 76. 76. 76.  0.
  0.  0.  0.  0.  0.  0.  0.  0.  0.  0.  0.  0.  0.  0.  0.  0.  0.  0.
1 1.0 — DATA SET 9
                                 INITIAL CONDITION
  0.100.100.100.100.100.100.100.100.100.100.100.100.100.100.100.100.  0.
  0.100.100.100.100.100.100.100.100.100.100. 33. 33.100.100.100.100.  0.
  0.100.100.100.100.100.100.100.100.100.100.100.100.100.100.100.100.  0.
  0.100.100.100.100.100.100.100.100.100.100.100.100.100.100.100.100.  0.
  0.100.100.100.100.100.100.100.100.100.100.100.100.100.100.100.100.  0.
  0.100.100.100.100.100.100.100.100.100.100.100.100.100.100.100.100.  0.
  0.100.100.100.100.100.100.100.100.100.100.100.100.100.100.100.100.  0.
  0.  0.  0.  0.  0.  0.  0.  0.  0.  0.  0.  0.  0.  0.  0.  0.  0.  0.
```

Δz; Δx; size of initial time step(sec); time increment multiplier; storage coefficient(should be a non-zero value); dispersivity; porosity

which replace lines E500-E540 on pages 55 and 56 in Konikow and Bredehoeft (1978). Note that dz/dt is expressed by equation (10), and DRO = $\Delta\rho$ (in g/cm^3), UMNW = μ_{nw} (in poise), and QZ = q_z (in ft/sec). Similar to grdx, in a gravity-driven natural gradient system, grdz = cos α. In the program segments given above, we take ρ_{nw} = 1.46 g/cm^3 and μ_w/μ_{nw} = 1.72. We keep the hydraulic gradient and velocities at the cell boundaries constant by replacing E590, E610, E620, and E640 on page 56 with

```
E 580
C            ---VELOCITIES AT CELL BOUNDARIES---
          GRDX=-SIN(ALPHA)
        VXBDY(IX,IY)=PERMX*GRDX*PORINV*DRWX(IX,IY)
          grdy=COS(ALPHA)
        VYBDY(IX,IY)=PERMY*GRDY*PORINV*ANFCTR*DRWZ(IX,IY)
```

Additional DIMENSION statements are added between lines E200-E210 to include new variables in the program

```
      DIMENSION RKNW(20,20),RKW(20,20),DKRNW(20,20),DKRW(20,20),
     1DENMX(20,20),DDENMX(20,20),UP(20,20),DUP(20,
     220),DN(20,20),DDN(20,20),DRWX(20,20),DRWZ(20,20)
```

Furthermore, the Data Sets given in Table 3 include proper initial conditions for the problem studied. Note that Konikow and Bredehoeft (1978) consider an initially clear (i.e., $C = 0$ at $t = 0$) aquifer. This would correspond to 100% water saturation in our problem (i.e., $S_w = 100$) as given by the last block of numbers and Data Set 9 in Table 3. In Data Set 6, two 1's in the third row refer to the referral code of pulse source points. The 0's in Data Set 6 indicate $S_w = 100\%$. In Data Set 7, Table 3 shows

1	Referral code to source point
1.0	Code for leakance from the source
83.0	Source concentration ($S_{wr} = 0.83$)
0.0	Diffusive recharge
0	OVERRD

In the case of pulse source, a slug of hydrocarbon initially ($t = 0$) was injected into the aquifer at a concentration $S_w = 0.33$; input modifications are shown in Data Set 9. In Data Set 7, the source concentration is taken as 0.83 since after $t = 0$, some hydrocarbon will remain in the pores at a level $S_{or} = 0.17$ so $S_w = 1 - S_{or} = 0.83$. After an initial pulse, water saturation will go back to 83% at the source nodes. Similarly, initial conditions are placed on the second row ($S_{wr} = 33\%$) instead of the first one. Figure 13 on page 29 of Konikow and Bredehoeft (1978), shows the location of a slug of tracer for a pulse source.

As we do not include observation wells, we eliminate Data Set 1 by setting NUMOBS (number of observation points) equal to zero. We also do not include pumping wells so we eliminate Data Set 2 by setting NREC (number of pumping or injection wells) equal to zero. Thus, the coordinates of observation and pumping wells in Data Sets 1 and 2 are eliminated.

With these modifications to subroutine VELO and Input Data, we use subroutine CNCON and other subroutines of the program without changes. Subroutine CNCON, in this case, computes the change in water saturation at each node and at each particle for the given time increment. Note that in the original Konikow and Bredehoeft (1978) program, CNCON computed solute concentrations.

ACKNOWLEDGMENTS

The authors appreciate the comments of an anonymous reviewer which greatly improved the presentation of the material.

REFERENCES

Buckley, S. E. and M. C. Leverett. 1942. Mechamism of fluid displacement in sands. Transactions of AIME. v. 146, pp. 107-117.

Byer, H. G., W. Blankenship, and R. Allen. 1981. Groundwater contamination by chlorinated hydrocarbons: causes and prevention. Civil Engineering, ASCE. March, pp. 54-55.

Corapcioglu, M. Y. and A. Baehr. 1987. A compositional multiphase model for groundwater contamination by petroleum products, I. Theoretical consideration. Water Resources Research. v. 23, no. 1, pp. 191-200.

Corapcioglu, M. Y. and M. A. Hossain. 1986. Migration of chlorinated hydrocarbons in groundwater. Proceedings of the Conference on Petroleum and Organic Chemicals in Ground Water, Nov. 12-14, 1986, Houston, Texas. National Water Well Association, Dublin, OH. pp. 33-52.

Corapcioglu, M. Y. and M. A. Hossain. 1988. Groundwater contamination by high-density immiscible hydrocarbon slugs in gravity-driven gravel aquifers. (Submitted for publication.)

Faust, C. R. 1985. Transport of immiscible fluids within and below the unsaturated zone: a numerical model. Water Resources Research. v. 21, no. 4, pp. 587-596.

Konikow, L. F. and J. D. Bredehoeft. 1978. Computer model of two dimensional solute transport and dispersion in groundwater. Techniques of Water Resources Investigations of the U.S. Geological Survey. U.S. Government Printing Office, Washington, DC. Book 7, Chapter C2.

Lin, C., G. F. Pinder, and E. F. Wood. 1982. Water and trichloroethylene on immiscible fluids in porous media. Princeton University. Water Resources Progress Report, 83-WR-2. October.

Schwille, F. 1981. Groundwater pollution in porous media by fluids immiscible with water. In Quality of Groundwater, ed. W. Van Duijvenbooden, P. Glasbergen, and H. van Lelyveld. Elsevier, The Netherlands, pp. 451-463.

Villaume, J. F. 1985. Investigations at sites contaminated with dense, non-aqueous phase liquids (NAPLs). Ground Water Monitoring Review. v. 5, no. 2, Spring, pp. 60-74.

* * * * *

M. Akhter Hossain received his B.S. in Civil Engineering from Bangladesh University of Engineering and Technology, Dhaka in 1982 and his M.S. from the University of Delaware in 1986 under the supervision of Dr. Corapcioglu. After his graduation in 1982, he worked as a research lecturer for two years at the Institute of Flood Control and Drainage Research of the Bangladesh University of Engineering and Technology. Specifically, his research interests include the development and application of computer models in microcomputers, and ground-water contamination by hydrocarbons.

An Associate Professor of Civil Engineering at Washington State University, M. Yavuz Corapcioglu received his Ph.D. in Civil Engineering (1975) from Cornell University. His research interests include ground-water flow, transport and fate of pollutants in ground water, hydrocarbon contamination, land subsidence, and mathematical modeling. He has directed various ground-water pollution projects funded by federal and private agencies.
Dr. Corapcioglu has over 50 publications to his credit. He coedited Transport Phenomena in Porous Media *(Martinus Nijhoff, 1984) and* Advances in Transport Phenomena in Porous Media *(Martinus Nijhoff, 1987).*

COMPUTER NOTES

APPROXIMATE AND ANALYTICAL SOLUTIONS FOR SOLUTE TRANSPORT FROM AN INJECTION WELL INTO A SINGLE FRACTURE

by Chia-Shyun Chen[a] and S. R. Yates[b]

Introduction

In dealing with problems related to land-based nuclear waste management, a number of analytical and approximate solutions were developed to quantify radionuclide transport through fractures contained in the porous formation (e.g., Neretnieks, 1980; Rasmuson and Neretnieks, 1981; Tang *et al.*, 1981; Sudicky and Frind, 1982; Barker, 1982; Hodgkinson and Lever, 1983; Rasmuson, 1984; Neretnieks and Rasmuson, 1984; Chen, 1986). By treating the radioactive decay constant as the appropriate first-order rate constant, these solutions also can be used to study injection problems of a similar nature subject to first-order chemical or biological reactions. In these works, the fracture is idealized by a pair of parallel, smooth plates separated by an aperture of constant thickness. Using this macroscopic approach, Chen (1986) gave solutions to different cases regarding the injection of radioactive material into a fractured formation. The planar fracture was assumed to have a constant aperture thickness, 2b, and intersect the well with a radius r_0 (see Figure 1). Water containing radioactive constituents was discharged into the fracture through the well under a constant flow rate of Q. The injected radionuclides moved primarily through the fracture in a steady, radial flow field where the velocity as a function of radial distance, r, is described by

$$V(r) = A/r \qquad (1)$$

where $A = Q/(4\pi b)$ as the advection parameter.

[a] Department of Geosciences, New Mexico Institute of Mining and Technology, Socorro, New Mexico 87801.

[b] U.S. Salinity Laboratory, USDA/ARS, Department of Soil and Environmental Science, University of California, Riverside, California 92521.

Received October 1987, revised April 1988, accepted April 1988.

Discussion open until July 1, 1989.

Ground water was assumed to be immobile in the underlying and overlying porous formations due to their low permeabilities. However, the injected radionuclides were able to move from the fracture into the porous matrix by molecular diffusion (the matrix diffusion) due to possible concentration gradients across the interface between the fracture and the porous matrix (i.e., at z = 0). Two models (Models I and II) were studied by Chen (1986). Model I assumed advection and longitudinal dispersion as the transport mechanisms in the fracture, while Model II considered only advection. Both models included matrix diffusion. Solutions of these two models are different under transient conditions but converge to the same solution at steady state for commonly occurring conditions. Compared to the steady-state solutions of Model I, the steady-state solutions of Model II are mathematically simpler and thus are recommended for use when dealing with steady-state conditions of the stated problem. In addition to quantifying a "worst case" scenario, the steady-state solutions can be used to determine the maximum transport distance of the injected radionuclides in the fracture. For time-dependent conditions, however, the transient solutions of Model I are suggested because they are more generalized in the sense that the longitudinal dispersion process in the fracture is taken into account.

These transient and steady-state solutions have potential usefulness for quantitative study of problems where radioactive material is injected into a fractured formation for disposal or for tracer tests. They also can be employed to check the accuracy of portions of pertinent three-dimensional numerical codes; for axial symmetric systems the radial dimension is a combination of the horizontal x and y Cartesian dimension (i.e., $r^2 = x^2 + y^2$), and the matrix diffusion normal to the radial direc-

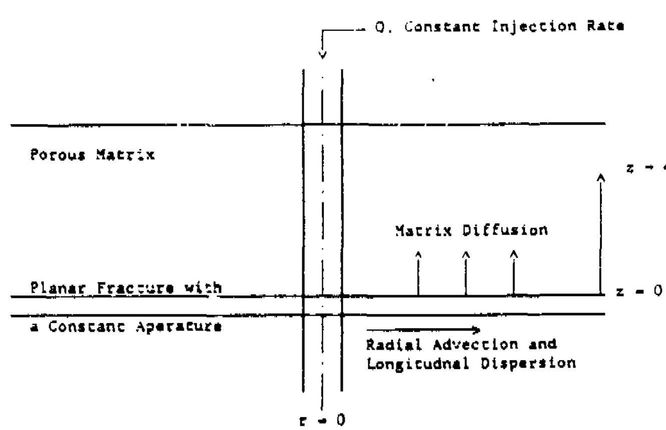

Fig. 1. Schematic of radionuclide transport from an injection well into a single, planar fracture situated in porous formation.

tion adds the third dimension, z. Consequently, these solutions could be used to check two-dimensional areal flow with matrix diffusions in the vertical direction.

By making use of the Stehfest method (Stehfest, 1970a, b), the transient solutions were determined by numerically inverting the solutions to Model I in the Laplace domain, which involve the transcendental Airy functions. Calculation of the transient solutions is not straightforward, and the purpose of this paper is to document a contained FORTRAN program, which computes the Stehfest inversion, the Airy functions, and gives the concentration distributions in the fracture as well as in the porous matrix for both transient and steady-state cases. A formula determining the maximum transport distance is given here.

Mathematical Model and Solutions

The mathematical model and its solutions are briefly discussed here. Detailed discussions of development of the model and derivation of the solutions are provided in Chen (1986).

The dispersion theory for solute transport in porous media is adopted, and the longitudinal dispersivity in the fracture is assumed to be constant. Hence, the longitudinal dispersion coefficient for the radial flow field neglecting molecular diffusion can be written as

$$D_r = \alpha_1 V \tag{2}$$

where V is the steady-state, radial ground-water velocity described by (1); and α_1 is the constant longitudinal dispersivity.

The governing equations of the model can be formulated as

$$D_m \frac{\partial^2 C_2}{\partial z^2} - \lambda R_2 C_2 = R_2 \frac{\partial C_2}{\partial t} \tag{3}$$

$$\frac{\alpha_1 A}{r} \frac{\partial^2 C_1}{\partial r^2} - \frac{A}{r} \frac{\partial C_1}{\partial r} + \frac{n_2 D_m}{b} \left. \frac{\partial C_2}{\partial z} \right|_{z=0} - \lambda R_1 C_1 = R_1 \frac{\partial C_1}{\partial t} \tag{4}$$

where λ is the decay coefficient for the radionuclides (or the first-order rate constant for chemical or biological transformation); C_1 and C_2 are concentrations in the fracture and in the porous matrix, respectively; D_m, n_2, and R_2 are, respectively, the effective molecular diffusion coefficient, the porosity, and the retardation factor for the linear-isotherm adsorption in the porous matrix; and α_1, b, and R_1 are, respectively, the dispersivity, half aperture thickness, and retardation factor in the fracture.

The initial condition for (3) and (4) is

$$C_1(r,0) = C_2(z,0) = 0 \tag{5}$$

which states that no contaminants exist in the system prior to injection.

The boundary condition at the interface of the fracture and the porous matrix is given by the continuity of concentrations as

$$C_1(r,t) = C_2(z,t); \qquad z = 0 \tag{6}$$

as $r \to \infty$ and $z \to \infty$, a bounded condition is prescribed for C_1 and C_2 as

$$C_1(\infty,t) = C_2(\infty,t) \text{ is bounded}; \quad r^2 + z^2 \to \infty \tag{7}$$

Two different boundary conditions for decay and nondecay sources are considered at the well bore. The decay boundary condition is

$$C_1(r_0,t) = C_0 e^{-\lambda t}/C_0 = e^{-\lambda t} \tag{8}$$

which may be relevant to injecting a radioactive substance with a short half-life. Due to the rapid decay, the concentration of the substance in the well bore cannot remain at a constant level but decreases with time following the exponential law as stated in (8).

The nondecay boundary condition, however, may be used if the concentrations at the injection well remain at a constant level because of the long half-life of the injected radioactive materials; that is,

$$C_1(r_0,t) = C_0/C_0 = 1 \tag{9}$$

In fact, if $\lambda t \leqslant 0.01$, the boundary conditions (8) and (9) are approximately equivalent since (8) yields a source concentration which like (9) is approximately equal to unity. Therefore, use of the decay or nondecay condition at the injection well does not cause significant difference in the calculated results provided $\lambda t \leqslant 0.01$.

Transient Solutions by Numerical Inversion

Analytical solutions to (3) and (4) subject to (5) through (8) or (9) can be determined by the Laplace transform technique. In appropriate dimensionless forms, the solutions for the decay boundary condition (8) in the Laplace domain is

$$G_1(\rho,p) = \frac{1}{p+\alpha_1} \exp\left[(\rho-\rho_0)/2\right] \frac{Ai[\beta^{1/3} y]}{Ai[\beta^{1/3} y_0]} \tag{10a}$$

$$G_2(\rho,p) = G_1 \cdot \exp\left[-\xi(p+\alpha_1)^{1/2}\right] \tag{10b}$$

where G_1 and G_2 denote the concentration distributions in the fracture; and within the porous matrix in the Laplace domain, respectively, p is the Laplace transform parameter of the dimensionless time τ defined by

$$\tau = At/R_1 \alpha_1^2$$

and the symbol Ai(x) represents the Airy function. The dimensionless radial distance ρ, the dimensionless vertical distance ξ, and other dimensionless parameters are defined in the Nomenclature.

The analytical Laplace inversion of (10) gives closed form solutions of C_1 and C_2 for the problem. As shown by Chen (1986), however, approximate solutions determined by numerically inverting (10) with the Stehfest method (Stehfest, 1970a, b) yield accurate results for practical purposes. Specifically, C_1 and C_2 for the decay boundary condition are obtained by numerically inverting G_1 and G_2 given in (10) with the following finite series of N terms

$$C_1(\rho,\tau) \cong p \sum_{n=1}^{N} W_n G_1(\rho, np); \quad p = \ln(2)/\tau \quad (11a)$$

$$C_2(\rho,\tau) \cong p \sum_{n=1}^{N} W_n G_2(\rho, np); \quad p = \ln(2)/\tau \quad (11b)$$

During the inversion calculation, p is inversely related to τ, and N must be an even integer. The weighting factors, W_n, are determined with the rational function given by Stehfest (1970a, b). These weighting factors are only dependent on the value of N chosen; that is, they need to be determined only once for any numerical inversions so long as N is fixed. In the computer examples provided in the Appendix, 16 weighting factors (i.e., N = 16) are given. It was found that 16 weighting factors provided sufficiently accurate results on an IBM-AT compatible microcomputer or on a DEC-20 main frame. Double-precision calculations are suggested when using the program. It should be noted that the arguments in the Airy functions are also dependent on p and hence on N and τ (see Nomenclature).

The Airy functions in (10) are calculated using appropriate formulae given by Abramowitz and Stegun (1970). Arguments of the Airy functions in (10) are always positive. The first 16 terms of the power series given by Abramowitz and Stegun (1970, equation 10.4.2) are used to evaluate Ai(x) when $0 \leq x < 3$. For the condition, $3 \leq x \leq 5$, Ai(x) is determined using a two-step procedure. Firstly, the modified Bessel function of the second kind of order $\frac{1}{3}$, $K_{1/3}(x)$, is calculated by the integral formula of equation 9.6.24 in Abramowitz and Stegun (1970). Secondly, the calculated $K_{1/3}(x)$ is converted to Ai(x) using the mathematical identity of equation 10.4.14 in Abramowitz and Stegun (1970). This method of determining Ai(x) for $3 \leq x \leq 5$ increases the computational stability of the algorithm. For $x > 5$, the first 14 terms of the asymptotic expansion given by equation 10.4.59 in Abramowitz and Stegun (1970) are employed for evaluating Ai(x). If a computer with sufficient precision is available, Ai(x) can be calculated by using the power series in the range $0 \leq x \leq 5$, and by the asymptotic expansion for $x > 5$ as mentioned above. In this event, the two-step computation for $3 \leq x \leq 5$ is not required. When $x > 5$, Ai(x) becomes small and can cause exponential underflow problems. Therefore, Ai(x) is scaled by a multiplying factor, $x^{1/4} \exp[(2/3)x^{3/2}]$. To recover the actual value for the Airy function during the calculations, the result is multiplied by $x^{-1/4} \exp[-(2/3)x^{3/2}]$. This approach for evaluating Ai(x) was suggested by Hsieh (1986).

In a similar manner, C_1 for the nondecay boundary condition can be determined by replacing

$$G_1(\rho,p) = (1/p)\exp[(\rho - \rho_0)/2] \frac{Ai[\beta^{1/3} y]}{Ai[\beta^{1/3} y_0]} \quad (12)$$

in (11a), and C_2 can be obtained by introducing (12) to (10b) and (11b).

The effect of the nondecay boundary condition is to replace the term $1/(p + \alpha_1)$ in (10) by the term 1/p. The calculation for the nondecay case follows identical procedures as the decay case. Hence, determination of concentration distributions for both the decay and nondecay boundary conditions requires only a slightly different calculation in the program.

Exact Steady-State Solution

Under steady-state conditions (i.e., injection time approaches infinity), the decay boundary condition yields a zero source concentration at the injection well, leading to a trivial solution of zero concentration everywhere in the system. However, nontrivial steady-state solutions exist for $\lambda > 0$ and a nondecay boundary condition; that is,

$$C_1 = \exp[(-E_1\lambda - E_2\lambda^{1/2})\bar{r}] \quad (13a)$$

$$C_2 = C_1 \exp[-z(R_2\lambda/D_m)^{1/2}] \quad (13b)$$

The longitudinal dispersivity is absent in (13) because the longitudinal dispersion in the fracture was neglected. Although Chen (1986) noted that longitudinal dispersion in the fracture could be neglected for steady-state conditions without introducing noticeable error based on one problem, we have verified that this conclusion is true for general conditions unless the parameter α is greater than approximately 10, which is unreasonably high and would rarely occur for practical problems. Therefore, (13) provides a useful steady-state solution for the stated problem.

The ultimate extent with which the concentration front can move in the fracture can be approximated with (13a). If the concentration front is taken as the location where x percent of the injected concentration takes place, then this ultimate moving distance is approximately equal to

$$r_x = \left[\frac{2 \ln(1/x)}{E_1 \lambda + E_2 \lambda^{1/2}} \right]^{1/2} \tag{14}$$

which is derived from (13a) by setting C_1 to x and the well radius is neglected. For example, if the frontal concentration is taken as 0.05, then the associated ultimate moving distance is

$$r_{0.05} = 2.5 \left[E_1 \lambda + E_2 \lambda^{1/2} \right]^{-1/2} \tag{15}$$

Examples

To illustrate the solutions contained herein, several hypothetical examples were created. To provide for the implementation of the computer program by future users, the data used to create the examples are reported in Appendix 2. To use the program, which is listed in Appendix 1, aquifer and chemical properties are required. The properties used for the following example are: half aperture thickness (b), well radius (r_0), flow rate into the fracture (Q), dispersivity (α_1), effective diffusion coefficient (D_m), and matrix porosity (n_2), respectively; 5.0×10^{-5} m, 0.1 m, 3.65 m^3/day, 0.1 m, 1.0×10^{-3} m^2/day, and 0.01 m^3/m^3. Other required parameters include the decay coefficient and retardation constant, which are 0.01 day^{-1} and 1.0, respectively. For each calculation, 16 Stehfest weighting coefficients and double precision were used.

Figure 2 shows the concentration distribution as a function of radial distance at several times and for two different boundary conditions at the well. The solid and dotted lines indicate, respectively, the concentration profiles based on the nondecay and decay boundary conditions. For the injection time equal to 0.01 day, the solutions determined by the two different boundary conditions are practically the same (see Figure 2) because the relationship $\lambda t \leq 0.01$ is satisfied. Under steady-state conditions, the solid line calculated by (12) with a large value of time is almost identical as the

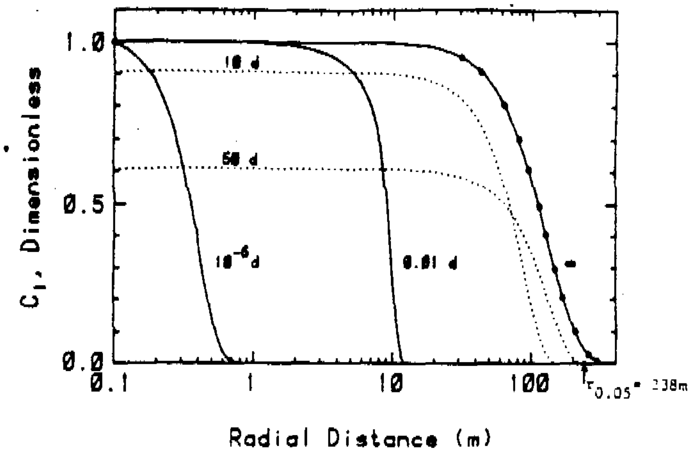

Fig. 2. Concentration with respect to time and radial distance in the fracture. The solid and dotted lines indicate the results from the nondecay and decay cases, respectively. The model coefficients are given in Appendix 2.

dots which resulted from the zero-dispersivity approximation, equation (13). This coincidence indicates that longitudinal dispersion in the fracture is not important for steady-state conditions. The ultimate moving distance, $r_{0.05}$, determined with equation (15), is about 238 m, which is found in Figure 2 by graphic interpolation.

Figure 3 is a diagram of the concentration distributions in the porous matrix for the example contained in Figure 2. In Figure 3a, the concentration profiles of C_2 at a radial distance of 1.0, 5.0, and 10.0 m and a time of 0.01 day is shown. In Figure 2b, the concentration profiles are for steady-state and radial distances of 1.0, 100.0, and 150.0 m. The dots indicate the results from the approximate solution. As was shown for the fracture, the zero-dispersivity approximation produces almost the same results as the more rigorous exact solution for this example.

Figure 4 contains a transient and steady-state contour diagram of the concentration in the fracture and porous matrix. For clarity, the fracture has been enlarged. The dotted line in Figure 4a indicates the position of the well bore. In Figure 4b, again it can be shown that equation (15) is a valid approximation for the ultimate moving distance, $r_{0.05}$.

Nomenclature

Dimensional Parameters

A	advection parameter equal to $Q/(4\pi b)$, m^2/s.
b	half fracture aperture, m.
C_0	concentration at the well bore, kg/m^3.
D_m	effective diffusion coefficient of porous matrix, m^2/s.

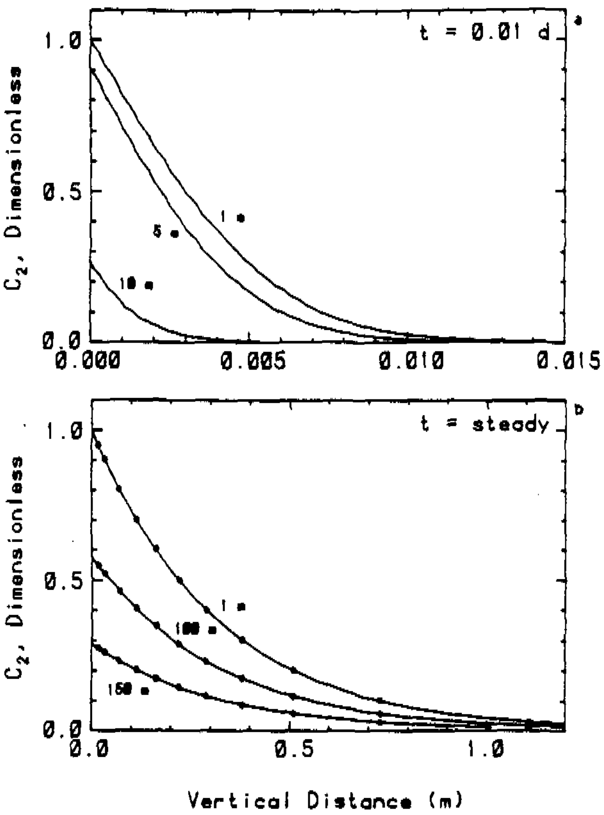

Fig. 3. Concentration in the porous media for times 0.01 d (a) and at steady-state (b). The dots in (b) indicate the results from equation (13). The model coefficients are given in Appendix 2.

D_r	longitudinal dispersion coefficient, m^2/s.
E_1	R_1/A, s/m^2.
E_2	$n_2(R_2D_m)^{1/2}/(bA)$, $s^{1/2}/m^2$.
Q	constant injection rate, m^3/s.
r	radial distance, m.
r_0	well radius, m.
$\tilde{r}$	$(r^2 - r_0^2)/2$, m^2.
t	time, s.
V	ground water in fracture defined by (1), m/s.
z	vertical distance in the porous matrix, m.
α_1	dispersivity of fracture, m.
λ	radioactive decay constant or first-order rate constant for chemical or biological reactions, s^{-1}.

Dimensionless Parameters

C_1, C_2	normalized concentration in fracture and in porous matrix, respectively.
n_2	porosity of porous matrix.
R_1, R_2	retardation factors in fracture and in porous matrix.
p	Laplace transform parameter.
y =	$\rho + 1/(4\beta)$.
y_0 =	$\rho_0 + 1(4\beta)$.
α =	$(n_2\alpha_1/b)(R_2D_m/R_1A)^{1/2}$.
α_1 =	$R_1\lambda\alpha_1^2/A$.
β =	$p + \alpha_1 + \alpha(p + \alpha_1)^{1/2}$.
ξ	$(z/\alpha_1)(R_2A/R_1D_m)^{1/2}$, dimensionless vertical distance.
τ	$At/(R_1\alpha_1^2)$, dimensionless time.
ρ	r/α_1, dimensionless radial distance.
ρ_0	r_0/α_1, dimensionless well radius.

Function

Ai(x) Airy function.

Disclaimer

Although a portion of the research described in this article has been funded wholly or in part by the United States Environmental Protection Agency, it has not been subjected to the Agency's peer and administrative review and therefore may not necessarily reflect the views of the Agency, and no official endorsement should be inferred.

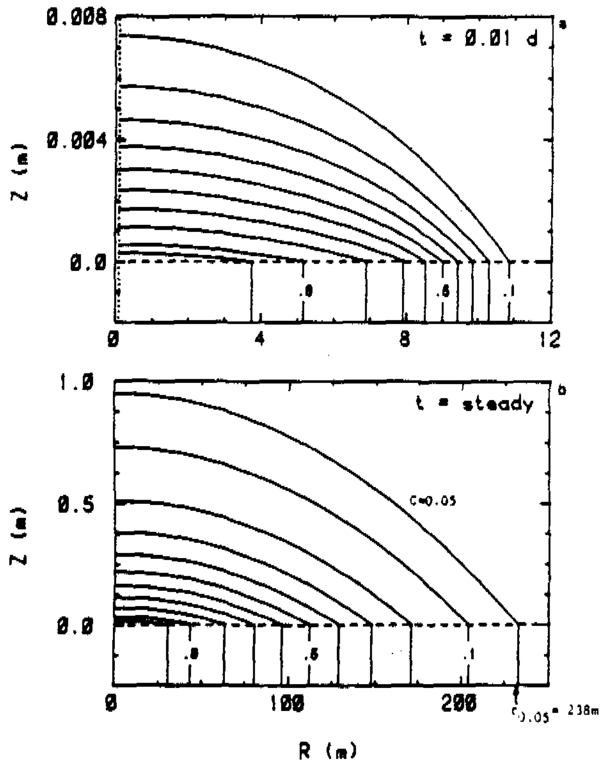

Fig. 4. Contour diagram of the concentration with respect to position and time. For t = 0.01 d (a), the contour levels are: 0.95, 0.9, 0.8, . . . , 0.1. For t = steady-state (b), the contour levels are: 0.95, 0.9, 0.8, . . . , 0.1, and 0.05. The dotted line in (a) indicates the position of the well bore.

Appendix 1. Program Source Code

```
C*****************************************************************************
C
C       THIS PROGRAM COMPUTES THE LAPLACE INVERSION OF THE RADIAL
C       DISPERSION EQUATION FOR VELOCITY DEPENDENT FLOW AND RADIOACTIVE
C       DECAY GIVEN BY CHEN(1986) USING THE LAPLACE INVERTION METHOD OF
C       STEHFEST(1970)
C
C*****************************************************************************
C
C    INPUT INFORMATION:
C    ******************
C
C         Input parameters can be provided to the program from either
C         a disk file or the keyboard.  In either case, the parameters
C         that must be supplied are:
C
C    INTERACTIVE INPUT (for opening files)
C    *************************************
C
C        IN          - Input file number.  IN=1 for disk, IN=5 for
C                       keyboard.
C
C        FILE        - IF IN=1, then give the input file name.
C
C
C        IO          - Output unit number.  IO=2 for disk, IO=5 for
C                       terminal, IO=6 for printer.
C
C        FILE        - IF IO=2, then give the output file name.
C
C
C
C    MODEL INPUT DATA (either from a disk file or interactively)
C    ***********************************************************
C
C    RECORD 1:  (free format)
C
C        TITLE(3)    - Three lines of title or problem description.
C
C        IBC         - Steering parameter for the boundary condition at
C                       the well.  If IBC=0; then a decay boundary.
C                       If IBC=1; then a non-decay boundary.
C
C        N           - Number of Stehfest weighting coefficients.  For
C                       IBM-AT compatible computers use between 10 to 16.
C
C        R1          - Retardation coefficient for the fracture surface.
C
C        R2          - Retardation coefficient for the porous matrix.
C
C        D           - Dispersivity of the fracture.
C
C        B           - Fracture aperature thickness.
C
C        N2          - Porosity of the porous matrix.
C
C        Dm2         - Effective diffusion coefficient for the porous
C                       matrix.
C
C        LAM         - Radioactive decay coefficient.
C
C        Q           - Flow into the fracture.
C
C
C    RECORD 2:
C
C        NR          - Number of radial coordinates where a concentration
C                       is to be calculated.
C
C        Ro          - The radius of the wellbore.
C
C        R           - The radial distance where the first concentration
C                       is to be calculated.
C
C        DR          - The distance between consecutive radial distances.
C                       A concentration will be determined at R + (i-1)DR,
C                       for i=1,2,3,...,NR.
C
C
C    RECORD 3:
C
C        NT          - Number of times the concentration is to be calculated.
C
C        T(NT)       - The NT values of time.  The maximum size for this
C                       array is 10.
C
C
C    RECORD 4:
C
C        NZ          - Number of vertical coordinates (in the porous matrix)
C                       where a concentration is to be calculated.  Note: the
C                       total number of concentrations calculated will be:
C                       NR*NZ*NT.
C
C        DZ          - The distance between consecutive vertical distances.
C
C*****************************************************************************
C
C    IMPORTANT VARIABLES
C
C        RHOO        - Dimensionless well radius
C        DRHO        - Incremental dimensionless radial distance
C        RHO         - Dimensionless radius
C        DXI         - Incremental dimensionless vertical distance
C        XI          - Dimensionless vertical distance
C        TAU         - Dimensionless time
C        A           - Advection parameter
C        ALF1        - Parameter relating to the radioactive decay
C        ALF         - Parameter relating to the diffusive leakage
C
C*****************************************************************************
      IMPLICIT DOUBLE PRECISION (A-H,O-Z)
      DOUBLE PRECISION LAM,N2,T(15),V(30),G(30),H(15),XR(30)
     # ,AI0(30),Z0(30)
      CHARACTER FILE*20,TITLE(3)*70,MES1(2)*46,MES2(2)*48
      COMMON IN,IT,IO,IL
      DATA MES1(1)/'Vertical concentrations will not be calculated'/
     #,MES1(2)/'Vertical concentrations will be calculated'/
     #,MES2(1)/'A decay boundary condition exists at the well'/
     #,MES2(2)/'A constant boundary condition exists at the well'/
      DATA INN,IOO,ITT/1,2,5/,IA/30/,IB/15/
C
C     ----- read steering parameters -----
      IT=ITT
      WRITE(IT,900)
      READ(IT,*) IN
      IF(IN.EQ.0) CALL VT100
      IF(IN.EQ.1) CALL VT52
C
      CALL VTPOSI
      WRITE(IT,*)' GIVE INPUT  DEVICE NUMBER (1=dsk, 5=tty) '
      READ(IT,*) IN
      IF(IN.EQ.INN) THEN
      CALL VTPOSI
      WRITE(IT,*)' GIVE INPUT  FILE NAME'
      READ(IT,'(A)') FILE
      OPEN(UNIT=IN,FILE=FILE,STATUS='OLD',MODE='READ')
      ELSE
      ENDIF
C
      CALL VTPOSI
      WRITE(IT,*)' GIVE OUTPUT DEVICE NUMBER (2=dsk, 5=tty, 6=lp)'
      READ(IT,*) IO
      IL=55
      IF(IO.EQ.5) IL=20
      IF(IO.EQ.IOO) THEN
      CALL VTPOSI
      WRITE(IT,*)' GIVE OUTPUT FILE NAME'
      READ(IT,'(A)') FILE
      OPEN(UNIT=IO,FILE=FILE,STATUS='NEW')
      ELSE
      ENDIF
C
C     ----- read in input parameters of the fracture -----
      IF(IN.EQ.1) THEN
      READ(IN,'(A)') (TITLE(I),I=1,3)
      READ(IN,*) IBC
      READ(IN,*) N,R1,R2,D,B,N2,DM2,LAM,Q
      READ(IN,*) NR,RO,R,DR
      READ(IN,*) NT,(T(I),I=1,NT)
      READ(IN,*) NZ,DZ
      ELSE
C
C     ----- interactive input option -----
      CALL INTRAC(TITLE,IBC,N,R1,R2,D,B,N2,DM2,LAM,Q,NR,RO,R,DR,
     #NZ,DZ,NT,T)
      ENDIF
C
C     ----- write out input parameters -----
      IFZN=0
      IF(NZ.GT.0) IFZN=1
      IF(IO.EQ.IT) CALL VTPOS1
      WRITE(IO,905)
      WRITE(IO,910) (TITLE(I),I=1,3)
      WRITE(IO,915)
      WRITE(IO,920) MES1(IFZN+1),MES2(IBC+1)
      IF(D.NE.0.D00) WRITE(IO,925) N
      IF(D.EQ.0.D00) WRITE(IO,930)
      IF(IO.EQ.IT) CALL VTWAIT
      WRITE(IO,935) D,R1,B,DM2,R2,N2,LAM,Q
      IF(IO.EQ.IT) CALL VTWAIT
C
C     ----- go to appropriate analytical solution -----
C     -----    model1 if D > 0, otherwise model2    -----
      IF(D.NE.0.D00) CALL MODEL1(IA,IB,IBC,N,R1,R2,D,B,N2,DM2,LAM,Q
     # ,NR,RO,R,DR,NZ,DZ,NT,T,V,G,H,XR,AI0,Z0)
      IF(D.EQ.0.D00) CALL MODEL2(IB,IBC,R1,R2,B,N2,DM2,LAM,Q,NR,RO,R
     # ,DR,NZ,DZ,NT,T)
C
C     ----- format statements -----
  900 FORMAT(36(/),' GIVE THE TERMINAL TYPE:',//,5X,'0 = VT100',/,
     # 5X,'1 = VT52',T50,'==> ',$)
  905 FORMAT(/,1X,78(1H*),/,1X,'*',76X,'*')
  910 FORMAT(1X,'*',3X,A,3X,'*')
  915 FORMAT(1X,'*',76X,'*',/,1X,78(1H*))
  920 FORMAT(///,1X,'PROBLEM SPECIFICATIONS',/,1X,22(1H=),//,1X,
     #A46,/,1X,A48)
  925 FORMAT(1X,I2,' Stehfest weighting factors will be used to invert t
     #he Laplace transform')
  930 FORMAT(1X,'The dispersivity of the fracture is zero.  Will use the
     # approximate solution')
  935 FORMAT(///1X,'INPUT PARAMETERS'/,1X,16(1H=),//,
     #1X,'Dispersivity of the fracture [L]..............',10(1H.)
     #,1PE13.6,/,
     #1X,'Retardation coefficient for fracture walls [0]',10(1H.)
     #,1PE13.6,/,
     #1X,'Half width of fracture aperature [L]..........',10(1H.)
     #,1PE13.6,/,
     #1X,'Diffusion coefficient of porous matrix [L*L/T]',10(1H.)
     #,1PE13.6,/,
     #1X,'Retardation coefficient for porous matrix [0].',10(1H.)
     #,1PE13.6,/,
     #1X,'Porosity of the porous matrix [0].............',10(1H.)
     #,1PE13.6,/,
     #1X,'Radioactive decay constant [1/T]..............',10(1H.)
     #,1PE13.6,/,
     #1X,'Constant injection rate [L*L*L/T].............',10(1H.)
     #,1PE13.6)
      END
C
C*****************************************************************************
C
C       SUBROUTINE MODEL1 -- CALCULATES THE LAPLACE INVERSION SOLUTION
C                            OF Chen (1985) WHEN THE DISPERSIVITY IS
C                            GREATER THAN ZERO.
C
C*****************************************************************************
      SUBROUTINE MODEL1(IA,IB,IBC,N,R1,R2,D,B,N2,DM2,LAM,Q,NR,RO
     # ,R,DR,NZ,DZ,NT,T,V,G,H,XR,AI0,Z0)
      IMPLICIT DOUBLE PRECISION (A-H,O-Z)
```

```
      DOUBLE PRECISION LAM,N2,V(IA),XR(IA),T(IB),AI0(IA),Z0(IA),G(IA),
     #H(IB)
      COMMON IN,IT,IO,IL
      COMMON /ARGU/ A13,ALF,BETA,BETA3
C
C     ----- calculate the problem constants -----
      RHO0 = R0/D
      DRHO = DR/D
      RHOI = R/D
      PI   = 2.000*DATAN(1.D+30)
      A    = Q/(4.000*PI*B)
      ALF  = N2*D*DSQRT(R2*DM2/(R1*A))/B
      ALF1 = R1*LAM*D*D/A
      DXI  = DZ*DSQRT(R2*A/(R1*DM2))/D
      A13=1.D0/3.D0
      A23=2.000/3.000
      Aln2=DLOG(2.D0)
C
C     ----- print out calculated parameters -----
      WRITE(IO,900) A,RHO0,DRHO,ALF,ALF1
      IF(NZ.GT.0) WRITE(IO,905) DXI
C
C     ----- determine the Stehfest weighting coefficients -----
      IF(T(1).LT.0.000.AND.NT.EQ.1) GOTO 15
      CALL LINV(IA,IB,N,V,G,H)
      IF(IO.EQ.IT) CALL VTWAIT
      WRITE(IO,910)
      DO 10 I=1,N/2
      II = N/2 + I
      WRITE(IO,915) I,V(I),II,V(II)
   10 CONTINUE
      CALL VTWAIT
C
C     ----- calculate a concentration profile for each time -----
   15 IF(IO.EQ.IT) CALL VTPOSI
      WRITE(IO,920)
      IF(IO.EQ.IT) CALL VTWAIT
C
C     ----- new time -----
      DO 20 K=1,NT
      TAU = A*T(K)/(R1*D*D)
      RHO = RHOI
C
      IF(IO.EQ.IT) CALL VTPOS1
      IF(T(K).LT.0.000) WRITE(IO,925)
      IF(T(K).GE.0.000) WRITE(IO,930) T(K),TAU
      WRITE(IO,935)
C
C     ----- determine Ai0 and Z0 (only once) -----
      IF(T(K).LT.0.000) THEN
      IF(IBC.EQ.0) WRITE(5,940)
      IF(IBC.EQ.0) RETURN
      IF(LAM.EQ.0.000) WRITE(IO,945)
      IF(LAM.EQ.0.000) GOTO 20
C
C     ----- find values for steady state case -----
      Y0  = ARG(ALF1,RHO0)
      Z0(1) = A23*(Y0)**1.500
      IOPT=1
      IF(Y0.LT.3.000) IOPT=-1
      IF(Y0.GE.5.000) IOPT= 0
      AI0(1) = AI(Y0,IOPT)
      ELSE
C
C     ----- find values for time-decendent case -----
      YMN = ARG(DBLE(FLOAT(N))*Aln2/TAU+ALF1,RHO0)
      YMX = ARG(Aln2/TAU+ALF1,RHO0)
      IOPT=1
      IF(YMX.LT.3.000) IOPT=-1
      IF(YMN.GT.5.000) IOPT= 0
C
      DO 25 L=1,N
      PA1=DBLE(FLOAT(L))*Aln2/TAU+ALF1
      Y0 = ARG(PA1,RHO0)
      Z0(L) = A23*Y0**1.500
      AI0(L)= AI(Y0,IOPT)
   25 CONTINUE
      ENDIF
C
C     ----- calculate the concentrations in the fracture -----
      LO=0
      DO 30 IR=1,NR
      DD=0.500*(RHO-RHO0)
      XP=0.D0
      IF(T(K).LT.0.000) THEN
C
C     ----- calculate the steady-state values -----
      Y  = ARG(ALF1,RHO)
      IF(Y.LT.5.D0) THEN
      Z = A23*(Y)**1.500
      C1=DEXP(DD+Z0(1)-Z)*AI(Y,1)*(Y0/Y)**0.2500/AI0(1)
      ELSE
      DXP=(Y0/Y)**.2500
      XP = A23*(Y0**1.500-Y**1.500)
      C1=DXP*DEXP(DD+XP)
      ENDIF
      ELSE
C
C     ----- calculate the time-dependent values -----
      YMN = ARG(DBLE(FLOAT(N))*Aln2/TAU+ALF1,RHO)
      YMX = ARG(Aln2/TAU+ALF1,RHO)
      IOPT=1
      IF(YMX.LT.3.000) IOPT=-1
      IF(YMN.GT.5.000) IOPT= 0
C
C     ----- Stehfest numerical integration method -----
      DO 35 L=1,N
      PA1 = DBLE(FLOAT(L))*Aln2/TAU+ALF1
      Y    = ARG(PA1,RHO)
      Z    = A23*Y**1.500
      FACT = DEXP(DD+Z0(L)-Z)*(Z0(L)/Z)**.25
C
C     ----- if IBC=1, C=1.0 at the well bore -----
      IF(IBC.EQ.1) PA1=PA1-ALF1
      AIFN = AI(Y,IOPT)
      XR(L)=V(L)*((AIFN*FACT)/(AI0(L)*PA1))
      XP = XP + XR(L)
   35 CONTINUE
      C1=XP*Aln2/TAU
      ENDIF
C
C     ----- print out result -----
      R = D*RHO
      LO=LO+1
      IF(C1.LT.0.000) C1=0.000
      WRITE(IO,950) LO,R,0.000,C1
      IF(LO.EQ.NR .AND. NZ.EQ.0) GOTO 30
      IF(FLOAT(LO/IL).EQ.FLOAT(LO)/FLOAT(IL)) CALL VTWAIT
      IF(FLOAT(LO/IL).EQ.FLOAT(LO)/FLOAT(IL)) WRITE(IO,935)
C
C     ----- calculate concentration in porous matrix -----
      XI=DXI
      DO 40 IZ=1,NZ
      IF(T(K).LT.0.000) THEN
C
C     ----- calculate steady state concentraton -----
      C2=C1*DEXP(-XI*SQRT(ALF1))
      Z = D*XI/DSQRT(R2*A/(R1*DM2))
      ELSE
C
C     ----- calculate time-dependent concentration -----
      ZP=0.000
      DO 45 L=1,N
      PA1 = L*Aln2/TAU+ALF1
      ZZ  = DEXP(-XI*DSQRT(PA1))
      ZP  = ZP + ZZ*XR(L)
   45 CONTINUE
      C2=ZP*Aln2/TAU
      ENDIF


C     ----- print out results -----
      Z = D*XI/DSQRT(R2*A/(R1*DM2))
      LO=LO+1
      IF(C2.LT.0.000) C2=0.000
      WRITE(IO,950) LO,R,Z,C2
      IF(LO.EQ.NR*NZ) GOTO 40
      IF(FLOAT(LO/IL).EQ.FLOAT(LO)/FLOAT(IL)) CALL VTWAIT
      IF(FLOAT(LO/IL).EQ.FLOAT(LO)/FLOAT(IL)) WRITE(IO,935)
   40 XI =XI+DXI
   30 RHO=RHO+DRHO
   20 IF(K.NE.NT) CALL VTWAIT
C
C     ----- format statements -----
  900 FORMAT(///1X,'CALCULATED PARAMETERS'/1X,22(1H*)//
     #1X,'Advection parameter (A).........................',10(1H.),
     #1PE13.6,/,
     #1X,'Dimensionless radius of the well (RHO0).......',10(1H.)
     #,1PE13.6,/,
     #1X,'Dimensionless distance between radii (DRHO)...',10(1H.)
     #,1PE13.6,/,
     #1X,'Ratio of diffusive loss to injection (ALPHA)..',10(1H.)
     #,1PE13.6,/,
     #1X,'Dimensionless radioactive decay constant (ALPHA1)',7(1H.)
     #,1PE13.6)
  905 FORMAT(1X,'Dimensionless vertical spacing (DXI)..........'
     # ,10(1H.),1PE13.6)
  910 FORMAT(///1X,'STEHFEST WEIGHTING FACTORS'/1X,27(1H=)//
     #5X,'I',12X,'V(I)',27X,'II',11X,'V(II)')
  915 FORMAT(1X,I5,1PE20.7,20X,I5,1PE20.7)
  920 FORMAT(16X,'CONCENTRATION DISTRIBUTION'
     #,/,16X,26(1H=),//)
  925 FORMAT(5X,'Time = Steady State',/)
  930 FORMAT(5X,'Time = ',1PE15.5,10X,'Tau = ',1PE15.5,/)
  935 FORMAT(5X,'I',14X,'R',16X,'Z',15X,'C/Co')
  940 FORMAT(5X,'ERROR: IBC must = 1 for a steady state solution')
  945 FORMAT(5X,'ERROR: Lambda cannot be zero for a steady state
     # solution.',/,12X,'The concentration is 1.0 for X < infinity',/)
  950 FORMAT(1X,I5,5X,F12.3,5(5X,F12.4))
      RETURN
      END
C
C***********************************************************************
C
C
C        SUBROUTINE NAME: MODEL2 -- THIS PROGRAM CALCULATES THE SOLUTION
C                                   OF Chen (1986) WHEN THE DISPERSIVITY
C                                   IS ZERO.
C
C***********************************************************************
      SUBROUTINE MODEL2(IB,IBC,R1,R2,B,N2,DM2,LAM,Q,NR,R0,R
     # ,DR,NZ,DZ,NT,T)
      IMPLICIT DOUBLE PRECISION (A-H,O-Z)
      DOUBLE PRECISION LAM,N2
      DIMENSION T(IB)
      COMMON IN,IT,IO,IL
C
C     ----- calculate problem constants -----
      PI = 2.000*DATAN(1.D+30)
      A  = Q/(4.000*PI*B)
      E1 = R1/A
      E2 = N2*DSQRT(R2*DM2)/A/B
      RI = R
      WRITE(IO,900) A,E1,E2
      CALL VTWAIT
      IF(IO.EQ.IT) CALL VTPOSI
      WRITE(IO,905)
      IF(IO.EQ.IT) CALL VTWAIT
C
C     ----- calculate concentration for each time -----
      DO 10 K=1,NT
      IF(IO.EQ.IT) CALL VTPOS1
      IF(T(K).LT.0.000) WRITE(IO,910)
      IF(T(K).GE.0.000) WRITE(IO,915) T(K)
      WRITE(IO,920)
C
C     ----- calculate the concentration in the fracture -----
      Z=0.000
      R=RI
      LO=0
C
      DO 15 IR=1,NR
      RR=R*R/2.-R0*R0/2.
      Z=0.000
      IF(T(K).LT.0.000) THEN
C
```

```
C       ----- steady-state solution -----
        ARG1 = -E1*LAM*RR - E2*DSQRT(LAM)*RR
        IF(IBC.EQ.0.AND.LAM.NE.0.0D0) C1 = 0.0D0
        IF(IBC.NE.0.AND.LAM.NE.0.0D0) C1=DEXP(ARG1)
        IF(IBC.NE.0.AND.LAM.EQ.0.0D0) C1=1.0D0
        ELSE
C
C       ----- time-dependent solution -----
        T1=T(K)-E1*RR
        IF(T1.LE.0.0) GOTO 25
        ARG1=E2*RR/DSQRT(T1)/2.0
        ARG2=DSQRT(LAM*T1)
        EXP1=E2*RR*DSQRT(LAM)
        EXP2=E1*RR*LAM
C
C       ----- calculation for a decay boundary condition -----
        IF(IBC.EQ.1) GOTO 20
        C1=DEXF(-LAM*T(K),ARG1)
        GOTO 30
C
C       ----- calculation for a non-decay boundary condition -----
   20   C1=0.5D0*(DEXF(-EXP1-EXP2,ARG1-ARG2)
     #   +DEXF(EXP1-EXP2,ARG1+ARG2))
        GOTO 30
   25   C1=0.0
   30   CONTINUE
        ENDIF
C
C       ----- print out results -----
        LO=LO+1
        WRITE(IO,925) LO,R,Z,C1
        IF(LO.EQ.NR .AND. NZ.EQ.0) GOTO 35
        IF(FLOAT(LO/IL).EQ.FLOAT(LO)/FLOAT(IL)) CALL VTWAIT
        IF(FLOAT(LO/IL).EQ.FLOAT(LO)/FLOAT(IL)) WRITE(IO,920)
C
C       ----- calculate concentration in porous media -----
   35   Z=DZ
        DO 40 N=1,NZ
        IF(T(K).LT.0.0D0) THEN
C
C       ----- steady-state solution (only non-decay boundary allowed) -----
        IF(IBC.NE.0) C2 = DEXP(ARG1 - Z*DSQRT(R2*LAM/DM2))
        ELSE
C
C       ----- time-dependent solution -----
        IF (T1.LE.0.0) GOTO 50
        ZZ=Z*DSQRT(R2/DM2)
        ARG1=(E2*RR+ZZ)/DSQRT(T1)/2.0
        IF(IBC.EQ.1) GOTO 45
C
C       ----- decay boundary condition -----
        C2=DEXF(-LAM*T(K),ARG1)
        GOTO 55
C
C       ----- non-decay boundary condition -----
   45   C2=0.5D0*(DEXF(-EXP1-EXP2-DSQRT(LAM)*ZZ,ARG1-ARG2)
     #       +DEXF(EXP1-EXP2-DSQRT(LAM)*ZZ,ARG1+ARG2))
        GOTO 55
   50   C2=0.0
   55   CONTINUE
        ENDIF
C
C       ----- print out results -----
        LO=LO+1
        WRITE(IO,925) LO,R,Z,C2
        IF(LO.EQ.NR*NZ) GOTO 40
        IF(FLOAT(LO/IL).EQ.FLOAT(LO)/FLOAT(IL)) CALL VTWAIT
        IF(FLOAT(LO/IL).EQ.FLOAT(LO)/FLOAT(IL)) WRITE(IO,920)
   40   Z=Z+DZ
   15   R=R+DR
   10   IF(K.NE.NT) CALL VTWAIT
        RETURN
C
C       ----- format statements -----
  900   FORMAT(///1X,'CALCULATED PARAMETERS'/1X,22(1H*)//
     #1X,'Advection parameter (A)........................',10(1H.),
     #1PE13.6,/,
     #1X,'Ratio of retardation in fracture to "A" (E1)..',10(1H.)
     #,1PE13.6,/,
     #1X,'Factor E2.......................................',10(1H.)
     #,1PE13.6)
  905   FORMAT(16X,'CONCENTRATION DISTRIBUTION'
     #,/,16X,26(1H=),//)
  910   FORMAT(5X,'Time = Steady State',/)
  915   FORMAT(5X,'Time = ',1PE15.5,/)
  920   FORMAT(5X,'I',14X,'R',16X,'Z',15X,'C/Co')
  925   FORMAT(1X,I5,5X,F12.3,5(5X,F12.4))
        END
C
C***********************************************************************
C
C         FUNCTION ARG -- CALCULATES THE ARGUMENT FOR THE AIRY FUNCTION
C
C***********************************************************************
        DOUBLE PRECISION FUNCTION ARG(P,R)
        IMPLICIT DOUBLE PRECISION (A-H,O-Z)
        COMMON /ARGU/ A13,ALF,BETA,BETA3
C
        BETA   = P+ALF*DSQRT(P)
        BETA3  = BETA**A13
        ARG = BETA3*(R + 0.25D0/BETA)
        RETURN
        END
C
C***********************************************************************
C
C       SUBROUTINE DEXF -- EVALUATES EXP(A)ERFC(B) IN DOUBLE PRECISION
C
C***********************************************************************
        DOUBLE PRECISION FUNCTION DEXF(A,B)
        IMPLICIT DOUBLE PRECISION (A-H,O-Z)
        DATA P/.3275911D0/,A1/.254829592D0/,A2/.284496736D0/
     # ,A3/1.421413741D0/,A4/1.453152027D0/,A5/1.061405429D0/
C
        DEXF=0.0D0
        IF((DABS(A).GT.82.D0).AND.(B.LE.0.0D0)) RETURN
        IF(B.NE.0.0) GOTO 10
        DEXF=DEXP(A)
        RETURN
   10   C=A-B*B
        IF((DABS(C).GT.82.D0).AND.(B.GT.0.D0)) RETURN
        IF(C.LT.-82.0D0) GOTO 25
        X=DABS(B)
        IF(X.GT.3.0D0) GOTO 15
        T = 1.D0/(1.0D0+P*X)
        Y = T*(A1-T*(A2-T*(A3-T*(A4-A5*T))))
        GOTO 20
   15   Y = .5641896D0/(X+.5D0/(X+1.D0/(X+1.5D0/(X+2.D0/(X+2.5D0/(X+1.D0
     #))))))
   20   DEXF = Y*DEXP(C)
   25   IF(B.LT.0.0D0) DEXF = 2.D0*DEXP(A)-DEXF
        RETURN
        END
C
C***********************************************************************
C
C       FUNCTION AI(ZA,IOPT) -- THIS FUNCTION SUBROUTINE COMPUTES THE
C                               AIRY FUNCTION FOR POSITIVE ARGUMENTS.
C
C       IF IOPT = -1, USE THE SMALL ARGUMENT SERIES SOLUTION
C       IF IOPT =  0, USE THE LARGE ARGUMENT SERIES SOLUTION
C       IF IOPT =  1, USE THE INTEGRAL SOLUTION METHOD
C
C       THE AIRY FUNCTION IS SCALED (MULTIPLIED) BY:
C
C          (Z**0.25)*EXP(U), WHERE U=(2./3.)*(Z**1.5)
C
C***********************************************************************
        DOUBLE PRECISION FUNCTION AI(ZA,IOPT)
        IMPLICIT DOUBLE PRECISION (A-H,O-Z)
        DOUBLE PRECISION XG(10),WG(10)
        COMMON IN,IT,IO,IL
        DATA C1,C2/.3550280538878D0,.2588194037928D0/
        DATA COEF1,COEF2,COEF3,COEF4,COEF5,COEF6/9.555526226877D-29,
     1   4.235605597020D-32,1.661021802753D-35,1.013578212294D-29,
     2   4.309431174718D-33,1.624974047782D-36/
        DATA V/.3333333333333333D0/,PISQR3/5.441398093D0/,
     # PIRT2/3.5449077018D0/,PI/3.141592653590D0/,PID4/7.853981634D-1/
     #,A23/.66666666666666667D0/
        DATA NG/10/,XG/.765265211334973D-1,.227785851141645D0,
     #.373706088715419D0,.510867001950827D0,.636053680726515D0,
     #.746331906460150D0,.839116971822218D0,.912234428251325D0,
     #.963971927277913D0,.993128599185094D0/
        DATA WG/.152753387130725D0,.149172986472603D0,
     #.142096109318382D0,.131688638449176D0,.118194531961518D0,
     #.101930119817240D0,.832767415767047D-1,.626720483341090D-1,
     #.406014298003869D-1,.176140071391521D-1/
C
C       ----- function statements -----
        FN(Y) = DEXP(-ZK*DCOSH(Y))*DCOSH(V*Y)
        DACOSH(Y) = DLOG(Y+DSQRT(Y*Y-1.0D0))
C
        IF(ZA.LT.0.D0) WRITE(IO,900)
        IF(ZA.LT.0.D0) STOP
        IF(IOPT) 10,20,30
C
C       ----- series expansion for Ai(ZA)  (for 0.0 =< ZA < 3.0) -----
   10   P=ZA**3
        F=1.D0+P*( 1.666666666667D-01+P*( 5.555555555556D-03+
     1        P*( 7.716049382716D-05+P*( 5.845491956603D-07+
     2        P*( 2.783567598382D-09+P*( 9.096626138505D-12+
     3        P*( 2.165863366311D-14+P*( 3.923665518679D-17+
     4        P*( 5.589267120625D-20+P*( 6.424444966235D-23+
     5        P*( 6.083754702874D-26+P*( 4.828376748313D-29+
     6        P*( 3.258014000211D-32+P*( 1.891994192922D-35+
     7        P*(      1.D-10*COEF1+P*(      1.D-10*COEF2+
     8        P*(      1.D-10* COEF3))))))))))))))))))
        G=ZA*(1.D0+P*( 8.333333333333D-02+P*( 1.984126984127D-03+
     1             P*( 2.204585537919D-05+P*( 1.413195857640D-07+
     2             P*( 5.888316073501D-10+P*( 1.721729846053D-12+
     3             P*( 3.726687978470D-15+P*( 6.211146630783D-18+
     4             P*( 8.215802421670D-21+P*( 8.834196152333D-24+
     5             P*( 7.873615109032D-27+P*( 5.911122454228D-30+
     6             P*( 3.789181060403D-33+P*( 2.098106899448D-36+
     7             P*(      1.D-10*COEF4+P*(      1.D-10*COEF5+
     8             P*(      1.D-10*COEF6))))))))))))))))))
        AI=C1*F-C2*G
        U=A23*ZA**1.5D0
        AI=(ZA**0.25D0)*DEXP(U)*AI
        RETURN
C
C       ----- asymptotic expansion for Ai(ZA)  (for ZA > 5.0D0) -----
   20   ZK=A23*ZA**1.5D0
        P=1.D0/ZK
        A=1.D0+P*(-6.944444444444D-02+P*( 3.713348765432D-02+
     1        P*(-3.799305912780D-02+P*( 5.764919041267D-02+
     2        P*(-1.160990640255D-01+P*( 2.915913992307D-01+
     3        P*(-8.776669695100D-01+P*( 3.079453030173D+00+
     4        P*(-1.234157333235D+01+P*( 5.562278536591D+01+
     5        P*(-2.784650807776D+02+P*( 1.533169432013D+03+
     6        P*(-9.207206599726D+03)))))))))))))
        AI=A/PIRT2
        RETURN
C
C       ----- integral representation for Ai(ZA) (for 3.0 =< ZA =< 5.0) -----
   30   ZK = 2.0D0*(ZA**1.5D0)/3.0D0
        TMP = 70.D0/ZK
        IF(TMP.LE.1.0D0) THEN
        XL=20.0D0/ZK
        ELSE
        XL = DACOSH(TMP)
        ENDIF
C
        BA2 = XL/2.D0
        SUM = 0.D+0
        SUM1 = 0.D+0
C
        DO 35 I=1,NG
        Y =  BA2*(XG(I) + 1.0D0)
        Y1= -BA2*(XG(I) - 1.0D0)
        SUM = SUM + WG(I)*FN(Y)
        SUM1 = SUM1 + WG(I)*FN(Y1)
   35   CONTINUE
C
        SUM = BA2*(SUM+SUM1)
        AI = DEXP(ZK)*(ZA**0.75D0)*SUM/PISQR3
```

```
      RETURN
C
900   FORMAT (' *** WARNING *** SUBROUTINE AI(Z) WILL NOT EVALUATE A
     # NON-POSITIVE ARGUMENT OF AI(Z).')
      END
C
C*************************************************************************
C
C     SUBROUTINE LINV  --  FINDS THE STEHFEST WEIGHTING COEFFICIENTS
C
C*************************************************************************
      SUBROUTINE LINV(IA,IB,N,V,G,H)
      IMPLICIT DOUBLE PRECISION (A-H,O-Z)
      DIMENSION G(IA),V(IA),H(IB)
C
      G(1)=1.D0
      NH=N/2
      DO 10 I=2,N
      G(I)=G(I-1)*DBLE(I)
   10 CONTINUE
      H(1)=2.D0/G(NH-1)
C
      DO 20 I=2,NH
      FI=DBLE(I)
      IF(I.EQ.NH) GOTO 15
      H(I)=(FI**NH)*G(2*I)/(G(NH-I)*G(I)*G(I-1))
      GOTO 20
   15 H(I)=(FI**NH)*G(2*I)/(G(I)*G(I-1))
   20 CONTINUE
      ISN=2*(NH-(NH/2)*2)-1
C
      DO 25 I=1,N
      V(I)=0.D0
      K1=(I+1)/2
      K2=I
      IF(K2.GT.NH)K2=NH
      DO 40 K=K1,K2
      IF(2*K-I.EQ.0) GOTO 30
      IF(I.EQ.K) GOTO 35
      V(I)=V(I)+H(K)/(G(I-K)*G(2*K-I))
      GOTO 40
   30 V(I)=V(I)+H(K)/G(I-K)
      GOTO 40
   35 V(I)=V(I)+H(K)/G(2*K-I)
   40 CONTINUE
      V(I)=ISN*V(I)
      ISN=-ISN
   25 CONTINUE
      RETURN
      END
C
C*************************************************************************
C
C     SUBROUTINE INTRAC -- ALLOWS INTERACTIVE INPUT
C
C     (This subroutine and the calling statement in the main program
C     can be removed if interactive input is not required)
C*************************************************************************
C
      SUBROUTINE INTRAC(TITLE,IBC,N,R1,R2,D,B,N2,DM2,LAM,Q,NR,RO
     # ,R,DR,NZ,DZ,NT,T)
      IMPLICIT DOUBLE PRECISION (A-H,O-Z)
      DOUBLE PRECISION N2,LAM
      DIMENSION T(10)
      CHARACTER TITLE(3)*70
      COMMON IN,IT,IO,IL
C
  800 FORMAT(1X,A50,$)
  805 FORMAT(1X,A50)
      CALL VTPOSI
      DO 10 I=1,3
      WRITE(IT,805)' GIVE A LINE OF TITLE                                  '
   10 READ(IT,'(A)') TITLE(I)
      CALL VTPOSI
      WRITE(IT,805)' GIVE 0: for DECAYING BOUNDARY CONDITION               '
      WRITE(IT,800)' or   1: for CONSTANT CONCENTRATION BOUNDARY       ==> '
      READ(IT,*) IBC
      CALL VTPOSI
      WRITE(IT,800)' GIVE THE NUMBER OF WEIGHTING FACTORS (N]          ==> '
      READ(IT,*) N
      CALL VTPOSI
      WRITE(IT,800)' GIVE RETARDATION FACTOR [FRACTURE: R1]            ==> '
      READ(IT,*) R1
      CALL VTPOSI
      WRITE(IT,800)' GIVE RETARDATION FACTOR [POROUS MATRIX: R2]       ==> '
      READ(IT,*) R2
      CALL VTPOSI
      WRITE(IT,800)' GIVE DISPERSIVITY IN THE FRACTURE (d]             ==> '
      READ(IT,*) D
      CALL VTPOSI
      WRITE(IT,800)' GIVE HALF FRACTURE APERATURE DIMENSION (b]        ==> '
      READ(IT,*) B
      CALL VTPOSI
      WRITE(IT,805)' GIVE POROSITY OF POROUS MATRIX [n ]                   '
      WRITE(IT,800)'                                  2                ==> '
      READ(IT,*) N2
      CALL VTPOSI
      WRITE(IT,805)' GIVE DIFFUSION COEFFICIENT IN MATRIX (Dm ]            '
      WRITE(IT,800)'                                         2         ==> '
      READ(IT,*) DM2
      CALL VTPOSI
      WRITE(IT,800)' GIVE RADIOACTIVE DECAY CONSTANT [lambda]          ==> '
      READ(IT,*) LAM
      CALL VTPOSI
      WRITE(IT,800)' GIVE THE INJECTION RATE [Q]                       ==> '
      READ(IT,*) Q
      CALL VTPOSI
      WRITE(IT,805)' GIVE THE NUMBER OF RADII [NT], WELL RADIUS (RO),      '
      WRITE(IT,805)' START RADIUS [R] AND DISTANCE BETWEEN RADII (DR)      '
      WRITE(IT,800)'                                                   ==> '
      READ(IT,*) NR,RO,R,DR
      CALL VTPOSI
      WRITE(IT,805)' GIVE THE NUMBER OF TIMES THE CONCENTRATION            '
      WRITE(IT,800)' PROFILE IS TO BE CALCULATED [NT]                  ==> '
      READ(IT,*) NT
      CALL VTPOSI
      DO 15 I=1,NT
      CALL VTPOSI
      WRITE(IT,810) I
   15 READ(IT,*) T(I)
  810 FORMAT(1X,' GIVE THE ',I2,'th TIME [T(I)]',20X,'==> ',$)
      CALL VTPOSI
      WRITE(IT,805)' GIVE THE NUMBER OF VERTICAL POSITIONS WHERE A         '
      WRITE(IT,805)' POROUS MATRIX CONCENTRATION IS TO BE CALCULATED       '
      WRITE(IT,800)'                                                   ==> '
      READ(IT,*) NZ
      IF(NZ.EQ.0) RETURN
      WRITE(IT,800)' GIVE THE SPACING BETWEEN VERTICAL POSITIONS       ==> '
      READ(IT,*) DZ
      RETURN
      END
C
C
C*************************************************************************
C
C     SUBROUTINES VT*** -- VIDEO DRIVERS FOR VT-100 AND VT-52
C
C*************************************************************************
      SUBROUTINE VT100
      CHARACTER*1 ESC
      DATA ESC /#1B/
      WRITE(5,900) ESC
  900 FORMAT ('+',1A1,'<')
      RETURN
      END
C
      SUBROUTINE VT52
      CHARACTER*1 ESC
      DATA ESC /#1B/
      WRITE(5,900) ESC
  900 FORMAT ('+',1A1,'[?2l')
      RETURN
      END
C
      SUBROUTINE VTPOSI
      CHARACTER*1 ESC
      CHARACTER CMD1*5,CMD2*3
      DATA ESC /#1B/,ILINE/8/,ICOL/1/
      DATA CMD1 /'[1;1f'/,
     # CMD2 /'[2J'/
C
      WRITE(5,900) ESC,CMD1,ESC,CMD2
      WRITE(5,905)  ESC,ILINE,ICOL
      RETURN
C
      ENTRY VTPOS1
      WRITE(5,900) ESC,CMD1,ESC,CMD2
  900 FORMAT ('+',A,A,A,A,$)
  905 FORMAT ('$' A1,'[',I2.2,';',I3.3,'f')
      RETURN
      END
C
      SUBROUTINE VTWAIT
      CHARACTER*1 ESC
      CHARACTER CMD1*5,CMD2*3
      COMMON IN,IT,IO,IL
      DATA ESC /#1B/,ILINE/24/,ICOL/1/
      DATA CMD1 /'[1;1f'/,
     # CMD2 /'[2J'/
C
C     ----- if output device is the printer -----
      IF(IO.EQ.IT) GOTO 10
      WRITE(IO,900)
      RETURN
C
C     ----- if output device is the terminal -----
   10 WRITE(5,905)  ESC,ILINE,ICOL
      WRITE(IO,910)
      READ(IT,915) TMP
      WRITE(5,920) ESC,CMD1,ESC,CMD2
      RETURN
C
  900 FORMAT('1')
  905 FORMAT('$',A1,'[',I2.2,';',I3.3,'f')
  910 FORMAT('+ Type return to continue >>> ',$)
  915 FORMAT(G1.0)
  920 FORMAT('+',A,A,A,A,$)
      END
```

Appendix 2. Examples of Program Input and Output

```
     Example input data set

1
16 1.0 1.0 0.1 5.0E-5 .01 1.0E-3 .01 3.65
10 0.1 1.0 1.0
1  .01
5 .002
```

```
****************************************************************************
*                                                                          *
*                                                                          *
*       Example input data set                                             *
*                                                                          *
*                                                                          *
****************************************************************************

PROBLEM SPECIFICATIONS
======================

Vertical concentrations will be calculated
A constant boundary condition exists at the well
16 Stehfest weighting factors will be used to invert the Laplace transform
```

```
INPUT PARAMETERS
****************

Dispersivity of the fracture (L)........................ 1.000000E-01
Retardation coefficient for fracture walls (0).......... 1.000000E+00
Half width of fracture aperature (L).................... 5.000000E-05
Diffusion coefficient of porous matrix (L*L/T).......... 1.000000E-03
Retardation coefficient for porous matrix (0)........... 1.000000E+00
Porosity of the porous matrix (0)....................... 1.000000E-02
Radioactive decay constant (1/T)........................ 1.000000E-02
Constant injection rate (L*L*L/T)....................... 3.650000E+00


CALCULATED PARAMETERS
*********************

Advection parameter (A)................................. 5.809155E+03
Dimensionless radius of the well (RHOO)................. 1.000000E+00
Dimensionless distance between radii (DRHO)............. 1.000000E+01
Ratio of diffusive loss to injection (ALPHA)............ 8.298001E-03
Dimensionless radioactive decay constant (ALPHA1)....... 1.721421E-08
Dimensionless vertical spacing (DXI).................... 4.820438E+01


STEHFEST WEIGHTING FACTORS
**************************
```

I	V(I)	II	V(II)
1	-3.9682540E-04	9	-1.0525395E+09
2	2.1337302E+00	10	2.2590133E+09
3	-5.5101667E+02	11	-3.3997020E+09
4	3.3500161E+04	12	3.5824505E+09
5	-8.1266511E+05	13	-2.5914961E+09
6	1.0076184E+07	14	1.2270498E+09
7	-7.3241383E+07	15	-3.4273456E+08
8	3.3905963E+08	16	4.2841819E+07

```
CONCENTRATION DISTRIBUTION
**************************

Time =     1.00000E-02          Tau =     5.80916E+03
```

I	R	Z	C/Co
1	1.000	.0000	.9961
2	1.000	.0020	.6494
3	1.000	.0040	.3659
4	1.000	.0060	.1758
5	1.000	.0080	.0713
6	1.000	.0100	.0243
7	2.000	.0000	.9857
8	2.000	.0020	.6353
9	2.000	.0040	.3521
10	2.000	.0060	.1655
11	2.000	.0080	.0654
12	2.000	.0100	.0215
13	3.000	.0000	.9682
14	3.000	.0020	.6118
15	3.000	.0040	.3296
16	3.000	.0060	.1493
17	3.000	.0080	.0563
18	3.000	.0100	.0175
19	4.000	.0000	.9427
20	4.000	.0020	.5777
21	4.000	.0040	.2981
22	4.000	.0060	.1274
23	4.000	.0080	.0447
24	4.000	.0100	.0128
25	5.000	.0000	.9066
26	5.000	.0020	.5311
27	5.000	.0040	.2568
28	5.000	.0060	.1008
29	5.000	.0080	.0320
30	5.000	.0100	.0081
31	6.000	.0000	.8560
32	6.000	.0020	.4696
33	6.000	.0040	.2055
34	6.000	.0060	.0713
35	6.000	.0080	.0196
36	6.000	.0100	.0042
37	7.000	.0000	.7904
38	7.000	.0020	.3870
39	7.000	.0040	.1456
40	7.000	.0060	.0424
41	7.000	.0080	.0095
42	7.000	.0100	.0016
43	8.000	.0000	.6861
44	8.000	.0020	.2774
45	8.000	.0040	.0842
46	8.000	.0060	.0191
47	8.000	.0080	.0031
48	8.000	.0100	.0003
49	9.000	.0000	.5012
50	9.000	.0020	.1548
51	9.000	.0040	.0347
52	9.000	.0060	.0052
53	9.000	.0080	.0004
54	9.000	.0100	.0000
55	10.000	.0000	.2643
56	10.000	.0020	.0561
57	10.000	.0040	.0072
58	10.000	.0060	.0001
59	10.000	.0080	.0000
60	10.000	.0100	.0000

References

Abramowitz, M. and I. A. Stegun. 1970. Handbook of Mathematical Functions. Dover, New York. 1046 pp.

Barker, J. A. 1982. Laplace transform solutions for solute transport in fissured aquifers. Adv. Water Resour. v. 5, pp. 98-104.

Chen, C. S. 1986. Solutions for radionuclide transport from an injection well into a single fracture in a porous formation. Water Resour. Res. v. 22, no. 4, pp. 508-518.

Hodgkinson, D. P. and D. A. Lever. 1983. Interpretation of a field experiment on the transport of sorbed and nonabsorbed tracers through a fracture in crystalline rock. Radioact. Waste Manage., Nucl. Fuel Cycle. v. 4, no. 2, pp. 129-158.

Hsieh, P. 1986. A new formula for the analytical solution of the radial dispersion problem. Water Resour. Res. v. 22, no. 11, pp. 1597-1605.

Neretnieks, I. 1980. Diffusion in the rock matrix: an important factor in radionuclide retardation? J. Geophys. Res. v. 85, no. B8, pp. 4379-4397.

Neretnieks, I. and A. Rasmuson. 1984. An approach to modeling radio-nuclide migration in a medium with strongly varying velocity and block sizes along the flow path. Water Resour. Res. v. 20, no. 12, pp. 1823-1836.

Rasmuson, A. 1984. Migration of radionuclides in fissured rock: analytical solutions for the case of constant source strength. Water Resour. Res. v. 20, no. 10, pp. 1435-1442.

Rasmuson, A. and I. Neretnieks. 1981. Migration of radionuclides in fissured rock: the influence of micropore diffusion and longitudinal dispersion. J. Geophys. Res. v. 86, no. B5, pp. 3749-3758.

Stehfest, H. 1970a. Numerical inversion of Laplace transforms. Commun. ACM. v. 13, no. 1, pp. 47-49.

Stehfest, H. 1970b. Remark on algorithm 368, numerical inversion of Laplace transforms. Commun. ACM. v. 13, no. 10, p. 624.

Sudicky, E. A. and E. O. Frind. 1982. Contaminant transport in fractured porous media: analytical solutions for a system of parallel fractures. Water Resour. Res. v. 18, no. 6, pp. 1634-1642.

Tang, D. H., E. O. Frind, and E. A. Sudicky. 1981. Contaminant transport in fractured porous media: analytical soltuion for a single fracture. Water Resour. Res. v. 18, no. 3, pp. 555-564.

* * * * *

Chia-Shyun Chen is an Associate Professor of Hydrology in the Geoscience Department of New Mexico Institute of Mining and Technology. He did his M.S. and Ph.D. in the Agricultural Engineering Department of Colorado State University and Texas A & M University, respectively. Prior to joining academics, he worked in a consulting firm for three years working on numerical simulation of transport problems under field conditions. His research interest is mathematical modeling of transport phenomena in subsurface hydrology.

Scott R. Yates received his B.S. in Geology from the University of Wisconsin in 1980, M.S. in Hydrology from New Mexico Institute of Mining and Technology in 1982, and Ph.D. in Soil and Water Science from the University of Arizona in 1985. He is currently a Soil Scientist for the USDA/ARS at the U.S. Salinity Laboratory in Riverside, California. His research interests include soil physics, modeling the fate and transport of contaminants in variably saturated media, and geostatistics.

Regional Hydrology

Ground-Water Modeling: Applications[a]

by James W. Mercer and Charles R. Faust[b]

ABSTRACT

The numerical models used in ground-water studies are general computer programs that can be applied to a variety of hydrogeological conditions. These programs are based on approximations to the governing partial differential equations for ground-water flow and transport. To use these models requires an understanding of the physical problem and field data. Although program input data and output results are quantitative, the appropriate application of numerical models remains a partly subjective procedure. To use models, the hydrologist must assess the merits of alternative numerical methods, evaluate available data, estimate data where missing or absent, and interpret computed results. The review of previous model applications can provide valuable insight on how these tasks may be approached.

INTRODUCTION

The effective application of numerical models to field problems in ground-water hydrology is ironically a qualitative procedure. The hydrologist must first decide whether a numerical model is necessary for project objectives. If needed, he is then faced with the decision of which numerical method is best for his problem. Once a particular method or computer program is selected, he must assess the reliability of data that are needed to run the program and the quality of the data that will be used to verify computed results. Because available data are never as comprehensive as desired, he will probably have to fill in data gaps with estimated, interpolated, or extrapolated values. Although running the computer program is fairly straightforward, interpreting or analyzing the output can be very difficult. The computed results may not compare well with observed data. It is then necessary to adjust and refine input data and rerun the computer program until some satisfactory agreement is obtained. This refinement procedure is known as model calibration. A calibrated model may be used for future forecasting, but care must be taken to avoid unwarranted prediction.

The above discussion suggests that a successful model application requires a combination of experience with (1) hydrologic principles, (2) numerical methods, (3) the aquifer to be modeled, and (4) model use. Model use is the topic of this paper, fourth in this series. In the previous papers we (1) provided an overview of numerical modeling, (2) presented and discussed the partial-differential equations on which numerical models are based, and (3) reviewed commonly-used numerical methods. If we accept that model use is a subjective procedure, then one way to gain experience is to see how other problems have been approached using modeling techniques.

There are several good review articles on models used in ground-water studies. Prickett (1975) presents a review of the available literature on ground-water modeling. In addition to Prickett's work, Narasimhan and Witherspoon (1977) present an overview on ground-water modeling. Anderson (1979) summarizes the literature concerned with modeling solute transport while Mercer and Faust (1979) summarize the literature dealing with modeling heat transport. Because of these articles,

[a]This is the fourth in a series of papers on ground-water modeling.

[b]GeoTrans, Inc., P.O. Box 2550, Reston, Virginia 22090.

Discussion open until March 1, 1981.

we do not present a literature review. Instead, in this paper we consider, in detail, three examples. The first deals with ground-water flow in a glacial aquifer. The second application involves the analysis of a pollution problem. The final example illustrates the potential for using models to aid in data collection.

GROUND-WATER SUPPLY EXAMPLE

This particular example was chosen for discussion because it is typical of many applications (only limited data are available), and it provides a qualitative comparison of two alternative numerical methods. This application was first presented by Pinder and Bredehoeft (1968). It represents the use of a ground-water flow model to analyze an aquifer system composed of glaciofluvial deposits. It includes a history match with limited data and a prediction using a finite-difference model. This problem was later simulated by Pinder and Frind (1972) using a Galerkin, finite-element model. Based on this field application and numerical experiments, they present a discussion on the relative merits of both numerical techniques.

Problem

The village of Musquodoboit Harbour, Nova Scotia (location map is shown in Figure 1) depends entirely on domestic wells for a water supply. Unfortunately, bedrock wells are of poor quality, and shallow wells cannot meet demands during summer months. Field studies indicate a nearby, unconsolidated deposit containing good quality water. Can this deposit provide an adequate water supply for Musquodoboit Harbour?

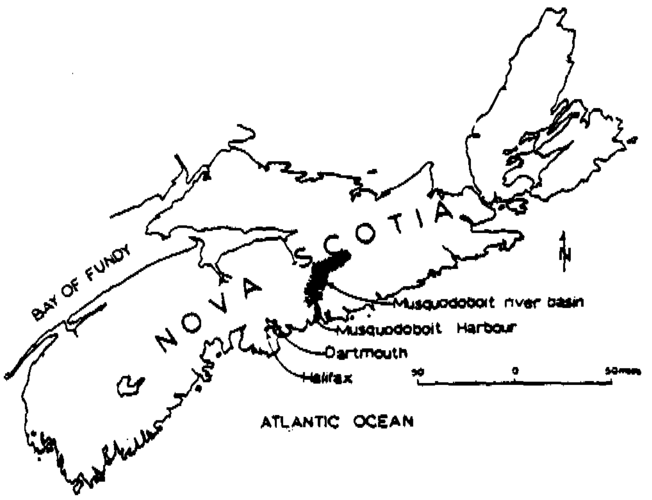

Fig. 1. Location map of the Musquodoboit River basin (from Pinder and Bredehoeft, 1968).

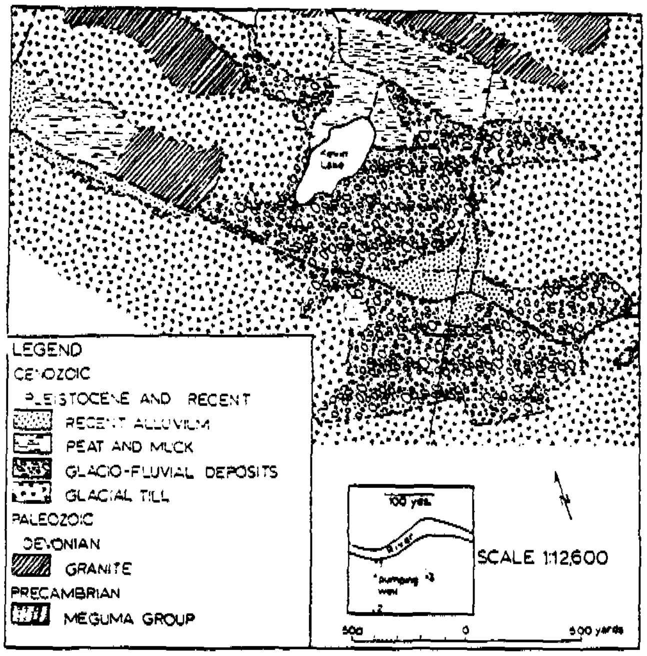

Fig. 2. Geologic map of Musquodoboit Harbour, Nova Scotia. Inset is the well configuration for the pump test conducted on this aquifer (numbered wells are observation wells) (from Pinder and Bredehoeft, 1968).

Hydrogeology

According to Pinder and Frind, the aquifer is adjacent to the Musquodoboit River ¼-mile northwest of the village of Musquodoboit Harbour (see the geologic map in Figure 2). The aquifer is a glaciofluvial deposit consisting of coarse sand, gravel, cobbles, and boulders deposited in a typical U-shaped glacial valley cut into the slates and quartzites of the Meguma group and granite intrusives of Devonian age. The contrast in permeability between the granitic and metamorphic rocks and the glaciofluvial valley fill is so great (approximately 10^6) that the bedrock is considered as impermeable in the aquifer analysis. The aquifer, which is up to 62 feet thick, is extensively overlain by recent alluvial deposits of sand, silt, and clay. The alluvial deposits are less permeable and act as confining beds. A cross section through the valley is given in Figure 3.

Aquifer Analysis

A pumping test was conducted to evaluate the aquifer transmissivity and storage coefficient, and to estimate recharge from the river. The test was run for 36 hours using a well discharging at 0.963 cubic feet per second (432 gallons per minute) and three observation wells (see insert of Figure 2 for locations). The test was discontinued when the water level in the pumping well became stable.

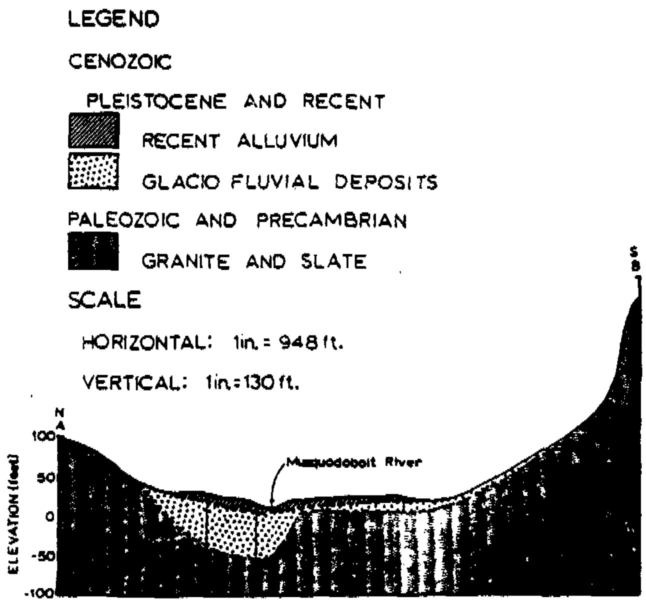

Fig. 3. Geologic cross section, Musquodoboit Harbour area, Nova Scotia (from Pinder and Bredehoeft, 1968).

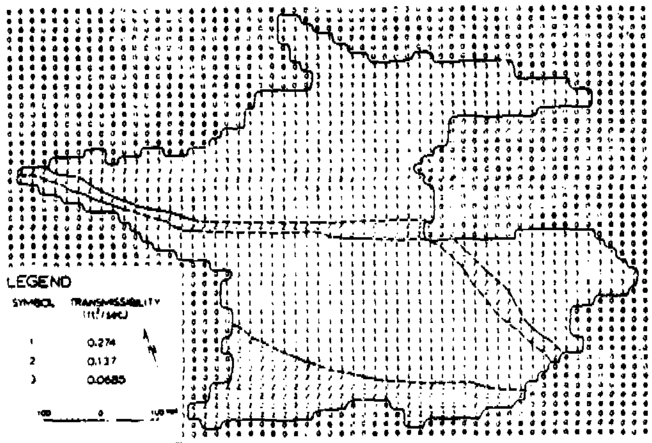

Fig. 5. Finite-difference grid showing the modified transmissivity matrix adjusted on the basis of three additional test well logs and digital model results (from Pinder and Bredehoeft, 1968).

Initial estimates of aquifer parameters were calculated using the Theis curve and the early segment of the drawdown curves for the observation wells. Results are shown in Figure 4. The values are somewhat variable, and because of the close proximity of boundaries, the pumping-test results are difficult to analyze using standard analytical methods.

Although not included in the original report, the late time data may also be analyzed using Jacob's method for distance drawdown data (Jacob, 1950). The transmissivity calculated by this method is 0.288 ft^2/s, which is about five times smaller than the values determined from the early time data.

Aquifer Model

The boundary used in the model is the contact between the valley-fill deposits and the bedrock.

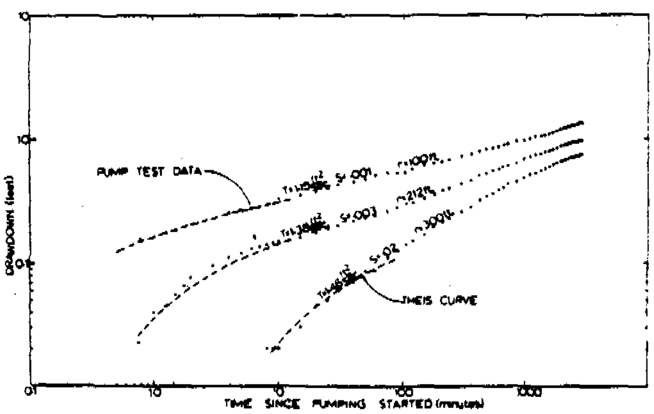

Fig. 4. Time-drawdown curves for a pump test conducted at the Musquodoboit Harbour aquifer (from Pinder and Bredehoeft, 1968).

Because of the very low permeability of the bedrock, the boundary condition is considered no-flow. A uniform 45 by 57 rectangular grid was used by Pinder and Bredehoeft, and is shown in Figure 5. Note that approximately half the nodes are outside the aquifer area and are not included in the calculation. The aquifer is considered to be confined; however, steady-state leakage is allowed through the river bottom.

According to Pinder and Frind, this grid could be redesigned with approximately 25% of the nodes by introducing a variable grid. Furthermore, a model based on Galerkin's approximation in conjunction with deformed isoparametric quadrilaterals was used to examine this problem and contained 96 nodes and 44 elements (see Figure 6). The flexibility introduced through the use of irregular elements is apparent in the definition of the impermeable boundaries and the river. Often, however, the subsurface geometry is not that well known. The shape and distribution of the internal elements demonstrate how an understanding of the hydrologic system can guide the hydrologist in the selection of an efficient nodal arrangement. On the other hand, a poorly designed model may be inefficient and may provide inaccurate results.

History Match

The history match consisted of reproducing the pump-test results. An initial estimate of transmissivity was made based on the pump-test analysis and the geologic information. Approximately 37 computer runs were made with the finite-difference model, varying aquifer parameters until a satisfactory match was obtained.

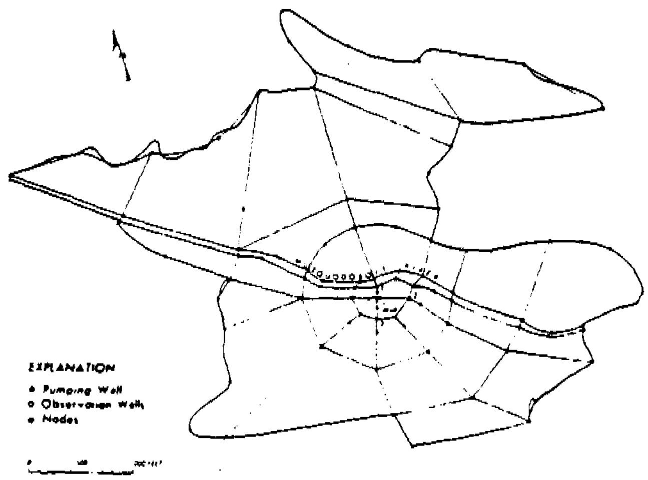

Fig. 6. Element configuration for Galerkin analysis of Musquodoboit Harbour aquifer (from Pinder and Frind, 1972).

The final transmissivity distribution used in the model is shown in Figure 5. Using the same data, the problem was again simulated with the finite-element model. A comparison of finite-difference and finite-element drawdowns is shown in Figure 7. These may be compared with the observed drawdowns in Figure 4. Note that by using drawdowns, the initial conditions for this linear problem are simply initial drawdown is equal to zero everywhere.

According to Pinder and Bredehoeft,

"A decrease in transmissibility results in a greater drawdown after a given period of pumping. The storage coefficient affects the shape of the time-drawdown curve before equilibrium is reached in the aquifer system. The most pronounced effect of an increase in the storage coefficient was a decrease in the drawdown during the early periods of pumping. Steady-flow conditions in the aquifer depend upon the quantity of water entering the system through the river bed. The closest approximation to the pump test results was obtained using a permeability value (for the confining material) of 0.00002 feet/sec for 10-foot thickness of river bottom. The shape of the time-drawdown curve was changed markedly by adjusting this value as little as 0.000005 feet/sec."

The aquifer is not confined everywhere and, in parts, behaves as a water-table aquifer. Although the saturated thickness does not change much with time because the drawdown is small, the storage coefficient is time-dependent due to drainage of the aquifer system. To account for this the following crude approximation was made. The initial value for the storage coefficient of 0.003 was allowed to increase linearly with time to a maximum of 0.06 after 10 minutes, over the entire aquifer.

Prediction

The areal head distribution in the aquifer after 206.65 days of pumping at a rate of 0.963 cfs is shown in Figure 8. Because of the aquifer's high transmissivity, a rapidly expanding, flat cone of depression develops. The influence of the Musquodoboit River is observed within a minute after pumping begins, and after 300 minutes the drawdown at the closest impermeable boundary is greater than 0.1 feet.

The drawdown for long pumping periods was computed for the three observation wells used in the pumping test (Figure 9). It is interesting to note that the steeply rising time-drawdown curve levels off rapidly after approximately 273 days of pumping, and has essentially attained steady state after 5,000 days. Based on this study, it was concluded that the aquifer could easily supply the village of Musquodoboit Harbour indefinitely at a rate of 0.963 cfs (approximately 0.6 mgd). This quantity of water was more than adequate to supply the village needs for the immediate future.

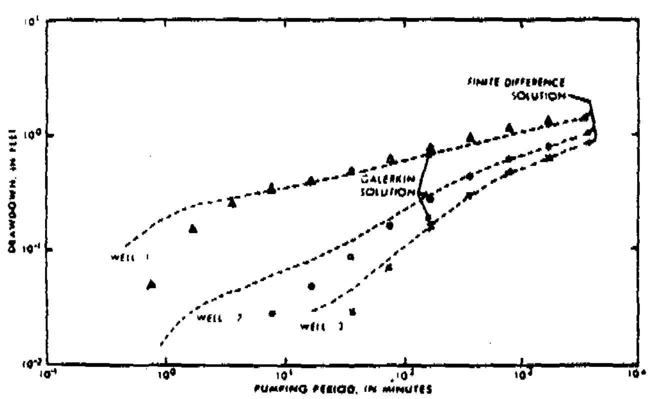

Fig. 7. Comparison of finite-difference and Galerkin solution at Musquodoboit Harbour (from Pinder and Frind, 1972).

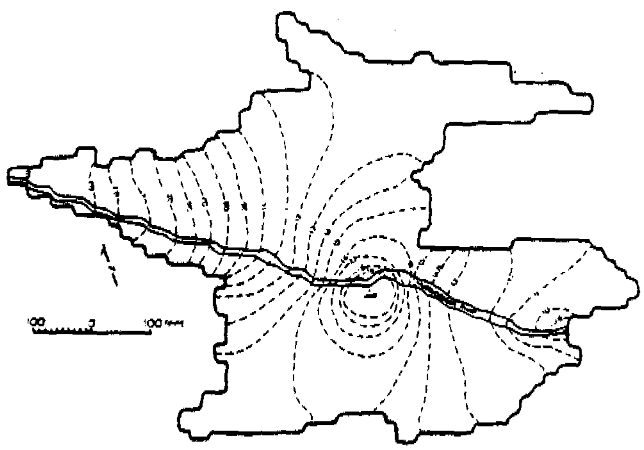

Fig. 8. Potentiometric surface determined from the digital model after 206.65 days of pumping at a rate of 0.963 cfs (from Pinder and Bredehoeft, 1968).

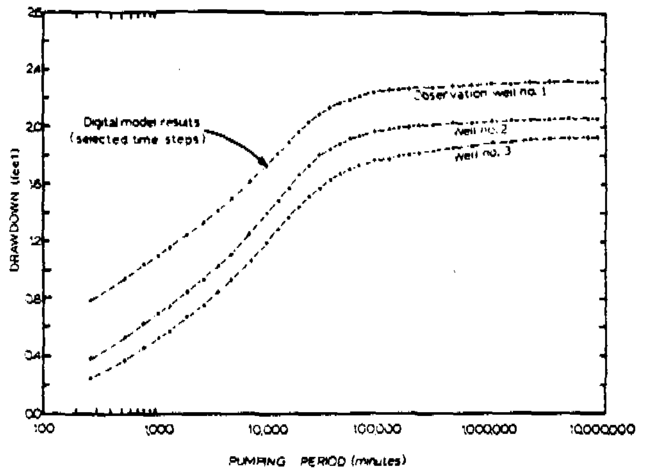

Fig. 9. Time-drawdown curves obtained from the digital model (from Pinder and Bredehoeft, 1968).

Discussion

In the Musquodoboit example, the subjective aspects of model application are evident. The first task was to determine if a numerical model was necessary. Pumping-test data suggested that because of boundary effects, analytical techniques may not be adequate. The authors, therefore, decided to use a numerical model, and performed the necessary developmental work.

Evaluation of available data involved reducing information from geologic reports to a form usable in the model (that is, boundary conditions, aquifer thickness, etc.). The pumping-test data were also analyzed to provide estimates of transmissivity and storage coefficient. These values were refined via model calibration. This took 37 runs and necessitated the assumption of an arbitrary time-dependent change in the storage coefficient.

It is interesting that the final transmissivity value in the vicinity of the pumping well (see Figure 5) was close to the value calculated using Jacob's method for the late time data. Although effort was spent to match early time data, the arbitrary time-dependent storage coefficient probably had little effect on the predictive results because after 10 minutes of pumping a constant value was used. The predictive results are more limited by the lack of data for both later times and greater distances from the pumping well.

In addition to making predictions, this application considered two different types of models. Conclusions regarding the relative merits of the two numerical methods are provided by Pinder and Frind as:

1. "The analysis of the aquifer at Musquodoboit Harbour indicates that a carefully designed model using deformed elements may provide the same accuracy as a finite difference model that used many more nodes."

The relative cost, however, will depend mainly on the matrix solution technique used for each method.

2. "The theoretical development of the Galerkin method of approximation is possibly more abstract than finite difference theory and the development of an efficient computer code for the Galerkin procedure is a formidable task."

3. "Experience has shown that errors in the input of nodal locations in the Galerkin model can lead to problems that are difficult to detect. This problem does not arise in the finite difference model because the entire grid is specified by the spacing between rows and columns."

4. "In the final analysis the primary advantage of the Galerkin approach to digital modeling of aquifer systems is its flexibility in application."

GROUND-WATER POLLUTION EXAMPLE

Konikow (1977) presents a good example of a solute-transport model applied to a chemical pollution problem at the Rocky Mountain Arsenal, near Denver, Colorado. The model couples a finite-difference solution to the ground-water flow equation with the method-of-characteristics solution to the solute-transport equation.

Problem

Liquid waste by-products from the manufacturing of chemicals for warfare and pesticides were disposed into unlined ponds from 1943-1956. The wastes contained chloride concentrations of several thousand mg/l. In 1954, severe crop damage occurred to fields irrigated with ground water along the South Platte River. This prompted the construction of an asphalt-lined evaporation pond. The purpose of this study was to demonstrate the application of a numerical solute-transport model to a complex field problem involving contaminant movement in an alluvial aquifer.

Hydrogeology

The location of the study area is shown in Figure 10, and the major hydrologic features are presented in Figure 11. The records of about 200 observation points were used to determine the hydrogeologic characteristics of the alluvial aquifer, including saturated thickness and transmissivity of the aquifer. Observed chloride concentration for 1956 is shown in Figure 12 and a water-table configuration is given in Figure 13. The major features to be noted are the areas where the alluvium is absent or unsaturated most

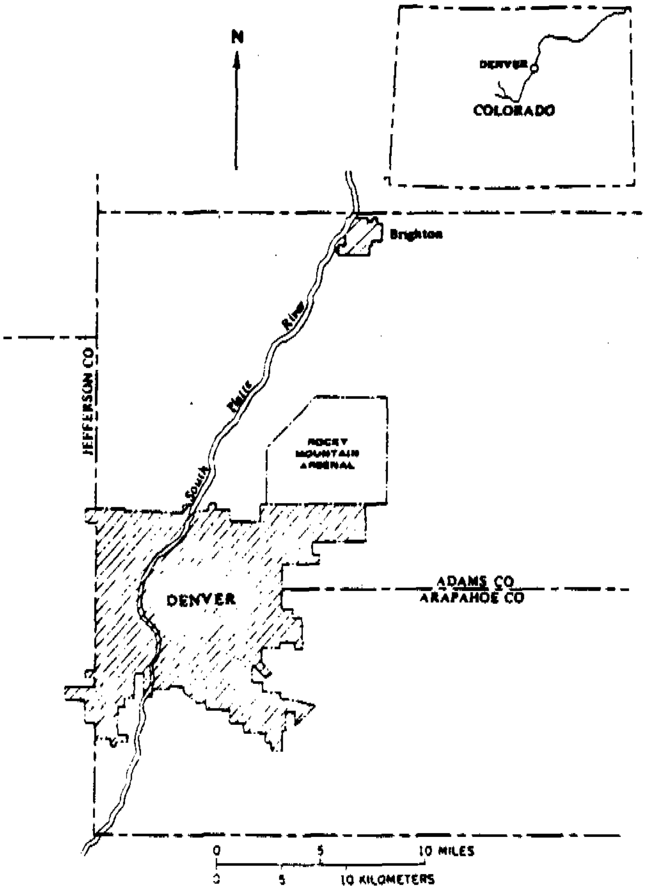

Fig. 10. Location of study area (from Konikow, 1977).

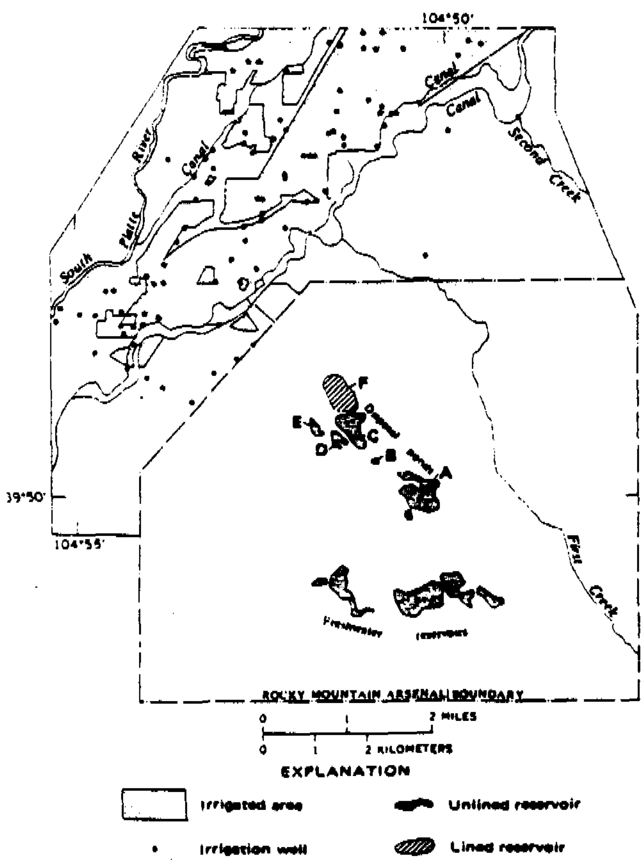

Fig. 11. Major hydrologic features. Letters indicate disposal-pond designations assigned by the U.S. Army (from Konikow, 1977).

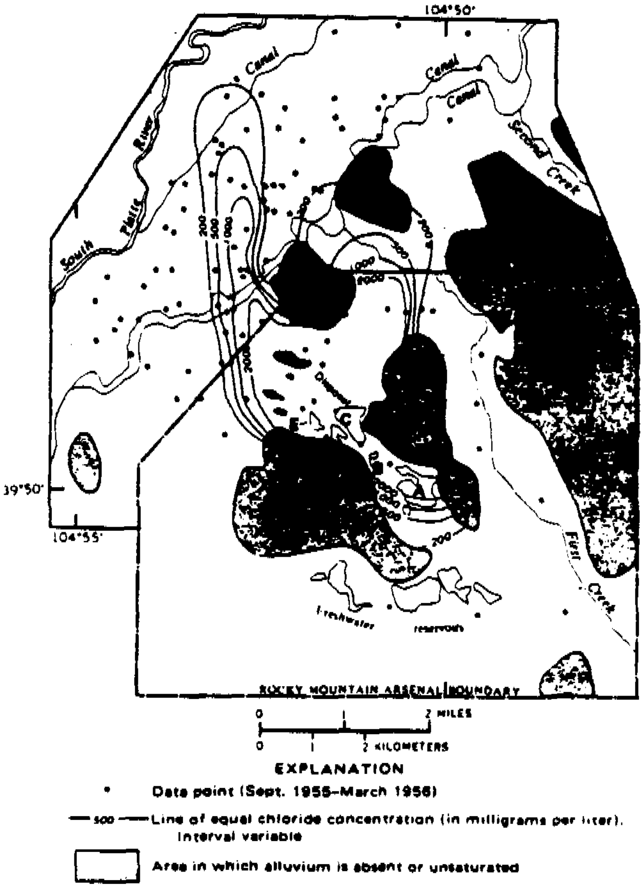

Fig. 12. Observed chloride concentration, 1956 (from Konikow, 1977).

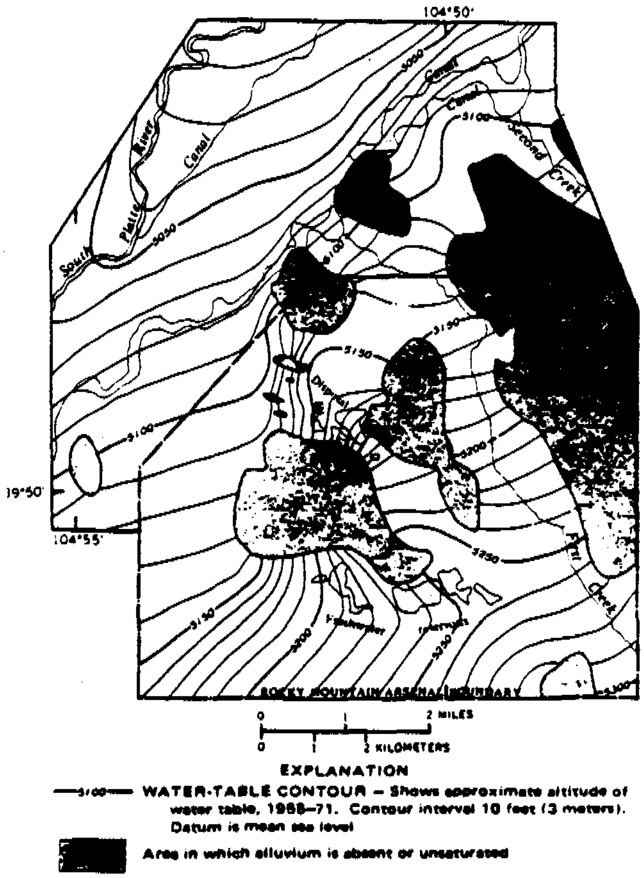

Fig. 13. General water-table configuration in the alluvial aquifer in and adjacent to the Rocky Mountain Arsenal, 1955-71 (from Konikow, 1977).

of the time. Bedrock below the alluvium is considered impermeable for the purposes of the model analysis.

Aquifer Analysis

The transmissivity of the alluvial aquifer in this area ranged from 0 to over 200,000 ft²/d (over 1,800 m²/d), and the saturated thickness was generally less than 60 feet (18 m). No field data were available for effective porosity and dispersivity of the aquifer. These were determined by trial and evaluated through a sensitivity analysis.

Aquifer Model

Konikow states:

> "The limits of the modeled area were selected to include the entire area having chloride concentrations over 200 mg/l and the areas downgradient to which the contaminants would likely spread, and to closely coincide with natural boundaries and divides in the ground-water flow system. The model includes an area of approximately 34 mi² (88 km²)."

The modeled area was subdivided into a finite-difference grid of blocks 1,000 feet (305 m) on a side (see Figure 14). The grid is 25 columns by 38 rows, but because of the boundaries, only 516 nodes are actually used to compute heads. The boundary conditions for flow are indicated in Figure 14. Constant-head boundaries were specified where it was believed that either recharge or underflow into or out of the modeled area was sufficient to maintain a nearly constant water-table altitude at that point in the aquifer. Leakage was allowed from the canal.

No data were available to describe the chloride concentrations in the aquifer when the Arsenal began its operations. Because more recent measurements indicated that the normal background concentration may be as low as 40 mg/l, an initial chloride concentration of 40 mg/l was assumed to have existed uniformly throughout the aquifer in 1942.

Recharge and discharge into and out of the aquifer had to be estimated. Recharge from the disposal ponds varied from 0 to 1.08 ft³/s with concentrations that ranged up to 4,000 mg/l (but were reduced significantly after 1956). The ponds were treated as constant-head nodes.

History Match

Insufficient field data were available to accurately calibrate a transient-flow model. Therefore, the hydraulic history of the aquifer

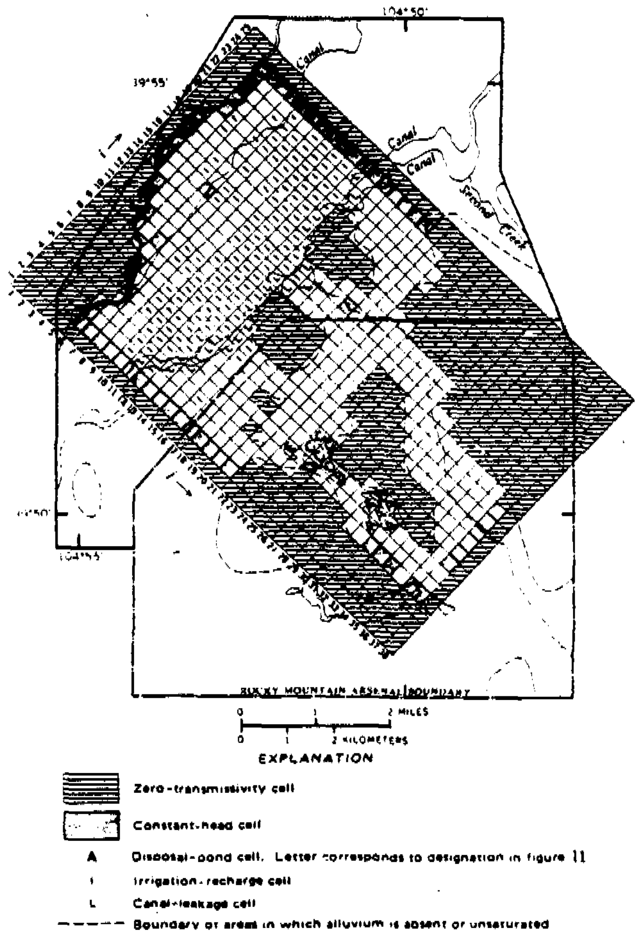

Fig. 14. Finite-difference grid used to model the study area (from Konikow, 1977).

was approximated by simulating four separate steady-flow periods which differed on the basis of the disposal pond operations. The computed chloride concentration at the end of one of the periods, 1956, is given in Figure 15. This compares well with that observed given in Figure 12. A comparison of observed and computed chloride concentration patterns indicated that an effective porosity of 30 percent and longitudinal and transverse dispersivities of 100 feet (30 m) were best.

The problem was simulated for a 30-year period, 1943 to 1972, and numerous comparisons of chloride distributions are given in the original reference.

Prediction

During the history-match portion of this study, leakage from pond C was found to be relatively important in flushing pollution out of the aquifer. To further assess this leakage, two simulations were made over the time period 1972-1980. In the first simulation, pond C was represented as full of fresh water; the computed chloride concentrations for this case are shown in Figure 16. For the second simulation, recharge of fresh water from pond C was kept to a minimum; the computed chloride concentrations for this case are shown in Figure 17. With artificial recharge, only one small area north of the Arsenal would contain chloride concentrations between 200 and 500 mg/l; for the second case, there are two relatively large areas of contamination.

Possible changes in water management in the area were also considered. These might, for example, involve maintaining withdrawal wells along parts of the northern boundary to intercept the contaminated ground water. To demonstrate the value of a solute-transport model as a planning tool, two sinks were incorporated into the model and their steady-state effects on the chloride concentrations were evaluated. Assuming the wells begin operating in 1968 and that pond C remains full after 1968 results in the computed chloride concentrations in Figure 18. Intercept wells would only slightly increase the rate of water-quality improvement between 1968 and 1980 in the area between the source and the sinks. Also

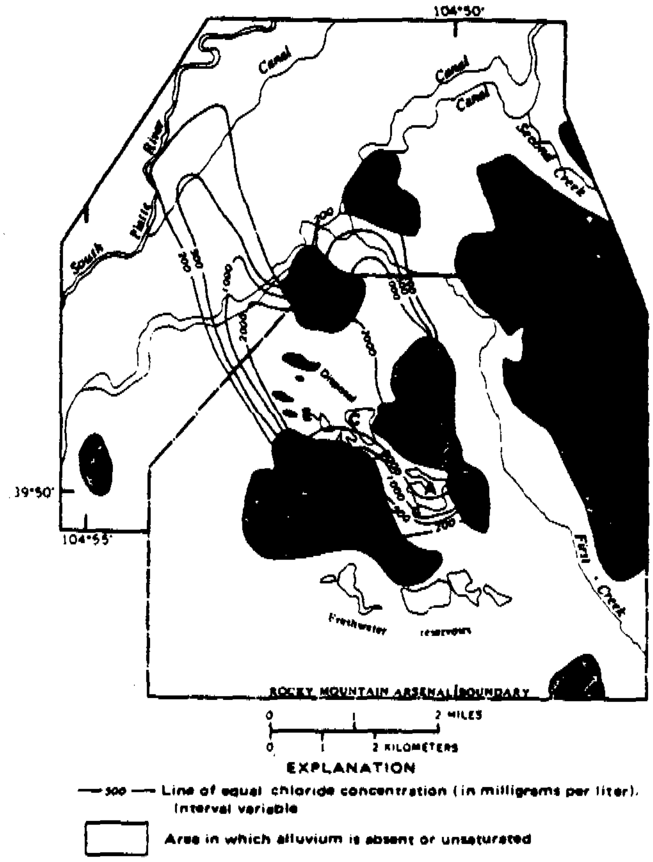

Fig. 15. Computed chloride concentration, 1956 (from Konikow, 1977).

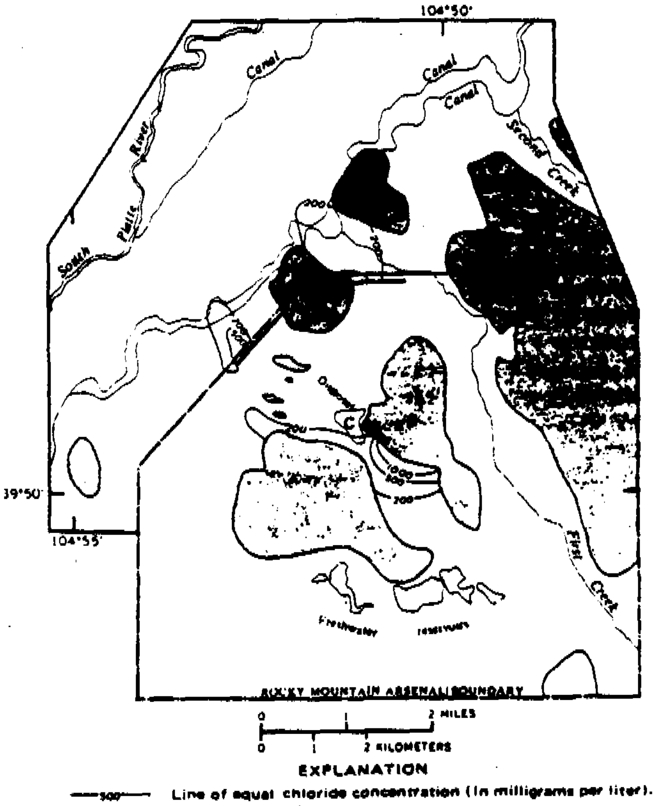

Fig. 16. Chloride concentration predicted for 1980, assuming that pond C is filled with fresh water during 1972-80 (from Konikow, 1977).

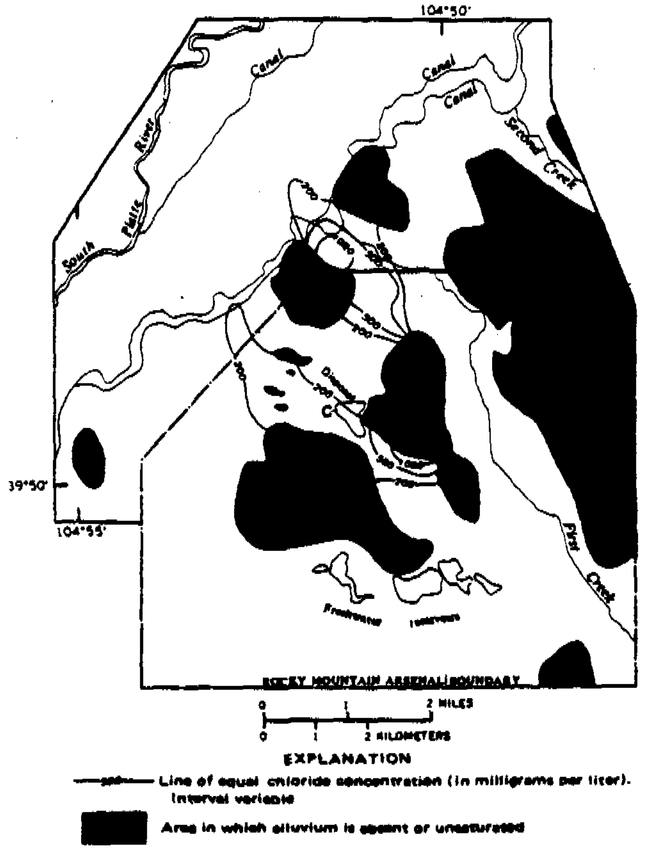

Fig. 17. Chloride concentration predicted for 1980, assuming that recharge from pond C is minimal during 1961-80 (from Konikow, 1977).

note that the intercept wells should be placed further downgradient to effect a more thorough cleanup.

According to Konikow,

"Analysis of the simulation results indicates that the geologic framework of the area markedly restricted the transport and dispersion of dissolved chemicals in the alluvium. Dilution, from irrigation recharge and seepage from unlined canals, was an important factor in reducing the level of chloride concentrations downgradient from the Arsenal. Similarly, recharge of uncontaminated water from the unlined ponds since 1956 has helped to dilute and flush the contaminated ground water."

Discussion

As with the example for Musquodoboit Harbour, the Rocky Mountain Arsenal example illustrates the presence of some subjective aspects in model applications. In addition, this example shows the additional complexity typical of solute transport problems. The additional complexity leads to some practical considerations: (1) input data determination, preparation, and evaluation are more difficult; (2) some data are likely to be missing for both model and input and for history

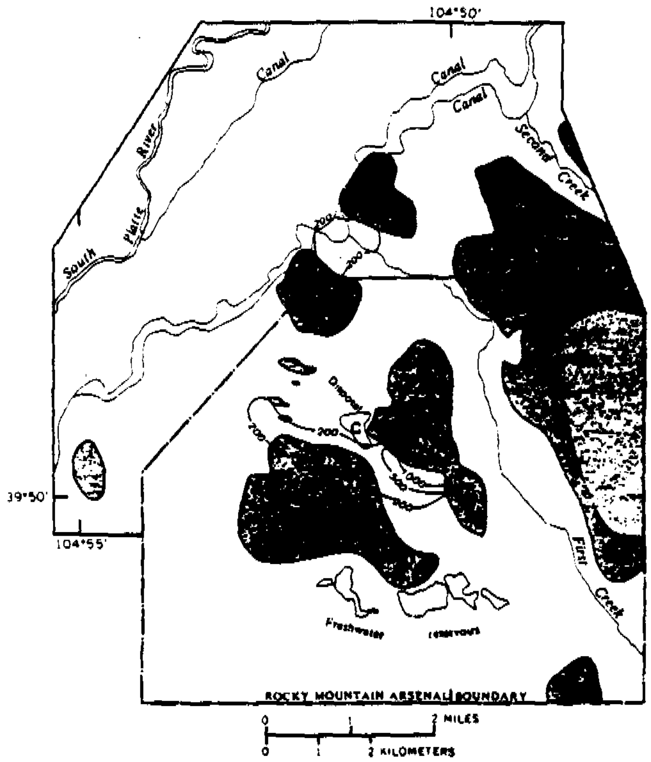

EXPLANATION

—500— Line of equal chloride concentration (in milligrams per liter). Interval variable

Area in which alluvium is absent or unsaturated

Fig. 18. Chloride concentration predicted for 1980, assuming that artificial recharge from pond C is coupled with drainage through two hydraulic sinks (from Konikow, 1977).

matching; and (3) some assumptions based on qualitative arguments are necessary.

In this example, additional data were needed for dispersion coefficients, effective porosity, initial and observed concentrations, and recharge from the disposal ponds and from irrigation. Insufficient data made calibration of transient ground-water flow not possible, so four steady-state flow periods were assumed. Comparisons with observed and computed chloride concentrations were made to determine the "best fit" values of dispersion coefficients and porosity.

Konikow also concluded that the stringent data requirements for applying the solute-transport model pointed out deficiencies in data existing at the start of the investigation. The subsequent analysis and reinterpretation of hydrogeologic and chemical data led to a revised and improved conceptual model of flow and contaminant transport in the alluvium.

The conclusions and predictions based on model results, though quantitatively nonunique, provided a great deal of qualitative insight into reclamation alternatives. In this particular situation, the relative merits of the various proposed remedial measures would have been extremely difficult to assess without the use of a model (also see Warner, 1979).

DATA-COLLECTION DESIGN EXAMPLE

In practice, models have been applied generally to field problems after data have been collected. However, models also can be used to help in data collection. In this example, we consider the use of a model to help design two-well tracer tests in a relatively porous limestone. Results from the tracer tests will be used to determine field dispersivity values for subsequent solute transport studies.

Problem

Denmark is presently undertaking a drilling program to evaluate the potential for storage of radioactive waste in salt domes. In particular, the focus is on data collection in order to more fully evaluate the geology and safety of such storage for two potential dome sites. The hydrological data collected at the sites will play a major role in the final evaluation.

As part of this study, a need for the field dispersivities that characterize the carbonate strata overlying the salt domes was identified. To determine these values, a conventional two-well tracer test will be used. This test involves injecting water containing a nonreacting tracer in one well while withdrawing water from the second well, both having the same constant volumetric flow rate. The tracer concentration is measured in the withdrawal well as a function of time. This data can be analyzed to determine dispersivity values.

Because little data are available on the hydrologic properties at these sites, several questions were raised about the test design. Among the most important were:

1. What range of pumping rates is necessary?
2. What range of well spacing is adequate?
3. How long should the test take? and
4. Are three-dimensional effects important?

Hydrogeology

Other than a generalized stratigraphy, little of the hydrology of the test site is known, especially for the deeper units. In descending order, the units consist of: (1) an upper aquifer system of Quaternary and Miocene age composed of clay, till, sand and gravel, totalling about 200 m in thickness; (2) Tertiary clays having a low permeability and a thickness ranging from 200 to 400 m; (3) a lower aquifer system consisting of Paleocene and Cretaceous limestone and chalks with a thickness ranging between 200 and 500 m; and (4) a Precretaceous cap rock for the salt dome, having a low permeability. Based on this description, the lower aquifer system is considered to be confined, with fluid pressures slightly in excess of hydrostatic.

Analysis

To help answer the design questions discussed earlier, two models were used. The first model is an analytical solution for quasi-steady-state flow between a recharging-discharging well pair for partially penetrating wells in three dimensions (Hantush, 1961). The second model is based on finite-difference approximations to the ground-water flow and solute transport equations in three dimensions (INTERCOMP, 1976).

In order to use either of these models, it is necessary to estimate probable ranges of pertinent hydrologic parameters. Based on values obtained at other locations for units similar to the lower limestone aquifer system, the ranges in Table 1 are assumed. The well field consists of two wells with equal open intervals at the top of the aquifer (assumed to be 200 meters thick). Major design variables include injection flow rate,

Table 1.

Parameter or Design Variable	*Range*
hydraulic conductivity	1.0×10^{-4}-1.0×10^{-6} m/s
porosity	0.08-0.32
horizontal to vertical anistropy	100.0-1.0
longitudinal dispersivity	5.0-40.0 m
injection flow rate	1.61×10^{-3}-1.61×10^{-2} m^3/s
length of open interval	10-20 m
well spacing	20-40 m

length of the open interval and well spacing, which are also included in Table 1.

With the major hydrologic and design parameters estimated, a sensitivity analysis was performed, which involved both models. The main purpose of the analytical model was to estimate the length of time to run the test. In a standard tracer test, three injection periods occur: (1) injection at a constant flow rate with no tracer until quasi-steady state is achieved between the two wells, (2) continued injection at the same flow rate, but now introducing the tracer—the *slug period*, and (3) continued injection, now with the tracer eliminated. This procedure produces a concentration breakthrough curve at the withdrawal well that looks like an asymmetrical bell (see Figure 19). The shape of this curve is used to estimate dispersivity. In designing a tracer test, a common practice is to end the slug period when the tracer is first encountered in the withdrawal well. The analytical solution provides an estimate of when this occurs, if dispersion is neglected. The analytical results show that for a horizontal to vertical anisotropy ratio of 100 or

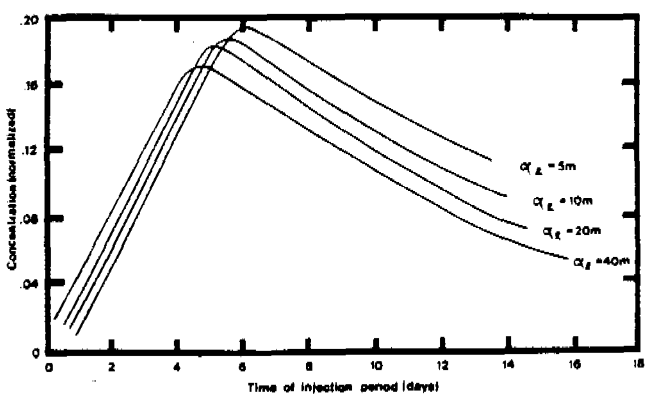

Fig. 19. Concentration breakthrough curves for the two-well tracer test at the withdrawal well, for different values of longitudinal dispersivity, α_ℓ. Transverse dispersivities are one-tenth as large as the longitudinal values for each case. Other data include: slug period, 4.63 days; porosity, 0.2; hydraulic conductivity, 1.0×10^{-5} m/s; well spacing, 40 m; open interval, 20 m; and pumping rate, 1.61×10^{-2} m^3/s.

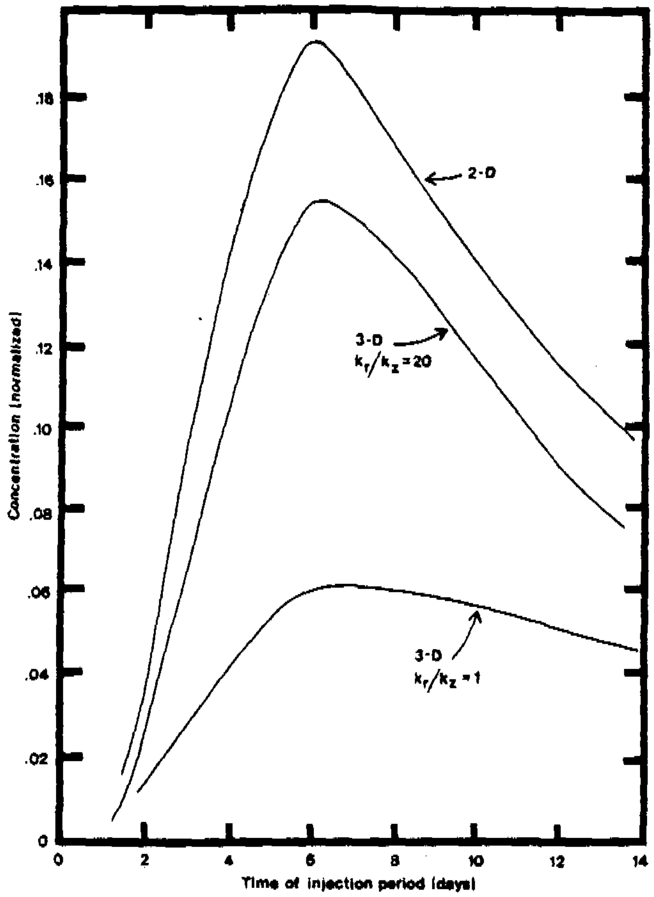

Fig. 20. Concentration breakthrough curves for different ratios of horizontal to vertical hydraulic conductivity, k_r/k_z. Longitudinal dispersion is 10 m; aquifer thickness is 140 m; all other data are the same as that given in Figure 19. Note that the three-dimensional results for partially penetrating wells approach the two-dimensional results as the anisotropy ratio increases.

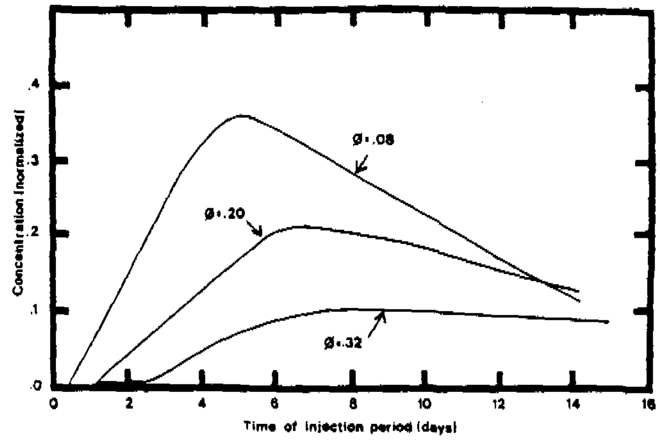

Fig. 21. Concentration breakthrough curves for different values of porosity, ϕ. Longitudinal dispersivity is 10 m; all other data are the same as that given for Figure 19.

larger, three-dimensional effects are not significant (see Figure 20). For isotropic conditions, results show the slug period is generally twice as long as for the corresponding anisotropic case.

In addition to providing the duration of the slug period, the analytical solution also determines the injection (and pumping) rate for the solute transport model. The injection rate was calculated assuming a head difference between wells of 160 m. If the injection rate required to sustain this difference exceeded 0.0161 m^3/s (about 360,000 gpd), then 0.0161 m^3/s was still used. With these data and injection constraints, sensitivity analysis using a two-dimensional, areal transport model was performed to assess the influence of porosity, dispersivity, and well spacing. To evaluate the importance of three-dimensional effects, a three-dimensional transport model was used in conjunction with different ratios of anisotropy. Some results from the sensitivity analysis are shown in Figures 19 through 22.

Discussion

In this final example, models are used before data are collected to provide insight into system behavior. The relative importance of the various hydrologic and design parameters were assessed and used to guide data collection. Conclusions (somewhat oversimplified here) of this study include: (1) For a given well spacing and head differential in the wells, the duration of the test will be related inversely to hydraulic conductivity and directly to porosity; (2) The major design criteria affecting the duration of the test are well spacing and head differential between the wells, which are related directly and inversely to the duration of the test; (3) Based on the range of possible hydrologic data and design criteria for the site, a single injection test may require from less than one month to two years to obtain sufficient

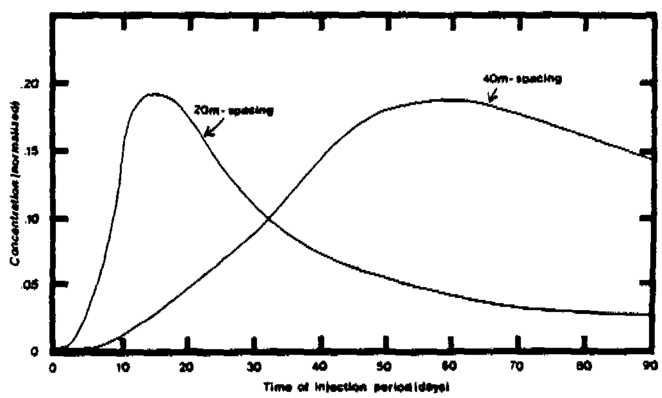

Fig. 22. Concentration breakthrough curves for two well spacings. Slug periods were 10.4 and 46.3 days with pumping rates of 1.80×10^{-3} and 1.61×10^{-3} m/s for spacings of 20 and 40 m, respectively. Other data include: hydraulic conductivity, 1.0×10^{-6} m/s; porosity, 0.2; open interval, 20 m; and anisotropy ratio, 100.

information about the system; (4) If the hydraulic conductivity of the aquifer is low, a small well spacing will be required in order to conduct the test in a reasonable amount of time; (5) The time required to reach a quasi-steady flow between wells will be short in comparison to the duration of the test; (6) Tests can be designed for a moderate injection rate of less than 1,500 m^3/day; and (7) Analysis of the field-test data can use a two-dimensional model if the anisotropy ratio is greater than 100; otherwise a three-dimensional model may be required.

Consideration of the model results led to recommendations, that are not presented in this article, on both test design and well drilling. As an example, it was recommended that single-well flow tests be performed on the first well before drilling the second. The resulting information would be useful in selecting appropriate well spacing for the next well.

This type of sensitivity analysis employing models may be used for other data collection programs. For example, model results could be used to guide the placement of monitor wells to help insure their success in detecting the possible movement of contaminants from disposal sites.

SUMMARY

The effective application of ground-water flow models involves several interrelated areas: model selection (need), computer program use, sensitivity analysis, system conceptualization, data collection design, history matching — calibration and prediction. The use of models cannot be considered a step-by-step procedure. Actually, it is an iterative process to which one never achieves a fully satisfactory conclusion. The reason for this is that when dealing with real systems, a model is never exact and complete data are never available. Consequently, considerable scientific judgement of a subjective or intuitive nature is necessary for any degree of success. For transport problems, the need for subjective judgement is greater than with ground-water flow.

ACKNOWLEDGMENTS

This effort was supported by the Holcomb Research Institute, Butler University, which is, in part, supported by EPA grant R-803713. The authors also wish to acknowledge the National Water Well Association's contribution for drafting, editing and publication. The authors wish to thank ELSAM, Denmark for granting permission to discuss the data-collection design example. We also appreciate the critical review provided by Lenny Konikow.

REFERENCES

Anderson, M. P. 1979. Using models to simulate the movement of contaminants through ground-water flow systems. Critical Reviews in Environmental Control. v. 9, issue 2, pp. 97-156.

Hantush, M. S. 1961. Drawdown around a partially penetrating well. Proc. Am. Soc. Civil Engrs. 87, HY4, pp. 83-98.

INTERCOMP. 1976. A model for calculating effects of liquid waste disposal in deep saline aquifers. U.S. Geol. Survey Water-Resources Inv. 76-61.

Jacob, C. E. 1950. Flow of groundwater. p. 346. In Engineering Hydraulics, edited by H. Rouse. New York, John Wiley and Sons.

Konikow, L. F. 1977. Modeling chloride movement in the alluvial aquifer at the Rocky Mountain Arsenal, Colorado. U.S. Geol. Survey Water-Supply Paper 2044, 43 pp.

Mercer, J. W. and C. R. Faust. 1979. A review of numerical simulation of hydrothermal systems. Hydrological Sciences Bulletin. 24 (3), pp. 335-343.

Narasimhan, T. N., and P. A. Witherspoon. 1977. Recent developments in modeling groundwater systems. Presented at the IBM Seminar on Regional Ground-water Hydrology and Modeling, Venice, Italy, May 25-26, 1976, 35 pp.

Pinder, G. F., and J. D. Bredehoeft. 1968. Application of the digital computer for aquifer evaluation. Water Resour. Res. v. 4, no. 5, pp. 1069-1093.

Pinder, G. F., and E. O. Frind. 1972. Application of Galerkin's procedure to aquifer analysis. Water Resour. Res. v. 8, no. 1, pp. 108-120.

Prickett, T. A. 1975. Modeling techniques for ground-water evaluation. In Advances in Hydroscience. V. T. Chow, (ed.). Academic Press, New York. pp. 1-145.

Warner, J. W. 1979. Digital-transport model study of Diisopropylmethylphosphonate (DIMP) ground-water contamination at the Rocky Mountain Arsenal, Colorado. U.S. Geol. Survey Open-File Report 79-676. 39 pp.

* * * * *

James W. Mercer attended Florida State University and University of Illinois, where he received his Ph.D. in Geology in 1973. Prior to graduation, he worked for Exxon Oil Corporation and the Desert Research Institute, University of Nevada. Most recently, he worked for the U.S. Geological Survey, and is currently President of GeoTrans, Inc. Dr. Mercer has taught ground-water modeling at the U.S.G.S. and at George Washington University. He has also coauthored several articles on modeling transport problems in ground water.

Charles R. Faust received his B.S. and Ph.D. in Geology from Pennsylvania State University in 1967 and 1976. Until recently, he was a Hydrologist with the Water Resources Division, U.S. Geological Survey. His interests there involved thermal pollution in rivers, geothermal reservoir simulation, and fluid flow in fractured rocks. Presently he is a principal with GeoTrans, Inc., where he is interested in quantitative evaluation of hazardous waste and radionuclide migration in fractured rocks.

Microcomputer Model of Artificial Recharge Using Glover's Solution

by D. Molden, D. K. Sunada, and J. W. Warner[a]

ABSTRACT

An interactive program written for an APPLE II+ 48K computer is presented which solves Glover's (1960) analytical solution for recharge from a rectangular basin. The program is capable of graphically displaying the rise and decline of the recharge mound for either an infinite homogeneous medium or for a stream aquifer system.

INTRODUCTION

Advances in technology are rapidly increasing the speed and storage capabilities of microcomputers, enabling them to perform more tasks that were previously reserved for main frame computers. But, unlike the many programs available for main frame computers, at present there are relatively few ground-water programs available for microcomputers. The program presented here is a model of artificial recharge, written in BASIC for use on the APPLE II+ 48K microcomputer (APPLE II+ is a trademark of APPLE computer). Glover's (1960) solution for a rectangular basin with a constant recharge rate and the principle of superposition are used to model the growth and decline of a recharge mound in the cases of an infinite, homogeneous aquifer and for a stream aquifer system. The model can also be used to calculate discharge from the recharge basin into a stream for various times. The results of the model are displayed both graphically and numerically. The program is interactive, allowing for easy data input and program execution.

Analytical solutions have been derived for the problem of artificial recharge from circular and rectangular recharge basins and for various assumed initial and boundary conditions (Baumann, 1952; Glover, 1960; Hantush, 1967; Hunt, 1971; Rao and Sarma, 1981). Most of these analytical solutions have not been used extensively by practicing hydrologists because the solutions often involve complex integrals which are poorly behaved and difficult to evaluate (Sunada *et al.*, 1982). Hand-held programmable calculators are capable of solving many simple problems, such as those involving the well function. However, the analytical solutions for artificial recharge are typically too complex and impractical to solve on handheld calculators. Conventional solution of the artificial recharge problem on large main frame computers has been by numerical methods, such as finite-difference and finite-element methods. The microcomputer is ideally suited to solve many types of problems, such as that of artificial recharge, which do not require the enormous capabilities of the main frame computer. The advent of the microcomputer has added greater importance and usefulness of many analytical solutions, such as that for artificial recharge. The increasing capabilities of microcomputers coupled with their increasing personal availability, primarily due to their decreasing cost, are destined to make the microcomputer an indispensable tool of the hydrologist.

[a]Graduate Student, Professor, and Assistant Professor, respectively, Department of Civil Engineering, Colorado State University, Fort Collins, Colorado 80523.

Received February 1983, revised October 1983, accepted October 1983.

Discussion open until July 1, 1984.

MATHEMATICAL BASIS OF RECHARGE FROM RECTANGULAR SOURCES

Glover's (1960) solution for constant recharge from a rectangular basin (Figure 1) has the form

$$H = \frac{Rt}{4S} \int_0^1 \left(\operatorname{erf}\frac{u_2}{\sqrt{\tau}} - \operatorname{erf}\frac{u_1}{\sqrt{\tau}}\right)\left(\operatorname{erf}\frac{u_4}{\sqrt{\tau}} - \operatorname{erf}\frac{u_3}{\sqrt{\tau}}\right) d\tau \quad (1)$$

where

$$u_1 = \left(\frac{x - W/2}{4T/St}\right) \qquad u_2 = \left(\frac{x + W/2}{4T/St}\right)$$

$$u_3 = \left(\frac{y - L/2}{4T/St}\right) \qquad u_4 = \left(\frac{y + L/2}{4T/St}\right)$$

and

H = mound height (L),

R = recharge rate (L/T),

S = storage coefficient (dimensionless),

T = transmissivity (L^2/T),

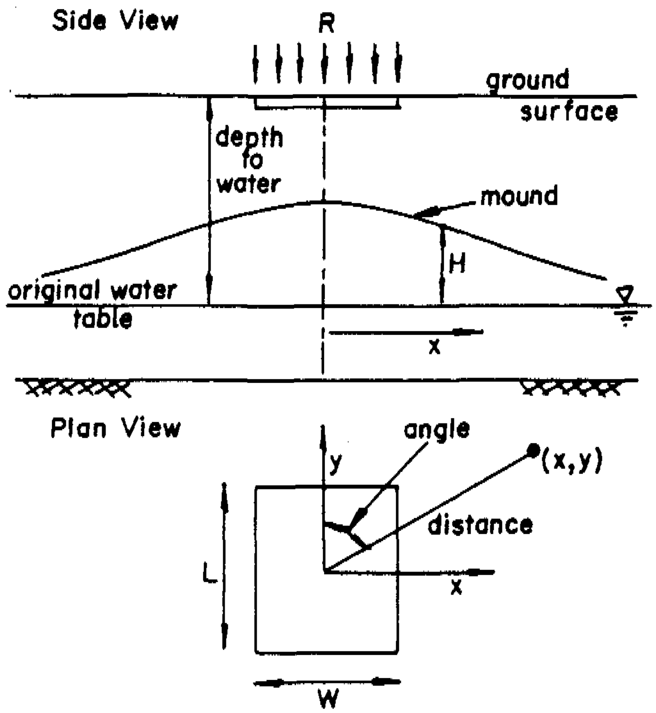

Fig. 1. Definition sketch of artificial recharge from a rectangular basin.

W = basin width (L),

L = basin length (L),

x, y = Cartesian coordinates (L),

t = time (T),

τ = dummy variable of integration,

erf(u) = error function.

Glover's solution is for a homogeneous, isotropic unconfined aquifer with constant recharge and an initially horizontal water table. For Glover's solution to be valid, the mound rise should be small compared to the initial saturated thickness of the aquifer.

To utilize Glover's solution it is necessary to evaluate the integral in equation (1). This integral is difficult to solve which is a major reason why Glover's solution is not used more extensively by practicing hydrologists. Both Simpson's rule in 10 steps and Gaussian Quadrature with up to 20 points (Abramowitz and Stegun, 1972) were tried to solve equation (1) directly, but neither method gave completely satisfactory results over a large range of data inputs. In evaluating Glover's solution, Simpson's rule applied directly to equation (1) gave the least satisfactory solution. Gaussian Quadrature applied directly to equation (1) gave satisfactory answers in most but not all cases that were simulated.

Hantush (1967) provides a better means of evaluating equation (1) by integration by parts. Performing the multiplication indicated in equation (1), Glover's solution is written as

$$H = \frac{Rt}{4S}\left[\int_0^1 \operatorname{erf}\frac{u_2}{\sqrt{\tau}}\operatorname{erf}\frac{u_4}{\sqrt{\tau}}\,d\tau - \int_0^1 \operatorname{erf}\frac{u_2}{\sqrt{\tau}}\operatorname{erf}\frac{u_3}{\sqrt{\tau}}\,d\tau - \int_0^1 \operatorname{erf}\frac{u_1}{\sqrt{\tau}}\operatorname{erf}\frac{u_4}{\sqrt{\tau}}\,d\tau + \int_0^1 \operatorname{erf}\frac{u_1}{\sqrt{\tau}}\operatorname{erf}\frac{u_3}{\sqrt{\tau}}\,d\tau\right]. \quad (2)$$

Hantush shows that the integrals in equation (2) can be evaluated as

$$\int_0^1 \operatorname{erf}\frac{u_i}{\sqrt{\tau}}\operatorname{erf}\frac{u_j}{\sqrt{\tau}}\,d\tau = \operatorname{erf}(u_i)\operatorname{erf}(u_j) + (4/\pi)\,u_i u_j W(u_i^2 + u_j^2) + (2/\sqrt{\pi})\,[u_i e^{-u_i^2}\operatorname{erf}(u_j) + u_j e^{-u_j^2}\operatorname{erf}(u_i)] - 2\,[u_i^2 M^*(u_i, u_j) + u_j^2 M^*(u_j, u_i)] \quad (3)$$

where

$$M^*(u_i, u_j) = \frac{u_j}{\pi u_i}\int_{-1}^{1}\frac{\exp[-u_i^2(1 + r^2)]}{1 + r^2}\,dv \quad (4)$$

$$r = (v + 1)\frac{u_j}{2u_i} \quad (5)$$

and W(u) = well function.

For implementation of equation (2) on the microcomputer, expressions for the error function and well function are used and the integral in the function M^* is numerically evaluated by Gaussian Quadrature. In the program the error function is evaluated by a polynomial approximation (Abramowitz and Stegun, 1972).

For $u \geqslant 0$, the error function is given by

$$\operatorname{erf}(u) = 1 - (e_1 b + e_2 b^2 + e_3 b^3 + e_4 b^4 + e_5 b^5)e^{-u^2} \quad (6)$$

where

$b = 1/(1 + pu)$ $\quad e_4 = -1.453152027$

$e_1 = .254829592$ $\quad e_5 = 1.06140543$

$e_2 = -.284496736$ $\quad p = .3275911$

$e_3 = 1.421413741$

and erf(−u) = −erf(u). The error in equation (6) is in the order of 10^{-7}.

The well function is found by approximations given by Huntoon (1980) and Abramowitz and Stegun (1972). For values of $u \leqslant 1$, the program uses

$$W(u) = a_0 - \ln(u) + a_1 u + a_2 u^2 + a_3 u^3 + a_4 u^4 + a_5 u^5 \quad (7)$$

where

$a_0 = -.57721566 \qquad a_3 = \ .05519968$

$a_1 = \ .99999193 \qquad a_4 = -.00976004$

$a_2 = -.24991055 \qquad a_5 = \ .00107857.$

For values of $1 \leqslant u \leqslant \infty$, the program uses

$$W(u) = \frac{1}{u\exp(u)} \; \frac{u^4 + b_1u^3 + b_2u^2 + b_3u + b_4}{u_4 + c_1u^3 + c_2u^2 + c_3u + c_4} \qquad (8)$$

where

$b_1 = \ 8.57332874 \qquad c_1 = \ 9.57332235$

$b_2 = 18.0590170 \qquad c_2 = 25.6329561$

$b_3 = \ 8.63476089 \qquad c_3 = 21.0996531$

$b_4 = \ .267773734 \qquad c_4 = \ 3.95849692$

In the program the integral in M^* is evaluated using six-point Gaussian Quadrature given by

$$M^*(u_i, u_j) = \frac{u_j}{\pi u_i} \sum_{k=1}^{6} \frac{\exp[-u_i^2(1 + r^2)]}{1 + r^2} \cdot V_k \qquad (9)$$

where

$$r \quad = (A_k + 1)\,\frac{u_j}{2u_i}, \qquad (10)$$

A_k = abscissas of Guassian Quadrature,

V_k = weights of Guassian Quadrature.

The abscissas and weights are

$A_1 = -A_6 = 0.238619186 \qquad V_1 = V_6 = 0.467913935$

$A_2 = -A_5 = 0.661209386 \qquad V_2 = V_5 = 0.360761573$

$A_3 = -A_4 = 0.932469514 \qquad V_3 = V_6 = 0.171324492$

USE OF SUPERPOSITION

The principle of superposition (McWhorter and Sunada, 1977) is used to obtain additional solutions for the case of a finite aquifer or for the case of a variable recharge rate. Superposition in time is used to calculate the decline of the recharge mound after recharge is stopped. With a stream in the vicinity, superposition in space is used to calculate mound profile and discharge to the stream with time.

At the end of the recharge period an image basin at the same location as the real basin begins withdrawal (negative recharge) while the real basin continues to recharge. The mound height due to the real basin is added to the drawdown due to the discharging image basin to give the actual mound height:

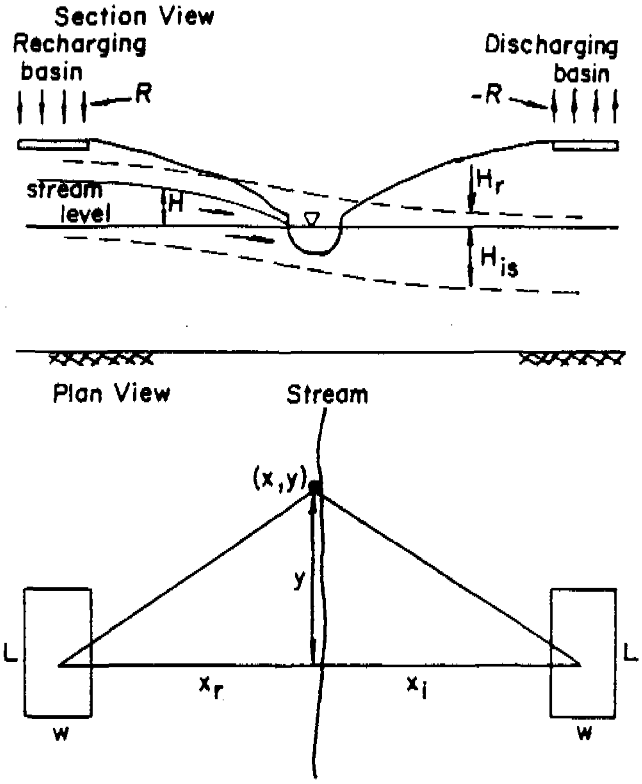

Fig. 2. Definition sketch of the use of superposition when a stream is in the vicinity (x_r = real x coordinate; x_i = image x coordinate).

$$H = H_r + H_{it} \qquad (11)$$

where

H_r = mound height contribution from the real basin,

H_{it} = mound height contribution from the image basin superimposed in time.

If a stream is in the vicinity, an image discharging basin is set up on the opposite side of the stream equidistant from the real basin (Figure 2). The drawdown from the image basin is superimposed onto the mound height contribution from the real basin to give the actual mound height

$$H = H_r + H_{is} \qquad (12)$$

where

H_{is} = drawdown contribution from the image basin superimposed in space.

If the end of the recharge period has been reached and a stream is in the vicinity, an image basin at the same location as the real basin begins discharging and another image basin at the same location as the image basin opposite the stream begins recharging. The mound height at a selected location is given by

$$H = H_r + H_{is} + H_{it} + H_{its} \tag{13}$$

where

H_{its} = mound height contribution from the image basin superimposed in time and space.

DISCHARGE TO THE STREAM

The integral equation for flow to a stream is (McWhorter and Sunada, 1977)

$$Q_T = \int_{-\infty}^{\infty} \left(T \frac{\partial H}{\partial x}\right) dy \tag{14}$$

where

Q_T = total discharge to the stream (L^3/T).

The integral is evaluated numerically by computing the integrand at selected intervals along the stream and integrating the distribution by the method of trapezoids. The numerical evaluation yields the expression for discharge

$$Q_T = 2 \sum_{i=1}^{n} \frac{[(T\,\partial H/\partial x)_{i-1} + (T\,\partial H/\partial x)_i]\,\Delta y_i}{2} \tag{15}$$

where

Δy_i = the interval between points i-1 and i along the length of the stream,

n = number of locations that stream discharge per unit length was calculated.

The value of n is selected by the program so that the discharge between locations n-1 and n is less than 0.1% of the total discharge calculated up to location n. The quantity $\partial H/\partial x$ is approximated by computing the mound height at 1 foot away from the stream denoted by H^1. Because the head at the stream is constant and known (selected to be zero in this case) the discharge is approximated by

$$Q_T = T \sum_{i=1}^{n} [H^1_{i-1} + H^1_i]\,\Delta y_i. \tag{16}$$

Figure 3 is a plot of discharge to the stream vs. time, with values obtained from the program using the data in Figure 5.

PROGRAM DESCRIPTION

Taking full advantage of the capabilities of the microcomputer, this interactive program is written to be self-explanatory and easy to use. The graphics are employed for quick visual study. An example run is described to demonstrate the flow of the program. The figures represent what would be shown on the screen.

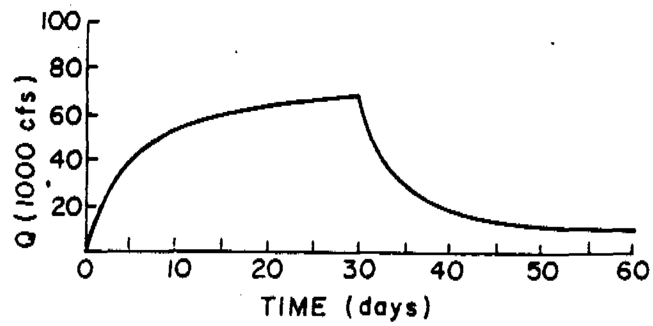

Fig. 3. Discharge to the stream vs. time.

The program can be easily operated by persons with very little knowledge of computers, yet many advantages of computer use are available. The program works by a "turn key" system; that is, the disk containing the program is inserted, the computer turned on and the program execution begins. The user is prompted at each step, often with a variety of options. Data are easily entered or changed; results are quickly obtained and readily compared.

When starting the program, a menu presents the user with selection of model options (Figure 4). For our example, option 1 is selected to model artificial recharge in an aquifer with a fully penetrating stream. The recharge parameters and their values are then displayed on the screen (Figure 5). To change a value, the number corresponding to the recharge parameter to be changed is input. The old value is displayed and the user asked to input a new value (Figure 6). The updated parameter list is again displayed and the process repeated until Ø is typed. The program then checks for any value which is out of range. A message will inform the user if there are any mistakes and appropriate values must be entered. With no mistakes, the program begins execution.

```
                    ARTIFICIAL RECHARGE

        OPTIONS
             1) STREAM IN VICINITY
             2) NO STREAM IN VICINITY
             3) READ FILES
             4) EXIT

        TYPE THE NUMBER OF YOUR CHOICE 1
```

Fig. 4. Screen display. Model options: artificial recharge will be modeled with a stream in the vicinity.

In this example, both mound profile and discharge to the stream are calculated. As values for head are calculated at selected distance they are plotted on the graphics screen with the values of time, distance and mound height shown beneath the plot (Figure 7). Upon completion of the plot, the user is asked to type C to continue. The graphics screen is then cleared and discharge to the stream is calculated. The display gives the distance along the stream, the mound height at one foot away from the stream, and the discharge per unit length at that point as the points are calculated (Figure 8). When the discharge per unit length becomes negligible, the total discharge to the stream is given.

To reexamine and study the problem, the user is presented with a variety of output options (Figure 9). The "data display" option gives a list of the recharge parameters used. The "results display" tabulates the numerical values of the results. A hard copy of the data and results can be obtained with the "results printout" option. The graphics are quickly recreated by the "graphics display" option. Data and results can be stored on the disk

```
 1) RECHARGE RATE (FT/DAY)              2
 2) TRANSMISSIVITY (SQ.FT/DAY)          2500
 3) SPECIFIC YIELD                      .2
 4) BEGINNING TIME (DAYS)               30
    FINAL TIME (DAYS)                   30
    TIME INCREMENT (DAYS)               30
 5) END OF RECHARGE PERIOD (DAYS)       30
 6) BEGINNING DISTANCE (FT)             0
    FINAL DISTANCE (FT)                 500
    DISTANCE INCREMENT (FT)             50
 7) DEPTH TO WATER (FT)                 30
 8) BASIN WIDTH (FT)                    200
 9) BASIN LENGTH (FT)                   200
10) ANGLE FROM LENGTH AXIS (DEG)        0
11) DISTANCE TO STREAM                  250
12) CALCULATE MOUND PROFILE             YES
13) CALCULATE DISCHARGE TO STREAM       YES

TYPE THE NUMBER OF THE VARIABLE YOU
WISH TO CHANGE. TYPE 0 IF YOU WISH
TO CONTINUE WITHOUT CHANGING. 7
```

Fig. 5. Screen display. Parameter display: the depth to water will be changed.

```
DEPTH TO WATER = 30 FEET


INPUT NEW DEPTH TO WATER 20
```

Fig. 6. Screen display. The depth to water is changed from 30 to 20 feet.

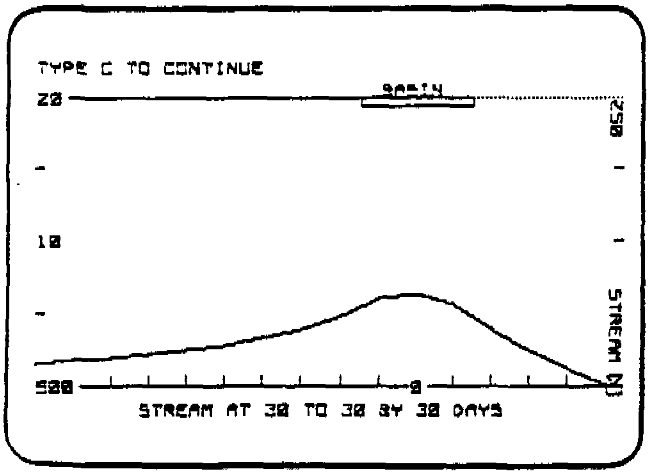

Fig. 7. Screen display. Mound profile at 30 days.

DISCHARGE TO STREAM

DISTANCE ALONG STREAM (FT)	HEAD AT 1 FOOT (FT)	DISCHARGE/UNIT LENGTH (SQ.FT/DAY)
30 DAYS		
0	.03881	97.03
50	.03739	93.48
100	.03353	83.83
200	.02329	58.23
400	9.86E-03	24.65
800	2.35E-03	5.88
1600	3.2E-04	.8
3200	0	0

TOTAL DISCHARGE = 68000 CUBIC FT./DAY

Fig. 8. Screen display. Discharge to the stream at 30 days.

```
OPTIONS
    1) DATA DISPLAY
    2) RESULTS DISPLAY
    3) GRAPHICS DISPLAY
    4) RESULTS PRINTOUT
    5) CREATE FILE
    6) ANOTHER RUN
    7) EXIT
TYPE THE NUMBER OF YOUR CHOICE 5
```

Fig. 9. Screen display. Output options: create file is chosen to store data on the disk.

```
READ FILES

DO YOU WISH TO SEE THE CATALOG
(Y/ES, N/O)? N

INPUT FILE NAME: NO STREAM

TYPE STOP TO RETURN TO THE MENU
```

Fig. 10. Screen display. Read files: the file "no stream" is read from the disk.

with the "create file" option. The "another run" option allows the user to go back to the original model option, retaining all the present values of the recharge parameters. The "create files" option is chosen and the name given to the file is "stream."

Next, the "another run" option is chosen and the original recharge option appears (Figure 4). "Read files" is then selected and the name of the file to be read is entered (Figure 10). The previously made file "no stream" is read from the disk. This file has exactly the same recharge parameters as "stream" but simulates recharge in an infinite aquifer. After the file has been read, the list of output options again appears on the screen with the exception that "create file" has been changed to "read another file." Up to 10 files can be read and simultaneously stored in memory. "Read another file" is chosen to read in the file "stream."

To compare the influence of a stream, the graphics will demonstrate any difference in mound profile. The "graphics display" option is chosen. The program has the capability of plotting several sets of points on the same graph enhancing comparison of solutions. "No stream" is chosen and plotted. The "graphics display" option is again chosen with "stream" to be plotted. The program asks if the same plot is to be used. In this manner, "stream" (dotted line) and "no stream" are plotted on the same graph (Figure 11). With a stream in the vicinity, the mound height is lower than an infinite aquifer and not symmetric around the center basin.

Glover (1960) also presents a solution for recharge from a circular basin using instantaneous slug injections. A comparison was made between the mound profile under a square basin using the data of "no stream" and a circular basin of the same area (Figure 12). Using 250 instantaneous injections took over 100 times the execution time required by the rectangular basin program, yet gave approximately the same solution, showing that this program could also be used to simulate recharge from a circular basin.

DISCUSSION

To calculate one point on the recharge mound takes about 13 seconds in interpreted basic and 6 seconds in compiled basic. To get a good graphical representation of the recharge mound height, it is usually adequate to calculate about 10 to 20 points, and total time of execution is usually only a few minutes. Memory requirements are not restrictive, as the program takes about 25K bytes of random access memory leaving about 15K bytes of memory for variables and 8K bytes for graphics

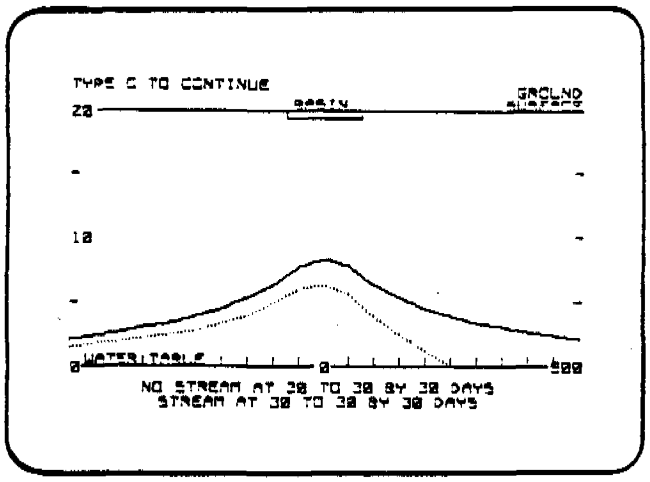

Fig. 11. Screen display. "Stream" (dotted line) and "no stream" are plotted on the same graph.

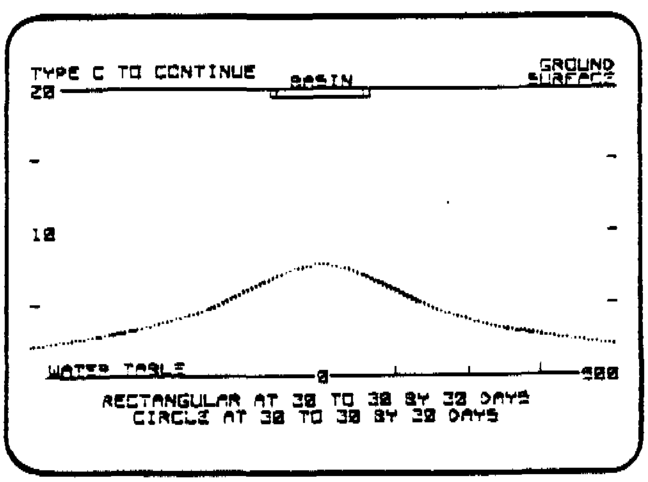

Fig. 12. Square basin (solid line) vs. circular basin (dotted line). The solution for the circular basin almost completely overlaps the solution for a rectangular basin.

in a 48K computer. The compiled version requires additional storage and will run on a 64K computer.

A major problem faced by hydrologists is to reduce the complex mathematical equations used in the study of ground water into results that can be readily understood by lay persons interested in water. By making programs which are very "user friendly" and which make extensive use of graphics, the ground-water hydrologist is much better able to communicate with nontechnical water users. This program was developed as part of a demonstration of artificial recharge in the San Luis Valley, Colorado, in cooperation with several local irrigation districts. The graphics features of the microcomputer were well suited to describe the effects of artificial recharge to nontechnical water users.

Using the program, the effects of various recharge strategies can be quickly investigated. For example, the user can study the effects of changing basin geometry, changing recharge rates and changing duration of recharge. The effects of different soil characteristics and boundary conditions can also be easily studied. The comparison of results for different case studies is enhanced by the capability of the program to plot several different case studies on the same graph.

CONCLUSIONS

The advent of microcomputers has given ground-water hydrologists another choice of tools for problem solving. The microcomputer is well suited to solve many types of problems, such as that of artificial recharge, which do not require the enormous capabilities of the large main frame computer. By making programs which are very "user friendly" and which make extensive use of graphics, the ground-water hydrologist is much better able to give a clear understanding of his results to the nontechnical water user. The program presented in this paper is one example of a large number of problems which could be solved on a microcomputer.

ACKNOWLEDGMENTS

The authors would like to thank the Office of Water Resources Technology and the Colorado State University Experiment Station Project 1-51101 for funding this project.

NOTE

A program listing is available, and can be obtained by request to *Ground Water.* A floppy disk for the APPLE II+ and documentation is available at duplication and mailing cost (approximately $20). Every effort has been made to provide an error-free program, but the authors do not take responsibility for any errors which may have been overlooked.

REFERENCES

Abramowitz, M. and I. A. Stegun. 1972. Handbook of Mathematical Functions with Formulas, Graphs and Mathematical Tables. 8th ed., Dover Publications, Inc., New York, NY. 1046 pp.

Baumann, P. 1952. Groundwater movement controlled through spreading. Transactions, ASCE. v. 117, pp. 1024-1060.

Glover, R. E. 1960. Mathematical Derivations as Pertain to Groundwater Recharge. Agricultural Research Service, USDA, Ft. Collins, Colorado.

Hantush, M. S. 1967. Growth and decay of groundwater mounds in response to uniform percolation. Water Resources Research. v. 3, pp. 227-234.

Hunt, B. W. 1971. Vertical recharge of unconfined aquifers. Journal of Hydraulics Div., ASCE. v. 97, no. HY7, pp. 1017-1030.

Huntoon, P. W. 1980. Computationally efficient polynomial approximations used to program the Theis equation. Ground Water. v. 18, no. 2, pp. 134-136, March-April.

McWhorter, D. and D. K. Sunada. 1977. Ground Water Hydrology and Hydraulics. Water Resources Publications, Ft. Collins, Colorado. 290 pp.

Rao, N. H. and P.B.S. Sarma. 1981. Ground-water recharge from rectangular areas. Ground Water. v. 19, no. 3, pp. 270-274.

Sunada, D. K., J. W. Warner, and D. J. Molden. 1983. Artificial Groundwater Recharge, San Luis Valley, Colorado. Colorado Water Resources Research Institute, Colorado State University, Ft. Collins, Colorado. Rep. No. 23.

* * * * *

David Molden is a graduate student in Civil Engineering at Colorado State University. He received his M.S. from Colorado State University in the ground-water program in 1982, and his B.S. from the University of Denver in 1977. He is presently a Ph.D. student at Colorado State University. He was a Peace Corps volunteer in Lesotho from 1977-1979.

Daniel K. Sunada is a Professor of Civil Engineering and leader of the ground-water program at Colorado State University. He has conducted research and written numerous papers and reports for the past 20 years. He has taught courses in ground-water engineering, ground-water hydraulics, drainage, pumping plants and basic courses in engineering. He is coauthor of a texbook which is used in several universities. For the past six years he has been heavily involved in international water management.

James W. Warner is an Assistant Professor of Civil Engineering in the ground-water program at Colorado State University. Formerly he worked as a ground-water hydrologist with the U.S.G.S. He has taught courses in ground water, ground-water modeling and basic engineering.

Mapping Recharge Areas Using a Ground-Water Flow Model — A Case Study

by Mary W. Stoertz[a] and Kenneth R. Bradbury[b]

ABSTRACT

We have developed a method to calculate ground-water recharge rates using the mass-balance equation, water-table elevation data, estimates of hydraulic conductivity, and aquifer thickness data, and have applied this method to produce a map of the recharge and discharge patterns for a ground-water basin in central Wisconsin. This recharge mapping method is simplified using a modified computer program, the USGS Modular Groundwater Flow Model (McDonald and Harbaugh, 1984). The modeled recharge pattern compares favorably with a recharge map based on field observations. Because recharge rates are extremely sensitive to hydraulic conductivity, the magnitudes of the calculated rates are less reliable than the patterns of recharge and discharge areas. However, introducing stream discharge data constrains the model to produce net recharge rates averaged over the basin which agree with estimates of the basin yield. Because the method is insensitive to the position of lateral boundaries, it can be used to map recharge over areas within basins that are not physically bounded. Recharge maps made with this method can be used to design ground-water monitoring networks and as frameworks for interpreting geochemical or potentiometric data.

INTRODUCTION

Of the many factors which control a well's susceptibility to contamination from the surface, the areal distribution of recharge and discharge is one of the most difficult to measure or predict, often requiring installation of extensive networks of multilevel piezometers in which water levels are measured frequently (e.g., Faustini, 1985; Sophocleous and Perry, 1984, 1985; Rehm *et al.*, 1982).

[a]University of Wisconsin-Madison, Department of Geology and Geophysics, 1215 W. Dayton St., Madison, Wisconsin 53706.

[b]Wisconsin Geological and Natural History Survey, 3817 Mineral Point Road, Madison, Wisconsin 53705.

Received January 1988, revised June 1988, accepted July 1988.

Discussion open until September 1, 1989.

This paper describes a method for mapping recharge and discharge areas using an existing water-table map. Like Freeze's (1967) method of mapping recharge and discharge areas, vertical fluxes derived from Darcy's Law are contoured to produce a map. In applying Darcy's Law, however, Freeze (1967) determined the vertical hydraulic gradient with a three-dimensional mathematical model. In contrast, we obtain a water balance for each water-table cell by calculating fluxes between the water-table cell and its four adjacent cells. Heads specified for each cell determine the hydraulic gradients. The recharge or discharge rate is interpreted as the deficit or surplus in the water balance. Other studies of recharge that are similar in concept to this one have been presented by Stallman (1956), Tanaka and Hollowell (1966), Cooley *et al.* (1971), Weeks and Sorey (1973), and Lappala (1978).

We apply the method areally in two dimensions to a ground-water basin in Portage County, Wisconsin and verify the resulting recharge map by comparing it to a field-based recharge map of the same basin.

OVERVIEW OF THE METHOD APPLIED IN TWO DIMENSIONS

The recharge mapping method described here is based on the steady-state mass-balance equation, and is illustrated in Figure 1 for one-dimensional flow in a homogeneous aquifer. The flux Q between two adjacent cells is calculated by Darcy's Law, using observed heads h, hydraulic conductivities K, and aquifer thickness, all of which must be specified. Heads in cells are *fixed*, so the entire water table is represented as a specified-head surface. Cell D (Figure 1) loses more water to cell C than it gains from cell E, according to Darcy's Law which determines the flux between the constant-head cells; there is a net mass deficit for cell D. To maintain the observed head, h_D, water must be added as recharge, R_D. Similarly, vertical

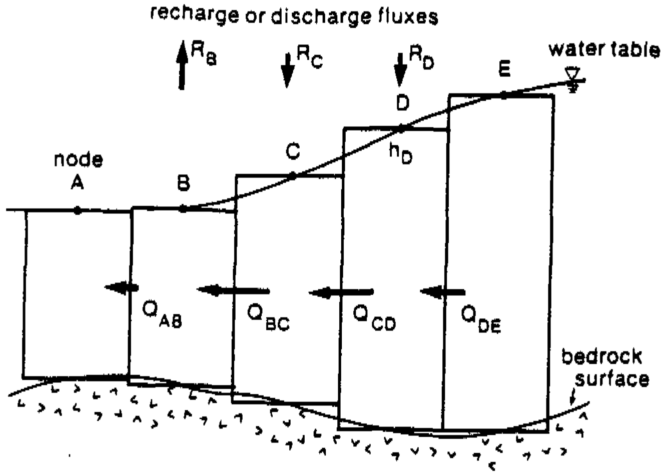

Fig. 1. Schematic of the recharge mapping method.

discharge R_B from cell B will offset a mass surplus for cell B. To extend this schematic to two dimensions, the mass balance is calculated using the four cells adjacent to each water-table cell. Contouring the values of the recharge and discharge rates for each water-table cell produces a recharge/discharge map.

The USGS Modular Groundwater Flow Model (McDonald and Harbaugh, 1984) contains a procedure to calculate the mass budget for individual cells. The Appendix gives modifications of the model to include flows between specified-head cells in its cell-by-cell budget calculations.

APPLICATION TO CENTRAL WISCONSIN

The Buena Vista Groundwater Basin occupies an area of 170 mi² in central Wisconsin (Figure 2). The unconfined aquifer is composed of medium to coarse moderately sorted outwash sand, ranging in thickness from 50 to 150 ft with the depth to water from 5 to 60 ft. The aquifer is bounded below by igneous and metamorphic bedrock and in places by sandstone. The surface relief is about 150 ft, primarily due to the series of moraines forming the eastern no-flow boundary of the basin. The Wisconsin River bounds the basin on the west, and the northern and southern boundaries correspond to flowlines determined from a water-table map (Lippelt and Hennings, 1981). Comparison of seasonal water-table maps and a water-table map prepared from well-construction reports spanning several decades indicates that these flowline boundaries do not shift significantly (Blanchard and Bradbury, 1987). Faustini (1985) showed that

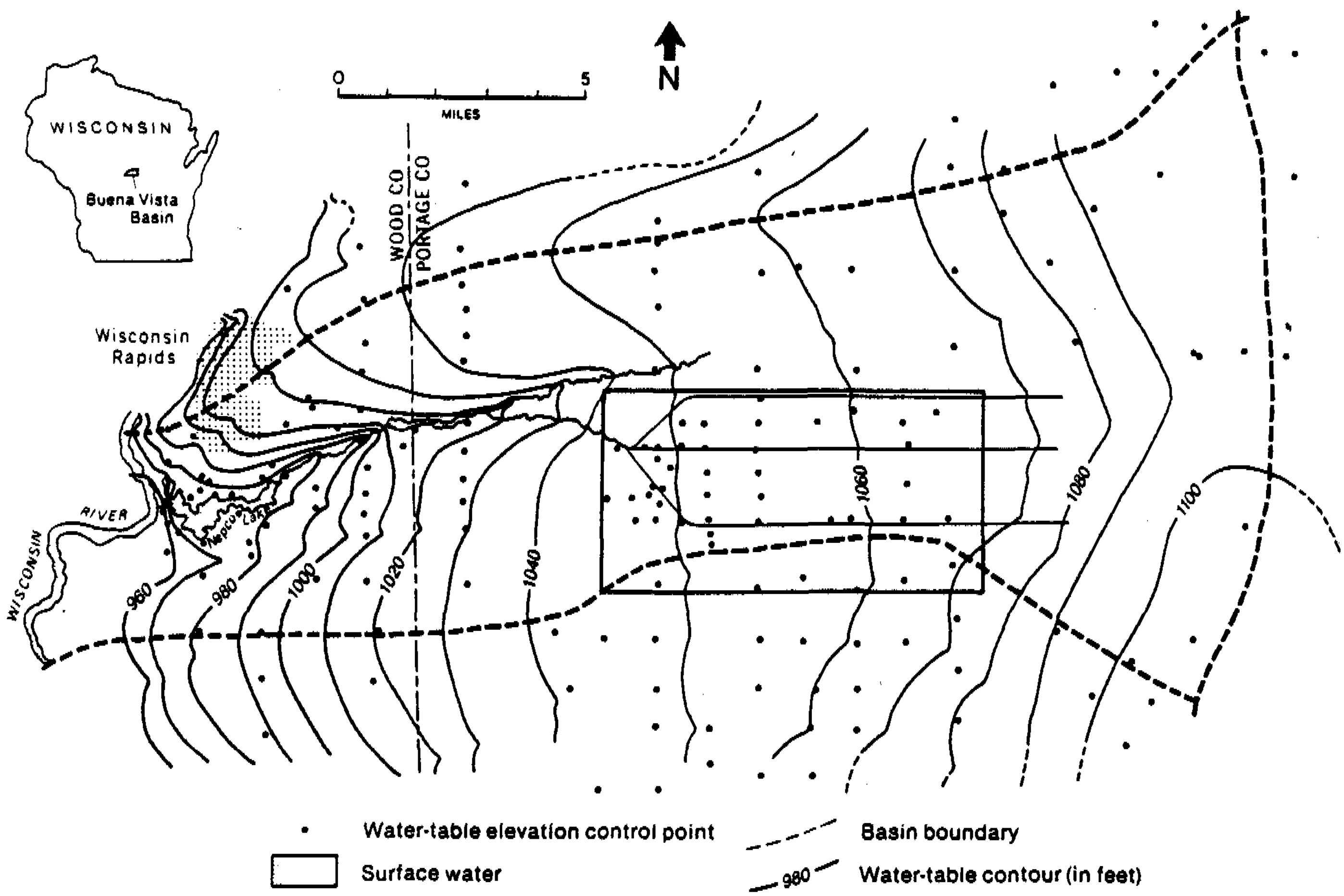

Fig. 2. Map of the Buena Vista Basin showing August 1984 field-observed water-table contours. Locations of water-level control points and surface drainage are shown, along with outline of the ditch subarea.

Table 1. Summary of Hydraulic Conductivity Values (in ft/s) as Determined by Various Methods

Method	*Number of samples*	*Lower endpoint* ——95% C.I.*	*Upper endpoint* ——	*Geometric mean*	*Standard deviation of log (K)*
Aquifer pumping test	11	6.2×10^{-4}	1.3×10^{-2}	2.9×10^{-3}	0.98
Specific capacity test	266	1.9×10^{-3}	2.2×10^{-3}	2.1×10^{-3}	0.25
Slug test	48	4.2×10^{-4}	1.2×10^{-3}	7.2×10^{-4}	0.79
Permeameter test	8	2.2×10^{-5}	8.2×10^{-3}	4.3×10^{-4}	1.53
Grain size analysis	71	8.9×10^{-4}	1.8×10^{-3}	1.2×10^{-3}	0.68

* The large 95% confidence intervals for pumping and permeameter tests are due to the small number of data points rather than scatter in the values.

the Buena Vista Groundwater Basin behaves as a closed basin with respect to ground water; i.e., ground water does not cross the boundaries except where it flows into the Wisconsin River. Detailed studies of the drainage ditches in the central basin (Faustini, 1985), corroborated by theoretical studies of these ditches as flow boundaries (Zheng and Anderson, 1985), show that local flow systems are well-developed within the basin.

Hydraulic Conductivity

Several hundred measurements of hydraulic conductivity have been made in the vicinity of the Buena Vista Groundwater Basin using pumping tests (Weeks, 1964, 1969; Holt, 1965; Weeks and Stangland, 1971; Karnauskas, 1977; Rothschild, 1982), specific capacity tests (Bradbury and Rothschild, 1985), slug tests (Allen, 1985), permeameter tests (Stoertz, 1985), and grain-size analyses (Brownell, 1986). Although several hydrostratigraphic units are discernible (Brownell, 1986), the aquifer is generally homogeneous as indicated by the narrow confidence intervals for specific capacity tests, slug tests, and grain-size analyses (Table 1). We treat the aquifer as homogeneous and use the geometric mean of pumping test conductivities as an initial estimate of the hydraulic conductivity of the whole basin.

Water Table

Figure 2 shows the August 1984 water table (Faustini, 1985), measured over several days following a week without rain. Because vertical gradients were relatively stable and storage changes were small, we view this water-table map as a steady-state map corresponding to late summer

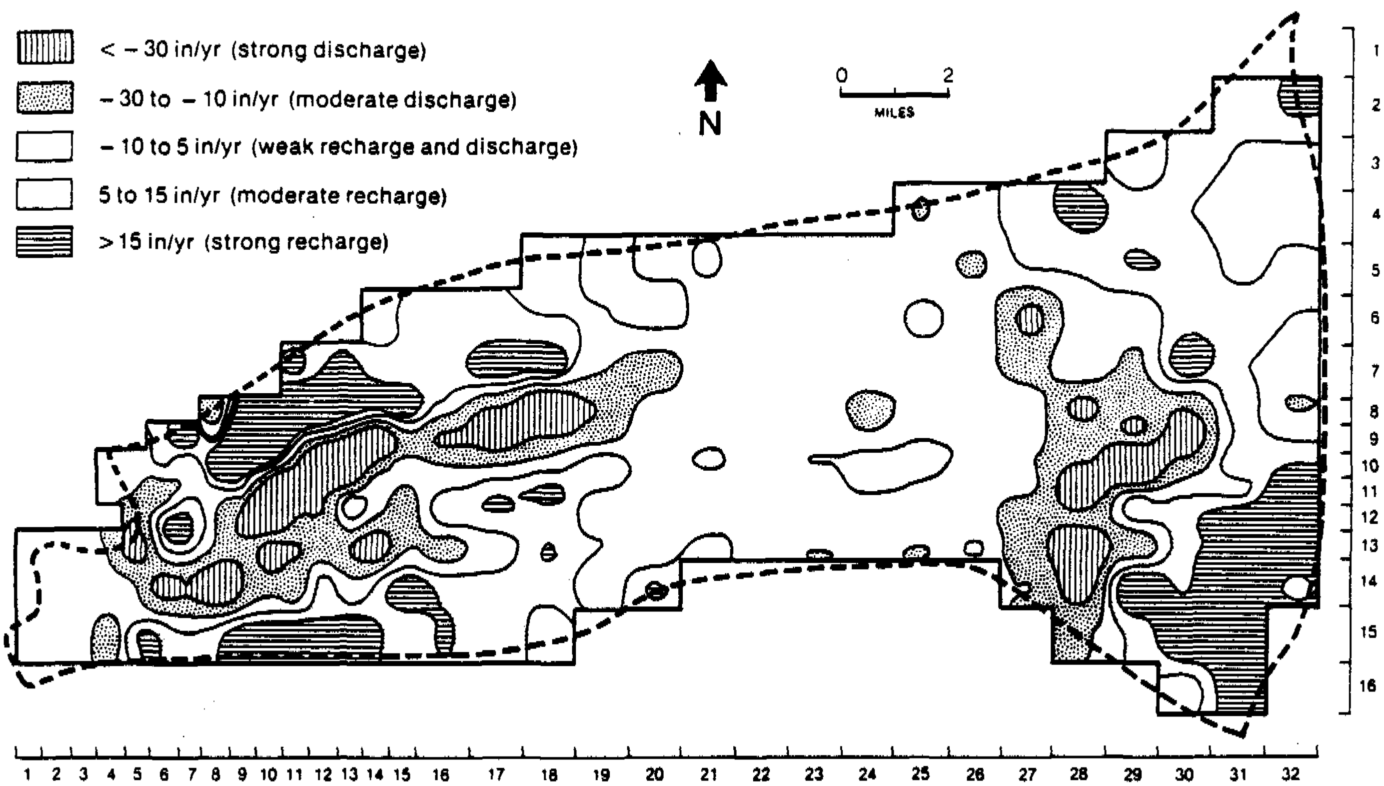

Fig. 3. Modeled map of recharge and discharge rates for the Buena Vista Basin, based on the August 1984 water-table map and a hydraulic conductivity value of 3.0 E-3 ft/sec. Basin outline (dashed) is the same as in Figure 2.

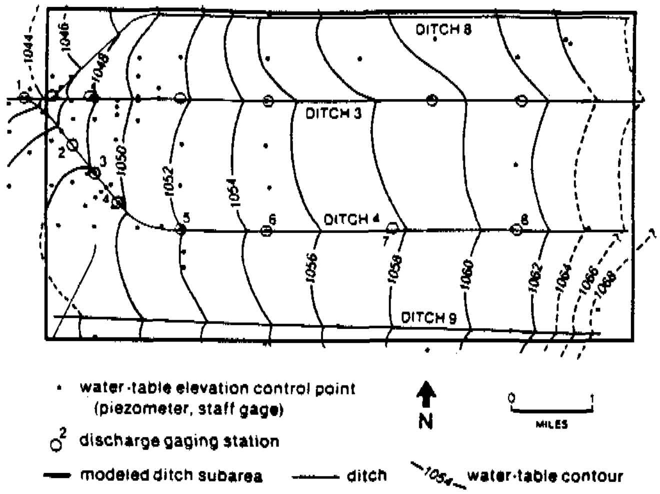

Fig. 4. Map of the ditch subarea showing water-table contours for July 2, 1984. Locations of water-level control points, gaging stations, and surface drainage are shown.

seasonal conditions. We argue that the water table in very permeable aquifers can be viewed as a series of quasi-steady-state profiles interrupted by brief periods of intense recharge. The primary influences on water-table profiles between recharge events are fairly steady fluxes, including a steady feeding of the aquifer from water traveling through the unsaturated zone in recharge areas, and a steady draining of the aquifer by evapotranspiration and ditch discharges. The resulting water table, while seasonal, is therefore fairly steady.

Model

The data just described, including boundary conditions, hydraulic conductivity, and water-table configuration, were used with a modified version of the USGS Modular Groundwater Flow Model (McDonald and Harbaugh, 1984). Modifications are described in the Appendix. The basin was modeled on a 16 by 32 grid, and the resulting recharge/discharge map is shown in Figure 3.

Calibration to Streamflow

Because the method is based on Darcy's Law, the calculated flux between adjacent cells varies in direct proportion to the hydraulic conductivity which is inherently uncertain. Additional information about the flow system, such as measurements of fluxes (e.g., streamflow or pump discharges), must be used to constrain the hydraulic conductivity.

Faustini (1985) measured streamflow at eight gaging stations along Ditch 4 in the central basin, and one day later made a detailed water-table map of a subarea of the basin including Ditch 4 (Figure 4, also outlined in Figure 2). Ditch stages were used in constructing the map and were assumed to be close to the underlying aquifer heads. The streamflow data allow calibration of hydraulic conductivity to streamflow but require a finer-meshed model of the ditch subarea (Figure 5) to give sufficient resolution to capture the details of the water-table map near the ditches. By applying the recharge/discharge mapping method to the ditch subarea, we can compute the discharges from nodes along the ditches and then compare them to the field-measured discharges for each segment of the ditch. Modeled and measured discharge gains between the upstream gage (Gage 8) and the downstream gage (Gage 1) for three different values of hydraulic conductivity are plotted in Figure 6. Stream sediments, aquatic vegetation, and local variations in

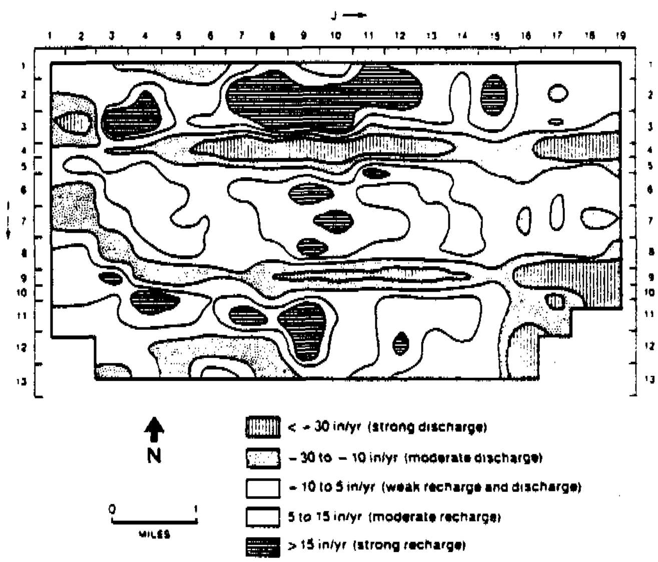

Fig. 5. Map of recharge and discharge rates for the ditch subarea based on the July 2, 1984 water-table map.

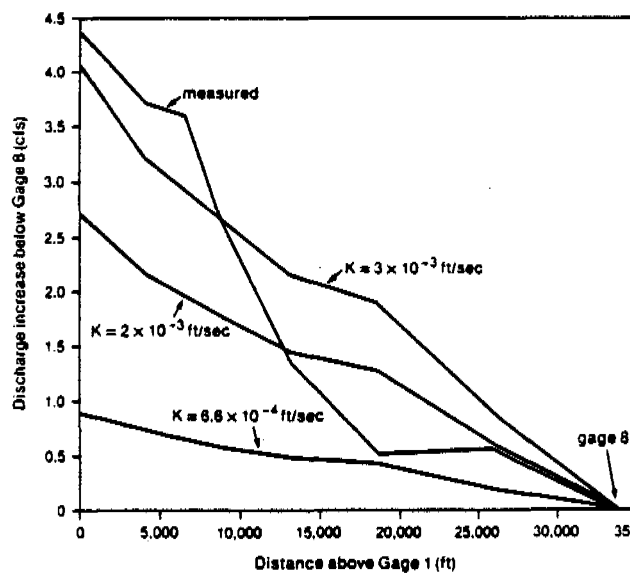

Fig. 6. Comparison of measured and modeled ditch discharges for the ditch subarea. Modeled discharges are shown for three hydraulic conductivity values.

hydraulic conductivity affect stream discharges, so the model cannot reproduce exactly the discharge increases. We nevertheless get an acceptable fit to the changes in ground-water discharge along the ditch using a value of K of 3×10^{-3} ft/sec which agrees with the geometric mean of conductivities from pumping tests in the Buena Vista Basin (Table 1). Moreover, basin yield estimates using this hydraulic conductivity value agree with estimates from previous studies in the area. This estimate of hydraulic conductivity was used to prepare the map in Figure 3.

Field Verification

We verified the modeled recharge pattern (Figure 3) by comparing it to a field-based recharge map (Figure 7) prepared by Faustini (1985) using topography, piezometric patterns, seepage measurements in stream sediments, and water-table response to precipitation, as indicators of recharge. Faustini (1985) did not assign rates to his various recharge and discharge zones, but instead differentiated them on the basis of whether they were part of regional, intermediate, or local flow systems. It is therefore possible to compare only the pattern and not the rates of recharge and discharge in Figures 3 and 7. In both figures, recharge occurs at the upper (eastern) end of the basin, and along the north and south flanks of the lower basin. Discharge occurs along streams and at the break in slope below the moraine in the east. The recharge patterns in the ditch area are poorly reproduced due to the large cell dimensions relative to the size of the ditches. The map for the ditch subarea (Figure 5) shows that with an appropriate discretization, the modeled discharge pattern near the ditches matches the field-measured pattern.

The model results are summarized in the first row of Table 2. Recharge areas cover 57.5% of the basin, and discharge areas cover 42.5% of the basin. Recharge rates averaged over recharge cells average 13 in./yr, while discharge rates (over only discharge cells) average −17.6 in./yr. Because the system is assumed to be at steady state, the volume of recharge must equal the volume of discharge. Since recharge areas are larger than discharge areas, the rates are higher in discharge areas. While recharge areas will not always be larger than discharge areas

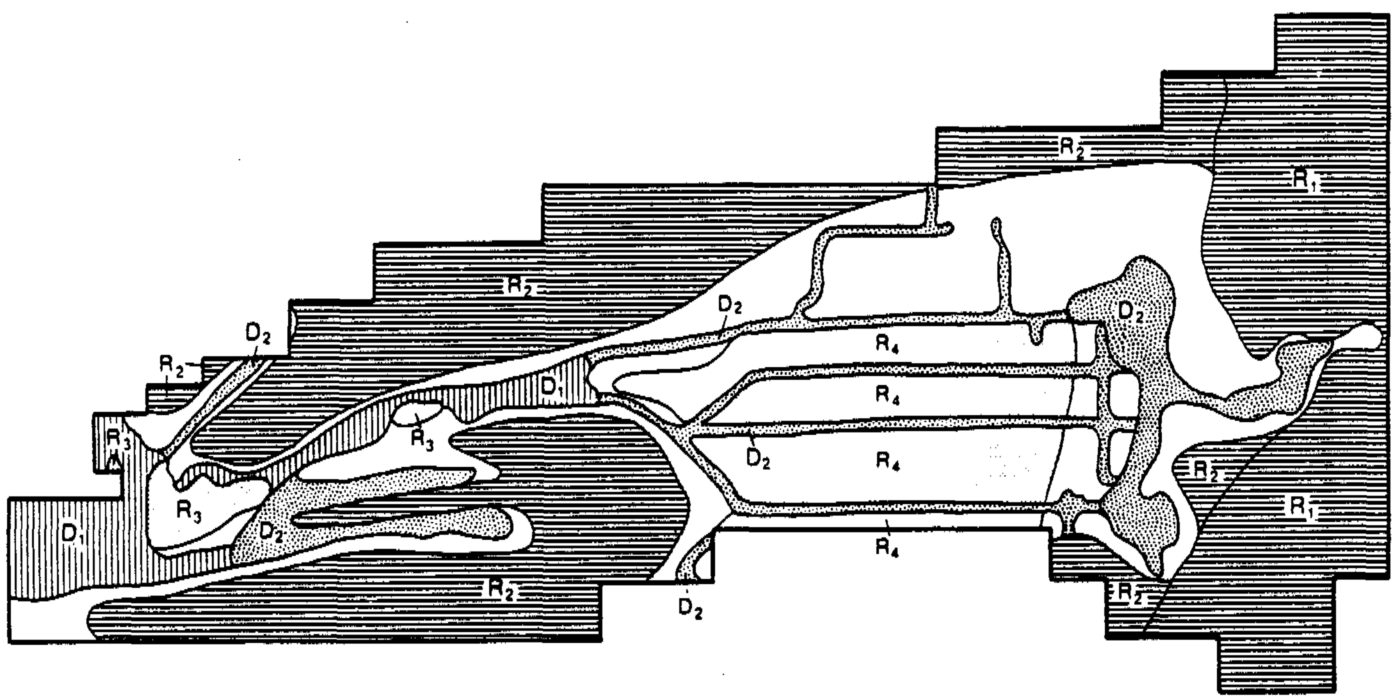

D1 Primary discharge area.

D2 Local (or intermediate) discharge area.

Transitional between recharge and discharge.

R3 Recharge induced by a dam.

R4 Recharge area for local (or intermediate) flow system.

R2 Secondary recharge area associated with groundwater divide between streams tributary to the regional discharge stream.

R1 Primary recharge area associated with a regional groundwater divide.

Fig. 7. Recharge map based on field observations (after Faustini, 1985, Plate 7).

Table 2. Comparison of Recharge and Discharge Rates and Areas, and Basin Yield, for Various Models

Model	*K, ft/sec*	*Recharge area* (% of total)	*Discharge area* (% of total)	*Average recharge* (in./yr)	*Average discharge* (in./yr)	*Basin yield* (in./yr)
8/84	3×10^{-3}	57.5	42.5	13.0	−17.6	7.5
8/84	2×10^{-3}	57.5	42.5	8.6	−11.7	5.0
Coarse	3×10^{-3}	57.4	42.6	8.0	−10.8	4.6
Fine	3×10^{-3}	54.5	45.5	24.1	−28.6	13.0
4/84	3×10^{-3}	57.2	42.8	15.9	−21.3	9.1
12/83	3×10^{-3}	56.3	43.7	13.1	−16.9	7.4
Ditch	3×10^{-3}	58.9	41.1	11.2	−21.0	6.6

Average recharge = (Total recharge)/(Total recharge area).
Average discharge = (Total discharge)/(Total discharge area).
Basin yield = (Total flux through system)/(Total area).
Total recharge = Total discharge, at steady state.

(e.g., Freeze and Witherspoon, 1967, Figures 1c and 4a), Freeze and Cherry (1979, p. 197) observe that "discharge areas commonly constitute only 5-30% of the surface area of a watershed."

Two checks on these rates were used: first, net annual recharge rates cannot exceed precipitation (31 in./yr in Portage County), and should be considerably less because of evapotranspiration. In applying the method, however, calculated rates exceed precipitation at several cells. A high-recharge cell may be caused by a lens of low-conductivity material that was not detected in drilling and therefore not included in the model. Unexpectedly high rates may also be caused by interpolation errors in discretizing the water table.

A second check on the magnitudes of the mapped rates is to compare the net annual recharge for the entire model to the annual basin yield. The net annual recharge is calculated by dividing the recharge volume by the total model area. For a steady-state model, the volumetric recharge rate equals the volumetric discharge rate, so either can be used to calculate basin yield. Holt (1965) estimated that the annual discharge from streams in the region averages 10.3 in./yr, or 6.8 in./yr during dry periods. The net annual recharge for this model is 7.45 in./yr for August 1984. Because the August water table was measured during a relatively dry period, the calculated net recharge rate over the entire basin agrees with Holt's (1965) estimate of the basin yield.

SENSITIVITY ANALYSIS

We checked the method's sensitivity to discretization, hydraulic conductivity, and head by changing each of these in turn, and observing how the change affected the recharge pattern and rates.

Discretization

To test the sensitivity of the mapping method to cell spacing, we used three different discretizations, with nodal spacings of 0.25 to 0.5 miles ("fine" grid, not shown), 0.5 to 1.0 miles (Figure 3), and 1 to 2 miles ("coarse" grid, not shown). Comparing the basin yields for these three models (Table 2, last column) shows that cell spacing affects the modeled yields profoundly, raising the question of how one should choose the cell spacing. Ideally, one would continue refining the grid until changes between successive simulations become acceptably small. Like other hydrologic parameters, however, recharge appears to be scale-dependent: the apparent recharge for a basin increases as the cell spacing decreases. Local flow systems, which account for much of the recharge and discharge within a basin, occur at all scales, so by using a smaller cell spacing, one accounts for more local flow and hence more recharge. Where the cell spacing is larger than local flow path lengths, water discharges in the same cell as it is recharged, resulting in zero net recharge. With increasing cell spacing, one overlooks increasing amounts of "intranodal flow" (Feinstein, 1986). At the limit net recharge is zero if a closed basin is viewed as a single cell, and net recharge should approach net infiltration if a fine cell spacing is used.

Increased recharge with small cell spacing can also be an artifact of the data collection and modeling. In detailed water-table maps constructed using geophysical methods, the water table is not artificially smoothed by interpolation between piezometers and can be quite irregular (Geoff Bohling, 1988, pers. comm.). If equally detailed hydraulic conductivity data are not available, calculated recharge rates may be unrealistically high because water-table irregularities arise from both recharge and conductivity variation. We conclude that

1. Recharge may be scale-dependent. This idea could be tested using mathematical models.

2. The choice of cell spacing is constrained by data availability. If one wishes to equate recharge with basin yield, a cell spacing that captures the general water-table curvature is appropriate. In defense of this vague guideline, we are in much the same position as someone establishing guidelines for piezometer placement: in both cases, one wishes to avoid over-interpolation.

Hydraulic Conductivity

Changing the hydraulic conductivity for the entire basin does not affect the pattern of recharge and discharge, but rates are affected. In many hydrogeologic problems, recharge rates are of less interest than the distribution of recharge and discharge areas. In these problems it is not necessary to constrain the conductivity with flux measurements since the patterns are insensitive to the magnitude of hydraulic conductivity. Even in heterogeneous aquifers, only relative hydraulic conductivity values may be known, but the patterns will still be valid.

Hydraulic Head

Water-table maps for April 1984 and December 1983 were used to make seasonal recharge maps as a test of the method's sensitivity to head changes. Comparison of the April and August maps (not shown) indicates that local flow systems are developed or enhanced during the spring, especially in the central basin where the water table is shallow (5-15 ft). The basin yield increases to 9.1 in./yr during the spring (Table 2), and average recharge and discharge rates both increase by about 20%. Comparison of the December and August maps shows decreased activity of local flow systems during the winter, especially in the eastern basin where the water table is relatively deep (30-60 ft). The basin yield, average recharge rate, and average discharge rate are similar to those of a dry season. Comparing all the seasonal maps, it is interesting that while fluxes nearly double, the percentage of the basin being recharged remains about the same, approximately 57%, and the general patterns of recharge and discharge are similar from season to season.

THREE-DIMENSIONAL ASPECTS

Modeling the inherently three-dimensional recharge process with a two-dimensional model seems paradoxical: the assumption of horizontal flow is implicit in a two-dimensional areal model, but the flow of interest is the vertical component. We view recharge not as a vector, but as an addition of water to the aquifer. Provided the full thickness of the aquifer is modeled and the lower boundary is impermeable, recharged water effectively flows horizontally when moving toward discharge areas. Where vertical gradients are very large, however, the appropriate hydraulic heads to assign to nodes in a two-dimensional model are not water-table elevations, but averaged heads one would measure in an aquifer screened over its entire thickness.

In complex hydrogeologic settings, three-dimensional models may be necessary. The recharge mapping method for three-dimensional models is similar to the method in two dimensions; the water table is fixed, as in the two-dimensional case, but the heads in the lower layers are calculated with the mathematical model. The flux is calculated between each water-table cell and five adjacent cells, including one below the cell of interest.

CONCLUSIONS

We have presented, demonstrated, and field-checked a method for making recharge maps that is readily available because it is adapted to the USGS Modular Groundwater Flow Model (McDonald and Harbaugh, 1984). The advantage of this method over field measurements of recharge is its dependence on data commonly available from well logs. The method must be used cautiously in the following cases:

1. If head data are widely spaced, the method may not have sufficient resolution to make management decisions about individual wells or properties.

2. Where hydrogeologic data are scarce, predicted recharge and discharge rates must be viewed with skepticism because there is a nonunique relationship between the recharge/discharge pattern and the shape of the water table.

3. If flow is strongly three-dimensional, the method must be applied using a three-dimensional analysis.

Despite these limitations which apply to ground-water flow modeling in general, the method described here is a useful tool for aquifer management. The method can be used to assist field studies, decreasing costs by indicating areas where contaminants might be entering the flow system. The method also should be useful in interpreting concentration data for natural ions, environmental isotopes, and contaminants. The combination of horizontal flow vectors drawn from a water-table map and recharge patterns obtained from the mapping method produces a pseudo-three-dimensional flow map. Such a map provides, at least roughly, the advective flow regime needed to interpret ground-water movement.

ACKNOWLEDGMENTS

This research was supported by the Wisconsin Geological and Natural History Survey. Several graduate students at the University of Wisconsin-Madison contributed to the development of the method, including Doug Rumbaugh, Daniel Feinstein, and Chunmiao Zheng. Tom Osborne and Jim Krohelski provided helpful reviews.

APPENDIX

Modification of the USGS Modular Ground-water Flow Model (McDonald and Harbaugh, 1984) permits the user to calculate recharge to and discharge from a water table. This Appendix describes modifications of the computer code and how to apply the technique.

Code Modifications

Two-Dimensional Models

The example in this paper is a case where flow can be treated as two-dimensional (thin, extensive, permeable aquifer) in which case only one layer is used in the USGS model. Because the water table is specified, there are no active (IBOUND>0) cells, so the model's solution routines are not needed. Some computers require that the solution routines be skipped to avoid terminating the program. Execution goes directly to the budget calculations. The solution routines can be skipped by omitting the following 19 lines from MAIN (McDonald and Harbaugh, 1984, p. 50):

MAIN – Remove the following 19 lines:

```
DO 300 KPER=1,NPER
DO 200 KSTP=1,NSTP
DO 100 KITER=1,MXITER
IF(IUNIT(9).GT.0) CALL SIP1AP(...5 lines total...)
IF(IUNIT(11).GT.0) CALL SOR1AP(...4 lines total...)
IF(ICNVG.EQ.1) GO TO 110
100 CONTINUE
KITER=MXITER
110 CONTINUE
IF(ICNVG.EQ.0) STOP
200 CONTINUE
300 CONTINUE
```

Because the model as originally written does not calculate flows between adjacent inactive (IBOUND.LE.0) cells, subroutine SBCF1F, which calculates flow from specified-head cells to active cells, must be modified to include flows between specified-head cells. Six lines require modification, as follows:

SBCF1F – In the following lines, change .LE. to .EQ.:

```
IF(IBOUND(J-1,I,K).LE.0)GO TO 30
IF(IBOUND(J+1,I,K).LE.0)GO TO 60
IF(IBOUND(J,I-1,K).LE.0)GO TO 90
IF(IBOUND(J,I+1,K).LE.0)GO TO 120
IF(IBOUND(J,I,K-1).LE.0)GO TO 150
IF(IBOUND(J,I,K+1).LE.0)GO TO 180
```

In effect, the flux calculations will be skipped only for no-flow cells, not specified-head cells.

Three-Dimensional Models

Although this paper discusses recharge mapping for a single-layer two-dimensional model, the method is similar for creating a recharge map for the upper layer in a three-dimensional model. Because there are active cells in the layers below the water table, MAIN does not have to be modified as in the two-dimensional case. The changes to SBCF1F are the same as for the two-dimensional case.

Data Entry

Two packages are used: the block-centered flow package (BCF), and output control (OC). If the model is three-dimensional, either the strongly implicit procedure (SIP) or the slice-successive overrelaxation (SOR) package will be used as well.

Basic Package Input

The IBOUND array for the water-table layer will be filled with 0's and −1's. Set all the water-table cells to −1, and cells outside the problem domain to 0. This makes the water table a specified-head surface. The observed heads are entered in the starting-head array (Shead). Head values for the center of each cell are obtained by interpolating between potentiometric contours, either by hand or with a computerized interpolation routine.

Block-Centered Flow Package Input

The simulation is treated as steady state (ISS = 1). The cell-by-cell flow terms must be printed for each specified-head cell, so ICBCFL = −1.

Hydraulic conductivities values for each cell are read in array HY. Bedrock surface (aquifer bottom) elevations are read in array BOT.

Output Control Input

This package enables printing of cell-by-cell flow terms; they are not printed if the default output is used. ICBCFL = 1 to print cell-by-cell flow terms.

Presentation

To contour the recharge and discharge rates, most contouring programs require an input file containing the array dimensions (NROW,NCOL), the cell spacings (DELR(J),DELC(I)), and a listing of fluxes by row and column. Preparing such a file involves reformatting the USGS Model's ouput file.

REFERENCES

Allen, R. M. 1985. Slug test determination of hydraulic conductivity in the Central Sand Plain of Wisconsin. Wisconsin Geological and Natural History Survey, unpublished report.

Blanchard, M. and K. R. Bradbury. 1987. A comparison of office-derived versus field-derived water-table maps for a sandy unconfined aquifer. Ground Water Monitoring Review. v. 7, no. 2, pp. 74-78.

Bradbury, K. R. and E. R. Rothschild. 1985. A computerized technique for estimating the hydraulic conductivity of aquifers from specific capacity data. Ground Water. v. 23, no. 2, pp. 240-245.

Brownell, J. R. 1986. Stratigraphy of unlithified deposits in the Central Sand Plain of Wisconsin. University of Wisconsin, M.S. thesis. 172 pp.

Cooley, R. L., J. W. Fordham, and J. A. Westphal. 1971. Hydrology of the Truckee Meadows, Nevada. Center for Water Resources Research, Desert Research Institute, University of Nevada System. Project Report No. 15. 49 pp.

Faustini, J. M. 1985. Delineation of groundwater flow patterns in a portion of the Central Sand Plain of Wisconsin. University of Wisconsin, M.S. thesis. 117 pp.

Feinstein, D. T. 1986. A three-dimensional model of flow to the sandstone aquifer in northeastern Wisconsin with discussion of contamination potential. University of Wisconsin, M.S. thesis. 240 pp.

Freeze, R. A. 1967. Quantitative interpretation of regional groundwater flow patterns as an aid to water balance studies. International Association of Scientific Hydrology, General Assembly of Berne. Publication 78. pp. 154-173.

Freeze, R. A. and J. A. Cherry. 1979. Groundwater. Prentice-Hall, Inc., Englewood Cliffs, NJ. 604 pp.

Freeze, R. A. and P. A. Witherspoon. 1967. Theoretical analysis of groundwater flow: 2. Effect of water-table configuration and subsurface permeability variation. Water Resources Research. v. 3, pp. 623-634.

Holt, C.L.R., Jr. 1965. Geology and water resources of Portage County, Wisconsin. U.S. Geological Survey Water-Supply Paper 1796. 77 pp.

Karnauskas, R. J. 1977. The hydrogeology of the Nepco Lake watershed in central Wisconsin with a discussion of management implications. University of Wisconsin, M.S. thesis. 249 pp.

Lappala, E. G. 1978. Quantitative hydrogeology of the Upper Republican Natural Resources District, southwest Nebraska. U.S. Geological Survey Water-Resources Investigations 78-38. 200 pp.

Lippelt, I. D. and R. G. Hennings. 1981. Irrigable lands inventory—phase I. Groundwater and related information. Wisconsin Geological and Natural History Survey Miscellaneous Paper 81-1.

McDonald, M. G. and A. W. Harbaugh. 1984. A modular three-dimensional finite-difference ground-water flow model. U.S. Geological Survey Open-File Report 83-875. 528 pp.

Rehm, B. W., G. H. Groenewold, and W. M. Peterson. 1982. Mechanisms, distribution and frequency of groundwater recharge in an upland area of western North Dakota. North Dakota Geological Survey. Report of Investigation No. 75. 72 pp.

Rothschild, E. R. 1982. Hydrogeology and contaminant transport modeling of the Central Sand Plain of Wisconsin. University of Wisconsin, M.S. thesis. 135 pp.

Sophocleous, M. and C. A. Perry. 1984. Experimental studies in natural groundwater-recharge dynamics. Assessment of recent advances in instrumentation. Journal of Hydrology. v. 70, pp. 369-382.

Sophocleous, M. and C. A. Perry. 1985. Experimental studies in natural groundwater-recharge dynamics: the analysis of observed recharge events. Journal of Hydrology. v. 81, pp. 297-332.

Stallman, R. W. 1956. Numerical analysis of regional water levels to define aquifer hydrology. Transactions of the American Geophysical Union. v. 37, no. 4, pp. 451-460.

Stoertz, M. W. 1985. Evaluation of groundwater recharge in the Central Sand Plain of Wisconsin. University of Wisconsin, M.S. thesis. 159 pp.

Tanaka, H. H. and J. R. Hollowell. 1966. Hydrology of the alluvium of the Arkansas River, Muskogee, Oklahoma, to Fort Smith, Arkansas. U.S. Geological Survey Water-Supply Paper 1809-T. 42 pp.

Weeks, E. P. 1964. Use of water-level recession curves to determine the hydraulic properties of glacial outwash in Portage County, Wisconsin. U.S. Geological Survey Professional Paper 501-B. pp. 181-184.

Weeks, E. P. 1969. Determining the ratio of horizontal to vertical permeability by aquifer test analysis. Water Resources Research. v. 5, no. 1, pp. 196-214.

Weeks, E. P. and M. L. Sorey. 1973. Use of finite-difference arrays of observation wells to estimate evapotranspiration from ground water in the Arkansas River Valley, Colorado. U.S. Geological Survey Water-Supply Paper 2029-C. 27 pp.

Weeks, E. P. and H. G. Stangland. 1971. Effects of irrigation on streamflow in the Central Sand Plain of Wisconsin. U.S. Geological Survey Open-File Report. 113 pp.

Zheng, C. and M. P. Anderson. 1985. Significance of streams as hydrogeological boundaries. EOS. v. 66, no. 46, p. 888.

* * * * *

Mary W. Stoertz received her B.S. in Geology (1981) from the University of Washington and her M.S. in Hydrogeology (1985) from the University of Wisconsin-Madison, where she currently is working toward a Ph.D. in Hydrogeology and Civil Engineering. Her research areas include natural ground-water recharge, ground-water parameter estimation, and measuring and modeling flow in the unsaturated zone.

Kenneth R. Bradbury received his B.A. (1974) from Ohio Wesleyan University, his A.M. (1977) from Indiana University, and his Ph.D. (1982) from the University of Wisconsin-Madison. Currently a Research Hydrogeologist with the Wisconsin Geological and Natural History Survey, his interests include ground-water field techniques, ground-water parameter estimation, and ground-water modeling.

Statistics

COMPUTER NOTES

THREE-DIMENSIONAL, CROSS-SEMIVARIOGRAM CALCULATIONS FOR HYDROGEOLOGICAL DATA

by Jonathan D. Istok[a], Richard M. Cooper[b], and Alan L. Flint[c]

Abstract. Geostatistics is a powerful tool for the analysis of hydrogeological data, but few well-documented computer programs for performing the necessary calculations have been presented in the technical literature. This is especially true for applications that require either three-dimensional or multivariate analyses. This paper describes a FORTRAN subroutine, VARIO, that can be used to compute experimental direct- and cross-semivariograms from a set of sample data, for any specified direction in one-, two-, or three-dimensional space. The subroutine combines into groups those sample pairs that fall within predetermined angular tolerances of the specified direction. The number of sample pairs used to compute the value of the experimental semivariogram at each value of separation can be specified in four different ways, depending on the nature of the available data. Written in FORTRAN 77, VARIO can be used on any computer that supports a FORTRAN 77 compiler. Source code listing, user instructions, and example input and output data for VARIO are presented.

Introduction

Whenever we make measurements at points distributed in space, we may refer to the quantity we are measuring as a *regionalized variable.* Some examples of regionalized variables in the field of hydrogeology are hydraulic conductivity, transmissivity, porosity, water-table elevation, ground-water temperature, and ground-water contaminant concentrations. The term *geostatistics* refers to a set of statistical procedures (1) for describing the spatial correlation displayed by regionalized variables, and (2) for using theoretical models of this spatial correlation to obtain local and global estimates for regionalized variables over the sample space. Geostatistical procedures are proving to be useful for solving a variety of practical problems in hydrogeology including determining values of aquifer parameters for input into numerical models of ground-water flow and solute transport (Delhomme, 1976; Neuman and Yakowitz, 1980; Vauclin *et al.*, 1983), mapping ground-water levels over large areas, and determining the severity of ground-water contamination at hazardous waste sites (Cooper and Istok, 1988a, b). Several reference texts are available that describe the theory of geostatistics (David, 1977; Journel and Huijbregts, 1978; Clark, 1979), but few well-documented computer programs have been presented in the technical literature. This is especially true for applications that require three-dimensional or multivariate analyses.

Essential to a geostatistical analysis are *direct-* and *cross-semivariograms* (defined in the Theory section). In the case of one- and two-dimensional problems, computer programs may be easily written to compute direct-semivariograms (Journel and Huijbregts, 1978). However, many problems in hydrogeology are truly three-dimensional and the use of direct-semivariograms based on a one- or two-dimensional approximation of the problem domain is not realistic. Also, in many situations (e.g., when more than one type of measurement is made at each sample point) it may be useful to study several regionalized variables simultaneously. If we determine that some of the regionalized variables are intercorrelated, the use of direct-semivariograms (which only display the spatial correlation of a single regionalized variable) is not sufficient. Instead, a multivariate geostatistical analysis is required, and this necessitates the use of direct-semivariograms computed for each regionalized variable and cross-semivariograms computed for each pair of intercorrelated regionalized variables. Procedures for the general problem of computing cross-semivariograms in three-dimensional space are more complex and for this reason are not widely used. To our knowledge, a computer program for performing these calculations previously has not been reported in the technical literature.

The objective of this paper is to describe a FORTRAN subroutine, VARIO, that can be used to compute direct- or cross-semivariograms from a set of sample data for any specified direction in

---

[a] Assistant Professor, Department of Agricultural Engineering, Oregon State University, Corvallis, Oregon 97331.

[b] Water Resources Engineer, Water Resources Division, South Florida Water Management District, P.O. Box V, West Palm Beach, Florida 33402.

[c] Hydrologist, U.S. Geological Survey, Mercury, Nevada 89023.

Received April 1987, revised February 1988, accepted Feburary 1988.

Discussion open until March 1, 1989.

one-, two-, or three-dimensional space. The subroutine can be used as either an exploratory tool, or as one component of a general purpose geostatistical software package. Future papers will describe subroutines for fitting theoretical models to the semivariograms computed by VARIO, and for using the fitted models to obtain local and global estimates for regionalized variables over the sample space. It is hoped that the publication of these subroutines will promote a more widespread use of geostatistics in the field of hydrogeology.

Theory

We are concerned here with a set of measurements made at an arbitrary number of sample points distributed in one-, two-, or three-dimensional space. The position of a sample point could be specified in a variety of ways, depending on the type of measurement. For example, if the measurements were made on core or ground-water samples, the position of each sample point would probably be specified by the location of the borehole, the elevation of the drill collar, and the depth from the drill collar to the center of the sample. To simplify the following discussion, however, we will assume that the position of each sample point has been specified by a set of coordinates represented by the vector x with components (x_u), (x_u, x_v), or (x_u, x_v, x_w) according to whether a one-, two-, or three-dimensional sample space is considered. The collection of sample points is represented by the set $(x_1, \ldots, x_N)$ where N is the number of sample points. At each sample point x_k, as many as M types of measurements may be made, and these are represented by the set $\{z_1(x_k), \ldots z_M(x_k), k = 1 \text{ to } N\}$.

For the following geostatistical procedures to be strictly valid, it is required that (1) the sizes (e.g., the volume or the mass) of all the samples are the same, (2) the same sampling procedures are used to obtain each sample, (3) the same measurement procedures are used for each measurement of the same type, and (4) the dimensions of the samples are much smaller than the dimensions of the sample space. These requirements are collectively referred to as the requirement for *constant* and *point support.* These requirements are satisfield approximately in most applications encountered in hydrogeology, but in cases where they are not, an additional procedure called *regularizaton* may be required (Rendu, 1978).

For many geostatistical techniques, it is also required that the regionalized variables are *normally distributed* (e.g., when using kriging to estimate the value of a variable at a point, deviations from a normal distribution may result in biased estimates). The probability that the regionalized variables are normally distributed may be determined from any of several statistics, e.g., the chi-squared statistic (Henley, 1981), the Kolmogorov-Smirnov statistic (Henley, 1981), or the Shapiro-Wilk statistic (SAS Institute, 1985). In many cases, a log-transformation will improve the fit of the regionalized variables to a normal distribution (Cooper and Istok, 1988b). A class of geostatistical methods called *indicator* geostatistics has been developed for the case where the regionalized variables are not normally distributed (Journel and Isaaks, 1984).

Procedure for Semivariogram Calculation

The first step in a geostatistical analysis is *structural analysis,* the determination of the statistical structure of the spatial correlation displayed by the experimental data. The first step in a structural analysis is to perform a detailed review of all the available data to determine if some or all the spatial correlation displayed by the data can be attributed to known geologic, geographic, topographic, or other factors. Particular attention should be paid to factors that cause trends or discontinuities in the data. For example, an observed trend in measured values of saturated thickness in an alluvial aquifer may be caused by the pattern of deposition (e.g., in an alluvial fan). Faults and nonconformities can often cause abrupt changes in measured values of regionalized variables. For example, measured values of porosity might change abruptly along a transect if the transect crosses a fault that juxtaposes two different lithostratigraphic units.

The next step in a structural analysis is to try to develop a theoretical model to quantify the pattern of spatial correlation displayed by the data and, in general, this requires the calculation of several experimental *direct-* and *cross-semivariograms.*

The experimental *direct-semivariogram,* $\gamma_{ii}(h)$, is a measure of the spatial correlation displayed by pairs of measured values of a single variable i. The experimental *cross-semivariogram,* $\gamma^*_{ij}(h)$, is a measure of the spatial correlation displayed by pairs of measured values, of two different variables i and j. Both types of semivariograms are defined by

$$\gamma^*_{ij}(h) = \frac{1}{2N(h)} \sum_{i=1}^{N(h)} [z_i(x_k) - z_i(x_k + h)]\,[z_j(x_k) - z_j(x_k + h)] \qquad (1)$$

where h is the vector separating a pair of sample points, and N(h) is the number of pairs of samples that are separated by the same vector h. Equation (1) defines the cross-semivariogram for regionalized variables i and j. When only one regionalized variable is considered, $j = i$, and equation (1) defines the direct-semivariogram for the regionalized variable i.

In a geostatistical analysis, semivariograms usually will be calculated for several specified directions for h. If all the semivariograms are equivalent, the *regionalization* (the underlying natural phenomenon that the regionalized variable represents) is said to be *isotropic*. When the spatial structure of a regionalized variable is not the same in every direction chosen for h, we say that the regionalization is *anisotropic*. The source of anisotropy depends on the type of regionalized variable studied. For example, anisotropy in the physical or chemical properties of alluvial aquifers may be caused by depositional processes. Similarly, anisotropy in ground-water contaminant distributions may be caused by dispersion or by an anisotropic ground-water flow pattern. Whatever the source, anisotropy in a regionalization will cause experimental semivariograms to be anisotropic. Since we will seldom know prior to our analysis if the regionalization is isotropic, we must be able to calculate semivariograms as a function of both the direction and magnitude of h

$$\gamma^*_{ij}(h) = \gamma^*_{ij}(\alpha, \beta, |h|) \qquad (2)$$

where α and β are two angles that define the orientation of h in three-dimensional space (see below), and $|h|$ is the magnitude of h. Thus, to perform a geostatistical structural analysis on a set of measured values of a regionalized variable, a procedure is needed to compute the values of experimental semivariograms for any specified direction and magnitude of h.

Conceptually, this procedure is simple. The steps are as follows:

1. Select a particular direction h_0 by specifying the angles α_0 and β_0 and the distance $|h_0|$.

2. Find all possible pairs of sample points that are aligned in the specified direction.

3. If a direct-semivariogram is to be computed, retain only those pairs of sample points that have measured values of the regionalized variable for which the direct-semivariogram is being computed. If a cross-semivariogram is to be computed, retain only those pairs of sample points that have measured values of the *two* specified regionalized variables for which the cross-semivariogram is being computed.

4. Group the sample pairs into categories of $|h|$ and substitute the measured values at each pair of retained sample points into equation (1).

In practice, performing these calculations can be difficult, primarily because the number of samples available for a geostatistical analysis is usually small and because the measurement points are usually irregularly distributed over the sample space. This means that if we limit the semivariogram calculations to only those pairs of samples points that are *exactly* aligned in the specified direction, an insufficient number of pairs of sample points will be available to accurately define the values of $\gamma^*_{ij}(h)$ [e.g., Journel and Huijbregts, 1978, p. 194, suggest that a minimum of 30 to 50 pairs of sample points are required for each value of $\gamma^*_{ij}(h)$]. This problem often can be avoided by performing the semivariogram calculations using those pairs of sample points that are *approximately* aligned in the specified direction. This is done by specifying angular tolerances for α_0 and β_0, $\Delta\alpha_0$ and $\Delta\beta_0$.

Consider a pair of sample points x_1 and x_2. In three-dimensional space, each point is defined by a set of coordinates (x_u, x_v, x_w). The separation vector $h = x_2 - x_1$ has components

$$h_u = x_u)_2 - x_u)_1 \qquad (3a)$$

$$h_v = x_v)_2 - x_v)_1 \qquad (3b)$$

$$h_w = x_w)_2 - x_w)_2 \qquad (3c)$$

where the term $x_u)_1$, for example, is the x_u coordinate of sample point x_1. The position of h in space also can be defined by two angles, α_h and β_h in the $x_u - x_v$ and $x_v - x_w$ planes where

$$\alpha_h = \arctan(h_v/h_u) \qquad (4a)$$

$$\beta_h = \arccos(h_w/|h|) \qquad (4b)$$

and $|h| = \sqrt{h_u + h_v + h_w}$ is the magnitude of h.

Following the procedure outlined above, the pair of measured values at the points x_1 and x_2 are used in the calculation of $\gamma^*_{ij}(\alpha_0, \beta_0, |h|)$ only if h is aligned with the specified direction h_0. Alignment of the pair of sample points with the specified direction is indicated if

$$\alpha_0 - \Delta\alpha_0 \leqslant \alpha_h \leqslant \alpha_0 + \Delta\alpha_0 \qquad (5a)$$

and $$\beta_0 - \Delta\beta_0 \leqslant \beta_h \leqslant \beta_0 + \Delta\beta_0 \qquad (5b)$$

These criteria are illustrated in Figure 1. If we wish to compute semivariograms for the isotropic case (i.e., the case that the experimental semivariograms are independent of α_0 and β_0), the criteria in equation (5) still can be used if $\Delta\alpha_0$ and $\Delta\beta_0$ are both set equal to 180°.

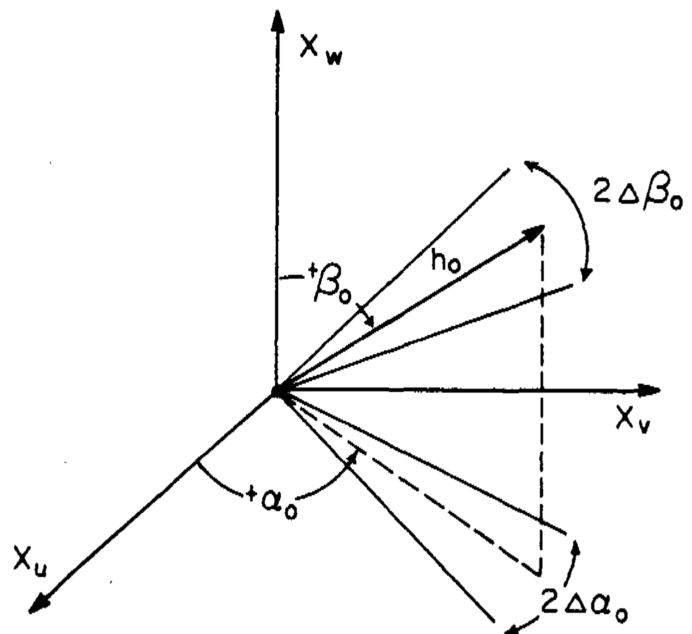

$-90° \leq \alpha_0 \leq 90° \quad 0 \leq \Delta\alpha_0 \leq 180°$

$-90° \leq \beta_0 \leq 90° \quad 0 \leq \Delta\beta_0 \leq 180°$

Fig. 1. Definition of angles and angular tolerances used to specify a direction h_0.

Once all the pairs of sample points aligned with a specified h_0 have been identified, they are grouped into categories of $|h|$. In general, four different methods can be used to perform the grouping operation. The choice of which method to use for a particular problem will depend on the number of sample points and on the way that the sample points are distributed in space. One criteria, for example, is that pairs of sample points with greatly different values of $|h|$ should not be combined because this will result in a smoothing of the semivariogram. The initial step for all these methods is the same; the pairs of aligned sample points are sorted, from smallest to largest, using the value of $|h|$ for each pair. Then the sample pairs are combined into groups by one of four methods:

Method 1: Divide the range of $|h|$ values into intervals of constant size. $|h|$ values are grouped according to the interval in which they occur. The number of pairs of sample points in each group will be different.

Method 2: Divide the range of $|h|$ values into intervals of variable size. $|h|$ values are grouped according to the interval in which they occur. The number of pairs of sample points in each group will be different.

Method 3: Specify the number of sample pairs to place in each group. The number of pairs of sample points in each group will be the same. The size of the intervals of $|h|$ is variable.

Method 4: Put each unique value of $|h|$ into a separate group. The number of pairs of sample points in each group will be different.

Whichever method is used, the measured values of the regionalized variable(s) for each pair of sample points in a group are substituted into equation (1) to compute the value of γ_{ij}^* for that group. The mean value of $|h|$ for a group (which is the value that will be plotted on the semivariograms) then can be computed by averaging the $|h|$ values for all the pairs of sample points in the group.

Computer Implementation—Subroutine VARIO

The FORTRAN subroutine VARIO was written to implement the procedures described above. VARIO can compute either direct- or cross-semivariograms from a set of sample data, for any specified direction in one-, two-, or three-dimensional space. The maximum number of sample points is limited only by the available computer memory and can be adjusted by changing the value of parameter MAX1, currently set at 100. Each sample point can have any number of regionalized variables in addition to the x_u (x_u, x_v), or (x_u, x_v, x_z) coordinates of the point. The subroutine has been tested and compiled on IBM compatible microcomputers using the Microsoft FORTRAN 77 compiler (version 3.3). The particular machines used had 640 Kbytes of RAM.

The definitions of FORTRAN variables used in VARIO are in Table 1, and the source code

Table 1. Variables Passed to VARIO from Calling Program

DIM	= Dimension of problem (1, 2, or 3).
ALPHA	= Specified direction in X_u - X_v plane (-90° ≤ ALPHA ≤ 90°).
DALPHA	= Tolerance for alpha (0 ≤ DALPHA ≤ 180°).
BETA	= Specified direction in X_v-X_v plane (-90° ≤ BETA ≤ 90°).
DBETA	= Tolerance for beta (0 ≤ DBETA ≤ 180°).
REVI	= Column number of first regionalized variable.
REVJ	= Column number of second regionalized variable. If REVI = REVJ then a direct-semivariogram be computed. REVI = REVJ then a cross-semivariogram will be computed.
LOGTRAN	= Flag to indicate if semivariograms will be computed on the natural logarithm of the values of the regionalized variable. If LOGTRAN = 1, natural logarithms of the values of the regionalized variable(s) will be used. If LOGTRAN = 0, the original values of the regionalized variable(s) will be used.
METHOD	= Choice of grouping method to use for |h| (1, 2, 3, or 4).
LIMITS(1)	= Interval size(s) for |h| if METHOD = 1 or 2. Number of sample pairs in each group if METHOD = 3. Not used if METHOD = 4.
.	
.	
.	
LIMITS(30)	
INFILE	= Input data file name (≤ 20 characters).
OUTFILE	= Output data file name (≤ 20 characters).
TITLE1	= First title for OUTFILE (≤ 80 characters).
TITLE2	= Second title for OUTFILE (≤ 80 characters).

```
      SUBROUTINE VARIO(DIM,ALPHA,DALPHA,BETA,DBETA,REVI,REVJ,
     1         LOGTRAN,METHOD,LIMITS,TITLE1,TITLE2,INFILE,OUTFILE)
      PARAMETER (MAX1=100, MAX2=2000)
      INTEGER DIM, METHOD, GROUPN, GN, GCOUNT, GNUM, REVI, REVJ
      REAL LIMITS(30), LOWXY, LOWYZ
      CHARACTER*20 INFILE, OUTFILE
      CHARACTER*80 TITLE1, TITLE2
      COMMON /BLK1/ XUVW(MAX1,3)
      COMMON /BLK2/ GROUPH(MAX2), GROUPZ(MAX2), GROUPN(MAX2)
      COMMON /BLK3/ GH(MAX2), GN(MAX2), NREF(MAX2), GCOUNT, GNUM
      COMMON /BLK4/ Z(MAX1,2)
      DATA PI/3.141592654/
C
C ..... OPEN INPUT AND OUTPUT DATA FILES
C
      OPEN(5, FILE=INFILE)
      OPEN(6, FILE=OUTFILE, STATUS='NEW')
C
C ..... WRITE HEADINGS TO OUTPUT FILE
C
      WRITE (6,10) TITLE1, TITLE2
 10   FORMAT (15X,A80/15X,A80/)
      WRITE (6,20) INFILE, DIM
 20   FORMAT (11X,'INPUT DATA FILE: ',A20,6X,'DIMENSIONS: ',I2/)
      WRITE (6,30) ALPHA, BETA, DALPHA, DBETA
 30   FORMAT (11X,'SPECIFIED DIRECTION:'//
     1        23X,'ALPHA = ',F6.2,5X,'BETA = ',F6.2/
     2        22X,'DALPHA = ',F6.2,4X,'DBETA = ',F6.2/)
      IF (REVI .EQ. REVJ) THEN
        WRITE (6,40) REVI
 40     FORMAT (11X,'DIRECT-SEMIVARIOGRAM FOR REGIONALIZED',
     1           ' VARIABLE ',I2)
      ELSE
        WRITE (6,50) REVI, REVJ
 50     FORMAT (11X,'CROSS-SEMIVARIOGRAM FOR REGIONALIZED',
     1           ' VARIABLES ',I2,' AND ',I2)
      ENDIF
      WRITE (6,60)
 60   FORMAT (6X,68('-')/
     1        18X,'GROUP',5X,'AVERAGE',5X,'NO. OF'/
     2        19X,'NO.',9X,'H',8X,'PAIRS',11X,'GAMMA(H)'/
     3        18X,5('-'),5X,7('-'),5X,6('-'),8X,11('-')/)
C
C ..... CONVERT ANGLES FROM DEGREE TO RADIANS
C
      CON = PI / 180.
      ALPHA = ALPHA * CON
      DALPHA = DALPHA * CON
      BETA = BETA * CON
      DBETA = DBETA * CON
      UPXY = ALPHA + DALPHA / 2.0
      LOWXY = ALPHA - DALPHA / 2.0
      UPYZ = BETA + DBETA / 2.0
      LOWYZ = BETA - DBETA / 2.0
C
C ..... CHECK FOR VALID INPUT VALUES. IF CHECKS FAIL,  PRINT ERROR
C       MESSAGE AND STOP
C
      IF ((DIM .LT. 1) .OR. (DIM .GT. 3)) CALL ERROR(1)
      IF ((REVI .LT. 1) .OR. (REVJ .LT. 1)) CALL ERROR(3)
      IF ((LOGTRAN .GT. 1) .OR. (LOGTRAN .LT. 0)) CALL ERROR(4)
      IF ((METHOD .GT. 4) .OR. (METHOD .LT. 1)) CALL ERROR(5)
      CON = PI / 2.
      IF ((ALPHA .GT. CON) .OR. (ALPHA .LT. -CON) .OR.
     1    (BETA .GT. CON) .OR. (BETA .LT. -CON) .OR.
     2    (DALPHA .GT. PI) .OR. (DALPHA .LT. 0.) .OR.
     3    (DBETA .GT. PI) .OR. (DBETA .LT. 0.)) CALL ERROR(6)
C
C ..... I N I T I A L I Z A T I O N
C
      DO 70 I=1, MAX2
        GROUPH(I) = 0.
        GROUPZ(I) = 0.
        GROUPN(I) = 0
        GH(I) = 0.
        GN(I) = 0
        NREF(I) = 0
 70   CONTINUE
      GNUM = 0
      GCOUNT = 0
C
C ..... READ FROM INPUT FILE: (XUVW(1,I),I=1,DIM),  Z(1,1) AND  Z(1,2)
C                                      ...             ...          ...
C                             (XUVW(NX,I),I=1,DIM), Z(NX,1) AND Z(NX,2)
C
      IF (REVJ .LT. REVI) THEN
        I = REVI
        REVI = REVJ
        REVJ = I
      ENDIF
      NX=1
      IF (REVI .EQ. 1) THEN
        IF (REVJ .EQ. 1) THEN
 80       READ(5,*,END=140) (XUVW(NX,I),I=1,DIM),Z(NX,1)
          IF (Z(NX,1) .NE. -999.) NX = NX + 1
          GOTO 80
        ELSEIF (REVJ .EQ. 2) THEN
 90       READ(5,*,END=140) (XUVW(NX,I),I=1,DIM),Z(NX,1),Z(NX,2)
          IF (Z(NX,1).NE.-999. .AND. Z(NX,2).NE.-999.) NX = NX + 1
          GOTO 90
        ELSEIF (REVJ .GT. 2) THEN
 100      READ(5,*,END=140) (XUVW(NX,I),I=1,DIM),Z(NX,1),
     1                   (DMY,I=1,REVJ-REVI-1),Z(NX,2)
          IF (Z(NX,1).NE.-999. .AND. Z(NX,2).NE.-999.) NX = NX + 1
          GOTO 100
        ENDIF
```

Fig. 2. Source code listing for VARIO (continued).

```
      ELSE
        IF (REVJ .EQ. REVI) THEN
 110      READ(5,*,END=140) (XUVW(NX,I),I=1,DIM),(DMY,I=1,REVI-1),
     1                      Z(NX,1)
          IF (Z(NX,1) .NE. -999.) NX = NX + 1
          GOTO 110
        ELSEIF (REVJ .EQ. REVI + 1) THEN
 120      READ(5,*,END=140) (XUVW(NX,I),I=1,DIM),(DMY,I=1,REVI-1),
     1                      Z(NX,1),Z(NX,2)
          IF (Z(NX,1).NE.-999. .AND. Z(NX,2).NE.-999.) NX = NX + 1
          GOTO 120
        ELSE
 130      READ(5,*,END=140) (XUVW(NX,I),I=1,DIM),(DMY,I=1,REVI-1),
     1                  Z(NX,1),(DMY,I=1,REVJ-REVI-1),Z(NX,2)
          IF (Z(NX,1).NE.-999. .AND. Z(NX,2).NE.-999.) NX = NX + 1
          GOTO 130
        ENDIF
      ENDIF
 140  NX=NX - 1
      IF (NX .GT. MAX1) THEN
        WRITE(*,150) ' DATA ',NX,MAX1
 150    FORMAT(A,'SIZE OF',I5,' EXCEEDS MAXIMUM SIZE OF',I5/' STOP!')
        GOTO 180
      ENDIF
C
C ..... FIND ALL ALIGNED PAIRS OF MEASUREMENT POINTS, AND PUT THE
C       COMPUTED SEPARATION AND MEASURED VALUES FOR THE PAIR INTO
C       TEMPORARY STORAGE (ONE-DIMENSIONAL PROBLEMS)
C
      IF (REVJ .EQ. REVI) THEN
        REVJ = 1
      ELSE
        REVJ = 2
      ENDIF
      REVI = 1
      CALL FINDPTS(DIM,METHOD,LOGTRAN,NX,1,REVI,REVJ,UPXY,LOWXY,UPYZ,
     1             LOWYZ)
      IF (GCOUNT .GT. MAX2) THEN
        WRITE(*,150) ' EXPANDED DATA ',GCOUNT,MAX2
        GOTO 180
      ENDIF
      CALL SETGROUP(METHOD, LIMITS)
      CALL FINDPTS(DIM,METHOD,LOGTRAN,NX,2,REVI,REVJ,UPXY,LOWXY,UPYZ,
     1             LOWYZ)
      DO 160 I=1, GCOUNT
        IF (GROUPN(I) .NE. 0) THEN
          GROUPH(I) = GROUPH(I) / GROUPN(I)
          GROUPZ(I) = GROUPZ(I) / (2 * GROUPN(I))
        ENDIF
        WRITE (6,170) I, GROUPH(I), GROUPN(I), GROUPZ(I)
 160  CONTINUE
 170  FORMAT (17X,I4,6X,G8.3,7X,I3,5X,G15.7)
 180  CLOSE(5,STATUS='KEEP')
      CLOSE(6,STATUS='KEEP')
      RETURN
      END
C
      SUBROUTINE SWAP(M, N)
      L=M
      M=N
      N=L
      RETURN
      END
C
      SUBROUTINE FINDPTS(DIM,METHOD,LOGTRAN,NX,NCHOICE,REVI,REVJ,UPXY,
     1                   LOWXY,UPYZ,LOWYZ)
      PARAMETER (MAX1=100, MAX2=2000)
      INTEGER DIM, GROUPN, GN, METHOD, GCOUNT, GNUM, REVI, REVJ
      REAL LOWXY, LOWYZ, HU, HV
      LOGICAL CHANGE
      COMMON /BLK1/ XUVW(MAX1,3)
      COMMON /BLK2/ GROUPH(MAX2), GROUPZ(MAX2), GROUPN(MAX2)
      COMMON /BLK3/ GH(MAX2), GN(MAX2), NREF(MAX2), GCOUNT, GNUM
      COMMON /BLK4/ Z(MAX1,2)
      REAL XU(MAX1), XV(MAX1), XW(MAX1)
      EQUIVALENCE (XU,XUVW(1,1)), (XV,XUVW(1,2)), (XW,XUVW(1,3))
      DATA PI/3.141592654/
      IF (DIM .EQ. 1) THEN
        DO 140 J = 1, NX - 1
          DO 140 I = J + 1, NX
            IF ((XU(J) .EQ. XU(I)) .OR. (Z(J,REVI) .LE. -990) .OR.
     1          (Z(J,REVJ) .LE. -990.) .OR. (Z(I,REVI) .LE. -990.)
     2          .OR. (Z(I,REVJ) .LE. -990.)) GOTO 140
            HU=XU(I) - XU(J)
            DIST=SQRT(HU**2)
            CALL COMPUTE(LOGTRAN, ZVALUE, I, J, REVI, REVJ)
            CALL ADDREC(METHOD, NCHOICE, DIST, ZVALUE)
 140    CONTINUE
C
C       FIND ALL ALIGNED PAIRS OF MEASUREMENT POINTS, AND PUT THE
C       COMPUTED SEPARATION AND MEASURED VALUES FOR THE PAIR INTO
C       TEMPORARY STORAGE (TWO-DIMENSIONAL PROBLEMS)
C
      ELSE IF (DIM .EQ. 2) THEN
        DO 150 J=1, NX-1
          DO 150 I=J+1, NX
            IF ((XU(J) .EQ. XU(I)) .AND. (XV(J) .EQ. XV(I)) .OR.
     1        (Z(J,REVI) .LE. -990.) .OR. (Z(J,REVJ) .LE. -990.) .OR.
     2          (Z(I,REVI) .LE. -990.) .OR. (Z(I,REVJ) .LE. -990.))
     3          GOTO 150
C
C       FIND THE SEEPARATION VECTOR FOR A PAIR OF SAMPLE POINTS
C
              HU=XU(I) - XU(J)
              HV=XV(I) - XV(J)
              DIST=SQRT(HU**2 + HV**2)
C
```

```
C       DETERMINE IF THE PAIR OF POINTS IS ALIGNED WITH THE SPECIFIED
C       DIRECTION (IN THE XU-XV PLANE)
C
              M=I
              N=J
              IF (XU(N) .EQ. XU(M)) THEN
                 ANGLE1=PI / 2.0
                 IF ((ANGLE1.GT.UPXY).OR.(ANGLE1.LT.LOWXY)) THEN
                    ANGLE1=PI / (-2.0)
                    CALL SWAP(M,N)
                 ENDIF
              ELSE
                 ANGLE1=ATAN(HV / HU)
              ENDIF
              IF ((ANGLE1 .LE. UPXY) .AND.
     1            (ANGLE1 .GE. LOWXY)) THEN
                  CALL COMPUTE(LOGTRAN, ZVALUE, M, N, REVI, REVJ)
                  CALL ADDREC(METHOD, NCHOICE, DIST, ZVALUE)
              ENDIF
150       CONTINUE
C
C       FIND ALL ALIGNED PAIRS OF MEASUREMENT POINTS, AND PUT THE
C       COMPUTED SEPARATION AND MEASURED VALUES FOR THE PAIR INTO
C       TEMPORARY STORAGE (THREE-DIMENSIONAL PROBLEMS)
C
          ELSE
            DO 160 J=1, NX-1
              DO 160 I=J+1, NX
                IF (((XU(J) .EQ. XU(I)) .AND. (XV(J) .EQ. XV(I))
     1              .AND. (XW(J) .EQ. XW(I))) .OR.
     2              (Z(J,REVI) .LE. -990.).OR.(Z(J,REVJ) .LE. -990.)
     3              .OR. (Z(I,REVI) .LE. -990.) .OR.
     4              (Z(I,REVJ) .LE. -990.)) GOTO 160

C
C       FIND THE SEPARATION VECTOR FOR A PAIR OF SAMPLE POINTS
C
                HU=XU(I) - XU(J)
                HV=XV(I) - XV(J)
                HW=XW(I) - XW(J)
                DIST=SQRT(HU**2 + HV**2 + HW**2)
C
C       DETERMINE IF THE PAIR OF POINTS IS ALIGNED WITH THE SPECIFIED
C       DIRECTION (IN THE XU-XV AND XV-XW PLANES)
C
                M=I
                N=J
                CHANGE=.FALSE.
                IF (XU(J) .EQ. XU(I)) THEN
                  ANGLE1=PI / 2.0
                  IF ((ANGLE1.GT.UPXY).OR.(ANGLE1.LT.LOWXY)) THEN
                    ANGLE1=PI / (-2.0)
                    CALL SWAP(M,N)
                    CHANGE=.TRUE.
                  ENDIF
                ELSE
                  ANGLE1=ATAN(HV / HU)
                ENDIF
                ANGLE2=ACOS(ABS(HW) / DIST)
                IF (HW .LT. 0.0) THEN
                  ANGLE2=-ANGLE2
                  IF (.NOT. CHANGE) CALL SWAP(M,N)
                ENDIF
                IF ((ANGLE1 .LE. UPXY) .AND. (ANGLE1 .GE. LOWXY)
     1              .AND. (ANGLE2 .LE. UPYZ) .AND.
     2              (ANGLE2 .GE. LOWYZ)) THEN
                  CALL COMPUTE(LOGTRAN, ZVALUE, M, N, REVI, REVJ)
                  CALL ADDREC(METHOD, NCHOICE, DIST, ZVALUE)
                ENDIF
160         CONTINUE
        ENDIF
        RETURN
        END
C
      SUBROUTINE SETGROUP(METHOD, LIMITS)
        PARAMETER (MAX1=100, MAX2= 2000)
      COMMON/BLK2/GROUPH(MAX2), GROUPZ(MAX2), GROUPN(MAX2)
      COMMON/BLK3/GH(MAX2), GN(MAX2), NREF(MAX2), GCOUNT, GNUM
      REAL LIMITS(30)
      REAL GH, GROUPH, DIST
      INTEGER  METHOD, GROUPN, GN, GCOUNT, GNUM, TEMP
      DO 170 I=1, GCOUNT-1
        L=I
        DO 180 J=I, GCOUNT
          IF (GROUPH(J) .LT. GROUPH(L)) L=J
180     CONTINUE
        X=GROUPH(L)
        GROUPH(L)=GROUPH(I)
        GROUPH(I)=X
        N=GROUPN(L)
        GROUPN(L)=GROUPN(I)
        GROUPN(I)=N
170   CONTINUE
      IF (METHOD .EQ. 1) THEN
        GNUM=GROUPH(GCOUNT) / LIMITS(1) + 1
        DO 220 I=1, GNUM
          GH(I)=LIMITS(1) * I
220     CONTINUE
      ELSE IF (METHOD .EQ. 2) THEN
           GNUM=1
230        IF (LIMITS(GNUM) .GT. 0) THEN
             GH(GNUM)=LIMITS(GNUM)
             GNUM=GNUM + 1
             GOTO 230
           ENDIF
           GNUM=GNUM - 1
      ELSE IF (METHOD .EQ. 3) THEN
             MAX=LIMITS(1)
             TEMP=MAX
             GNUM=0
             KOUNT=1
             DO 240 I=1, GCOUNT
250             GNUM=GNUM + 1
                IF (GROUPN(I) .GT. TEMP) THEN
                  GH(GNUM)=GROUPH(I)
                  GN(GNUM)=TEMP
                  NREF(GNUM)=KOUNT
                  GROUPN(I)=GROUPN(I) - TEMP
C                 WRITE (6,*) GH(GNUM), TEMP, NREF(GNUM)
                  KOUNT=KOUNT + 1
                  TEMP=MAX
                  GOTO 250
                ELSE IF (GROUPN(I) .LT. TEMP) THEN
                       GH(GNUM)=GROUPH(I)
                       GN(GNUM)=GROUPN(I)
                       NREF(GNUM)=KOUNT
C                      WRITE (6,*) GH(GNUM),GROUPN(I),NREF(GNUM)
                       TEMP=TEMP - GROUPN(I)
                     ELSE
                       GH(GNUM)=GROUPH(I)
                       GN(GNUM)=TEMP
                       NREF(GNUM)=KOUNT
C                      WRITE (6,*) GH(GNUM), TEMP, NREF(GNUM)
                       KOUNT=KOUNT + 1
                       TEMP=MAX
                ENDIF
240          CONTINUE
           ELSE
             GNUM=GCOUNT
             DO 275 I=1, GNUM
               GH(I)=GROUPH(I)
275          CONTINUE
      ENDIF
      DO 990 I=1, MAX2
        GROUPH(I)=0.
        GROUPZ(I)=0.
        GROUPN(I)=0
990   CONTINUE
      DO 995 I=1, GNUM
        GH(I)=GH(I)*1.0001
995   CONTINUE
      GCOUNT=0
      RETURN
      END
C
      SUBROUTINE COMPUTE(LOGTRAN, ZVALUE, M, N, REVI, REVJ)
      PARAMETER (MAX1=100, MAX2=2000)
      COMMON/BLK4/Z(MAX1,2)
      INTEGER REVI,REVJ
C
      Z1=Z(N,REVI)
      Z2=Z(N,REVJ)
      Z3=Z(M,REVI)
      Z4=Z(M,REVJ)
      IF (LOGTRAN .EQ. 1) THEN
        Z1=LOG10(Z1)
        Z2=LOG10(Z2)
        Z3=LOG10(Z3)
        Z4=LOG10(Z4)
      ENDIF
      IF (REVI .EQ. REVJ) THEN
        ZVALUE=(Z1 - Z3)**2
      ELSE
        ZVALUE=(Z1 - Z3) * (Z2 - Z4)
      ENDIF
      RETURN
      END
C
       SUBROUTINE ADDREC(METHOD, NCHOICE, DIST, ZVALUE)
       PARAMETER (MAX1=100, MAX2=2000)
       COMMON/BLK2/GROUPH(MAX2), GROUPZ(MAX2), GROUPN(MAX2)
       COMMON/BLK3/GH(MAX2), GN(MAX2), NREF(MAX2), GCOUNT, GNUM
       INTEGER METHOD, GROUPN, GN, GCOUNT, GNUM
       REAL GH, GROUPH, DIST
       LOGICAL FOUND
       DATA TOL/1.0001/
       IF (NCHOICE .EQ. 1) THEN
         FOUND=.FALSE.
         M=1
         DO 800 N=1,GCOUNT
           M=N
           IF ((DIST .GE. GROUPH(N)*(TOL-0.0002)) .AND.
     1         (DIST .LE. GROUPH(N)*TOL)) THEN
             FOUND=.TRUE.
             GOTO 810
           ENDIF
800      CONTINUE
810      IF (.NOT. FOUND) THEN
           GCOUNT=GCOUNT + 1
           M=GCOUNT
           GROUPH(M)=DIST
           GROUPN(M)=0
         ENDIF
         GROUPN(M)=GROUPN(M) + 1
       ELSE IF (METHOD .EQ. 3) THEN
            DO 750 N=1, GNUM
              M=N
              IF ((DIST .LT. GH(N)) .AND. (GN(N).NE.0)) GOTO 760
750         CONTINUE
760         GROUPH(NREF(M))=GROUPH(NREF(M)) + DIST
            GROUPZ(NREF(M))=GROUPZ(NREF(M)) + ZVALUE
            GROUPN(NREF(M))=GROUPN(NREF(M)) + 1
            GN(M)=GN(M) - 1
            IF (NREF(GNUM) .GT. GCOUNT) GCOUNT=NREF(GNUM)
```

Fig. 2. Source code listing for VARIO (continued).

```
            ELSE
               M=1
               GCOUNT=GNUM
               DO 770 N=1, GCOUNT
                  M=N
                  IF (DIST .LT. GH(N)) GOTO 780
770            CONTINUE
780            GROUPH(M)=GROUPH(M)  + DIST
               GROUPZ(M)=GROUPZ(M)  + ZVALUE
               GROUPN(M)=GROUPN(M)  + 1
            ENDIF
      RETURN
      END

C
       SUBROUTINE ERROR(NUM)
       INTEGER NUM
       IF (NUM .EQ. 1) THEN
          WRITE (*,610)
       ELSE IF (NUM .EQ. 2) THEN
               WRITE (*,,620)
            ELSE IF (NUM .EQ. 3) THEN
                    WRITE (*,630)
                 ELSE IF (NUM .EQ. 4) THEN
                         WRITE (*,640)
                      ELSE IF (NUM .EQ. 5) THEN
                              WRITE (*,650)
                           ELSE
                              WRITE (*,660)
       ENDIF
610    FORMAT (' PROGRAM ABORTED - INVALID DIMENSION GIVEN')
620    FORMAT (' PROGRAM ABORTED - EXCEED ARRAY''S LIMITS')
630    FORMAT (' PROGRAM ABORTED - INVALID COLUMNS GIVEN')
640    FORMAT (' PROGRAM ABORTED - INVALID CODE FOR NATURAL LOGARITHM',
   1           ' OPERATION')
650    FORMAT (' PROGRAM ABORTED - INVALID CODE FOR GROUPING OPERATION')
660    FORMAT (' PROGRAM ABORTED - EXCEED DEGREE BOUNDS')
       STOP
       END
```

Fig. 2. Source code listing for VARIO.

listing is in Figure 2. All program control information is passed to VARIO through the argument list in the calling statement. The dimension of the problem is specified with the integer variable DIM. The direction for which the semivariogram is to be computed is specified by the real variables ALPHA (= α, in Theory section and in Figure 1), DALPHA (= $\Delta\alpha$), BETA (= β), and DBETA (= $\Delta\beta$).

REVI and REVJ are used to specify the column numbers (on the input data file) that correspond to the regionalized variable(s) to be used in the semivariogram calculations. If REVI = REVJ, then a direct-semivariogram will be computed. If REVI ≠ REVJ, then a cross-semivariogram will be computed. For example, if REVI = REVJ = 2, a direct-semivariogram will be computed for the regionalized variable that corresponds to the second column of the input data file. If REVI = 1 and REVJ = 3, a cross-semivariogram will be computed for the pair of regionalized variables that corresponds with the first and third columns of the input data file. LOGTRAN indicates if the semivariograms are to be computed using the natural logarithm of the values of the regionalized variable(s). METHOD is used to specify the grouping method to use for $|h|$. If METHOD = 1, then method 1 (described in Theory section) will be used. The interval size for h is specified by the value of LIMITS(1). If METHOD = 2, then method 2 will be used. The interval sizes for h for each group are specified by the values of LIMITS(1) to LIMITS(30). If METHOD = 3, then method 3 will be used. The number of pairs of sample points to place in each group is specified by the value of LIMITS(1). If METHOD = 4, then method 4 will be used and the array LIMITS is not used.

VARIO reads the coordinates of the sample points and the measured values of the regionalized variable(s) for each sample point from the data file specified by the character variable "INFILE". VARIO reads data from INFILE using "free-format" FORTRAN read statements. The form this data file should be in for one-, two-, and three-dimensional problems is shown in Figure 3. The computed semivariograms are written to the data file specified by the character variable "OUTFILE". The two character variables TITLE1 and TITLE2 are used to label the output data file.

Example input data for VARIO are given in Tables 2 and 3. The first example is for a two-dimensional problem (DIM=2) used as an example by Clark (1979). Direct-semivariograms are computed for three directions (α = 0°, 45°, and 90°) for a single regionalized variable. The results shown in Table 4 are for grouping method 1. The average value of $|h_0|$, the number of pairs of measurement points, and the value of $\gamma^*_{ij}(\alpha_0, \beta_0, |h_0|)$, labeled GAMMA(H) on the output file, are computed for each group.

The second example is a three-dimensional

DIM = 1

$X_u(1)$	Z(1,1)	• • •	Z(1,10)
$X_u(2)$	Z(2,1)	• • •	Z(2,10)
⋮	⋮		⋮
$X_u(NX)$	Z(NX,1)	• • •	Z(NX,10)

DIM = 2

$X_u(1)$	$X_v(1)$	Z(1,1)	• • •	Z(1,10)
$X_u(2)$	$X_v(2)$	Z(2,1)	• • •	Z(2,10)
⋮	⋮	⋮		⋮
$X_u(NX)$	$X_v(NX)$	Z(NX,1)	• • •	Z(NX,10)

DIM = 3

$X_u(1)$	$X_v(1)$	$X_w(1)$	Z(1,1)	• • •	Z(1,10)
$X_u(2)$	$X_v(2)$	$X_w(2)$	Z(2,1)	• • •	Z(2,10)
⋮	⋮	⋮	⋮		⋮
$X_u(NX)$	$X_v(NX)$	$X_w(NX)$	Z(NX,1)	• • •	Z(NX,10)

Fig. 3. Input data file structure for VARIO.

Table 2. Example Input Data+ for VARIO for a Two-Dimensional Problem (DIM=2)

x_u, *ft*	x_v, *ft*	*Fe, %*	x_u, *ft*	x_v, *ft*	*Fe, %*
0	0	38	100	300	37
100	0	37	200	300	37
200	0	35	300	300	35
400	0	30	400	300	38
600	0	29	500	300	37
700	0	30	600	300	37
800	0	32	700	300	33
0	100	36	800	300	34
100	100	35	0	400	42
200	100	36	200	400	43
300	100	35	300	400	42
400	100	34	400	400	39
500	100	33	500	400	39
600	100	32	600	400	41
700	100	29	700	400	40
800	100	28	800	400	38
0	200	35	0	500	44
100	200	38	200	500	40
300	200	35	300	500	42
400	200	37	400	500	40
500	200	36	500	500	39
600	200	36	600	500	37
700	200	35	700	500	36
0	300	37			

Table 3. Example Input Data for VARIO for a Three-Dimensional Problem (DIM=3)

x_u	x_v	x_w	*Bromide*	*Chloride*	*Bromoform*
---	*m*	---	---	g/m^3 ---	mg/m^3
0.0	0.0	2.9	82	240	27.2
		2.5	178	579	24.8
		2.3	96	267	3.1
		2.1	4	34	0.1
0.0	1.0	3.1	0	3	0.0
		2.9	165	553	0.4
		2.7	212	570	31.9
		2.3	147	472	4.1
1.0	2.0	3.0	103	315	0.0
		2.8	177	558	23.0
		2.6	210	663	20.0
		2.2	30	95	0.4
1.0	3.0	3.0	0	3	0.1
		2.8	151	472	4.2
		2.6	76	230	3.4
		2.2	5	25	0.1
		1.6	174	582	13.9
2.0	4.0	2.7	2	6	1.4
		2.3	2	5	0.1
		1.5	0	2	0.1
2.0	5.0	2.7	118	348	0.1
		2.5	186	632	9.5
		2.3	165	520	3.6
		2.1	8	58	0.1
		1.7	10	28	0.1

problem (DIM=3). Cross-semivariograms are computed for two pairs of regionalized variables. In both cases, the regionalization is considered to be isotropic. The results shown in Table 5 were calculated using grouping method 1, and the results shown in Table 6 were calculated using grouping method 3.

Summary

A general procedure is presented for calculating direct- and cross-semivariograms, from a set of sample data, for any specified direction in one-, two-, or three-dimensional space. Four different algorithms are presented for combining sample pairs into groups, and these should handle most problems that occur in practice. A FORTRAN subroutine is presented for implementing the procedure on any computer that supports a

Table 4. Output from VARIO for Example Input Data in Table 2

```
     TWO-DIMENSIONAL EXAMPLE GIVEN IN CLARK (1979)

INPUT DATA FILE: TABLE2                            DIMENSIONS:  2
SPECIFIED DIRECTION:
             ALPHA =     .00      BETA =     .00
            DALPHA =     .00     DBETA =     .00

DIRECT-SEMIVARIOGRAM FOR REGIONALIZED VARIABLE  1
------------------------------------------------------------------
             GROUP      AVERAGE       NO. OF
              NO.          H          PAIRS      GAMMA(H)
             -----      -------       ------     ---------
               1        100.00          36            1.46
               2        200.00          33            3.30
               3        300.00          27            4.31
               4        400.00          23            6.70
               5        500.00          17            8.88
               6        600.00          14           13.04
               7        700.00           9           15.56
               8        800.00           4           15.63

******************************************************************

     TWO-DIMENSIONAL EXAMPLE GIVEN IN CLARK (1979)

INPUT DATA FILE: TABLE2                            DIMENSIONS:  2
SPECIFIED DIRECTION:
             ALPHA =   90.00      BETA =     .00
            DALPHA =     .00     DBETA =     .00

DIRECT-SEMIVARIOGRAM FOR REGIONALIZED VARIABLE  1
------------------------------------------------------------------
             GROUP      AVERAGE       NO. OF
              NO.          H          PAIRS      GAMMA(H)
             -----      -------       ------     ---------
               1        100.00          36            5.35
               2        200.00          27            9.87
               3        300.00          21           18.88
               4        400.00          13           27.54
               5        500.00           5           26.10

******************************************************************

     TWO-DIMENSIONAL EXAMPLE GIVEN IN CLARK (1979)

INPUT DATA FILE: TABLE2                            DIMENSIONS:  2
SPECIFIED DIRECTION:
             ALPHA =   45.00      BETA =     .00
            DALPHA =    1.00     DBETA =     .00

DIRECT-SEMIVARIOGRAM FOR REGIONALIZED VARIABLE  1
------------------------------------------------------------------
             GROUP      AVERAGE       NO. OF
              NO.          H          PAIRS      GAMMA(H)
             -----      -------       ------     ---------
               1        141.42          31            3.89
               2        282.84          22            5.89
               3        424.26          14            8.54
               4        565.69           8            8.69
               5        707.11           3             .33
```

Table 5. Output from VARIO for Example Input Data in Table 3

```
THREE-DIMENSIONAL EXAMPLE

INPUT DATA FILE: TABLE 3                        DIMENSIONS:  3
SPECIFIED DIRECTION:
         ALPHA =     .00      BETA =     .00
        DALPHA = 180.00      DBETA = 180.00

CROSS-SEMIVARIOGRAM FOR REGIONALIZED VARIABLES 1 AND  2
```

GROUP NO.	AVERAGE H	NO. OF PAIRS	GAMMA(H)
1	.20	11	15599.23
2	.40	12	22309.46
3	.60	7	24103.71
4	.80	6	17290.92
5	1.00	10	16162.55
6	1.04	21	22529.24
7	1.17	12	19155.54
8	1.28	5	22555.30
9	1.40	1	50373.00
10	1.44	25	17112.40
11	1.57	7	14918.36
12	1.68	1	1380.00
13	1.77	3	22559.50
14	1.92	1	35485.00
15	2.06	1	.00
16	2.26	48	22159.15
17	2.34	11	19731.18
18	2.45	9	14242.39
19	2.59	3	16487.17
20	2.69	2	33246.25
21	3.17	18	10673.75
22	3.23	19	20348.63
23	3.35	1	44255.00
24	3.42	2	14538.75
25	3.64	9	34442.22
26	3.80	1	60208.00
27	3.87	1	45457.50
28	3.94	1	.00
29	4.48	16	12864.63
30	4.54	13	27013.23
31	4.67	3	16856.83
32	5.39	14	14496.43
33	5.43	5	18562.60
34	5.52	1	7632.00

FORTRAN 77 compiler. Copies of VARIO, and an example main program and data files can be obtained by sending a formatted 5¼-inch floppy diskette (360 Kb format) to the senior author. Future papers will present procedures and subroutines that use the experimental semivariograms computed by VARIO to fit theoretical semivariogram models, to calculate extension variances, and for kriging and cokriging. It is hoped that the increased availability of programs and subroutines for geostatistical analysis will encourage the more widespread use of these methods by practicing ground-water hydrologists.

Table 6. Output from VARIO for Example Input Data in Table 3

```
THREE-DIMENSIONAL EXAMPLE

INPUT DATA FILE: TABLE 3                        DIMENSIONS:  3
SPECIFIED DIRECTION:
         ALPHA =     .00      BETA =     .00
        DALPHA = 180.00      DBETA = 180.00

CROSS-SEMIVARIOGRAM FOR REGIONALIZED VARIABLES 1 AND  3
```

GROUP NO.	AVERAGE H	NO. OF PAIRS	GAMMA(H)
1	.37	30	569.83
2	.97	30	417.80
3	1.22	30	489.81
4	1.50	30	477.45
5	2.21	30	384.58
6	2.30	30	641.21
7	2.81	30	454.69
8	3.29	30	638.87
9	4.29	30	698.03
10	5.13	30	450.45

Acknowledgments

This work was supported by the U.S. Geological Survey and the Oregon Agricultural Experiment Station. Larry Yuen and Janet Lee wrote the VARIO computer program.

References

Clark, I. 1979. Practical Geostatistics. Applied Science Publishers, London.

Cooper, R. M. and J. D. Istok. 1988a. Geostatistics applied to groundwater pollution. 1. Methodology. Journal of Environmental Engineering, Amer. Soc. Civil Engrs. In press.

Cooper, R. M. and J. D. Istok. 1988b. Geostatistics applied to groundwater pollution. 2. Application. Journal of Environmental Engineering, Amer. Soc. Civil Engrs. In press.

David, M. 1977. Geostatistical Ore Reserve Estimation. Elsevier Scientific Publishing Co., New York.

Delhomme, J. P. 1976. Kriging in the hydrosciences. In: Advances in Water Resources. v. 1, pp. 251-256.

Henley, S. 1981. Nonparametric Geostatistics. Applied Science Publishers, Halstead Press, John Wiley and Sons, New York.

Journel, A. G. and C. J. Huijbregts. 1978. Mining Geostatistics. Academic Press, New York.

Journel, A. G. and E. H. Isaaks. 1984. Conditional indicator simulation: Application to a Saskatchewan uranium deposit. Mathematical Geology. v. 16, no. 7, pp. 685-718.

Neuman, S. P. and S. Yakowitz. 1980. A statistical approach to the inverse problem of aquifer hydrology. 1. Theory. Water Resources Research. v. 15, no. 4, pp. 845-860.

Rendu, J. M. 1978. An introduction to geostatistical methods of mineral evaluation. South African Institute of Mining and Metallurgy, Johannesburg.

SAS Institute, Inc. 1985. SAS Procedures Guide for Personal Computers, Version 6. Cary, NC.

Vauclin, M., S. R. Vieira, G. Vachaud, and D. R. Nielsen. 1983. The use of cokriging with limited field soil observations. Soil Soc. Am. J. v. 47, p. 184.

* * * * *

Jonathan D. Istok is an Assistant Professor in the Departments of Agricultural and Civil Engineering at Oregon State University, specializing in statistical and mathematical modeling of ground-water flow and solute transport.

Richard M. Cooper is a Water Resources Engineer with the Water Resources Division of the South Florida Water Management District, specializing in surface-water hydrology.

Alan L. Flint is a Hydrologist with the U.S. Geological Survey, specializing in soil physics. Dr. Flint is project chief for two components of the site characterization study for the proposed high-level nuclear waste repository at Yucca Mountain, Nevada.

Unsaturated Zone

COMPUTER NOTES

A GALERKIN FINITE-ELEMENT PROGRAM FOR SIMULATING UNSATURATED FLOW IN POROUS MEDIA

by R. Khaleel[a] and T.-C. Yeh[b]

Abstract. A fully documented Galerkin finite-element FORTRAN program is presented for solving the one-dimensional, transient flow equation in unsaturated porous media. Material balance error summaries are presented to demonsrrate accuracy of the numerical scheme. Comparison of our simulated results with other existing numerical solutions using the Galerkin scheme provided excellent agreement.

Introduction

Unsaturated flow typically involves nonuniform, time-dependent moisture contents and flow fields. The partial differential equation governing unsaturated flow in porous media is nonlinear, and is not readily amenable to accurate analytical solutions. In recent years, the Galerkin finite-element technique has been used to solve the transient, unsaturated flow equation (e.g., Neuman, 1973; van Genuchten, 1978; Yeh, 1981; Huyakorn and Pinder, 1983). In the Galerkin approach, the dependent variable—the pressure head—is approximated by a series of basis (or shape) functions and associated time-dependent coefficients. The approximating series are then substituted into the governing equations and the resulting errors (residuals) minimized through the use of weighted-residual theorems (Zienkiewicz, 1977). The integral equations derived in this manner are evaluated using the finite-element method of discretization, resulting in a set of (quasi)-linear equations which can be solved using appropriate matrix equation solvers.

In this paper, a Galerkin finite-element solution of one-dimensional unsaturated flow equation is developed using linear basis or shape functions. A fully documented listing of the FORTRAN program is provided. Material balance error summaries are presented to demonstrate accuracy of the numerical scheme. Results obtained using our program are compared with other existing numerical solutions.

Numerical Model

The pressure head form of the differential equation describing one-dimensional, vertical flow of water in an unsaturated homogeneous and isotropic soil profile, can be written as:

$$\mathcal{L}(\psi) = \frac{\partial}{\partial z}\,[K(\psi)\frac{\partial}{\partial z}(\psi - z)] - C^*(\psi)\frac{\partial \psi}{\partial t} = 0 \qquad (1)$$

where $\mathcal{L}$ is the differential operator defined in the flow region; ψ is the pressure head, L; $K(\psi)$ is the hydraulic conductivity, LT^{-1}; $C^*(\psi) = \partial\theta/\partial\psi$ is the specific water capacity, L^{-1}; $\theta(\psi)$ is the volumetric water content; z is cartesian coordinate (positive in the downward direction), L; and t is time, T. Both ψ and K are assumed to be single-valued function of θ.

The initial conditions are

$$\psi(z, 0) = \psi_0(z) \qquad (2)$$

and the boundary conditions are the usual Dirichlet (constant pressure) and Neuman (flux type) conditions:

$$\psi(z, t) = \psi_{\Gamma_1}(z, t) \quad \text{on } \Gamma_1 \qquad (3a)$$

and

$$K(\psi)(\frac{\partial \psi}{\partial z} - 1)\,n_i + q_{\Gamma_2}(z, t) = 0 \quad \text{on } \Gamma_2 \qquad (3b)$$

[a]Assistant Professor of Hydrology, Department of Geoscience, New Mexico Institute of Mining and Technology, Socorro, New Mexico 87801.
[b]Assistant Professor, Department of Environmental Sciences, University of Virginia, Charlottesville, Virginia 22903.
Received July 1984, accepted September 1984.
Discussion open until July 1, 1985.

where $\Gamma_1 + \Gamma_2 = \Gamma$, the boundary of the region; q_{Γ_2} is the surface flux prescribed along the Neuman boundary Γ_2; and n_i is the unit outward normal on Γ_2.

The finite-element equations are formulated using the Galerkin technique (Neuman *et al.*, 1974). A trial function can be selected of the form

$$\hat{\psi}(z, t) = \sum_{i=1}^{n} \psi_i(t) N_i(z) \tag{4}$$

where N_i are the element shape functions; ψ_i are undetermined coefficients which become the nodal values of the function ψ; and n is the total number of nodes in the finite-element grid system. For a one-dimensional linear element e, the shape functions are

$$N_1 = 1 - \frac{z}{L_e} \tag{5a}$$

and

$$N_2 = \frac{z}{L_e} \tag{5b}$$

where L_e is the length of element e. Upon substituting the trial function (4) into (1) and setting the resulting residual orthogonal to all N_i's, one obtains a set of n integral equations in the flow domain Ω:

$$\int_{\Omega} \mathcal{L}(\hat{\psi}) N_i \, dz = 0 \quad i = 1, 2, \ldots n \tag{6}$$

which, upon integration by parts on the second derivative term in (6), can be solved for the unknowns ψ_i.

A functional representation is used to express the variable parameters K and C within a linear element with two nodes, as weighted averages of the corresponding nodal values of the element.

$$K(z) = \sum_{\ell=1}^{2} K_\ell(\psi_\ell) N_\ell(z) \tag{7a}$$

and

$$C^*(z) = \sum_{\ell=1}^{2} C_\ell^*(\psi_\ell) N_\ell(z) . \tag{7b}$$

The same shape functions as those of the trial function (4) are used here. The final finite-element equations are written in the matrix form as

$$[A]\{\psi\} + [B]\{\frac{\partial \psi}{\partial t}\} = \{F\} \tag{8}$$

where for a typical one-dimensional linear element e, the elements of the matrices and the right-hand vector in (8) are:

$$a_{ij}^e = \int_{L_e} \sum_{\ell=1}^{2} N_\ell K_\ell \frac{\partial N_i}{\partial z} \frac{\partial N_j}{\partial z} dz, \quad i, j = 1, 2 \tag{8a}$$

$$b_{ij}^e = \int_{L_e} \sum_{\ell=1}^{2} N_\ell C_\ell^* N_i N_j \, dz, \tag{8b}$$

$$f_i^e = \int_{L_e} \sum_{\ell=1}^{2} N_\ell K_\ell \frac{\partial N_i}{\partial z} dz - \int_{\Gamma_2} N_i q_{\Gamma_2} d\Gamma . \tag{8c}$$

Because of the nonlinear nature of the differential equation, the solution is iterative at each time step. Using a time weighting factor ϵ, where $0 \leqslant \epsilon \leqslant 1$, equation (8) is discretized in time as

$$[A](\epsilon\{\psi\}^{k+1} + (1-\epsilon)\{\psi\}^k) + \frac{1}{\Delta t^k}[B](\{\psi\}^{k+1} - \{\psi\}^k) = \{F\} \tag{9}$$

where k indicates a point t^k in time, and $\Delta t^k = t^{k+1} - t^k$. The matrix [B] in (8) is diagonalized by a procedure known as "lumping." According to this procedure, we calculate the elements in [B] as

$$b_{ii}^e = \int_{L_e} \sum_{\ell=1}^{2} N_\ell C_\ell^* N_i \, dz \quad i = j \tag{10a}$$

$$b_{ij}^e = 0 \quad i \neq j \tag{10b}$$

Experience indicates that a stable solution is obtained with the lumped mass matrix. A lumping procedure similar to that just described was successfully applied by Neuman (1973) to a number of seepage problems.

Following the mass lumping procedure for matrix [B] and performing necessary integrations, the element matrix for an interior element becomes:

$$\frac{\epsilon}{2L_e}\begin{bmatrix} (K_1 + K_2) & -(K_1 + K_2) \\ -(K_1 + K_2) & (K_1 + K_2) \end{bmatrix}\begin{Bmatrix} \psi_1 \\ \psi_2 \end{Bmatrix}^{k+1} +$$

$$\frac{L_e}{\Delta t}\begin{bmatrix} C_1^*/3 + C_2^*/6 & 0 \\ 0 & C_1^*/6 + C_2^*/3 \end{bmatrix}\begin{Bmatrix} \psi_1 \\ \psi_2 \end{Bmatrix}^{k+1} =$$

$$\frac{(\epsilon - 1)}{2L_e}\begin{bmatrix} (K_1 + K_2) & -(K_1 + K_2) \\ -(K_1 + K_2) & (K_1 + K_2) \end{bmatrix}\begin{Bmatrix} \psi_1 \\ \psi_2 \end{Bmatrix}^{k} +$$

$$\frac{L_e}{\Delta t}\begin{bmatrix} C_1^*/3 + C_2^*/6 & 0 \\ 0 & C_1^*/6 + C_2^*/3 \end{bmatrix}\begin{Bmatrix} \psi_1 \\ \psi_2 \end{Bmatrix}^{k} +$$

$$\begin{Bmatrix} -(K_1 + K_2)/2 \\ (K_1 + K_2)/2 \end{Bmatrix} \tag{11}$$

The variable coefficients in (9) are evaluated at one-half the time step. At the beginning of the iteration, estimates of $\psi_i^{k+1/2}$ are obtained by linear extrapolation:

$$\psi_i^{k+1/2} = \psi_i^k + \frac{\Delta t^k}{2\Delta t^{k-1}} (\psi_i^k - \psi_i^{k-1}) \tag{12}$$

These are used in determining the variable parameters $K(\psi)$, $\theta(\psi)$, and $C^*(\psi)$; and in updating coefficient matrices [A], [B], and the right-hand vector {F} in (9). A tridiagonal system of linear algebraic equations is generated at each iteration and solved for ψ_i^{k+1} at all nodes by gaussian elimination (Carnahan *et al.*, 1969). Due to the nonlinear nature of (9), these estimates for ψ_i^{k+1} must be improved (Neuman *et al.*, 1974). At each iteration, an improved estimate of $\psi_i^{k+1/2}$ is obtained by averaging the most recent estimate of ψ_i^{k+1} with ψ_i^k, the value obtained in the previous time step:

$$\psi_i^{k+1/2} = 1/2(\psi_i^k + \psi_i^{k+1}) \tag{13}$$

After having reevaluated $K(\psi)$, $\theta(\psi)$, and $C^*(\psi)$ based on $\psi_i^{k+1/2}$; and coefficient matrices [A], [B], and right-hand vector {F}, equation (9) is again solved for improved estimates of ψ_i^{k+1}. The iterative procedure is continued until the relative change in pressure head between two successive iterations is within a prescribed tolerance.

Computer Program

The computer program is written in FORTRAN for the DEC 2060 computer at New Mexico Tech computer center. A reprint of the program used in solving an infiltration problem (Warrick *et al.*, 1971) is given in Appendix A.

The FORTRAN code consists of a main program and eight subroutines. The main program accepts the input data and governs the sequence of operations to be performed. Initial segment of the main program (up to statement number 169) controls the type of input data, their sequence, and printing. Actual simulation of the problem starts at statement 179 (LA is simply an integer number to indicate simulation increments). Equation (12) is programmed in statement 195, whereas equation (13) is programmed in statement 329.

The iterative segment of the program for solving the nonlinear equations starts at statement 203. In statements 207 through 251, we set up the individual matrix elements [equation (11)]. The RH arrays are generated for use in the MATBAL subroutine.

After assembly of individual matrices, the global matrices are formed in statements 257 through 305. The program, in its present form, can handle two types of boundary conditions: (1) a constant pressure boundary; and (2) a constant flux boundary. The global matrix for the interior nodes is formulated in statements 276 through 285. The global matrix for the top boundary condition is formulated in statements 257 through 272. For the lower boundary condition, the global matrix is formulated in statements 289 through 305.

The variable time step size used during simulation is calculated in statements 360 through 367. At each time step, the equation for calculating Δt is given by

$$\Delta t^{k+1} = \min\left(\frac{\Delta t^k}{\epsilon^k} * \mathrm{TOL},\ 0.1 * \frac{\mathrm{DELZ}}{\mathrm{Q}(1)}\right)$$

and is programmed in statement 364. The variables TOL, DELZ, and Q(1) are defined in the initial segment of the main program. The variable ϵ^k is defined as

$$\epsilon^k = \max_i \left| \frac{\psi_i^k - \psi_i^{k-1}}{\psi_i^k} \right|$$

and is programmed in statements 313 through 319.

Subroutine INTERP is used to linearly interpolate for values in the soil hydraulic properties. It is used only when the parameter INT equals 1. When INT = 0, functional relationships are used to describe the soil hydraulic properties.

The five functional subroutines FNCTP, FNCPT, FNCZT, FNCPK, and FNCPC are used to obtain, respectively, (1) pressure head ψ given moisture content θ, (2) moisture content θ given pressure head ψ, (3) θ as a function of the depth Z for the initial condition, (4) hydraulic conductivity K as a function of ψ, and (5) water capacity C^* as a function of ψ.

Subroutine TRIDIA is used to solve the tridiagonal system of equations generated by equation (9). It is adapted from a similar subroutine given by Carnahan *et al.* (1969). The arrays A, B, C, and D formulated in statements 257 through 305 during global assembly procedure are inputs to the TRIDIA subroutine. The solution vector of ψ values is contained in array ANS and returned to the main program.

The material balance errors are calculated in subroutine MATBAL. Both differential and cumulative material balance errors are calculated at each time step. The equations used in MATBAL to calculate inflow, outflow, and change in storage are developed following equation (11).

Application

Our computer code was used to solve the infiltration flow problem as described by Warrick *et al.* (1971). Other finite-element solutions for this particular problem are available (van Genuchten, 1978). Our simulation results could therefore be compared with those of van Genuchten.

Warrick *et al.* (1971) obtained experimental data from a 6.1-m by 6.1-m square field plot of Panoche clay loam having an approximate initial water content of 0.20. The soil was wetted with 7.62 cm of 0.20 N $CaCl_2$ solution, followed immediately by tracer-free water. The total infiltration time was 17.5 hours.

Functional relationships (INT = 0) for θ, ψ, K, and $C^*(\psi)$ were given by van Genuchten (1978) for Panoche clay loam soil (Warrick *et al.*, 1971).

$$\theta(\psi) = \begin{cases} 0.6829 - 0.09524\,\ell n\,|\psi|, & \psi \leq -29.484 \\ 0.4531 - 0.02732\,\ell n\,|\psi|, & -29.484 < \psi \leq -14.495 \end{cases} \quad \ldots .(14a)$$

$$\psi(\theta) = \begin{cases} -1300\exp(-10.5\theta), & \theta \leq .3606 \\ -1.59 \times 10^7 \exp(-36.6\theta), & \theta > .3606 \end{cases} \quad (14b)$$

$$K(\psi) = \begin{cases} 19.34 \times 10^5\,|\psi|^{-3.4095}, & \psi \leq -29.484 \\ 516.8\,|\psi|^{-0.97814}, & -29.484 < \psi \leq -14.495 \end{cases} \quad (14c)$$

$$C^*(\psi) = \begin{cases} 0.09524/|\psi|, & \psi \leq -29.484 \\ 0.02732/|\psi|, & -29.484 < \psi \leq -14.495 \end{cases} \quad (14d)$$

where the hydraulic conductivity, K is in cm/day; and the pressure head, ψ is in cm.

The initial and boundary conditions are as follows:

$$\theta(z,0) = \begin{cases} 0.15 + 0.0008333\,z, & 0 < z \leq 60 \\ 0.2000 & 60 < z \leq 125 \end{cases} \quad (15a)$$

$$\psi(0,t) = -14.495 \qquad \theta_0 = 0.38 \qquad (15b)$$

$$\psi(125,t) = -159.19 \qquad \theta_\ell = 0.20 \qquad (15c)$$

where the distance z is in cm; and time t is in days.

The following were the input data (main program, Appendix A) for our test problem:

Interpolation parameter, INT = 0;

Saturated hydraulic conductivity, KSAT = 37.8 cm/day;

Saturated moisture content, POR = 0.38;

Total number of nodes, NODES = 51;

Spatial increment, DELZ = 2.5 cm;

Initial time step size, DELT = 1 sec;

Convergence criterion, TOL = 0.01;

Time weighting factor, EPS = 0.5;

Maximum iterations during a time step, MAXIT = 10;

Maximum size of time step, DELMAX = 1000 sec.

The variables NP and NPT (main program, Appendix A) were given dummy integer values when the parameter INT = 0. For node 1, the boundary conditions were given by: type of boundary condition, NBC(1) = 0, the pressure head value, BC(1) = −14.495 cm, and Q(1) = 0. For node 51, the boundary conditions were: NBC(51) = 0, BC(51) = −159.19 cm, and Q(51) = 0. The initial conditions were provided by calling subroutines FNCZT and FNCTP.

Figure 1 is a comparison of water content profiles obtained using our unsaturated flow

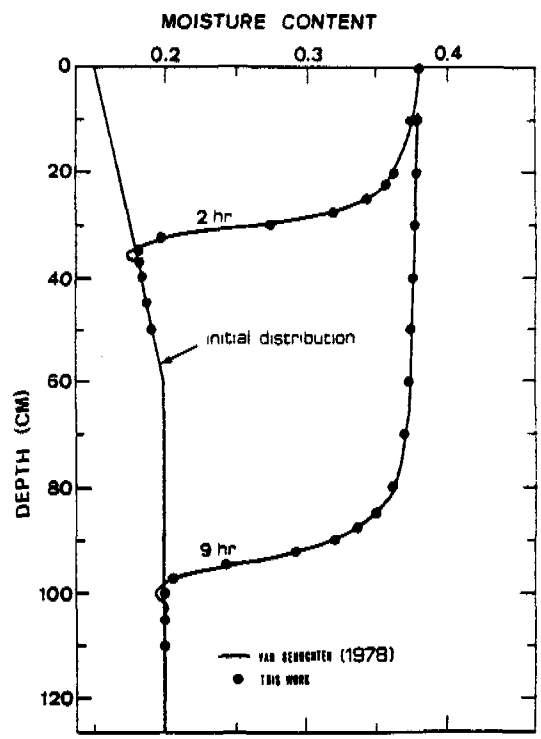

Fig. 1. Moisture content profiles at two and nine hours for the Panoche clay loam soil (Warrick *et al.*, 1971): Δz = 2.5 cm and ϵ = 0.5.

program with those obtained by van Genuchten (1978) using his mass-lumped linear finite-element (MFE) program for the Panoche clay loam soil. As discussed earlier, a variable time increment size was used during simulation. A total of 86 time steps were needed for the nine-hour simulation. Frequently it required no more than four or five iterations to converge to a relative pressure head tolerance value of 0.01; at no time did it require more than seven iterations. As suggested by equation (14d), there is a discontinuity in $C(\psi)$ at $\psi = -29.484$ cm. However, these same functional relationships (14) were also used by van Genuchten (1978). An indication of accuracy of our numerical results is given by the material balance error analysis. The cumulative material balance error at the end of the nine-hour simulation was of the order of 10^{-5} percent of the total inflow rate. We used a single precision in our computer code; use of double precision would have further improved these errors. Our numerical results are nearly identical to those of van Genuchten (1978); the two solutions were indistinguishable from each other on the plots (Figure 1). However, this is to be expected since both our and van Genuchten's method used identical numerical schemes.

References

Carnahan, B., H. A. Luther, and J. O. Wilkes. 1969. Applied Numerical Methods. John Wiley & Sons, N.Y.

Huyakorn, P. S. and G. F. Pinder. 1983. Computational Methods in Subsurface Flow. Academic Press, N.Y.

Neuman, S. P. 1973. Saturated-unsaturated seepage by finite elements. ASCE, J. of Hydraulics Div. v. 99, HY 12, pp. 2233-2251.

Neuman, S. P., R. A. Feddes, and E. Bresler. 1974. Finite element simulation of flow in saturated-unsaturated soils considering water uptake by plants. Third Annual Rept., Project No. AIO-SWC-77, Israel Institute of Technology, Haifa.

van Genuchten, M. T. 1978. Mass transport in saturated-unsaturated media: one-dimensional solutions. Water Resourc. Program, Princeton Univ. Techn. Rept. 78-WR-11, Princeton, N.J.

Warrick, A. W., J. W. Biggar, and D. R. Nielsen. 1971. Simultaneous solute and water transfer for an unsaturated soil. Water Resour. Res. v. 7, no. 5, pp. 1216-1225.

Yeh, G. T. 1981. On the computation of Darcian velocity and mass balance in the finite element modeling of groundwater flow. Water Resour. Res. v. 17, no. 5, pp. 1529-1534.

Zienkiewicz, O. C. 1977. The Finite Element Method. McGraw-Hill Book Co., N.Y.

* * * * *

Raz Khaleel is an Assistant Professor of Hydrology at the New Mexico Institute of Mining and Technology. He received the Ph.D. degree from Texas A&M University. Some of his current research interests include studies involving multiphase fluid flow in porous media and interaction of surface water/ground water.

T.-C. Jim Yeh is an Assistant Professor in the Department of Environmental Sciences at the University of Virginia. He received the Ph.D. degree from New Mexico Institute of Mining and Technology. He is primarily interested in stochastic modeling of subsurface fluid flow.

Appendix A. A Finite-Element Program to Simulate Unsaturated Flow

```
C
C-----UNSAT.FOR-----WRITTEN BY R. KHALEEL  AND  T.C. YEH-----N.M.I.M.T.-----
C
C       THIS IS A FINITE ELEMENT PROGRAM TO SIMULATE
C       ONE-DIMENSIONAL UNSATURATED FLOW.
C
C
C       INPUT INFORMATION:
C
C       BEFORE EXECUTING THIS PROGRAM, YOU SHOULD CREATE AN INPUT
C       FILE WHICH CONSISTS OF THE FOLLOWING:
C
C       (1)     SOIL TYPE NAME (NOT TO EXCEED 10 CHARACTERS)
C
C       (2)     FUNCTIONAL RELATIONS OR TABULAR INPUT
C
C                       INT--- 0 FUNCTIONAL RELATIONSHIPS USED FOR
C                                MOISTURE CHARACTERISTIC CURVES
C                              1 TABULAR INPUT DATA
C
C       (3)     HYDRAULIC CONDUCTIVITY AND SUCTION RELATIONSHIP
C               (NP AND KSAT)
C                       NP----NO. OF PSI-K PAIR
C                       KSAT--SATURATED HYDRAULIC CONDUCTIVITY
C
C       (4)     XP AND XK PAIR
C                       XP--PSI
C                       XK--RELATIVE HYDRAULIC CONDUCTIVITY
C       NOTE!!  XP SHOULD BE IN A DESCENDING ORDER
C
C       (5)     SOIL MOISTURE RETENTION DATA (XPP AND XTHE)
C                       XPP--PSI
C                       XTHE--MOISTURE CONTENT
C       NOTE!!  XPP SOULD BE IN A DESCENDING ORDER
C
C       (6)     NODES, DELZ, DELT, TMAX, TOL, MAXIT, TPRIN
C                       NODES--NO. OF NODAL POINTS
C                       DELZ--INTERVAL BETWEEN NODAL POINTS
C                       DELT--TIME INTERVAL
C                       TMAX--MAXIMUM SIMULATION TIME
C                       TOL---TOLERANCE
C                       EPS---TIME WEIGHTING FACTOR
C                       MAXIT-MAXIMUM NO. OF ITERATIONS
C
C       (7)     TOP BOUNDARY CONDITION (NBC(1), BC(1), Q(1))
C                       NBC(1)--0 FOR CONSTANT HEAD BOUNDARY
C                               1 FOR FLUX BOUNDARY
C                       BC(1)---HEAD VALUE FOR THE CONSTANT HEAD BOUNDARY
C                       Q(1)----FLUX FOR FLUX BOUNDARY
C
C       (8)     BOTTOM BOUNDARY CONDITION (NBC(2), BC(2), Q(2))
C                       SAME AS ABOVE
C       (9)     INITIAL CONDITION
C
C       ALL THE INPUT DATA SHOULD BE IN A FREE FORMAT
C       UNITS OF PARAMETERS SHOULD BE CONSISTENT WITH KSAT
C
C
C
        DOUBLE PRECISION NAME, FILN
        REAL KSAT, L
        DIMENSION XP(51),XK(51),XC(51),YP(51),XTHE(51),XPP(51),
     *  PPSI(51),PSIH(51),NBC(2),BC(2),Q(2),PP(51),SP(2,2,51),
     *  RHS(2,2,51),R(2,51),TPSI(51),RH(2,2,51)
        COMMON A(51),B(51),C(51),D(51),PSI(51)
        COMMON DELT,DELZ,EPS,NODES,TWIN,TWOUT,TWEN,TWUT,WS,WS1,WIS,
     *  DWIN,DWOUT,DELMAX,POR,TMAX,TIME
        DATA TWIN,TWOUT,TWEN,TWUT,WS,WIS/0.,0.,0.,0.,0.,0./
C
        WRITE(5,1)
1       FORMAT(' ' ,'       INPUT FILE NAME IN A10')
        READ(5,2) FILN
2       FORMAT(A10)
        WRITE(5,999)
999     FORMAT(' DO YOU WANT TO HAVE A HARD COPY?  YES=3, NO=5')
        READ(5,*)NPRT
        OPEN(UNIT=6,FILE='WARRICK.DAT',ACCESS='SEQIN',DEVICE='DSK')
        READ(6,3)NAME
3       FORMAT(A10)
        WRITE(NPRT,1001)NAME
1001    FORMAT(' ',10X,5('-'),A10,'SOIL PROPERTIES ',10('-')//)
        READ(6,*) INT
C
C       READ SOIL PROPERTIES
C
        READ(6,*)NP,KSAT
        IF (INT. EQ. 0) GO TO 770
        WRITE(NPRT,1002)
1002    FORMAT(' ',10X,10('-'),'PSI',13('-'),'KR',10('-'),//)
        DO 10 I=1,NP
        READ(6,*)XP(I),XK(I)
        XP(I)=-XP(I)
        WRITE(NPRT,1003)XP(I),XK(I)
1003    FORMAT(' ',10X,2E16.5)
10      CONTINUE
770     CONTINUE
C
C       READ PSI AND THETA RELATION
C
        READ(6,*)NPT,POR
        IF (INT .EQ. 0) GO TO 772
        WRITE(NPRT,1004)
1004    FORMAT(' ',/,10X,10('-'),'PSI',13('-'),'THETA',13('-'),/)
        DO 20 I=1,NPT
        READ(6,*)XPP(I),XTHE(I)
        XPP(I)=-XPP(I)
        WRITE(NPRT,1005)XPP(I),XTHE(I)
1005    FORMAT(' ',10X,2F16.5)
20      CONTINUE
C
C       DETERMINE PSI AND MOISTURE CAPACITY RELATIONSHIP
```

```
C
      WRITE(NPRT,1015)
 1015 FORMAT(' ',/,10X,10('-'),'PSI',10('-'),'  C ',10('-'),/)
      NPC=NPT-1
      DO 30 I=1,NPC
      XC(I)=(XTHE(I)-XTHE(I+1))/(XPP(I)-XPP(I+1))
      YP(I)=0.5*(XPP(I)+XPP(I+1))
      WRITE(NPRT,1006)XP(I),XC(I)
 1006 FORMAT(' ',10X,2F16.5)
   30 CONTINUE
  772 CONTINUE
C
C     READ PARAMETERS
C
      READ(6,*)NODES,DELZ,DELT,TMAX,TOL,EPS,MAXIT,DELMAX
      WRITE(NPRT,1007)NODES,DELZ,DELT,TMAX,TOL,EPS,MAXIT,DELMAX
 1007 FORMAT(' ',//,10X,'  TOTAL NO. OF NODES= ',I4,/,
     * ' ',10X,'    DELZ= ',F16.5,/,11X,'    DELT= ',F16.5,/,
     * 11X,'   TMAX= ',F16.5,/,11X,'TOLERANCE= ',F16.5,/,
     * 11X,'  TIME WEIGHTING FACTOR, EPS = ',F16.5,/,
     * 11X,'  MAXIT= ',I4,/,11X,'  MAXIMUM DELT=',F16.5,/,
     * //11X,'  BOUNDARY CONDITIONS -------',
     * 13X,'  NODE',' TYPE','    PSI   ','     Q     ')
      NODE1=NODES-1
      NELEM=NODE1
      L=DELZ
      NELEM1=NELEM-1
C
C     INITIAL CONDITION AND BOUNDARY CONDITION
C
      DO 35 I=1,2
      N=1
      IF (I.EQ.2)N=NODES
      READ(6,*)NBC(I),BC(I),Q(I)
      WRITE(NPRT,11) N,NBC(I),BC(I),Q(I)
   11 FORMAT(' ',10X,2I5,2F10.2)
      PSI(N)=BC(I)
      PPSI(N)=PSI(N)
      TPSI(N)=PPSI(N)
   35 CONTINUE
      WRITE(NPRT,1008)
 1008 FORMAT(' ',/,10X,10('-'),' INITIAL CONDITION',10('-'),/)
      Z=0.
      IF (INT .EQ. 1) GO TO 96
      DO 402 I=2,NODE1
      Z=Z+DELZ
      CALL FNCZT (Z,THETA)
      CALL FNCTP (THETA,PSI(I))
  402 CONTINUE
      GO TO 404
   96 READ(6,*)(PSI(I),I=2,NODE1)
  404 CONTINUE
      DO 40 I=2,NODE1
      PPSI(I)=PSI(I)
      TPSI(I)=PPSI(I)
   40 CONTINUE
      WRITE(NPRT,1009)(I,PSI(I),I=1,NODES)
 1009 FORMAT(5(I4,F10.3))
C
C     SIMULATION STARTS HERE
C
      TIME=0.0
      LA=0
C
C     TIME LOOP
C
 1000 CONTINUE
      LA=LA+1
      TIME=TIME+DELT
      WRITE(NPRT,1030)TIME
 1030 FORMAT(' ',/,10('-'),'SIMULATION TIME = ',E13.5,10('-'),
     * //)
C
C     PREDICT PSI AT T+1/2 TIME STEP BY LINEAR EXTRAPOLATION
C
      TWEN=TWIN
      TWUT=TWOUT
      WS1=WS
      DWIN=0.
      DWOUT=0.
      IF(LA.GT.1) DTT=0.5*DELT/DT1
      DO 100 I=1,NODES
      IF(LA.GT.1)PSIH(I)=PPSI(I)+DTT*(PPSI(I)-TPSI(I))
      IF(LA.LE.1) PSIH(I)=PPSI(I)
  100 CONTINUE
      ITER=0
C
C     ITERATION LOOP
C
  900 CONTINUE
      ITER=ITER+1
C
C     SET UP ELEMENT STIFFNESS MATRIX
C
      DO 200 K=1,NELEM
      XK1=1.0
      XK2=1.0
      C1=0.0
      C2=0.0
      IF (INT .EQ. 0) GO TO 780
      IF(PSIH(K).LT.0.0)CALL INTERP(XP,XK,PSIH(K),XK1,NP)
      IF(PSIH(K+1).LT.0.0)CALL INTERP(XP,XK,PSIH(K+1),XK2,NP)
      IF(PSIH(K).LT.0.0)CALL INTERP(YP,XC,PSIH(K),C1,NPC)
      IF(PSIH(K+1).LT.0.0)CALL INTERP(YP,XC,PSIH(K+1),C2,NPC)
      GO TO 785
  780 CONTINUE
      IF (PSIH(K).LT.0.0)CALL FNCPK(PSIH(K),XK1)
      IF (PSIH(K+1).LT.0.0)CALL FNCPK(PSIH(K+1),XK2)
      IF (PSIH(K).LT.0.0)CALL FNCPC(PSIH(K),C1)
      IF (PSIH(K+1).LT.0.0)CALL FNCPC(PSIH(K+1),C2)
  785 CONTINUE
      XK1=XK1*KSAT
      XK2=XK2*KSAT
C
C     DETERMINE INDIVIDUAL ELEMENTS IN EACH ELEMENT MATRIX
C
      A11=(XK1+XK2)*0.5/L
      A12=-A11
      A21=A12
      A22=A11
      B11=L*(C1/3.0+C2/6.0)/DELT
      B12=0.0
      B21=B12
      B22=L*(C1/6.0+C2/3.0)/DELT
      SF(1,1,K)=EPS*A11+B11
      SF(1,2,K)=EPS*A12+B12
      SF(2,1,K)=EPS*A21+B21
      SF(2,2,K)=EPS*A22+B22
      RHS(1,1,K)=(EPS-1.)*A11+B11
      RHS(1,2,K)=(EPS-1.)*A12+B12
      RHS(2,1,K)=(EPS-1.)*A21+B21
      RHS(2,2,K)=(EPS-1.)*A22+B22
      RH(1,1,K)=B11
      RH(1,2,K)=B12
      RH(2,1,K)=B21
      RH(2,2,K)=B22
      R(1,K)=-0.5*(XK1+XK2)
      R(2,K)= 0.5*(XK1+XK2)
  200 CONTINUE
C
C     ASSEMBLE THE ELEMENT STIFFNESS MATRICES INTO A GLOBAL MATRIX
C
C     TOP BOUNDARY CONDITION
C
      IF(NBC(1).EQ.0)GOTO 210
C
C     CONSTANT FLUX BOUNDARY CONDITION
C
      A(1)=SF(1,1,1)
      B(1)=SF(1,2,1)
      D(1)=RHS(1,1,1)*PPSI(1)+RHS(1,2,1)*PPSI(2)-R(1,1)+Q(1)
      GOTO 220
C
C     CONSTANT HEAD BOUNDARY CONDITION
C
  210 A(1)=0.0
      B(1)=1.0
      C(1)=0.0
      D(1)=BC(1)
  220 CONTINUE
C
C     INTERIOR NODES
C
      DO 250 K=1,NELEM1
      K1=K+1
      A(K1)=SF(2,1,K)
      B(K1)=SF(2,2,K)+SF(1,1,K1)
      C(K1)=SF(1,2,K1)
      AA=RHS(2,1,K)
      BB=RHS(2,2,K)+RHS(1,1,K1)
      CC=RHS(1,2,K1)
      D(K1)=AA*PPSI(K)+BB*PPSI(K+1)+CC*PPSI(K+2)+R(2,K)+R(1,K1)
  250 CONTINUE
C
C     LOWER BOUNDARY
C
      IF(NBC(2).EQ.0) GOTO 260
C
C     CONSTANT FLUX BOUNDARY CONDITION
C
      A(NODES)=SF(2,1,NELEM)
      B(NODES)=SF(2,2,NELEM)
      D(NODES)=RHS(2,1,NELEM)*PPSI(NODES)+RHS(2,2,NELEM)
     * *PPSI(NODES)+R(2,NELEM)-Q(2)
      GOTO 270
C
C     CONSTANT HEAD BOUNDARY CONDITION
C
  260 A(NODES)=0.0
      B(NODES)=1.0
      C(NODES)=0.0
      D(NODES)=BC(2)
  270 CONTINUE
C
C     CALL TRIDIA
C
      CALL TRIDIA(NODES)
C
C     TEST OF CONVERGENCE
C
      EPSLON=0.0
      DO 300 I=2,NODE1
      CHG=ABS((PSI(I)-PP(I))/PSI(I))
      IF (CHG.LT.EPSLON)GOTO 300
      EPSLON=CHG
      NMAX=I
  300 CONTINUE
      WRITE(NPRT,1110)ITER,EPSLON,NMAX
 1110 FORMAT(1X,' MAX. RELATIVE CHANGE IN PRESSURE HEAD DURING '
     * ,' ITERATION'
     * ,I3,' WAS ',E13.5,' AT NODE ',I4)
      IF (EPSLON.LE.TOL.AND.ITER.NE.1) GOTO 500
C
C     IMPROVE THE PSIH VALUE FOR NEXT ITERATION
C
      DO 350 I=1,NODES
      PSIH(I)=0.5*(PPSI(I)+PSI(I))
      PP(I)=PSI(I)
  350 CONTINUE
      IF(ITER.LT.MAXIT)GOTO 900
      WRITE(NPRT,1010)ITER
 1010 FORMAT(' ',/,'******* MAX. NO. OF ITERATION EXCEEDED AT ',
     * I4/)
  500 CONTINUE
      WRITE(NPRT,1120)
 1120 FORMAT(' ',/,13X,'Z',13X,'PSI',6X,'THETA',/)
      Z=0.0
      IF (INT.EQ.1) GOTO 610
      DO 605 I=1,NODES
      CALL FNCPT (PSI(I),THETA)
      IF (PSI(I).GE.0.0) THETA=POR
      WRITE (NPRT,1011) Z,PSI(I),THETA
      Z=Z+DELZ
  605 CONTINUE
      GOTO 620
  610 DO 600 I=1,NODES
      CALL INTERP(XPP,XTHE,PSI(I),THETA,NPT)
      IF(PSI(I).GE.0.0)THETA=POR
      WRITE(NPRT,1011)Z,PSI(I),THETA
 1011 FORMAT(' ',10X,F6.2,F16.4,2X,F7.4)
      Z=Z+DELZ
  600 CONTINUE
  620 CONTINUE
C
      CALL MATBAL (NPRT,PPSI,R,RH,Q,NBC)
C     DETERMINE A TIME STEP SIZE FOR NEXT TIME STEP
C
      DT1=DELT
      IF (NBC(1) .EQ. 1) GO TO 47
      Q(1)=(PSI(1)-PSI(2)+DELZ)*EPS*R(2,1)/DELZ +
     & (PPSI(1)-PPSI(2)+DELZ)*(1.-EPS)*R(2,1)/DELZ
   47 DELT=AMIN1(DELT/EPSLON*TOL,0.1*DELZ/Q(1))
      IF (ITER .GT. 5) DELT=0.5*DELT
      IF (DELT .GT. DELMAX) DELT=DELMAX
      IF (TIME+DELT .GE. TMAX) DELT=TMAX-TIME
C
C     STORE THE PSI VALUES FOR NEXT TIME STEP
C
      DO 700 I=1,NODES
      TPSI(I)=PPSI(I)
      PPSI(I)=PSI(I)
  700 CONTINUE
C
      IF(TIME.GE.TMAX)STOP
      GOTO 1000
      END
C
C-----------------------------------------------------------------------
C
      SUBROUTINE INTERP(X,Y,XX,YY,N)
      DIMENSION X(N),Y(N)
C
C     LINEAR INTERPOLATION
C
      DO 10 I=2,N
      IF(XX.GT.X(I).AND.I.LT.N)GOTO 10
      AA=Y(I-1)+(XX-X(I-1))*(Y(I)-Y(I-1))/(X(I)-X(I-1))
      YY=AA
      GOTO 20
   10 CONTINUE
   20 RETURN
      END
C
C-----------------------------------------------------------------------
C
      SUBROUTINE TRIDIA(NN)
      COMMON A(51),B(51),C(51),D(51),ANS(51)
      DIMENSION BB(51),GG(51)
C
```

```
C         SET UP BB AND GG ARRAYS
C
          BB(1)=B(1)
          GG(1)=D(1)/B(1)
          DO 10 I=2,NN
          I1=I-1
          BB(I)=B(I)-A(I)*C(I1)/BB(I1)
          GG(I)=(D(I)-A(I)*GG(I1))/BB(I)
10        CONTINUE
C
C         PERFORM BACK SUBSTITUTION
C
          ANS(NN)=GG(NN)
          N1=NN-1
          DO 15 J=1,N1
          I=NN-J
          ANS(I)=GG(I)-C(I)*ANS(I+1)/BB(I)
15        CONTINUE
          RETURN
          END

C-----------------------------------------------------------------------
C
C---  NOTE! THE FOLLOWING FIVE FUNCTIONAL SUBROUTINES SPECIFICALLY APPLY TO
C           PANOCHE CLAY LOAM (WARRICK ET AL., 1971) ONLY.  USE ANOTHER
C           FUNCTIONAL RELATION FOR A DIFFERENT SOIL -----
C-----------------------------------------------------------------------
C
          SUBROUTINE FNCTP(XX,YY)
          IF (XX.LE.0.360622341 YY=-1300.*EXP(-10.5*XX)
          IF (XX.GT.0.360622341 YY=-1.59E07*EXP(-36.6*XX)
          RETURN
          END
C---------------   ------------------------------------------------
C
          SUBROUTINE FNCPT(XX,YY)
          IF (XX.LE.-29.484) YY=0.6829-0.09524*ALOG(ABS(XX))
          IF (XX.GT.-29.484.AND.XX.LE.-14.495) YY=0.4531-
     &    0.02732*ALOG(ABS(XX))
          RETURN
          END
C-----------------------------------------------------------------
C
          SUBROUTINE FNCTT(XX,YY)
          IF (XX.GT.60.0) YY=0.20
          IF (XX.LE.60.0) YY=0.15+0.0008333*XX
          RETURN
          END
C-----------------------------------------------------------------
C
          SUBROUTINE FNCPK(XX,YY)
          IF (XX.LE.-29.484) YY=19.34E05/37.3*(ABS(XX))**(-3.4095)
          IF (XX.GT.-29.484.AND.XX.LE.-14.495)YY=516.8/
     &    37.3*(ABS(XX))**(-0.97814)
          RETURN
          END
C-----------------------------------------------------------------
C
          SUBROUTINE FNCPC(XX,YY)
          IF (XX.LE.-29.484) YY=0.09524/ABS(XX)
          IF (XX.GT.-29.484.AND.XX.LE.-14.495) YY=
     &    0.02732/(ABS(XX))
          RETURN
          END

C-----------------------------------------------------------------
C
          SUBROUTINE MATBAL (NPRT,PPSI,R,RH,Q,NBC)
          DIMENSION PPSI(51),R(2,51),RH(2,2,51),Q(2),NBC(2)
          COMMON A(51),B(51),C(51),D(51),PSI(51)
          COMMON DELT,DELZ,EPS,NODES,TWIN,TWOUT,TWEN,TWUT,WS,WS1,WIS,
     &    DWIN,DWOUT,DELMAX,POR,TMAX,TIME
          TWIN=TWEN
          TWOUT=TWUT
C
C         COMPUTES WATER INFLOW OR OUTFLOW THROUGH THE UPPER BOUNDARY
C
          IF (NBC(1) .EQ. 1) GO TO 1
          Q(1)=(PSI(1)-PSI(2)+DELZ)*EPS*R(2,1)/DELZ*DELT
     &    - (PPSI(1)-PPSI(2)+DELZ)*(1.-EPS)*R(2,1)/DELZ*DELT
1         CONTINUE
          IF (Q(1) .GT. 0.0) GO TO 11
          DWOUT=DWOUT-Q(1)
          GO TO 12
11        DWIN=DWIN+Q(1)
12        CONTINUE
C
C         COMPUTES WATER INFLOW OR OUTFLOW THROUGH LOWER BOUNDARY
C
          IF (NBC(2) .EQ. 1) GO TO 2
          Q(2)=-(PSI(NODES-1)-PSI(NODES)+DELZ)*EPS*R(2,NODES-1)/DELZ*DELT
     &    - (PPSI(NODES-1)-PPSI(NODES)+DELZ)*(1.-EPS)*R(2,NODES-1)/DELZ
     &    *DELT
2         CONTINUE
          IF (Q(2) .GT. 0.) GO TO 13
          DWOUT=DWOUT-Q(2)
          GO TO 14
13        DWIN=DWIN+Q(2)
14        CONTINUE
C
C         COMPUTES CHANGE IN WATER STORAGE
C
          DWS=0.
          NODE1=NODES-1
          DO 140 K=2,NODE1
          DWS=DWS+(RH(2,2,K-1)+RH(1,1,K))*(PSI(K)-PPSI(K))*DELT
140       CONTINUE
          WS=WS+DWS
          WS2=WS+WIS
          TWIN=TWIN+DWIN
          TWOUT=TWOUT+DWOUT
          DWDIFF=DWIN-DWOUT
          TWDIFF=TWIN-TWOUT
          DERRW=ABS(DWS-DWDIFF)
          RERRW=ABS(WS-TWDIFF)
          WRITE (NPRT,475)
          WRITE (NPRT,471)
          WRITE (NPRT,473) DWIN,DWOUT,DWDIFF,DWS,TWIN,TWOUT,TWDIFF,
     &    WS,WIS,WS2,DERRW,RERRW
471       FORMAT (/31X,'* * * * MATERIAL BALANCE ERROR ANALYSIS * * * * ')
473       FORMAT (/,1X,'INC. WATER IN =',E11.4,T30,'INC. WATER OUT =',
     &    E11.4,T60,'INC. WATER IN & OUT =',E11.4,T95,'INC. WATER STRG.
     &    CHANGE =',E11.4,/1X,'CUM. WATER IN =',E11.4,T30,'CUM. WATER
     &    OUT =',E11.4,T60,'CUM. WATER IN & OUT =',E11.4,T95,'CUM.
     &    WATER STRG. CHANGE =',E11.4,/,' INTL. WATER STRG. =',E11.4,T30,
     &    'CUM. WATER STRG. =',E11.4,T60,'INC. WATER ERROR, % =',E11.4,
     &    T95,'CUM. WATER ERROR, % =',E11.4)
475       FORMAT (26('*****'))
          RETURN
          END
```

A Three-Dimensional Analytical Model to Aid in Selecting Monitoring Locations in the Vadose Zone

by C.R. McKee and A.C. Bumb

Abstract

Monitoring of the vadose zone is a potentially complex, time-consuming, and expensive problem. The location of monitoring points and selection of monitoring instruments can be optimized by using computer models. Numerical models developed for this purpose in the past have often been expensive and difficult to use. This paper describes a fast, three-dimensional, approximate analytical solution to the moisture content in the unsaturated zone. An analytical solution is available for steady-state drainage, whereas an approximate analytical solution is available for the transient case. The model will handle an arbitrary distribution of fluid sources, as well as vertical and horizontal impermeable boundaries.

The model may be applied to predict the incursion of fluid from accidental leakage or infiltration over large areas from unlined ponds and land treatment sites. The model is quite useful as an aid in designing monitoring or premonitoring programs near hazardous waste sites. Examples are presented to demonstrate the model's utility in estimating the maximum spread of a contaminant, the extent to which the fluid may spread with depth, the regions of high and low capillary pressure, and the non-linear behavior of the saturation when drainage from several sources in considered. These results are useful for the placement of monitoring locations and the selection of appropriate instruments, and as a tool in working with regulatory agencies to design monitoring programs. A glimpse of the future is necessary for today's planning. Computer models are some of the most useful crystal balls we have available.

Introduction

Computer models for predicting unsaturated flow near waste sites have become more numerous and prevalent in recent years, although their use has yet to become widespread. A review of such models has been given by Oster (1982). The use of models in the unsaturated zone is complicated by a lack of data and the need for the operator to be familiar with numerical analysis of non-linear problems. Moreover, the assessment of the impact at a hazardous waste site is a time-dependent problem in three dimensions (Adams et al. 1983), which further suggests its complexity. Furthermore, instabilities can arise, requiring a linearization of the saturation vs. capillary pressure curve (Segol 1982). Comparatively few hydrologists and geohydrologists have the necessary mathematical and computer training to handle such difficulties. Indeed, many of these problems continue to be the object of present-day research. The authors have developed a computer model that is free of the problems associated with the use of numerical models, yet is three-dimensional and can be run rapidly on a microcomputer by the experienced hydrogeologist.

The problems associated with monitoring and predicting the fate of hazardous waste in the vadose zone can lead to considerable expense (see, e.g., Devary and Schalla 1983) and these programs, if not well planned, may not obtain the necessary data, resulting in delays that further escalate costs. Everett et al. (1982), in an excellent review of monitoring systems, point out that premonitoring programs are necessary because they provide clues on potential mobility rates and valuable information for the design of a vadose zone monitoring system. The approach they advocate appears largely intuitive and based on previous experience. Personal experience, unfortunately, is difficult to quantify and pass on to other investigators. Hence, the use of premonitoring data as input to a mathematical model to predict the direction and rate of migration of contaminants is advocated. Most investigations do not have sufficient *funds available in the premonitoring* stage to obtain the extensive data required for numerical modeling. Thus, the recommended approach is to use an analytical model. This will allow optimum use of the monitoring budget to concentrate sensors and sampling devices in the most likely avenues of pollutant migration. The authors' experience in working with regulatory agencies is that they often require a worst-case analysis, using a mathematical model, to predict paths of contaminant migration in case containment mechanisms fail. The monitoring systems are then designed, based upon this analysis, for early detection of contaminant migration.

According to Everett et al. (1982), a vadose zone monitoring program consists of premonitoring followed by an active monitoring program. Premonitoring consists of assessing the hydrologic and geochemical properties of the vadose zone. In this study, "premonitoring" is synonymous with the term "site characterization." Here, the authors are interested only in the hydrologic characterization of the vadose zone. Lack of a chemical assessment is not a significant problem because anions, many complexes, and some organics travel with little or no adsorption. Some chemicals may affect fluid mobility, and this can be readily incorporated in models using different mobility rates. Chemical movement in the vapor phase may be important, but is not considered here. Tracking the infiltration front usually represents a worst-case analysis. If this shows unacceptable migration, then a geochemical site characterization may be necessary.

Selection of a Computer Model

The mathematics of unsaturated or multiphase flow are well known (they are reviewed by Bear 1979, Corey 1977). The equations have also been tested in numerous hydrologic, agricultural and petroleum laboratories. Nonetheless, the equations remain very difficult to solve either analytically or numerically due to their non-linearity and tendency to form sharp fronts. Sharp fronts, in turn, are the result of a non-linear dependence of the hydraulic conductivity on saturation. Ground water velocity increases with saturation, causing waves or perturbations to catch up to the infiltration front. The process is analogous to the formation of shock waves in hydrodynamics.

Procedures in modeling unsaturated flow are reviewed or illustrated by Lappala (1982), Segol (1982), Sharma (1982), and Dagan and Bresler (1983). These procedures or steps may include: (1) site characterization to obtain field data for a model; (2) selection of a mathematical model; (3) selection of a method to obtain a solution from the mathematical model; (4) prediction and comparison with field data; and (5) history matching and improvement of the model selected.

According to Dagan and Bresler (1983), accurate site characterization in the case of unsaturated flow is a time-consuming process. Moreover, the error due to spatial variability, which is random in many cases, can be much larger than that due to model approximation. The reason for the difficulty stems not only from the usual geologic variability but also from the large array of parameters that must be determined. These include the non-linear functional dependence of saturation on capillary pressure of suction and the corresponding relationship between effective saturation and hydraulic conductivity. Approximately eight parameters are required to characterize a given soil type depending upon the functional forms selected to describe the capillary pressure, saturation, and hydraulic conductivity curves. Because it is often difficult to obtain the desired accuracy for necessary measurements, and because unsaturated flow properties are often unknown and must be inferred from measurements in the literature on materials having similar composition, the selection of an elaborate method to solve the equations would appear unwarranted. This is not a serious limitation because simple approximate methods, even in a spatially variable field, generally lead to predictions as accurate as field data for the saturation over the entire field (Dagan and Bresler 1983).

A typical approach to the problem is to state that because the equations are non-linear and because heterogeneities exist, a finite difference or finite element approach is the only practical method of obtaining a solution. The authors do not agree with this viewpoint, and indeed believe that in many cases there are strong reasons for considering an approximate analytical solution instead. The alternatives will be compared to justify this approach.

Once the basic site characterization is complete and a mathematical model describing the physical situation is at hand, the next step is to select a solution technique for the equations. The major mathematical solution techniques include finite difference, finite element, analytical, and combined analytical and numerical methods.

Finite Difference and Finite Element Models

For steady-state problems, using regular meshes and the common triangular elements, it is easy to show that both the finite element method (FEM) and the finite difference method (FDM) result in identical difference equations (Allen 1955, Zienkiewicz 1977). Higher-order FEM have not proven as useful in solving unsaturated flow equations. Higher-order methods involve more computational time per discretization point, which is compensated for by using fewer points. However, this works only if the functions are smooth and interpolation can be performed with high accuracy (Finlayson 1980). Because unsaturated flow often results in rapid changes in saturation, higher-order methods must still use more points to define these areas, which often makes them prohibitive in cost (Abou-Kassem and Aziz 1982, Ewing 1983).

FEM enjoys advantages over FDM in ease of interpolating data and fitting odd boundaries. However, for steady-state and transient problems with variable coefficients in two dimensions, FEM has some disadvantages (Emery and Carson 1971). These include long execution times and large storage requirements, which may be an order of magnitude larger than using FDM, as well as potential inaccuracies in the treatment of sources and transient terms. For three-dimensional problems, the storage and execution time favor FDM by the square of the matrix band width over two dimensions. Both, however, become unwieldy in storage and execution time in three dimensions when fine zoning is required. According to Brebbia (1981), the finite element method, in many cases, constitutes an inaccurate and expensive technique, whose early claims were often exaggerated.

While these differences are of interest, it is noted that efficiency considerations generally dictate that lower-order methods be employed. Except for storage and execution times, the stability and accuracy of the two methods are similar.

For regular meshes both FDM and FEM are spatially accurate to second-order terms (square of the nodal point spacing multiplying the higher-order derivatives of the dependent variable). However, most practical problems require the use of irregular meshes that are only accurate to first-order terms. Upstream weighting of conductivities and fully implicit weighting are frequently used to preserve stability, and these, again are only first-order accurate. As long as the functions involved are smooth, the higher-order derivatives in the error terms remain bounded. When sharp fronts are present, however, the higher-order derivatives become very large and can cause substantial error. Under this condition, order-of-error concepts lose their value, and the solution of the difference equation will generally not converge to that of the partial differential equation.

Lax's equivalence theorem for linear equations is often invoked to show that if stability of the difference equations occurs, then the solution will converge to that of the differential equation (Smith 1978). However, both the FEM (Segol 1982) and the FDM (Sharma 1982) formulations are unstable (implying lack of convergence to the differential equation) unless the saturation vs. capillary pressure curves are linearized. But if non-linear material properties are to be linearized, why measure the non-linear soil properties in the first place? Upstream weighting of conductivities and the commonly used fully implicit technique are deceptive terms to increase stability. These methods effectively add diffusion terms to the solution, which were not present in the original differential equation.

For low-order FEM and FDM, grid orientation effects can also distort the solution. (For a discussion, see Aziz and Settari 1979). The calculated displacement fronts will appear vastly different depending on whether the leading edge of the infiltration front is moving parallel to or diagonally along the mesh. Both answers are calculated incorrectly! Grid orientation effects are eliminated using higher-order FDM (Yanosik and McCracken 1973, Abou-Kassem and Aziz 1982) and FEM (Settari et.al. 1977), but again at additional expense and complexity.

In the authors' experience, some instabilities can be eliminated by using a grid that is smaller than the displacement head p_d (see Brooks and Corey 1964, for definition). However, as Segol (1981) states, "This usually requires the nodal spacing of the finite element grid to be small (on the order of centimeters or tens of centimenters) to avoid numerical instabilities. It is impractical to design such a fine mesh for a field problem because of economic considerations."

The preceding remarks serve to illustrate the authors' reservations concerning the use of FEM and FDM for solving the equations of unsaturated flow. In general, their power and accuracy for solving highly non-linear equations are often overstated. The thousands of waste sites requiring analysis, compared with the relatively few geohydrologists familiar with advanced numerical techniques, and the questionable accuracy of these techniques in practical use, has motivated the authors to re-examine the utility of purely numerical solutions and proceed instead in another direction: that of analytical solutions.

Analytical Solutions

Included in this category are analytical, quasi-analytical, and approximate analytical solutions. Following Philip (1969), the authors define analytical solutions as those found completely by mathematical analysis. Quasianalytical solutions are those that have a well-defined mathematical form, but require numerical techniques for their evaluation; integral equations and iterative successive approximation methods fall in this category. Approximate analytical solutions include situations in which the solution does not exactly satisfy the differential equation, but the error can be shown to be negligible for specified conditions. The latter approach broadens the range of possible applications and increases the flexibility of analytical solutions, and is the approach followed in this article.

The advantages of the analytical solution the authors are proposing are: (1) it is three-dimensional; (2) no numerical dissipation or damping coefficients are required; and (3) it is fast enough to run on microcomputers. The computer model can handle arbitrary distribution of unlined ponds, land treatment areas, and/or leakage from surface sites, directional permeability, vertical impermeable and constant-head boundaries, and horizontal impermeable boundaries. For certain cases, time-dependent solutions are available. Among the disadvantages are that the boundary geometry must be regular, permeability may not vary spatially (although directional permeability is included, which may sometimes account for layering effects), and the model should not be used near the water table if mounding of the phreatic surface is appreciable. These drawbacks will be removed in the future using combined analytical and numerical techniques.

Theory

The governing equation for the movement of fluid in an unsaturated medium was first obtained by Richards (1931). When conservation of mass is applied using Darcy's law, as modified by Buckingham (1907), and allowing that the gravity vector need not coincide with a positive coordinate axis, the governing equation for unsaturated flow is (in general terms)

$$\nabla \cdot \left\{ \underset{\sim}{K}(S) \nabla \left(p_c(S) + \frac{\vec{g} \cdot \vec{R}}{|g|} \right) \right\} = -\phi \frac{\partial S}{\partial t} \qquad (1a)$$

where $\underset{\sim}{K}$ is the permeability tensor; p_c is the capillary pressure head or suction, measured in units of head of the wetting fluid; $\overline{R}$ is the radius vector from the source; S is saturation, t is time; and ϕ is porosity. When z is defined positive downward, with gravitational force downward, in a homogeneous medium, the result is

$$\nabla \cdot \left\{ K(S) \nabla \left(p_c(S) + z \right) \right\} = -\phi \frac{\partial S}{\partial t} \qquad (1b)$$

On the other hand, if z is taken as positive upward, then the sign of z is negative in Equation 1b. In this article z is taken as positive downward.

A general solution for Equation 1b is not available because of its non-linear character, which arises from the interrelationship of K, p_c, and S. For certain cases, analytical solutions are available (Philip 1969). This article describes an analytical solution that is computationally faster than numerical procedures, yet maintains the time and three-dimensional spatial dependence. The solution is obtained by simplifying Equation 1b using a Kirchhoff transformation. The simplified differential equation is

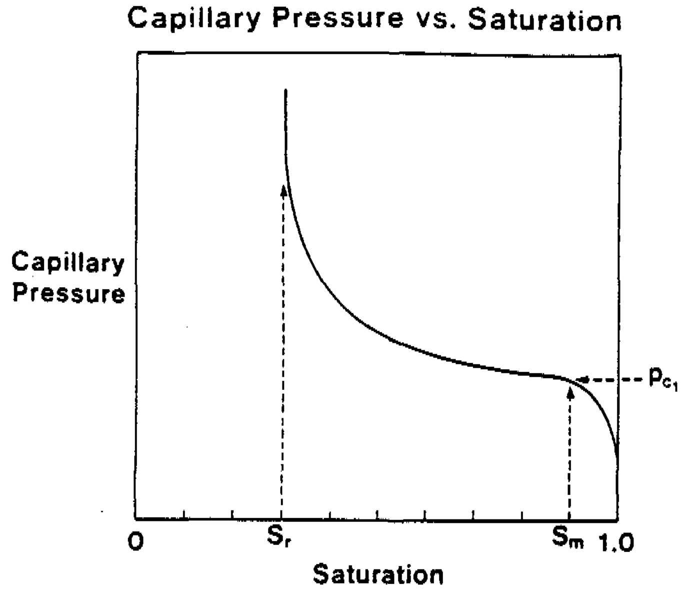

Figure 1. Typical plot of capillary pressure as a function of saturation to illustrate the selection of S_r, S_m, and p_{c_1}.

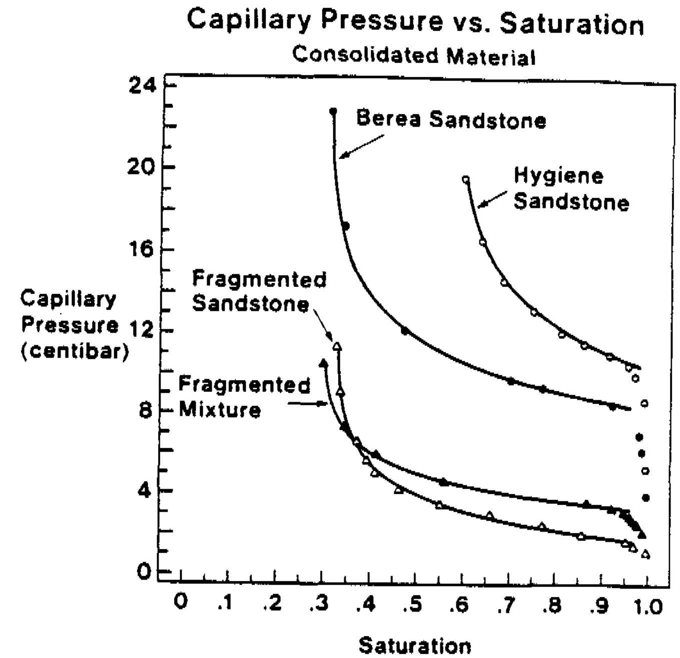

Figure 2. Curve fits (solid lines) to match data from Brooks and Corey (1964) for consolidated material. Data were converted to an equivalent water-air system using Brooks and Corey's Equation 17.

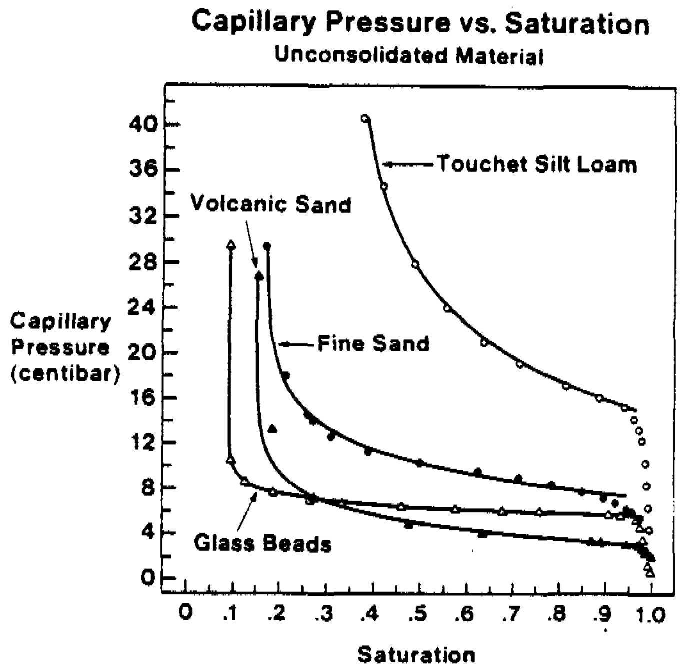

Figure 3. Curve fits (solid lines) to match data from Brooks and Corey (1964) for unconsolidated material. Data were converted to an equivalent water-air system using Brooks and Corey's Equation 17.

linear for some specific functional relationships between K, S, and p_c, described in the following section. An analytical solution can then be obtained for an unbounded medium, while for a bounded medium, a modified method of images is used.

Functional Dependence of p_c and K on S

Many empirical relationships for saturation vs. capillary pressure and saturation vs. hydraulic conductivity have been suggested (Corey 1977, Bumb 1987). The specific functional relationships for the dependence of capillary pressure and hydraulic conductivity on saturation, which will be used to transform Richards' equation, are

$$S_e = \frac{S - S_r}{S_m - S_r} = \exp\left(-\frac{p_c - p_{c_1}}{\beta}\right) \qquad (2)$$

and

$$K = K_o S_e^n \qquad (3)$$

where K_o is saturated hydraulic conductivity; n is an exponent in Equation 3; p_{c_1} is a parameter in Equation 3; S_e is effective saturation; S_m is maximum saturation; S_r is residual or irreducible saturation, and β is a parameter in Equation 2. When capillary pressure is equal to p_{c_1}, effective saturation is 1.0, and actual saturation is equal to the maximum saturation. In general, the more uniform the pore size distribution, the smaller β becomes. Equation 2 is referred to as a Boltzmann distribution. It is not valid for $p_c > p_{c_1}$, since it will yield values of S_e greater than unity.

To establish the validity of the functional relationship between p_c and S, Equation 2 is used to fit experimental data for capillary pressure vs. saturation. For plotted capillary pressure vs. saturation data, the values of S_r, S_m, and p_{c_1} are approximately established as shown in Figure 1. Once approximate values of S_r and S_m are selected, p_{c_1} and β can be obtained using standard curve-fitting techniques (minimization of absolute error, least-squares method, relative least-squares method, etc.). Depending on the quality of the curve fit, S_r and S_m may need to be adjusted and the curve-fitting technique reapplied to obtain final parameter values.

Equation 2 was fitted to data from eight samples studied by Brooks and Corey (1966) and one sample from a low-level waste management site in the Powder River Basin in Wyoming. Figures 2, 3 and 4 show the data points along with the curves obtained from Equation 2 using the values of parameters given in Table 1. As can be seen, the curve fits are excellent in the interval S_r to S_m.

Expressions defining the relationship between S and p_c are more commonly found in the form of a power law (Corey 1977). These, however, are also empirical relationships. Curve-fitting techniques are required to select the values of the adjustable parameters, and their range of validity is also restricted (Bumb 1987). Thus, these relationships suffer the same restrictions as Equation 2. Equation 2, however, has the advantage of permitting Richards' equation to be transformed to a linear equation for certain cases. This fact, and the fact that a reasonable fit to experimental data is obtained, provide the justification for using Equation 2.

TABLE 1
Properties of the Soils Used in the Examples

Sample	S_r (%)	S_m (%)	P_{c_1} (cb)	β (cb)
Powder River Basin soil	27.7	95.0	3.97	78.09
Touchet silt loam*	36.0	96.5	14.99	8.32
Fine sand*	17.4	94.5	7.39	3.32
Hygiene Sandstone*	58.0	97.5	10.56	3.27
Berea Sandstone*	31.0	96.0	8.48	2.75
Volcanic sand*	15.5	98.0	3.05	2.19
Fragmented sandstone*	33.0	97.0	1.67	1.70
Fragmented mixture*	30.0	96.0	3.27	1.47
Glass beads*	9.5	97.0	5.63	0.91

*Converted to equivalent water-air system using Equation 17 of Brooks and Corey (1964).

A power-law expression relating relative permeability and effective saturation has been proposed by several authors (Corey 1954, Irmay 1954, Averjanov 1962). These expressions are equivalent to Equation 3, the values of K_o, S_m, S_r being defined by the data, leaving n as an adjustable parameter. Corey (1954) proposed a value of 4 for the exponent in Equation 3, while Irmay (1954) proposed a value of 3. Reiss (1980) suggested a value of 1 for a smooth fracture. Using data from Brooks and Corey (1964) and Irmay (1954), our curve-fitting procedures suggested n to be in the interval from 2 to 3 for consolidated and unconsolidated material. By analyzing drawdown test data from a saturated coal seam in the presence of desorbing methane, Bumb (1987) and McKee and Bumb (1987) obtained $n = 3$, in agreement with Irmay's theoretical result. The case for $n = 1$ is particularly attractive, because then an analytical solution for the transient case can be obtained. For $n \neq 1$, Richards' time-dependent equation does not transform to a linear equation and successive approximations may be used to obtain a solution.

Analytical Solutions

A new variable, θ, is defined using a Kirchhoff transformation, to reduce the non-linearity of Equation 1b:

$$\theta = \int_{p_c}^{\infty} K \, dp_c = \frac{\beta}{n} K \tag{4}$$

Then, using Equations 2 and 3 and assuming an isotropic medium, Equation 1b is transformed to

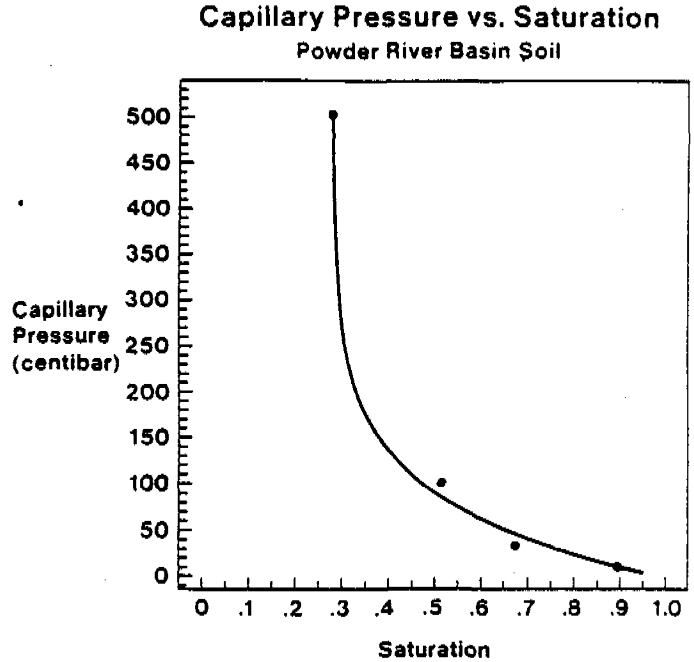

Figure 4. Curve fit to match data for PRB soil.

$$\frac{\partial^2\theta}{\partial x^2} + \frac{\partial^2\theta}{\partial y^2} + \frac{\partial^2\theta}{\partial z^2} - \alpha \frac{\partial\theta}{\partial z} = \frac{1}{D}\frac{\partial\theta}{\partial t} \tag{5a}$$

where

$$\alpha = \frac{n}{\beta} \tag{5b}$$

and

$$D = \frac{\beta K_0}{\phi(S_m - S_r)} S_e^{n-1} \tag{5c}$$

As can be seen from Equation 5c, the non-linearity involving θ for the term in brackets becomes unity only for $n = 1$. For $n = 1$, the coefficient of the diffusivity, D, simplifies to

$$D = \frac{\beta K_0}{\phi(S_m - S_r)} \qquad \text{for } n = 1 \tag{5d}$$

The same result can be obtained for anisotropic media by scaling the coordinate system using the following transformations:

$$x = x^* \sqrt{k_y/k_x} \tag{5e}$$

$$y = y^* \sqrt{k_x/k_y} \tag{5f}$$

$$z = z^* \left[\sqrt{\frac{k_x/k_y}{k_z}}\right]^{1/2} \tag{5g}$$

and

$$\alpha = \frac{n}{\beta}\left[\frac{k_z}{\sqrt{k_x/k_y}}\right]^{1/2} \tag{5h}$$

where x^*, y^* and z^* are the actual coordinates in the anisotropic media and coincide with the principal axis of permeability.

Note that Equation 5a is a linear differential equation for $n = 1$ in the transient case and for all values of n at steady-state. The boundary and initial conditions are obtained by recognizing (1) that the medium is initially assumed to be at uniform saturation; (2) that far from the point source the medium will be unaffected; and (3) that there is a source of constant strength (infiltration rate) at the draining site.

Time-Dependent Solution for n = 1

The solution to Equation 5a for $n = 1$ is obtained by analogy with the problem of heat transfer from a point source of constant strength moving through a uniform medium. The solution for a source at the origin is (Carslaw and Jaeger 1959)

$$\Delta\theta = \theta - \theta_o = \frac{Q}{8\pi\sqrt{\pi D}} \int_0^t dt' \frac{\exp\left[-\frac{(z - \alpha D(t-t'))^2 + x^2 + y^2}{4D(t-t')}\right]}{(t-t')^{3/2}} \tag{6a}$$

where θ_o is the value of θ at initial saturation, and $\Delta\theta$ is the change in θ. Evaluating the integral for a source with infiltration rate Q at x',y',z' results in

$$\theta - \theta_o = \frac{Qe^{\alpha(z-z')/2}}{8\pi R}\left(e^{\alpha R/2}\,\mathrm{erfc}\left[\frac{R}{2\sqrt{Dt}} + \frac{\alpha\sqrt{Dt}}{2}\right] + e^{-\alpha R/2}\,\mathrm{erfc}\left[\frac{R}{2\sqrt{Dt}} - \frac{\alpha\sqrt{Dt}}{2}\right]\right) \tag{6b}$$

where

$$R = \sqrt{(x-x')^2 + (y-y')^2 + (z-z')^2} \tag{6c}$$

This solution is for a point source. Areal leakage for land treatment facilities can be obtained by superposition of a large number of point sources. Superposition can be used to sum any number of solutions of the form of 6b, since 5a is linear when $n = 1$ or in the steady-state case. Saturation as a function of space and time is obtained using the inverse transformation from Equations 2, 3, and 4,

$$S = S_r + (S_m - S_r)\left(\frac{n\theta}{\beta K_o}\right)^{1/n} \tag{7}$$

Time-Dependent Solution for n ≠ 1

As noted earlier, governing Equation 5a is non-linear when $n \neq 1$. However, the non-linearity occurs only in the coefficient of diffusivity, D. The non-linearity for D (Equation 5c) is in the S_e term. To be conservative, the authors evaluate the coefficient of diffusivity by substituting unity for S_e. By doing so, diffusivity is overestimated, and therefore the spreading of soil moisture content is overestimated. In the limiting case of large times, time-dependent model calculations are the same as steady-state model calculations, indicating some confidence in the approximation.

Steady-State Solution

If the steady-state case is considered, the $n = 1$ restriction may be removed because the governing equation,

$$\frac{\partial^2\theta}{\partial x^2} + \frac{\partial^2\theta}{\partial y^2} + \frac{\partial^2\theta}{\partial z^2} - \alpha\frac{\partial\theta}{\partial z} = 0 \tag{8}$$

is linear for all values of n. Non-linearity, however, is preserved in the inversion to capillary head and saturation. The solution for the steady-state case is

$$\theta - \theta_o = \frac{Q}{4\pi R}\exp\left\{-\frac{\alpha}{2}\left(R - (z - z')\right)\right\} \tag{9}$$

This result is also from Carslaw and Jaeger (1959), as noted by Philip (1969).

Boundaries

The solutions presented in the preceding section are valid for a vadose zone of infinite depth and extent. These assumptions are questionable for many situations, particularly when the physical boundaries of the vadose zone are near the leakage or infiltration. A common example is leakage under a lined pond, where the lining forms a horizontal impermeable boundary. Solution techniques for impermeable boundaries can be developed using the approximate method of images and non-linear superposition for partial differential equations. Because the results are different for horizontal and vertical boundaries, they are presented separately.

Horizontal Impermeable Boundary Above the Source

When no flow through the soil surface is allowed, and the source is at a depth d below the surface, Raats (1972) gives the following equation:

$$\theta_d - \theta_o = \Delta\theta_\infty[r,z-d] + e^{-\alpha d}\,\Delta\theta_\infty[r,z+d] - \frac{Q\alpha}{4\pi}\,e^{\alpha z}\,E_1\left[\frac{\alpha}{2}\left(z+d+\sqrt{r^2+(z+d)^2}\right)\right] \tag{10}$$

where E_1 is the exponential integral function. Equation 10 is also applicable with appropriate definitions of d for any impermeable boundary above the source.

Horizontal Impermeable Boundary Below the Source

For an impermeable boundary at $z = a$, the no-flux condition is represented by:

$$\text{flux} = -K\frac{\partial}{\partial z}\left(p_c + \frac{\vec{g}\cdot\hat{e}_z z}{|\vec{g}|}\right) = 0 \quad \text{at } z = a \tag{11}$$

where $\hat{e}_z$ is a unit vector in the positive z direction. This condition represented in terms of the Kirchhoff transformation variable θ is

$$\text{flux} = \left.\frac{\partial\theta}{\partial z}\right|_{z=a} - \frac{\vec{g}\cdot\hat{e}_z}{|\vec{g}|}\left.K\right|_{z=a} = 0 \tag{12}$$

The theory of images, as illustrated in Figure 5, has been used extensively in the hydrology of saturated flow to model impermeable and constant-head boundaries (see, for example, Muskat 1946), and in conduction of heat in solids to model perfect insulation or constant temperature (Carslaw and Jaeger 1959). For these applications, θ would represent the potential (head or temperature) and the no-flow boundary condition given by $\nabla \cdot \theta = 0$ at the boundary. In that case the exact method of images results in $\theta = \theta_R + \theta_I$, where θ_R is the solution for the real source and θ_I is the solution for the image source. In the saturated flow case $(\alpha + 0)$, the real and image solutions have the same mathematical form, but the presence of gravity causes an asymmetry between them for unsaturated flow. The authors' modified method of images has the same form as the classical method of images, namely

$$\Delta\theta = \Delta\theta_R + \Delta\theta_I^h \tag{13}$$

In Equation 13, θ_R is the solution due to a "real" point source at (x′,y′,z′) in an infinite medium (which may be either Equation 6b, time-dependent, or Equation 9, steady-state) and θ_I^h is the solution due to an "image" point source for a horizontal boundary at (x′,y′, 2a-z′) in an infinite medium with gravitational force acting upward:

$$\Delta\theta_I^h = \theta_I^h - \theta_o = \frac{Qe^{-\alpha(z-2a+z')/2}}{8\pi R_I}\left\{e^{\alpha R_I/2}\,\mathrm{erfc}\left(\frac{R_I}{2\sqrt{Dt}} + \frac{\alpha\sqrt{Dt}}{2}\right) + e^{\alpha R_I/2}\,\mathrm{erfc}\left(\frac{R_I}{2\sqrt{Dt}} + \frac{\alpha\sqrt{Dt}}{2}\right)\right\} \tag{14a}$$

where

$$R_I = \sqrt{(x-x')^2 + (y-y')^2 + (z-(2a-z'))^2} \tag{14b}$$

The steady-state image solution is also obtained by changing the sign of (z–z′) in Equation 9 and replacing R with R_I. Notice that the flow due to the "real" solution (θ_R) will be downward (gravity pulling water downward), while the flow due to the "image" solution (θ_I^h) will be upward (the direction of gravity is reversed). The flux due to a real source in which gravity is downward is then

$$\mathrm{flux}_R = \left(\frac{\partial\theta_R}{\partial z} - K\right)\Bigg|_{z=a} \tag{15}$$

and the flux due to an image source in which gravity is upward is

$$\mathrm{flux}_I = \left(\frac{\partial\theta_I}{\partial z} + K\right)\Bigg|_{z=a} \tag{16}$$

and the total flux at the boundary is given by

$$\mathrm{flux} = \mathrm{flux}_R + \mathrm{flux}_I = 0 \tag{17}$$

which is satisfied as shown in the appendix, and hence the solution is Equation 13. The error introduced by reversing the sign of gravity is evident when Equation 13 is substituted into differential Equation 5 as all the terms do not cancel (see appendix). The remaining terms vanish exponentially with distance from the real source.

Vertical Impermeable Boundary

The vertical impermeable boundary at x = b is represented by

$$\frac{\partial}{\partial_x}\left(p_c + z\right) = 0 \tag{18}$$

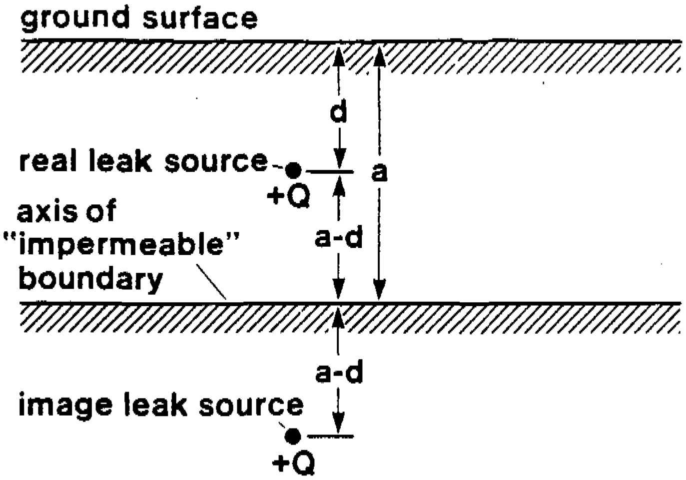

Figure 5. Schematic of real and image sources used to model a horizontal "impermeable" barrier under the real source.

or, equivalently,

$$\frac{\partial\theta}{\partial x} = 0 \tag{19}$$

This is easily satisfied, with no change in the sign of gravity, by

$$\nabla\theta = \nabla\theta_R + \nabla\theta_I^v \tag{20}$$

where θ_R is the solution due to the "real" point source and θ_I^v is the solution due to the "image" point source located at (2b-x′,y′,z′); θ_I^v is obtained by substituting (2b-x′) for x′ in Equation 6a.

Flux and Velocity

The flux in the unsaturated zone is given by

$$\mathrm{flux} = -K\,\nabla\cdot\left(p_c + \frac{\vec{g}\cdot\hat{e}_z z}{|\vec{g}|}\right) \tag{21}$$

where $\hat{e}_z$ is a unit vector in the positive z direction. Note that p_c is in units of head of water (or wetting fluid). The x, y, and z components of flux in terms of θ are

$$\text{x component of flux} = \frac{\partial\theta}{\partial x} \tag{22a}$$

$$\text{y component of flux} = \frac{\partial\theta}{\partial y} \tag{22b}$$

$$\text{z component of flux} = \frac{\partial\theta}{\partial z} - \frac{\vec{g}\cdot\hat{e}_z}{|\vec{g}|}\,\frac{n}{\beta}\,\theta \tag{22c}$$

Derivatives of θ are easily calculated from the expression for θ. Equation 22 is linear; therefore, the method of superposition can be used to obtain flux. If a horizontal impermeable boundary below the source exists, Equation 22 will have the appropriate sign with the second term on the right.

The cross-sectional area for particle movement is reduced by a factor of ϕS. Therefore, the particle velocity, v, is obtained from flux using

$$v = \frac{\mathrm{flux}}{\phi S} \tag{23}$$

Application of the Computer Model to Monitoring

There are at least six ways in which computer modeling can aid in designing an effective monitoring program: (1) The maximum spread, both laterally and vertically, of contaminants from a leak or waste site can be estimated. Most monitoring should be concentrated in this region, with sparse monitoring outside it to check that the movement of fluid is as anticipated; (2) The model will indicate whether fluid from the site tends to spread with depth. Accordingly, samplers and instruments, such as moisture blocks, can be set at depths where they will be most likely to intercept fluids from the source; (3) Regions beneath the waste site or leak can be classified into areas with low and high soil moisture suction or capillary pressure head values (most moisture movement occurs at less than a few meters of suction head). This information can be used to identify the most accessible flow region for instrumentation, because the high flow region will transport contaminants most rapidly; (4) One can, from the computer output of suction and saturation, estimate the range of suction and saturation values expected in the vertical plume. This range can be used to select the optimum instrumentation to measure moisture content and potential, and the appropriate sampling units such as lysimeters. Many types of instruments are available; however, they often work over limited ranges in soil moisture and suction. Computer calculations will help reduce the uncertainty in selecting appropriate instruments to carry out the desired function. (5) The non-linear nature of hydraulic conductivity and capillary pressure/saturation must be considered when leakage occurs from multiple adjacent sources in the same area. Superposition of flows from multiple sources can create an unanticipated region of higher flow between the sources; and (6) The computer model can be used as an aid in working with regulatory agencies to lend assurance that an adequate monitoring plan has been, or will be, implemented.

Two different soil types will be used to illustrate the preceding concepts. The first, termed Touchet Silt Loam (TSL), was studied by Brooks and Corey (1964) and has 0.54 ft^{-1} (1.77 m^{-1}) for the value of α when n = 3. The second is a sample taken from the Powder River Basin (PRB) in Wyoming in conjunction with an investigation for an experimental low-level waste disposal facility. For this soil, α is 0.057 ft^{-1} (0.189 m^{-1}), again for n = 3. According to Philip (1969), α for most soils lies in the range of 1.52 to 0.06 ft^{-1} (5 to 0.2 m^{-1}). Note that α is proportional to $1/\beta$ and that large β values correspond to a wide range of pore sizes. Hence, TSL soil contains an average range of pore sizes for the soils Philip (1969) studied, while PRB soil is within the range expected but toward the lower range of α, indicative of a wide range of pore sizes.

These two soil types were chosen because they exhibit very different behavior of the vertical unsaturated flow plumes, and they serve to illustrate the points the authors have made for the use of a computer model. In all cases, the effective saturation, S_e, is plotted in the accompanying figures. The real saturation can be obtained using the values of S_m and S_r found in Table 1. When $S_e = 0$, the soil is at residual saturation, S_r, where soil water movement is negligible. The permeability of the PRB soil was measured at 0.4 darcy, or a hydraulic conductivity of 1.15 ft/day (0.35 m/day) for water movement, and a porosity of 34.5 percent. TSL was assumed the same so that the effect of α on the saturation profile can be illustrated.

Vertical permeability is normally less than horizontal permeability. A ratio of horizontal to vertical permeability of 4 was selected based on measurements conducted on shallow aquifers. It is assumed a layered soil will exhibit the same behavior. If S_e is the same for both soils, then the hydraulic conductivity will be the same for soils with the same saturated hydraulic conductivity. For the following examples, it is assumed that initially the soils are at irreducible saturation. All the steady-state examples use n = 3 to relate effective saturation to hydraulic conductivity, i.e., $K = K_0 S_e^3$.

Point Source Leakage

Point source leakage is typical of the behavior of leaks from buried pipes or tanks. The three-dimensional axisymmetric solution for TSL and PRB soils is given in Figure 6. The leakage rate is assumed to be 52.8 gpd (200 liters/day). Note that at 33 feet (10m) below the source, the fluid has spread laterally to 33 feet (10m) for TSL and 72 feet (22m) for PRB soil using the S_e = 5 percent contours to illustrate the penetration of the fluid. For equivalent increases in effective saturation, S_e, the plume for PRB soil is much wider. However, from a contaminant transport perspective, TSL maintains higher soil moisture content directly under the leak, resulting in faster movement of the fluid. At 100 feet (30m) horizontally from the leak and 100 feet (30m) deep, TSL should not transport contaminants, whereas PRB soil will. The relative siting of monitoring instruments is obvious from the two plots of effective saturation.

Uniform Pond Leakage

Figure 7 shows a cross section of an unlined pond or land treatment site 49.2 feet (15m) by 98.4 feet (30m). Infiltration of 9.17 gpm (50 m^3/day) is assumed, which is approximately 30 percent of the maximum soil infiltration rate. This allows for a flow reduction due to fines at the surface. The results of calculations in the TSL and PRB soils are given in Figure 8. Note that at 80 feet (24m) from the edge of the pond for TSL [120 feet (37m) from the origin along the major axis] instrumentation would have to be buried at a depth of 100 feet (30m) to intercept appreciable amounts of fluid seepage from the site. However, the PRB pond calculation indicates considerable saturation at the same distance from near the surface to the maximum depth calculated. The velocity, which increases with saturation, shows more gradual variation. At 65 feet (20m) deep and less than 30 feet (10m) away from the pond, the effective saturation is 38 percent, which is very close to saturation under the pond in PRB soil. A sample at this point would therefore be predicted to be representative of that under the pond. For TSL, the

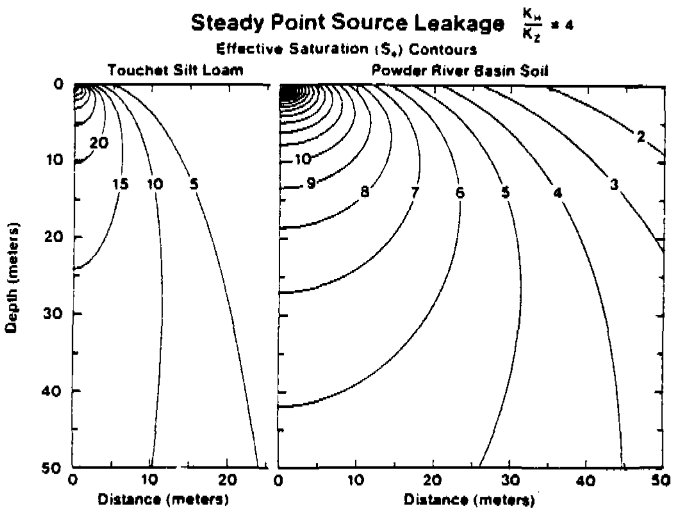

Figure 6. Steady point-source leakage compared for a soil with TSL and PRB soil properties. The relative spreading of the plume in the two cases indicates very different monitoring approaches. Fluid would move most rapidly directly under the leak in a TSL soil. The leakage rate in both cases is 5.28 gpd (200 liters/day).

maximum effective saturation of 80 percent occurs directly under the pond where the flow is highest. In this case, for an existing site, directional drilling would have to be used to sample or install instruments in the most active region of flow.

Multipond Calculation

The layout for two ponds is given in Figure 9. This problem was chosen because it is a true three-dimensional calculation with no axis of symmetry to reduce the amount of calculation required. If this were done accurately with a finite difference or finite element computer program using a 3-foot (1 m) grid spacing, approximately 15 million nodal points would be required. Needless to say, it would not be in the realm of possibility to run this problem on today's computers. This problem demonstrates the advantagės of the analytical approach, particularly to aid in understanding the flow patterns.

Saturation contours for TSL and PRB soils are shown in Figures 10 and 11, respectively. The flows for each pond combine to produce the highest saturation between the ponds. This is due to the rapid non-linear increase in the hydraulic conductivity as the saturation increases. The area between the ponds is the predicted zone of greatest flow, and monitoring should address this area first.

The spreading of fluid is again radically different for the two cases. The TSL needs monitoring close to the ponds, while the PRB soil will influence a larger area. Absolute saturations between the ponds will be in the 45 to 60 percent range. Figure 12 shows the components of particle velocities projected on the cross-sectional plane shown in Figure 9 for TSL soil. Information on velocities (and flux) is important in determining how fast contaminants are moving and in designing leak detection networks.

Time-Dependent Calculations

The principal utility of time-dependent calculations is to estimate arrival time of contaminants at selected loca-

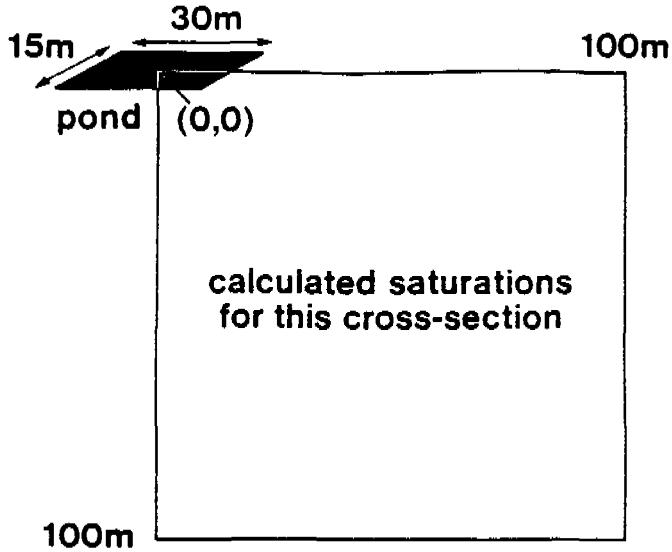

Figure 7. Cross section for uniform steady infiltration calculation, performed for half the pond along the major axis. Uniform infiltration from the pond at a rate of 9.17 gpm (50 m^3/day) is assumed.

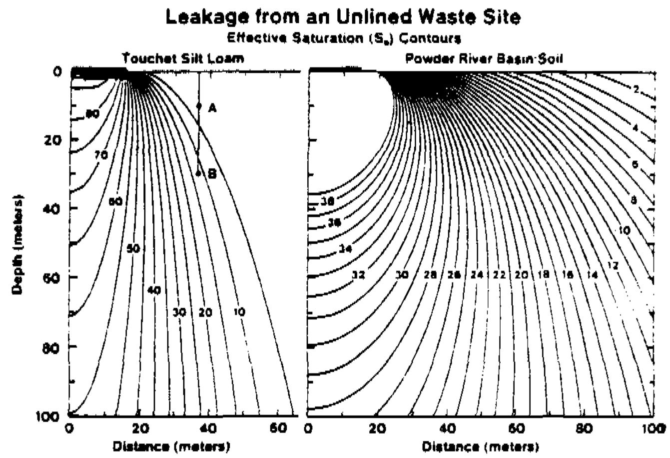

Figure 8. Steady-state effective saturation contours for two different soil types for the cross section shown in Figure 7. Maximum flow and saturation occur directly under the TSL waste site and can be accessed only by directionally drilled holes. The same saturation values are accessible for monitoring near the edge of the PRB site.

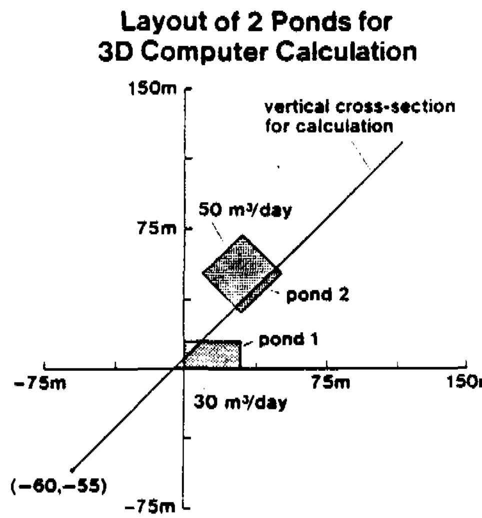

Figure 9. Plan view of two asymmetrical ponds for three-dimensional computer calculation. The calculation is performed in a vertical plane along the cross-section line.

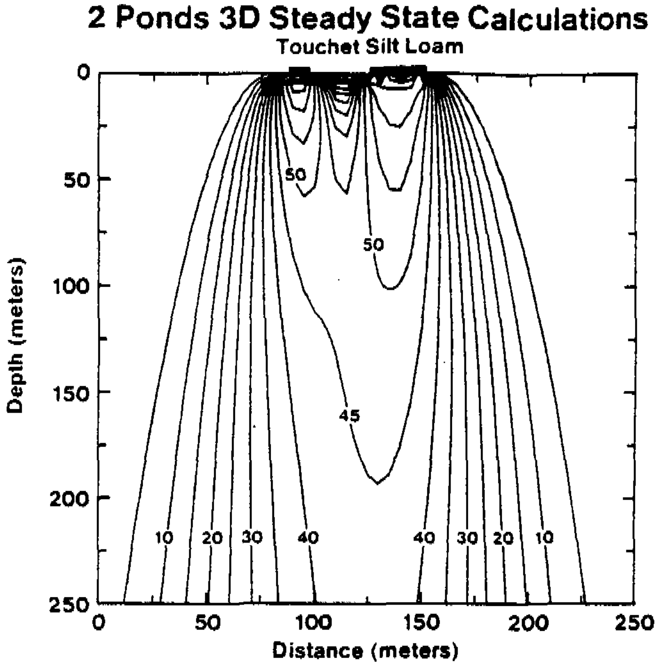

Figure 10. Steady-state effective saturations along cross section shown in Figure 9 for TSL soil. The highest flow occurs between the two ponds.

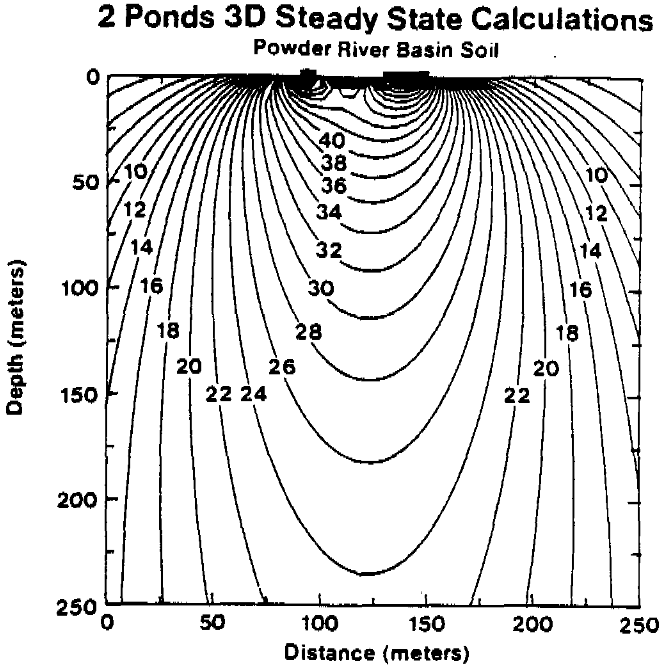

Figure 11. Steady-state effective saturations along cross section shown in Figure 9 for PRB soil. Monitoring in this case should be concentrated between the ponds since this is the region of highest flow and saturation.

tions and to gauge when instruments should begin to respond. The results for n = 1 and n = 3 are given in Figures 13 and 14, respectively. The time-dependent calculation is exact for n = 1. For n = 3 the coefficient of the time-dependent term (D) is the same as for n = 1; however, the spatial part (α) contains the correct terms. The calculation can only be regarded as an approximation of the transient behavior. This deficiency will be removed in future work. Large differences in saturation profile again persist for the two soil types, although they are not shown.

Notice that for n = 1, it takes almost 50 days for 1 percent effective saturation to reach 100 feet (30m) below the center of the pond. However, in Figure 14 for n = 3, the 5 percent S_e contour reaches the same point in less than 10 days. Although the time-dependent solution for $n \neq 1$ is approximate, faster arrival times (greater spreading) for n = 3 compared to n = 1 are also indicated from steady-state calculations (Figures 13 and 14). This is surprising since higher values of n result in lower relative permeability, and one would intuitively expect that lower permeability would result in longer travel times. The preceding statement applies to linear differential equations written in pressure. The governing equation for the vadose zone in terms of capillary pressure (Equation 1) is highly non-linear; it becomes linear only in terms of θ (Equation 5). Note that this equation is analogous to the equation for heat transfer from a constant-strength source moving through a uniform medium. In the analogous problem, α would correspond to the speed of the moving heat source. Since α is proportional to n, one would expect more spreading of heat (and saturation) for higher velocities of the heat source (higher n).

Summary and Conclusions

State-of-the-art for modeling unsaturated flow was reviewed, with the conclusion that approximate analytical solutions offer unique advantages—primarily ease and economy of running the program and freedom from a host of numerical instabilities and damping coefficients that were not present in the original differential equation. The disadvantages include a lack of spatial variation in hydraulic conductivity.

Six reasons were given for using a model to guide the installation of instrumentation in the vadose zone. The primary reasons are that instruments can be selected to optimally respond to the saturation and soil potential

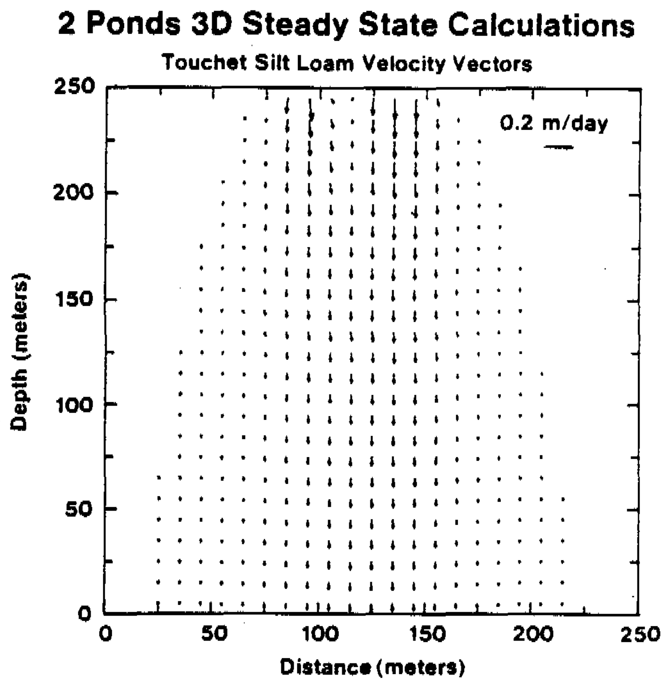

Figure 12. Steady-state velocity vectors along the cross section shown in Figure 9 for TSL soil.

condition in situ. Instrumentation can be located in the areas of the highest fluid mobility to afford the earliest detection of contaminant escape. Also, the model can be used in working with regulatory agencies to justify and optimize the design of a monitoring system. The model is not advocated as the final solution for a site, but rather as a tool with which to guide and develop a vadose zone monitoring program. The final model must, of course, include the effects of site-specific geometrical constraints and heterogeneities.

Acknowledgments

We wish to express our appreciation to J.T. Laman, T.L. Deshler and R.H. Jacobson for helpful comments and discussions; to M.S.P. Ramesh for helping in coding the program; and to J.M. Reverand for technical editing. The model described here is available as a proprietary computer code, VADOSE, from In-Situ Inc., Laramie, Wyoming.

Appendix: Calculations for Horizontal Boundary Conditions

From Equations 15, 16, and 17, it is known that the flux at the impermeable boundary is given by

$$\text{Flux} = \left(\frac{\partial\theta_R}{\partial z} - K + \frac{\partial\theta_I}{\partial z} + K\right)\Bigg|_{z=a} \qquad \text{(A-1)}$$

From Equations 6 and 14, it can be shown that

$$\frac{\partial\theta_R}{\partial z}\bigg|_{z=a} = -\frac{\partial\theta_I^h}{\partial z}\bigg|_{z=a} \qquad \text{(A-2)}$$

Substitution of Equation A-2 into Equation A-1 yields

$$\text{Flux}\bigg|_{z=a} = 0 \qquad \text{(A-3)}$$

Hence the image solution

$$\nabla\theta = \nabla\theta_R + \nabla\theta_I^h \qquad \text{(A-4)}$$

satisfies the no-flux criterion. However, when the "image" solution for a horizontal boundary is substituted in the differential equation, all the terms do not cancel. This is due to reversing the sign of gravity for the "image" solution. The remaining terms for the steady-state case are

$$\frac{Q}{4\pi}\left\{\frac{2(z-z')}{R^3}\alpha + \left(\frac{1}{R} + \frac{(z-z')}{R^2}\right)\alpha^2\right\}e^{-0.5\alpha(R+z-z')} \qquad \text{(A-5)}$$

Since α is a small number, these remaining terms are negligible. As long as R and z are positive, the error term decays exponentially. Similarly, it can be shown that the remaining terms for the transient differential equation are also negligible. Thus, this image solution technique, while not exact, is still a preferred approximation to an otherwise very complex proolem.

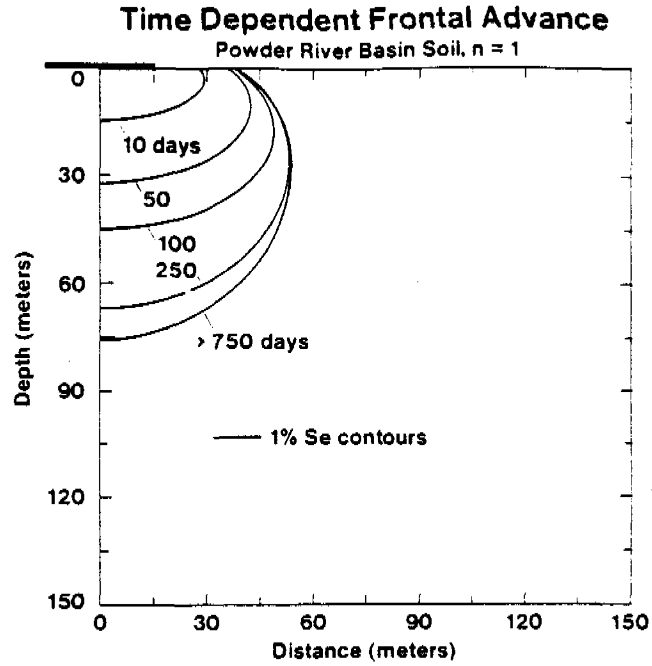

Figure 13. Time-dependent frontal (1 percent effective saturation) advance for PRB soil and the pond layout shown in Figure 7. The exponent relating effective saturation to hydraulic conductivity is 1; therefore, for this case, the analytical solution is correct.

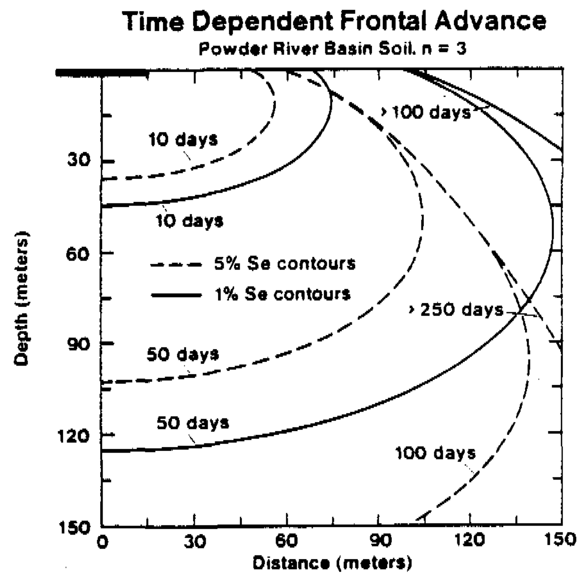

Figure 14. Time-dependent front (1 percent effective saturation) advance for PRB soil and the pond layout shown in Figure 7. The exponent relating effective saturation to hydraulic conductivity is 3, and thus, this calculation is only a rough approximation. Fluid spreads much more rapidly in this case.

Nomenclature

a = distance to impermeable boundary [L]

d = depth to the source [L]

D = parameter defined in Equation 5d [L^2/T]

e_z = unit vector in the positive z direction

K = hydraulic conductivity [L/T]

K_o = hydraulic conductivity at maximum saturation [L/T]

n = power in the power-law relationship for K as a function of soil saturation

p_{c_l} = displacement pressure head obtained by extrapolating the capillary pressure curve to S = 1 [L]

P_c = capillary pressure head [L]

Q = flow rate or strength of point source [L^3/T]

R = distance from point source [L]

R_I = distance from image point source [L]

S = saturation of the soil

S_e = effective saturation

S_m = maximum saturation

S_r = irreducible or residual saturation

t = time since drainage began [T]

v = velocity of particles

x,y,z = Cartesian coordinates, z defined positive downward [L]

x',y',z' = location of point source [L]

α = constant defined in Equation 5b [L^{-1}]

β = adjustable parameter in the saturation vs. capillary pressure relation, Equation 2 [L]

θ = dependent variable defined by Kirchhoff transformation, Equation 4 [M^2/T]

θ_o = value of θ at initial conditions

θ_R = dependent variable for real point source in an infinite medium [M^2/T]

θ_I^h = dependent variable for image point source for a horizontal impermeable boundary in an infinite medium [M^2/T]

θ_I^v = dependent variable for image point source for a vertical impermeable boundary in an infinite medium [M^2/T]

ϕ = porosity

References

Abou-Kassem, J.H. and K. Aziz. 1982. Grid Orientation During Steam Displacement. Soc. Petr. Eng. of AIME, SPE Paper 10497.

Adams, W.M., S.W. Wheatcraft and J.W. Hess. 1983. Downhole Sensing Equipment for Hazardous Waste Site Investigations. Proc. National Conf. on Management of Uncontrolled Hazardous Waste Sites, Washington, D.C., Oct.-Nov. 1983, pp. 108-113. Hazardous Materials Control Research Inst., Silver Spring, Maryland.

Allen, D.N. 1955. Relaxation Methods. McGraw-Hill, New York.

Arnold, E.M., G.W. Gee and R.W. Nelson, eds. 1982. Proc. Symposium on Unsaturated Flow and Transport Modeling, held at Seattle, March 1982. Sponsored by the Office of Nuclear Material Safety and Safeguards of the U.S. Nuclear Regulatory Commission. NUREG/CP-0030, PNL-SA-10325.

Averjanov, S.F. 1962. About Permeability of Subsurface Soils in Case of Incomplete Saturation. The Theory of Groundwater Movement, by P.Y. Poluarinova-Kochina, trans. J.M.R. DeWiest. Princeton Univ. Press, Princeton, New Jersey.

Aziz, K. and A. Settari. 1979. Petroleum Reservoir Simulation. Applied Science Publishers, London.

Bear, J. 1979. Hydraulics of Groundwater. McGraw-Hill, New York.

Brebbia, C.A. 1981. Progress in Boundary Element Methods, v. 1. John Wiley & Sons, New York.

Brooks, R.H. and A.T. Corey. 1964. Hydraulic Properties of Porous Media. Hydrology Paper No. 3, Colorado State University, Ft. Collins, Colorado.

Buckingham, E. 1907. U.S. Dept. Agr., Bur. Soils Bull. 38.

Bumb, A.C. 1987. Unsteady-State Flow of Methane and Water in Coalbeds. Ph. D. thesis, Dept. of Chemical Engineering, University of Wyoming, Laramie.

Carslaw, H.S. and J.C. Jaeger. 1959. Conduction of Heat in Solids, 2nd ed. Oxford Univ. Press, New York.

Corey, A.T. 1954. The Interrelation Between Gas and Oil Relative Permeabilities. Producer's Monthly, v. 19, no. 1.

Corey, A.T. 1977. Mechanics of Heterogeneous Fluids in Porous Media. Water Resources Publications, Fort Collins, Colorado.

Dagan, G. and E. Bresler. 1983. Unsaturated Flow in Spatially Variable Fields, 1. Derivation of Models of Infiltration and Redistribution. Water Resour. Res., v. 19, pp. 413-420.

Devary, J.L. and R. Schalla. 1983. Improved Methods of Flow System Characterization. Proc. National Conf. on Management of Uncontrolled Hazardous Waste Sites, Washington, D.C., Oct.-Nov. 1983, pp. 117-122. Hazardous Materials Control Research Inst., Silver Springs, Maryland.

Emery, A.F. and H.W. Carson. 1971. An Evaluation of the Use of the Finite-Element Method in the Computation of Temperature. J. Heat Transfer, May 1971, pp. 136-145.

Everett, L.G., L.G. Wilson and L.G. McMillion. 1982. Vadose Zone Monitoring for Hazardous Waste Sites. Ground Water, v. 20, no. 3, pp. 312-324.

Ewing, R. 1983. University of Wyoming, Laramie, Wyoming. Private Communication.

Finlayson, B.A. 1980. Nonlinear Analysis in Chemical Engineering. McGraw-Hill, New York.

Irmay, S. 1954. On the Hydraulic Conductivity of Unsaturated Soils. Trans. AGU, v. 35, no. 3, pp. 463-467.

Lappala, E.G. 1982. Recent Developments in Modeling Variably Saturated Flow and Transport. Arnold et al., eds., 1982, pp. 35-54.

McKee, C.R. and A.C. Bumb. 1987. Flow-Testing Coalbed Methane Production Wells in the Presence of Water and Gas. SPE Formation Evaluation, December 1987, pp. 599-608.

Muskat, M. 1946. The Flow of Homogeneous Fluids Through Porous Media. J.W. Edwards, Ann Arbor, Michigan.

Oster, C.A. 1982. Review of Ground-Water Flow and Transport Models in the Unsaturated Zone. Battelle Pacific Northwest Laboratory, Richland, Washington, report for U.S. Nuclear Regulatory Commission, NUREG/CR-2917, PNL-4427.

Philip, J.R. 1969. Theory of Infiltration. Advances in Hydroscience, ed. V.T. Chow, v. 5, pp. 215-296. Academic Press, New York.

Raats, P.A.C. 1971. Steady Infiltration from Point Sources, Cavities, and Basins. Soil Sci. Soc. Amer. Proc., v. 35, pp. 689-694.

Reiss, L.H. 1980. The Reservoir Engineering Aspects of Fractured Formations. Gulf Pub. Co., Houston, TX.

Richards, L.A. 1931. Capillary Conduction of Liquids Through Porous Mediums. Physics, v. 1, pp. 318-333.

Segol, G. 1982. Unsaturated Flow Modeling as Applied to Field Problems. Arnold et al., eds., 1982, pp. 35-54.

Settari, A., H.S. Price and T. Dupont. 1977. Development and Application of Variational Methods for Simulation of Miscible Displacement in Porous Media. Soc. Petr. Eng. J., v. 17, no. 3, pp. 228-246.

Sharma, D. 1982. Fluid Dynamics and Mass Transfer in Variably Saturated Porous Media: Formulation and Applications of a Mathematical Model. Arnold et al., eds., 1982, pp. 179-210.

Smith, G.D. 1978. Numerical Solution of Partial Differential Equations: Finite Difference Methods. 2nd ed. Oxford Univ. Press, Oxford, United Kingdom.

Yanosik, J.L. and T.A. McCracken. 1979. A Nine-Point, Finite Difference Reservoir Simulator for Realistic Prediction of Adverse Mobility Ratio Displacements. Soc. Petr. Eng. J., v. 19, no. 4, pp. 253-262.

Zienkiewicz, O.C. 1977. The Finite Element Method, 3rd ed., p. 430. McGraw-Hill, New York.

Biographical Sketches

Chester R. McKee, president of In-Situ Inc. (P.O. Box I, 210 S. Third St., Laramie, WY 82070), holds a B.S. in physics from Duquesne University, and an M.S. and a Ph.D. in physics from the New Mexico Institute of Mining and Technology. His research interests include ground water modeling, contaminant migration, saturated and unsaturated permeability testing, and in situ mining. He has published numerous technical papers on hydrodynamics, explosive fracturing, subsidence, hydrology and ground water restoration.

Amar C. Bumb is manager of the computer technology division of In-Situ Inc. (P.O. Box I, 210 S. Third St., Laramie, WY 82070). He specializes in hydrology and computer applications. He received his B.E. with honors in chemical engineering from the Birla Institute of Technology and Science in Pilani, India, and his M.S.Ch.E. and Ph.D. from the University of Wyoming. His research interests include in situ mining, optimum well field design, ground water restoration, hydrodynamics, and multiphase flow.

FOCUS

Simulation of Vapor Transport Through the Unsaturated Zone — Interpretation of Soil-Gas Surveys

by Lyle R. Silka

Abstract

Soil-gas surveys are becoming more widely accepted as a tool for the preliminary determination of the extent of soil and ground water contamination by volatile organic compounds (VOCs). The interpretation of the results of published soil-gas surveys has been necessarily limited and qualitative due to a lack of adequate models. There has been considerable effort in the recent past to characterize the transport and fate of pesticides in soil. However, the behavior of pesticides generally differ substantially from those of VOCs.

This paper presents a computer model developed to simulate the diffusive transport of VOC vapor through unsaturated soils using a two-dimensional, finite-difference, solution to Fick's second law of diffusion. An effective diffusion coefficient that incorporates the effects of tortuosity, moisture content, and soil organic carbon content is computed. Although the model has not been validated due to the unavailability of adequate field or laboratory data, nevertheless, sensitivity analyses demonstrate the importance of soil moisture and, secondarily, organic matter content in controlling the migration of VOC vapor through the unsaturated zone. The interpretation of soil-gas surveys can be complicated by unknown spatial heterogeneities in soil moisture and organic carbon content, temporal variations in moisture content, extent of contaminant migration as a non-aqueous phase liquid and by the unknown extent of VOC liquid and contaminated ground water.

Introduction

Volatile organic chemicals (VOCs) have been identified nationwide as one of the more ubiquitous groups of hazardous chemicals present in contaminated ground water. A major reason for this is the widespread use of VOCs in the manufacture of pesticides, plastics, paints, pharmaceuticals, solvents and textiles, as well as constituents of petroleum products. Due to the presence of VOCs at many sites of contamination, there has been increasing interest in the sampling and measurement of VOCs in soil gas to estimate their extent in soils and ground water. With the recent development of the portable gas chromatograph, the quantitative and semiquantitative field analysis of VOCs in soil gas is now a reality.

Portable gas chromatography, a relatively new technology, has been shown to be especially applicable to the investigation of soil and ground water contamination through the analysis of shallow soil gas. Under diffusive transport, VOCs volatilize from ground water and move upward through the unsaturated zone, ultimately venting to the atmosphere. This process provides a means to delineate areas of subsurface contamination through the analysis of VOCs in the shallow soil gas. Also, it has been shown empirically that the concentration of VOCs in samples of shallow soil gas are related to the concentration of VOCs in ground water (Glaccum et al. 1983, Lappala and Thompson 1983a and b, Swallow and Gschwend 1983, and Marrin 1984). Soil-gas surveys are recognized as a valuable tool, both alone and in conjunction with other remote-sensing techniques, that can provide data on the location and extent of soil and ground water contamination and can aid in the design of more detailed ground water studies involving soil borings and monitoring well networks.

The successful interpretation of a soil-gas survey depends on several factors, including the size and age of the source, the moisture content and organic carbon content of the unsaturated zone, and the volatility and solubility of the VOC. Prior to conducting a soil-gas survey, the effects of these factors should be evaluated in order to optimize the design of the soil-gas survey. Through a review of theory and application of a computer model, this paper presents an evaluation of the operational limitations of soil-gas surveys.

Behavior of VOCs in the Subsurface

Transport Mechanisms

The transport of VOCs from a source through unsaturated soil may be by mass flow as a solute in percolating water or by diffusion as a vapor in soil gas. Mass flow as a vapor due to advective migration may be important in the upper few feet of the unsaturated zone. Advective vapor migration in the shallow soil may be induced by diurnal temperature and barometric variations. Barometric, or atmospheric pressure changes are not considered here because, on the scale of typical soil-gas investigations, changes in barometric pressure would produce minor vertical piston-type fluctuations in the soil gas as the air alternately compresses and expands. The alternating up and down movement of the soil gas under the influence of the barometric fluctuations would tend to approach an average condition.

However, pressure and temperature gradients can become important near subsurface structures such as basements and utilities that are vented to the atmosphere. Nazaroff et al. (1987) found that pressure and temperature gradients may be transmitted to the subsurface by residential houses with basements and could induce significant advective transport of soil gas to lateral distances of 20 feet (6m). Although this paper does not address these influences and considers vapor migration under isothermal and isostatic conditions, the influences of atmospheric wind-induced pressure gradients and temperature-induced thermal gradients near subsurface structures should be considered in the interpretation of soil-gas surveys.

For VOCs that have low solubility limits in water, as is generally the case with the chlorinated solvents, diffusive transport in soil gas can predominate (Spencer and Farmer 1980). When a liquid VOC is spilled on the soil or leaks from a tank into the soil, the VOC will begin to partition into the liquid and vapor phases and become dissolved in soil moisture and adsorbed onto the surfaces of soil minerals and organic matter. The degree of partitioning of the VOC among these four components will depend on the volatility and water solubility of the VOC, the soil moisture content, and the nature of soil solids.

Partitioning Between Liquid and Soil Gas

The saturated equilibrium concentration of a VOC in air above a volatile liquid is expressed by Raoult's law and is described by a partition coefficient that is dependent on the vapor pressure of the VOC and the temperature (Thibodeaux 1979). At equilibrium, the mole fraction of a VOC in the air space above the pure VOC liquid at a specified temperature is expressed as:

$$y = p/p_T \qquad (1)$$

where y is the mole fraction of the VOC, p is the vapor pressure of the VOC, and p_T is the total pressure in the air space.

Equation 1 provides a means to estimate the source concentration of a VOC vapor in the soil gas above a free VOC liquid spill. Vapor pressures for many VOCs at ambient temperatures are available in the literature (for example, Perry and Chilton 1973, and Callahan et al. 1979).

Partitioning Between Soil Gas and Soil Moisture

Partitioning between the VOC vapor in the soil gas and VOC dissolved in soil moisture may be expressed as the ratio of its concentration in each of the two phases (Equation 2). At equilibrium, this ratio is constant for constant temperature and is governed by the relationship expressed as Henry's law, i.e., (Thibodeaux 1979):

$$K_H = C_G/C_L \qquad (2)$$

where K_H is Henry's law constant for the VOC at a specified temperature, C_G is the concentration of the VOC in soil gas, and C_L is the concentration of the VOC in the water.

The Henry's law constant may also be expressed as a function of the VOC vapor pressure, the concentration of the VOC in water, and temperature as (Thibodeaux 1979):

$$K_H = 16.04 p_a M_a / T C_L \qquad (3)$$

where M_a is the gram molecular weight of the VOC, T is the temperature (in degrees Kelvin), and the other parameters are as previously defined.

Dilling (1977) reports values of Henry's law constant for numerous chlorinated solvents with those for selected VOCs presented in Table 1. Empirically derived values of Henry's law constants reported by Dilling (1977), Swallow and Gschwend (1983), and Lappala and Thompson (1983) are in reasonable agreement with the calculated values of K_H, keeping in mind the temperature dependence of K_H.

Partitioning Between Soil Moisture and Soil Solids

In addition to the partitioning of the VOC between the vapor and aqueous phases, some of the VOC will be adsorbed onto the soil minerals to a lesser extent and onto soil organic matter to a greater extent. Although no research in this area is known to this author, adsorption of VOC vapor on to organic matter may be an important sink for VOC transport in soil gas. In order to estimate the possible importance of adsorption onto organic matter, results of research on the adsorption of aqueous VOCs have been utilized. Although not specifically directed at the current problem, the results from the experiments with aqueous solutions of VOCs may prove applicable, because soil solids will be surrounded by water layers of at least several molecules thick for even the driest soils. The process of partitioning of the VOC between the soil gas and the soil solids then becomes a two-step process of partitioning from the vapor into the water and subsequently from the water onto the soil solids.

Since no known research has been directed at the problem of determining the partitioning of VOCs in a three-phase system, the validity of the approach utilized

TABLE 1
Reported Values of Henry's Law Constant, Vapor Pressure and Solubility at 25 C for Selected Chlorinated Solvents

Chemical	Solubility in Water (ppm)	Vapor Pressure (mm Hg)	Henry's Law Constant Calculated (Measured) (Dimensionless)
1,1,2,2-Tetrachloroethane	3000	6.5	0.019
1,1,2-Trichloroethane	4420	23	0.038
1,1-Dichloroethane	8700	82	0.050 (.040)[1]
Tetrachloroethylene	140	18.6	1.2 (0.5)[2] (0.43)[1]
Trichloroethylene	1100	74	0.49 (0.33)[3]
trans-Dichloroethylene	6300	326	0.27
cis-Dichloroethylene	3500	206	0.31

Source: Dilling (1977).
Notes:
[1] Empirical values reported by Dilling (1977).
[2] Empirical values will vary from calculated values due to differences in temperature.
[3] Empirical values reported by Lappala and Thompson (1983).

for this model is unknown. Nevertheless, as described later, to the extent that Jury et al. (1984) tested this approach, they reported finding good agreement between calculated and empirically derived values for the effective diffusion coefficient.

At equilibrium, the degree of partitioning between the soil solids and the soil moisture is expressed as:

$$K_D = S/C_L \tag{4}$$

where K_D is the partition coefficient or distribution coefficient (with units of l^3/m), S is the mass of chemical adsorbed per unit dry mass of soil solids, and C_L is the concentration of the chemical in the soil moisture.

For aqueous solutions, it has been observed that strongly hydrophobic organic chemicals tend to adsorb more strongly onto the soil solids. Empirical studies by Karickhoff et al. (1979) found that K_D was proportional to the organic carbon content of the soil, as well as the octanol:water partition coefficient (K_{OW}), a measure of the hydrophobicity of an organic chemical. For the equilibrium condition, this relationship has been expressed as (Karickhoff et al. 1979, which is essentially the same relationship determined by Rao et al. 1985):

$$K_D = 0.63 K_{OW} f_{oc} \tag{5}$$

where K_D is the distribution coefficent of Equation 4, f_{oc} is the soil organic carbon content, and K_{OW} is the octanol:water partition coefficient.

The amount of carbonaceous matter in the soil is the dominant factor controlling the extent of adsorption of dissolved organic chemicals. Karickhoff et al. (1979) also found that the particle size of the mineral fraction was important. For example, the distribution coefficients for pyrene and methoxychlor on the sand-sized fraction were approximately 100 times less than the distribution coefficient for the silt- and clay-sized fraction, due primarily to the lower organic carbon content of the sand (Karickhoff et al. 1979). Table 2 presents data for K_{OW} and calculated values of K_D using Equation 5 for selected VOCs. From the example calculations of distribution coefficients in Table 2, these VOCs are not strongly adsorbed onto the soil solids due to their relatively low octanol-water partition coefficients. Pentachlorophenol, in comparison, with a log K_{OW} of 4.74, has a K_D of 35, i.e., pentachlorophenol will be preferentially adsorbed to the soil solids by a factor of 100 to 1000 times greater than the chlorinated solvents listed in Table 2.

VOC Vapor Diffusion in Soil Gas

As previously stated, the primary transport mechanism for VOCs in the unsaturated soil is by diffusion through the soil gas. The distribution of VOC concentration in the soil gas can be modeled by Fick's second law, which in one dimension is expressed as (Thibodeaux 1979):

$$C/dt = Dd^2C/dz^2 \tag{6}$$

where C is concentration of the VOC in air, D is the diffusion coefficient, and z is the distance traveled.

Assuming the outer boundary condition is zero concentration, Equation 6 can also be expressed as (Thibodeaux 1979):

$$\frac{C_{(z,t)}}{C_{(z=0,t=0)}} = \mathrm{erf}[z/(4Dt)^{0.5}] \tag{7}$$

where $C_{(z,t)}$ is the concentration (as mole fraction) at a distance z and time t, $C_{(z=0,t=0)}$ is the initial concentration, and erf is the error function.

Swallow and Gschwend (1983) conducted limited

TABLE 2
Reported Values of Log Octanol: Water Partition Coefficient and Calculated Values of Distribution Coefficient for Selected Chlorinated Solvents

Chemical	Log Octanol:Water Partition Coefficient[4]	Calculated Distribution Coefficient[5]		
		Fraction Organic Carbon		
		0.001	0.01	0.03
1,1,2,2-Tetrachloroethane	2.56	0.23	2.3	6.9
1,2,2-Trichloroethane	2.17	0.09	0.9	2.7
1,1-Dichloroethane	1.79	0.04	0.4	1.2
Tetrachloroethylene	2.88	0.48	4.8	14.4
Trichloroethylene	2.29	0.12	1.2	3.6
trans-Dichloroethylene	1.48	0.02	0.2	0.6
cis-Dichloroethylene	1.48	0.02	0.2	0.6

Notes:
[4]From Callahan et al. 1979.
[5]Calculated from $K_D = 0.63 K_{OW} f_{oc}$.

controlled laboratory experiments using a glass tank. Although their experimental design prevented a direct measurement of the concentration of VOCs in the unsaturated zone, Swallow and Gschwend (1983) concluded that volatilization can be adequately modeled by Fick's second law.

Diffusion Coefficient in Soil Gas

The diffusion coefficient for VOC vapor in air was estimated by Jury et al. (1983 and 1984) to be 4.6 ft^2/d (0.43 m^2/d) based on studies by Brattain in 1929 of the gas diffusion coefficient of intermediate molecular weight organic chemicals. However, Bruell and Hoag (1986) reported values of the diffusion coefficient for benzene in air of from 8.0 to 8.4 ft^2/d (0.74 and 0.78 m^2/d).

The diffusion coefficient in soil gas has been found to be reduced from that in air by a tortuosity factor which accounts for decreased cross-sectional area for flow and increased length of the flow path. Jury et al. (1983 and 1984) concluded that the Millington-Quirk tortuosity formula has been proven useful for describing pesticide soil diffusion coefficients. More recently, Bruell and Hoag (1986) confirmed the validity of the Millington-Quirk model in column experiments. Jury et al. (1983) estimated the diffusion coefficient in soil gas by determining the effect of the Millington-Quirk tortuosity formula on the diffusion coefficient in air by:

$$D_G = Da^{10/3}/n^2 \quad (8)$$

where D_G is the diffusion coefficient in soil gas, D is the diffusion coefficient in air, a is the volumetric air content of the soil, and n is the total soil porosity.

Since the VOC vapor may partition between the gas, liquid, and solid phases, an effective diffusion coefficient can be formulated that incorporates that partitioning. The removal of VOCs from the soil gas by partitioning into the soil moisture and soil organic matter results in a reduction in the apparent diffusion rate, and consequently, the apparent, or effective, diffusion coefficient. Jury et al. (1983) developed the following relationship between the diffusion coefficient in soil gas from Equation 8 and the effective diffusion coefficient:

$$D_e = D_G/[(bK_D/K_H) + w/K_H + a] \quad (9)$$

where D_e is the effective diffusion coefficient in soil gas corrected for effects of partitioning, D_G is the diffusion coefficient corrected for tortuosity using Equation 8, b is the bulk dry density of the soil, K_D is the soil partition coefficient from Equation 5, K_H is Henry's law constant from Equation 3, w is the volumetric soil moisture content, and a is the volumetric air content, where n (total porosity) = a + w.

Jury et al. (1984) report that the model for the effective diffusion coefficient expressed in Equation 9 gives results that are in good agreement with empirically derived values of D_e.

Model Description

Although several investigators have developed models for the simulation of the transport of organic chemicals in the soil (for example, Leistra 1973, Jury et al. 1983 and 1984, Rao et al. 1985), these models are limited in their application to the simulation of the diffusion of VOCs in soil gas. In general, the previous models were developed for application to the modeling of pesticide movement and fate in soils. The models are one-dimensional analytical solutions that do not allow for heterogeneous soil properties and initial conditions. Also, these models incorporate transport of the chemical in the liquid phase, as the models were intended for the study of the leaching of pesticides from soils (Jury et al. 1983). In the case of the model developed by Rao et al. (1985), transport by vapor diffusion was omitted.

Corapcioglu and Baehr (1987) described a one-dimensional, finite-difference model of VOC transport through the unsaturated zone. Although their model simulates multiphase transport in vapor, water and immiscible liquid, and accounts for partitioning, adsorption, and transformations, the vertical, one-dimensional nature of their model limits its application to the interpretation of soil-gas survey results that are two- to three-dimensional in nature.

To correct for these limitations, a two-dimensional vapor diffusion model was developed and described previously (Silka 1986). This model is a finite-difference, forward-difference approximation relative to time, and is based on Fickian diffusive transport. (Although unavailable to this author at this writing, Striegl (1987) subsequently reported on the development of a similar model).

Model Assumptions

The model is based on the following assumptions.

Assumption 1	Diffusion is described by Fick's second law.
Assumption 2	Partitioning coefficients are linear and system is at equilibrium with respect to partitioning, i.e., Equations 3 and 5 are valid.
Assumption 3	The Millington-Quirk tortuosity formula defined in Equation 8 is valid.
Assumption 4	The soil properties of bulk density, b, and total porosity, n, are homogeneous.
Assumption 5	The diffusion coefficient in air, D, is constant.
Assumption 6	The soil gas is isostatic and at atmospheric pressure, i.e., there is no pressure-gradient induced advective vapor flux.
Assumption 7	The soil system is isothermal, i.e., there is no thermal-gradient induced convective vapor flux.
Assumption 8	The VOC is conservative, i.e., the VOC is unaffected by biotransformation, hydrolysis, or redox reactions.

The model allows for heterogeneous initial concentrations with either constant concentration sources or instantaneous spike sources. The diffusion coefficients may be varied over the finite-difference grid and in the x and y directions by weighting coefficients. The effects of partitioning are incorporated by using the effective diffusion coefficient as defined in Equation 9.

Since the finite-difference equation is solved using the forward-difference approximation relative to time, the maximum size of the time steps must meet the following criterion for the solution to be stable. For two dimensions where dx = dy = x, (i.e., the grid spacing is the same in both directions and equal to X):

$$dt < 0.25X^2\, a/D_e \qquad (10)$$

where dt is the maximum time step, X is the grid spacing, a is the volumetric air content, and D_e is the effective diffusion coefficient (after Wang and Anderson 1982).

Model Verification and Validation

To date, the verification of the vapor diffusion model has been limited to comparisons with computed results from the one-dimensional analytical solution presented in Equation 7. At this time, it is difficult to adequately validate the vapor diffusion model against real field data due to the lack of good data.

An adequate validation problem requires information on the moisture content and organic matter content of the soil, the soil texture, as well as the concentration and distribution of the source. Further complications arise when one considers that field conditions are dynamic, i.e., always changing. This problem is especially acute for soil moisture content, which, over the large scale, fluctuates seasonally. Also, field data are not available in sufficient detail to allow description of the spatial variability of soil conditions resulting in necessary oversimplification of the physical setting. Jury (1986) lists several potential problems that must be considered to successfully carry out a field validation experiment of a vapor diffusion model:

1. Lateral and vertical variability of transport and retention parameters may introduce heterogeneities and anisotropy not included in the model;
2. Macropores, cracks, plant root holes and animal burrows may create discontinuities difficult to account for in the model;
3. Time-dependent boundary conditions, such as depth to water table and seasonally saturated zones may alter the system geometry from that modeled;
4. Problems with validity of measurement techniques for characterizing field properties may introduce model error;
5. Scale effects may be important in the field that are not accounted for in the model, such as temperature variation.

Although not available at the time of this writing, Striegl (1987) published an account of an apparently successful modeling of the diffusion of methane from a waste disposal trench in Illinois using a two-dimensional finite-difference solution of Fickian diffusion similar to the model described here.

Implications for Soil-Gas Surveys

Delineating Surface Contamination

Previously, this author has presented the results of sensitivity analyses using the model 2D-DIFF to assist in designing and interpreting soil-gas surveys for contaminated soil and leaking underground storage tanks (Silka 1986, and Ferre and Silka 1987, respectively). With regard to the use of soil-gas surveys for identifying shallow contaminated soil (Silka 1986), the optimum grid spacing for the soil-gas survey was found to be primarily dependent upon soil moisture and the value of Henry's law constant, and, to a lesser degree, organic matter content. Figure 1 illustrates the dependence of the effective diffusion coefficient on K_H and fraction of pore volume occupied by water (w/n). The reduction in D_e is represented by the ratio of D_e/D_G, where D_G is the diffusion coefficient corrected by the Millington-Quirk tortuosity formula in Equation 8. Therefore, in dry soil D_e/D_G is unity.

Obviously, optimum conditions for soil-gas surveys are obtained when dry soil conditions have prevailed prior to the survey. Since moist soil is the rule, though, especially in the more humid regions, the optimum grid spacing will generally be less than 100 feet (30.5m). For VOCs with even moderate values of K_H, for example, trichloroethylene (TCE) with K_H of 0.4 and 1,1,2,2-tetrachloroethane (TET) with K_H of 0.02, the reduction in the effective diffusion coefficient is sufficient to reduce their distance of migration. Compared to a VOC with a K_H of 0.0, TCE would migrate on the order of only 60 percent of the distance, while TET would migrate on the order of only about 20 percent of the distance of the unretarded VOC within the same time period. In homogeneous soils, the maximum extent of the migration of vapor through soil gas will be limited by the thickness of the unsaturated zone. However, many soils are heterogeneous and stratified, and greater lateral migration may occur.

Mapping Ground Water Plumes

Several observations reported in the literature concerning the interpretation of soil-gas surveys for ground water plume mapping have been investigated using the model 2D-DIFF. It has been reported that concentrations of VOCs in soil gas decrease from the source at the water table to the surface by up to 5 orders of magnitude (Lappala and Thompson 1983). This field observation follows from the diffusive transport equation. Since the soil-gas system is bounded below by an essentially constant concentration source and above by a constant zero-concentration boundary (i.e., the atmosphere), the vapor concentration will decrease logarithmically from the water table to the surface in an ideal, homogeneous soil.

Figures 2 and 3 show two cases for the distribution of vapor concentration with distance above the centerline of a plume of contaminated ground water where the water table is at a depth of 32.8 feet (10m). The concentration is presented in dimensionless units. Figure 2 shows the results for a relatively dry soil having only 8 percent water content (a=0.32, w=0.08) and a VOC with a K_H of 0.02. Figure 3 shows the results for a wetter soil with a 20 percent water content (a=0.2, w=0.2). In both cases, there is greater than a 3 to 5 order of magnitude change in the VOC concentration in soil gas from the water table to the surface, even when the concentration profile approaches steady-state.

For the dryer soil (Figure 2), the higher effective diffusion coefficient results in the concentration profile approaching steady-state faster than the wetter soil case (Figure 3). Thus, the dryer soil conditions will result in a more responsive concentration profile as compared to the wetter soil. Shallow soil-gas measurements in the dryer setting will better reflect the distribution of the VOC in the ground water at that point in time.

More recently, Evans and Thompson (1986) concluded that aerobic biodegradation of hydrocarbon vapors was the cause of lower than expected concentrations, <10 $\mu g/L$, in shallow soil gas at depths of less than

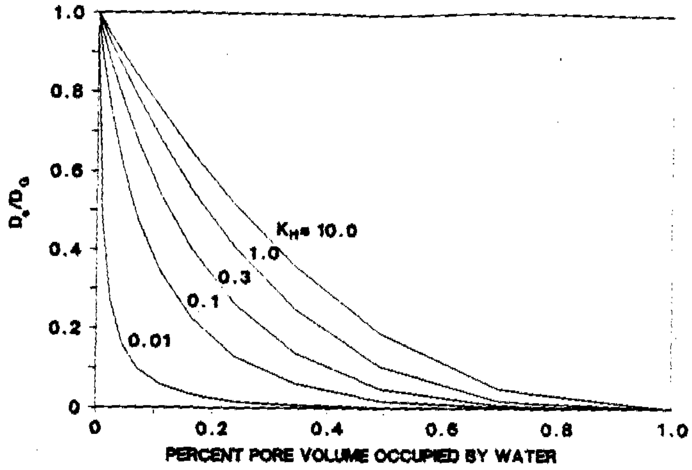

Figure 1. Dependence of the effective diffusion coefficient, expressed as the ratio of D_e/D_G, on moisture content, expressed as the fraction of total porosity occupied by water, and Henry's law coefficient, K_H.

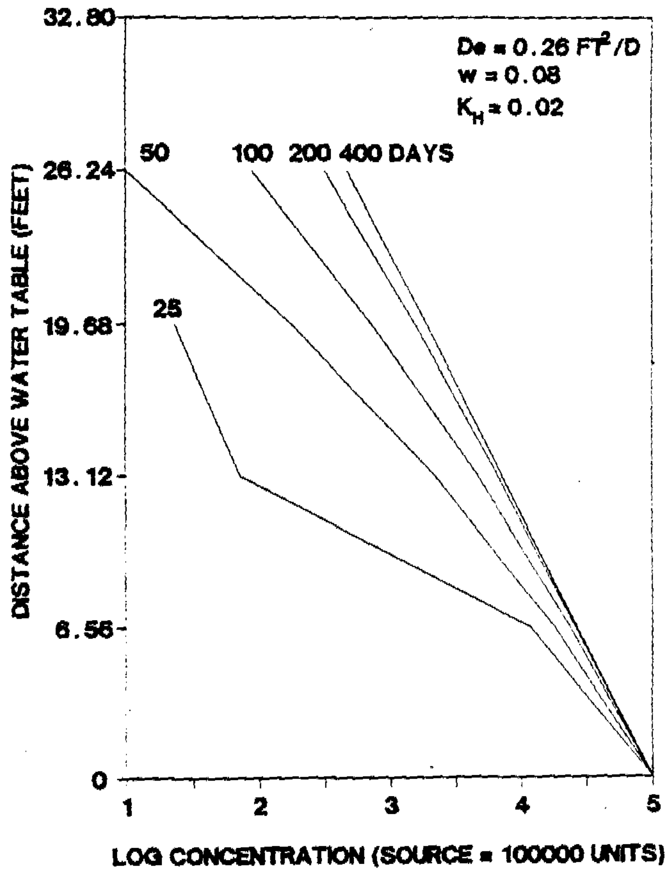

Figure 2. VOC concentration in soil gas vs. time and distance above the water table under nearly dry soil conditions (w=0.08).

5 feet (1.5m) when compared to the >1000 $\mu g/L$ concentrations in the 6- to 14-foot interval (1.8 to 4.3m). However, they also reported at least one instance when the concentration gradient reversed and decreased with depth below the 6- to 14-foot (1.8 to 4.3m) interval.

In order to substantiate the interpretation that biodegradation was occurring, active microbial populations and degradation by-products, such as CO_2 generation should be confirmed in the soil column. Since these data are lacking for their particular site, alternative explanations may be just as viable. For example, the lower-than-expected concentration in the uppermost 5 feet (1.5m)

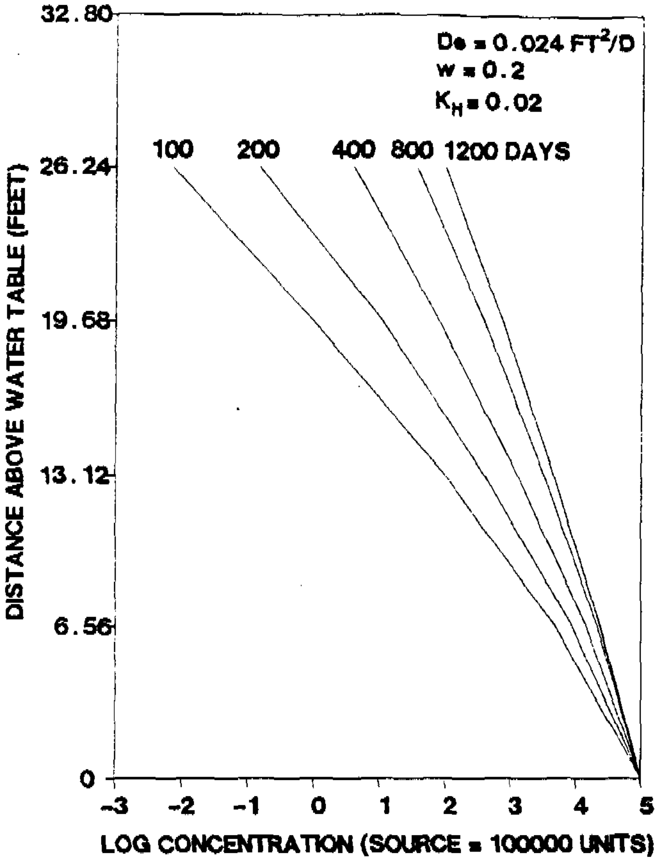

Figure 3. VOC concentration in soil gas vs. time and distance above the water table under wet soil conditions (w=0.02).

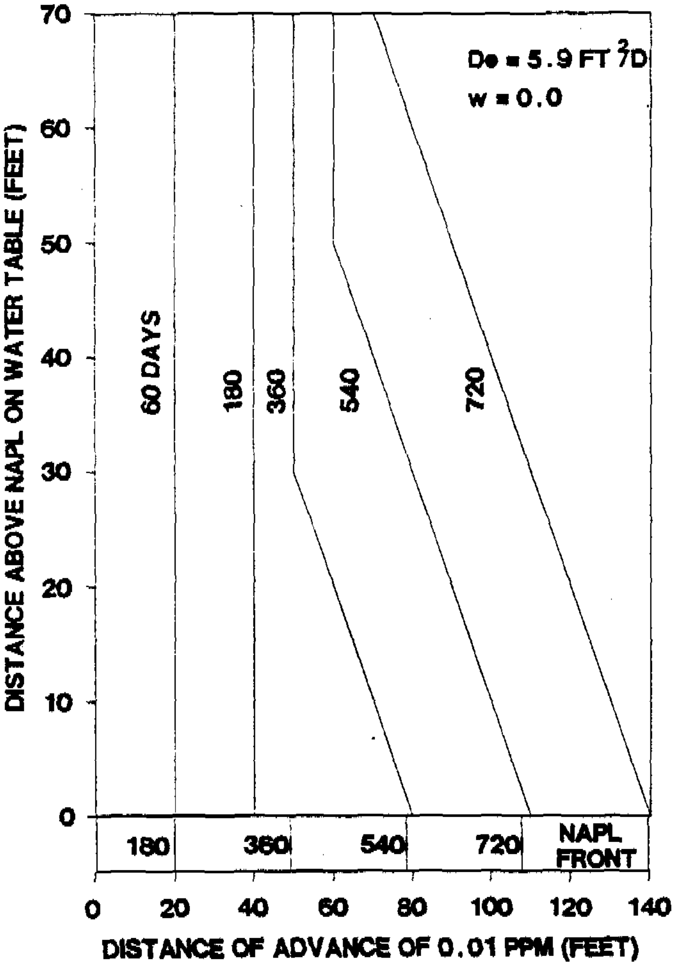

Figure 4. Extent of migration of 0.01 ppm contour for VOC in soil gas from a vertical spill source and advancing NAPL front floating on the water table dry soil conditions.

could be due to the normal decrease in concentration expected under the concentration gradient established by diffusion alone. Inspection of Figures 2 and 3 shows that transient concentration profiles can produce a concentration decrease of greater than 3 orders of magnitude from the 6- to 14-foot (1.8 to 4.3m) interval to the less than 6-foot (1.8m) interval. Considering that the concentration decrease due to the diffusion gradient would be greater in wetter soils, biodegradation is not necessary to explain the observed decrease.

Evans and Thompson (1986) also reported the observation that vapor concentrations decrease rapidly, by 2 to 3 orders of magnitude, just beyond the edge of the ground water contamination zone. Simulations were conducted using 2D-DIFF for an advancing front of a non-aqueous phase liquid (NAPL) floating on the water table. The model was set up with a constant saturated vapor concentration of 6000 ppm at the NAPL-soil gas interface and an initial concentration of 6000 ppm along the left side to represent the downward path of liquid VOC migration. Two variations were run, one with a vapor diffusion rate that was faster than the NAPL front velocity, and the second with a vapor diffusion rate that was slower than the NAPL front velocity. Figures 5 and 6 show the results in terms of the relative positions of the NAPL front and the 0.01 ppm concentration contour. The results presented in these figures can be applied to the case of only dissolved VOC in a ground water plume by dividing 0.01 ppm by 6000 ppm, i.e., the contours in the figures would be equivalent to 1.6×10^{-6} times the concentration of the VOC in the soil gas just above the water table.

Figure 4 indicates that for a source front, i.e., NAPL or dissolved contaminant plume, that moves slower than the diffusion rate, the VOC does diffuse beyond the plume edge as observed by Evans and Thompson (1986), up to a height of 40 feet (12.2m) above the water table. Above a height of 40 feet (12.2m) from the water table, the vapor front falls behind the liquid front. However, Figure 5 indicates that when the diffusion rate in soil gas is less than the velocity of the source front, the VOC distribution in the soil gas will lag behind the source front or edge of the plume at a much lower height above the water table. In the case illustrated in Figure 5, the VOC diffusion in the soil gas begins to lag behind the front at a height of about 15 feet (4m) above the water table. The lag increases to about 60 feet (18.3m) at a height of 30 feet (9.2m) above the water table. Therefore, it may not always be the case that the soil-gas survey will detect VOCs beyond the edge of the plume, and, in fact, may underestimate the extent of the plume.

Discriminating Between Ground Water and Surface Sources

A problem that arises in the course of soil-gas surveys for detection of surface sources, but more so, for mapping ground water contamination, is the potential interference caused by VOC vapors from another source. The interferences are especially problematic in highly industrialized areas with multiple contaminant sources. Based on sensitivity runs, the vapor concentration due to a contaminant source may be sufficient out to several hundred feet to mask the detection of vapors emanating from contaminated ground water when vapor concentrations due to ground water contamination are much less than those due to the diffusion from a surface source. This potential problem was first recognized by Marrin (1984).

Computer simulations reported previously (Silka 1986) were used to estimate the potential interference from the upward diffusion of VOC vapors emanating from contaminated ground water. For the modeling, it was assumed that the highest VOC concentration in ground water underlying the area of the soil-gas survey was 100 ppb. The depth to the water table was 30 feet (9.2m). This level of ground water contamination could result in soil-gas concentrations in the upper 3 feet (0.9m) of soil as high as 150 ppb.

In comparison, a surface source of TCE, with a saturated vapor concentration of 72,000 ppm, could cause a concentration in soil gas at a distance of 100 feet (30.5m) of as high as 72 ppm. Even with a relatively low saturated vapor concentration, for example TET at 6000 ppm, the concentration in soil gas at a distance of 100 feet (30.5m) could be several parts per million. Vapor concentrations of less than a part per million due to diffusion from contaminated ground water would be completely masked by such surface sources.

Conclusions

Previous investigators have shown that VOC vapor migration through the unsaturated zone is primarily under diffusive transport. The vapor diffusion is adequately described by Fick's second law, and the effects of partitioning between soil-gas and soil moisture can be incorporated into the model by the use of Henry's law coefficient. Adsorption of VOCs onto soil organic matter is accounted for by the empirical relationship between the octanol-water partition coefficient and the liquid-solid partition coefficient.

Design of soil-gas surveys should be developed with an understanding of the potential extent and distribution of contaminants in the subsurface. Preliminary modeling of the diffusive transport using a model such as 2D-DIFF can provide useful criteria for designing the survey and interpretation of subsequent results. Modeling results presented here and in a previous paper (Silka 1986) demonstrate the importance of soil moisture content to the design of the soil-gas survey. Optimum conditions for soil-gas surveys occur when lengthy, dry soil conditions have preceded the survey, which usually occur during July, August and September over much of the United States.

Interpretation of soil-gas survey results are hampered by unknown or poorly defined parameters, such as soil porosity, moisture content, organic matter content, as well as source attributes. In general, the variation in soil moisture will have the greatest influence on the rate of diffusion of VOC vapors through the unsaturated zone, especially for those VOCs with small values of K_H. Slight increases in soil moisture dramatically reduce the effective diffusion rate and increase the time required for concentrations in soil gas to approach steady-state values. Dry

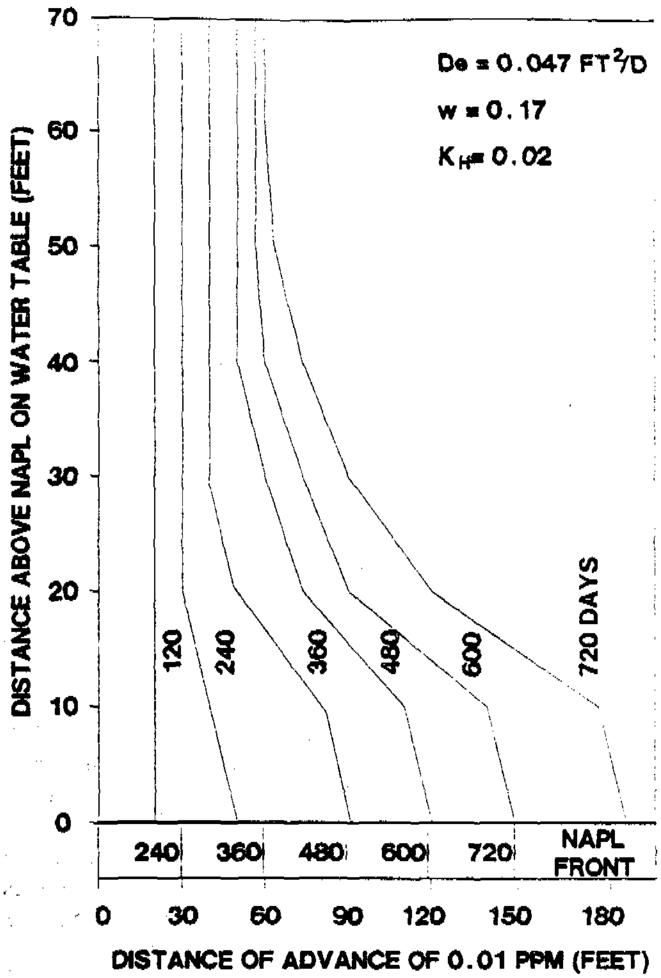

Figure 5. Extent of migration of 0.01 ppm contour for VOC in soil gas from a vertical spill source and advancing NAPL front floating on the water table under slightly moist soil conditions (w=0.17).

soils in arid regions may allow quasi-steady-state concentration profiles to be approached. However, steady-state conditions probably are never approached in the humid, temperate regions where frequent, episodic wet and dry periods occur.

References

Bruell, C.J. and G.E. Hoag. 1986. The Diffusion of Gasoline-Range Hydrocarbon Vapors in Porous Media, Experimental Methodologies. Proc. of the NWWA/API Conference on Petroleum Hydrocarbons and Organic Chemicals in Ground Water—Prevention, Detection and Restoration. National Water Well Association, pp. 420-443.

Callahan, M.A., et al. 1979. Water Related Environmental Fate of 129 Priority Pollutants, v. II EPA-440/4-79-029b. Environmental Protection Agency, Washington, D.C.

Corapcioglu, M.Y. and A.C. Baehr. 1987. A Compositional Multiphase Model for Ground Water Contamination by Petroleum Products. I—Theoretical Considerations. Water Resources Research, v. 23, no. 1, pp. 191-200.

Dilling, W.L. 1977. Interphase Transfer Processes. II. Evaporation Rates of Chloro Methanes, Ethanes, Ethylenes, Propanes and Propylenes from Dilute Aqueous Solutions. Comparisons with Theoretical

Predictions. Environ. Sci. Technol., v. 11, no. 4, pp. 405-409.

Evans, O.D. and G.M. Thompson. 1986. Field and Interpretation Techniques for Delineating Subsurface Petroleum Hydrocarbon Spills Using Soil Gas Analysis. Proc. of the NWWA/API Conference on Petroleum Hydrocarbons and Organic Chemicals in Ground Water—Prevention, Detection and Restoration. National Water Well Association, pp. 444-455.

Ferre, P.T. and L.R. Silka. 1987. Application of the Soil-Gas Survey to Underground Storage Tank Monitoring and Leak Detection. Proc. of the Assoc. of Ground Water Scientists and Engineers Conference, Focus: Eastern Regional Ground Water Issues, pp. 187-205.

Glaccum, R., N. Michael, R. Evans and L. McMillion. 1983. Correlation of Geophysical and Organic Vapor Analyzer Data Over a Conductive Plume Containing Volatile Organics. Proc. of the Third National Symposium on Aquifer Restoration and Ground-Water Monitoring, May 25-27, 1983, Columbus, Ohio, National Water Well Association, pp. 421-427.

Jury, W.A. 1986. Chemical Movement Through Soil. Hern, S.C. and S.M. Melancon, Editors. Vadose Zone Modelling of Organic Pollutants. Lewis Publishers Inc., Chelsea, Michigan, pp. 135-158.

Jury, W.A., W.F. Spencer and W.J. Farmer. 1983. Behavior Assessment Model for Trace Organics in Soil: I. Model Description. Jour. of Environ. Qual., v. 12, no. 4, pp. 558-564.

Jury, W.A., W.F. Spencer and W.J. Farmer. 1984. Behavior Assessment Model for Trace Organics in Soil: IV. Review of Experimental Evidence. Jour. of Environ. Qual., v. 13, no. 4, pp. 580-586.

Karickhoff, S.W., D.S. Brown and T.A. Scott. 1979. Sorption of Hydrophobic Pollutants on Natural Sediments. Water Research, v. 13, pp. 241-248.

Lappala, E.G. and G.M. Thompson. 1983a. Detection of Ground Water Contamination by Shallow Soil Gas Sampling in the Vadose Zone. Proc. of the Characterization and Monitoring of the Vadose (Unsaturated) Zone, December 8-10, 1983, Las Vegas, Nevada, National Water Well Association, pp. 659-679.

Lappala, E.G. and G.M. Thompson. 1983b. Detection of Ground Water Contamination by Shallow Soil Gas Sampling in the Vadose Zone. Proc. of the National Conference on Management of Uncontrolled Hazardous Waste Sites, November 7-9, 1984, Washington, D.C., Hazardous Materials Control Research Institute, Silver Spring, Maryland, pp. 20-28.

Leistra, M. 1973. Computation Models for the Transport of Pesticides in Soil. Residue Review, v. 49, pp. 87-130.

Marrin, D.L. 1984. Remote Detection and Preliminary Hazard Evaluation of Volatile Organic Contaminants in Ground Water. Ph.D. Dissertation. University of Arizona.

Nazaroff, W.W., S.R. Lewis, S.M. Doyle, F.A. Moed and A.V. Nero. 1987. Experiments on Pollutant Transport from Soil into Residential Basements by Pressure-Driven Air Flow. Environ. Sci. and Tech., v. 21, no. 5, pp. 459-466.

Perry, H.P. and C.H. Chilton, Editors. 1973. Chemical Engineers Handbook. 5th edition, McGraw-Hill Book Co., New York.

Rao, P.S.C., A.G. Hornsby, D.P. Kilcrease and P. Nkedi-Kizza. 1985. Sorption and Transport of Hydrophobic Organic Chemicals in Aqueous and Mixed Solvent Systems: Model Development and Preliminary Evaluation. Jour. Environ. Qual., v. 14, no. 3, pp. 376-383.

Silka, L.R. 1986. Simulation of the Movement of Volatile Organic Vapor Through the Unsaturated Zone as It Pertains to Soil-Gas Surveys. Proc. of the NWWA/API Conference on Petroleum Hydrocarbons and Organic Chemicals in Ground Water—Prevention, Detection and Restoration. National Water Well Association, pp. 204-224.

Spencer, W.F. and W.J. Farmer. 1980. Assessment of the Vapor Behavior of Toxic Organic Chemicals. R. Haque, Editor. Dynamics, Exposure and Hazard Assessment of Toxic Chemicals. Ann Arbor Science. Ann Arbor, Michigan.

Striegl, R.G. 1987. Transport of Methane in the Unsaturated Zone. Proc. of the Association of Ground Water Scientists and Engineers Program, Focus: Contaminant Hydrogeology. NWWA Annual Meeting and Expo, September 14-16, 1987.

Swallow, J.A. and P.M. Gschwend. 1983. Volatilization of Organic Compounds from Unconfined Aquifers. Proc. of the Third National Symposium on Aquifer Restoration and Ground Water Monitoring, National Water Well Association, pp. 327-333.

Thibodeaux, L.J. 1979. Chemodynamics. Environmental Movement of Chemicals in Air, Water and Soil. John Wiley & Sons, New York. 501 pp.

Wang, H.F. and M.P. Anderson. 1982. Introduction to Groundwater Modeling. W.H. Freeman and Co. San Francisco, p. 70.

Biographical Sketch

Lyle R. Silka is president of HYDROSYSTEMS Inc. (2042 Peach Orchard Dr., Falls Church, VA 22043). He has more than 15 years of experience in hazardous waste site characterization, risk and liability assessment, evaluation of remedial actions, and computer modeling applications. From 1976 to 1980, he was a hydrogeologist with the U.S. Environmental Protection Agency in Washington, D.C., involved in regulatory development under RCRA and program implementation under Superfund. From 1980 to 1983, he was senior hydrogeologist with GeoTrans Inc. in Herndon, Virginia. Currently, Silka is directing the remedial investigation/feasibility study of a Superfund site in Virginia and is the principal technical advisor for responsible parties at three other Superfund sites in Washington, Oregon and Virginia. Silka has applied soil-gas surveys for the detection of subsurface VOC contamination as part of environmental audits at 12 industrial sites and is directing research into the transport and fate of VOCs in the unsaturated zone. Silka has published more than 20 professional papers and is a member of the NWWA Association of Ground Water Scientists and Engineers, Association of Engineering Geologists, the Geological Society of America, and the American Chemical Society.